

**Springer Theses**  
Recognizing Outstanding Ph.D. Research

Paul-Hermann Balduf

# Dyson–Schwinger Equations, Renormalization Conditions, and the Hopf Algebra of Perturbative Quantum Field Theory



Springer

# **Springer Theses**

Recognizing Outstanding Ph.D. Research

## **Aims and Scope**

The series “Springer Theses” brings together a selection of the very best Ph.D. theses from around the world and across the physical sciences. Nominated and endorsed by two recognized specialists, each published volume has been selected for its scientific excellence and the high impact of its contents for the pertinent field of research. For greater accessibility to non-specialists, the published versions include an extended introduction, as well as a foreword by the student’s supervisor explaining the special relevance of the work for the field. As a whole, the series will provide a valuable resource both for newcomers to the research fields described, and for other scientists seeking detailed background information on special questions. Finally, it provides an accredited documentation of the valuable contributions made by today’s younger generation of scientists.

**Theses may be nominated for publication in this series by heads of department at internationally leading universities or institutes and should fulfill all of the following criteria**

- They must be written in good English.
- The topic should fall within the confines of Chemistry, Physics, Earth Sciences, Engineering and related interdisciplinary fields such as Materials, Nanoscience, Chemical Engineering, Complex Systems and Biophysics.
- The work reported in the thesis must represent a significant scientific advance.
- If the thesis includes previously published material, permission to reproduce this must be gained from the respective copyright holder (a maximum 30% of the thesis should be a verbatim reproduction from the author’s previous publications).
- They must have been examined and passed during the 12 months prior to nomination.
- Each thesis should include a foreword by the supervisor outlining the significance of its content.
- The theses should have a clearly defined structure including an introduction accessible to new PhD students and scientists not expert in the relevant field.

Indexed by zbMATH.

Paul-Hermann Balduf

# Dyson–Schwinger Equations, Renormalization Conditions, and the Hopf Algebra of Perturbative Quantum Field Theory

Doctoral Thesis accepted by  
Humboldt University of Berlin, Germany



Springer

*Author*  
Dr. Paul-Hermann Balduf  
Combinatorics and Optimization  
University of Waterloo  
Waterloo, ON, Canada

*Supervisor*  
Prof. Dr. Dirk Kreimer  
Humboldt-Universität zu Berlin  
Berlin, Germany

ISSN 2190-5053

Springer Theses

ISBN 978-3-031-54445-3

<https://doi.org/10.1007/978-3-031-54446-0>

ISSN 2190-5061 (electronic)

ISBN 978-3-031-54446-0 (eBook)

© The Editor(s) (if applicable) and The Author(s), under exclusive license to Springer Nature Switzerland AG 2024

This work is subject to copyright. All rights are solely and exclusively licensed by the Publisher, whether the whole or part of the material is concerned, specifically the rights of translation, reprinting, reuse of illustrations, recitation, broadcasting, reproduction on microfilms or in any other physical way, and transmission or information storage and retrieval, electronic adaptation, computer software, or by similar or dissimilar methodology now known or hereafter developed.

The use of general descriptive names, registered names, trademarks, service marks, etc. in this publication does not imply, even in the absence of a specific statement, that such names are exempt from the relevant protective laws and regulations and therefore free for general use.

The publisher, the authors, and the editors are safe to assume that the advice and information in this book are believed to be true and accurate at the date of publication. Neither the publisher nor the authors or the editors give a warranty, expressed or implied, with respect to the material contained herein or for any errors or omissions that may have been made. The publisher remains neutral with regard to jurisdictional claims in published maps and institutional affiliations.

This Springer imprint is published by the registered company Springer Nature Switzerland AG  
The registered company address is: Gewerbestrasse 11, 6330 Cham, Switzerland

Paper in this product is recyclable.

*Wir sindameisen und bauen an schwerem  
gerät*

*Elisa Weinkötz*<sup>1</sup>

---

<sup>1</sup> E. Weinkötz, “Gedichte”, in 27. open mike Wettbewerb für junge Literatur (Allitera Verlag, München, 2019), p. 182.

# Supervisor's Foreword

*Quantum Field Theory is a monster.* What a wonderful sentence to open a thesis dedicated to the complexities and miracles of quantum field theory.

The monster is treated with care and respect starting from a first chapter introducing perturbative quantum field theory. The chapter is a rather complete if succinct account of its foundations and its incarnation for the practitioner: Feynman graphs. The chapter ends with the introduction of Dyson–Schwinger equations, the entrance door for a treatment beyond perturbation theory.

The next chapter introduces the Hopf algebra theory of renormalization. It starts with the treatment of power series so as to allow the renormalization of Dyson–Schwinger equations later on. It then pays tribute to the consideration of perturbative quantum field theory order by order and graph by graph.

Chapter 3 returns to full Green functions in kinematic renormalization. It emphasizes that we can read renormalization as the choice of suitable boundary conditions for those Dyson–Schwinger equations. Iterating this choice reproduces the perturbative renormalization by the Hopf algebra structure introduced before. The renormalization group is here studied in accordance with the group structure emanating from Hopf algebra of Feynman graphs.

These first three chapters can be read as an introduction to renormalization and quantum field theory based on Hopf algebraic structures underlying any perturbative expansion. They constitute Paul's beautiful pedagogical account of 25 years of work in that area.

Chapter 4 then treats non-kinematic renormalization with a focus on recent research of Paul Balduf. It provides an exhaustive discussion of renormalization after regularization by a complex parameter, most prominently through the popular dimensional regularization and ensuing minimal subtraction.

The results enrich our conceptual understanding of the monster's fearsome incarnations profoundly. Indeed, the conceptual differences by renormalization through minimal subtraction in dimensional as compared to kinematic renormalization have never been systematically addressed before. It is a relief to see this finally treated with care.

Chapter 5 changes track. Apart from work on renormalization Paul also considered the invariance of a quantum field theory under diffeomorphisms of its defining quantum fields. The naive answer of the path integral approach—*The theory is invariant!*—is as wrong as is the definition of the path integral unsatisfactory. He gives precise conditions under which the naive answer is correct.

As this chapter was not the main topic of his thesis we are given in succinct manner a trove of fascinating results which invite the reader's curiosity. It includes a digression on quantum gravity studying its Feynman rules in comparison to a theory obtained by field diffeomorphisms.

The final chapter gives conclusions. As it befits a true opus, these are as much a summary of what has been achieved as an outlook to future work on the asymptotics of perturbation theory by numerical quadrature.

Behind its technical details Paul's thesis is a masterful account of recent research. It amasses an enormous set of results reflecting the richness of its subject. Indeed it allows only for one conclusion: The monster is quite charming.

Berlin, Germany  
February 2024

Prof. Dr. Dirk Kreimer

# Preface

Quantum field theory is a monster: Unmanageable in terms of the sheer number of different, sometimes contradictory, principles, formalisms, definitions, and results that have been amassed in the past 100 years, often without clear relation to each other. It suffers from mathematical conundrums, incomprehensible heuristic constructions, and being declared hopeless or obsolete once every few years, while at the same time its computational techniques are being used successfully in ever more remote areas of research.

For the present thesis, this has two consequences: Firstly, I spent extraordinarily much effort on explaining the background of relevant constructions, discussing their relations and demonstrating the logical order of their development, as well as the practical applicability in 151 examples. And secondly, I tried to refer not only to modern reviews, but also to historical original work, in order to acknowledge the context and motivation of these constructions. At five occasions, complete sections are marked as *Digression*, they are not relevant for the understanding of the thesis, but contain additional remarks, motivations, or related topics I found interesting.

More than 70 years after its inception, text books about quantum field theory are now readily available for the general audience, e.g., [1–5], as well as for almost any profession, from mathematicians [6] over economists [7] to gifted amateurs [8]. Nevertheless, Chap. 1 is a self-contained introduction to make the thesis accessible to readers without a background in quantum field theory. Conversely, in Chap. 2, I review the mathematical formalism, before introducing the concept of renormalization. Chapter 3 concerns the renormalization group, which lies at the heart of the thesis. Most of my own new results are contained in Chap. 4, where I examine different renormalization schemes. Finally, Chap. 5 contains the results of a second research project, concerning transformations of the field variable. Chapter 6 is a summary of key findings of the thesis, and a short outlook to future work. The appendix is—apart from the bibliography—mostly for entertainment.

Occasionally, I quote from works in their original language German or French. A friend mocked this as “a very continental attitude”, a verdict I can live with. The

reader can rest assured that those quotes only serve to illustrate some qualitative remarks of mine, and that they are completely irrelevant for the main text.

Kreuzberg, Germany  
October 2022

Paul-Hermann Balduf

## References

1. A. Das, *Lectures on Quantum Field Theory* (World Scientific, Singapore, 2010)
2. C. Itzykson, J.-B. Zuber, *Quantum Field Theory* (Dover publications, Mineola, New York, 2005)
3. N. Nakanishi, I. Ojima, *Covariant Operator Formalism of Gauge Theories and Quantum Gravity* (World scientific, 1990), <https://www.worldscientific.com/doi/abs/10.1142/0362>
4. S. Weinberg, *The Quantum Theory of Fields. Volume 1: Foundations*, vol. 1 (Cambridge University Press, Cambridge, 1996), <https://doi.org/10.1017/CBO9781139644167>
5. M.E. Peskin, D.V. Schroeder, 6R. Ticciati, *Quantum Field Theory for Mathematicians*, (1995), <https://cds.cern.ch/record/257493>
6. R. Ticciati, *Quantum Field Theory for Mathematicians*, Encyclopedia of Mathematics and Its Applications (Cambridge University Press, Cambridge, 1999), <https://www.cambridge.org/core/books/quantum-field-theory-for-mathematicians/4783BB717856D3572422F05714CA3D5A>
7. B. E. Baaquie, *Quantum Field Theory for Economics and Finance—Econophysics*, Financial Physics and Social Physics (Cambridge, 2018), <https://www.cambridge.org/de/academic/subjects/physics/econophysics-and-financial-physics/quantum-field-theory-economics-and-finance>
8. T. Lancaster, S. Blundell, *Quantum Field Theory for the Gifted Amateur*, First Edition (Oxford University Press, Oxford, 2014)

# Acknowledgements

First of all, I thank my supervisor Dirk, who is always optimistic and confident in his doctoral candidates' work. A doctorate is probably never truly easy, and even less so when one is working on an individual highly specialized project during a pandemic. This endeavor would have been impossible without Dirk trusting and encouraging me that it will eventually succeed. Renormalization group theory is a subject that, on the one hand, is old enough that most of the recent publications simply assume the basics without precise definitions, and, on the other hand, it is obscure enough that tiny inaccuracies in notation or interpretation of formulas can quickly make a calculation pointless or even wrong. The only way for me to comprehend the different historic and modern perspectives on renormalization, regularization, renormalization group, and renormalization conditions was to spend several months on re-doing old calculations, changing definitions, reading old papers, and re-doing calculations once again. During that time I did not write any paper, and I did not produce any result that had not, from some perspective, been known for decades. Dirk believed that this undertaking is ultimately worthwhile, and he gave me as much time as I needed to finish it, even when I could not exactly explain to him what I was trying to achieve other than understand the renormalization group. From Dirk, I have learned that one can actually understand things in quantum field theory, not merely do calculations and follow ad hoc recipes. Besides, despite being retired, he still answers my messages more quickly than most of my friends.

I am thankful for discussions, comments, and suggestions by people I met during conferences, in Berlin or online. Among them, I want to mention especially David Broadhurst, Karen Yeats, Gerald Dunne, John Gracey, Oliver Schnetz, Michael Borinsky, Erik Panzer, Marko Berghoff, David Prinz, Maximilian Mühlbauer, and René Klausen.

In terms of language, consistency, and orthography, the thesis has profited immensely from Daniel's proofreading and comments, who continued to find missing hyphens in proofs even after I started printing them \tiny. Cordula has contributed to design and insisted that not all text be printed \tiny, even if it would have made the thesis shorter.

Alexandra, my friends, and my family have not seen me much in the past months, I thank them for supporting me with food and encouragement.

Finally, during the last 3 years HU-Docs has become something like a second family. With public life shut down and conferences cancelled, it was a relief to see new faces every week, if only virtually, to learn about each other's research, and hear stories from all over the world. I thank all members of the HU-Docs board for this supporting environment, and for making an active club life possible in the challenging times of a pandemic.

# Contents

<b>1</b>	<b>Introduction to Perturbative Quantum Field Theory</b>	1
1.1	Conventions	2
1.2	From Classical Field Theory to Perturbative QFT	4
1.2.1	Classical Field Theory	4
1.2.2	Canonical Quantization	11
1.2.3	2-Point Correlation Functions	13
1.2.4	$n$ -Point Correlation Functions of the Free Field	18
1.2.5	The S-Matrix	20
1.2.6	Perturbative Computation of the S-Matrix	23
1.2.7	The Path Integral	25
1.2.8	Digression: History and Alternative Ways to Compute the S-Matrix	27
1.3	Feynman Graphs	30
1.3.1	Graphical Representation of Feynman Integrals	30
1.3.2	Basic Definitions	32
1.3.3	Graph Matrices	36
1.3.4	Graph Polynomials	42
1.3.5	Feynman Rules in Position Space	46
1.3.6	Feynman Rules in Momentum Space	48
1.3.7	Feynman Rules in Parametric Space	52
1.3.8	Symmetry Factors	58
1.3.9	Digression: Electrical Networks	62
1.3.10	1PI Graphs	65
1.3.11	Dyson–Schwinger Equations	67
	References	72
<b>2</b>	<b>Hopf Algebra Theory of Renormalization</b>	81
2.1	Combinatorics and Hopf Algebras	82
2.1.1	Formal Power Series	82
2.1.2	Divergent Power Series	85
2.1.3	Basics of Hopf Algebra Theory	91

2.1.4	Faà di Bruno Hopf Algebra . . . . .	102
2.1.5	Connes-Kreimer Hopf Algebra . . . . .	109
2.1.6	Fixed-Point Equations for Rooted Trees . . . . .	113
<b>2.2</b>	<b>Renormalization . . . . .</b>	<b>115</b>
2.2.1	Renormalization of a Formal Power Series . . . . .	116
2.2.2	Classification of Feynman Amplitudes . . . . .	118
2.2.3	Hopf Algebra of Feynman Graphs . . . . .	121
2.2.4	Renormalized Feynman Rules . . . . .	127
2.2.5	Dyson-Schwinger Equations Revisited . . . . .	130
<b>2.3</b>	<b>Divergences and Renormalizability . . . . .</b>	<b>135</b>
2.3.1	Divergences of Feynman Graphs . . . . .	135
2.3.2	Analytic Regularization . . . . .	138
2.3.3	Dimensional Regularization . . . . .	140
2.3.4	Renormalizability . . . . .	146
<b>2.4</b>	<b>Digression: Order of Derivatives and Dimension of Spacetime . . . . .</b>	<b>153</b>
	<b>References . . . . .</b>	<b>155</b>
<b>3</b>	<b>Renormalized Green Functions in Kinematic Renormalization . . . . .</b>	<b>163</b>
<b>3.1</b>	<b>Renormalization and Momentum-Dependence . . . . .</b>	<b>164</b>
3.1.1	Angles and Scales . . . . .	164
3.1.2	Expansion in Logarithmic Momenta . . . . .	164
3.1.3	Mellin Transforms . . . . .	168
<b>3.2</b>	<b>Renormalization Group in Kinematic Renormalization . . . . .</b>	<b>172</b>
3.2.1	Callan-Symanzik Equation . . . . .	172
3.2.2	Counterterms and $\epsilon$ -dependence . . . . .	178
3.2.3	Grouplike Green Functions . . . . .	183
3.2.4	Digression: History and Variants of the Renormalization Group . . . . .	186
<b>3.3</b>	<b>Dyson-Schwinger Equations, Third Act . . . . .</b>	<b>188</b>
3.3.1	Propagator-DSE as Differential Equation . . . . .	188
3.3.2	Insertions into a Single Edge . . . . .	190
3.3.3	Leading-Log Expansion . . . . .	194
3.3.4	Non-physical Spacetime Dimension . . . . .	196
<b>3.4</b>	<b>Asymptotics and Nonperturbative Contributions in MOM . . . . .</b>	<b>199</b>
3.4.1	Multiedge DSE at $D = 4$ . . . . .	199
3.4.2	Stokes Constant as a Function of the Exponent of the Invariant Charge . . . . .	203
3.4.3	Multiedge DSE at $D = 6$ . . . . .	205
3.4.4	Toy Model . . . . .	207
	<b>References . . . . .</b>	<b>208</b>
<b>4</b>	<b>Renormalization Group and DSEs in Non-kinematic Renormalization . . . . .</b>	<b>215</b>
<b>4.1</b>	<b>Non-kinematic Renormalization Schemes . . . . .</b>	<b>216</b>
4.1.1	General Infinitesimal Feynman Rules . . . . .	216

4.1.2	Renormalization Group Functions at the Physical Dimension .....	220
4.1.3	Properties of Minimal Subtraction .....	225
4.1.4	Renormalization Scheme Independent Quantities .....	227
4.2	Recursively Solving a DSE .....	229
4.2.1	Expansion of the Kernel of the DSE .....	229
4.2.2	Series Solution of the DSE .....	231
4.2.3	Expansions of the Renormalized Green Function .....	236
4.2.4	Exact Solutions of the Toy Model .....	240
4.3	Shifted Kinematic Renormalization Point .....	242
4.3.1	Shifted Green Function .....	242
4.3.2	Shifted Counterterms .....	245
4.3.3	Shifted Renormalization Group Functions .....	248
4.4	MS as a Shifted MOM Scheme .....	252
4.4.1	Relation Between MS and MOM .....	253
4.4.2	Brute-Force Computation .....	254
4.4.3	Relation of the Shift to Renormalization Group Functions .....	255
4.4.4	Deriving the Shift from the MOM Solution .....	258
4.5	Shift Between MS and MOM in Non-linear Examples .....	261
4.5.1	Multiedge DSE in $D = 4$ Dimensions .....	261
4.5.2	Multiedge DSE in $D = 6$ Dimensions .....	265
4.5.3	Toy Model .....	268
4.5.4	The Chain Approximation in $D = 4$ .....	270
	References .....	273
<b>5</b>	<b>Field Diffeomorphisms and Symmetries .....</b>	<b>275</b>
5.1	Symmetries and Hopf Ideals .....	276
5.1.1	Symmetries .....	276
5.1.2	Ward Identities .....	278
5.1.3	Hopf Ideals .....	282
5.1.4	Tadpoles .....	284
5.2	Diffeomorphisms of Scalar Fields .....	287
5.2.1	Digression: The Numerous Problems of Quantum Gravity .....	287
5.2.2	Field Diffeomorphisms .....	291
5.2.3	Diffeomorphism Feynman Rules in Position Space .....	293
5.2.4	Diffeomorphism Feynman Rules in Momentum Space .....	296
5.2.5	Propagator Cancellations and the Connected Perspective .....	297
5.2.6	Two-Point Function in Momentum Space .....	301
5.3	Exponential Diffeomorphism .....	304
5.3.1	Field Transformations .....	304

5.3.2	Correlation Functions of the Exponential Diffeomorphism .....	307
5.4	Divergences of Field Diffeomorphisms .....	310
5.4.1	Metacounterterms .....	310
5.4.2	Metacounterterms for Less Than 3 Edges Offshell .....	312
5.4.3	1PI Counterterms .....	316
5.4.4	Ward Identities of the Field Diffeomorphism .....	321
	References .....	324
<b>6</b>	<b>Conclusion</b> .....	331
6.1	Summary .....	331
6.2	Outlook: Numerical Integration of Feynman Periods .....	333
6.2.1	Symmetries of the Period .....	333
6.2.2	Numerical Quadrature .....	335
6.2.3	Results .....	337
	References .....	340
	<b>Author’s Curriculum Vitae</b> .....	343
	<b>Appendix A: Curious Quotes from the Literature</b> .....	349
	<b>Appendix B: Statistics</b> .....	353
	<b>Appendix C: Lied vom Schreiberling</b> .....	355
	<b>Appendix D: List of Examples</b> .....	357
	<b>Bibliography</b> .....	361

# Chapter 1

## Introduction to Perturbative Quantum Field Theory



The first chapter is a short, but largely self-contained, introduction to perturbative quantum field theory and its description in terms of Feynman graphs.

For the later chapters, which are based on details of the process of renormalization, the most important aspects of quantum field theory are the combinatorics of Feynman graphs, and their scale-dependence or energy-dependence. Both these effects can most easily be studied for a quantum field theory where the field is a single scalar quantity, as opposed to e.g., a vector-valued field. The main difference between the present chapter and typical quantum field theory courses is that we concentrate our attention on scalar fields, as opposed to quantum electrodynamics or quantum chromodynamics. The first part of the chapter, Sect. 1.2, is a concise review of quantization. Its main purpose is to set the stage and introduce the most fundamental constructions, such as Green functions, the Dyson series, or the path integral. It should on a technical level be accessible to a reader who has no formal education in quantum field theory.

The second part of the present chapter, Sect. 1.3, deals with Feynman graphs and Feynman rules in a way that is significantly more mathematical than what is common in introductory physics courses. Still, this part is intended to be understandable for a reader without formal education in graph theory. We introduce several mathematical constructions such as graph matrices and graph polynomials, and study their properties for Feynman graphs. The goal with this approach is to be able to work with Feynman graphs and their Feynman integrals in a relatively rigorous, systematic fashion, without resorting to ad-hoc arguments later in the thesis. To the physicist reader, this might at first appear overly technical, but it will pay off in later chapters when the combinatorial properties of symmetry factors, Dyson–Schwinger equations, and renormalization, turn out to be entirely plausible and natural.

## 1.1 Conventions

The following notation and conventions should be familiar to the physicist reader.

Definitions will be indicated by “ $\coloneqq$ ”, where  $A \coloneqq B$  means that  $A$  is defined to be equal to  $B$ . The real numbers are  $\mathbb{R}$ , the natural numbers  $\mathbb{N}$  do not include zero, and  $\mathbb{N}_0 = \mathbb{N} \cup \{0\}$ . The sign  $\propto$  means “exactly proportional to”, while  $\sim$  denotes “of the order” or “approximately proportional to”. With  $\stackrel{!}{=}$  we denote “is demanded to be equal”. The center dot  $\cdot$  is used to visually highlight a multiplication. It does not indicate a special type of multiplication, such as a scalar product between vectors.

Integrals act as operators on products to the right of them, but not on sums:

$$\int dx \left( f(x)g(x) + h(x) \right) \neq \int dx f(x)g(x) + h(x) = \left( \int dx f(x)g(x) \right) + h(x).$$

An integral without explicit integration domain is meant to cover the entire space.

In this thesis, we assume a flat  $D$ -dimensional spacetime. A point in this spacetime is a  $D$ -vector, that is an ordered tuple

$$\underline{x} := (x^0, \mathbf{x}) := (x^0, x^1, \dots, x^{D-1}),$$

consisting of one time coordinate  $x^0$  and a  $(D - 1)$ -dimensional vector  $\mathbf{x}$  which denotes the position in space.

**Definition 1.** The  $D$ -dimensional real vector space together with the pseudo scalar product Eq.(1.1) is called *Minkowski space*  $\mathbb{M}^D$ . The *Minkowski metric* is the  $D \times D$ -matrix

$$\eta := \text{diag}(1, -1, \dots, -1) = \begin{pmatrix} 1 & 0 & \dots & 0 \\ 0 & -1 & \dots & 0 \\ \vdots & & \ddots & \vdots \\ 0 & \dots & 0 & -1 \end{pmatrix}.$$

The magnitude of a vector is given by the pseudo scalar product

$$\underline{x}\underline{y} := \sum_{i=0}^{D-1} \sum_{j=0}^{D-1} x^i \eta_{ij} y^j = \sum_{i=0}^{D-1} x^i y_i =: x_i y^i \quad (1.1)$$

where “pseudo” indicates that the quantity  $\underline{x}^2 = \underline{x}\underline{x}$  might be negative for certain vectors  $\underline{x}$ . In Eq.(1.1), we have introduced Einstein’s sum convention: If an index (the  $i$  in the last formula) appears twice, it is being summed over.

Occasionally, we use *Euclidean spacetime*, where the metric is  $\mathbb{1}_{D \times D} = \text{diag}(1, \dots, 1)$ . The transition between Euclidean and Minkowski metric is formally

achieved by exchanging  $x^0 = t \leftrightarrow i\tau$ . This can be interpreted as continuation to imaginary times, and is called *Wick rotation*.

**Definition 2 ([5, 6]).** Let  $\eta$  be the Minkowski metric (Definition 1). A *Lorentz transformation* is a transformation of coordinates  $x'^\mu = \Lambda^\mu_\nu x^\nu$ , where the transformation matrix  $\Lambda$  satisfies

$$\Lambda^\mu_\rho \Lambda^\nu_\sigma \eta_{\mu\nu} = \eta_{\rho\sigma}, \quad \text{or short} \quad \Lambda^T \eta \Lambda = \eta.$$

Transformations between different inertial frames are given by the group of Lorentz transformations. In  $D = 4$  spacetime dimensions, a Lorentz transformation has 6 parameters, representing rotations around 3 axes and changes in the relative velocity along 3 axes. The Lorentz group is closely related to causality [7].

**Definition 3 ([8]).** A *Poincaré transformation* is a transformation of coordinates  $x'^\mu = \Lambda^\mu_\nu x^\nu + a^\mu$ , where  $\Lambda$  is a Lorentz transformation (Definition 2) and  $a$  is a  $D$ -dimensional constant vector.

We use *natural units*, that is, we choose the units such that the speed of light is  $c = 1$  and the reduced Planck constant [9] is  $\hbar = 1$ . Thereby, all quantities we encounter have the same unit, which one can choose to be mass.

**Definition 4.** If, in natural units, a quantity has the unit  $(\text{mass})^n$  for some  $n$ , we say it has *mass dimension*  $n$ . Equivalently, the unit  $(\text{length})^n$  amounts to a mass dimension  $-n$ .

A Fourier transform involves a factor  $2\pi$ , which we include into the momentum-integral,

$$\tilde{f}(k) = \int dx f(x) e^{ikx} \Leftrightarrow f(x) = \int \frac{dk}{2\pi} \tilde{f}(k) e^{-ikx}.$$

**Definition 5 ([10]).** Let  $\nu \in \mathbb{R}$  and  $-\nu \notin \mathbb{N}_0$ . The *Euler Gamma function* is defined as

$$\Gamma(\nu) := \int_0^\infty dt t^{\nu-1} e^{-t}.$$

For later use, we note here two formulae regarding the  $D$ -dimensional Fourier transforms of a monomial. Let  $\nu \in \mathbb{C}$  with real part  $-\nu \notin \mathbb{N}_0$  and  $\nu - D/2 \notin \mathbb{N}_0$ , and  $n \in \mathbb{N}$ , then [11, pp. 155, 163]

$$\begin{aligned} \int \frac{d^D k}{(2\pi)^D} \frac{1}{(\underline{k}^2)^\nu} e^{-i\underline{k}\underline{x}} &= \frac{1}{4^\nu \pi^{\frac{D}{2}}} \frac{\Gamma\left(\frac{D}{2} - \nu\right)}{\Gamma(\nu)} (\underline{x}^2)^{\nu - \frac{D}{2}} \\ \int \frac{d^D k}{(2\pi)^D} (\underline{k}^2)^n e^{-i\underline{k}\underline{x}} &= (-1)^n (\partial_\mu \partial^\mu)^n \delta(\underline{x}), \quad n \in \mathbb{N}. \end{aligned} \quad (1.2)$$

The  $D$ -dimensional Euclidean Gaussian [12] integral is

$$\int \frac{d^D \underline{k}}{(2\pi)^D} e^{i\alpha \underline{k}^2 - i\underline{k}\underline{x}} = \left( \frac{i}{4\pi\alpha} \right)^{\frac{D}{2}} e^{-\frac{i\underline{x}^2}{4\alpha}}. \quad (1.3)$$

Similarly, if the quadratic function of  $n$  variables in the exponent involves a matrix  $A$ , we have

$$\int \frac{d^n \vec{u}}{(2\pi)^{\frac{n}{2}}} e^{-\frac{1}{2} \vec{u}^T A \vec{u}} = \frac{1}{(\det A)^{\frac{1}{2}}}. \quad (1.4)$$

## 1.2 From Classical Field Theory to Perturbative QFT

This thesis concerns perturbative quantum field theory (QFT). Before we discuss the technical points, the present section is a brief introduction to the subject. The content is readily available in any QFT course or textbook, such as [1–4]. The reader familiar with the basics is invited to skip directly to Sect. 1.3.

### 1.2.1 Classical Field Theory

Colloquially, a field is an object which takes a value depending on a point in space-time. In the present thesis, we almost exclusively consider scalar fields, this means that the value of the field is a single, real number (as opposed to a vector or a matrix) at each point. More formally, a field is a function  $\phi : \mathbb{M}^D \rightarrow \mathbb{R}$ . A *field theory* is a set of fields, together with so-called *equations of motion* which describe the behavior of these fields.

One way to specify a field theory is through the corresponding Lagrangian density, short *Lagrangian*. It contains the field variables and information about how the fields interact with themselves or with each other.

**Definition 6.** A *Lagrangian* is a function  $\mathcal{L}$  with the following properties:

1.  $\mathcal{L}(\underline{x})$  can depend on  $\underline{x}$ , on  $\phi(\underline{x})$ , and on finitely many derivatives of  $\phi(\underline{x})$ , all evaluated at the same spacetime point  $\underline{x}$  (“locality”).
2.  $\mathcal{L}(\underline{x})$  is a scalar under Poincaré transformations (Definition 3),  $\mathcal{L}(\underline{x}) \mapsto \mathcal{L}(\Lambda \underline{x})$ .
3.  $\mathcal{L}(\underline{x})$  depends on the field  $\phi(\underline{x})$  only via the value  $\phi(\underline{x})$  itself and its first derivatives  $\partial_\mu \phi(\underline{x})$ , not via higher derivatives of  $\phi(\underline{x})$ .
4.  $\mathcal{L}(\underline{x})$  has mass dimension (Definition 4)  $D$  in a  $D$ -dimensional spacetime. Equivalently, the action (Definition 7) carries no units.

We write  $\mathcal{L}(\underline{x})$  or equivalently  $\mathcal{L}(\phi, \partial_\mu \phi)$  for  $\mathcal{L}(\underline{x}, \phi(\underline{x}), \partial_\mu \phi(\underline{x}))$ .

We restrict ourselves to Lagrangians that do not depend on  $\underline{x}$  explicitly. Property 2 implies that the field variables are representations of the Poincaré group (Definition 3). A closer inspection of the structure of this group [6] reveals that fields, and in a quantum theory their corresponding particles, can be classified according to a half-integer parameter *spin* and a real, non-negative parameter *mass*. Property 3 is subtle. At this point, we take it as an axiom without obvious physical reason, but we will explore the motivation and implications in Sect. 2.4.

**Definition 7.** The *action* is the  $D$ -dimensional spacetime integral of the Lagrangian,

$$S[\phi] := \int d^D \underline{x} \mathcal{L}(\underline{x}).$$

### Example 1: Free scalar field, Lagrangian.

The Lagrangian density of the free scalar field reads

$$\mathcal{L} = \frac{1}{2} \partial_\mu \phi(\underline{x}) \partial^\mu \phi(\underline{x}) - \frac{1}{2} m^2 \phi^2(\underline{x}).$$

In this,

- The prefactors  $\frac{1}{2}$  are convention.
- The first summand,  $\frac{1}{2} \partial_\mu \phi(\underline{x}) \partial^\mu \phi(\underline{x})$ , is called *kinetic term*. For each field, a Lagrangian density needs to have one kinetic term, which is the product of two field variables and involves at least one derivative.
- The second summand,  $\frac{1}{2} m^2 \phi^2(\underline{x})$ , is called *mass term*. It is quadratic in the field without derivative. The constant  $m \in \mathbb{R}$  has mass dimension (Definition 4)  $[m] = 1$ . The mass term is optional, fields can be massless.

Both summands in the free Lagrangian density are quadratic in the field variable. Since the Lagrangian has mass dimension  $[\mathcal{L}] = D$ , the field variable must have mass dimension

$$[\phi] = \frac{D - 2}{2}.$$

The characteristic property of a free field theory is that the Lagrangian is quadratic in the field variables, it can therefore be expressed with a differential operator  $\hat{s}$  in the form

$$\mathcal{L} = \frac{1}{2} \phi \hat{s} \phi. \quad (1.5)$$

**Definition 8.** The *offshell variable*  $s_p$  is the Fourier transform of the free field differential operator from Eq. (1.5),

$$s_p \cdot e^{i \underline{p} \underline{x}} := \hat{s} e^{i \underline{p} \underline{x}},$$

A momentum  $\underline{p}$  is said to be *onshell* if  $s_p = 0$ , otherwise  $\underline{p}$  is called *offshell*. For numbered momenta, we use the shorthand notation  $s_{i+j} := s_{p_i + p_j}$ .

### Example 2: Scalar field, field differential operator.

The Lagrangian from Example 1 amounts to the field differential operator  $\hat{s} = -\partial_\mu \partial^\mu - m^2$  and the offshell variable  $s_p = \underline{p}^2 - m^2$ . A particle is onshell if  $\underline{p}^2 = m^2$ .

The corresponding massless theory is obtained by setting  $m = 0$ , i.e.,

$$\mathcal{L} = -\frac{1}{2} \phi \partial_\mu \partial^\mu \phi, \quad \hat{s} = -\partial_\mu \partial^\mu, \quad s_p = \underline{p}^2.$$

Any summand of higher than second power represents an interaction between fields. We only consider interactions that are monomials in the field, which amounts to a Lagrangian

$$\mathcal{L} = \frac{1}{2} \partial_\mu \phi(\underline{x}) \partial^\mu \phi(\underline{x}) - \frac{1}{2} m^2 \phi^2(\underline{x}) - \sum_{n=3}^{\infty} \frac{\lambda_n}{n!} \phi^n(\underline{x}). \quad (1.6)$$

Here, the parameters  $\lambda_n$  are called *coupling constants*. In classical field theory they take a pre-defined finite numerical value. From now on, we will mostly skip the argument  $(\underline{x})$ , understanding that all terms in a Lagrangian are to be evaluated at the same point.

**Example 3:  $\phi^n$  theory, Lagrangian.**

The so-called  $\phi^n$  theory is a model with only a single interaction monomial  $\propto \phi^n$ . The most popular examples are  $\phi^3$  theory and  $\phi^4$  theory. The Lagrangian of  $\phi^n$  theory is

$$\mathcal{L} = \frac{1}{2} \partial_\mu \phi \partial^\mu \phi - \frac{1}{2} m^2 \phi^2 - \frac{\lambda_n}{n!} \phi^n.$$

Following Definition 6 and Example 1, we conclude the mass dimension of the coupling constant

$$[\lambda_n] = D - n \frac{D-2}{2}, \quad \Rightarrow \quad [\lambda_3] = 3 - \frac{1}{2}D, \quad [\lambda_4] = 4 - D.$$

**Example 4: Liouville theory, Lagrangian.**

A typical example of non-polynomial interaction are theories of Liouville-type [13]

$$\mathcal{L} = \frac{1}{2} \partial_\mu \phi \partial^\mu \phi - c \exp(\lambda \cdot \phi).$$

In this case  $[\phi] = \frac{D-2}{2}$  and  $[\lambda] = \frac{2-D}{2}$  and  $[c] = D$ .

The classical equations of motion can be obtained by requesting that the action (Definition 7) be invariant under infinitesimal changes of the field  $\phi$ ,

$$\delta S[\phi] \stackrel{!}{=} 0. \quad (1.7)$$

A series expansion of the Lagrangian in the field variable, assuming the properties of Definition 6 are fulfilled, leads to the Lagrangian equation of motion,

$$\frac{\partial \mathcal{L}}{\partial \phi} - \frac{d}{dx^\mu} \left( \frac{\partial \mathcal{L}}{\partial (\partial_\mu \phi)} \right) = 0. \quad (1.8)$$

Here, all functions and derivatives are to be taken at the same spacetime point. Equation (1.8) is a second order partial differential equation, it requires two initial conditions: The field  $\phi(0, \mathbf{x})$  at the starting time and its time derivative  $\partial_0 \phi(0, \mathbf{x}) =: \dot{\phi}(0, \mathbf{x})$ , both for the entire space.

### Example 5: Free scalar field, classical solution.

The free Lagrangian from Example 1 results in

$$\frac{\partial \mathcal{L}}{\partial \phi} = -m^2 \phi, \quad \frac{\partial \mathcal{L}}{\partial(\partial_\mu \phi)} = \partial_\mu \phi$$

and the Lagrangian equation of motion, Eq. (1.8), is the Klein–Gordon equation [14–16]

$$(\partial_\mu \partial^\mu + m^2) \phi(\underline{x}) = 0. \quad (1.9)$$

Its solutions in infinitely large spacetime are superpositions of plane waves of the form

$$\phi(\underline{x}) = A \cdot \sin(\underline{k} \cdot \underline{x}) + B \cdot \cos(\underline{k} \cdot \underline{x}), \quad (1.10)$$

where  $A$  and  $B$  are arbitrary constants and  $\underline{k}^2 - m^2 = 0$ . The last equation means that  $\underline{k}$  is onshell (Definition 8). Since Eq. (1.9) is a *linear* partial differential equation, any sum of such solutions is a solution as well. Physically, this means that any number of such waves can exist simultaneously without disturbing each other, there is no interaction between them, the theory is a *free* field as claimed.

We remark that a mode expansion, that is, an expansion into fundamental solutions of the differential operator, is fruitful in field theory much more generally. For example, the *quasinormal modes* [17] framework allows to treat the behavior of the electromagnetic field (Example 7) in finite size cavities. Also dissipation can be included by allowing for complex energies  $k^0$ , which effectively give rise to exponentially decaying solutions. In QFT, this amounts to unstable particles, see [18].

### Example 6: Interacting scalar fields, classical equations of motion.

$\phi^n$  theory from Example 3 leads to the equation of motion

$$(\partial^\mu \partial_\mu + m^2) \phi(\underline{x}) + \frac{\lambda}{(n-1)!} \phi^{n-1}(\underline{x}) = 0.$$

Liouville theory from Example 4 produces  $\partial^\mu \partial_\mu \phi(\underline{x}) + \lambda \exp(\lambda \cdot \phi(\underline{x})) = 0$ .

Both differential equations are non-linear in the field variable  $\phi(\underline{x})$ , a superposition of two solutions is not a solution. Hence, they describe a field with self-interaction, not a free field. One can obtain a perturbative solution in terms of iterated integrals by recursively inserting the *Green functions* (Eq. (1.24)) of the free field, see e.g., [19].

### Example 7: Classical electrodynamics.

The electromagnetic field describes many familiar phenomena in physics, such as light, heat radiation, radio waves, or the attraction between atoms. Due to its high popularity, we will occasionally use the electromagnetic field as an example. Classical electrodynamics can be formulated in terms of a scalar potential  $\Phi(\underline{x})$  and a vector potential  $\mathbf{A}(\underline{x})$ . In the relativistic formulation, the two are merged into the 4-component vector potential  $A^\mu(\underline{x}) := (\Phi(\underline{x}), \mathbf{A}(\underline{x}))$ . The field strength tensor  $F_{\mu\nu} := \partial_\mu A_\nu - \partial_\nu A_\mu$  is a  $4 \times 4$ -matrix, its entries are the classical electric field  $\mathbf{E}$  and magnetic field  $\mathbf{B}$ :

$$F_{\mu\nu} = \begin{pmatrix} 0 & E_x & E_y & E_z \\ -E_x & 0 & -B_z & B_y \\ -E_y & B_z & 0 & -B_x \\ -E_z & -B_y & B_x & 0 \end{pmatrix}.$$

Recall that we defined the speed of light to be  $c = 1$ , otherwise, the  $E$ -fields appear as  $\frac{E_j}{c}$  in  $F_{\mu\nu}$ . The Lagrangian of electrodynamics is

$$\mathcal{L} = -\frac{1}{4} F_{\mu\nu} F^{\mu\nu}.$$

Let  $\epsilon^{\mu\nu\rho\sigma}$  be a completely antisymmetric tensor with  $\epsilon^{1234} = 1$ . The Euler Lagrange equations of motion (Eq.(1.8)) arising from  $\mathcal{L}$  are the vacuum Maxwell equations [20]

$$\partial_\mu F^{\mu\nu} = 0, \quad \partial_\mu \epsilon^{\mu\nu\rho\sigma} F_{\rho\sigma} = 0.$$

In terms of  $\mathbf{E}$  and  $\mathbf{B}$ , the first equation reads  $\nabla \cdot \mathbf{E} = 0$  and  $\nabla \times \mathbf{B} - \partial_t \mathbf{E} = 0$ , and the second equation is  $\nabla \cdot \mathbf{B} = 0$  and  $\nabla \times \mathbf{E} + \partial_t \mathbf{B} = 0$ .

The electromagnetic field interacts with fermions, most notable electrons. In classical electrodynamics, they appear as point charges or continuous charge densities. For later, it will be useful to introduce a fermionic field  $\psi(\underline{x})$  which carries a charge  $e \in \mathbb{R}$  and a mass  $m \in \mathbb{R}_+$ . This field is a Dirac spinor [21], that is a vector in spinor space, operated on by the Dirac matrices  $\gamma^\mu$ , and  $\bar{\psi} := \psi^\dagger \gamma^5$  is the adjoint spinor. The Lagrangian of the fermion field is

$$\mathcal{L} = \bar{\psi} (i \gamma^\mu \partial_\mu - m) \psi.$$

The coupling between the electromagnetic and the fermionic field has a particular structure, called *gauge-covariant derivative*, which will be motivated in Example 128,

$$D_\mu := \partial_\mu - i e A_\mu.$$

The Lagrangian of the electromagnetic field, coupled to the fermion field, is then

$$\mathcal{L} = \bar{\psi} (i\gamma^\mu D_\mu - m) \psi - \frac{1}{4} F_{\mu\nu} F^{\mu\nu}.$$

The equations of motion Eq.(1.8) arising from this Lagrangian are the Dirac equation for the fermion field, and the Maxwell equations for the electromagnetic field, where the fermion density  $\bar{\psi}\psi$  now appears as a source term:

$$(i\gamma^\mu \partial_\mu - m) \psi(\underline{x}) = 0 \\ \partial_\mu \epsilon^{\mu\nu\rho\sigma} F_{\rho\sigma} = 0, \quad \partial_\mu F^{\mu\nu} = e\bar{\psi}\psi.$$

For the construction of a quantum field theory, we need the Hamiltonian description of classical field theory. To this end, we introduce the canonical conjugate momentum field,

$$\pi := \frac{\partial \mathcal{L}}{\partial(\partial_0 \phi)}, \quad (1.11)$$

where  $\partial_0 \phi =: \dot{\phi}$  is the time-derivative of  $\phi$ . We assume that Eq.(1.11) is invertible so that we can express  $\dot{\phi}$  as a function of  $\pi$ .

**Definition 9.** The *Hamiltonian density* is defined as the Legendre transform (to be defined formally in Definition 55) of the Lagrangian density,

$$\mathcal{H}(\underline{x}) := \pi(\underline{x}) \dot{\phi}(\pi) - \mathcal{L}(\phi, \dot{\phi}(\pi)).$$

The Hamiltonian density is a function of  $\phi$  and  $\pi$ , there is no dependence on  $\dot{\phi}$  any longer. The function  $\dot{\phi}(\pi)$  is the inverse of Eq.(1.11).

### Example 8: Free scalar field, Hamiltonian density.

The Hamiltonian density of a free field (Example 1) reads

$$\mathcal{H}(\underline{x}) = \frac{1}{2} \pi^2(\underline{x}) + \frac{1}{2} (\nabla \phi(\underline{x}))^2 + \frac{1}{2} m^2 \phi^2(\underline{x}).$$

**Definition 10.** The *Hamilton function*, or *Hamiltonian*, is the spatial integral of the Hamiltonian density (Definition 9),

$$H := \int d^{D-1}\mathbf{x} \mathcal{H}(\mathbf{x}, t).$$

From Eq.(1.8) and Definition 10 one derives the *Hamiltonian equations of motion*,

$$\dot{\phi}(t, \mathbf{x}) = \frac{\delta H}{\delta \pi(t, \mathbf{x})}, \quad \dot{\pi}(t, \mathbf{x}) = -\frac{\delta H}{\delta \phi(t, \mathbf{x})}. \quad (1.12)$$

**Definition 11.** The *Poisson bracket* of two functionals  $A[\phi, \pi]$  and  $B[\phi, \pi]$  is defined as

$$\{A, B\}(t) := \int d^{D-1}\mathbf{x} \left( \frac{\delta A}{\delta \phi(t, \mathbf{x})} \frac{\delta B}{\delta \pi(t, \mathbf{x})} - \frac{\delta B}{\delta \phi(t, \mathbf{x})} \frac{\delta A}{\delta \pi(t, \mathbf{x})} \right).$$

By explicit calculation, we find

$$\begin{aligned} \{\phi(t, \mathbf{x}), \pi(t, \mathbf{y})\} &= \delta(\mathbf{x} - \mathbf{y}) \\ \{\phi(t, \mathbf{x}), \phi(t, \mathbf{y})\} &= 0 = \{\pi(t, \mathbf{x}), \pi(t, \mathbf{y})\}. \end{aligned} \quad (1.13)$$

The equations of motion Eq.(1.12) can be expressed with Poisson brackets (Definition 11) as

$$\dot{\phi}(t, \mathbf{x}) = \{\phi(t, \mathbf{x}), H\}, \quad \dot{\pi}(t, \mathbf{x}) = \{\pi(t, \mathbf{x}), H\}. \quad (1.14)$$

### 1.2.2 Canonical Quantization

Canonical quantization produces a quantum field theory out of a given classical field theory in Hamilton formalism. Concretely, it amounts to two formal steps:

1. Promote the field variable  $\phi(t, \mathbf{x})$  and the canonical momentum  $\pi(t, \mathbf{x})$  to operators on a suitable Hilbert space of states.
2. Replace the Poisson brackets Eq.(1.13)  $\{ , \}$  by commutators  $-i\hbar[ , ]$  between the operators.

There are numerous justifications, constraints and technical details to this procedure both from the physics and the mathematics side. While the first formulation in the 1920s [22–25] was based on physical intuition, a contemporary approach called *deformation quantization* [26–29] is more mathematically rigorous. The interested

reader finds more modern perspectives about quantization in [30–33], an amusing collection of “mathematical surprises” in [34], and some examples of contradictions and open problems in [35–38].

A more sophisticated version of canonical quantization is based on operators acting on smooth test functions and avoids the notion of a “field at spacetime point  $\underline{x}$ ”. For Minkowski spacetime, this gives rise to the *Wightman axioms* [39, 40], in Euclidean spacetime one has the *Osterwalder-Schrader axioms* [41, 42]. For completeness, we state the Wightman axioms, following [37], without introducing all technical terms.

**Definition 12.** A quantum field theory can be defined by the *Wightman axioms*:

1. All states of the system are vectors in a separable Hilbert space which is equipped with a strongly continuous unitary representation of the Poincaré group  $P_+^\uparrow$ . There is a unique vacuum state  $|0\rangle$  which is invariant under Poincaré transformations (Definition 3).
2. The spectrum of the energy-momentum operator  $p_\mu$  lies in the closed forward light cone, that is,  $p_\mu p^\mu \geq 0$ .
3. For each Schwartz function  $f$  there are operators  $\phi_1(f), \dots, \phi_n(f)$  (“quantum fields”) and their adjoints  $\phi_1^\dagger(f), \dots, \phi_n^\dagger(f)$ , defined on a dense subset  $D$  of the Hilbert space containing the vacuum and stable under actions of the Poincaré group.
4. The quantum fields transform covariantly under the Poincaré group.
5. If the support of  $f, g$  is spacelike separated then  $[\phi(f), \phi(g)] = 0$ .

The free scalar quantum field in infinitely large spacetime can be expanded in modes like the classical free field (Example 5),

$$\phi(\underline{x}) = \int \frac{d^{D-1} \mathbf{k}}{(2\pi)^{D-1}} \frac{1}{2\omega(\mathbf{k})} (a(\mathbf{k}) e^{-ikx} + a^\dagger(\mathbf{k}) e^{ikx}). \quad (1.15)$$

We have introduced  $\omega(\mathbf{k}) := \sqrt{\mathbf{k}^2 + m^2}$ . The operator-valued coefficients  $a(\mathbf{k})$  and  $a^\dagger(\mathbf{k})$  are called *annihilation- and creation operators*. Replacing the Poisson brackets Eq. (1.13) by commutators leads to the fundamental commutation relations

$$\begin{aligned} [a(\mathbf{k}), a^\dagger(\mathbf{k}')] &= (2\pi)^{D-1} 2\omega(\mathbf{k}) \hbar \delta(\mathbf{k} - \mathbf{k}'), \\ [a(\mathbf{k}), a(\mathbf{k}')] &= 0 = [a^\dagger(\mathbf{k}), a^\dagger(\mathbf{k}')]. \end{aligned} \quad (1.16)$$

The Hamilton function (Definition 10) becomes the Hamiltonian operator of the free field theory, which computes the energy of a state. Further, it governs time-evolution via the quantized version of the Hamiltonian equation of motion (Eq. (1.14)),

$$\dot{\phi}(t, \mathbf{x}) = [\phi(t, \mathbf{x}), H(t)]. \quad (1.17)$$

We are operating in the *Heisenberg picture* of quantum mechanics: The operators are time-dependent, while the states are not. An explicit calculation of various commutators reveals that the operator  $a^\dagger(\mathbf{k})$  increases the momentum of a state by  $\mathbf{k}$  and the energy by  $\omega(\mathbf{k})$ , this justifies the interpretation that  $a^\dagger(\mathbf{k})$  creates one non-interacting particle of momentum  $\mathbf{k}$  and mass  $m$ . The vacuum  $|0\rangle$  does not contain a particle which could be annihilated,

$$a(\mathbf{k})|0\rangle = 0, \quad \langle 0|a^\dagger(\mathbf{k}) = 0, \quad \forall \mathbf{k}. \quad (1.18)$$

In general, it is possible to add a position-independent constant to the Lagrangian Eq. (1.6) and to the field Eq. (1.15). Such constant amounts to a shift of the vacuum expectation value of the field, which is, for example, relevant when the field is coupled to gravity. However, for the QFTs considered in the present thesis, the absolute value of the field is not observable, therefore we choose this constant to vanish. Equation (1.18) then implies

$$\langle 0|\phi(x)|0\rangle = 0. \quad (1.19)$$

### 1.2.3 2-Point Correlation Functions

Following the general principle of the Copenhagen interpretation of quantum mechanics [43], it is impossible to directly observe quantum fields. The only quantities accessible to measurements are *observables*, given by hermitian operators.

The requirement in the Wightman axioms (Definition 12), that the subset spanned by quantum fields be dense in the Hilbert space, means that all states in it can be reasonably expressed by products of quantum field operators  $\phi(x), \phi^\dagger(x)$ . This entails that all observables are expressible in terms of vacuum expectation values of products of fields. In practice, one can circumvent the somewhat arcane notion of operator-valued distributions, and their precise physical interpretation, by taking the correlation functions as primary objects. Alternatively, instead of the Wightman axioms for the field operators, a quantum field theory can also be defined by an equivalent set of axioms for its corresponding *Wightman distributions* in the first place [37, 39].

**Definition 13.** The *Wightman distributions* are the vacuum expectation values of a product of  $n$  quantum fields, given by  $n$  Schwartz functions:

$$\tilde{W}^{(n)}(f_1, \dots, f_n) := \langle 0|\phi(f_1) \cdots \phi(f_n)|0\rangle.$$

Using the Fourier expansion Eqs. (1.15) and (1.18), the 2-point distribution is

$$\tilde{W}^{(2)}(f_1, f_2) = \int \frac{d^D \underline{k}}{(2\pi)^D} 2\pi\theta(p^0)\delta(\underline{k}^2 - m^2)\tilde{f}_1^*(\underline{k})\tilde{f}_2(\underline{k}). \quad (1.20)$$

Here,  $\tilde{f}_j$  are the Fourier transforms of the Schwartz functions  $f_j$ .

If one demands the Schwartz functions  $f_j(\underline{x})$  to be localized arbitrarily closely around some spacetime points  $\underline{x}_j$ , then the Wightman distributions (Definition 13) become the local *Wightman functions*  $\tilde{W}^{(n)}(\underline{x}_1, \dots, \underline{x}_n)$ . Colloquially, this limit is denoted by  $f_j \rightarrow \delta(\underline{x} - \underline{x}_j)$  in position space, or  $\tilde{f}_j(\underline{p}) \rightarrow e^{i\underline{k}\underline{x}_j}$  in momentum space. In doing so, one leaves the territory of well-defined axiomatic QFT. The functions  $\tilde{W}^{(n)}$  will generally have singularities, see Sect. 1.2.8. By replacing  $\tilde{f}_j(\underline{p}) \rightarrow e^{i\underline{p}\underline{x}_j}$ , one obtains the “local” limit of the distribution in Eq. (1.20),

$$\tilde{W}^{(2)}(\underline{x}_1, \underline{x}_2) = \int \frac{d^D \underline{k}}{(2\pi)^D} 2\pi\theta(k^0)\delta(\underline{k}^2 - m^2)e^{-i\underline{k}(\underline{x}_1 - \underline{x}_2)} = \int \frac{d^{D-1} \mathbf{k}}{(2\pi)^{D-1}} \frac{e^{i\underline{k}(\underline{x}_1 - \underline{x}_2)}}{2\sqrt{\mathbf{k}^2 + m^2}}.$$

This function depends only on the difference  $\underline{x}_1 - \underline{x}_2$ . Further, it is manifestly singular in the case  $\underline{x}_1 = \underline{x}_2$ . The integrand  $\theta(p^0)\delta(\underline{p}^2 - m^2) =: \delta_+(\underline{p}^2 - m^2)$  has a physical interpretation, it ensures that only the positive energy  $p^0 = +\sqrt{\mathbf{p}^2 + m^2} \equiv +\omega(\mathbf{p})$  contributes. One uses the residue theorem (see Fig. 1.1) to rewrite

$$\tilde{W}^{(2)}(\underline{z}) = 2\pi i \int \frac{d^{D-1} \underline{k}}{(2\pi)^D} \frac{-i}{2\omega(\mathbf{k})} e^{i\underline{k}\underline{z}} = \int \frac{d^{D-1} \underline{k}}{(2\pi)^D} \int dp^0 \frac{i}{(k^0 - \omega(\mathbf{p}))(k^0 + \omega(\mathbf{p}))} e^{-ik^0 z^0} e^{i\underline{k}\underline{z}}. \quad (1.21)$$

In this, we have to integrate  $k^0$  around the right pole of  $((k^0 - \omega(\mathbf{p}))(k^0 + \omega(\mathbf{p}))^{-1} = (\underline{k}^2 - m^2)^{-1}$ . The function is holomorphic everywhere else, the integration path can be extended to include the full real axis, passing the poles on the right side, see Fig. 1.1.

In Eq. (1.21), it is still cumbersome to remember the different integration contours of Fig. 1.1. They can be enforced by introducing an infinitesimal  $\epsilon > 0$  and using

$$\tilde{W}^{(2)}(\underline{z}) = \lim_{\epsilon \rightarrow 0} \text{sgn}(z^0) \int \frac{d^4 \underline{k}}{(2\pi)^4} \frac{i}{\underline{k}^2 - m^2 + \text{sgn}(z^0)i\epsilon} e^{-i\underline{k}\underline{z}}. \quad (1.22)$$

In this case, no information about the integration contour of  $k^0$  needs to be provided, see Fig. 1.2: It extends along the real axis and it is closed either above or below, depending on the sign of  $z^0$ , such that  $e^{-i\underline{k}\underline{z}}$  decays on the semi-circle for  $|\Im p^0| \rightarrow \infty$ . This setup is called *i* $\epsilon$ -prescription.

The Wightman functions have a straightforward relation to the field operators  $\phi$ , but for the computation of physical observables, the *time-ordered correlation functions* are more relevant [44–47].

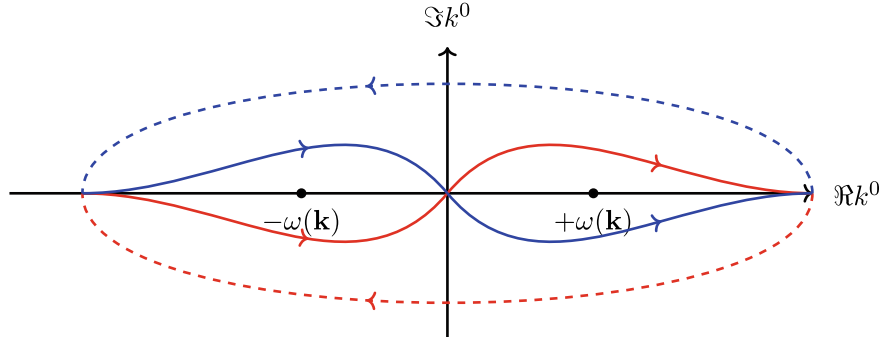


**Fig. 1.1** Integration contour for the Wightman propagator for  $z^0 > 0$  (red) and  $z^0 < 0$  (blue). In both cases, the integral runs along the real line in positive direction “ $\rightarrow$ ” and it encloses only the right pole

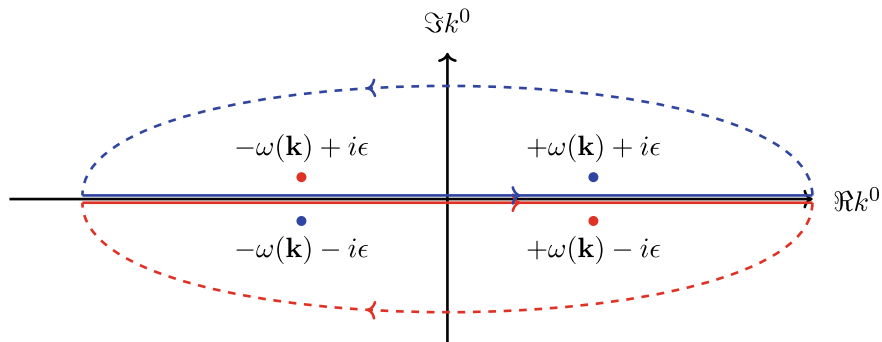


**Fig. 1.2** Poles of Eq.(1.22). For  $z^0 > 0$  (red), the integral needs to be closed on the negative imaginary  $k^0$ -plane to make  $e^{-ik^0 z^0}$  decay. In that case, only the right pole (red) at  $+\omega(\mathbf{k})$  is enclosed. Analogously for  $z^0 < 0$  (blue), again only the right pole is enclosed

**Definition 14.** The (not necessarily connected, ) time-ordered *n-point functions*, or *Green functions*, are the correlation functions of *n* field operators,

$$\tilde{G}^{(n)}(\underline{x}_1, \dots, \underline{x}_n) := \langle 0 | T (\phi(\underline{x}_1) \cdots \phi(\underline{x}_n)) | 0 \rangle.$$

Here, the operator  $T$  switches the order of its arguments such that the factors are sorted with respect to the time coordinate  $x^0$ , where the largest time stands to the left. We write  $\tilde{G}_F^{(n)}$  if  $\phi$  is a free field, and  $\tilde{G}^{(n)}$  for interacting fields.

**Definition 15.** The *Feynman propagator* is the time-ordered 2-point Green function (Definition 14) of a free field. By Lorentz covariance, it depends only on the difference of its two arguments,

$$G_F(\underline{x}_1 - \underline{x}_2) = G_F(\underline{x}_1, \underline{x}_2) := \tilde{G}^{(2)}(\underline{x}_1, \underline{x}_2) - \tilde{G}^{(1)}(\underline{x}_1)\tilde{G}^{(1)}(\underline{x}_2).$$

In Definition 15, we have included the subtraction of 1-point-functions for completeness, this qualifies  $G_F$  as the *connected* 2-point function (Definition 20). Within our setup, this makes no difference because the second summand vanishes thanks to Eq. (1.19). The Feynman propagator (Definition 15) is related to the Wightman propagator (Definition 13) by

$$G_F(\underline{x}_1, \underline{x}_2) = G_F(\underline{z}) = \begin{cases} W^{(2)}(\underline{z}), & z^0 > 0 \\ W^{(2)}(-\underline{z}), & z^0 < 0. \end{cases} \quad (1.23)$$

An inspection of Eq. (1.22) shows that Eq. (1.23) amounts to taking the right pole for  $z^0 > 0$  and the left pole for  $z^0 < 0$  in Fig. 1.2. That can be achieved by leaving out the factor “ $\text{sgn}(z^0)$ ” in the  $i\epsilon$ -prescription Eq. (1.22). The Feynman propagator is given by

$$G_F(\underline{z}) = \int \frac{d^D k}{(2\pi)^D} \frac{i}{\underline{k}^2 - m^2 + i\epsilon} e^{-ik\underline{z}}. \quad (1.24)$$

Again, it is automatically implied on which side the contour needs to be closed, as shown in Fig. 1.3. Equation (1.24) is a Fourier transform, we read off the Feynman propagator in momentum space:

$$G_F(\underline{p}) = \frac{i}{\underline{p}^2 - m^2 + i\epsilon} = \frac{i}{s_p + i\epsilon} =: \frac{i}{s_p} \quad (1.25)$$

In the last equation, we have used the offshell variable  $s_p$  (Definition 8). From now on, the summand  $+i\epsilon$  is always implied, even if we do not write it explicitly.

From the momentum-space representation Eq. (1.25), it follows that the Feynman propagator is a Green function of the Klein–Gordon equation, that is, it fulfils

$$(\partial_\mu \partial^\mu + m^2) G_F(\underline{z}) = -i\delta(\underline{z}). \quad (1.26)$$

This explains the name *propagator*: it describes how the field at  $\underline{z}$  reacts to a point-like “source” at  $\underline{0}$ . The poles in the propagator are the eigenvalues of the time-evolution (Eq. (1.17)), even if we were to set up a free quantum field on more exotic timelike hypersurfaces [48]. All other possible combinations of signs for  $i\epsilon$  in Eqs. (1.22) and (1.25) amount to solutions of Eq. (1.26) which differ only in the boundary conditions.

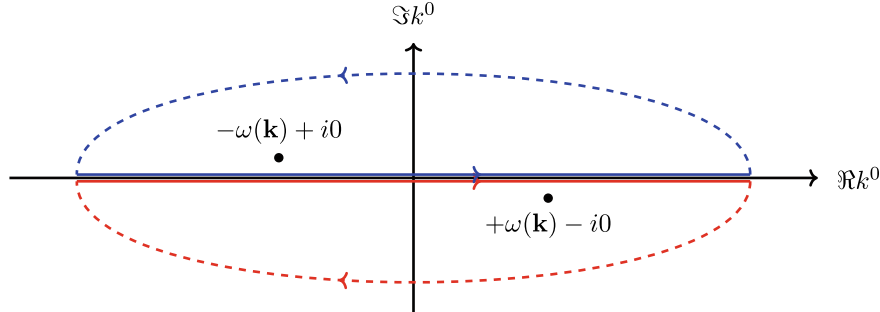


**Fig. 1.3** Integration path of the Feynman propagator (Definition 15) in the complex  $k^0$ -plane for  $z^0 > 0$  (red) and  $z^0 < 0$  (blue)

Using the Fourier transforms given in Eq. (1.2), we can solve the integral Eq. (1.24) for the massless Feynman propagator in position space, and obtain

$$G_F(\underline{x}) = \frac{\Gamma\left(\frac{D}{2}\right)}{4\pi^{\frac{D}{2}}} \frac{i}{(\underline{x}^2)^{\frac{D}{2}-1}}. \quad (1.27)$$

For the massive field, the Feynman propagator in position space is given by Bessel functions, for example in four spacetime dimensions [49, p. 30]:

$$G_F(\underline{x}) = \frac{m}{4\pi^2} \begin{cases} \frac{1}{\sqrt{\underline{x}^2}} \frac{i\pi}{2} H_1^{(1)}\left(m\sqrt{\underline{x}^2}\right), & \underline{x}^2 > 0 \\ \frac{1}{\sqrt{-\underline{x}^2}} K_1\left(m\sqrt{-\underline{x}^2}\right), & \underline{x}^2 < 0. \end{cases} \quad (1.28)$$

Both the massive and the massless propagator scale like  $(\underline{x}^2)^{-1}$  in the limit  $\underline{x}^2 \rightarrow 0^+$ . This seemingly mundane statement has profound consequences for the theory of renormalization, see Sect. 2.3.1: For the high-energy behavior of a quantum field theory, it is largely irrelevant if the involved quanta are massive or not.

Finally, we want to mention a remarkable result from axiomatic QFT, underlining the conceptual importance of particularly the 2-point functions:

**Theorem 1** (Jost–Schroer–Federbush–Johnson–Pohlmeier [50–52]). If the 2-point Wightman distribution  $W^{(2)}$  of a quantum field theory equals that of a free quantum field theory with mass  $m \geq 0$ , then the theory in question is a free theory of that mass.

### 1.2.4 *n*-Point Correlation Functions of the Free Field

The Feynman propagator (Eq. (1.24)) is the time-ordered 2-point correlation function of a free field. We now compute the time-ordered correlation functions (Definition 14) of ( $n > 2$ ) factors of the free quantum field. To do that, we split the field Eq. (1.15) into positive and negative frequency solutions,  $\phi(\underline{x}) = \phi^-(\underline{x}) + \phi^+(\underline{x})$ , where

$$\phi^-(\underline{x}) := \int \frac{d^3 p}{(2\pi)^3} \frac{1}{2\omega(\mathbf{p})} a^\dagger(\mathbf{p}) e^{i \underline{p} \cdot \underline{x}}, \quad \phi^+(\underline{x}) := \int \frac{d^3 p}{(2\pi)^3} \frac{1}{2\omega(\mathbf{p})} a(\mathbf{p}) e^{-i \underline{p} \cdot \underline{x}}.$$

**Definition 16.** A product of quantum field operators is *normal ordered* if all annihilation operators appear to the right of all creation operators. It is denoted  $: \phi(\underline{x}_1) \cdots \phi(\underline{x}_n) :$ .

By Eq. (1.18), the vacuum expectation value of any normal ordered product vanishes. An explicit calculation shows that

$$T(\phi(\underline{x})\phi(\underline{y})) = : \phi(\underline{x})\phi(\underline{y}) : + \begin{cases} [\phi^+(\underline{x}), \phi^-(\underline{y})], & x^0 > y^0 \\ [\phi^+(\underline{y}), \phi^-(\underline{x})], & x^0 < y^0. \end{cases} = : \phi(\underline{x})\phi(\underline{y}) : + \overline{\phi(\underline{x})\phi(\underline{y})} \quad (1.29)$$

We have defined the contraction  $\overline{\phi\phi}$  as a shorthand for the conditional commutator expression. Taking the vacuum expectation value, the left hand side, by Definition 14, equals the Feynman propagator, while the normal ordered product vanishes. Consequently  $\langle 0 | \phi(\underline{x})\phi(\underline{y}) | 0 \rangle = G_F(\underline{x}, \underline{y})$ . By induction, any time-ordered product can be expanded into a sum where each term is a product of normal-ordered and pairwise contracted factors like in Eq. (1.29).

**Theorem 2** (Wick [53]). For a free scalar quantum field  $\phi$ , the time-ordered (Definition 14) and normal ordered (Definition 16) products of fields fulfil

$$(1) \quad T(\phi(\underline{x}_1) \cdots \phi(\underline{x}_n)) = : \phi(\underline{x}_1) \cdot \phi(\underline{x}_n) : + \text{sum of all contractions}$$

$$(2) \quad \tilde{G}_F^{(n)} = \langle 0 | T(\phi(\underline{x}_1) \cdots \phi(\underline{x}_n)) | 0 \rangle = \begin{cases} \text{sum of all complete contractions} & n \text{ even} \\ 0 & n \text{ odd.} \end{cases}$$

Here, a *contraction* is a product of Feynman propagators (Definition 15) between pairs of the spacetime points, where all remaining non-contracted field operators are normal ordered. A *complete contraction* is a product where all factors are contracted and no normal ordered factor prevails.

There is an obvious graphical notation for Wick's theorem: Any single contraction  $\overline{\phi(x_1)}\phi(x_2)$  involves precisely two distinct points in spacetime, hence, it can be drawn as a line joining the points  $x_1$  and  $x_2$ . Wick's theorem then states that the  $n$ -point function will be the sum of all ways of joining the  $n$  distinct points pairwise with edges.

### Example 9: Free scalar field, Four-point function.

Let  $\phi(x_j) =: \phi_j$ , then

$$\begin{aligned} T(\phi_1\phi_2\phi_3\phi_4) &=: \phi_1\phi_2\phi_3\phi_4 : + : \phi_1\phi_2 : \phi_3\phi_4 : + 5 \text{ similar terms} \\ &+ \overline{\phi_1}\phi_2\phi_3\phi_4 + \overline{\phi_1}\phi_2\phi_3\phi_4 + \overline{\phi_1}\phi_2\phi_3\phi_4, \\ \tilde{G}_F^{(n)} &= \langle 0 | T(\phi_1\phi_2\phi_3\phi_4) | 0 \rangle \\ &= G_F(x_1, x_2)G_F(x_3, x_4) + G_F(x_1, x_3)G_F(x_2, x_4) + G_F(x_1, x_4)G_F(x_2, x_3). \end{aligned}$$

Denoting the spacetime points as points in a plane, the 4-point function of the free field has the following graphical representation:

$$\tilde{G}_F^{(4)} = \langle 0 | T(\phi_1\phi_2\phi_3\phi_4) | 0 \rangle = \begin{array}{c} x_1 \\ \bullet \\ \vdots \\ x_2 \end{array} + \begin{array}{c} x_3 \\ \bullet \\ \vdots \\ x_4 \end{array} + \begin{array}{c} x_1 & x_3 \\ \bullet & \bullet \\ \hline x_2 & x_4 \end{array} + \begin{array}{c} x_1 & x_3 \\ \bullet & \bullet \\ \diagdown & \diagup \\ x_2 & x_4 \end{array}$$

Clearly, the  $n$ -point functions vanish for odd  $n$ : There is no way to connect an odd number of points into pairs.

We often encounter symmetric sums over all permutations of certain terms, therefore we introduce a shorthand notation:

**Definition 17.** Let  $f(x_1, \dots, x_n)$  be a function of  $n \in \mathbb{N}$  arguments. The expression  $\langle k \rangle f(x_1, x_2, \dots, x_n)$  denotes the sum over all  $k \in N$  different permutations of arguments in the function  $f(x_1, \dots, x_n)$ .

### Example 10: Permutations of four-point amplitude.

The four-point amplitude from Example 9 is the sum over three permutations (Definition 17),

$$\tilde{G}_F^{(4)}(x_1, x_2, x_3, x_4) = \langle 3 \rangle G_F(x_1, x_2)G_F(x_3, x_4).$$

In this notation, we assumed the known symmetry  $G_F(x_1, x_2) = G_F(x_2, x_1)$  of the Feynman propagator Eq. (1.24).

The derivation of Wick's theorem made use of operator identities in QFT, but there is an entirely different perspective, concerning multivariate normal distributions [12]:

**Theorem 3** (Isserlis [54]). Let  $x_1, \dots, x_n$  be independent random variables, normal distributed with zero mean,  $\mathbb{E}(x_j) = 0 \forall j$ . Let  $\mathcal{P}$  be the set of all partitions of  $\{1, \dots, n\}$  into pairs, then

$$\mathbb{E}(x_1 \cdots x_n) = \sum_{p \in \mathcal{P}} \prod_{\{j,k\} \in p} \mathbb{E}(x_j x_k).$$

A normal distribution is the ground state wave function of a quantum-mechanical harmonic oscillator. In this sense, a free quantum field can be thought of as an infinite collection of uncoupled harmonic oscillators.

We remark that, instead of using  $\tilde{G}^{(n)}$  (Definition 14), one can formulate perturbative QFT in terms of  $W^{(n)}$  (Definition 13) [55]. This was originally proposed by Schwinger [56–58], but it involves rather intransparent nested commutators. Feynman's and Dyson's formulation entirely in terms of  $\tilde{G}^{(n)}$ , see e.g., [59], avoids this problem. Still, an analysis of the relationship between  $\tilde{G}^{(n)}$  and  $W^{(n)}$  is fruitful even if one is eventually only interested in  $\tilde{G}^{(n)}$ , because it reveals certain analytic properties of  $\tilde{G}^{(n)}$ , compare Sect. 1.2.8.

### 1.2.5 The S-Matrix

For an interacting theory, it is useful to introduce the notion of *scattering processes*. A scattering process amounts to a transition of the system from some *asymptotic state*  $\Psi_1$  at the infinite past to some new asymptotic state  $\Psi_2$  at the infinite future, where we assume that interactions take place only in the intermediate process but not in the asymptotic states. Effectively, the asymptotic states are assumed to be states of a free field, which is sometimes called *adiabatic hypothesis*, see e.g., [60]. We do especially require that the asymptotic states are physically valid states of the system. That includes that the momenta of all particles are onshell (Definition 8) and all symmetries of the system are satisfied.

The existence of asymptotic free states faces considerable mathematical obstacles known as *Haag's theorem* [37, 61]. For example, Theorem 1 prevents any state of an interacting theory to truly propagate like a free field, because a theory with the propagator of a free field is a free theory altogether. These problems however have been circumvented by a more careful construction, known as *Haag–Ruelle theory* [62–64], which sharply distinguishes between states themselves being equal, and expectation values of certain operators being equal.

Moreover, the naive relationship between states of an interacting and a free quantum field theory also rises concerns from a philosophical perspective [65]: In an interacting theory, the state generated by the field operators  $\phi(x_1)\phi(x_2)|0\rangle$  will in

general not have twice the energy of a single particle  $\phi(\underline{x})|0\rangle$ , therefore it is strictly no longer obvious in what sense this state is to be interpreted as “two quanta”. We will however resort to the assumption that the asymptotic states resemble free quanta “close enough” to be indistinguishable by real-world experiments, which can never measure the *complete* 2-point function or the *exact* energy of a state.

**Definition 18** ([66, 67]). The *S-matrix* is the operator that takes the asymptotic initial state to the asymptotic final state,

$$\Psi_2 =: S\Psi_1.$$

The *S-matrix* becomes an actual (infinitely large) matrix as soon as we define a basis for the space of asymptotic states. Each state contains a countable number of particles. For a fixed number  $n$  of particles, one can take any basis of the corresponding  $n$ -particle Hilbert space  $H_n$ , for example the states with well-defined onshell (Definition 8) momenta. They can be written in terms of field operators in momentum space,

$$|0\rangle, \quad |\phi(\underline{k}_1)\rangle, \quad |\phi(\underline{k}_1)\phi(\underline{k}_2)\rangle, \quad \dots \quad \text{where } s_{k_j} = 0 \forall j.$$

The space of asymptotic states is the direct sum  $\bigoplus_{n=0}^{\infty} H_n$  of the  $n$ -particle Hilbert spaces, or equivalently the symmetric tensor algebra of  $H_1$ , this is a *Fock space* [68]. The *S-matrix* elements in momentum space are then given by expectation values of the form

$$\langle \phi(\underline{k}_1) \cdots \phi(\underline{k}_n) | S | \phi(\underline{k}_{n+1}) \cdots \phi(\underline{k}_m) \rangle \quad \text{where } s_{k_j} = 0 \forall j. \quad (1.30)$$

Similarly, matrix elements can be defined in position space. The *LSZ-formula* makes the link between the *S-matrix* (which is observed in scattering experiments) and the time-ordered Green functions.

**Theorem 4** (Lehmann–Symanzik–Zimmermann formula [47]). The *S-matrix* element for a  $2 \rightarrow 2$ -scattering between particles with 4-momenta  $\underline{p}_i$  and masses  $m_i$  is given by

$$\langle \phi(\underline{p}_1) \phi(\underline{p}_2) | S | \phi(\underline{p}_3) \phi(\underline{p}_4) \rangle \propto \int \cdots \int d^D \underline{x}_1 \cdots d^D \underline{x}_4 \left[ e^{i(\underline{p}_1 \underline{x}_1 + \underline{p}_2 \underline{x}_2 - \underline{p}_3 \underline{x}_3 - \underline{p}_4 \underline{x}_4)} \right. \\ \left( \prod_{i=1}^4 (\partial_{\mu,i} \partial^{\mu,i} + m_i^2) \right) \tilde{G}^{(4)}(\underline{x}_1, \underline{x}_2, \underline{x}_3, \underline{x}_4) \left. \right].$$

Here,  $\partial_{\mu,i}$  is short for  $\frac{\partial}{\partial x_i^{\mu}}$  and  $\tilde{G}^{(4)}$  is the time-ordered Green function (Definition 14) of the interacting field.

The overall factor is a normalization factor for the wave functions. We will see in Sect. 2.3.4 that this factor needs to be fixed by experiment. The LSZ-formula (Theorem 4) can be generalized for more than four external particles by including additional terms for the new arguments  $x_j$ .

Note that the only difference between incoming and outgoing particles is their sign in the exponential. If we flip all 4-momenta of outgoing particles  $(\underline{p}_1, \underline{p}_2) \rightarrow (-\underline{p}_1, -\underline{p}_2)$ , then the formula becomes completely symmetric with respect to incoming and outgoing particles. From now on, we will count all external momenta of scattering processes as pointing towards the interaction.

The S-matrix elements Eq. (1.30) are *onshell* by definition, whereas the time-ordered correlation functions  $\tilde{G}^{(4)}(\underline{x}_1, \underline{x}_2, \underline{x}_3, \underline{x}_4)$  are not restricted. Their relationship in the LSZ-formula (Theorem 4) becomes more clear if one considers the Green functions in momentum space:

$$\tilde{G}^{(4)}(\underline{p}_1, \underline{p}_2, \underline{p}_3, \underline{p}_4) := \int \cdots \int d^D \underline{x}_1 \cdots d^D \underline{x}_4 e^{-i(\underline{p}_1 \cdot \underline{x}_1 + \underline{p}_2 \cdot \underline{x}_2 + \underline{p}_3 \cdot \underline{x}_3 + \underline{p}_4 \cdot \underline{x}_4)} \tilde{G}^{(4)}(\underline{x}_1, \underline{x}_2, \underline{x}_3, \underline{x}_4).$$

**Theorem 5** (LSZ formula in momentum space). Let  $\underline{p}_j$  be the onshell (Definition 8) external momenta. The S-matrix elements in momentum space are given, up to overall factors, by the *amputated* time-ordered Green functions (Definition 14) in momentum space, where *amputated* means that the 2-point function of external particles, including its quantum corrections, is to be left out. Equivalently, the S-matrix elements are the residues of the poles of time-ordered Green functions when the external momenta are put onshell.

$$\langle \phi(\underline{p}_1) \phi(\underline{p}_2) | S | \phi(\underline{p}_3) \phi(\underline{p}_4) \rangle \propto \left( \prod_{i=1}^4 \left( \underline{p}_i^2 - m_i^2 \right) \right) \tilde{G}^{(4)} \left( \underline{p}_1, \underline{p}_2, \underline{p}_3, \underline{p}_4 \right).$$

Conversely, the LSZ formula gives a criterion for the existence of external states, or particles: If  $\tilde{G}^{(n)}(\underline{p}_i, \dots)$  has a pole at  $\underline{p}_i^2 - m_i^2$ , then there is a particle of mass  $m_i$  participating in this type of scattering.

The S-matrix elements computed by the LSZ theorem are not yet the total scattering cross sections observed in real-world experiments, but only *scattering amplitudes*. To obtain cross-sections, one first needs to square the amplitudes, and secondly, integrate over *phase space*, which is the space of all possible, but unobservable, configurations of the system. These can be angles or energies outside the range of the detector, unobserved types of particles, or integrals over energy-bins of a detector with limited resolution. The phase space integration is outside the scope of this work, but we remark that it is closely related to the Feynman integrals to be introduced in Theorem 6 via *loop-tree duality* [69–74].

### 1.2.6 Perturbative Computation of the S-Matrix

The Lagrangian of an interacting field, Eq. (1.6), gives rise to a Hamiltonian density (Definition 9)

$$\mathcal{H} = \underbrace{\frac{1}{2}\pi^2(\underline{x}) + \frac{1}{2}(\nabla\phi(\underline{x}))^2 + \frac{1}{2}m^2\phi^2(\underline{x})}_{=: \mathcal{H}_0} + \underbrace{\sum_{n=3}^{\infty} \frac{\lambda_n}{n!}\phi^n(t, \mathbf{x})}_{=: \mathcal{H}_I}. \quad (1.31)$$

Here, we have separated the Hamiltonian  $\mathcal{H}_0$  of the free field (Example 8). Spatial integration leads to the Hamiltonian (Definition 10)

$$H(t) = H_0(t) + \sum_{n=3}^{\infty} \int d^{D-1}\mathbf{x} \frac{\lambda_n}{n!} \phi^n(t, \mathbf{x}) =: H_0(t) + H_I(t). \quad (1.32)$$

The sum of interaction terms constitutes the *interacting Hamiltonian*  $H_I$ . With this definition, we can formally separate the evolution of free fields, governed by  $H_0$ , from the interaction  $H_I$  which we will treat perturbatively. As remarked below Eq. (1.17), the free fields  $\phi(\underline{x})$  constructed via canonical quantization are in the Heisenberg picture of quantum mechanics, they are time-dependent operators acting on time-independent state vectors.

For interacting fields, we use the free field operators as basis vectors, governed again by the Heisenberg equation (1.17), where  $H_0$  replaces  $H$ . Due to the presence of  $H_I$  in Eq. (1.32), the state vectors, i.e., the coefficients of the expansion in free fields, are now time-dependent as well. Their time evolution is given by an unitary *time evolution operator*

$$|\Psi(t)\rangle = U(t, t_0)|\Psi(t_0)\rangle. \quad (1.33)$$

One possible way to obtain the time evolution operator is via the formal time-ordered exponential of the interaction Hamiltonian, called *Dyson Series* [59],

$$U(t, t_0) = T \left( \exp \left( -i \int_{t_0}^t d\tau H_I(\tau) \right) \right). \quad (1.34)$$

Here, “formal” means that the exponential generates a series expansion and we make no claim about convergence, see Sect. 2.1.1. To concretely compute  $U(t, t_0)$ , one expands the exponential and obtains a series of integrals over time-ordered products of the interacting Hamiltonian,

$$U(t, t_0) = \mathbb{1} + \sum_{k=1}^{\infty} \frac{(-i)^k}{k!} \int \cdots \int_{t_0}^t d\tau_1 \cdots d\tau_k T(H_I(\tau_1) \cdots H_I(\tau_k)).$$

The Hamiltonian Eq.(1.32) is itself a spatial integral over the Hamiltonian density Eq.(1.31), which in turn consists of powers of the field operators, hence

$$U(t, t_0) = \mathbb{1} + \sum_{k=1}^{\infty} \frac{(-i)^k}{k!} \int \cdots \int_{t_0}^t d\tau_1 \cdots d\tau_k \int \cdots \int_{-\infty}^{\infty} dx_1 \cdots dx_k \cdot \\ \cdot T \left( \left( \sum_{n_1=3}^{\infty} \frac{\lambda_{n_1}}{n_1!} \phi^{n_1}(\tau_1, x_1) \right) \cdots \left( \sum_{n_k=3}^{\infty} \frac{\lambda_{n_k}}{n_k!} \phi^{n_k}(\tau_k, x_k) \right) \right).$$

We remark that the Dyson series Eq.(1.34) is not the only way to compute the time evolution operator; a second possibility is given by the *Magnus expansion* [75]. On the level of series coefficients, the Magnus expansion is a reorganization of terms, which is well understood combinatorially [76, Sect. 8], [77].

The adiabatic hypothesis asserts that in the limit  $t \rightarrow \infty, t_0 \rightarrow -\infty$ , the states approach the states of a free field, and are hence time-independent. In this limit, the time evolution operator becomes the S-matrix,

$$S = \lim_{t \rightarrow \infty} \lim_{t_0 \rightarrow -\infty} U(t, t_0). \quad (1.35)$$

In the adiabatic limit, the combined integrals now run over all Minkowski space for each of the spacetime points. Exchanging summation and time-ordering, we identify time-ordered  $n$ -point Green functions (Definition 14)  $\tilde{G}_F^{(n)}$  of a *free* field. Equation(1.35) refers to  $S$  as an operator. If we let the initial and final states be the vacuum, we obtain

$$S_0 := \langle \Omega | S | \Omega \rangle = 1 + \sum_{k=1}^{\infty} \frac{(-i)^k}{k!} \sum_{n_1=3}^{\infty} \frac{\lambda_{n_1}}{n_1!} \cdots \sum_{n_k=3}^{\infty} \frac{\lambda_{n_k}}{n_k!} \int \cdots \int dx_1 \cdots dx_k \cdot \\ \cdot \tilde{G}_F^{(n_1+\cdots+n_k)} \left( \underbrace{x_1, \cdots, x_1}_{n_1 \text{ times}}, \cdots, \underbrace{x_k, \cdots, x_k}_{n_k \text{ times}} \right). \quad (1.36)$$

$S_0$  is not an operator, but a series in the masses and coupling constants (which, in practice, will often be divergent, see Sect. 2.1.2). The quantity  $S_0$  is not directly observable.

The time evolution between non-vacuum states is a Green function  $\tilde{G}^{(n)}$  (of the interacting field) between those states. In the limit of infinite future and past, owing to the adiabatic hypothesis, the external states are free field states, hence generated by products of  $\phi(x)$  operators. The resulting Green functions are singular for onshell external momenta, one needs to amputate external edges with the LSZ-formula (Theorem 4) to obtain the observable S-matrix elements. Moreover, a naive expansion of the Dyson series always produces a factor of  $S_0$ , consisting of Green functions between vacuum states that are unrelated to any other asymptotic states, and we divide by this factor to obtain the non-trivial part of the result.

**Theorem 6.** The Dyson series takes the following form for interacting Green functions in position space (Definition 14), where  $\tilde{G}_F^{(n)}$  are the  $n$ -point time ordered Green functions of a free field (Definition 14) given by Theorem 2, and  $S_0$  is the vacuum  $S$ -matrix (Eq.(1.36)):

$$\tilde{G}^{(n)}(\underline{z}_1, \dots, \underline{z}_j, \underline{y}_1, \dots, \underline{y}_i) = \frac{1}{S_0} \sum_{k=1}^{\infty} \frac{(-i)^k}{k!} \sum_{n_1=3}^{\infty} \frac{\lambda_{n_1}}{n_1!} \dots \sum_{n_k=3}^{\infty} \frac{\lambda_{n_k}}{n_k!} \\ \int \dots \int d\underline{x}_1 \dots d\underline{x}_k \cdot \tilde{G}_F^{(j+n_1+\dots+n_k+i)}(\underline{z}_1, \dots, \underline{z}_j, \underbrace{\underline{x}_1, \dots, \underline{x}_1}_{n_k \text{ times}}, \dots, \underbrace{\underline{x}_k, \dots, \underline{x}_k}_{n_1 \text{ times}}, \underline{y}_1, \dots, \underline{y}_i).$$

The integrals appearing in this series are called *Feynman integrals*.

It appears at first that by the Dyson series (Theorem 6), even the amplitudes of interacting QFT are reduced to free 2-point functions just as for the free field in Wick's Theorem 2. But note two striking differences:

1. Wick's theorem involves only finitely many summands, whereas the Dyson series requires us to add up infinitely many terms.
2. In Wick's theorem, all we have to do is multiply known functions. For the Dyson series, we have to *integrate* such products. Compare also Sect. 5.2.3.

### 1.2.7 The Path Integral

Instead of canonical quantization as outlined in Sect. 1.2.2, one can also use the *path integral* formalism [44–46, 78, 79]. Here, the fundamental object is the path integral, which is a formal integral over all possible field configurations  $\mathcal{D}\phi$ , weighted with an imaginary Boltzmann factor of their respective classical action (Definition 7):

$$Z[J] := \int \mathcal{D}\phi e^{iS[\phi] + i \int d^D \underline{x} J(\underline{x})\phi(\underline{x})}. \quad (1.37)$$

We have introduced a *source field*  $J(\underline{x})$  such that the functional derivative of  $Z[J]$  with respect to  $J(\underline{x})$  produces factors  $\phi(\underline{x})$  in the path integral. Equivalently, Eq.(1.37) can be interpreted as an infinite dimensional Fourier transform of the functional  $e^{iS[\phi]}$  [80, Sect. 3.4].

The path integral is very much analogous to statistical mechanics. A Wick rotation to Euclidean spacetime eliminates the imaginary units and  $Z$  turns into the partition function of a statistical system with infinitely many degrees of freedom [81, 82]. Just like in statistical physics, the vacuum expectation value of products of fields, that is, the correlation functions (Definition 13), can be computed by including the corresponding terms into the integral and normalizing the result:

$$\begin{aligned}
\langle 0 | T(\phi(\underline{x}_1) \cdots \phi(\underline{x}_n)) | 0 \rangle &= \frac{\int \mathcal{D}\phi \phi(\underline{x}_1) \cdots \phi(\underline{x}_n) e^{iS[\phi] + i \int d^D \underline{x} J(\underline{x}) \phi(\underline{x})}}{\int \mathcal{D}\phi e^{iS[\phi] + i \int d^D \underline{x} J(\underline{x}) \phi(\underline{x})}} \Big|_{J(\underline{x}) \equiv 0} \\
&= \frac{(-i)^n}{Z[0]} \frac{\delta}{\delta J(\underline{x}_1)} \cdots \frac{\delta}{\delta J(\underline{x}_n)} Z[J] \Big|_{J(\underline{x}) \equiv 0}.
\end{aligned} \tag{1.38}$$

In the sense of Eq.(1.38),  $Z[J]$  is a *generating functional* of the time-ordered Green functions. The path integral framework does not have any notion of operator-valued distributions and therefore circumvents many of their conceptual problems (Sect. 1.2.2). Also, it comes with a physical interpretation along the lines of “quantum field theory means summing over all possible fields, weighting them with their classical action”. However, this view is deceptive: The path integral is a mathematically highly non-trivial object which can, in relevant cases, not be computed in any conventional sense. Also, the path integral is dominated entirely by non-continuous “trajectories” [83, 84], which have little in common with the classical “path of a particle”.

The free part, analogous to Eq.(1.31), of the path integral (1.38) is a Gaussian integral which can be solved analytically. A series expansion in the coupling constants  $\lambda_n$  of the remaining interaction Lagrangian then leads to the same Feynman integrals and Feynman graphs as does canonical quantization in Theorem 6. One even recovers the  $i\epsilon$ -prescription (Eq.(1.22)) for the propagator from the path integral [85].

Conversely, knowing Feynman integrals as series coefficients, one can *define* the path integral as their formal generating functional, irrespective of convergence issues:

$$\sum_{n=0}^{\infty} \frac{1}{n!} i^n \langle T(\phi(\underline{x}_1) \cdots \phi(\underline{x}_n)) \rangle J(\underline{x}_1) \cdots J(\underline{x}_n) =: Z[J]. \tag{1.39}$$

In this sense, the path integral or the canonical quantization procedure are equivalent, and either one produces Feynman integrals (Theorem 6) as a perturbation series. In Sect. 1.3.11, we will motivate *Dyson–Schwinger equations* from perturbation theory, they can also be derived from the path integral (e.g., [19]), or one takes Dyson–Schwinger equations as primary objects and derives from them the perturbation series.

The pragmatic view in the present thesis will therefore be that Feynman integrals are the correct series coefficients of the  $S$ -matrix, irrespective of the mathematical truth of their derivation. This is in the spirit of ’t Hooft and Veltman [85]:

Whatever approach is used, the result is always that the S-matrix is expressed in terms of a certain set of Feynman diagrams. [...] The situation must be reversed: Diagrams form the basis from which everything must be derived. [...] Using diagrams as a starting point seems [...] to be a capitulation in the struggle to go beyond perturbation theory. It is unthinkable to accept as a final goal a perturbation theory, and it is not our purpose to forward such a notion. On the contrary, it becomes more and more clear that perturbation theory is a very useful device to discover equations and properties that may hold true even if the perturbation expansion fails.

As for the last sentence, much progress has been reached in the last 50 years in the framework of *resurgence*, which we comment on in Sect. 2.1.2.

### 1.2.8 Digression: History and Alternative Ways to Compute the S-Matrix

We have seen in Theorem 6 that we can compute the S-matrix as an infinite series of Feynman integrals. Following this approach naively, however, has shortcomings. Amongst them

1. The whole derivation was based on quantum field operators, whose physical significance is not completely clear, see Sect. 1.2.2. Even if the resulting formulas for observables are apparently correct, their “derivation” from classical field theory is questionable.
2. Feynman graphs are often divergent. This problem is for most of the physically relevant cases solved by *renormalization* (Sect. 2.2).
3. The individual integrals are hard to solve and the number of Feynman integrals grows rapidly with rising order in the Dyson series (see Sect. 6.2), or with rising number of external particles. The resulting functions are highly non-trivial.
4. The perturbation series diverges even if individual integrals are finite. It appears unclear what information it carries about the true, non-perturbative solution. This is to some extent solved by *resurgence* (Sect. 2.1.2).

As an illustration for the third problem, take the anomalous magnetic momentum in QED, which, with decades of effort, has been computed perturbatively to 4th (!) order [86]

$$\frac{g}{\mu_B} = 1 + 0.5 \left( \frac{\alpha}{\pi} \right) - 0.3285 \left( \frac{\alpha}{\pi} \right)^2 + 1.181 \left( \frac{\alpha}{\pi} \right)^3 - 1.912 \left( \frac{\alpha}{\pi} \right)^4 + \dots$$

The numerical coefficients are known to thousands of digits. At order 4, individual Feynman integrals take values in the 100s or 1000s. All these large numbers almost completely cancel, leaving the result  $-1.912$ . See also [87].

One possibility to, at least partially, overcome the computational problem 3. is the massive use of numerical calculations. Firstly, one can resort to numerical quadrature of Feynman integrals, compare for example Sect. 6.2. Secondly, the framework of

lattice QFT [88, 89] aims at an ab-initio simulation of quantum fields in a small, discretized region of Euclidean spacetime, where QFT essentially becomes statistical physics [82, 90].

An alternative approach to computing  $S$ -matrix element goes broadly by the name of (constructive/axiomatic)  *$S$ -matrix theory*. It consists of several different, closely related methods with the aim of establishing as many general properties as possible which a sensible  $S$ -matrix must fulfil. Trivial examples are Lorentz covariance and macroscopic conservation laws for charges and momentum, another line of thought is the intuition that a scattering process of many particles with local interactions should decompose into “elementary” clusters in a consistent manner [91]. A more sophisticated examination concerns the analytic structure of scattering amplitudes. Being not based on QFT, analogous statements exist, for example, for the  $S$ -matrix in classical optics, where they relate scattering amplitudes to the optical resonances of a system [17, 92, 93].

The goal of constructive  $S$ -matrix theory is to establish sufficiently many conditions such that the whole  $S$ -matrix is fixed by them. In the early days of quantum field theory, the main motivation was to circumvent the technical and conceptual difficulties of canonical quantization outlined above. In the best case, constructive  $S$ -matrix theory would be able to replace quantum field theory altogether and produce all observables without any reference to an unobservable “microscopic” theory. This is in the spirit of Heisenberg’s dictum [24] from 1920s quantum mechanics:

Die anschauliche Deutung der Quantenmechanik ist bisher noch voll innerer Widersprüche, die sich im Kampf der Meinungen um Diskontinuumus- und Kontinuumstheorie, Korpuskeln und Wellen auswirken. Schon daraus möchte man schließen, daß eine Deutung der Quantenmechanik mit den gewohnten kinematischen und mechanischen Begriffen jedenfalls nicht möglich ist. Die Quantenmechanik war ja gerade aus dem Versuchen entstanden, mit jenen gewohnten kinematischen Begriffen zu brechen und an ihre Stelle Beziehungen zwischen konkreten experimentell gegebenen Zahlen zu setzen.

Heisenberg himself doubled down on this perspective in his introduction of the  $S$ -matrix [67], and it eventually lead to an understanding of *renormalization* (Sect. 2.2). Interestingly, the same principle was also the crucial ingredient for the second revolution in 20th-century physics, Einstein’s general relativity [94]

Eine Antwort auf diese Frage [das Mach’sche Paradox] kann nur dann als erkenntnistheoretisch befriedigend anerkannt werden, wenn die als Grund angegebene Sache eine *beobachtbare Erfahrungstatsache* ist; denn das Kausalitätsgesetz hat nur dann den Sinn einer Aussage über die Erfahrungswelt, wenn als Ursachen und Wirkungen letzten Endes nur *beobachtbare Tatsachen* auftreten.

In the 1960s, the technical problems 1. and 2. were largely sorted out for quantum electrodynamics, and Feynman integral calculations became a widely used tool in quantum field theory. In hindsight, Weinberg remarks about this period [95]

One problem with the S-matrix program was in formulating what is meant by the analyticity of the S-matrix. What precisely are the analytic properties of a multi-particle S-matrix element? I don't think anyone ever knew. I certainly didn't know [...]. By the mid-1960's it was clear that S-matrix theory had failed in dealing with the one problem it had tried hardest to solve, that of pion-pion scattering.

By Theorem 6, Feynman integrals are supposed to be summands of the  $S$ -matrix element and therefore they naturally inherit many of its analytic properties. Consequently, the approaches of axiomatic-constructive S-matrix theory and perturbative quantum field theory heavily informed each other. Notable outcomes of this interplay are, amongst others, the *Källen-Lehmann representation* of the 2-point function [47, 96], the Landau equations [97], *Cutkosky's theorem* [98–101], and a classification of particles and their propagators in terms of the Lorentz group [102–106]. The correspondence between Wightman functions (Definition 13) and time-ordered Green functions (Definition 14) noted in Sects. 1.2.3 and 1.2.4 gives rise to the *Steinman relations* [107, 108] for the latter. Expressing the Feynman propagator in terms of Wightman propagators is the starting point for the *cutting formula* [18, Sect. 2].

The success of such analytic considerations in perturbation theory has been unbroken. Still today, extended and refined versions are routinely used in the computation of Feynman integrals, see for example [109–112]; the reader interested in historic anecdotes will also enjoy [113]. Another aspect is to use analytic properties in order to restrict the class of functions appearing as solutions of certain Feynman integrals, and specify their properties and relations, see for example [114–119]. These methods nowadays primarily attack the third problem above, the difficulty to solve individual Feynman integrals. They add to the vast amount of identities and methods to simplify Feynman integrals, some of which are [120–124].

Another contemporary branch of analytic methods goes by the label *on-shell methods*. It has proven especially valuable for amplitudes with complicated Lorentz structure. These are notably QCD amplitudes with many external particles [125–132], and theories with higher spin [133–136].

But even after decades of successful perturbative QFT, the second original motivation for  $S$ -matrix theory is still relevant, namely the computation of scattering amplitudes when the microscopic theory is not understood. Quantum gravity has so far resisted every attempt to be described by a convincing quantum field theory, see Sect. 5.2.1, but still it is possible to deduce many features of the graviton-scattering S-matrix from general considerations without knowing the microscopic theory, e.g., [115, 137–144]. Conversely, there are dozens of hypothetical microscopic explanations for quantum gravity, ranging from string theory [145–147] over causal dynamic triangulation [148, 149] and causal sets [150–156] to causal fermionic systems [157, 158]. For these approaches,  $S$ -matrix theory can be a guideline and criterion to check their predictions for plausibility.

### Summary of Sect. 1.2

1. Starting from classical field theory (Sect. 1.2.1), one can construct quantum field theory “by analogy” (Sect. 1.2.2) in a process called *canonical quantization*.
2. We have discussed in detail the 2-point functions of a free quantum field (Sect. 1.2.3) and how they determine all  $n$ -point functions via Wick’s theorem (Theorem 2).
3. All information about an interacting quantum field theory is encoded in its  $S$ -matrix (Sect. 1.2.5), which can be computed perturbatively with the Dyson series (Theorem 6) in terms of Feynman integrals.
4. The path integral provides another way to define a QFT, leading to the same Feynman integrals as a perturbative solution (Sect. 1.2.7).
5. A brute-force computation of Feynman integrals is inefficient, and there are numerous advanced tricks for improvement. Moreover, there are approaches to quantum scattering amplitudes which do not involve Feynman integrals at all (Sect. 1.2.8).

## 1.3 Feynman Graphs

Feynman graphs appear as a graphical notation of the perturbative solution to a QFT. In the present section, we discuss their central properties.

### 1.3.1 Graphical Representation of Feynman Integrals

The correlation functions of the interacting theory are, by the Dyson series (Theorem 6), expressed in terms of *Feynman integrals* over products of propagators (Definition 15). These integrals inherit the graphical notation of Wick’s theorem, introduced in Sect. 1.2.4, we obtain *Feynman graphs* [45].

From Theorem 6 we learn that these graphs can involve vertices of valence  $k$  if and only if the Lagrangian (Eq. (1.6)) contains an interaction term  $\frac{-\lambda_k}{k!} \phi^k$ . Conversely, there is exactly one field operator at each of the external coordinates  $\underline{z}_1, \dots, \underline{y}_i$ , which therefore show up as 1-valent vertices in the Feynman graphs; to compute the interacting  $G^{(n)}$ , we need to sum over all possible graphs which have exactly  $n$  external 1-valent vertices, but arbitrarily many internal ones. The vacuum  $S$ -matrix (Eq. (1.36)) amounts to the sum over all graphs without external vertices. Dividing through the vacuum  $S$ -matrix in Theorem 6 entails that we can leave out all graphs

which are disconnected from all of the external points of  $G^{(n)}$ . Eventually, the Dyson series (Theorem 6) takes the form

$$\tilde{G}^{(n)}(\underline{x}_1, \dots, \underline{x}_n) = \sum_{\Gamma \in \tilde{\Gamma}^{(n)}} \text{sym}(\Gamma) \cdot \mathcal{F}[\Gamma](\underline{x}_1, \dots, \underline{x}_n). \quad (1.40)$$

Here,  $\tilde{\Gamma}^{(n)}$  is the set of all graphs with  $n$  external vertices corresponding to the points  $\underline{x}_1, \dots, \underline{x}_n$ . We have absorbed all combinatorial prefactors into the *symmetry factor*  $\text{sym}(\Gamma)$  which will be discussed in Sect. 1.3.8. All integrals and coupling constants are absorbed into the *Feynman rules*  $\mathcal{F}(\Gamma)$ , to be discussed in Sect. 1.3.5. The graphs in  $\tilde{\Gamma}^{(n)}$  have at most  $n$  connected components (Definition 22).

In the Feynman integral, two spacetime points  $\underline{x}, \underline{y}$  are joined by a propagator  $G_F(\underline{x}, \underline{y})$  (Eq. (1.24)) if and only if there is an edge between the two vertices representing  $\underline{x}$  and  $\underline{y}$  in the corresponding Feynman graph. Conversely, if a graph  $\Gamma$  has two connected components  $\Gamma = \gamma_1 \cup \gamma_2$ , that is two subgraphs which are not connected to each other, then the corresponding variables in the Feynman integral are independent. We conclude:

$$\Gamma = \gamma_1 \cup \gamma_2, \gamma_1 \cap \gamma_2 = \emptyset \Rightarrow \mathcal{F}[\Gamma] = \mathcal{F}[\gamma_1] \cdot \mathcal{F}[\gamma_2]. \quad (1.41)$$

**Definition 19.** The *connected combinatorial Green function*  $\tilde{\Gamma}^{(n)}$  is the set of all connected (Definition 22) Feynman graphs with  $n$  external edges, including their symmetry factor (Theorem 15) and powers of coupling constants.

**Definition 20.** The *connected analytic Green function*  $\tilde{G}^{(n)}$  is the restriction of the analytic Green function Eq. (1.40) to only connected graphs (Definition 19), namely  $\tilde{G}^{(n)} = \sum_{\Gamma \in \tilde{\Gamma}^{(n)}} \mathcal{F}(\Gamma)$ .

Equivalently, the connected Green function  $\tilde{G}^{(n)}$  arises from the non-connected Green functions  $\tilde{G}^{(n)}$  (Definition 14) by subtraction of all products of smaller valence,

$$\begin{aligned} \tilde{G}^{(1)}(\underline{x}) &= \tilde{G}^{(1)}(\underline{x}), & \tilde{G}^{(2)}(\underline{x}_1, \underline{x}_2) &= \tilde{G}^{(2)}(\underline{x}_1, \underline{x}_2) - \tilde{G}^{(1)}(\underline{x}_1)\tilde{G}^{(1)}(\underline{x}_2) \\ \tilde{G}^{(3)}(\underline{x}_1, \underline{x}_2, \underline{x}_3) &= \tilde{G}^{(3)}(\underline{x}_1, \underline{x}_2, \underline{x}_3) - \langle 3 \rangle \cdot \tilde{G}^{(2)}\tilde{G}^{(1)} - \tilde{G}^{(1)}(\underline{x}_1)\tilde{G}^{(1)}(\underline{x}_2)\tilde{G}^{(1)}(\underline{x}_3), & \dots \end{aligned}$$

Here,  $\langle 3 \rangle$  denotes permutations (Definition 17). In terms of generating functionals, the relationship between  $\tilde{G}$  and  $\tilde{G}$  is that of exponentiation or logarithm. If  $Z[J]$  is the generating series of all Green functions (Eq. (1.39)), then the connected Green functions are generated by  $W[J] := \ln Z[J]$  [82, 159]. Finally, we exclude all graphs which contain self-loops, or tadpoles (Definition 30). A more detailed account of this decision will be given in Sect. 5.1.4.

**Example 11:**  $\phi^3$  theory, connected Feynman graphs.

Consider the connected 2-point graphs (Definition 19) of  $\phi^3$  theory (Example 3). There is a single graph without loops, namely an edge. Next there is one 1-loop graph, the 1-loop multiedge. At two loops, there are already four graphs. In this example, we write the coupling constants as explicit prefactors, they can alternatively be included into the definition of the graphs.

$$\bar{\Gamma}^{(2)} = \text{---} + \lambda_3^2 \frac{1}{2} \text{---} \bullet \bullet \text{---} + \lambda_3^4 \left( \frac{1}{4} \text{---} \bullet \bullet \text{---} \bullet \bullet \text{---} + \frac{1}{2} \text{---} \bullet \bullet \text{---} \bullet \bullet \text{---} + \frac{1}{2} \text{---} \bullet \bullet \text{---} \bullet \bullet \text{---} \right) + \dots$$

There are infinitely many more graphs contributing to  $\bar{\Gamma}^{(2)}$ . Similarly,  $\bar{\Gamma}^{(3)}$  starts with

$$\begin{aligned} \bar{\Gamma}^{(3)} = & \lambda_3 \text{---} \bullet \text{---} + \lambda_3^3 \left( \text{---} \bullet \text{---} \bullet \text{---} \bullet \text{---} + \langle 3 \rangle \frac{1}{2} \text{---} \bullet \bullet \text{---} \bullet \bullet \text{---} \right) \\ & + \lambda_3^5 \langle 3 \rangle \left( \frac{1}{2} \text{---} \bullet \bullet \text{---} \bullet \bullet \text{---} + \frac{1}{2} \text{---} \bullet \bullet \text{---} \bullet \bullet \text{---} + \text{---} \bullet \bullet \text{---} \bullet \bullet \text{---} \right) + \lambda_3^5 \frac{1}{2} \text{---} \bullet \bullet \text{---} \bullet \bullet \text{---} + \dots \end{aligned}$$

The factor  $\langle 3 \rangle$  means that these graphs can be oriented in 3 different ways (Definition 17). The very last graph is symmetric under exchange of the three external edges and does not obtain a factor  $\langle 3 \rangle$ . Altogether, there are 15 different connected graphs contributing up to loop order 2.

### 1.3.2 Basic Definitions

**Definition 21.** A non-amputated Feynman graph  $\Gamma$  is a graph given by disjoint vertex sets  $(V_\Gamma, V_{\Gamma,\text{ext}})$  and edge sets  $(E_\Gamma, E_{\Gamma,\text{ext}})$  where

1.  $V_\Gamma$  are called *internal vertices* of  $\Gamma$ . The valence (Definition 23) of them is at least 3.
2.  $V_{\Gamma,\text{ext}}$  are called *external vertices* of  $\Gamma$ . They have valence 1.
3.  $E_\Gamma$  are the *internal edges* of  $\Gamma$ . An edge  $e \in E_\Gamma$  is an ordered pair  $e = \{v_1, v_2\}$  where both  $v_j \in V_\Gamma$ .
4.  $E_{\Gamma,\text{ext}}$  are the *external edges* of  $\Gamma$ . An edge  $e \in E_{\Gamma,\text{ext}}$  is an ordered pair  $e = \{v_1, v_2\}$  where  $v_1 \in V_\Gamma$  and  $v_2 \in V_{\Gamma,\text{ext}}$ .

5. Every edge comes with a *mass*  $0 \leq m_e \in \mathbb{R}$  and a power (also called *index*)  $\nu_e \in \mathbb{R}$  and a 4-momentum  $\underline{k}_e$ . Unless otherwise specified, we will assume that  $\nu_e = 1$ .

This definition allows for *multigraphs*, that is, graphs with multiple parallel edges between the same two vertices. Also, the two end-vertices of an internal edge can be the same vertex, which is called *tadpole* in physics and *loop* in mathematics (not to be confused with *loop* in the physical nomenclature, Definition 29). Further, Definition 21 is a *directed* graph which is not strictly necessary for a scalar theory since the scalar Feynman propagator Eq. (1.24) is symmetric with respect to exchanged arguments. However, we will use the direction of edges to fix the direction of the edge-momentum  $\underline{k}_e$ .

Moreover, a Feynman graph according to Definition 21 need not be connected.

**Definition 22.** A graph is *connected* if for any two vertices, there is a path of edges to go from the first vertex to the second one. A *connected component*  $\gamma \subset \Gamma$  is a connected graph  $\gamma$  that is not connected to the remainder  $\Gamma \setminus \gamma$ .

**Definition 23.** The *valence* (=degree) of a vertex is the number of edges incident to it, regardless of direction of the edges. A graph is  $j$ -regular if and only if all its vertices have valence  $j$ .

Thanks to the LSZ formula (Theorem 5), we will mostly be working with amputated graphs.

**Definition 24.** An (amputated) *Feynman graph*  $\Gamma$ , derived from a non-amputated Feynman graph  $\Gamma'$  (Definition 21), is a graph given by disjoint vertex sets,  $V_\Gamma = V_{\Gamma,\text{int}} \cup V_{\Gamma,\text{ext}}$  and an edge set  $E_\Gamma$  where

1.  $V_{\Gamma,\text{ext}}$  are called *external vertices* of  $\Gamma$ . They have valence at least 2. These are the vertices  $v \in V_{\Gamma'}$  that used to be connected to external edges of  $\Gamma'$ . Especially,  $V_{\Gamma,\text{ext}} \subseteq V_{\Gamma'}$  and  $V_{\Gamma,\text{ext}} \not\subseteq V_{\Gamma',\text{ext}}$ .
2.  $V_{\Gamma,\text{int}}$  are called *internal vertices* of  $\Gamma$ . Their valence is at least 3. In  $\Gamma'$ , they were not adjacent to any external edge.
3. The edges  $E_\Gamma = E_{\Gamma'}$  are the *internal edges* of  $\Gamma'$ .
4. To every edge  $e \in E_\Gamma$  we assign a mass  $0 \leq m_e \in \mathbb{R}$  and a power  $\nu_e \in \mathbb{R}$  and a 4-momentum  $\underline{k}_e$ . Unless otherwise specified, we assume that  $\nu_e = 1$ .

The information about which vertices are external and internal is not trivial, it can in general not be reconstructed from (a drawing of) the graph  $\Gamma$  alone without knowing the underlying  $\Gamma'$ . If we know that  $\Gamma'$  is  $j$ -regular (Definition 23) then those vertices  $v \in \Gamma$  with valence lower than  $j$  are exactly the ones where, in  $\Gamma'$ , external edges used to be attached.

**Definition 25.** A *subgraph*  $\gamma \subseteq \Gamma$  of a Feynman graph  $\Gamma$  (Definition 24) is a Feynman graph such that  $E_\gamma \subseteq E_\Gamma$  and  $\gamma$  contains all the vertices adjacent to any edges  $e \in E_\gamma$ . That is,  $\gamma$  may contain disconnected (Definition 22) vertices, but no edges without their end vertices.

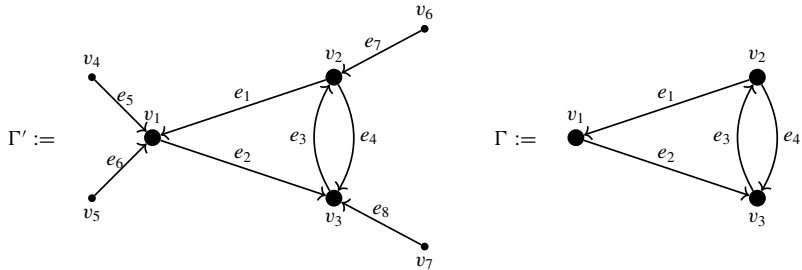
**Definition 26.** The *residue*  $\text{res}(\Gamma)$  of a non-amputated Feynman graph  $\Gamma$  (Definition 21) is the product of its external edges,  $\text{res}(\Gamma) = \prod_{e \in E_{\Gamma,\text{ext}}} e$ . Especially, the residue of a single vertex is the product of edges adjacent to it.

The physical interpretation of Feynman graphs is that each edge represents a field variable. In that case, the residue is a monomial in the field variables.

**Definition 27.** Let  $\gamma \subset \Gamma$  be a proper subgraph (Definition 25) of a Feynman graph  $\Gamma$ . The *contracted graph*  $\frac{\Gamma}{\gamma}$  is the graph  $\Gamma$ , but every connected component of  $\gamma$  is replaced by its residue, that is, by a single vertex.

### Example 12: Dunce's cap.

Traditionally, one chooses as an example the following Feynman graph, known as the *dunce's cap*:



Here  $\Gamma'$  is the graph including external vertices and external edges (Definition 21), while in  $\Gamma$ , the external edges have been amputated (Definition 24), following Theorem 5.

For  $\Gamma'$ , the internal vertices are  $V_{\Gamma'} = \{v_1, v_2, v_3\}$  while the external vertices are  $V_{\Gamma',\text{ext}} = \{v_4, v_5, v_6, v_7\}$ . Likewise, the internal edges are  $E_{\Gamma'} = \{e_1, e_2, e_3, e_4\}$  and the external edges are  $E_{\Gamma',\text{ext}} = \{e_5, e_6, e_7, e_8\}$ . This graph is 4-regular (Definition 23), and it is connected (Definition 22). The external edges are directed inwards by convention, the orientation of inner edges is fixed arbitrarily. Each edge represents the propagation of the same type of field  $\phi$ , hence the residue (Definition 26) of the unamputated graph is  $\text{res}(\Gamma') = \phi^{|E_{\Gamma',\text{ext}}|} = \phi^4$ .

In the amputated graph  $\Gamma$ , all three vertices are *external* vertices,  $V_{\Gamma,\text{ext}} = \{v_1, v_2, v_3\}$  since all of them used to be connected to an external edge prior to amputation. The residue of  $\Gamma$  is not well-defined, unless one specifies the valence of the external vertices. If we provide the information that the unamputated graph is 4-regular (Definition 26), then one can infer the amputated external edges and that  $\text{res}(\Gamma) = \phi^4$ .

**Definition 28.** A *circuit* in a Feynman graph  $\Gamma$  (Definition 24) is a sequence of edges that form a closed path, where edges and vertices are allowed to be visited more than once, and not all edges or vertices of  $\Gamma$  have to be used.

**Definition 29.** A *cycle*, or *loop* is a circuit that visits no vertex more than once. The set of *loops*  $L_\Gamma$  of a Feynman graph  $\Gamma$  (Definition 24) is a basis of the graph's cycle space, that is, a choice of linearly independent loops. For a given graph  $\Gamma$ , this choice need not be unique. The *loop number*  $|L_\Gamma|$  is the dimension of the cycle space, it is unique for a fixed  $\Gamma$ . In mathematical terminology,  $|L_\Gamma| = b_1(\Gamma)$  is the first Betti number.

By Definition 29, a cycle, does not contain any edge more than once. We consider two cycles identical if they only differ by the order of edges they contain.

**Definition 30.** A *tadpole* graph is a amputated Feynman graph (Definition 24) that has only one external vertex. A *tadpole* subgraph  $\gamma \subset \Gamma$  is a graph  $\gamma$  that is connected to the remainder  $\Gamma \setminus \gamma$  by only a single vertex.

**Theorem 7** (Euler's formula [160]). For a connected (Definition 22) graph  $\Gamma$ , the number of edges  $|E_\Gamma|$ , vertices  $|V_\Gamma|$  and loops  $|L_\Gamma|$  are related by

$$|E_\Gamma| - |V_\Gamma| + 1 = |L_\Gamma|.$$

It is sometimes useful to rephrase Euler's formula in terms of the number of external edges  $|E_{\Gamma,\text{ext}}|$  and the number of  $j$ -valent vertices,  $n_j$ .

$$\sum_{j=3}^{\infty} (j-2)n_j = |E_{\Gamma,\text{ext}}| - 2 + 2|L_\Gamma|. \quad (1.42)$$

Especially, if  $\Gamma$  is  $n$ -regular (Definition 23) then  $n_n = |V_\Gamma|$  and  $n_{j \neq n} = 0$  and

$$(n-2)|V_\Gamma| = |E_{\Gamma,\text{ext}}| - 2 + 2|L_\Gamma|, \quad |E_{\Gamma,\text{int}}| = \frac{|E_{\Gamma,\text{ext}} - n|}{n-2} + \frac{n}{n-2}|L_\Gamma|. \quad (1.43)$$

### Example 13: Dunce's cap, loops.

A possible choice of loops (Definition 29) for the dunce's cap (Example 12) is

$$L_{\Gamma'} = \{\{e_1, e_2, -e_4\}, \{e_3, e_4\}\}.$$

We have used different signs to account for the direction of edges along the loop. The dunce's cap has loop number (Definition 29)  $|L'_{\Gamma}| = 2$ . Euler's formula (Theorem 7) is fulfilled:  $8 - 7 + 1 = 2$ . Since  $\Gamma'$  is 4-regular, Eq. (1.43) holds:  $(4-2) \cdot 3 = 6 = 4 - 2 + 2 \cdot 2$ .

The amputated graph  $\Gamma$  has the same set of loops and therefore still has loop number  $|L_\Gamma| = 2$ . Despite the missing edges, it still satisfies Theorem 7:  $4 - 3 + 1 = 2$ .

### 1.3.3 Graph Matrices

In order to handle larger graphs algorithmically, it is useful to express them not as a set of edges and vertices as in Definition 24, but rather in terms of matrices, which encode these elements.

**Definition 31.** The *incidence matrix*  $I_\Gamma$  of a Feynman graph  $\Gamma$  (Definition 24) is a  $|E_\Gamma| \times |V_\Gamma|$  matrix whose entries correspond to edges  $\{v_1, v_2\} = e \in E_\Gamma$  and vertices  $v \in V_\Gamma$ ,

$$(I_\Gamma)_{e,v} := \begin{cases} 1 & v = v_1 \\ -1 & v = v_2 \\ 0 & \text{else.} \end{cases}$$

**Lemma 8.** The *cycle space*  $\text{Cyc}(G)$  (Definition 29) is the kernel of the transpose incidence matrix (Definition 31),

$$\text{Cyc}(G) = \left\{ \vec{e} \in \mathbb{R}^{|E_\Gamma|} \mid I_\Gamma^T \vec{e} = \vec{0} \right\}.$$

Lemma 8 is very useful in computer calculations because it gives a simple algebraic way to obtain a choice of loops, see Example 14.

**Definition 32.** The undirected *adjacency matrix*  $A_\Gamma$  of a Feynman graph  $\Gamma$  (Definition 24) is a  $|V_\Gamma| \times |V_\Gamma|$  matrix where the entry  $(A_\Gamma)_{i,j}$  is the number of edges – regardless of direction – between vertices  $v_i$  and  $v_j$ .

**Definition 33.** The undirected *degree matrix*  $D_\Gamma$  of a Feynman graph  $\Gamma$  (Definition 24) is a  $|V_\Gamma| \times |V_\Gamma|$  matrix where the entry  $(D_\Gamma)_{i,i}$  is the valence (Definition 23) of  $v_i$ , and  $(D_\Gamma)_{i,j \neq i} = 0$ .

**Lemma 9** (e.g., [161]). Let  $I_\Gamma$  be the incidence matrix (Definition 31),  $A_\Gamma$  the adjacency matrix (Definition 32) and  $D_\Gamma$  the degree matrix (Definition 33) of a graph  $\Gamma$  (Definition 24). The following two expressions coincide, and they define the  $|V_\Gamma| \times |V_\Gamma|$  *Laplace matrix*  $M_\Gamma$ :

$$M_\Gamma := I_\Gamma^T I_\Gamma = D_\Gamma - A_\Gamma.$$

There are straightforward generalizations of Definitions 32 and 33 for directed multi-graphs: For the adjacency matrix, let  $(A_\Gamma)_{i,j}$  be the number of edges directed from  $i$  to  $j$ . A tadpole (Definition 30) at  $v_i$  corresponds 1 to  $(A_\Gamma)_{i,i}$ . For the degree matrix, let  $(D_\Gamma)_{i,i}$  be the number of directed edges entering  $v_i$ . For our applications, due to the use of scalar fields, it will be sufficient to consider undirected matrices.

**Example 14: Dunce's cap, graph matrices.**

Consider the dunce's cap from Example 12. The incidence matrix of  $\Gamma'$  is

$$I_{\Gamma'} = \begin{pmatrix} -1 & 1 & 0 & 0 & 0 & 0 & 0 \\ 1 & 0 & -1 & 0 & 0 & 0 & 0 \\ 0 & -1 & 1 & 0 & 0 & 0 & 0 \\ 0 & 1 & -1 & 0 & 0 & 0 & 0 \\ 1 & 0 & 0 & -1 & 0 & 0 & 0 \\ 1 & 0 & 0 & 0 & -1 & 0 & 0 \\ 0 & 1 & 0 & 0 & 0 & -1 & 0 \\ 0 & 0 & 1 & 0 & 0 & 0 & -1 \end{pmatrix}$$

We note that the 4 external edges result in a  $4 \times 4$  block identity matrix  $-\mathbb{1}_{4 \times 4} \subset I_{\Gamma'}$ . The incidence matrix of the amputated graph is the remainder after removing said block,

$$I_{\Gamma} = \begin{pmatrix} -1 & 1 & 0 \\ 1 & 0 & -1 \\ 0 & -1 & 1 \\ 0 & 1 & -1 \end{pmatrix}.$$

From this matrix, one obtains the loops (Definition 29) with the simple calculation

$$I_{\Gamma}^T \vec{e} = \vec{0} \quad \Rightarrow \quad \vec{e} = (a, a, b, b - a), \quad a, b \in \mathbb{R}.$$

Choosing, for example,  $a = 1$  and  $b = 0$ , we have  $\vec{e} = (1, 1, 0, -1)$ , which amounts to the loop  $\{e_1, e_2, -e_4\}$ . The choice  $a = 0$  and  $b = 1$  yields the loop  $\{e_3, e_4\}$ . This reproduces the loops from Example 13. Note how the result respects the direction of edges in the loop.

The undirected adjacency matrix and degree matrix of  $\Gamma$  are

$$A_{\Gamma} = \begin{pmatrix} 0 & 1 & 1 \\ 1 & 0 & 2 \\ 1 & 2 & 0 \end{pmatrix}, \quad D_{\Gamma} = \begin{pmatrix} 2 & 0 & 0 \\ 0 & 3 & 0 \\ 0 & 0 & 3 \end{pmatrix}.$$

The two matrices in Lemma 9 coincide and give rise to the Laplace matrix

$$M_{\Gamma} = \begin{pmatrix} 2 & -1 & -1 \\ -1 & 3 & -2 \\ -1 & -2 & 3 \end{pmatrix}.$$

For comparison, the directed Laplace matrix (with directions as indicated in Example 12) is

$$M_\Gamma = \begin{pmatrix} 1 & 0 & -1 \\ -1 & 1 & -1 \\ 0 & -1 & 2 \end{pmatrix}.$$

**Definition 34.**

1. A *tree* is a connected Feynman graph (Definition 24) with zero loops (Definition 29). Those trees which contribute to a given amplitude are called *treelevel graphs*.
2. A *j-forest* is a disjoint set of exactly  $j$  trees, that is, a Feynman graph with exactly  $j$  connected components and zero loops.

For a tree  $T$ , Euler's formula (Theorem 7) specializes to

$$|V_T| = |E_T| + 1. \quad (1.44)$$

**Lemma 10** (Cayley's formula, [162–164]). There are  $|V_T|^{|V_T|-2}$  labelled trees with distinguishable (=labelled) vertices.

**Definition 35.** Let  $\Gamma$  be a connected Feynman graph (Definition 24).

1. A *spanning tree* of  $\Gamma$  is a connected subgraph  $T \subseteq \Gamma$  (Definition 25) such that  $T$  is a tree and  $V_T = V_\Gamma$ ,  $V_{T,\text{ext}} = V_{\Gamma,\text{ext}}$ . By  $T_\Gamma^{(1)}$  we denote the set of all spanning trees of  $\Gamma$ .
2. A *spanning j-forest* of a Feynman graph  $\Gamma$  is a subgraph  $F \subseteq \Gamma$  (Definition 25) such that  $F$  is a forest with exactly  $j$  components, and  $V_F = V_\Gamma$ ,  $V_{F,\text{ext}} = V_{\Gamma,\text{ext}}$ . By  $T_\Gamma^{(j)}$  we denote the set of all spanning  $j$ -forests of  $\Gamma$ .

Since our definition of Feynman graph (Definition 24) is a directed graph, its spanning trees will be directed as well. Under the name *directed acyclic graphs*, directed trees are prominently used in blockchain technology [165].

**Theorem 11** (Matrix tree theorem, Kirchhoff's theorem [162, 163, 166]). Let  $M_\Gamma$  be the Laplace matrix (Definition 37) and let  $M_\Gamma(i, j)$  be  $M_\Gamma$  where the row  $i$  and the column  $j$  are deleted. Then,  $(-1)^{i+j} \det M_\Gamma(i, j)$  is the number of spanning trees in  $\Gamma$ , irrespective of the choice of  $(i, j)$ .

If, instead,  $M_\Gamma$  is the directed Laplace matrix, then  $\det M_\Gamma(i, i)$  is the number of directed spanning trees in  $\Gamma$ , originating from  $v_i$ .

### Example 15: Dunce's cap, trees.

For the dunce's cap Example 12, we have

$$M_\Gamma(3, 3) = \begin{pmatrix} 2 & -1 \\ -1 & 3 \end{pmatrix}, \quad \det M_\Gamma(3, 3) = 5,$$

indicating by Theorem 11 that  $\Gamma$  has 5 different spanning trees. Explicitly, they are

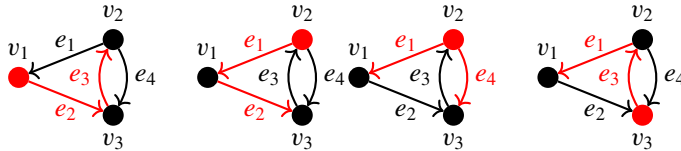
$$T_\Gamma = \{\{e_1, e_2\}, \{e_1, e_3\}, \{e_1, e_4\}, \{e_2, e_3\}, \{e_2, e_4\}\}.$$

The cofactors of the directed Laplacian matrix (Example 14) are

$$M_{\Gamma'}(1, 1) = \begin{pmatrix} 1 & -1 \\ -1 & 2 \end{pmatrix}, \quad M_{\Gamma'}(2, 2) = \begin{pmatrix} 1 & -1 \\ 0 & 2 \end{pmatrix}, \quad M_{\Gamma'}(3, 3) = \begin{pmatrix} 1 & 0 \\ -1 & 1 \end{pmatrix}.$$

Consequently, there are  $\{1, 2, 1\}$  oriented spanning trees starting at vertices  $\{v_1, v_2, v_3\}$ :

$$\{\{e_2, e_3\}, \quad \{\{e_1, e_2\}, \{e_1, e_4\}\}, \quad \{e_1, e_3\}\}.$$



The spanning  $j$ -forests (Definition 35) of the dunce's cap are

$$T_\Gamma^{(2)} = \{\{\{e_1\}, \{v_3\}\}, \{\{e_2\}, \{v_2\}\}, \{\{e_3\}, \{v_1\}\}, \{\{e_4\}, \{v_1\}\}\},$$

$$T_\Gamma^{(3)} = \{\{\{v_1\}, \{v_2\}, \{v_3\}\}\}, \quad T_\Gamma^{(j \geq 4)} = \emptyset.$$

There are numerous generalizations and alternative proofs of matrix tree theorems [167]. One useful type of generalization concerns labelled, or weighted, edges. This

way, instead of merely counting the number of certain objects, one obtains explicit information about which edges are involved. We collect the edge variables in a  $|E_\Gamma| \times |E_\Gamma|$  diagonal matrix

$$Y_\Gamma := \text{diag}(a_1, \dots, a_{|E_\Gamma|}). \quad (1.45)$$

Note that  $Y_\Gamma^{-1}$  is a diagonal matrix with entries  $\frac{1}{a_e}$ .

Recall that in Lemma 8, we have characterized the cycle space as the kernel of the (not edge-labelled) incidence matrix. This construction can be generalized to the labelled matrix  $I_\Gamma^T Y_\Gamma^{-1}$  to give rise to a *weighted cycle space*. The complement of the cycle space is called cut space.

**Definition 36.** The *weighted cut space*  $\text{Cut}(\Gamma)$  of a connected graph  $\Gamma$  is the column space of  $Y_\Gamma^{-1} I_\Gamma$ , where  $I_\Gamma$  is the incidence matrix (Definition 31) and  $Y$  is as in Eq. (1.45):

$$\text{Cut}(G) := \{\vec{e} \in \mathbb{R}^{|E_\Gamma|} \mid \vec{e} = Y_\Gamma^{-1} I_\Gamma \vec{v}, \vec{v} \in \mathbb{R}^{|V_\Gamma|}\}.$$

By Definition 36, each vector of edges  $\vec{e} \in \text{Cut}(\Gamma)$  is induced by a vector of vertices  $\vec{v} \in \mathbb{R}^{|V_\Gamma|}$ . Indeed, if we take  $\vec{v} \in V_\Gamma$  as a binary vector  $\vec{v} \in \{0, 1\}^{|V_\Gamma|}$ , then the corresponding  $\vec{e} = Y_\Gamma^{-1} I_\Gamma \vec{v}$  gives the (weighted) edges which will be cut if all the selected vertices are removed from the graph. The Euler formula (Theorem 7), together with the fact that the column space of a matrix is orthogonal to its kernel, implies the following statements:

**Lemma 12.** Let  $\Gamma$  be a connected graph. Its weighted cycle space (Lemma 8 where  $I_\Gamma^T Y_\Gamma^{-1}$  replaces  $I_\Gamma^T$ ) and weighted cut space (Definition 36) are subspaces of  $\mathbb{R}^{|E_\Gamma|}$ , and they satisfy

1.  $\dim(\text{Cyc}(\Gamma)) = |E_\Gamma| - |V_\Gamma| + 1$
2.  $\dim(\text{Cut}(\Gamma)) = |V_\Gamma| - 1$
3. The weighted cycle space and the weighted cut space are orthogonal with respect to the dot product

$$\langle \vec{v}, \vec{w} \rangle = \vec{v} \cdot \vec{w}, \quad \vec{v} \in \text{Cut}(\Gamma), \vec{w} \in \text{Cyc}(\Gamma)$$

**Example 16: Dunce's cap, cut space and cycle space.**

The incidence matrix of the (amputated) dunce's cap has been given in Example 14. The matrix  $Y_\Gamma$  (Eq.(1.45)) has size  $4 \times 4$ , and  $(Y_\Gamma^{-1} I_\Gamma)$  has three columns. Two of them are linearly independent, consequently, the cut space (Definition 36) is 2-dimensional. One choice of basis is obtained by  $\vec{v}_1 := (1, 0, 0)^T$  and  $\vec{v}_2 := (0, 1, 0)^T$ ,

$$\text{Cut}(\Gamma) = \text{Span} \left\{ \begin{pmatrix} -\frac{1}{a_1} \\ \frac{1}{a_1} \\ \frac{1}{a_2} \\ 0 \end{pmatrix}, \begin{pmatrix} \frac{1}{a_1} \\ 0 \\ -\frac{1}{a_3} \\ \frac{1}{a_4} \end{pmatrix} \right\} = \text{Span} \{ \vec{e}_1, \vec{e}_2 \} \subset \mathbb{R}^4.$$

Indeed, these two vectors can be identified with two different ways to cut  $\Gamma$  into two pieces. More precisely,  $\vec{e}_1$  is the cut obtained by removing the vertex  $v_1$ , and  $\vec{e}_2$  is the cut induced by removing  $v_2$ , as expressed by the vectors  $\vec{v}_1, \vec{v}_2$ . All other possible vertex-induced cuts can be obtained as linear combinations.

From a generalization of Example 14 to weighted incidence matrix, we obtain the weighted cycle space

$$\text{Cyc}(\Gamma) = \ker(I_\Gamma^T Y_\Gamma^{-1}) = \text{Span} \left\{ \begin{pmatrix} a_1 \\ a_2 \\ 0 \\ -a_4 \end{pmatrix}, \begin{pmatrix} 0 \\ 0 \\ a_3 \\ a_4 \end{pmatrix} \right\} \subset \mathbb{R}^4.$$

By computing the inner product  $\vec{e}_1 \cdot \vec{e}_2$  between pairs of basis vectors, one confirms that indeed  $\text{Cut}(\Gamma)$  and  $\text{Cyc}(\Gamma)$  are orthogonal, as claimed in Lemma 12.

### 1.3.4 Graph Polynomials

**Definition 37.** Let  $\Gamma$  be a Feynman graph (Definition 24) with incidence matrix  $I_\Gamma$  (Definition 31), and  $Y_\Gamma$  as in Eq.(1.45). The *labelled Laplace matrix*

$$M_\Gamma := I_\Gamma^T Y_\Gamma I_\Gamma$$

is a  $|V_\Gamma| \times |V_\Gamma|$ -matrix with entries

$$(M_\Gamma)_{i,j} := - \sum_e a_e, \text{ where } e \text{ joins } v_i \text{ with } v_j \text{ and } i \neq j,$$

$$(M_\Gamma)_{i,i} := \sum_e a_e, \text{ where } e \text{ is incident to } v_i.$$

If we use the matrix  $Y_\Gamma^{-1}$  instead of  $Y_\Gamma$ , we obtain a Laplace matrix where all variables are dual,  $a_e \leftrightarrow \frac{1}{a_e}$ , it is hence called *dual* labelled Laplace matrix.

**Theorem 13** (Labelled Kirchhoff's theorem). Let  $\Gamma$  be a connected graph. Let  $M_\Gamma$  be the labelled Laplace matrix (Definition 37) and  $M_\Gamma(i, j)$  the same matrix with row  $i$  and column  $j$  deleted. Then, regardless of which  $(i, j)$  are chosen,

$$(-1)^{i+j} \det M_\Gamma(i, j) =: \tilde{\psi}_\Gamma(\{a_e\})$$

is the same polynomial in the edge variables  $\{a_e\}$ , called *Kirchhoff polynomial*. Every monomial in  $\tilde{\psi}_\Gamma$  corresponds to a spanning tree (Definition 35) of  $\Gamma$ ,

$$\tilde{\psi}_\Gamma(\{a_e\}) = \sum_{T \in T_\Gamma^{(1)}} \prod_{e \in T} a_e.$$

**Definition 38.** Let  $\Gamma$  be a connected Feynman graph with amputated external edges. The *first Symanzik polynomial*  $\psi_\Gamma$  is defined to be the dual Kirchhoff polynomial (Theorem 13). It, too, is given by a sum over spanning trees  $T_\Gamma^{(1)}$  (Definition 35):

$$\psi_\Gamma(\{a_e\}) := \tilde{\psi}_\Gamma\left(\left\{\frac{1}{a_e}\right\}\right) \cdot \prod_{e \in E_\Gamma} a_e = \sum_{T \in T_\Gamma^{(1)}} \prod_{e \notin T} a_e.$$

Intuitively, the polynomial is identical no matter which row and column  $(i, j)$  are deleted because each edge ends in two vertices. Therefore, knowing all but one vertices allows to reconstruct the missing information. If, however, a larger subset of the rows and columns is deleted, one obtains a different polynomial. These are the *Dodgson polynomials*, they are useful for a study of subgraphs of Feynman graphs and for gauge theories [168–170]. The fact that a determinant can be expanded in determinants of submatrices translates to *Dodgson identities* for sums and products of Dodgson polynomials.

### Example 17: Dunce's cap, first Symanzik polynomial.

For the dunce's cap (Example 12) one finds the labelled Laplace matrix (Definition 37)

$$M_\Gamma = \begin{pmatrix} a_1 + a_2 & -a_1 & -a_2 \\ -a_1 & a_1 + a_3 + a_4 & -a_3 - a_4 \\ -a_2 & -a_3 - a_4 & a_2 + a_3 + a_4 \end{pmatrix}.$$

The Kirchhoff polynomial is

$$\begin{aligned}\tilde{\psi}_\Gamma &= \det M_\Gamma(1, 1) = (a_1 + a_3 + a_4)(a_2 + a_3 + a_4) - (a_3 + a_4)(a_3 + a_4) \\ &= a_1 a_2 + a_1 a_3 + a_1 a_4 + a_2 a_3 + a_2 a_4.\end{aligned}$$

The monomials exactly correspond to the spanning trees stated in Example 15. Conversely, the first Symanzik polynomial (Definition 38) is

$$\psi_\Gamma = a_3 a_4 + a_2 a_4 + a_2 a_3 + a_1 a_4 + a_1 a_3.$$

In quantum field theory, a 4-momentum  $\underline{k}_e$  is associated to each edge of a Feynman graph (Definition 24). Take a spanning 2-forest  $F = \{T_1, T_2\} \in T_\Gamma^{(2)}$  (Definition 35). It divides the graph  $\Gamma$  into exactly two connected components. We consider the edges of  $\Gamma$  which lead from one component to the other,

$$C_F := \{e \in E_\Gamma | e = \{v_1, v_2\}, v_1 \in T_i, v_2 \in T_{j \neq i}\}.$$

Note that in general  $C_F \neq \Gamma \setminus \{T_1 \cup T_2\}$ . Now let

$$Q(F) := \sum_{e \in C_F} \bar{k}_e, \quad (1.46)$$

where  $\bar{k}_e = \underline{k}_e$  if the edge  $e$  is directed from  $T_1$  to  $T_2$ , and  $\bar{k}_e = -\underline{k}_e$  if  $e$  is directed from  $T_2$  to  $T_1$ . Hence,  $Q(F)$  is the total momentum flowing from the first component  $T_1$  of the spanning forest  $F$  into the second component  $T_2$ . Due to momentum conservation in Feynman graphs,  $Q(F)$  is at the same time the total external momentum entering  $T_1$ , or leaving  $T_2$ .

**Definition 39.** Let  $\Gamma$  be a connected amputated Feynman graph (Definition 24). Let  $Q(F)$  be defined as in Eq. (1.46). The *second Symanzik polynomial* is given by

$$\phi_\Gamma := \sum_{F \in T_\Gamma^{(2)}} Q(F)^2 \prod_{e \notin F} a_e - \psi_\Gamma \sum_{e \in E_\Gamma} m_e^2 a_e.$$

We remark that the signs in Definition 39 might change if one works in Euclidean instead of Minkowski spacetime (Definition 1), depending on conventions. For more details, compare [171, 172].

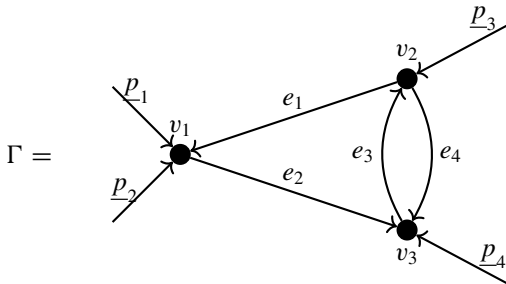
**Lemma 14.**

1. The first Symanzik polynomial (Definition 38) is homogeneous of degree  $|L_\Gamma|$  (Definition 29) in the variables  $\{a_e\}$ , and no  $a_e$  appears with higher than first power.
2. The second Symanzik polynomial (Definition 39) is homogeneous of degree  $|L_\Gamma| + 1$  in  $\{a_e\}$ .
3. The second Symanzik polynomial is homogeneous of degree two in masses and momenta.

**Proof** By Eq. (1.44), a spanning tree contains exactly  $|V_\Gamma| - 1$  edges. Using Theorem 7, the number of edges not in the spanning tree is  $|E_\Gamma| - |V_\Gamma| + 1 = |L_\Gamma|$ , the number of edges not in a spanning 2-forest is  $|L_\Gamma| + 1$ . The remaining points follow from the definitions.  $\square$

**Example 18: Dunce's cap, second Symanzik polynomial.**

We define the external momenta of the dunce's cap as follows:

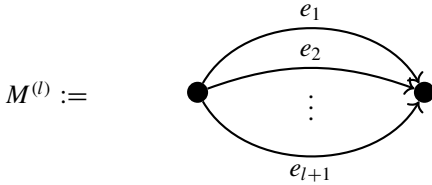


The total external momentum is zero,  $p_1 + p_2 + p_3 + p_4 = \underline{0}$ , this allows to express any sum of three momenta by the fourth one. The spanning 2-forests of the dunce's cap are listed in Example 15, the first Symanzik polynomial has been computed in Example 17. The second Symanzik polynomial (Definition 39) is

$$\begin{aligned} \phi_\Gamma = & \underline{p}_4^2 a_2 a_3 a_4 + \underline{p}_3^2 a_1 a_3 a_4 + (\underline{p}_1 + \underline{p}_2)^2 a_1 a_2 a_4 + (\underline{p}_1 + \underline{p}_2)^2 a_1 a_2 a_3 \\ & - (a_3 a_4 + a_2 a_4 + a_2 a_3 + a_1 a_4 + a_1 a_3) \left( m_1^2 a_1 + m_2^2 a_2 + m_3^2 a_3 + m_4^2 a_4 \right). \end{aligned}$$

### Example 19: Multiedges, Symanzik polynomials.

The amputated  $l$ -loop multiedge graph consists of  $l + 1$  parallel edges.



Each edge is a spanning tree and there is exactly one spanning 2-forest, hence  $M^{(l)}$  has the following Symanzik polynomials (Definitions 38 and 39):

$$\psi_{M^{(l)}} = \sum_{e=1}^{l+1} \frac{1}{a_e} \prod_{n=1}^{l+1} a_n, \quad \phi_{M^{(l)}} = +\underline{p}^2 \prod_{e=1}^{l+1} a_e - \psi_{M^{(l)}} \sum_{e=1}^{l+1} m_e^2 a_e.$$

Especially

$$\psi_{M^{(1)}} = a_1 + a_2, \quad \phi_{M^{(1)}} = \underline{p}^2 a_1 a_2 - (a_1 + a_2)(m_1^2 a_1 + m_2^2 a_2).$$

### 1.3.5 Feynman Rules in Position Space

**Definition 40.** We will use the term *Feynman rules* with two closely related, but not quite identical, meanings:

1. The *Feynman rules of a theory* are a set of vertices, edges, and rules how to connect them to build Feynman graphs of that theory.
2. The *Feynman rules*  $\mathcal{F}$  in a closer sense are a map that takes a Feynman graph and returns the contribution of this graph to a scattering amplitude, which is given by the Feynman integral.

We have already established the first point in Sect. 1.3.1. The second point, how exactly to construct the Feynman integral  $\mathcal{F}(\Gamma)$  from a given graph  $\Gamma$ , follows from Theorems 6 and 2. In the spirit of Sects. 1.2.2 and 1.2.8, we take the resulting algorithm as a definition, rather than a theorem, in order to avoid a technical discussion about the precise relation between quantum fields and Feynman amplitudes.

**Example 20:  $\phi^3$  theory, Feynman rules in position space.**

Consider  $\phi^3$  theory with the Lagrangian from Example 3, and  $m = 0$ . By Sect. 1.3.1, it gives rise to Feynman graphs which contain (a single type of) edges, and 3-valent vertices. The Feynman rules of these graphical building blocks are

$$\mathcal{F}[\text{---}] = \frac{\Gamma(\frac{D}{2})}{4\pi^{\frac{D}{2}}} \frac{1}{(\underline{x}^2)^{\frac{D}{2}-1}}, \quad \mathcal{F}[\text{---} \bullet \text{---}] = -i\lambda_3.$$

The Feynman rules of a graph without internal vertices are just the product of the Feynman rules of its building blocks. If the graph  $\Gamma$  contains internal vertices, then  $\mathcal{F}[\Gamma]$  is an integral.

**Definition 41.** Let  $\Gamma = (V_{\Gamma,\text{int}}, V_{\Gamma,\text{ext}}, E_\Gamma)$  be a Feynman graph (Definition 24). The corresponding *Feynman integral in position space*  $\mathcal{F}[\Gamma]$  is obtained by the following steps:

1. Identify each internal vertex  $v_i$  with a spacetime point  $\underline{x}_i$ .
2. Identify each external vertex with a spacetime point  $\underline{y}_i$  of an external particle.
3. For each internal scalar edge  $e = \{\underline{x}_1, \underline{x}_2\}$ , write one Feynman propagator (Eqs. (1.27) and (1.28))  $(G_F(\underline{x}_2 - \underline{x}_1, m))^{\nu_e}$ , where  $m_e$  is the mass of the particle and  $\nu_e$  the propagator power,  $\nu_e = 1$  unless otherwise mentioned. Use other propagators for other types of field where appropriate.
4. Write one integral  $\int d^D \underline{x}_i$  for each of the internal spacetime points  $\underline{x}_i$ .
5. For each internal  $n$ -valent vertex, multiply the expression by the appropriate vertex Feynman rule, for a scalar vertex this is a factor  $-i\lambda_n$ .

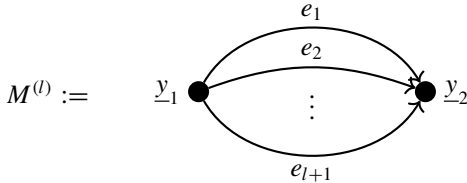
The Feynman integral  $\mathcal{F}[\Gamma]$  resulting from Definition 41 is a  $nD$ -fold integral, where  $D$  is the dimension of spacetime and  $n$  the number of internal vertices. The integral is a function of the positions  $\underline{y}_i$  of external particles, and of the mass(es) of particles. Conceptually, it has the following form:

$$\mathcal{F}[\Gamma] \left( \{\underline{y}_i\}, \{m_i\} \right) = \prod_{v \in V_\Gamma} (-i\lambda_{|v|}) \cdot \int \cdots \int d^D \underline{x}_1 \cdots d^D \underline{x}_n \prod_{e \in E_\Gamma} (G_F(\underline{x}_{e_1}, \underline{x}_{e_2}, m_e))^{\nu_e}. \quad (1.47)$$

Here, the points  $\{\underline{x}_{e_1}, \underline{x}_{e_2}\}$  of the edges can be either internal points  $\underline{x}_i$  or external points  $\underline{y}_i$  of the underlying Feynman graph.

### Example 21: Multiedges, Feynman integral in position space.

The amputated 1-loop multiedge (Example 19) involves two external vertices  $\underline{y}_1, \underline{y}_2$  and no internal vertices,



By Lorentz invariance, the function  $\mathcal{F}[M^{(l)}]$  can not depend on the two individual positions, but only on the magnitude of the difference  $\underline{y} := \underline{y}_2 - \underline{y}_1$ . We assume that all masses are equal and all propagator powers are  $\nu_e = 1$ . If there is one external edge at each vertex, the vertices have valence  $(l + 2)$  and come with a coupling constant  $\lambda_{l+2}$ . As the graph has no internal vertices, the Feynman rules in position space (Definition 41) do not involve any integration and the contribution of such a graph to a scattering amplitude is the  $(l + 1)$ -th power of the massive Feynman propagator (Eq. (1.24)),

$$\mathcal{F}[M^{(l)}](\underline{y}^2) = (-i\lambda_{l+2})^2 \prod_{e=1}^{l+1} G_F(\underline{y}, m) = -\lambda_{l+2}^2 (G_F(\underline{y}))^{l+1}.$$

### 1.3.6 Feynman Rules in Momentum Space

To compute scattering processes with the LSZ formula (Theorem 5), it is often convenient to know Green functions in momentum space instead of position space. The series expansion of Green functions in terms of Feynman graphs in momentum space is exactly the same as in position space, Eq. (1.40). In computing the Fourier transform of the individual summands (Eq. (1.47)), one finds that the Feynman integral itself can be formulated directly in momentum space, as we show in the following.

Consider a non-amputated Feynman graph with  $|V_{\Gamma, \text{ext}}|$  external vertices and  $|V_{\Gamma, \text{int}}|$  internal vertices and  $|E_\Gamma|$  edges. Its position space Feynman integral involves  $|V_{\Gamma, \text{int}}|$  integrals  $\int d^D \underline{x}$  over the internal vertices. Perform a Fourier transform of the  $|V_{\Gamma, \text{ext}}|$  external positions  $\underline{y}_j$ , this introduces  $|V_{\Gamma, \text{ext}}|$  integrals  $\int d^D \underline{y}_j e^{i \underline{p}_j \cdot \underline{y}_j}$ . Now replace each Feynman propagator  $G_F(\underline{z})$  with the Fourier transform  $G_F(\underline{k}_e)$  (Eq. (1.24)). This introduces  $|E_\Gamma|$  integrals  $\int d^D \underline{q}_j e^{-i \underline{k}_e \cdot \underline{z}_e}$ . The Feynman integral Eq. (1.47) now takes the form

$$\mathcal{F}[\Gamma] \left( \underline{p}_1, \dots, \underline{p}_{|V_{\Gamma, \text{ext}}|} \right) = \prod_{v \in V_{\Gamma}} (-i \lambda_{|v|}) \cdot \int \cdots \int d^D \underline{x}_1 \cdots d^D \underline{x}_{|V_{\Gamma, \text{int}}|} d^D \underline{y}_1 \cdots d^D \underline{y}_{|V_{\Gamma, \text{ext}}|}$$

$$\left( \prod_{e \in E_{\Gamma}} \int \frac{d^D k_e}{(2\pi)^D} \right) \left( \prod_{j \in V_{\Gamma, \text{ext}}} e^{i \underline{p}_j \cdot \underline{y}_j} \right) \left( \prod_{e \in E_{\Gamma}} e^{-i k_e \cdot z_e} \right) \prod_{e \in E_{\Gamma}} (G_F(\underline{k}_e))^{\nu_e}.$$

Here,  $z_e = \underline{x}_{v_j} - \underline{x}_{v_i}$  is the difference between two vertex positions which are joined by an edge  $e = \{v_i, v_j\}$ . Algebraically, this difference is given by the incidence matrix (Definition 31),  $z_e = (I \vec{x})_e$ , where  $\vec{x} = (\underline{x}_1, \dots, \underline{x}_{|V_{\Gamma}|})$  are the vertex positions. We similarly introduce a vector of edge momenta  $\vec{k} := (k_1, \dots, k_{|E_{\Gamma}|})$ . The exponent in the product  $\prod_e e^{i k_e (I \vec{x})_e}$  is then equivalent to the dot product  $i \vec{k} \cdot (I \vec{x}) = i (I^T \vec{k}) \cdot \vec{x}$ .

Only  $|V_{\Gamma, \text{ext}}| \leq |V_{\Gamma}|$  of the vertices have a non-vanishing external momentum, but to unify the notation, we set  $\underline{p}_v := \underline{0}$  for all remaining vertices, and assemble all external momenta to a vector  $\vec{p} = (\underline{p}_1, \dots, \underline{p}_{|V_{\Gamma}|})$ . Then, the integrals  $d\underline{x}_j$  and  $d\underline{y}_j$  together mean that we integrate over *all* vertices of the graph, and the factors  $e^{i \underline{p}_j \cdot \underline{y}_j}$  and  $e^{-i k_e z_e}$  can be combined to a product

$$\mathcal{F}[\Gamma](\vec{p}) = \prod_{v \in V_{\Gamma}} (-i \lambda_{|v|}) \left( \prod_{v \in V_{\Gamma}} \int d^D \underline{x}_v \right) \left( \prod_{e \in E_{\Gamma}} \int \frac{d^D k_e}{(2\pi)^D} \right) e^{i (\vec{p} - I^T \vec{k}) \cdot \vec{x}} \prod_{e \in E_{\Gamma}} (G_F(\underline{k}_e))^{\nu_e}. \quad (1.48)$$

The integrals over vertex positions can be done analytically, and they turn the exponential into a product of delta functions,

$$\mathcal{F}[\Gamma](\vec{p}) = \prod_{v \in V_{\Gamma}} (-i \lambda_{|v|}) \cdot \left( \prod_{e \in E_{\Gamma}} \int \frac{d^D k_e}{(2\pi)^D} \right) \prod_{v \in V_{\Gamma}} \delta \left( \underline{p}_v - (I^T \vec{k})_v \right) \prod_{e \in E_{\Gamma}} (G_F(\underline{k}_e))^{\nu_e}. \quad (1.49)$$

There is one delta function for each vertex, they enforce momentum conservation. For the external vertices, this merely says that the momentum in the external edge is equal to the external momentum entering at the external vertex. Hence, at this point it is convenient to make the transition to an amputated graph, and simply leave out those trivial ‘‘external’’ delta functions. One of the remaining delta functions can be rewritten to express overall momentum conservation between all external momenta, by convention, this delta function is not written explicitly.

The remaining delta functions allow to eliminate  $|V_{\Gamma, \text{int}}| - 1$  of the integrations  $\int d^D \underline{k}_e$  over edge momenta. Only those momenta remain undetermined which are in the kernel of the incidence matrix. As remarked below Definition 31, the kernel of  $I$  is the cycle space (Definition 29), and a basis for this vector space is a choice of linearly independent loops  $L_{\Gamma}$  of the graph. Consequently, the remaining non-trivial integrals in Eq. (1.49) are those over loop momenta,

$$\mathcal{F}[\Gamma](\vec{p}) = \prod_{v \in V_\Gamma} (-i \lambda_{|v|}) \cdot \left( \prod_{l \in L_\Gamma} \int \frac{d^D k_l}{(2\pi)^D} \right) \prod_{e \in E_\Gamma} (G_F(\underline{k}_e))^{\nu_e}. \quad (1.50)$$

In Eq.(1.50), the internal momenta  $\{\underline{k}_e\}$  and  $\{\underline{k}_l\}$  and the external momenta  $\{\underline{p}_v\}$  are implicitly related via momentum conservation at each vertex. The freedom to choose an arbitrary linearly independent set of cycles as the loops in Definition 29 corresponds to the freedom of choosing a set of internal momenta as integration variables.

**Definition 42.** Let  $\Gamma$  be a Feynman graph and  $\{\underline{p}_i\}$  a set of external momenta, pointing towards the graph. The Feynman integral in momentum space is obtained by the following procedure, called *Feynman rules in momentum space*:

1. Assign to each internal edge  $e$  a  $D$ -momentum  $\underline{k}_e$ .
2. For all momenta  $\{\underline{k}_i\}$  flowing into a vertex, including potentially external momentum  $\underline{p}_v$ , enforce momentum conservation  $\underline{0} = \sum_i \underline{k}_i$ . This will reduce the total number of independent internal momenta  $k_i$  to  $|L_\Gamma|$ .
3. For each internal edge  $e$ , write a corresponding momentum-space Feynman propagator (for scalar fields Eq. (1.25)) with mass  $m_e$ , propagator power  $\nu_e$  and momentum  $k_e$  corresponding to that edge.
4. Integrate over the  $|L_\Gamma|$  independent internal momenta,  $\int \cdots \int \frac{d^D k_1}{(2\pi)^D} \cdots \frac{d^D k_{|L_\Gamma|}}{(2\pi)^D}$ .
5. For each internal  $n$ -valent scalar vertex, multiply the integral by one factor  $-i \lambda_n$ . For other vertices, use the appropriate vertex Feynman rule.

### Example 22: $\phi^3$ theory, Feynman rules in momentum space.

In momentum space, the Feynman rules of  $\phi^3$  theory (Example 3) are

$$\mathcal{F}\left[\begin{array}{c} \text{---} \\ \text{---} \end{array}\right] = \frac{i}{p^2 - m^2}, \quad \mathcal{F}\left[\begin{array}{c} \text{---} \\ \text{---} \\ \bullet \end{array}\right] = -i \lambda_3.$$

The Feynman rules of a treelevel graph (Definition 34) are the product of the Feynman rules of its components.

In general,  $|V_\Gamma| \neq |L_\Gamma|$ . This means that the number of  $D$ -dimensional integrations in position space (Definition 41) is different from the number in momentum space (Definition 42). Compare Sect. 5.2.3 for a particularly striking example. The *treelevel* (Definition 34) Feynman graphs are the solution of the corresponding classical field theory; in momentum space, they do not involve any integrals at all. Loops represent quantum corrections.

### Example 23: Quantum electrodynamics.

Quantum electrodynamics (QED) is the quantized version of classical electrodynamics (Example 7). It is defined by the Lagrangian

$$\mathcal{L} = \bar{\psi} (i\gamma^\mu (\partial_\mu - ieA_\mu) - m) \psi - \frac{1}{4} F_{\mu\nu} F^{\mu\nu}.$$

The two involved fields correspond to two different types of particles. The particles represented by the field  $A^\mu$  are massless *photons*, they carry spin 1 (that is,  $A^\mu$  behaves like an ordinary vector under Lorentz transformations). In Feynman graphs, they are represented by a wavy line . Since  $A^\mu$  carries one Lorentz index, the Feynman propagator is a tensor with two indices, representing the two fields in  $\langle A^\mu(0) A^\nu(x) \rangle$ . The precise Feynman rule for the propagator depends on the chosen gauge (see Example 128), typically parametrized by a constant  $\xi \in \mathbb{R}$ :

$$\mathcal{F}\left[\text{---}\right] = \frac{i}{\underline{p}^2} \left( \eta^{\mu\nu} + \xi \frac{\underline{p}_\nu \underline{p}_\mu}{\underline{p}^2} \right).$$

The fermion  $\psi$  has spin  $\frac{1}{2}$  and is represented by an arrow in Feynman graphs. Its propagator is a tensor in spinor space, but a scalar with respect to Lorentz indices,

$$\mathcal{F}\left[\rightarrow\right] = \frac{i}{\gamma^\mu \underline{p}_\mu - m} = \frac{i}{\underline{p}^2 - m^2} \left( \gamma^\mu \underline{p}_\mu + m \right).$$

Observe that this propagator scales as  $|\underline{p}|^{-1}$ , and not  $|\underline{p}|^{-2}$ .

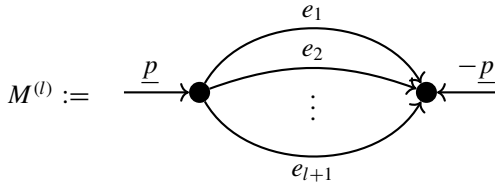
QED contains only a single type of interaction, given by the term  $ieA_\mu \bar{\psi} \psi$  in the Lagrangian. In Feynman graphs, it is represented as a 3-valent vertex with Feynman rule

$$\mathcal{F}\left[\text{---}\times\right] = ie\gamma^\mu.$$

The index of  $\gamma^\mu$  amounts to the Lorentz index of the incoming photon line.

### Example 24: Multiedges, Feynman integral in momentum space.

Consider the  $l$ -loop multiedge graph from Example 21. In momentum space, assign an external momentum  $\underline{p}$  to the external vertices:



By Lorentz invariance  $\mathcal{F}[M^{(l)}]$  is a function of the scale  $s := \underline{p}^2$  of the external momentum. The Feynman integral in momentum space reads

$$-\lambda_{l+2}^2 \left( \prod_{e=1}^l \int \frac{d^D k_e}{(2\pi)^D} \right) \frac{i^{l+1}}{\left( k_1^2 - m_1^2 \right)^{\nu_1} \cdots \left( k_l^2 - m_l^2 \right)^{\nu_l} \left( \left( \underline{p} - \cdots - \underline{k}_l \right)^2 - m_{l+1}^2 \right)^{\nu_{l+1}}}.$$

This is an  $(l \cdot D)$ -fold integral, while  $\mathcal{F}(M^{(l)})(\underline{y})$  in position space (Example 21) is merely a product. Instead of solving the momentum-space integral, the result can conveniently be found by Fourier-transforming the position-space expression [173].

### 1.3.7 Feynman Rules in Parametric Space

Integration in parametric space is described in [174]. We will only review the construction of the scalar momentum space version of parametric Feynman rules, loosely following the exposition in [172]. Note that some signs in the formulas will change if one uses Euclidean spacetime. An analogous construction can be done based on position space Feynman rules (Definition 41). For them, one uses the Gaussian integral Eq. (1.3) to obtain  $G_F(\underline{z})$  as a parametric integral [175, Eq. (1.10)] analogous to Eq. (1.51). Moreover, a generalization to gauge theories is possible using the *corolla polynomial* [176–178].

The goal of parametric space is to eliminate all integrals over  $D$ -vectors and instead rewrite the Feynman rules as integrals over one scalar *Schwinger parameter* for each edge. The first step is the integral representation of the Gamma function, Definition 5. With a change of integration variable, one obtains

$$(G_F(\underline{p}))^\nu = \frac{i}{(\underline{p}^2 - m^2)^\nu} = \frac{i}{\Gamma(\nu)} \int_0^\infty da \, a^{\nu-1} e^{-a(\underline{p}^2 - m^2)}. \quad (1.51)$$

This identity is sometimes called *Schwinger trick*, the variable  $a$  is the *Schwinger parameter*. Next, we insert the Schwinger trick (Eq. (1.51)) into the Feynman integral in momentum space (Eq. (1.48)), where the delta functions are written as exponential functions:

$$\begin{aligned} \mathcal{F}[\Gamma](\vec{p}) &= i^{|E_\Gamma|} \prod_{v \in V_\Gamma} (-i\lambda_{|v|}) \left( \prod_{v \in V_\Gamma \setminus v_0} \int d^D \underline{x}_v \right) \left( \prod_{e \in E_\Gamma} \int \frac{d^D \underline{k}_e}{(2\pi)^D} \right) \\ &\quad \left( \prod_{e \in E_\Gamma} \int_0^\infty \frac{da_e a_e^{\nu_e - 1}}{\Gamma(\nu_e)} \right) \exp \left( - \sum_{e \in E_\Gamma} a_e (\underline{k}_e^2 - m_e^2) + i \sum_{v \in V_\Gamma \setminus v_0} (\underline{p}_v - (I_\Gamma^T \vec{k})_v) \underline{x}_v \right). \end{aligned} \quad (1.52)$$

The integration over  $v_0$  has been consumed to produce an implicit overall delta function as described in Sect. 1.3.6. Consequently,  $I_\Gamma$  is the incidence matrix (Definition 31) with the first vertex removed. We introduce the diagonal matrix  $Y := \text{diag}(\vec{a})$ , such that  $\sum_e \underline{k}_e^2 a_e = \vec{k} Y \vec{k}$ . The exponent in Eq. (1.52) now is

$$-\vec{k}^T Y \vec{k} + \vec{m}^T Y \vec{m} + i \vec{p}^T \vec{x} - i \vec{k}^T I_\Gamma \vec{x} =: X. \quad (1.53)$$

We want to solve the  $d^D \underline{k}_e$  integrals analytically. In order to employ the standard formula (Eq. (1.4)) for Gaussian integrals, we need to find a matrix  $B$  such that the exponent has the form

$$X = -(\vec{k} + B)^T Y (\vec{k} + B) + R = -\vec{k}^T Y \vec{k} - B^T Y \vec{k} - \vec{k}^T Y B - B^T Y B + R. \quad (1.54)$$

Comparing coefficients with Eq. (1.53), we find  $i \vec{k}^T I_\Gamma \vec{x} = B^T Y \vec{k} + \vec{k}^T Y B$ . Consequently,

$$\frac{i}{2} Y^{-1} I_\Gamma \vec{x} = B, \quad \Rightarrow B^T Y B = -\frac{1}{4} \vec{x}^T I_\Gamma^T Y^{-1} I_\Gamma \vec{x} = -\frac{1}{4} \vec{x}^T M_\Gamma \vec{x},$$

where  $M_\Gamma = I_\Gamma^T Y^{-1} I_\Gamma$  is the dual labelled Laplace matrix (Definition 37). Like the incidence matrix  $I_\Gamma$ , also  $M_\Gamma$  is missing the row and column corresponding to  $v_0$ , it is the *reduced* dual labelled Laplace matrix. The remainder  $R$  in Eq. (1.54) can again be written as a square,

$$R = -\frac{1}{4} \vec{x}^T M_\Gamma \vec{x} + i \vec{p}^T \vec{x} + \vec{m}^T Y \vec{m} =: -\frac{1}{4} (\vec{x} + B_2)^T M_\Gamma (\vec{x} + B_2) + R_2,$$

where the new remainder  $R_2$  is independent of both  $\underline{k}_e$  and  $\underline{x}_v$ ,

$$B_2 = -2i M_\Gamma^{-1} \vec{p}, \quad \Rightarrow R_2 = \vec{m}^T Y \vec{m} - \vec{p}^T M_\Gamma^{-1} \vec{p}.$$

We now have rewritten the exponent Eq. (1.54) as the sum of two quadratic functions, one in  $\vec{k}$  and one in  $\vec{x}$ . The shifts  $B$  and  $B_2$  can be absorbed by a change of variable  $\vec{u} := \vec{k} + B$  and  $\vec{w} := \vec{x} + B_2$ , such that Eq. (1.52) takes the form

$$\begin{aligned} \mathcal{F}[\Gamma](\vec{p}) = i^{|E_\Gamma|} \prod_{v \in V_\Gamma} (-i \lambda_{|v|}) \left( \prod_{e \in E_\Gamma} \int_0^\infty \frac{da_e a_e^{\nu_e - 1}}{\Gamma(\nu_e)} \right) e^{\vec{m}^T Y \vec{m} - \vec{p}^T M_\Gamma^{-1} \vec{p}} \\ \left( \prod_{v \in V_\Gamma \setminus v_0} \int d^D \underline{w}_v \right) e^{-\frac{1}{4} \vec{w}^T M_\Gamma \vec{w}} \left( \prod_{e \in E_\Gamma} \int \frac{d^D \underline{u}_e}{(2\pi)^D} \right) e^{-\vec{u}^T Y \vec{u}}. \quad (1.55) \end{aligned}$$

The integrals in the second row can be evaluated with Eq. (1.4), keeping in mind that we have  $(|V_\Gamma| - 1)D$  vertex integrals and  $|E_\Gamma| D$  edge integrals, i.e.,  $D$  integrals for each row of the matrices  $M_\Gamma$  or  $Y$ :

$$\begin{aligned} \left( \prod_{v \in V_\Gamma \setminus v_0} \int d^D \underline{w}_v \right) e^{-\frac{1}{4} \vec{w}^T M_\Gamma \vec{w}} &= (2\pi)^{\frac{(|V_\Gamma|-1)D}{2}} \frac{1}{(\det \frac{M_\Gamma}{2})^{\frac{D}{2}}} = (4\pi)^{\frac{(|V_\Gamma|-1)D}{2}} \frac{1}{(\det M_\Gamma)^{\frac{D}{2}}}, \\ \left( \prod_{e \in E_\Gamma} \int \frac{d^D \underline{u}_e}{(2\pi)^D} \right) e^{-\vec{u}^T Y \vec{u}} &= (2\pi)^{-\frac{|E_\Gamma|D}{2}} \frac{1}{(\det(2Y))^{\frac{D}{2}}} = \frac{1}{(4\pi)^{\frac{|E_\Gamma|D}{2}}} \frac{1}{(\det Y)^{\frac{D}{2}}}. \end{aligned}$$

The matrix  $Y$  is diagonal, its determinant is simply  $\det Y = \prod_{e \in E_\Gamma} a_e$ . The determinant of the reduced Laplace matrix is, by Theorem 13 and Definition 38, the first Symanzik polynomial up to just this factor:  $\det Y \cdot \det M_\Gamma = \psi_\Gamma$ . With this, Eq. (1.55) takes the form

$$\begin{aligned} \mathcal{F}[\Gamma](\vec{p}) = i^{|E_\Gamma|} \prod_{v \in V_\Gamma} (-i \lambda_{|v|}) \left( \prod_{e \in E_\Gamma} \int_0^\infty \frac{da_e a_e^{\nu_e - 1}}{\Gamma(\nu_e)} \right) e^{\vec{m}^T Y \vec{m} - \vec{p}^T M_\Gamma^{-1} \vec{p}} \\ (4\pi)^{\frac{(|V_\Gamma|-|E_\Gamma|-1)D}{2}} \frac{1}{(\psi_\Gamma)^{\frac{D}{2}}}. \quad (1.56) \end{aligned}$$

In Eq. (1.56), the remaining exponential function involves the inverse Laplace matrix  $M_\Gamma^{-1}$ . As with every inverse matrix, this is a rational function, where the denominator is the determinant  $\det M_\Gamma$ . The latter is almost the first Symanzik polynomial. The numerator of the rational function is given by determinants of submatrices of  $M_\Gamma$ , these quantities are Dodgson polynomials, mentioned below Definition 38:

$$(M_\Gamma^{-1})_{i,j} = \frac{(-1)^{i+j} \det M_\Gamma(i, j)}{\det M_\Gamma}.$$

By a generalization of the labelled matrix tree theorem (Theorem 13), one finds that these particular Dodgson polynomials  $\det M_\Gamma(i, j)$  are sums over all spanning 2-forests. In fact, the two summands in the exponent in Eq. (1.56) precisely combine to give the second Symanzik polynomial (Definition 39):

$$\vec{m}^T Y \vec{m} - \vec{p}^T M_\Gamma^{-1} \vec{p} = \frac{-\psi_\Gamma \vec{p}^T M_\Gamma^{-1} \vec{p} + \psi_\Gamma \sum_{e \in E_\Gamma} m_e^2 a_e}{\psi_\Gamma} = -\frac{\phi_\Gamma}{\psi_\Gamma}.$$

Using Theorem 7, we identify the loop order  $|V_\Gamma| - |E_\Gamma| - 1 = -|L_\Gamma|$ , Eq.(1.56) finally takes the form

$$\mathcal{F}[\Gamma](\vec{p}) = \frac{i^{|E_\Gamma|}}{(4\pi)^{|L_\Gamma| \frac{D}{2}}} \prod_{v \in V_\Gamma} (-i\lambda_{|v|}) \prod_{e \in E_\Gamma} \int_0^\infty \frac{da_e}{\Gamma(\nu_e)} \frac{a_e^{\nu_e-1} \exp\left(-\frac{\phi_\Gamma}{\psi_\Gamma}\right)}{\psi_\Gamma^{\frac{D}{2}}}. \quad (1.57)$$

It is possible to do one more integration analytically. To that end, we scale all Schwinger parameters  $a_e \rightarrow t \cdot a_e$  and use homogeneity (Lemma 14). The integration over  $t$  then is the integral representation of the Gamma function (Definition 5), where the argument is the superficial degree of convergence.

**Definition 43.** For an amputated Feynman graph  $\Gamma$  (Definition 24), the *superficial degree of convergence* is defined as

$$\omega_\Gamma := \sum_{e \in E_\Gamma} \nu_e - |L_\Gamma| \frac{D}{2}.$$

The remaining integral is over a projective space, that is, over the parameters  $a_e$  where the sum is fixed to be unity:

$$\mathcal{F}[\Gamma](\vec{p}) = \frac{i^{|E_\Gamma|} \prod_{v \in V_\Gamma} (-i\lambda_{|v|})}{(4\pi)^{|L_\Gamma| \frac{D}{2}}} \Gamma(\omega_\Gamma) \prod_{e \in E_\Gamma} \int_0^\infty \frac{da_e}{\Gamma(\nu_e)} a_e^{\nu_e-1} \delta\left(1 - \sum_{e=1}^{|E_\Gamma|} a_e\right) \frac{1}{\psi_\Gamma^{\frac{D}{2}}} \left(\frac{\psi_\Gamma}{\phi_\Gamma}\right)^{\omega_\Gamma}. \quad (1.58)$$

### Example 25: Massless 1-loop multiedge.

We know the graph polynomials of multiedge graphs from Example 19. For the massless 1-loop case, the resulting Feynman integral Eq.(1.57) is the integral representation of Euler's beta function (e.g., [179]). Let  $s := \underline{p}^2$  be the external momentum squared. Then

$$\begin{aligned} \mathcal{F}[M^{(1)}](s) &= \frac{(-i\lambda_3)^2 i^2}{(4\pi)^{\frac{D}{2}} \Gamma(\nu_1) \Gamma(\nu_2)} \int_0^\infty da_1 \int_0^\infty da_2 a_1^{\nu_1-1} a_2^{\nu_2-1} \frac{\exp\left(-\frac{a_1 a_2 s}{a_1 + a_2}\right)}{(a_1 + a_2)^{\frac{D}{2}}} \\ &= \frac{\lambda_3^2}{(4\pi)^{\frac{D}{2}}} \frac{\Gamma(\nu_1 + \nu_2 - \frac{D}{2})}{\Gamma(\nu_1) \Gamma(\nu_2)} \frac{1}{s^{\nu_1 + \nu_2 - \frac{D}{2}}} \frac{\Gamma(\frac{D}{2} - \nu_1) \Gamma(\frac{D}{2} - \nu_2)}{\Gamma(D - \nu_1 - \nu_2)}. \end{aligned}$$

This result is widely known. One of the earlier articles showing a derivation is [180]. The superficial degree of convergence (Definition 43) is  $\omega = \nu_1 - \nu_2 - \frac{D}{2}$ , the prefactor is  $\Gamma(\omega)$  as expected from Eq. (1.58). As a remark, integrals of multiedges for non-scalar fields, or with propagator powers in the numerator, can be found in [120, 122, 181–184].

### Example 26: Massless $l$ -loop multiedges.

We found in Example 25 that the Feynman integral of the massless 1-loop multiedge itself has the form of a massless propagator  $\frac{1}{(k^2)^{\nu_e}}$ , but with the propagator power  $\nu_e := \nu_1 + \nu_2 - \frac{D}{2}$ . This means that we can insert the amputated 1-loop multiedge into another 1-loop multiedge and obtain an expression for the 2-loop multiedge without any explicit integration. Keeping track of the various prefactors, the result is

$$\begin{aligned} \mathcal{F}[M^{(2)}](s) &= \frac{-\lambda_4^2 i^3}{(4\pi)^2 \frac{D}{2}} \frac{\Gamma(\nu_1 + \nu_2 + \nu_3 - 2\frac{D}{2})}{\Gamma(\nu_1)\Gamma(\nu_2)\Gamma(\nu_3)} \frac{1}{s^{\nu_1 + \nu_2 + \nu_3 - 2\frac{D}{2}}} \\ &\cdot \frac{\Gamma(\frac{D}{2} - \nu_1)\Gamma(\frac{D}{2} - \nu_2)\Gamma(\frac{D}{2} - \nu_3)}{\Gamma(3\frac{D}{2} - \nu_1 - \nu_2 - \nu_3)}. \end{aligned}$$

By induction, one confirms a formula for arbitrary loop number  $l$ . To this end, define  $\nu := \sum_e \nu_e$ . The superficial degree of convergence (Definition 43) is  $\omega = \nu - l\frac{D}{2}$ .

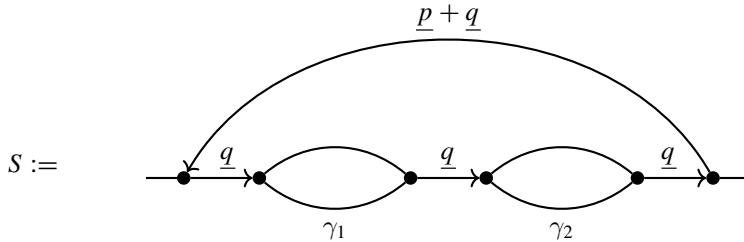
$$\mathcal{F}[M^{(l)}](s) = \frac{-\lambda_{l+2}^2 i^{l+1}}{(4\pi)^l \frac{D}{2}} \frac{\Gamma(\omega)}{\prod_e \Gamma(\nu_e)} \frac{1}{s^\omega} \frac{\prod_e \Gamma(\frac{D}{2} - \nu_e)}{\Gamma((l+1)\frac{D}{2} - \nu)}.$$

Again, the result includes the expected factor  $\Gamma(\omega)$ .

Unfortunately, the massless multiedges from Example 26, and the massless triangles where one external momentum vanishes, are essentially the only infinite class of 4-dimensional Feynman integrals that can be solved explicitly. As soon as a massive propagator is involved, the recursion becomes much more complicated, see [185, 186].

**Example 27: Second chain graph.**

We call the following graph in a massless  $\phi^3$  theory “second chain graph”  $S$ :



Assume that all propagator powers are  $\nu_e = 1$ . There are two subgraphs  $\gamma_1$  and  $\gamma_2$ . They are 1-loop multiedges and they carry the same momentum  $t := \underline{q}^2$ , hence, by Example 25,

$$\mathcal{F}[\gamma_1] = \mathcal{F}[\gamma_2] = \frac{\lambda_3^2}{(4\pi)^{\frac{D}{2}}} \frac{\Gamma(2 - \frac{D}{2})}{1} \frac{\Gamma(\frac{D}{2} - 1) \Gamma(\frac{D}{2} - 1)}{\Gamma(D - 2)} \frac{1}{t^{2 - \frac{D}{2}}}.$$

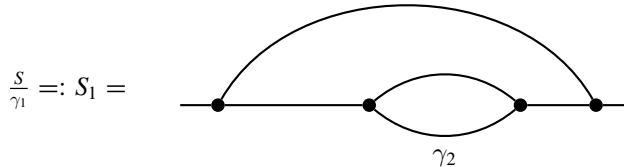
These two graphs are connected with three propagators  $\frac{i}{t}$  (Eq. (1.25)), each of which carries momentum  $t$ . The complete chain therefore has the value

$$\left( \frac{\lambda_3^2}{(4\pi)^{\frac{D}{2}}} \Gamma\left(2 - \frac{D}{2}\right) \frac{\Gamma(\frac{D}{2} - 1) \Gamma(\frac{D}{2} - 1)}{\Gamma(D - 2)} \right)^2 \frac{1}{t^{4-D}} \frac{i^3}{t^3}.$$

The value of this chain is again similar to a propagator, but with exponent  $7 - D$  and a prefactor. Hence, we can evaluate it once again with Example 25 and obtain (for  $s := \underline{p}^2$ )

$$\mathcal{F}[S] = \frac{-\lambda_3^6}{(4\pi)^{\frac{3}{2}D}} \frac{\Gamma^2(2 - \frac{D}{2}) \Gamma(8 - \frac{3}{2}D) \Gamma^5(\frac{D}{2} - 1) \Gamma(\frac{3}{2}D - 7)}{\Gamma^2(D - 2) \Gamma(7 - D) \Gamma(2D - 8)} \frac{1}{s^{8 - 3\frac{D}{2}}}.$$

Later, we will also need the graphs  $S_i$  where the subgraph  $\gamma_i$  is contracted (Definition 27),



Both  $S_1$  and  $S_2$  have the same value

$$\mathcal{F}[S_1] = \mathcal{F}[S_2] = \frac{i\lambda_3^4}{(4\pi)^D} \frac{\Gamma(2 - \frac{D}{2}) \Gamma(5 - D) \Gamma^3(\frac{D}{2} - 1) \Gamma(D - 4)}{\Gamma(D - 2) \Gamma(4 - \frac{D}{2}) \Gamma(\frac{3}{2}D - 5)} \frac{1}{s^{5-D}}.$$

Besides the three forms (Sects. 1.3.5–1.3.7) we discussed, there are several other ways to express Feynman integrals. We will not go into details because computational techniques for individual graphs are out of the scope of this thesis. The interested reader is referred to the literature. Examples include representations by the Lee–Pomeransky polynomial  $G_\Gamma := \psi_\Gamma + \phi_\Gamma$  [187], which can be understood as a special case of a GKZ hypergeometric function [124, 188–190], or the Baikov representation [191–193], or as solutions of differential or difference equations [121, 194–198]. For the various polynomials, it is also fruitful to consider their geometric realizations such as Newton polytopes, see e.g., [190, 199, 200].

### 1.3.8 Symmetry Factors

By Wick’s theorem (Theorem 2), the correlation functions  $\tilde{G}_F^{(n)}$  of the free field are given by “all contractions”. But, as soon as some of the arguments of  $\tilde{G}_F^{(n)}$  coincide, some of the contractions start to become identical.

#### Example 28: Contraction of the four-point function.

Consider the 4-point function from Example 9, but, for the time being, assume that  $\underline{x}_1 = \underline{x}_2$  and  $\underline{x}_3 = \underline{x}_4$ . Out of the three complete contractions, two now become identical:

$$\begin{aligned} \tilde{G}_F^{(4)}(\underline{x}_1, \underline{x}_2, \underline{x}_3, \underline{x}_4) &= \begin{array}{c} \text{---} \\ | \\ \bullet \quad \bullet \\ | \\ \text{---} \end{array} + \begin{array}{c} \bullet \quad \bullet \\ | \\ \bullet \quad \bullet \\ | \\ \text{---} \end{array} + \begin{array}{c} \bullet \quad \bullet \\ | \\ \bullet \quad \bullet \\ | \\ \times \end{array} \\ \Rightarrow \tilde{G}_F^{(4)}(\underline{x}_1, \underline{x}_1, \underline{x}_3, \underline{x}_3) &= \begin{array}{c} \text{---} \\ | \\ \bullet \\ | \\ \text{---} \end{array} + \begin{array}{c} \text{---} \\ | \\ \bullet \\ | \\ \text{---} \end{array} + \begin{array}{c} \bullet \quad \bullet \\ | \\ \bullet \quad \bullet \\ | \\ \text{---} \end{array} \end{aligned}$$

The fact that graphs can potentially become identical when vertices are merged gives rise to non-trivial combinatoric prefactors in the Dyson series (Eq. (1.40)). We will discuss the fundamental mechanism that leads to these *symmetry factors* by examining the two most basic examples.

Before going to the examples, we quickly recall why in many cases there is *no* non-trivial symmetry factor. Each  $k$ -valent vertex in a Feynman graph corresponds to an

interaction term  $\phi^k$ , which comes with a prefactor  $\frac{1}{k!}$  in the Lagrangian (Eq. (1.6)). Assume that in the Dyson series,  $k$  arguments of  $\tilde{G}_F^{(n)}$  are identified. That means, before identification, there were  $k$  distinct 1-valent vertices, which are now merged to a single  $k$ -valent vertex. The  $k$  adjacent edges had, in general,  $k!$  different permutations of which edge joins which of the original 1-valent vertices. Hence, there were  $k!$  different original graphs, which all become identical as soon as the vertices are merged. The resulting graph would have a prefactor  $k!$ , were it not for the factor  $\frac{1}{k!}$  in the Lagrangian which precisely cancels it. The resulting graph therefore has a prefactor of unity.

Similarly, the order  $n$  in the Dyson series is given by graphs with  $n$  internal vertices. In the Feynman integral, each internal vertex is integrated over the whole space. Therefore, all  $n$  vertices are interchangeable. All graphs which differ only by a labelling of the vertices are actually the same graph. For  $n$  vertices, this would give rise to a prefactor  $n!$ . But the Dyson series (Theorem 6) contains a prefactor  $\frac{1}{n!}$  for the order- $n$  term, arising from the exponential function. Once more, both prefactors cancel and the resulting graph appears with a prefactor of unity.

The mechanism outlined in the last two paragraphs works only as long as the initial edges or vertices were distinguishable. We will now see the two most basic cases where this is not the case, and why they give rise to non-trivial symmetry factors.

Firstly, examine a tadpole (Definition 30), such as in the first summand in Example 28: Each 2-valent vertex comes with a prefactor  $\frac{1}{2!}$ , but for each vertex there is only a single way to build the tadpole. The “other” way would be exchanging the two ends of the tadpole edge, which gives the same graph. Consequently, the first summand in  $\tilde{G}_F^{(4)}(\underline{x}_1, \underline{x}_1, \underline{x}_3, \underline{x}_3)$  has a prefactor  $\frac{1}{2} \cdot \frac{1}{2} = \frac{1}{4}$ . It is straightforward to see that, irrespective of the valence of the vertices, every tadpole produces a prefactor  $\frac{1}{2}$ .

Secondly, look at multiedges. The second and third summand in Example 28 are examples of 2-edge multiedges. Starting from  $\underline{x}_1$ , there are two ways of attaching an edge to  $x_3$ . They are symbolized by the two (identical) graphs in  $\tilde{G}_F^{(4)}(\underline{x}_1, \underline{x}_1, \underline{x}_3, \underline{x}_3)$ . But again, each of the two vertices has a factor  $\frac{1}{2}$ , and adding the two identical graphs, we obtain an overall factor  $\frac{1}{2} \cdot \frac{1}{2} + \frac{1}{2} \cdot \frac{1}{2} = \frac{1}{2}$ . In this case, not a tadpole, but a multiedge (Example 26) leads to the mismatch of prefactors: If there are  $n$  parallel edges, then there are  $n!$  ways of attaching them, but each of the two vertices comes with a prefactor  $\frac{1}{n!}$ . Therefore, a  $n$ -edge multiedge produces an overall symmetry factor  $n! \cdot \frac{1}{n!} \cdot \frac{1}{n!} = \frac{1}{n!}$ .

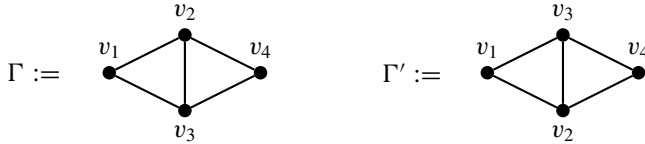
In general, one finds that such “overcompensation” of prefactors always occurs whenever a graph  $\Gamma$  has multiple subgraphs which can be interchanged without altering  $\Gamma$ . In the case of multiedges, these subgraphs were just the individual edges. Tadpoles are a limiting case, namely exchanging the order  $\{v_1, v_2\} \leftrightarrow \{v_2, v_1\}$  in an edge, which only ever leaves the graph unaltered if  $v_1 = v_2$ . For the exchange of more complicated subgraphs, it is helpful to introduce the notion of a *graph automorphism*.

**Definition 44.** An *isomorphism* between two undirected graphs  $\Gamma_1, \Gamma_2$ , where both edges and vertices are labelled, is a map  $f : E_{\Gamma_1} \rightarrow E_{\Gamma_2}, V_{\Gamma_1} \rightarrow V_{\Gamma_2}$  such that  $\{v_i, v_j\} = e \in E_{\Gamma_1}$  if and only if  $\{f(v_i), f(v_j)\} = f(e) \in E_{\Gamma_2}$ .

**Definition 45.** An *automorphism* of an amputated Feynman graph  $\Gamma$  (Definition 24) is an isomorphism  $f : \Gamma \rightarrow \Gamma$  (Definition 44). Additionally, we demand that an automorphism acts trivially on the external vertices  $V_{\Gamma, \text{ext}}$ , and that reversing the “direction” of a tadpole edge is considered an automorphism. The set of all automorphisms of a graph forms the *automorphism group*  $\text{Aut}(\Gamma)$ .

### Example 29: Automorphism group of a 2-loop graph.

Consider the following graph  $\Gamma$ , where  $v_1$  and  $v_4$  are external vertices:



The graph  $\Gamma'$  is an automorphism (Definition 45) of  $\Gamma$ : It is exactly the same drawing, but labels are exchanged, and every edge that was present in  $\Gamma$  is still present in  $\Gamma'$ . Since the external vertices  $v_1$  and  $v_4$  are fixed,  $\Gamma'$  is the only non-trivial automorphism of  $\Gamma$  and  $|\text{Aut}(\Gamma)| = 2$ . If we write the graphs as an abstract list of edges (instead of drawing them), then

$$\Gamma = \{\{v_1, v_2\}, \{v_2, v_4\}, \{v_2, v_3\}, \{v_1, v_3\}, \{v_3, v_4\}\} = \Gamma'.$$

The automorphism here is the exchange  $v_2 \leftrightarrow v_3$ , which leaves the list unchanged apart from the direction of the central edge,  $\{v_2, v_3\} \leftrightarrow \{v_3, v_2\}$ . But we are considering undirected graphs, so both edges are identical.

One can also consider  $\Gamma'$  as “a different way of drawing  $\Gamma$ ”. But this is not the point: There are infinitely many different ways of drawing the same graph on a plane. The automorphism is about exchanging labelled parts of the graph without changing the drawing.

**Theorem 15.** In the Dyson series (Eq.(1.40)), each graph appears with a *symmetry factor* which is the inverse of the size of its automorphism group (Definition 45),

$$\text{sym}(\Gamma) = \frac{1}{|\text{Aut}(\Gamma)|}.$$

**Proof** A mathematically rigorous proof can be found for example in [201, Sect. 2.3]. It is based on the *orbit-stabilizer-theorem*, namely that the size of a group equals the number of orbits times the size of each orbit, which is a specialization of the Cauchy–Frobenius–Burnside lemma [202, 203] or the Redfield–Pólya theorem [204, 205]. The case of multiedges and tadpoles has been discussed in detail above. What remains is the relabelling of vertices. The permutations of all  $|V_\Gamma|$  (labelled) vertices are the symmetric group  $S_{|V_\Gamma|}$  with size  $|V_\Gamma|!$ . The automorphism group  $\text{Aut}(\Gamma)$  is the stabilizer group of  $S_{|V_\Gamma|}$  acting on  $V_\Gamma$ . The orbit  $\text{Orb}(\Gamma)$  of  $S_{|V_\Gamma|}$  acting on the labelled graph  $\Gamma$  amounts to all the copies of  $\Gamma$  which are created by Wick’s theorem (Theorem 2). The Dyson series (Theorem 6) introduces a prefactor  $\frac{1}{|V_\Gamma|!}$ , the result is

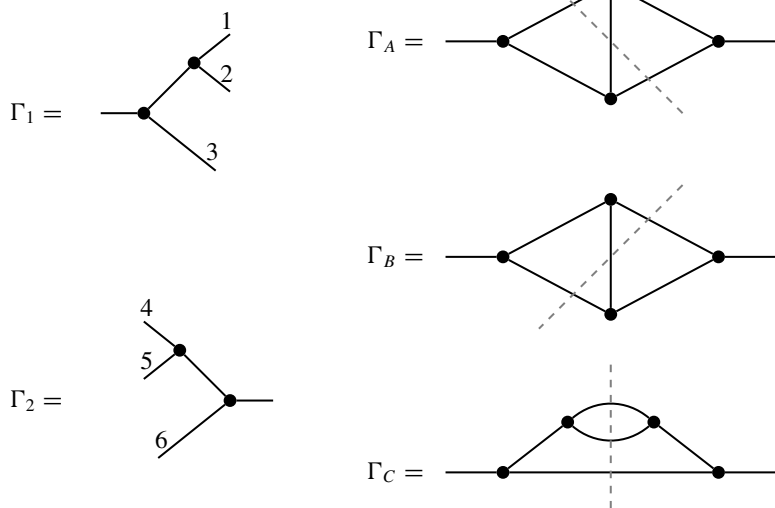
$$\frac{1}{|V_\Gamma|!} |\text{Orb}(\Gamma)| \cdot \Gamma = \frac{1}{|\text{Orb}(\Gamma)| |\text{Aut}(\Gamma)|} |\text{Orb}(\Gamma)| \cdot \Gamma = \frac{1}{|\text{Aut}(\Gamma)|} \cdot \Gamma$$

□

Symmetry factors are compatible with cutting, in the sense that summing all possible ways to cut a set of graphs into smaller components is the same as summing all subgraphs with all ways to join them. See [201, 206] or Example 30 for more details. This fact has important consequences for Dyson–Schwinger equations (Sect. 1.3.11) in gauge theories.

### Example 30: Cutting a 2-loop graph.

Choose  $\Gamma_1, \Gamma_2$  as indicated, then each of them has symmetry factor  $\frac{1}{2}$  (for the exchange of  $1 \leftrightarrow 2$  or  $4 \leftrightarrow 5$ ). The numbered edges are supposed to be internal in the final graph, so they are not excluded from graph automorphisms (Definition 45). There are  $3! = 6$  possibilities to join  $\Gamma_1$  to  $\Gamma_2$ , resulting in the graphs  $\Gamma_A, \Gamma_B, \Gamma_C$ .



Two of the 6 possible connections result in  $\Gamma_C$ , producing an overall factor of  $2 \cdot \frac{1}{2} \cdot \frac{1}{2}$ , which is the correct symmetry factor  $\text{sym}(\Gamma_C) = \frac{1}{2}$ . The 4 other possibilities produce the topology  $\Gamma_A = \Gamma_B$  with an overall factor  $4 \cdot \frac{1}{2} \cdot \frac{1}{2} = 1$ . There are two distinct ways of cutting this topology into  $\Gamma_1$  and  $\Gamma_2$ . The correct symmetry factor is respected in the sum over both cuts,  $2 \cdot \text{sym}(\Gamma_A) = 2 \cdot \frac{1}{2} = 1$ . This summation over all possible cuts, although it appears slightly odd at first, is exactly what one needs in QFT, for example for gauge theory [176, 207, 208], see Example 132, or field diffeomorphisms [206, 209], see Chap. 5.

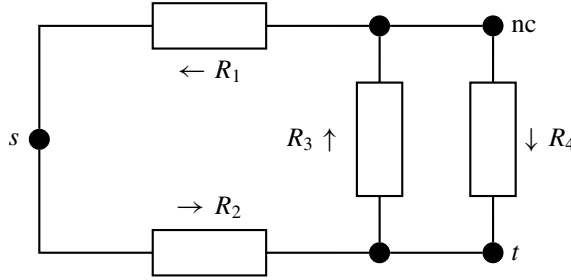
### 1.3.9 Digression: Electrical Networks

The theoretical analysis of electrical networks was first started by Ohm's discovery of the fundamental law  $U = R \cdot I$  for the voltage  $U$ , resistance  $R$  and current  $I$  in directed current circuits [210]. In 1847, Kirchhoff gave a more systematic treatment, accounting for charge conservation by his famous two rules (from today's perspective, these rules are a graph-discretized version of Maxwell's equations [20] for the electric field). In the present section, we will see what the original meaning of the Kirchhoff polynomial (Theorem 13) for electrical networks was.

To turn a graph into the customary type of drawing of an electrical network, the edges become resistors (inheriting the direction of the edge), and we add additional lines and dots to make the drawing rectangular. Each resistor has a conductance  $c_i := \frac{1}{R_i}$ . We assume that current flows from one vertex  $s$  to another vertex  $t$  through the network. All other vertices are not connected to any external potential, marked "nc", hence no current can enter or leave there.

**Example 31: Dunce's cap as an electrical network.**

Choosing arbitrarily one of the vertices as  $s$  and one as  $t$ , the dunce's cap (Example 12) becomes the following electrical network:



For any spanning tree  $T \in T_{\Gamma}^{(1)}$  (Definition 35), let its *weight* be the product of the conductances in the tree,  $c_T := \prod_{e \in T} c_e$ . Each spanning tree defines a unique directed path from  $s$  to  $t$ . Assume that a current of magnitude 1 flows from  $s$  to  $t$ . Then, Kirchhoff's theorem for electrical networks [161, 166] states that the current through  $R_i$  is

$$I_i = \frac{N(s, R_i^+, t) - N(s, R_i^-, t)}{\tilde{\psi}(\{c_e\})}. \quad (1.59)$$

Here,  $N(s, R_i^+, t)$  is the sum of the weights  $c_T$  of all spanning trees  $T$  which, on their way from  $s$  to  $t$ , pass through  $R_i$  in positive direction.  $N(s, R_i^-, t)$  is defined accordingly for negative direction, and  $\tilde{\psi}$  is the Kirchhoff polynomial (Theorem 13). Compare Example 15: sums of directed spanning trees arise from cofactors of the directed Laplacian matrix. For readability, we have skipped the physical units in Eq. (1.59).

**Example 32: Dunce's cap, currents in the edges.**

For the network shown in Example 31, we know the Symanzik polynomial from Example 17. The currents in the resistors are, by Eq. (1.59),

$$\begin{aligned} I_1 &= \frac{0 - (c_1 c_3 + c_1 c_4)}{c_1 c_2 + c_1 c_3 + c_1 c_4 + c_2 c_3 + c_2 c_4} \\ I_2 &= \frac{(c_2 c_3 + c_2 c_4 + c_1 c_2) - 0}{c_1 c_2 + c_1 c_3 + c_1 c_4 + c_2 c_3 + c_2 c_4} \\ I_3 &= \frac{(c_2 c_3) - (c_1 c_3)}{c_1 c_2 + c_1 c_3 + c_1 c_4 + c_2 c_3 + c_2 c_4} \\ I_4 &= \frac{(c_2 c_4) - (c_1 c_4)}{c_1 c_2 + c_1 c_3 + c_1 c_4 + c_2 c_3 + c_2 c_4}. \end{aligned}$$

Knowing all currents, we can reconstruct all other properties of the network. For example, by Ohm's law [210], the voltage between  $s$  and  $t$  is the voltage over  $R_2$ ,

$$\begin{aligned} U_{s \rightarrow t} = U_2 = R_2 I_2 &= \frac{1}{c_2} \frac{c_2 c_3 + c_2 c_4 + c_1 c_2}{c_1 c_2 + c_1 c_3 + c_1 c_4 + c_2 c_3 + c_2 c_4} \\ &= \frac{c_3 + c_4 + c_1}{c_1 c_2 + c_1 c_3 + c_1 c_4 + c_2 c_3 + c_2 c_4}. \end{aligned}$$

The voltage in turn delivers the total resistance of the network because the total current is 1 (where the unit Ampere is left out):  $R = U_{s \rightarrow t}/1 = U_{s \rightarrow t}$ . A manual calculation with the rules for parallel/serial resistors, known from high school physics, confirms this result.

Current conservation in electrical networks is analogous to momentum conservation in Feynman graphs. It is therefore not surprising that solving for the individual currents in an electrical network involves the same graph polynomial as does the resolution of all internal momenta in a Feynman graph with respect to a chosen set of loop momenta. The Schwinger trick Eq.(1.51) can be interpreted as minimizing the power dissipation of an electrical network, see [211].

The analogy between Feynman graphs and electrical networks has sometimes been mentioned in the literature, but concrete applications remain rare. In electrical networks, a triangle of resistors can always be replaced by a “star”, joining the three corners to a new central vertex. A similar relation for Feynman integrals is known as *uniqueness identity* [212–215],

$$\int d^D t \frac{1}{((x-t)^2)^a} \frac{1}{((y-t)^2)^b} \frac{1}{((z-t)^2)^c} \propto \frac{1}{((x-y)^2)^{\frac{D}{2}-a}} \frac{1}{((y-z)^2)^{\frac{D}{2}-b}} \frac{1}{((z-x)^2)^{\frac{D}{2}-c}}.$$

The uniqueness identity holds only for  $a + b + c = D$ , while the replacement of stars in electrical networks is always possible. In [216], the star-triangle relation for electrical circuits is used to restrict the analytic form of 1-loop massless 3-point functions. Notice that a triangle is the planar dual graph of a star. The Feynman period (Definition 98) satisfies a so-called Fourier-split identity [217], which means the value of the period does not change if certain subgraphs are replaced by their planar dual. As pointed out in [200], this can be interpreted as a generalization of the uniqueness identity.

### 1.3.10 1PI Graphs

In momentum space, the Feynman rules (Definition 42) require integration for every linearly independent loop. Conversely, if two Feynman graphs  $\Gamma_1, \Gamma_2$  are connected by only a single edge, then they can not be part of the same loop and hence the total integral factors,

$$\mathcal{F}[\Gamma_1 \cdot e \cdot \Gamma_2] = \mathcal{F}[\Gamma_1] \cdot \mathcal{F}[e] \cdot \mathcal{F}[\Gamma_2]. \quad (1.60)$$

**Definition 46.** An amputated Feynman graph  $\Gamma$  (Definition 24) is *1-particle irreducible* (1PI) if it is 2-edge connected. That is,  $\Gamma$  is connected and it stays connected (Definition 22) when any one of the internal edges is removed.

#### Example 33: $\phi^3$ theory, 1PI graphs.

In Example 11, we gave the first graphs contributing to the connected Green functions in  $\phi^3$  theory. The 1PI graphs are a subset of those. For the 2-point function, there is only one non-1PI graph, and the first 1PI graphs are

$$\begin{aligned} \Gamma^{(2)} = & \text{ — } + \lambda_3^2 \frac{1}{2} \text{ — } \bullet \text{— } \text{— } \bullet \text{— } \\ & + \lambda_3^4 \left( \frac{1}{2} \text{ — } \bullet \text{— } \text{— } \bullet \text{— } \text{— } \bullet \text{— } + \frac{1}{2} \text{ — } \bullet \text{— } \text{— } \bullet \text{— } \right) + \dots \end{aligned}$$

For the 3-point function, two of the topologies in Example 11 are connected but not 1PI. The 1PI ones are

$$\begin{aligned} \Gamma^{(3)} = & \lambda_3 \text{ — } \bullet \text{— } \text{— } + \lambda_3^3 \text{ — } \bullet \text{— } \text{— } \bullet \text{— } \\ & + \lambda_3^5 \langle 3 \rangle \left( \frac{1}{2} \text{ — } \bullet \text{— } \text{— } \bullet \text{— } \text{— } \bullet \text{— } + \text{ — } \bullet \text{— } \text{— } \bullet \text{— } \text{— } \bullet \text{— } \right) + \lambda_3^5 \frac{1}{2} \text{ — } \bullet \text{— } \text{— } \bullet \text{— } \text{— } \bullet \text{— } + \dots \end{aligned}$$

There are in total nine 1PI graphs contributing up to loop number 2, down from 15 connected graphs in Example 11.

**Definition 47.** The *combinatorial 1PI Green function*  $\Gamma^r$  is the sum of all 1PI graphs (Definition 46) with residue  $r$  (Definition 26), weighted with their symmetry factors (Theorem 15) and coupling constants, the latter rescaled to match the loop number (Definition 29).

$$\Gamma^r(\alpha) := \sum_{\Gamma \text{ 1PI}, \text{res}(\Gamma)=r} \alpha^{|L_\Gamma|} \text{sym}(\Gamma) \cdot \Gamma.$$

For a  $\phi^n$  theory, the residue are monomials of  $\phi$ , we write  $r = (j)$  to indicate the residue  $\phi^j$ . By  $\Gamma \in \Gamma^r$  we mean that  $\Gamma$  is 1PI and  $\text{res}(\Gamma) = r$ .

Observe that 1PI Green functions are not the same as amputated (Theorem 5) Green functions. The two classes coincide for 2-point and 3-point functions, but from 4 external edges on, the amputated Green function can contain an internal edge making it 1-particle reducible.

**Definition 48.** The 1PI Green function  $G^r$  is the combinatorial 1PI green function  $\Gamma^r$  (Definition 47), evaluated with the Feynman rules (Definition 40):

$$G^r := \mathcal{F}[\Gamma^r]$$

For 2-point graphs, the relation between connected and 1PI graphs is given by a geometric series. If we consider the functions as operators, this is a Neumann series [218]. The self energy  $\Sigma^{(2)}$  is the sum of all quantum corrections to the 2-point function. The connected 2-point function  $\bar{G}^{(2)}$  then equals the sum of any number of chains of the self-energy, all of them with the same momentum  $\underline{p}$  and connected by propagators  $\frac{i}{s_p}$  (Eq. (1.25)). By Eq. (1.60), the Feynman integral of a chain of graphs is the product of the individual integrals, consequently

$$\begin{aligned} \bar{G}^{(2)}(\underline{p}) &= \frac{i}{s_p} + \frac{i}{s_p} \Sigma^{(2)}(\underline{p}) \frac{i}{s_p} + \frac{i}{s_p} \Sigma^{(2)}(\underline{p}) \frac{i}{s_p} \Sigma^{(2)}(\underline{p}) \frac{i}{s_p} + \dots \\ &= \frac{i}{s_p} \sum_{k=0}^{\infty} \left( \frac{i}{s_p} \Sigma^{(2)}(\underline{p}) \right)^k = \frac{i}{s_p} \frac{1}{1 - \frac{i}{s_p} \Sigma^{(2)}(\underline{p})} =: \frac{i}{s_p G^{(2)}(\underline{p})}. \end{aligned} \quad (1.61)$$

**Definition 49.** The *1PI 2-point function* is defined as

$$G^{(2)}(\underline{p}) := 1 - \frac{i}{s_p} \Sigma^{(2)}(\underline{p})$$

where  $\Sigma^{(2)}(\underline{p})$  represents the *self energy*, the sum of all 1PI 2-point quantum corrections. Consequently, the connected 2-point function, replacing the treelevel propagator Eq.(1.25), is  $\bar{G}^{(2)}(\underline{p}) = \frac{i}{s_p G^{(2)}(\underline{p})}$ . For Definition 47, it is  $\bar{\Gamma}^{(2)} = \frac{1}{\Gamma^{(2)}}$ .

The relationship between connected and 1PI 2-point functions is consistent with the Feynman propagator (Eq.(1.25)). For example, instead of using the massive propagator, one can use the massless propagator and take the mass term of the Lagrangian (Example 1) as a 2-valent vertex. Then, every internal line in a graph can be dressed with infinitely many of these vertices, which eventually add up to the massive Feynman propagator.

1PI graphs are “building blocks” of connected Feynman graphs, in the same sense that trees are built of vertices, which in turn are generated by the classical action (Definition 7).

**Definition 50.** The *effective action*  $\Gamma[J]$  is the formal (Definition 53) generating functional of all 1PI Green functions.

If  $W[J]$  is the generating functional of connected amplitudes (Eq.(1.39)), then  $\Gamma[J]$  is the Legendre transform (Definition 55) of  $W[J]$  [81, 159, 219, 220]. We will discuss the correspondence between graphs and power series in Sect. 2.1.4. Among other things, it can be used to count graphs, see Example 57, or [201] for a detailed account.

### 1.3.11 Dyson–Schwinger Equations

So far, we have viewed the graphs appearing in the Dyson series (Eq.(1.40)) as isolated objects. But for a given graph  $\Gamma$ , the subgraphs  $\gamma \subset \Gamma$  are graphs themselves. This observation will now be used to organize the graphs in the Dyson series according to their residue (Definition 26). The resulting identity is called *Dyson–Schwinger equation*, and it can be stated in various equivalent forms. In the present section, we stay rather general and “qualitative”. More precise equations will be given in Sects. 2.2.5 and 3.3.

**Definition 51.** The *residues of the Lagrangian* are a set  $\mathcal{L}$  of pairs  $(g, T)$  associated to the monomials of the Lagrangian (Definition 6).  $g$  is the residue (Definition 26), that is, a monomial of field variables, while  $T$  is the tensor structure, that is, a monomial in masses or momenta.

We write  $\Gamma \in \mathcal{L}$  if there is a  $(g, T) \in \mathcal{L}$  such that  $\text{res}(\Gamma) = g$  and  $\Gamma$  projected onto  $T$  does not vanish at  $\underline{p} = \underline{0}, m = 0$ . As shown in Example 34, the second condition is not trivial.

**Example 34:**  $\phi^n$  theory, residues of the Lagrangian.

In massive  $\phi^n$  theory (Example 3), the kinetic term amounts to  $(\phi^2, \underline{p}^2) \in \mathcal{L}$ , the mass term contributes  $(\phi^2, m^2) \in \mathcal{L}$  and the interaction term is  $(\phi^n, 1) \in \mathcal{L}$ .

Assume now that  $\Gamma$  is a graph contributing to a 2-point function with momentum  $\underline{p}$ , but  $\mathcal{F}[\Gamma] \propto \underline{p}^4$ , then  $\Gamma \notin \mathcal{L}$  for the  $\phi^n$  theory.

Let  $\Gamma \in \Gamma^{(n)}$  be a graph contributing to the combinatorial 1PI  $n$ -point Green function (Definition 46). Into every edge  $e \in \Gamma$  one can insert any 2-valent graph  $\gamma \in \Gamma^{(2)}$ , and the result is a valid Feynman graph of  $\Gamma^{(n)}$ . Similarly, one can replace every  $j$ -valent vertex with any  $\gamma \in \Gamma^{(j)}$ . A closer inspection shows that such insertion, when done consistently, produces the correct symmetry factors (Theorem 15) for the newly created graphs.

**Definition 52.** Let  $\Gamma^{(n)}$  be the combinatorial 1PI  $n$ -point Green function (Definition 47). A *kernel graph*  $K \in \Gamma^{(n)}$  is a 1PI (Definition 46) Feynman graph with  $n$  external edges such that there is no proper subgraph  $\gamma \subset K$  with  $\gamma \in \mathcal{L}$  (Definition 51). The set of all kernel graphs for  $\Gamma^{(n)}$  is denoted  $\mathcal{K}^{(n)}$ .

**Theorem 16** (Dyson–Schwinger equations (DSEs) for Feynman graphs). The 1PI combinatorial Green function  $\Gamma^{(n)}$  (Definition 47) is given by a (possibly infinite) sum of kernel graphs (Definition 52)  $\mathcal{K}^{(n)}$ , and for each  $K \in \mathcal{K}^{(n)}$ , all  $j$ -valent vertices  $v_j \in K$  are replaced by the series  $\Gamma^{(j)}$ , and all edges by  $\bar{\Gamma}^{(2)} = \frac{1}{\Gamma^{(2)}}$  (Definition 49).

A special role is played by the 2-point function  $\Gamma^{(2)}$ : We insert the connected 2-point function, but the DSE is usually written for the 1PI 2-point function. The relationship Definition 49 entails that the DSE for the 2-point function contains a minus sign in front of all kernel graphs.

**Example 35:  $\phi^3$  propagator, combinatorial Dyson–Schwinger equation.**

Consider the 2-point function of  $\phi^3$  theory. The first graphs are shown in Example 33. The propagator DSE only involves a single kernel graph, which has symmetry factor  $\frac{1}{2}$  (Theorem 15). To avoid double-counting, one needs to disentangle the series into three parts, see also [207, 221, 222]. Again, we write the DSE for the 1PI 2-point function  $\Gamma^{(2)}$ , not for the connected one, see Definition 49.

$$\begin{aligned} \Gamma^{(3)} &=: \text{---} \bullet \text{---} \\ \bar{\Gamma}^{(2)} &=: \text{---} \bullet \text{---} \quad \bar{\Gamma}^{(2)} \text{---} \text{---} =: \text{---} \bullet \text{---} \\ \Gamma^{(2)} &= 1 - \lambda_3^2 \frac{1}{2} \text{---} \bullet \text{---} \text{---} \text{---} - \lambda_3^2 \text{---} \bullet \text{---} \text{---} \text{---} - \lambda_3^2 \frac{1}{2} \text{---} \bullet \text{---} \text{---} \text{---} \end{aligned}$$

Compare this to Theorem 1: We see that the presence of interaction, that is  $\Gamma^{(3)} \neq 0$ , necessarily alters the 2-point function.

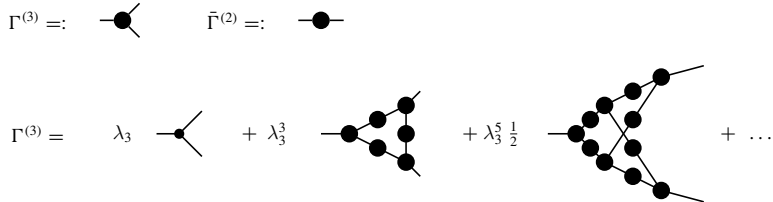
**Example 36:  $\phi^3$  propagator, simplified combinatorial DSE.**

A drastic simplification of the propagator DSE can be obtained by ignoring all quantum corrections to the vertex, that is setting  $\Gamma^{(3)} = \text{---} \bullet \text{---}$ . This produces a DSE where  $\Gamma^{(2)}$  is the only unknown function. Such DSEs will be discussed in detail in Sect. 3.3.2.

$$\Gamma^{(3)} =: \text{---} \bullet \text{---} \quad \bar{\Gamma}^{(2)} =: \text{---} \bullet \text{---} \quad \Rightarrow \quad \Gamma^{(2)} = 1 - \lambda_3^2 \frac{1}{2} \text{---} \bullet \text{---} \text{---} \text{---}$$

**Example 37:  $\phi^3$  vertex, combinatorial Dyson–Schwinger equation.**

Consider massless  $\phi^3$  theory (Example 3) where  $\mathcal{L} = \left\{ (\phi^2, \underline{p}^2), (\phi^3, 1) \right\}$  (Example 34). In Example 33, we depicted the first graphs contributing to the 1PI (Definition 46) 3-point function  $\Gamma^{(3)}$ . Indeed, some of them have subgraphs with 2 or 3 external edges which can be identified as coefficients of the series  $\Gamma^{(2)}$  and  $\Gamma^{(3)}$ . Without such subgraphs, there is one graph at order  $\lambda_3^3$  and one at order  $\lambda_3^5$  (in 3 different orientations). Into each edge we insert the *connected* 2-point function  $\bar{\Gamma}^{(2)}$  (see Eq. (1.61)).



Unlike the propagator DSE (Example 35), the vertex DSE involves infinitely many kernel graphs. Counting the different orientations, we now have three kernel graphs up to loop order 2, down from nine 1PI graphs in Example 33.

As it stands, Theorem 16 is a mildly interesting combinatoric statement about the sum of infinitely many graphs and their subgraphs. But these graphs ultimately represent Feynman integrals, and consequently, Theorem 16 actually amounts to a set of integral equations for the 1PI Green functions (Definition 48).

**Theorem 17** (Dyson–Schwinger integral equations [223–226]). The 1PI Green function  $G^{(n)}$  (Definition 92) is given by a series of integrals, encoded by kernel graphs (Definition 52), where the  $j$ -valent vertices are replaced by the 1PI Green function  $G^{(j)}$  and the edges are replaced by the function  $\bar{G}^{(2)}$  (Definition 49).

### Example 38: $\phi^3$ propagator, simplified integral DSE.

Consider the simplified propagator DSE of Example 36, that is, setting the vertex Green function to  $\mathcal{F}[\Gamma^{(3)}] = G^{(3)} \stackrel{!}{=} -i\lambda_3$ . Define the 2-point functions as in Definition 49. One then has, using  $(-i)^2 i^2 = 1$  and the propagator from Eq. (1.25),

$$G^{(2)}(\underline{p}) = 1 - \frac{i}{s_p} \lambda_3^2 \frac{1}{2} \int \frac{d^D k}{(2\pi)^D} \frac{1}{s_k s_{k+p}} (G^{(2)}(\underline{k}))^{-1} (G^{(2)}(\underline{k} + \underline{p}))^{-1}.$$

In both forms (Theorems 16 and 17), the Dyson–Schwinger equations are *fixed-point equations*, this means that the objects on the left hand side of these equations also appear in the right hand side. To solve a DSE, one needs to find a self-consistent solution. One possible approach is to consider all quantities as series in a coupling parameter and to solve the DSE recursively order by order. We will discuss this procedure in detail in Sect. 4.2.

Our formulation of Dyson–Schwinger equations are based on kernel graphs (Definition 52) which have one out of finitely many residues (Definition 26). This entails that only finitely many Dyson–Schwinger equations are coupled. On the other hand, one generally has to include an infinite set of kernel graphs. An alternative version involves only a small number of graphs for each residue, but all (infinitely many) equations are coupled. See e.g., [227] for an entertaining presentation. These DSEs

are again fixed-point equations, the most compact way to write them is if one identifies Green functions with derivatives of the path integral as in Eq. (1.38).

**Theorem 18** (Dyson–Schwinger equations for generating functionals). Let  $Z[J]$  be the path integral (Eq. (1.37)) and  $S[\phi]$  the classical action (Definition 7), then

$$\frac{\delta S[\phi]}{\delta \phi(\underline{x})} \Big|_{\phi \rightarrow \frac{\delta}{\delta J}} Z[J] = 0.$$

Observe the similarity to the classical equations of motion  $\delta S = 0$  (Eq. (1.7)).

As announced in Sect. 1.2.7, Dyson–Schwinger equations provide another possible way to define a quantum field theory. Their series expansion leads to the same set of Feynman rules as the definitions discussed so far. Indeed, that was their original motivation [224]:

The construction of these [Green functions] for coupled fields is usually considered from the viewpoint of perturbation theory. [...] It is desirable to avoid founding the formal theory of the Green's functions on the restricted basis provided by the assumption of expandability in powers and coupling constants.

### Summary of Sect. 1.3

1. Feynman integrals appearing in the Dyson series can be represented graphically as Feynman graphs, and it is sufficient to consider connected graphs (Sects. 1.3.1 and 1.3.2).
2. We reviewed graph theory and learned about various matrices and polynomials associated to graphs, and how they can be used to systematically compute quantities of interest (Sects. 1.3.3 and 1.3.4).
3. We established a concrete algorithm to turn a given Feynman graph into the corresponding integral in position space, called *Feynman rules* (Sects. 1.3.5).
4. Feynman rules can equivalently be formulated in momentum space (Sects. 1.3.6) or in parametric space (Sect. 1.3.7).
5. We derived the symmetry factor of Feynman graphs in the Dyson series, which is given by the size of the automorphism group (Sect. 1.3.8).
6. Connected graphs can be decomposed into 1PI graphs and it is usually sufficient to compute the 1PI ones (Sect. 1.3.10).
7. The structure of nested subgraphs of Feynman graphs is expressed by Dyson–Schwinger equations. They are fixed-point equations and can be formulated in various ways, either as a statement for sums of graphs, or for Green functions, or for generating functionals (Sect. 1.3.11).

## References

1. A. Das, *Lectures on Quantum Field Theory* (World Scientific, Singapore, 2010)
2. N. Nakanishi, I. Ojima, *Covariant Operator Formalism of Gauge Theories and Quantum Gravity* (World Scientific, 1990), 452 pp. <https://www.worldscientific.com/doi/abs/10.1142/0362>
3. S. Weinberg, *The Quantum Theory of Fields. Volume 1: Foundations*, vol. 1 (Cambridge University Press, Cambridge, 1996). <https://doi.org/10.1017/CBO9781139644167>
4. M.E. Peskin, D.V. Schroeder, *An Introduction to Quantum Field Theory* (1995), 842 p. <https://cds.cern.ch/record/257493>
5. H.A. Lorentz, Versuch Einer Theorie der Electrischen und Optischen Erscheinungen in Bewegten Körpern, in *Collected Papers*, vol. V, ed. by H.A. Lorentz (Springer, Netherlands, Dordrecht, 1895), pp. 1–138
6. E. Wigner, On unitary representations of the inhomogeneous Lorentz group. *Ann. Math.* **40**, 149 (1939)
7. E.C. Zeeman, Causality implies the Lorentz group. *J. Math. Phys.* **5**, 490–493 (1964)
8. M.H. Poincaré, Sur la dynamique de l'électron. *Rendiconti del Circolo Matematico di Palermo* **1884–1940**(21), 129–175 (1906)
9. M. Planck, Ueber irreversible Strahlungsvorgänge. *Annalen der Physik* **306**, 69–122 (1900)
10. L. Euler, De progressionibus transcendentibus seu quarum termini generales algebraice dari nequeunt. *Commentarii academiae scientiarum Petropolitanae*, 36–57 (1738)
11. R.P. Kanwal, *Generalized Functions, Theory and Applications*, 3rd edn. (Springer, 2004)
12. C.F. Gauss, *Theoria motus corporum coelestium in sectionibus conicis solem ambientium* (1809). <http://www.deutsche-digitale-bibliothek.de/item/3VB4VDOTEM5XBYLK3VV7VQY5JK6SJW0>
13. J. Liouville, Sur l'équation aux differences partielles  $d2\log du/dv^2a^2=0$ . *Journal de mathématiques pures et appliquées 1re serie* **18**, 71–72 (1853)
14. O. Klein, Elektrodynamik und Wellenmechanik vom Standpunkt des Korrespondenzprinzips. *Zeitschrift für Physik A Hadrons and nuclei* **41**, 407–442 (1927)
15. W. Gordon, Der Comptoneffekt nach der Schrödingerschen Theorie. *Zeitschrift für Physik* **40**, 117–133 (1926)
16. E. Schrödinger, Quantisierung als Eigenwertproblem. *Annalen der Physik* **386**, 109–139 (1926)
17. P.T. Kristensen, K. Herrmann, F. Intravaia, K. Busch, K. Busch, Modeling electromagnetic resonators using quasinormal modes. *Adv. Opt. Photon.* **12**, 612–708 (2020)
18. M. Veltman, Unitarity and causality in a renormalizable field theory with unstable particles. *Physica* **29**, 186–207 (1963)
19. A.A. Mahmoud, On the enumerative structures in quantum field theory (2020). [arXiv: 2008.11661](https://arxiv.org/abs/2008.11661)
20. J.C. Maxwell, A dynamical theory of the electromagnetic field. *Philos. Trans. R. Soc. Lond.* **155**, 459–512 (1865)
21. P.A.M. Dirac, R.H. Fowler, The quantum theory of the electron, in *Proceedings of the Royal Society of London. Series A, Containing Papers of a Mathematical and Physical Character*, vol. 117, pp. 610–624 (1928)
22. W. Heisenberg, Über quantentheoretische Umdeutung kinematischer und mechanischer Beziehungen. *Zeitschrift für Physik* **33**, 879–893 (1925)
23. M. Born, W. Heisenberg, P. Jordan, Zur Quantenmechanik. II. *Zeitschrift für Physik* **35**, 557–615 (1926)
24. W. Heisenberg, Über den anschaulichen Inhalt der quantentheoretischen Kinematik und Mechanik. *Zeitschrift für Physik* **43**, 172–198 (1927)
25. I.J.R. Aitchison, D.A. MacManus, T.M. Snyder, Understanding Heisenberg's "Magical" paper of July 1925: a new look at the calculational details, version 1. *Amer. J. Phys.* **72**, 1370–1379 (2004)

26. F. Bayen, M. Flato, C. Fronsdal, A. Lichnerowicz, D. Sternheimer, Deformation theory and quantization. II. Physical applications. *Ann. Phys.* **111**, 111–151 (1978)
27. F. Bayen, M. Flato, C. Fronsdal, A. Lichnerowicz, D. Sternheimer, Deformation theory and quantization. I. Deformations of symplectic structures. *Ann. Phys.* **111**, 61–110 (1978)
28. M. Kontsevich, Deformation, Quantization and Beyond. Rutgers Algebra Seminar (1997)
29. M. Kontsevich, Deformation quantization of poisson manifolds. *Lett. Math. Phys.* **66**, 157–216 (2003)
30. S.T. Ali, M. Engliš, Quantization methods: a guide for physicists and analysts. *Rev. Math. Phys.* **17**, 391–490 (2005)
31. S. Bates, A. Weinstein, *Lectures on the Geometry of Quantization*, 134 (1994)
32. N.M.J. Woodhouse, *Geometric Quantization*, 2nd edn. Oxford Mathematical Monographs (Oxford University Press, Oxford, New York, 1997), p. 320
33. P.C. Grange, E. Werner, Quantum Fields as Operator Valued Distributions and Causality (2007). [arXiv: math-ph/0612011](https://arxiv.org/abs/math-ph/0612011)
34. F. Gieres, Mathematical surprises and Dirac's formalism in quantum mechanics. *Rep. Progress Phys.* **63**, 1893–1931 (2000)
35. M.J. Gotay, H.B. Grundling, G.M. Tuynman, Obstruction results in quantization theory. *J. Nonlinear Sci.* **6**, 469–498 (1996)
36. D. Buchholz, R. Haag, “The quest for understanding in relativistic quantum physics”, version 2. *J. Math. Phys.* **41**, 3674–3697 (2000)
37. L. Kłaczynski, Haag's theorem in renormalisable quantum field theories. Doctoral Thesis (Humboldt-Universität zu Berlin, Mathematisch-Naturwissenschaftliche Fakultät, 2016). <https://edoc.hu-berlin.de/handle/18452/18100>
38. O. Müller, On the von Neumann rule in quantization (2019). [arXiv: 1903.10494](https://arxiv.org/abs/1903.10494)
39. A.S. Wightman, Quantum field theory in terms of vacuum expectation values. *Phys. Rev.* **101**, 860–866 (1956)
40. A.S. Wightman, L. Gårding, Fields as operator-valued distributions in relativistic quantum theory. *Ark. Fys.* **28**, 129–184 (1965)
41. K. Osterwalder, R. Schrader, Axioms for Euclidean Green's functions. *Commun. Math. Phys.* **31**, 83–112 (1973)
42. G. Mack, Osterwalder-Schrader positivity in conformal invariant quantum field theory, in *Trends in Elementary Particle Theory*, ed. by H. Rollnik, K. Dietz. Lecture Notes in Physics (1975), pp. 66–91
43. H.P. Stapp, The copenhagen interpretation. *Amer. J. Phys.* **40**, 1098–1116 (1972)
44. R.P. Feynman, Mathematical formulation of the quantum theory of electromagnetic interaction. *Phys. Rev.* **80**, 440–457 (1950)
45. R.P. Feynman, Space-time approach to quantum electrodynamics. *Phys. Rev.* **76**, 769–789 (1949)
46. R.P. Feynman, Space-time approach to non-relativistic quantum mechanics. *Rev. Mod. Phys.* **20**, 367–387 (1948)
47. H. Lehmann, Über Eigenschaften von Ausbreitungsfunktionen und Renormierungskonstanten quantisierter Felder. *Il Nuovo Cimento* **1943–1954**(11), 342–357 (1954)
48. S. Fubini, A.J. Hanson, R. Jackiw, New approach to field theory. *Phys. Rev. D* **7**, 1732–1760 (1973)
49. K. Huang, *Quantum Field Theory: From Operators to Path Integrals* (Wiley, New York, 1998), p.426
50. R. Jost, Properties of Wightman functions, in *Lectures on Field Theory and the Many-body Problem*, ed. by E.R. Caianiello (Academic, New York, 1961)
51. P.G. Federbush, K.A. Johnson, Uniqueness property of the twofold vacuum expectation value. *Phys. Rev.* **120**, 1926–1926 (1960)
52. K. Pohlmeyer, The Jost-Schroer theorem for zero-mass fields. *Commun. Math. Phys.* **12**, 204–211 (1969)
53. G.C. Wick, The evaluation of the collision matrix. *Phys. Rev.* **80**, 268–272 (1950)

54. L. Isserlis, On a formula for the product-moment coefficient of any order of a normal frequency distribution in any number of variables. *Biometrika* **12**, 134–139 (1918)
55. O. Steinmann, Perturbation theory of Wightman functions. *Commun. Math. Phys.* **152**, 627–645 (1993)
56. J. Schwinger, Quantum electrodynamics. I. A covariant formulation. *Phys. Rev.* **74**, 1439–1461 (1948)
57. J. Schwinger, Quantum electrodynamics. II. Vacuum polarization and self-energy. *Phys. Rev.* **75**, 651–679 (1949)
58. J. Schwinger, Quantum electrodynamics. III. The electromagnetic properties of the electron-radiative corrections to scattering. *Phys. Rev.* **76**, 790–817 (1949)
59. F.J. Dyson, The radiation theories of Tomonaga, Schwinger, and Feynman. *Phys. Rev.* **75**, 486–502 (1949)
60. P. Duch, Massless fields and adiabatic limit in quantum field theory (2017). [arXiv: 1709.09907](https://arxiv.org/abs/1709.09907)
61. R. Haag, On Quantum Field Theories. *Det Kongelige Danske Videnskabernes Selskab Matematisk-fysiske Meddelelser* **29**, 19 (1955)
62. H. Araki, K. Hepp, D. Ruelle, On the asymptotic behaviour of Wightman functions in space-like directions. *Helv. Phys. Acta* **35**, 164–174 (1962)
63. D.A. Slavnov, Asymptotic states in the quantum field theory. *Theor. Math. Phys.* **1**, 251–256 (1969)
64. N.N. Bogolubov, A.A. Logunov, A.I. Oksak, I.T. Todorov, G.G. Gould, Haag-Ruelle scattering theory, in *General Principles of Quantum Field Theory*. ed. by N.N. Bogolubov, A.A. Logunov, A.I. Oksak, I.T. Todorov. Mathematical Physics and Applied Mathematics (Springer, Netherlands, Dordrecht, 1990), pp. 486–502
65. D.L. Fraser, Haags theorem and the interpretation of quantum field theories with interactions. Doctoral Dissertation (2006). <http://d-scholarship.pitt.edu/8260/>
66. J.A. Wheeler, On the mathematical description of light nuclei by the method of resonating group structure. *Phys. Rev.* **52**, 1107–1122 (1937)
67. W. Heisenberg, Die beobachtbaren Größen in der Theorie der Elementarteilchen. *Zeitschrift für Physik* **120**, 513–538 (1943)
68. V. Fock, Konfigurationsraum und zweite Quantelung. *Zeitschrift für Physik* **75**, 622–647 (1932)
69. R.P. Feynman, Quantum theory of gravitation. *Acta Phys. Polon.* **24**, 697–722 (1963)
70. R. Runkel, Z. Szőr, J.P. Vesga, S. Weinzierl, Causality and loop-tree duality at higher loops. *Phys. Rev. Lett.* **123**, 059902 (2019)
71. J.J. Aguilera-Verdugo, F. Driencourt-Mangin, J. Plenter, S. Ramírez-Uribe, G. Rodrigo, G.F.R. Sborlini, W.J.T. Bobadilla, S. Tracz, Causality, unitarity thresholds, anomalous thresholds and infrared singularities from the loop-tree duality at higher orders. *JHEP* **12**, 163 (2019)
72. Z. Capatti, V. Hirschi, D. Kermanschah, A. Pelloni, B. Ruijl, Manifestly causal loop-tree duality (2020). [arXiv: 2009.05509](https://arxiv.org/abs/2009.05509) [hep-ph]
73. J.J. Aguilera-Verdugo, R.J. Hernandez-Pinto, G. Rodrigo, G.F.R. Sborlini, W.J.T. Bobadilla, Mathematical properties of nested residues and their application to multi-loop scattering amplitudes. *J. High Energy Phys.* **02**, 112 (2021)
74. M. Berghoff, D. Kreimer, Graph complexes and Feynman rules (2020). [arXiv: 2008.09540](https://arxiv.org/abs/2008.09540)
75. W. Magnus, On the exponential solution of differential equations for a linear operator. *Commun. Pure Appl. Math.* **7**, 649–673 (1954)
76. H. Figueroa, J.M. Gracia-Bondía, Combinatorial hopf algebras in quantum field theory. *Rev. Math. Phys.* **17**, 881–976 (2005)
77. C. Curry, K. Ebrahimi-Fard, B. Owren, The Magnus expansion and post-Lie algebras. *Math. Comput.* **89**, 2785–2799 (2020)
78. N. Wiener, Differential-space. *J. Math. Phys.* **2**, 131–174 (1923)
79. P.A.M. Dirac, The lagrangian in quantum mechanics. *Physikalische Zeitschrift der Sovjetunion* **3** (1933). [https://doi.org/10.1142/9789812567635\\_0003](https://doi.org/10.1142/9789812567635_0003)
80. A. Connes, M. Marcolli, Noncommutative geometry, quantum fields and motives, vol. 55. (Colloquium Publications, American Mathematical Society, Providence, Rhode Island, 2007). <http://www.ams.org/coll/055>

81. G. Jona-Lasinio, Relativistic field theories with symmetry-breaking solutions. Il Nuovo Cimento **1955–1965**(34), 1790–1795 (1964)
82. A. Wipf, *Statistical approach to quantum field theory: an introduction*, Lecture Notes in Physics, vol. 864 (Springer, Heidelberg; New York, 2013), 390 pp
83. F.A. Berezin, Feynman path integrals in a phase space. Soviet Physics Uspekhi **23**, 763–788 (1981)
84. L.F. Abbott, M.B. Wise, Dimension of a quantum-mechanical path. Amer. J. Phys. **49**, 37–39 (1981)
85. G. 't Hooft, M. Veltman, Diagrammar. Geneva (1973)
86. S. Laporta, High-precision calculation of the 4-loop contribution to the electron g-2 in QED. Phys. Lett. B **772**, 232–238 (2017)
87. P. Cvitanović, Asymptotic estimates and gauge invariance. Nuclear Phys. B **127**, 176–188 (1977)
88. K.G. Wilson, Confinement of quarks. Phys. Rev. D **10**, 2445–2459 (1974)
89. H.J. Rothe, *Lattice Gauge Theories: An Introduction*, 4th edn. (World Scientific Publishing Company, 2012). <https://doi.org/10.1142/8229>
90. J. Ginibre, Some applications of functional integration in statistical mechanics, in *Les Houches Summer School of Theoretical Physics: Statistical Mechanics and Quantum Field Theory* (1971), pp. 327–429
91. E.H. Wichmann, J.H. Crichton, Cluster decomposition properties of the S-matrix. Phys. Rev. **132**, 2788–2799 (1963)
92. F. Alpeggiani, N. Parappurath, E. Verhagen, L. Kuipers, Quasinormal-mode expansion of the scattering matrix. Phys. Rev. X **7**, 021035 (2017)
93. S.V. Lobanov, W. Langbein, E.A. Muljarov, Resonant-state expansion of three-dimensional open optical systems: light scattering. Phys. Rev. A **98**, 033820 (2018)
94. A. Einstein, Die Grundlage der allgemeinen Relativitätstheorie. Annalen der Physik **49**, 769 (1916)
95. S. Weinberg, What is quantum field theory, and what did we think it is? (1997). arXiv: [hep-th/9702027](https://arxiv.org/abs/hep-th/9702027)
96. G. Källén, On the definition of the renormalization constants in quantum electrodynamics (1952). <https://doi.org/10.5169/seals-112316>. <https://www.e-periodica.ch/digbib/view?pid=hpa-001:1952:25::814>
97. L.D. Landau, On analytic properties of vertex parts in quantum field theory. Nuclear Phys. **13**, 181–192 (1959)
98. S. Mandelstam, Determination of the Pion-Nucleon scattering amplitude from dispersion relations and unitarity. general theory. Phys. Rev. **112**, 1344–1360 (1958)
99. S. Mandelstam, Analytic properties of transition amplitudes in perturbation theory. Phys. Rev. **115**, 1741–1751 (1959)
100. R.E. Cutkosky, Singularities and discontinuities of Feynman amplitudes. J. Math. Phys. **1**, 429–433 (1960)
101. D. Amati, S. Fubini, Dispersion relation methods in strong interactions. Ann. Rev. Nuclear Sci. (1962)
102. S. Weinberg, Feynman rules for any spin. Phys. Rev. **133**, B1318–B1332 (1964)
103. S. Weinberg, Feynman rules for any spin. II. Massless particles. Phys. Rev. **134**, B882–B896 (1964)
104. S. Weinberg, Feynman rules for any spin. III. Phys. Rev. **181**, 1893–1899 (1969)
105. S. Weinberg, Photons and gravitons in S-matrix theory: derivation of charge conservation and equality of gravitational and inertial mass. Phys. Rev. B **135**, B1049–B1056 (1964)
106. S. Weinberg, Photons and gravitons in perturbation theory: derivation of Maxwell's and Einstein's equations. Phys. Rev. B **138**, B988–B1002 (1965)
107. O. Steinmann, Ueber den Zusammenhang zwischen den Wightmanfunktionen und den retardierten Kommutatoren. Doctoral Thesis (ETH Zurich, 1960). <https://www.research-collection.ethz.ch/handle/20.500.11850/135473>

108. O. Steinmann, Wightman-Funktionen und retardierte Kommutatoren. II. *Helv. Phys. Acta* **33** (1960)
109. E. Remiddi, Dispersion relations for Feynman graphs. *Helvetica Physica Acta* **54**, 364–382 (1982)
110. W.L. Van Neerven, Dimensional regularization of mass and infrared singularities in two-loop on-shell vertex functions. *Nuclear Phys. B* **268**, 453–488 (1986)
111. J. Bosma, M. Sogaard, Y. Zhang, Maximal cuts in arbitrary dimension. *J. High Energy Phys.* **2017**, 51 (2017)
112. E. Remiddi, Generalised cuts and Wick rotations, in *Proceedings of Loops and Legs in Quantum Field Theory — PoS(LL2018)* (2018), p. 086
113. E. Remiddi, SCHOONSCHIP, the largest time equation and the continuous dimensional regularisation. *Acta Phys. Polon. B* **52**, 513 (2021)
114. R. Britto, F. Cachazo, B. Feng, New recursion relations for tree amplitudes of gluons. *Nuclear Phys. B* **715**, 499–522 (2005)
115. R. Britto, F. Cachazo, B. Feng, E. Witten, Direct proof of tree-level recursion relation in Yang-Mills theory. *Phys. Rev. Lett.* **94**, 181602 (2005)
116. R. Zwicky, A brief introduction to dispersion relations and analyticity, in *Proceedings, Quantum Field Theory at the Limits: from Strong Fields to Heavy Quarks (HQ 2016), Dubna, Russia, 18–30 July 2016* (2017), pp. 93–120
117. S. Bloch, D. Kreimer, Feynman amplitudes and Landau singularities for one-loop graphs. *Commun. Number Theory Phys.* **4**, 709–753 (2010)
118. S. Bloch, D. Kreimer, Cutkosky rules and outer space (2015). [arXiv: 1512.01705](https://arxiv.org/abs/1512.01705)
119. S. Abreu, R. Britto, C. Duhr, E. Gardi, The diagrammatic coaction and the algebraic structure of cut Feynman integrals (2018). [arXiv: 1803.05894](https://arxiv.org/abs/1803.05894)
120. F.V. Tkachov, A theorem on analytical calculability of 4-loop renormalization group functions. *Phys. Lett. B* **100**, 65–68 (1981)
121. S. Laporta, High-precision calculation of multi-loop Feynman integrals by difference equations. *Int. J. Modern Phys. A* **15**, 5087 (2000)
122. K.G. Chetyrkin, F.V. Tkachov, Integration by parts: the algorithm to calculate Beta-functions in 4 loops. *Nuclear Phys. B* **192**, 159–204 (1981)
123. D. Broadhurst, Quadratic relations between Feynman integrals. *PoS LL2018*, 053 (2018)
124. H.J. Munch, Feynman integral relations from GKZ hypergeometric systems. *PoS LL2022*, 042 (2022)
125. F.A. Berends, W.T. Giele, Recursive calculations for processes with n gluons. *Nuclear Phys. B* **306**, 759–808 (1988)
126. L. Dixon, Calculating Scattering Amplitudes Efficiently (1996). [arXiv: hep-ph/9601359](https://arxiv.org/abs/hep-ph/9601359)
127. S.J. Parke, T.R. Taylor, Amplitude for n-Gluon scattering. *Phys. Rev. Lett.* **56**, 2459–2460 (1986)
128. N. Arkani-Hamed, J.L. Bourjaily, F. Cachazo, A. Postnikov, J. Trnka, On-shell structures of MHV amplitudes beyond the planar limit. *JHEP* **06**, 179 (2015)
129. S. Badger, Automating QCD amplitudes with on-shell methods. *J. Phys.: Conf. Ser.* **762**, 012057 (2016)
130. D. Forde, On-shell recursion relations for n-point QCD. *Cont. Adv. QCD* **2006**, 472–478 (2007)
131. C. Schwinn, S. Weinzierl, On-shell recursion relations for all Born QCD amplitudes. *J. High Energy Phys.* **04**, 072 (2007)
132. N. Arkani-Hamed, J.L. Bourjaily, F. Cachazo, A.B. Goncharov, A. Postnikov, J. Trnka, *Scattering Amplitudes and the Positive Grassmannian* (Cambridge University Press, 2016). [arXiv: 1212.5605](https://arxiv.org/abs/1212.5605)
133. L. Mason, D. Skinner, Scattering amplitudes and BCFW recursion in twistor space. *J. High Energy Phys.* **01**, 064 (2010)
134. T. Cohen, H. Elvang, M. Kiermaier, On-shell constructibility of tree amplitudes in general field theories. *J. High Energy Phys.* **2011**, (2011). [https://doi.org/10.1007/JHEP04\(2011\)053](https://doi.org/10.1007/JHEP04(2011)053)

135. D.A. McGady, L. Rodina, Higher-spin massless S matrices in four dimensions. *Phys. Rev. D* **90**, 084048 (2014)
136. N. Arkani-Hamed, T.-C. Huang, Y.-t. Huang, Scattering amplitudes for all masses and spins (2017). [arXiv: 1709.04891](https://arxiv.org/abs/1709.04891)
137. F. Cachazo, A. Strominger, Evidence for a new soft graviton theorem (2014). [arXiv: 1404.4091 \[hep-th\]](https://arxiv.org/abs/1404.4091)
138. W.-M. Chen, Y.-t. Huang, D.A. McGady, Anomalies without an action (2014). [arXiv: 1402.7062](https://arxiv.org/abs/1402.7062)
139. D. Neill, I.Z. Rothstein, Classical space-times from the S-matrix. *Nuclear Phys. B* **877**, 177–189 (2013)
140. P. Benincasa, C. Boucher-Veronneau, F. Cachazo, Taming tree amplitudes in general relativity. *J. High Energy Phys.* **2007**, 057–057 (2007)
141. N.E.J. Bjerrum-Bohr, J.F. Donoghue, P. Vanhove, On-shell techniques and universal results in quantum gravity. *J. High Energy Phys.* **02**, 111 (2014)
142. N.E.J. Bjerrum-Bohr, P.H. Damgaard, G. Festuccia, L. Planté, P. Vanhove, General relativity from scattering amplitudes. *Phys. Rev. Lett.* **121**, 171601 (2018)
143. M. Campiglia, A. Laddha, Sub-subleading soft gravitons: new symmetries of quantum gravity? *Phys. Lett. B* **764**, 218–221 (2017)
144. D. Meltzer, Dispersion formulas in QFTs, CFTs and holography. *J. High Energy Phys.* **2021**, 98 (2021)
145. N. Dragon, The relativistic string, in *Trends in Elementary Particle Theory*, ed. by H. Rollnik, K. Dietz. Lecture Notes in Physics (1975), pp. 331–351
146. A.M. Polyakov, Quantum geometry of bosonic strings. *Phys. Lett. B* **103**, 207–210 (1981)
147. W. Siegel, Introduction to string field theory (1988). [arXiv: hep-th/0107094](https://arxiv.org/abs/hep-th/0107094)
148. R. Loll, Discrete approaches to quantum gravity in four dimensions. *Living Rev. Relativ.* **1**, 13 (1998)
149. J. Ambjørn, A. Görlich, J. Jurkiewicz, R. Loll, J. Gizbert-Studnicki, T. Trześniewski, The semiclassical limit of causal dynamical triangulations. *Nuclear Phys. B* **849**, 144–165 (2011)
150. D. Finkelstein, Space-time code. *Phys. Rev.* **184**, 1261–1271 (1969)
151. J. Myrheim, *Statistical Geometry* (1978). <https://cds.cern.ch/record/293594>
152. L. Bombelli, J. Lee, D. Meyer, R.D. Sorkin, Space-time as a causal set. *Phys. Rev. Lett.* **59**, 521–524 (1987)
153. G. Brightwell, R. Gregory, Structure of random discrete spacetime. *Phys. Rev. Lett.* **66**, 260–263 (1991)
154. L. Bombelli, J. Henson, R.D. Sorkin, Discreteness without symmetry breaking: a theorem. *Modern Phys. Lett. A* **24**, 2579–2587 (2009)
155. D.M.T. Benincasa, F. Dowker, Scalar curvature of a causal set. *Phys. Rev. Lett.* **104**, 181301 (2010)
156. S. Surya, The causal set approach to quantum gravity. *Living Rev. Relativ.* **22**, 5 (2019)
157. F. Finster, The principle of the fermionic projector: an approach for quantum gravity? *Quantum Gravity* 263–281 (2006)
158. F. Finster, Causal fermion systems: classical gravity and beyond, in *The Sixteenth Marcel Grossmann Meeting* (2023), pp. 661–678
159. D.M. Jackson, A. Kempf, A.H. Morales, A robust generalization of the Legendre transform for QFT. *J. Phys. A: Math. Theor.* **50**, 225201 (2017)
160. L. Euler, Elementa doctrinae solidorum. *Novi Commentarii academiae scientiarum Petropolitanae*, 109–140 (1758)
161. B. Bollobás, *Modern Graph Theory* (Springer, New York, NY, 1998), 394 p. <https://doi.org/10.1007/978-1-4612-0619-4>
162. C.W. Borchhardt, Über eine Interpolationsformel für eine Art symmetrischer Functionen un über deren Anwendung. *Abhandlungen der Königlichen Akademie der Wissenschaften in Berlin*, 1–20 (1860)
163. A. Cayley, A theorem on trees. *Q. J. Pure Appl. Math.* **23**, 376–378 (1889)

164. J.W. Moon, *Counting Labelled Trees*. Canadian Mathematical Monographs 1 (William Clowes and Sons, London, 1970)
165. S. Nakamoto, Bitcoin: a peer-to-peer electronic cash system (2008). <https://bitcoin.org/bitcoin.pdf>
166. G. Kirchhoff, Ueber die Auflösung der Gleichungen, auf welche man bei der Untersuchung der linearen Verteilung galvanischer Ströme geführt wird. Annalen der Physik **148**, 497–508 (1847)
167. S. Chaiken, D.J. Kleitman, Matrix tree theorems. J. Comb. Theory Ser. A **24**, 377–381 (1978)
168. F. Brown, K. Yeats, Spanning forest polynomials and the transcendental weight of Feynman graphs. Commun. Math. Phys. **301**, 357–382 (2011)
169. K. Yeats, *A Combinatorial Perspective on Quantum Field Theory*, vol. 15. Springer Briefs in Mathematical Physics (Springer International Publishing, Cham, 2017). <http://link.springer.com/10.1007/978-3-319-47551-6>
170. M. Golz, Dodgson polynomial identities (2018). <arXiv: 1810.06220>
171. C. Bogner, S. Weinzierl, Feynman graph polynomials. Int. J. Modern Phys. A **25**, 2585–2618 (2010)
172. E. Panzer, Feynman integrals and hyperlogarithms. Doctoral Thesis (Humboldt-Universität zu Berlin, Berlin, 2015). <arXiv: 1506.07243>
173. C.G. Bollini, J.J. Giambiagi, Dimensional regularization in configuration space. Phys. Rev. D **53**, 5761–5764 (1996)
174. N. Nakanishi, *Graph Theory and Feynman Integrals*, vol. 11. Mathematics and Its Applications (Gordon and Breach, Science Publishers Inc, New York London Paris, 1971)
175. N.N. Bogoliubow, O.S. Parasiuk, Ueber die Multiplikation der Kausalfunktionen in der Quantentheorie der Felder. Acta Math. **97**, 227–266 (1957)
176. D. Kreimer, M. Sars, W.D. van Suijlekom, Quantization of gauge fields, graph polynomials and graph homology. Ann. Phys. **336**, 180–222 (2013)
177. D. Kreimer, K. Yeats, Properties of the corolla polynomial of a 3-regular graph. Electr. J. Combin. P41–P41 (2013)
178. D. Prinz, The corolla polynomial for spontaneously broken Gauge theories. Math. Phys. Anal. Geom. **19**, 18 (2016)
179. H. Amann, J. Escher, *Analysis*. 2., korrig. Aufl., 1. Nachdr, Grundstudium Mathematik (Birkhäuser, Basel, 2008), 415 pp
180. N.I. Usyukina, On a representation for the three-point function. Theor. Math. Phys. **22**, 210–214 (1975)
181. D.M. Capper, G. Leibbrandt, Ward identities in a general axial gauge. I. Yang-Mills theory. Phys. Rev. D **25**, 1002–1008 (1982)
182. D.M. Capper, G. Leibbrandt, Ward identities in a general axial gauge. II. Quantum gravity. Phys. Rev. D **25**, 1009–1018 (1982)
183. M.S. Milgram, H.C. Lee, Tables of divergent Feynman integrals in the axial and light-cone gauges. J. Comput. Phys. **59**, 331–346 (1985)
184. G. Kramer, B. Lampe, Integrals for two-loop calculations in massless QCD. J. Math. Phys. **28**, 945–956 (1987)
185. K. Bönisch, F. Fischbach, A. Klemm, C. Nega, R. Safari, Analytic structure of all loop Banana amplitudes. J. High Energy Phys. **05**, 066 (2021)
186. D. Kreimer, Bananas: multi-edge graphs and their Feynman integrals. Lett. Math. Phys. **113**, 38 (2023)
187. R.N. Lee, A.A. Pomeransky, Critical points and number of master integrals. J. High Energy Phys. **2013**, 165 (2013)
188. I.M. Gelfand, M.M. Kapranov, A.V. Zelevinsky, *Discriminants, Resultants, and Multidimensional Determinants* (Springer, 1994). <https://link.springer.com/book/10.1007/978-0-8176-4771-1>
189. P. Vanhove, Feynman integrals, toric geometry and mirror symmetry (2018) <arXiv: 1807.11466>

190. R.P. Klausen, Hypergeometric series representations of Feynman integrals by GKZ hypergeometric systems (2019). [arXiv: 1910.08651](https://arxiv.org/abs/1910.08651)
191. P.A. Baikov, Explicit solutions of the n-loop vacuum integral recurrence relations (1996). [arXiv: hep-ph/9604254](https://arxiv.org/abs/hep-ph/9604254)
192. P.A. Baikov, Explicit solutions of the 3-loop vacuum integral recurrence relations. Phys. Lett. B **385**, 404–410 (1996)
193. P.A. Baikov, A practical criterion of irreducibility of multi-loop Feynman integrals. Phys. Lett. B **634**, 325–329 (2006)
194. A.V. Kotikov, Differential equation method. The calculation of N-point Feynman diagrams. Phys. Lett. B **267**, 123–127 (1991)
195. A.V. Kotikov, Differential equations method. New technique for massive Feynman diagram calculation. Phys. Lett. B **254**, 158–164 (1991)
196. E. Remiddi, Differential equations for Feynman graph amplitudes. Il Nuovo Cimento A **110**, 1435–1452 (1997)
197. T. Gehrmann, E. Remiddi, Differential equations for two-loop four-point functions. Nuclear Phys. B **580**, 485–518 (2000)
198. E. Nasrollahpouramami, Periods of Feynman diagrams and GKZ D-modules (2016). [arXiv: 1605.04970](https://arxiv.org/abs/1605.04970)
199. C. Berkesch, J. Forsgård, M. Passare, Euler–Mellin integrals and A-hypergeometric functions (2013). [arXiv: 1103.6273](https://arxiv.org/abs/1103.6273)
200. E. Panzer, Hepp’s bound for Feynman graphs and matroids. Annales de l’Institut Henri Poincaré D **10**, 31–119 (2022)
201. M. Borinsky, *Graphs in Perturbation Theory: Algebraic Structure and Asymptotics*. Springer Theses (Springer International Publishing, Cham, 2018)
202. G. Frobenius, Ueber die Congruenz nach einem aus zwei endlichen Gruppen gebildeten Doppelmodul. Journal für die reine und angewandte Mathematik **101**, 273–299 (1887)
203. W. Burnside, *Theory of Groups of Finite Order* (Cambridge University Press, Cambridge, 1897). <https://www.gutenberg.org/ebooks/40395>
204. J.H. Redfield, The theory of group-reduced distributions. Amer. J. Math. **49**, 433–455 (1927)
205. G. Pólya, Kombinatorische Anzahlbestimmungen für Gruppen, Graphen und chemische Verbindungen. Acta Math. **68**, 145–254 (1937)
206. D. Kreimer, K. Yeats, Diffeomorphisms of quantum fields. Math. Phys. Anal. Geom. **20**, 16, 16 (2017)
207. D. Kreimer, Anatomy of a gauge theory. Ann. Phys. **321**, 2757–2781 (2006)
208. M. Berghoff, A. Knispel, Complexes of marked graphs in gauge theory. Lett. Math. Phys. **110**, 2417–2433 (2020)
209. P.-H. Balduf, Perturbation theory of transformed quantum fields. Math. Phys. Anal. Geom. **23**, 33 (2020)
210. G.S. Ohm, Vorläufige Anzeige des Gesetzes, nach welchem Metalle die Contaktelektricität leiten. Annalen der Physik **80**, 79–88 (1825)
211. J. Mathews, Application of linear network analysis to Feynman diagrams. Phys. Rev. **113**, 381–381 (1959)
212. M. D’eramo, L. Peliti, G. Parisi, Theoretical predictions for critical exponents at the  $\lambda$ -point of bose liquids. Lettere al Nuovo Cimento **1971–1985**(2), 878–880 (1971)
213. A.N. Vasil’ev, Yu.M. Pis’mak, Yu.R. Khononen, 1/n Expansion: calculation of the exponents eta and nu in the order 1/n<sup>2</sup> for arbitrary number of dimensions. Theor. Math. Phys. **47**, 465–475 (1981)
214. N.I. Usyukina, Calculation of many-loop diagrams of perturbation theory. Theor. Math. Phys. **54**, 78–81 (1983)
215. D.I. Kazakov, Calculation of Feynman diagrams by the ‘Uniqueness’ method. Theor. Math. Phys. **58**, 223–230 (1984)
216. A. Suzuki, Analytic result for the one-loop massless triangle Feynman diagram (2007)
217. S. Hu, O. Schnetz, J. Shaw, K. Yeats, Further investigations into the graph theory of  $\phi^4$ -periods and the  $c_2$  invariant. Annales de l’Institut Henri Poincaré D **9**, 473–524 (2022)

218. C.G. Neumann, *Untersuchungen ü ber das logarithmische und Newton'sche Potential* (B.G. Teubner, Leipzig, 1877)
219. B.S. DeWitt, R. Stora, *Relativity, Groups and Topology: No. 2: Summer School Proceedings* (Elsevier Science Ltd, Amsterdam; New York : New York, N.Y, 1984), 1360 pp
220. D.M. Jackson, A. Kempf, A.H. Morales, Algebraic combinatorial Fourier and Legendre transforms with applications in perturbative quantum field theory (2019). [arXiv: 1805.09812](https://arxiv.org/abs/1805.09812)
221. K. Yeats, Growth estimates for Dyson-Schwinger equations (2008). [arXiv: 0810.2249](https://arxiv.org/abs/0810.2249) [math-ph]
222. M.P. Bellon, E.I. Russo, Ward-Schwinger-Dyson equations in Phi3\_6 quantum field theory. *Lett. Math. Phys.* **111**, 42 (2021)
223. F.J. Dyson, The S matrix in quantum electrodynamics. *Phys. Rev.* **75**, 1736–1755 (1949)
224. J. Schwinger, On the Green's functions of quantized fields. I. *Proc. Natl. Acad. Sci.* **37**, 452–455 (1951)
225. J. Schwinger, On the Green's functions of quantized fields. II. *Proc. Natl. Acad. Sci.* **37**, 455–459 (1951)
226. M. Gell-Mann, F. Low, Bound states in quantum field theory. *Phys. Rev.* **84**, 350–354 (1951)
227. P. Cvitanovic, *Field Theory*. Nordita Lecture Notes (1983), 115 pp. <https://chaosbook.org/FieldTheory/pdf.html>

# Chapter 2

## Hopf Algebra Theory of Renormalization



The second chapter is a detailed account of renormalization theory. The goal is, in particular, to demonstrate that the modern Hopf-algebraic formulation is entirely natural and compatible with the more traditional approach.

We start in Sect. 2.1 with a review of formal power series and Hopf algebras. While well-known to mathematicians, these topics are not usually taught in physics courses, and the section includes basic definitions and examples in order to be accessible to physicists. The core finding is that a Hopf algebra is a systematic framework that encodes, in one way or another, the insertion of combinatorial objects into each other. The canonical example for this is the insertion of power series,  $f(g(x))$ , which lies at the heart of all renormalization and can naturally be visualized in terms of rooted trees.

We examine renormalization of Feynman integrals in Sect. 2.2. The original physical motivation for renormalization is that the predictions from quantum field theory contain unspecified “bare” parameters, such as coupling constants, and that one needs to systematically infer these values from a measurement in order to make concrete physical predictions. Essentially, this is a problem of reverting and inserting power series, but it can equivalently be formulated in terms of Feynman graphs, or in terms of Dyson–Schwinger equations for Green functions.

Section 2.3 deals with questions of finiteness of renormalized Green functions. We see that for many, but not all, theories, renormalization has the additional effect of removing certain divergent expressions. In order to make the divergences explicit in intermediate calculations, we introduce two popular regularization schemes, dimensional regularization and analytic regularization. The systematic approach to renormalization allows us to give a relatively general, concrete definition of what constitutes a renormalization scheme.

## 2.1 Combinatorics and Hopf Algebras

In this section, we introduce the mathematical background needed for the later work. The concepts are well-known, but usually not taught in physics courses. The mathematically experienced reader might want to skip directly to Sect. 2.2.

### 2.1.1 Formal Power Series

**Definition 53.** Let  $R$  be a commutative ring and  $t$  a formal parameter.  $R[[t]]$  denotes the ring of all formal power series in the parameter  $t$  with coefficients in  $R$ . A *formal power series*  $f \in R[[t]]$  is a sequence of coefficients  $f_j \in R$ , each of which is indexed by a power of the parameter  $t$ , and extracted by  $[t^j]f(t) = f_j$ :

$$f(t) = \sum_{j=0}^{\infty} f_j t^j.$$

As opposed to ordinary power series and analytic functions, a formal power series has no notion of convergence.  $t$  is merely a symbol to indicate coefficients, it is not supposed to have any numerical value. Operations such as differentiation, integration or series reversion are identities between series coefficients, which agree with the formulas for analytic functions if the power series converges. For example, a formal power series can be differentiated using  $f_j \mapsto (j+1)f_{j+1}$  even if the series  $f(t)$  does not converge to a differentiable function in the ordinary sense. A standard reference on formal series is [1], for further details see [2–4].

**Definition 54.** [[5], [6, p. 134]] Let  $k \in \mathbb{N}_0$ ,  $n \in \mathbb{N}_0$  and  $k \leq n$  be fixed. The *partial Bell polynomial* is given by

$$B_{n,k}(x_1, x_2, x_3, \dots) = \sum_S \frac{n!}{j_1! j_2! \cdots j_n!} \left(\frac{x_1}{1!}\right)^{j_1} \left(\frac{x_2}{2!}\right)^{j_2} \left(\frac{x_3}{3!}\right)^{j_3} \cdots \left(\frac{x_n}{n!}\right)^{j_n},$$

where the sum extends over all sets  $\{j_i\}_{i \in \{1, \dots, k\}}$  which satisfy

$$S := \{j_i \geq 0 \forall i, \quad j_1 + j_2 + j_3 + \dots + j_k = k \quad j_1 + 2j_2 + 3j_3 + \dots + (n-k)j_{n-k} = n\}.$$

The generating function of the Bell polynomials is

$$\sum_{n=0}^{\infty} \sum_{k=0}^n B_{n,k} (x_1, x_2, \dots) u^k \frac{t^n}{n!} = \exp \left( u \sum_{j=1}^{\infty} x_j \frac{t^j}{j!} \right). \quad (2.1)$$

### Example 39: Some values of Bell polynomials.

The Bell polynomials contain several sets of combinatorially interesting numbers and have various relations amongst themselves and to other polynomials, see for example [6–9]. Some straightforward evaluations are:

$$B_{0,0} = 1,$$

$$B_{n,0} = 0, \quad n > 0,$$

$$B_{n,k} = 0, \quad k > n,$$

$$B_{n,1} = x_n, \quad n > 0,$$

$$B_{n,n} = x_1^n, \quad n > 0,$$

$$B_{n,2} = \sum_{k=1}^{n-1} \frac{1}{2} \binom{n}{k} x_k x_{n-k},$$

$$B_{n,k}(1, 2, 3, \dots) = \binom{n}{k} k^{n-k},$$

$$B_{n,k}(1^0, 2^1, 3^2, 4^3, \dots) = \binom{n-1}{k-1} n^{n-k}.$$

The Bell polynomials encode all combinatoric information to solve two of the standard tasks of formal power series, finding the inverse of a series, and concatenating two series.

**Theorem 19.** (Lagrange inversion [10–12]) Let  $f(t) = f_1 t + f_2 t^2 + f_3 t^3 + \dots$  be a formal power series and  $f^{-1}(t) =: g_1 t + g_2 t^2 + g_3 t^3 + \dots$  its combinatorial inverse, that is,  $f^{(-1)}(f(t)) = t$ . Let  $B_{n,k}$  be the partial Bell polynomials (Definition 54). Then for all  $n \geq 1$ ,

$$(f^{-1})_n = g_n = \frac{1}{n!} \sum_{k=1}^{n-1} \frac{1}{f_1^{n+k}} B_{n-1+k, k} (0, -2! f_2, -3! f_3, \dots), \quad g_1 = \frac{1}{f_1}.$$

Alternatively, for power series of exponential type,

$$f(t) = \sum_{n=0}^{\infty} f_n \frac{t^n}{n!}, \quad \text{and} \quad f^{-1}(t) =: g(t) = \sum_{n=1}^{\infty} g_n \frac{t^n}{n!},$$

$$g_n = \sum_{k=1}^{n-1} \frac{1}{f_1^{n+k}} B_{n-1+k, k} (0, -f_2, -f_3, \dots), \quad g_1 = \frac{1}{f_1}.$$

**Example 40: First coefficients of the inverse series.**

For a series  $f(t) = t + f_2 t^2 + f_3 t^3 + \dots$ , the inverse series begins with

$$f^{-1}(t) = t - f_2 t^2 + (-f_3 + 2f_2^2) t^3 + (-f_4 - 5f_2^3 + 5f_2 f_3) t^4 + \dots$$

Similarly, for an exponential series  $f(t) = t + f_2 \frac{t^2}{2!} + f_3 \frac{t^3}{3!} + \dots$ , the coefficients are

$$\begin{aligned} f^{-1}(t) &= t - f_2 \frac{t^2}{2} + (3f_2^2 - f_3) \frac{t^3}{3!} + (-15f_2^3 + 10f_2 f_3 - f_4) \frac{t^4}{4!} \\ &\quad + (105f_2^4 - 105f_2^2 f_3 + 10f_3^2 + 15f_2 f_4 - f_5) \frac{t^5}{5!} + \dots \end{aligned}$$

It might appear unaesthetic that the summands in the individual parentheses are monomials of different order, or weight. However, if one subtracts 1 from each index, the weights match. This is natural if one interprets them as rooted trees, see Example 54.

**Theorem 20.** (Faà di Brunos formula [13]) Let  $f(t) = f_0 + f_1 t + f_2 t^2 + \dots$  and  $g(t) = g_1 t + g_2 t^2 + g_3 t^3 + \dots$  be formal power series. Then, the coefficients  $h_n$  of the concatenation  $f(g(t)) =: h_0 + h_1 t + h_2 t^2 + \dots$  are given by  $h_0 = f_0$  and the partial Bell polynomials (Definition 54):

$$h_n = \sum_{k=1}^n \frac{k!}{n!} f_k \cdot B_{n,k} (1!g_1, 2!g_2, \dots, (n+1-k)!g_{n+1-k}), \quad n \geq 1.$$

If, instead,

$$f(t) = \sum_{n=0}^{\infty} f_n \frac{t^n}{n!}, \quad g(t) = \sum_{n=1}^{\infty} g_n \frac{t^n}{n!}, \quad f(g(t)) =: h(t) = \sum_{n=0}^{\infty} h_n \frac{t^n}{n!},$$

then  $h_0 = f_0$  and

$$h_n = \sum_{k=1}^n f_k \cdot B_{n,k} (g_1, \dots, g_{n+1-k}), \quad n \geq 1.$$

**Example 41: First coefficients of the concatenation of series.**

Let  $f(t) = f_0 + f_1 t + f_2 t^2 + \dots$  and  $g(t) = g_0 + g_1 t + g_2 t^2 + g_3 t^3 + \dots$ , then by theorem 20

$$\begin{aligned} h(t) = & f_0 + f_1 g_0 t + (f_2 g_0^2 + f_1 g_1) t^2 + (f_3 g_0^3 + 2f_2 g_0 g_1 + f_1 g_2) t^3 \\ & + (f_4 g_0^4 + 3f_3 g_0^2 g_1 + f_2 g_0^2 + 2f_2 g_1 g_2 + f_1 g_3) t^4 + \dots \end{aligned}$$

In Definitions 9 and 50 we have mentioned the Legendre transform without formally defining it. For formal power series, it is once again a statement about combinatorics of their coefficients, irrespective of analytic properties of functions [2, 3].

**Definition 55.** Let  $f(t)$  be a formal power series (Definition 53) and let  $u(t) = \partial_t f(t)$  be its formal derivative. Further, let  $t(u)$  be the combinatorial inverse of  $u(t)$ , given by Lagrange inversion (Theorem 19). The *Legendre transform* of  $f$  is defined as the series

$$g(u) := -t(u) \cdot u + f(t(u)).$$

### 2.1.2 Divergent Power Series

Physics courses tend to focus heavily on Taylor expansions, supporting the impression that every physically sensible function should be identified with a convergent power series. A similarly radical view was also prominent in mathematics 200 years ago, as Borel [14] reproduces a famous quote by Abel (1826):

Les séries divergentes sont en général quelque chose de bien fatal et c'est une honte qu'on ose y fonder aucune démonstration.

However, by now it is established that divergent series can contain a large amount of information on the “true” function they are supposed to represent. First steps in that direction were already taken in the 1800s [15]. The modern treatment is based on *Borel resummation* and, more generally, *resurgence*. This is a very active field of research with an immense literature, a starting point can be one of the reviews [16–21]. More sophisticated examples related to physics can be found in [22–37].

**Example 42: Divergence of the QED perturbation series.**

Without any mathematical analysis of the growth behavior of coefficients, one can conclude from physical arguments that the Dyson series (Eq. (1.40)) in QED (Example 23) can not be convergent [38]. The perturbative expansion parameter is the fine structure constant  $\alpha$  [39], which has a positive value  $\alpha \approx \frac{1}{137} > 0$  in nature. If the Green functions of QED were convergent functions of  $\alpha$  around the expansion point  $\alpha = 0$ , then it would be possible to continue them to small negative  $\alpha$ , where they are still convergent. Physically, a negative value of  $\alpha$  corresponds to an “electrodynamics” where equal charges attract each other and opposite charges are repelled. By charge conservation, quantum fluctuations can only produce pairs of particles with opposite charges. In a world where  $\alpha < 0$ , these particles would repel each other instead of merging back to the vacuum. Consequently, if  $\alpha < 0$  the vacuum would “decay” into a large number of particles. The ground state of this theory would not be a vacuum state, but a state filled with matter. It would be unreasonable to assume that the Green functions of a field in such a state are “similar” to those in a vacuum state. Consequently, the Green functions of QED must abruptly have different properties as soon as  $\alpha$  becomes infinitesimally negative, they can not be analytic around  $\alpha = 0$ . Hence the (renormalized) perturbation series should not be expected to be convergent.

**Definition 56.** An *asymptotic power series* is a formal power series (Definition 53) where the remainder term  $R_N(t)$ , defined by

$$f(t) =: \sum_{n=0}^N f_n t^n + R_N(t),$$

fulfills

$$\lim_{t \rightarrow 0} t^{-N} |R_N(t)| = 0, \quad \text{for each fixed } N.$$

Every convergent power series is asymptotic, but the converse is not true. Observe that for a convergent power series one has, instead of a limit  $t \rightarrow 0$  as in Definition 56,

$$\lim_{N \rightarrow \infty} |R_N(t)| = 0, \quad t \text{ fixed.}$$

**Definition 57.** [[40]] For  $k \in \mathbb{N}$ , a formal power series  $\sum_{n=0}^{\infty} f_n t^n$  is called *Gevrey- $k$*  if

$$\sum_{n=0}^{\infty} \frac{f_n}{(n!)^k} t^n$$

has a non-zero radius of convergence.

**Definition 58.** Let  $f(t)$  be a formal power series. The *Borel transform* of  $f$  is the power series obtained by the mapping  $B : f_n \mapsto \frac{f_n}{n!}$ , that is

$$f(t) = \sum_{n=0}^{\infty} f_n t^n \quad \Leftrightarrow \quad B[f](u) = \sum_{n=0}^{\infty} \frac{f_n}{n!} u^n.$$

The complex  $u$ -plane is called *Borel plane*. The inverse mapping  $L : f_n \mapsto n! f_n$  is called *Laplace transform*.

The Borel transform is convergent near the origin if the original function is Gevrey-1 (Definition 57), and this is the case we will be dealing with for the rest of the thesis. For convergent power series, Definition 58 is consistent with the customary analytic definition of the Laplace transform (in the variable  $\frac{1}{t}$ ), given by the integral

$$L[f](t) = \frac{1}{t} \int_0^{\infty} du \ f(u) e^{-u \frac{1}{t}} = \int_0^{\infty} du \ e^{-u} f(ut),$$

upon recalling the definition of the Gamma function (Definition 5)  $\int_0^{\infty} du \ e^{-u} u^n = \Gamma(n+1) = n!$ .

### Example 43: Borel transform of factorially divergent series.

Consider the factorially divergent power series

$$f(t) := \sum_{n=0}^{\infty} (-1)^n n! t^n.$$

Its Borel transform (Definition 58) is analytic at the origin  $u = 0$ ,

$$B[f](u) = \sum_{n=0}^{\infty} (-1)^n \frac{n!}{n!} u^n = \frac{1}{1+u}.$$

It turns out that, starting from a divergent Gevrey-1 power series  $f(t)$ , performing the Borel transform and then the Laplace transform, one can potentially arrive at a well-defined function. The outcome is called *Borel resummation*  $S[f]$  of the series,

$$S[f](t) = L[B[f]](t) = \frac{1}{t} \int du B[f](u) e^{-u\frac{1}{t}}. \quad (2.2)$$

The fundamental reason why a Borel resummation can work is that the divergence of the original series corresponds to the Borel transform being non-holomorphic in the Borel plane. In doing the Laplace transform, one can chose an integration contour that avoids singularities in the Borel plane, and hence arrive at a finite result.

#### Example 44: Exponential integral.

The Borel resummation of Example 43 is

$$S[f](t) = \frac{1}{t} \int_0^\infty du \frac{1}{1+u} e^{-u\frac{1}{t}} = \frac{1}{t} e^{\frac{1}{t}} \int_1^\infty du \frac{e^{-u\frac{1}{t}}}{u} = \frac{1}{t} e^{\frac{1}{t}} E_1\left(\frac{1}{t}\right).$$

Here we have introduced the exponential integral (incomplete Gamma function)

$$E_1(z) := \int_1^\infty dt \frac{e^{-zt}}{t} = \int_z^\infty dt \frac{e^{-t}}{t}.$$

The exponential integral has, for  $z > 0$ , the convergent series representation

$$E_1(z) = -\gamma_E - \ln|z| - \sum_{k=1}^{\infty} \frac{(-z)^k}{k!k}.$$

By Borel resummation, we have replaced  $f(t)$  by a convergent series in  $z = \frac{1}{t}$ . Despite its intimidating looks, the Borel resummed function  $S[f](t)$  is finite at the origin  $t = 0$ , and its derivatives are exactly the coefficients of the original series  $f(t)$  from Example 43. Hence,  $f(t)$  is a tailor series of  $S[f](t)$  around  $t = 0$ , but this Taylor series diverges, while the function  $S[f](t)$  has a finite numeric value for  $t > 0$ .

Curiously, this example of resummation was given by Euler [41] 66 years before Abel's comment at the beginning of the present section.

Example 44 illustrates that the class of formal power series in one variable  $t$  is too small to capture Borel transforms, we at least need to allow for powers of exponentials such as  $e^{\frac{1}{t}}$ . Including also logarithms, the resulting class of series is a generalization of formal power series by the name of *transseries*, see [42] for an introduction.

**Definition 59.** [[43–45]] A *transseries* is a formal power series (Definition 53) in the three monomials  $t$ ,  $e^{-\frac{S_q}{t}}$  and  $\ln t$ . It has the form

$$f(t) = \sum_{p=0}^{\infty} \sum_{q=0}^{\infty} \sum_{l=1}^{q-1} c_{p,q,l} \cdot t^p \cdot e^{-q \cdot \frac{S_q}{t}} \cdot (\ln t)^l, \quad (2.3)$$

where  $c_{p,q,l}$  are constants and  $S_q(t)$  can be a transseries itself, but it is not allowed to nest infinitely many transseries this way.

The term  $q \cdot S$  is called the  *$q$ -instanton action*, in more general cases it can also be a non-trivial function  $S_q(t)$ . Transseries are sufficient to express all functions definable from addition, multiplication and exponentiation [46], and the field of transseries is closed under differentiation, integration, composition, inversion, Borel transforms and various other operations [47, 48].

As seen in Example 43, the Borel transform (Definition 58) of a Gevrey-1 (Definition 57) power series can have poles in the Borel plane. Assume that there is a simple pole at  $u = u_0$  closest to the origin,

$$B[f](u) = \phi(u) \left(1 - \frac{u}{u_0}\right)^{-\beta}, \quad (2.4)$$

where  $\phi(u)$  is smooth at  $u_0$  and  $\beta \in \mathbb{R}$ . This functional form has an implication for the series expansion  $B[f](u) =: \sum_{n=0}^{\infty} b_n u^n$  of  $B[f](u)$  near the origin  $u = 0$ . Namely for  $n \rightarrow \infty$  the coefficients asymptotically behave like

$$b_n \sim \frac{\Gamma(n + \beta)}{\Gamma(n + 1)\Gamma(\beta)} \frac{1}{u_0^n} \left( \phi(u_0) - \frac{(\beta - 1)u_0\phi'(u_0)}{(n + \beta - 1)} + \dots \right). \quad (2.5)$$

Since  $b_n$  are the coefficients of the Borel transform (Definition 58), the coefficients of the original function  $f(t)$  grow like

$$f_n \sim \frac{\Gamma(n + \beta)}{\Gamma(\beta)} \frac{1}{u_0^n} \left( \phi(u_0) - \frac{(\beta - 1)u_0\phi'(u_0)}{(n + \beta - 1)} + \dots \right). \quad (2.6)$$

A detailed discussion as well as many more examples and theorems regarding asymptotic power series can be found in the book [49].

**Definition 60.** If the coefficients of a formal power series  $f$  grow asymptotically like

$$f_n \sim S \cdot A^n \cdot \Gamma(n + \beta) \left(1 + \mathcal{O}\left(\frac{1}{(n + \beta - 1)}\right)\right), \quad n \rightarrow \infty,$$

then  $f$  is called a *factorially divergent power series* with *Stokes constant*  $S$ .

Owing to  $\Gamma(n + \beta)/\Gamma(n) \sim n^\beta$ , all factorially divergent power series are Gevrey-1 (Definition 57).

The relationship Eq. (2.6) is the first step towards a general theory of *resurgence*: We observe that the asymptotic factorial growth of the coefficients of a divergent power series contains information about poles in the Borel plane. The next step would be to examine the general form of the Laplace transform of Eq. (2.4), which is the Borel resummation of  $f(t)$ . One finds that the coefficients of the subleading corrections in Eq. (2.6) reappear as coefficients of the perturbative fluctuations around the 1-instanton term  $e^{-\frac{S}{t}}$  (Definition 59) of the resummed transseries.

On the other hand, the subleading corrections in Eq. (2.6) are given by derivatives  $\phi^{(n)}(u_0)$  of the function  $\phi(u)$  from Eq. (2.4). Assume that  $B[f](u)$  has a second pole, other than  $u = u_0$ , at  $u = u_1$ . Then the asymptotic growth of the expansion coefficients of  $\phi(u)$  around  $u_0$  will be dominated by the pole at  $u_1$ , in the same way that the pole at  $u_0$  determines the coefficients  $b_n$  in Eq. (2.5). This construction can be continued indefinitely, until eventually all correction coefficients in Definition 60 are expressed via the locations and exponents of poles of the Borel transform. They in turn determine the fluctuations around all  $q$ -instanton terms in the resummed function  $B[f](t)$  (Eq. (2.2)).

In this heuristic account, we have skipped all sorts of difficulties which can potentially appear. The detailed mathematical theory of resurgence was developed by Ecalle [50], by now there are comprehensive reviews such as [19, 20]. Some particularly instructive cases are used in [33] to compute asymptotic expansions.

In practical calculations, we often only know a finite set of coefficients  $\{f_n\}$  and we want to determine the subleading corrections of factorially divergent powerseries (Definition 60), after stripping off a known factorial growth. That is, we want to compute the constants  $\{a_j\}$  for in the asymptotic expansion

$$f_n \sim a_0 + a_1 \frac{1}{n} + a_2 \frac{1}{n^2} + \mathcal{O}\left(\frac{1}{n^3}\right), \quad n \rightarrow \infty. \quad (2.7)$$

Formally, the coefficients can be extracted from their definition, like  $a_0 = \lim_{n \rightarrow \infty} f_n$ , but this procedure is imprecise unless we know  $f_n$  for very high  $n$ . It is more practical to algebraically eliminate subleading corrections. Define a discrete series derivation operator

$$\Delta f_n := f_{n+1} - f_n. \quad (2.8)$$

With this operator, we find

$$\Delta(nf) = (n+1)f_{n+1} - nf_n = a_0 + \mathcal{O}\left(\frac{1}{n^2}\right).$$

The quantity  $\Delta(nf)$  can be expected to converge to  $a_0$  more quickly than  $f_n$  itself.

**Definition 61.** [[51]] Assume a sequence  $\{f_n\}$  behaves asymptotically like Eq. (2.7). Let  $\Delta(f) := \{f_{n+1} - f_n\}$ , then the order- $k$  Richardson extrapolation is the sequence

$$R_k[f] := \frac{1}{k!} \Delta^k (n^k f) = a_0 + \mathcal{O}\left(\frac{1}{n^{k+1}}\right).$$

The order- $k$  Richardson extrapolation operator is only applicable if we know at least  $k + 1$  elements of the sequence  $\{f_n\}$ . Moreover, the cancellations of small differences in computing  $\Delta^k(n^k f)$  usually require that we know the numbers  $f_n$  to arbitrary precision, and not just as numerical estimates.

The higher asymptotic coefficients  $a_{j>0}$  can be extracted by applying Richardson extrapolation (Definition 61) to a sequence where lower coefficients are subtracted, for example

$$\Delta(n^2(f - a_0)) = (n + 1)^2(f_{n+1} - a_0) - n^2(f_n - a_0) = a_1 + \mathcal{O}\left(\frac{1}{n^2}\right).$$

### 2.1.3 Basics of Hopf Algebra Theory

In the present section, we review those aspects of Hopf algebra theory which become important later in the thesis. A comprehensive introduction to Hopf algebras is contained in the book [52]. Here and in the following,  $\otimes$  denotes a tensor product while  $\circ$  denotes concatenation of maps.

**Definition 62.** Let  $K$  be a field. An associative, unital *algebra*  $A$  over  $K$  is a vector space endowed with two vector space homomorphisms

$$\begin{aligned} m : A \otimes A &\rightarrow A && \text{(product),} \\ \mathbb{1} : K &\rightarrow A && \text{(unit),} \end{aligned}$$

subject to the conditions

$$\begin{aligned} m \circ (m \otimes \text{id}) &= m \circ (\text{id} \otimes m) && \text{(associativity of } m\text{),} \\ m \circ (\mathbb{1} \otimes \text{id}) &= m \circ (\text{id} \otimes \mathbb{1}) = \text{id} && \text{(\mathbb{1} is a left and right unit).} \end{aligned}$$

Strictly speaking, there is a unit element  $1$  in the field  $K$ , and the homomorphism  $\mathbb{1}$ , and a unit element in the algebra. We will slightly abuse notation by calling the

latter also  $\mathbb{1}$ , namely we identify  $\mathbb{1}(1) =: \mathbb{1} \in A$ . Further, we will generally assume our algebras to be commutative, that is  $m(a, b) = m(b, a) \forall a, b \in A$ .

**Example 45: Algebra of quadratic matrices.**

For  $n \in \mathbb{N}$ , the  $n \times n$ -matrices are the elements of an algebra, where  $m$  is matrix multiplication and  $\mathbb{1}$  is the identity matrix.

**Definition 63.** Let  $K$  be a field. A coassociative counital *coalgebra*  $C$  over  $K$  is a vector space equipped with two vector space homomorphisms

$$\begin{aligned}\Delta : C &\rightarrow C \otimes C && \text{(coproduct),} \\ \tilde{\mathbb{1}} : C &\rightarrow K && \text{(counit),}\end{aligned}$$

subject to the conditions

$$\begin{aligned}(\text{id} \otimes \Delta) \circ \Delta &= (\Delta \otimes \text{id}) \circ \Delta && \text{(coassociativity of } \Delta\text{),} \\ (\tilde{\mathbb{1}} \otimes \text{id}) \circ \Delta &= (\text{id} \otimes \tilde{\mathbb{1}}) \circ \Delta = \text{id} && (\tilde{\mathbb{1}} \text{ is a left and right unit).}\end{aligned}$$

**Definition 64.** A coalgebra  $C$  is *cocommutative* if the two factors of the coproduct are interchangeable, that is, if for all elements  $h \in C$ ,

$$\Delta(h) = \sum_i h'_i \otimes h''_i = \sum_i h''_i \otimes h_i.$$

**Definition 65.** The *augmentation ideal*  $\text{Aug}$  is the kernel of  $\tilde{\mathbb{1}}$ . By  $P_{\text{Aug}}$  we denote the projection to the augmentation ideal such that the identity map is  $\text{id} = P_{\text{Aug}} + \tilde{\mathbb{1}}$ .

**Definition 66.** The *reduced coproduct* of a coalgebra  $C \ni h$  is

$$\Delta_1(h) := (P_{\text{Aug}} \otimes P_{\text{Aug}})\Delta(h).$$

**Definition 67.** Let  $C$  be a coalgebra. An element  $h \in C$  is called *primitive* if  $\Delta(h) = h \otimes 1 + 1 \otimes h$ , or equivalently  $\Delta_1(h) = 0$ . An element  $h \in C$  is called *grouplike* if  $\Delta(h) = h \otimes h$ .

**Example 46: Polynomials as algebra and coalgebra.**

Let  $K$  be a field. The polynomials  $K[t]$  in one variable  $t$  are an algebra, where  $m$  is the ordinary product and  $\mathbb{1}$  is the polynomial  $1t$ . For example, let  $K[t] \ni f = 1 + 3t^2$  and  $K[t] \ni g = 2 + t$ , then

$$m(f, g) = f \cdot g = (1 + 3t^2)(2 + t) = 2 + t + 6t^2 + 3t^3.$$

Polynomials can be given the structure of a coalgebra by the following construction: First, define the counit  $\tilde{\mathbb{1}}(t^n) := \delta_{n,0} \in K$ . Consequently, the augmentation ideal (Definition 65) are all those polynomials which are not constants.

Next, we let  $\Delta(t) := 1 \otimes t + t \otimes 1$ . This implies that the polynomial  $t$  is a primitive element (Definition 67). Then, by the homomorphism property  $\Delta(ab) = \Delta(a)\Delta(b)$ , one finds the coproduct of any monomial,

$$\Delta(t^n) = \sum_{j=0}^n \binom{n}{j} t^j \otimes t^{n-j}, \quad \tilde{\mathbb{1}}t^n = \delta_{n,0} \in K,$$

The two factors in the tensor product can be exchanged, the coproduct is cocommutative (Definition 64). By linearity, one obtains the coproduct of any polynomial, for example

$$\begin{aligned} \Delta(1 + 3t^2) &= 1 \cdot \Delta(t^0) + 3 \cdot \Delta(t^2) = 1 \otimes 1 + 3(1 \otimes t^2 + 2t \otimes t + t^2 \otimes 1), \\ \Delta(2 + t) &= 2(1 \otimes 1) + 1 \otimes t + t \otimes 1. \end{aligned}$$

**Definition 68.** Let  $K$  be a field. A *bialgebra*  $B$  over  $K$  is a vector space over  $K$  endowed with the vector space homomorphisms

$$\begin{array}{ll} m : B \otimes B \rightarrow B & (\text{product}), \\ \mathbb{1} : K \rightarrow B & (\text{unit}), \\ \Delta : B \rightarrow B \otimes B & (\text{coproduct}), \\ \tilde{\mathbb{1}} : B \rightarrow K & (\text{counit}), \end{array}$$

such that  $(B, m, \mathbb{1})$  is an algebra (Definition 62), and  $(B, \Delta, \tilde{\mathbb{1}})$  is a coalgebra (Definition 63), and  $\Delta$  and  $\tilde{\mathbb{1}}$  are morphisms of the algebra  $(B, m, \mathbb{1})$ . Explicitly, the latter requirement means

$$\begin{aligned}\Delta \circ m &= (m \otimes m) \circ (\text{id} \otimes \text{flip} \otimes \text{id}) \circ (\Delta \otimes \Delta), \\ \mathbb{1} \otimes \mathbb{1} &= \Delta \circ \mathbb{1}, \\ \tilde{\mathbb{1}} \otimes \tilde{\mathbb{1}} &= \tilde{\mathbb{1}} \circ \Delta, \\ \tilde{\mathbb{1}} \circ \mathbb{1} &= \text{id},\end{aligned}$$

where  $\text{flip}(a \otimes b) = b \otimes a$  denotes exchange of two arguments

### Example 47: Polynomials as bialgebra.

In Example 46, we saw that the polynomials  $K[t]$  form an algebra and a coalgebra. In fact, they form a bialgebra. It is straightforward to see that the product and the coproduct are compatible because the coproduct essentially is the binomial theorem. For the two example polynomials above, one can verify the compatibility by an explicit calculation:

$$\begin{aligned}\Delta \circ m(f, g) &= \Delta(2 + t + 6t^2 + 3t^3) \\ &= 2(1 \otimes 1) + 1 \otimes t + t \otimes 1 + 6(1 \otimes t^2 + 2t \otimes t + t^2 \otimes 1) \\ &\quad + 3(1 \otimes t^3 + 3t \otimes t^2 + 3t^2 \otimes t + t^3 \otimes 1) \\ &= m(1 \otimes 1 + 3(1 \otimes t^2 + 2t \otimes t + t^2 \otimes 1), 2(1 \otimes 1) + t \otimes 1 + 1 \otimes t) = m(\Delta f, \Delta g).\end{aligned}$$

**Definition 69.** A *Hopf algebra*  $H$  over  $K$  is a bialgebra (Definition 68) equipped with a linear map

$$S : H \rightarrow H \quad (\text{antipode})$$

such that

$$m(S \otimes \text{id}) \Delta = m(\text{id} \otimes S) \Delta = \mathbb{1} \circ \tilde{\mathbb{1}}.$$

The antipode automatically satisfies  $S(\mathbb{1}) = \mathbb{1}$ . Definitions 65 and 69 imply for the antipode:

$$S(h) = -m(S \otimes P_{\text{Aug}})(\Delta(h)), \quad h \in \text{Aug}. \quad (2.9)$$

For a primitive (Definition 67) element  $h \in H$  we immediately find

$$S(h) = -h. \quad (2.10)$$

Similarly, a grouplike element  $h \in H$  has  $S(h) = h^{-1}$ , such that  $m(h \otimes h^{-1}) = \mathbb{1}$ .

**Definition 70.** A Hopf algebra  $H$  is *graded* if

$$\begin{aligned} H &= \bigoplus_{k=0}^{\infty} H^{(k)}, \\ \Delta H^{(n)} &\subseteq \sum_{i+j=n} H^{(i)} \otimes H^{(j)} \\ H^{(i)} \cdot H^{(j)} &\subseteq H^{(i+j)}. \end{aligned}$$

For  $h \in H$ , the degree is denoted  $|h| \in \mathbb{N}_0$ , that is  $|h| = n \Leftrightarrow h \in H^{(n)}$ . We let  $Y : H \rightarrow H$  be the linear operator counting the degree,

$$Y(h) = |h| \cdot h \quad \forall h \in H.$$

The degree counting operator of Definition 70 is a *derivation*, that means, for  $h_1, h_2 \in H$  it fulfills

$$Y(h_1 \cdot h_2) = Y(h_1) \cdot h_2 + h_1 \cdot Y(h_2). \quad (2.11)$$

If, in a graded Hopf algebra,  $H^{(0)} = K\mathbb{1}$  (that is,  $H^{(0)}$  is 1-dimensional), then this Hopf algebra is called *connected*. In that case Eq. (2.9) is sufficient to uniquely define an antipode, therefore, every graded connected bialgebra is automatically a Hopf algebra.

### Example 48: Polynomials as Hopf algebra.

The bialgebra of polynomials (Example 47) is actually a graded, connected, cocommutative Hopf algebra  $H_P$ . The grade of a polynomial is the exponent of its highest monomial. The operator  $Y$  is a derivation (Eq. (2.11)), for example

$$\begin{aligned} Y((3t^2 + 1)(t^4 - t^2)) &= Y(3t^6 - 2t^4 - t^2) = 6(3t^6 - 2t^4 - t^2) = 6(3t^2 + 1)(t^4 - t^2) \\ &= 2(3t^2 + 1)(t^4 - t^2) + (3t^2 + 1)4(t^4 - t^2) \\ &= Y(3t^2 + 1) \cdot (t^4 - t^2) + (3t^2 + 1) \cdot Y(t^4 - t^2). \end{aligned}$$

$H_P$  is connected because there is a unique degree zero polynomial  $\mathbb{1} = 1 \in H_P$ , not to be confused with e.g. the polynomial 5, which is  $5 \in K$  multiplied with  $1 \in H_P$ . So the grade zero component (Definition 70) is indeed  $H_P^{(0)} = K \cdot \mathbb{1}$ .

Finally,  $H_P$  has an antipode. Trivially,  $S(\mathbb{1}) = \mathbb{1} \in H_P$ . The monomial  $t$  is primitive, its antipode is  $S(t) = -t$ . Using Eq. (2.9), we find the antipode

$$S(t^2) = -2 S(t)t - S(1)t^2 = 2t^2 - t^2 = t^2.$$

Generally  $S(t^n) = (-1)^n t^n = (-t)^n$ , as can be seen from the induction step

$$S(t^n) = - \sum_{k=0}^n \binom{n}{k} S(t^k) P_{\text{Aug}}(t^{n-k}) = - \sum_{k=0}^{n-1} \binom{n}{k} (-1)^k 1^{n-k} t^n = -(1-1)^n t^n + (-1)^n t^n.$$

**Definition 71.** A *Hopf ideal*  $I$  of a Hopf algebra  $H$  (Definition 69) is a subset  $I \subset H$  such that

$$\begin{aligned} H \cdot I &\subset I, \\ \Delta(I) &\subset H \otimes I + I \otimes H, \\ S(I) &\subset I. \end{aligned}$$

If  $I \subset H$  is a Hopf ideal then the quotient Hopf algebra mimics the usual construction of dividing a ring by an ideal: the elements are equivalent up to addition of elements of the ideal:

$$\frac{H}{I} := \{h \in H \text{ where } h_1 = h_2 \Leftrightarrow h_1 - h_2 \in I\}. \quad (2.12)$$

Expressed differently, dividing by an ideal means that all elements of the ideal are set to zero. Consequently, their coproduct and antipode are also set to zero.

**Lemma 21.** Let  $H$  be a Hopf algebra (Definition 69) and  $I \subset H$  a Hopf ideal (Definition 71). Then, the quotient  $U := \frac{H}{I}$  (Eq. (2.12)) is a sub Hopf algebra, that is,

$$\Delta(U) \subseteq U \otimes U, \quad S(U) \subseteq U.$$

We have seen in Definition 67 that primitive elements in the Hopf algebra are characterized by a particularly simple coproduct. This notion can be generalized, namely, we count how often a coproduct has to be applied recursively before the remainder becomes primitive.

**Definition 72.** The *iterated coproduct* of a Hopf algebra  $H$  is

$$\Delta^1 := \Delta, \quad \Delta^k := (\Delta \otimes \text{id} \otimes \cdots \otimes \text{id}) (\Delta \otimes \text{id} \cdots \otimes \text{id}) \cdots (\Delta \otimes \text{id}) \Delta.$$

It is well-defined thanks to coassociativity (Definition 63) of  $\Delta$ . Further, using the projector  $P_{\text{Aug}}$  (Definition 65), we define the iterated reduced coproduct,

$$\Delta_0 := P_{\text{Aug}}, \quad \Delta_1 := (P_{\text{Aug}} \otimes P_{\text{Aug}}) \Delta, \quad \Delta_k := P_{\text{Aug}}^{\otimes(k+1)} \Delta^k.$$

The iterated reduced coproduct is a generalization of the reduced coproduct  $\Delta_1$  from Definition 66. It induces the *coradical filtration*

$$H^0 \subset H^1 \subset \dots \quad \text{where} \quad H^n := \{x \in H \mid \Delta_n(x) = 0\}. \quad (2.13)$$

**Definition 73.** Let  $H \ni h$  be a Hopf algebra. Using the iterated coproduct (Definition 72), the *coradical degree* of  $h$  is defined as

$$\text{cor}(h) = n \Leftrightarrow \Delta_n = 0 \text{ and } \Delta_k \neq 0 \quad \forall k < n.$$

An element  $h \in H$  is primitive (Definition 67) if and only if it has coradical degree one. The coradical filtration is not to be confused with the grading (Definition 70). But there is the bound

$$\text{cor}(h) \leq |h| \quad \forall h \in H. \quad (2.14)$$

### Example 49: Polynomials, coradical degree.

Using the coproduct (Example 46) of polynomials, one finds that

$$\begin{aligned} \Delta^1(t^2) &= \Delta(t^2) = \mathbb{1} \otimes t^2 + 2t \otimes t + t^2 \otimes \mathbb{1}, & \Delta_1(t^2) &= 2t \otimes t \\ \Delta^2(t^2) &= \mathbb{1} \otimes \mathbb{1} \otimes t^2 + 2(\mathbb{1} \otimes t + t \otimes \mathbb{1}) \otimes t + \Delta(t^2) \otimes \mathbb{1}, & \Delta_2(t^2) &= 0 \end{aligned}$$

and hence  $\text{cor}(t^2) = 2$ . A simple inductive proof shows that  $\text{cor}(t^n) = n$ .

The homomorphisms of a Hopf algebra  $H$  can be given the structure of a cochain complex as follows [53–55]: For  $n \in \mathbb{N}_0$ , the  $n$ -cochains are the elements of  $\text{Hom}(H, H^{\otimes n})$ , that is, linear maps  $L_n : H \rightarrow H^{\otimes n}$ . Here,  $H^{\otimes 0} = K$  is the underlying field. The coboundary operator is defined as

$$b_n : \text{Hom}(H, H^{\otimes n}) \rightarrow \text{Hom}(H, H^{\otimes(n+1)}),$$

$$b_n L_n := (\text{id} \otimes L_n) \Delta + \sum_{j=1}^n \left( (-1)^j \text{id}^{\otimes(j-1)} \otimes \Delta \otimes \text{id}^{\otimes(n-j)} \right) L_n + (-1)^{n+1} L_n \otimes \mathbb{1}.$$

We will only need the first two instances,

$$b_0 L_0 = m (\text{id} \otimes L_0) \Delta - \mathbb{1} L_0,$$

$$b_1 L_1 = (\text{id} \otimes L_1) \Delta - \Delta L_1 + L_1 \otimes \mathbb{1}.$$

**Definition 74.** Let  $H$  be a Hopf algebra (Definition 69) and  $L_n$  be a homomorphism  $H \rightarrow H^{\otimes(n+1)}$ . If  $b_n L_n = 0$  then  $L_n$  is called  $n$ -cocycle. If  $L_n = b_{n-1} M_{n-1}$  for a homomorphism  $M_{n-1}$ , then  $L_n$  is called  $n$ -coboundary.

Automatically, every  $n$ -coboundary is also a  $n$ -cocycle because the coassociativity of  $\Delta$  (Definition 63) implies  $b_{n+1} \circ b_n = 0$ . The quotient space, that is, those  $n$ -cocycles which are not  $n$ -coboundaries, is called the  $n$ th *cohomology group*.

**Definition 75.** Let  $H$  be a Hopf algebra. A *Hochschild 1-cocycle* is a homomorphism  $B_+ : H \rightarrow H$  such that, for all  $h \in H$ ,

$$\Delta(B_+(h)) = B_+(h) \otimes \mathbb{1} + (\text{id} \otimes B_+) \Delta(h).$$

**Lemma 22.** Hochschild-1 cocycles  $B_+$  (Definition 75) have the following properties:

1. The reduced coproduct (Definition 66) is  $\Delta_1(B_+(h)) = h \otimes B_+(\mathbb{1}) + (\text{id} \otimes B_+) \Delta_1(h)$ .
2. If  $B_+$  is a 1-cocycle, then from any homomorphism  $L_0 : H \mapsto \mathbb{K}$  we obtain another 1-cocycle by adding the 0-coboundary  $b_0 L_0$  to  $B_+$ .

3.  $B_+(\mathbb{1})$  is primitive (Definition 67) and it has no freedom to add 0-coboundaries.
4.  $B_+$  increases the coradical degree (Definition 73) by exactly one.

**Proof** (1)  $(P_{\text{Aug}} \otimes P_{\text{Aug}})\Delta(B_+(h)) = (P_{\text{Aug}} \otimes P_{\text{Aug}})(\text{id} \otimes B_+)(\mathbb{1} \otimes h + h \otimes \mathbb{1} + \Delta_1(h))$ .  
(2) If we add a 0-coboundary  $L_1 = b_0 L_0$  then  $b_1(B_+ + L_1) = b_1 B_+ + b_1 b_0 L_0 = b_1 B_+$  since  $b_1 b_0 = 0$ . Hence,  $(B_+ + L_1)$  is a 1-cocycle, fulfilling  $\Delta(B_+(h) + L_1(h)) = (B_+(h) + L_1(h)) \otimes \mathbb{1} + (\text{id} \otimes (B_+ + L_1))\Delta(h)$ .  
(3) Every homomorphism  $L_0 : H \rightarrow K$  maps  $\mathbb{1} \mapsto 1 \in K$ . Therefore,  $b_0 L_0(\mathbb{1}) = (\text{id} \otimes L_0)(\mathbb{1} \otimes \mathbb{1}) - L_0(\mathbb{1}) \otimes \mathbb{1} = 0$ . Consequently, a 0-boundary necessarily vanishes when applied to  $\mathbb{1}$  and  $B_+(\mathbb{1}) + b_0 L_0(\mathbb{1}) = B_+(\mathbb{1})$ . Its coproduct is

$$B_+(\mathbb{1}) \otimes \mathbb{1} + (\text{id} \otimes B_+)(\mathbb{1} \otimes \mathbb{1}) = B_+(\mathbb{1}) \otimes \mathbb{1} + \mathbb{1} \otimes B_+(\mathbb{1}),$$

which certifies that  $B_+(\mathbb{1})$  is primitive (Definition 67).

(4) Induction on the coradical degree. Let  $h$  have coradical degree  $n$ , so  $\Delta_{n-1}(h) \neq 0$ .

$$\Delta(B_+(h)) = B_+(h) \otimes \mathbb{1} + (\text{id} \otimes B_+)(h \otimes \mathbb{1} + \mathbb{1} \otimes h + \Delta_1(h)) = \dots + h \otimes B_+(\mathbb{1}) + \dots$$

It is  $\Delta_n = (\Delta_{n-1} \otimes P_{\text{Aug}})\Delta$ . This coproduct does not vanish since  $P_{\text{Aug}} B_+(\mathbb{1}) \neq 0$  and  $\Delta_{n-1}(h) \neq 0$ . But all higher ones vanish since  $\Delta_1(B_+(\mathbb{1})) = 0$  by (2).  $\square$

**Definition 76.** Let  $H$  be a Hopf algebra (Definition 69) and  $A$  an algebra (Definition 62). An  $A$ -valued *character* is a map

$$\phi : H \rightarrow A,$$

linear under multiplication, that is,  $\phi(m_H(h_1, h_2)) = m_A(\phi(h_1) \otimes \phi(h_2))$  where  $m_H$  is the multiplication in  $H$  and  $m_A$  is the multiplication in  $A$ .

**Definition 77.** Let  $\phi, \psi : H \rightarrow A$  be two characters (Definition 76) from a Hopf algebra  $H$  to an algebra  $A$ . The *convolution product*  $\phi \star \psi$  is again a character, defined as

$$\phi \star \psi = m_A(\phi \otimes \psi)\Delta.$$

Together with the convolution product  $\star$ , the characters  $H \rightarrow A$  form a group  $G_A^H$ . Using Definition 69, one confirms that the inverse of a character  $\phi \in G_A^H$  is given by

$$\phi^{-1} = \phi \circ S. \quad (2.15)$$

Coassociativity of the coproduct (Definition 63) implies associativity of the convolution product,

$$(\phi_1 \star \phi_2) \star \phi_3 = \phi_1 \star (\phi_2 \star \phi_3).$$

### Example 50: Polynomials, Hopf algebra characters.

Let  $H_P = K[t]$  from Example 48. A group  $G_K^{H_P}$  of  $K$ -valued characters  $\phi_t$  on  $H_P$  is given by the evaluation at  $a \in K$ . Namely, let  $p \in H_P$ , then

$$\phi_a \in G_K^{H_P}, \quad \phi_a(p) = p(a) \in K.$$

This group  $G_K^{H_P}$  with operation  $\star$  is isomorphic to the group  $K$  under addition. Using the coproduct from Example 46, we see that the basis elements behave as expected:

$$(\phi_a \star \phi_b)(t^n) = m(\phi_a \otimes \phi_b) \Delta(t^n) = (a + b)^n = \phi_{a+b}(t^n).$$

The antipode from Example 48 gives the inverse character according to Eq. (2.15),

$$\begin{aligned} (\phi_a \star \phi_a^{-1})(t^n) &= m(\phi_a \otimes \phi_a \circ S) \sum_{j=0}^n \binom{n}{j} t^j \otimes t^{n-j} = m(\phi_a \otimes \phi_a) \sum_{j=0}^n \binom{n}{j} t^j \otimes (-t)^{n-j} \\ &= \sum_{j=0}^n \binom{n}{j} a^j \otimes (-a)^{n-j} = 0^n = \phi_0(t^n) = \phi_{a-a}(t^n). \end{aligned}$$

Recall that the neutral element of addition is indeed 0, not 1.

We remark that the behavior of many familiar functions under addition of their arguments can be expressed through a coalgebra [56]. Another such case, apart from polynomials, are trigonometric functions such as  $\sin(a + b) = \sin(a)\cos(b) + \cos(a)\sin(b) =: (\Delta \sin)(a, b)$ . Especially, the exponential function  $e^{a+b} = e^a \cdot e^b$  amounts to a grouplike (Definition 67) element,  $\Delta e^\cdot = e^\cdot \otimes e^\cdot$ . This case will become important later in Sect. 3.2.3.

**Theorem 23.** (Milnor-Moore-Cartier-Quillen [57, 58]) The dual of a Hopf algebra is the universal enveloping algebra of a Lie algebra.

The character group  $G_K^H$  (Definition 76) is a Lie group, see [59, 60] for details.

**Definition 78.** An *infinitesimal character* is a character (Definition 76)  $\sigma : H \rightarrow A$  which fulfills, for  $h_1, h_2 \in H$ ,

$$\sigma(h_1 h_2) = \tilde{\mathbb{1}}(h_1)\sigma(h_2) + \tilde{\mathbb{1}}(h_2)\sigma(h_1).$$

The set of all infinitesimal characters form a Lie algebra  $\mathfrak{g}_A^H$  with Lie bracket given by the convolution product (Definition 77):  $[\sigma_1, \sigma_2] := \sigma_1 \star \sigma_2 - \sigma_2 \star \sigma_1$ .

The elements of  $\mathfrak{g}_A^H$  act as generators of the Lie group  $G_A^H$  by the exponential map

$$G_A^H \ni \phi = \exp^\star(\sigma) := \sum_{n=0}^{\infty} \frac{1}{n!} \sigma^{\star n} = \tilde{\mathbb{1}} + \sigma + \frac{1}{2} \sigma \star \sigma + \dots \quad (2.16)$$

The action of the exponential map on the Hopf algebra  $H$  motivates the notions of primitive and grouplike elements (Definition 67): If  $p \in H$  is primitive, then

$$H \ni g := \mathbb{1} + p + \frac{1}{2} p^2 + \dots = \exp(p) \quad (2.17)$$

is grouplike, as can be verified by explicitly using  $\Delta(p) = p \otimes \mathbb{1} + \mathbb{1} \otimes p$ . In a Hopf algebra, the set of all grouplike elements forms a group under multiplication  $m$ .

### Example 51: Polynomials, infinitesimal characters.

Polynomials can trivially be identified with their Taylor series at the origin. Any character  $\phi_a$  (Example 50) is given by the series

$$\phi_a = \exp\left(a \left. \frac{\partial}{\partial t} \right|_{t=0}\right).$$

The infinitesimal characters are thus the first derivatives,  $\sigma_a = a\partial_t|_{t=0}$ . They extract the linear coefficient of a polynomial. They fulfil the condition Definition 78 because the product of two polynomials can only have a linear term if one of the two factors contains a constant term, and  $\tilde{\mathbb{1}}$  is exactly the projection onto constants. Concretely, for two monomials

$$\begin{aligned} \sigma_a(t^m) &= a\partial_t(t^m)|_{t=0} = am \cdot t^{m-1}|_{t=0} = am \cdot \delta_{m=1}, \\ \sigma_a(t^m \cdot t^n) &= a\partial_t(t^{m+n})|_{t=0} = a(m+n)\delta_{m+n=1} = \tilde{\mathbb{1}}(t^n)\sigma_a(t^m) + \tilde{\mathbb{1}}(t^m) \cdot \sigma_a(t^n). \end{aligned}$$

### 2.1.4 Faà di Bruno Hopf Algebra

In Sect. 2.1.3, we have used polynomials as a central example for a Hopf algebra, where the coproduct merely corresponds to the usual product between two polynomials. The Faà di Bruno Hopf algebra  $H_{\text{FdB}}$  [61–64] expresses formal power series, but, contrary to the polynomials, the coproduct operation is not multiplication of series, but concatenation. Also, the algebraic perspective is different: The algebra elements are no longer the power series themselves, but rather their coefficient extraction operators. Let  $f(t)$  be a formal power series (Definition 53), then the elements of  $H_{\text{FdB}}$  are the operators  $\mathfrak{C}_n$  for  $n \in \mathbb{N}$ , extracting the  $n$ th coefficient,

$$f \mathfrak{C}_n = f_n = [t^n] f(t) = \frac{1}{n!} \partial_t^n f(t) \Big|_{t=0}. \quad (2.18)$$

Observe the notation: The operator  $\mathfrak{C}_n$  extracts coefficients of the power series, and hence, it effectively acts to the left, and the notation is consistent with Sect. 2.1.3. A formal power series  $f(t)$  over a field  $K$  can then be viewed as a linear map that associates a value – the coefficient  $f_n \in K$  – to each of the algebra elements  $\mathfrak{C}_n$ :

$$\begin{aligned} f : H_{\text{FdB}} &\rightarrow K[t] \\ \{f_1, f_2, \dots\} &\mapsto f_1 t + f_2 t^2 + \dots \end{aligned}$$

We demand that this map is a character (Definition 76) of the Hopf algebra, where the product of power series is concatenation, not ordinary multiplication:

$$f \star g := f \circ g.$$

On the other hand, the concatenation product  $\star$  of characters amounts by definition to the coproduct in the Hopf algebra,

$$(f \star g) \mathfrak{C}_n = (f(g(t))) \mathfrak{C}_n = m \circ (f(t) \otimes g(t)) \Delta \mathfrak{C}_n. \quad (2.19)$$

In this way, one obtains the coproduct of the Faà di Bruno Hopf algebra. From Faà di Bruno's theorem 20, we know the coefficients of series concatenation, namely

$$(f \star g) \mathfrak{C}_n = \sum_{k=1}^n \frac{k!}{n!} f_k \cdot B_{n,k} (1!g_1, \dots, (n+1-k)!g_{n+1-k}).$$

In this formula,  $f_j$  and  $g_j$  are once again coefficients, extracted from the power series  $f, g$  by suitable operators  $\mathfrak{C}_j$ . Therefore, the coproduct of the Faà di Bruno Hopf algebra reads

$$\Delta \mathfrak{C}_n = \sum_{k=1}^n \frac{k!}{n!} \mathfrak{C}_k \otimes B_{n,k} (1!\mathfrak{C}_1, 2!\mathfrak{C}_2, \dots, (n+1-k)!\mathfrak{C}_{n+1-k}). \quad (2.20)$$

Generally,  $f(g(t))$  and  $g(f(t))$  are not the same series, while  $f(t)g(t)$  and  $g(t)f(t)$  are. Consequently, the coproduct of the polynomials (Example 46) is cocommutative (Definition 64), but the coproduct Eq. (2.20) of the Faà di Bruno Hopf algebra is not.

From Eq. (2.20), one obtains  $\Delta(\mathfrak{C}_1) = \mathfrak{C}_1 \otimes \mathfrak{C}_1$ , this element is grouplike (Definition 67). By rescaling all involved power series, we set  $\mathfrak{C}_1 = \mathbb{1} \in H_{\text{FdB}}$  to ensure that  $\mathfrak{C}_1$  has an inverse. The Faà di Bruno Hopf algebra is connected. The inverse character is given by the antipode Eq. (2.15). The antipode can be constructed either by demanding that the character  $f^{-1}$  be the inverse series under concatenation, or by using Eq. (2.9). Unsurprisingly, the result in both cases is the Lagrange inversion formula (theorem 19), where  $f_1 = 1$ :

$$S\mathfrak{C}_n = \frac{1}{n!} \sum_{k=1}^{n-1} (-1)^k B_{n-1+k,k} (0, 2!\mathfrak{C}_2, 3!\mathfrak{C}_3, \dots) = \frac{1}{n!} \sum_{k=1}^{n-1} B_{n-1+k,k} (0, -2!\mathfrak{C}_2, -3!\mathfrak{C}_3, \dots). \quad (2.21)$$

### Example 52: Faà di Bruno Hopf algebra, coproducts and antipodes.

The first coproducts Eq. (2.20) are

$$\begin{aligned} \Delta(\mathfrak{C}_2) &= \mathfrak{C}_2 \otimes \mathbb{1} + \mathbb{1} \otimes \mathfrak{C}_2, \\ \Delta(\mathfrak{C}_3) &= \mathfrak{C}_3 \otimes \mathbb{1} + \mathbb{1} \otimes \mathfrak{C}_3 + 2\mathfrak{C}_2 \otimes \mathfrak{C}_2, \\ \Delta(\mathfrak{C}_4) &= \mathfrak{C}_4 \otimes \mathbb{1} + \mathbb{1} \otimes \mathfrak{C}_4 + \mathfrak{C}_2 \otimes (\mathfrak{C}_2^2 + 2\mathfrak{C}_3) + 3\mathfrak{C}_3 \otimes \mathfrak{C}_2. \end{aligned}$$

Compare this with the coefficients in Example 41: The coproduct indeed computes the concatenation of series. Likewise, the antipodes agree with Example 40,

$$\begin{aligned} S\mathfrak{C}_2 &= -\mathfrak{C}_2, \\ S\mathfrak{C}_3 &= -\mathfrak{C}_3 + 2\mathfrak{C}_2^2, \\ S\mathfrak{C}_4 &= -\mathfrak{C}_4 + 5\mathfrak{C}_2\mathfrak{C}_3 - 5\mathfrak{C}_2^3. \end{aligned}$$

There is a beautiful graphical representation of the Faà di Bruno Hopf algebra as rooted trees, shown in Fig. 2.1. We identify  $\mathfrak{C}_n$  with a vertex with  $n$  lower edges, called *hairs*. This can be motivated intuitively:  $\mathfrak{C}_n$  corresponds to a term  $t^n$  in a power series, so it “accepts one input value”  $t$  and “returns”  $n$  copies of it, which it multiplies (Fig. 2.1).

A concatenation  $f \circ g$  of two functions corresponds to replacing the argument  $t$  of  $f(t)$  with the series  $g$ , so attaching the vertices of  $g$  at the lower ends of the

$$\mathfrak{C}_1 = \text{ } \bullet \text{ } \quad \mathfrak{C}_2 = \text{ } \bullet \text{ } \bullet \text{ } \quad \mathfrak{C}_3 = \text{ } \bullet \text{ } \bullet \text{ } \bullet \text{ } \quad \mathfrak{C}_4 = \text{ } \bullet \text{ } \bullet \text{ } \bullet$$

**Fig. 2.1** Identification of the Faà di Bruno Hopf Hopf algebra elements with trees

vertices of  $f$ . We obtain plane trees (that is, two trees that count as different if they can not be transformed into each other without crossing edges.) of depth two with arbitrary many vertices. A tree with  $n$  hairs contributes to  $(f \circ g)\mathfrak{C}_n$ , so to the coefficient  $t^n$  of  $f(g(t))$ . With the notation of Eq. (2.20), the left factor in the tensor product corresponds to the upper vertex, the right factor is the lower vertex. Note that each tree with  $n$  hairs corresponds to a partition of  $\{1, \dots, n\}$  into  $k$  non-empty sets, where  $k$  is the number of hairs of the upper vertex. In total,  $\Delta\mathfrak{C}_n$  is given by all these plane trees, so it is a sum over all such partitions. This is precisely the sum over Bell polynomials (Definition 54). Consequently, counting trees reproduces the formula Eq. (2.20) for the coproduct.

### **Example 53: Series concatenation as trees.**

Let us see explicitly how trees reproduce the coefficients of  $f(g(t))$  from Example 41. We show the trees and below them the corresponding terms in the coproduct (Example 52), where the left factor is the upper vertex and the right factor are the lower vertices.

$$\begin{array}{ccccccccc}
\text{Diagram 1} & + & \text{Diagram 2} & + & \text{Diagram 3} & + & \text{Diagram 4} & + 2 & \text{Diagram 5} \\
\mathfrak{C}_1 \otimes \mathfrak{C}_1 & + & \mathfrak{C}_2 \otimes \mathfrak{C}_1^2 & + & \mathfrak{C}_1 \otimes \mathfrak{C}_2 & + & \mathfrak{C}_3 \otimes \mathfrak{C}_1^3 & + 2 & \mathfrak{C}_2 \otimes \mathfrak{C}_2 \mathfrak{C}_1 \\
f_1 g_1 t & + & \left( f_2 g_1^2 + f_1 g_2 \right) t^2 & + & \left( f_3 g_1^3 + 2 f_2 g_2 g_1 + f_1 g_3 \right) t^3 & + \dots
\end{array}$$

Note how the combinatorial factor 2 exactly accounts for the two ways of attaching the lower vertices to the upper one, namely left or right. These two trees count as different because they can not be transformed into each other without crossing an edge (i.e. we are counting plane trees). On the other hand, the two resulting trees give the same contribution  $f_2 g_2 g_1$ , so instead of considering them independently, we only draw one of them and count it twice. The mechanism that gives rise to *two* trees, which are ultimately identical, is the same that transforms  $ab + ba \rightarrow 2ab$  if we compute  $(a + b)^2$ : The terms are the same due to commutativity of the product, but still we need both of them.

Knowing the coproduct, the antipode can be constructed recursively using Eq. (2.9). We skip the details, the end result is that the antipode is given by the sum of *all* trees, not just the ones of depth 2. Additionally, each vertex of the trees carries a factor  $-1$ . For any  $n$ ,  $S\mathfrak{C}_n$  corresponds to the sum of all those trees with exactly  $n$  leaves. There are infinitely many such trees which differ from each other just by adding chains of 2-valent vertices. These infinite sums, viewed as a geometric series, eventually correspond to the factors  $\frac{1}{f_1}$  in theorem 19, compare Eq. (1.61).

The condition  $f_1 = 1$ , or equivalently  $\mathfrak{C}_1 = \mathbb{1}$ , amounts to leaving out all such chains and keeping only non-trivial trees. Of course, formalizing the tree-counting with the help of set partitions reproduces the Lagrange inversion theorem 19 and Eq. (2.21).

### Example 54: Series inversion as trees.

Assume  $\mathfrak{C}_1 = \mathbb{1}$ , then there are no 2-valent vertices and the edges contribute a factor  $\mathbb{1}$  to the value of a tree. To improve readability, we also leave out all  $+$  signs between the various summands.

•						
$\mathbb{1}$	$(-\mathfrak{C}_2)$	$(-\mathfrak{C}_3)$	$2(-\mathfrak{C}_2)^2$	$(-\mathfrak{C}_4)$	$4(-\mathfrak{C}_2)^3$	$2(-\mathfrak{C}_2)(-\mathfrak{C}_3)$
$1t$	$-f_2 t^2$	$+ (-f_3 + f_2^2) t^3$	$+ (-f_4 + 5f_2 f_3 - 5f_2^3) t^4$			

Observe that different tree topologies contribute to the same monomial at order  $t^4$ . As claimed, the end result equals the inverse series given in Example 40.

$S\mathfrak{C}_n$  amounts to the sum of all trees with alternating signs. To facilitate notation, define

$$\mathfrak{B}_n := i^n S\mathfrak{C}_n. \quad (2.22)$$

This operator extracts the  $n$ th coefficient of the inverse of a given power series,

$$f(t)\mathfrak{B}_n = i^n [t^n] f^{-1}(t) = i^n n! \left. \frac{\partial^n f^{-1}(t)}{\partial t^n} \right|_{t=0}. \quad (2.23)$$

The antipode of  $\mathfrak{B}_n$  essentially extracts coefficients of  $f$ ,

$$f(t)(S\mathfrak{B}_n) = f^{-1}(t)\mathfrak{B}_n = i^n [t^n] f(t) = f(t)(i^n \mathfrak{C}_n).$$

### Example 55: Faà di Bruno Hopf algebra, inverse operators.

Using Eq. (2.21), one finds

$$\begin{aligned} \mathfrak{B}_4 &= (-\mathfrak{C}_4 + 5\mathfrak{C}_2\mathfrak{C}_3 - 5\mathfrak{C}_2^3) i^4, \\ \mathfrak{B}_5 &= (-\mathfrak{C}_5 + 6\mathfrak{C}_2\mathfrak{C}_4 + 3\mathfrak{C}_3^2 - 21\mathfrak{C}_2^2\mathfrak{C}_3 + 14\mathfrak{C}_2^4) i^5. \end{aligned}$$

Up to the factors  $i^n$ , we have merely exchanged the meaning of  $\mathfrak{C}_n$  and  $S\mathfrak{C}_n$  with  $S\mathfrak{B}_n$  and  $\mathfrak{B}_n$ . This appears to be a technical subtlety, but becomes convenient for the coproduct  $\Delta(\mathfrak{B}_n)$ . The latter now computes the coefficients of two concatenated *inverse* series. Note that by Coxeter's rule,  $f^{-1} \circ g^{-1} = (g \circ f)^{-1}$ , so

$$\begin{aligned} m(f \otimes g) \Delta(\mathfrak{B}_n) &= (f \circ g) \mathfrak{B}_n = (g^{-1} \circ f^{-1})^{-1} \mathfrak{B}_n = i^n (g^{-1} \circ f^{-1}) \mathfrak{C}_n \\ &= i^n m(g \otimes f) (S \otimes S) \Delta \mathfrak{C}_n = m(f \otimes g) i^n \text{flip}(S \otimes S) \Delta(\mathfrak{C}_n). \end{aligned}$$

Translating this to our graphical representation,  $\mathfrak{B}_j$  equals the sum of all plane trees with exactly  $j$  leaves. Observe the difference between  $\Delta(\mathfrak{B}_n)$  and  $\Delta(\mathfrak{C}_n)$  (Eq. (2.20)): For  $\Delta(\mathfrak{C}_n)$ , we sum over all trees of depth exactly two, where the upper vertex is the left factor in the tensor product, whereas for  $\Delta(\mathfrak{B}_n)$ , there is no restriction to the depth of trees, and the factors are exchanged, the upper part of the cut tree, which is a tree itself, represents the right factor in the tensor product. The lower part of the cut tree is a product of trees and appears to the left.

**Theorem 24.** Let  $\mathfrak{B}_n$  be the operator from eq. (2.22). In the graphical representation as rooted trees, where  $\mathfrak{B}_n$  corresponds to the sum of all trees with  $n$  leaves, the coproduct is given by

$$\Delta(\mathfrak{B}_n) = \sum_{C=R \cup P} \mathfrak{B}_P \otimes \mathfrak{B}_R.$$

Here,  $C$  is the set of all possible cuts of the trees which separate the root from the leaves, including the trivial cuts above the root or below the leaves. Each path in the trees from above the roots to below the leaves is cut exactly once.  $R$  denotes the component including the root,  $P$  is a disjoint union of trees containing all the leaves, and  $\mathfrak{B}_P$  denotes the product of all the  $\mathfrak{B}_j$  corresponding to the disjoint trees. The summands  $\mathfrak{B}_R, \mathfrak{B}_P$  correspond to individual trees, they become well-defined tree-sums  $\mathfrak{B}_n$  only in the sum over  $C$ .

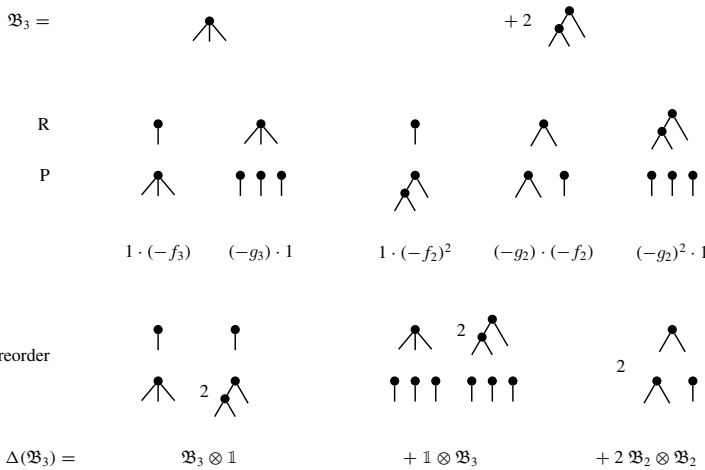
**Proof** The non-trivial assertion of this theorem is that, when summing over all cuts of all trees representing some  $\mathfrak{B}_n$ , the cut components once again add up to  $\mathfrak{B}_j$ , without any trees missing or doubled. On the one hand, this is a standard fact of enumerating *all* plane trees: One obtains exactly *all* trees by joining all smaller trees in all possible ways, and our cut formula reverses this operation. On the other hand, it can be shown by expressing everything in terms of  $\Delta(\mathfrak{C}_n)$ : Cutting the trees of depth two produces all trees of depth one, that is, vertices. Using eq. (2.22), we replace each vertex with  $j$  leaves with a sum of all trees with  $j$  leaves.  $\square$

**Example 56: Faà di Bruno Hopf algebra, coproduct of inverse operators.**

To understand the coproduct of theorem 24, let us examine  $\Delta(\mathfrak{B}_3)$  in detail. That means, we are looking for the coefficient of  $t^3$  in the concatenation

$$g^{-1}(f^{-1}(t)) = \dots + (-f_3 + 2f_2^2 - g_3 + 2g_2^2 + 2f_2g_2) \cdot t^3 + \dots$$

$\mathfrak{B}_3$  is represented by two different trees, both of which have 3 leaves. They are shown in the top row. Below them are all the possibilities of cutting them according to theorem 24. Next, we reorder the cut components to obtain  $\mathfrak{B}_j$ .



The individual trees we obtained in  $R$  and  $P$  are not necessarily Hopf algebra elements  $\mathfrak{B}_j$ , but, as expected, they appear in just the right multiplicities that the total sum consists of  $\mathfrak{B}_j$ . A similar construction produces the coproduct

$$\Delta(\mathfrak{B}_4) = \mathfrak{B}_4 \otimes \mathbb{1} + \mathbb{1} \otimes \mathfrak{B}_4 + \mathfrak{B}_2^2 \otimes \mathfrak{B}_2 + 2\mathfrak{B}_3 \otimes \mathfrak{B}_2 + 3\mathfrak{B}_2 \otimes \mathfrak{B}_3.$$

For more details about the Faà di Bruno Hopf algebra, see for example [64–66]. We remark that, instead of ordinary power series  $f(t) = f_1 t + f_2 t^2 + \dots$ , it is more customary to base the whole construction on exponential power series  $f(t) = f_1 \frac{t}{1!} + f_2 \frac{t^2}{2!} + \dots$ . This only changes numerical prefactors, namely, one then has to consider *all* permutations of lower edges, not only the planar ones. For example, the factor 2 in  $\Delta(\mathfrak{C}_3)$  becomes a 3, in accordance with the three ways to permute the leaves of the tree in Example 53.

At least two close cousins of the Faà di Bruno Hopf algebra are worth mentioning: Firstly, the Connes-Moscovici Hopf algebra  $H_{\text{CM}}$  which appears in the study of differential operators [67]. The simplest case of  $H_{\text{CM}}$  is almost isomorphic to  $H_{\text{FdB}}$ , only

that  $H_{\text{CM}}$  is slightly more general in that it allows the involved power series to have non-vanishing constant terms, and non-unit linear coefficients, see [64, Section 9] for details. This simple version of  $H_{\text{FdB}}$  is often expressed such that its basis elements  $\delta_k \in H_{\text{CM}}$  extract the coefficients of the *logarithm*  $\ln(\partial_t f^{-1}(t))$  of inverted power series. The elements  $\delta_k \in H_{\text{CM}}$  can again be represented by certain rooted trees [68], as shown in Example 60.

Secondly, the Butcher group [69–72] encodes the concatenation of Runge-Kutta numerical integration methods [73, 74]. If one expresses the involved functions as power series, it is not too surprising that the combinatorics of this process is once more expressible by joining certain rooted trees.

We mentioned the correspondence between trees and their generating formal power series in Sect. 1.3.10. Now we are in the position to understand the Legendre transform (Definition 55) graphically: Given some vertices, by inverting the series, compare to Eq. (2.23), it produces all possible trees made from these vertices. For details on counting graphs, see [2, 3, 33, 36, 75].

**Example 57:**  $\phi^3$  theory, counting treelevel graphs.

To illustrate how the Legendre transform can in principle be used to count graphs, consider  $\phi^3$  theory in  $D = 0$  spacetime dimensions. This means that there is no kinematic dependence, every Feynman graph evaluates to a constant number. Without integrals, the classical action (Definition 7) equals the Lagrangian (Example 3); it is the generating function of the vertices. The 3-valent vertex has amplitude  $\lambda_3$  and an edge has amplitude  $\frac{1}{p}$ . The Legendre transform (Definition 55) can be computed in closed form:

$$\begin{aligned} \mathcal{L}(t) &= \frac{1}{2}pt^2 - \frac{\lambda_3}{3!}t^3, \quad \frac{\partial \mathcal{L}}{\partial t} = pt - \frac{1}{2}\lambda_3t^2 \quad \left(\frac{\partial \mathcal{L}}{\partial t}\right)^{-1} = \frac{p - \sqrt{p^2 - 2\lambda_3t} - p}{\lambda_3} \\ - \left(\frac{\partial \mathcal{L}}{\partial t}\right)^{-1} \cdot t + \mathcal{L}\left(\left(\frac{\partial \mathcal{L}}{\partial t}\right)^{-1}\right) &= \frac{p^3}{3\lambda_3^2} - \frac{pt}{\lambda_3} - \frac{\left(p^2 - 2\lambda_3t\right)^{\frac{3}{2}}}{3\lambda_3^2} \\ &= -\frac{1}{p} \frac{t^2}{2!} - \frac{\lambda_3}{p^3} \frac{t^3}{3!} - 3 \frac{\lambda_3^2}{p^5} \frac{t^4}{4!} - 15 \frac{\lambda_3^3}{p^7} \frac{t^5}{5!} - 105 \frac{\lambda_3^4}{p^9} \frac{t^6}{6!} - \dots \\ &= -\sum_{n=2}^{\infty} (2n-5)!! \frac{\lambda_3^{n-2}}{p^{2n-3}} \frac{t^n}{n!}. \end{aligned}$$

In the resulting series, the coefficient of  $\frac{t^n}{n!}$  corresponds to all trees with  $n$  external edges. Powers of  $\lambda_3$  count vertices, powers of  $p^{-1}$  count edges. Hence, there are exactly  $(2n-5)!!$  trees with  $n$  external edges, and each of them contains  $(n-2)$  3-valent vertices and  $2n-3$  edges (of which  $n$  are external edges). These numbers of course satisfy the Euler characteristic Eq. (1.44).

### 2.1.5 Connes-Kreimer Hopf Algebra

As discussed in Sect. 2.1.4, the Faà di Bruno Hopf algebra has a natural interpretation as rooted trees, and its coproduct is given by cutting these trees into an upper and a lower part (Theorem 24). The elements  $\mathfrak{B}_n$  of the (inverse) Faà di Bruno Hopf algebra are the sums of all rooted trees with  $n$  leaves. The coproduct and the antipode in the Faà di Bruno Hopf algebra do not actually require that the Hopf algebra elements are sums of *all* rooted trees, it is possible to understand these operations for each individual tree. To this end, we need a Hopf algebra where the elements are not sums of trees, but individual trees. This is the Connes-Kreimer Hopf algebra of rooted trees  $H_{CK}$  [53, 67, 76, 77]. In fact, there are several closely related Hopf algebras of rooted trees, see also [64, 78–81], the latter with the cheerful introduction “We study here a type of algebra which deserves more attention than it has been given”.

In the following, we attach 1-valent vertices at the top and at the bottom of any tree, so the leaves are now vertices, not edges, and every edge is incident to precisely two vertices.

**Definition 79.** The *Connes-Kreimer Hopf algebra*  $H_{CK}$  is a graded (Definition 70) Hopf algebra (Definition 69) where the basis elements are non-plane rooted trees, that means, different ways of drawing trees count as the same element. Multiplication of trees is disjoint union, the unit is the empty tree, the counit annihilates all trees but the empty tree. The coproduct is given in analogy to Theorem 24: Let an admissible cut  $\emptyset \neq c \subseteq E_T$  be a subset of the edges of a tree  $T \in H_{CK}$  such that every path from the root of  $T$  to any of its leaves contains at most one edge  $e \in c$ . Removing  $c$  disconnects the tree, let  $R^c(T)$  be the component containing the root and  $P^c(T)$  all other components. Then  $T - c = P^c(T) \oplus R^c(T)$ . Let  $C(T)$  be the set of all cuts  $c$ , then the coproduct and antipode of  $H_{CK}$  are

$$\begin{aligned}\Delta(T) &= T \otimes \mathbb{1} + \mathbb{1} \otimes T + \sum_{\emptyset \neq c \in C} P^c(T) \otimes R^c(T) \\ S(T) &= -T - \sum_{\emptyset \neq c \in C} S(P^c(T))R^c(T).\end{aligned}$$

The degree of a tree is the number of vertices, counted by the operator  $Y : H_{CK} \rightarrow H_{CK}$  according to  $Y(T) = |T| \cdot T$  (Definition 70).

#### Example 58: Rooted trees, coproducts and antipodes.

Recall the reduced coproduct from Definition 72.

$$\Delta(\bullet) = \bullet \otimes \mathbb{1} + \mathbb{1} \otimes \bullet, \quad \Delta_1(\bullet) = 0, \quad S(\bullet) = -\bullet,$$

$$\Delta_1(\text{Λ}) = 2 \bullet \otimes \mathbb{I} + \bullet \bullet \otimes \bullet, \quad \Delta_2(\text{Λ}) = 2 \bullet \otimes \bullet \otimes \bullet,$$

$$S(\text{Λ}) = -\text{Λ} + 2 \bullet \mathbb{I} - \bullet \bullet \bullet.$$

Multiplicativity  $\Delta(h_1 h_2) = \Delta(h_1)\Delta(h_2)$  results in (compare  $\Delta(t^n)$  in Example 46)

$$\Delta(\underbrace{\bullet \bullet \cdots \bullet}_{n \text{ factors}}) = \sum_{j=0}^n \binom{n}{j} \underbrace{\bullet \bullet \cdots \bullet}_{n-j \text{ factors}} \otimes \underbrace{\bullet \bullet \cdots \bullet}_j.$$

The degree (Definition 70) is counted by  $Y$ , this operator is a derivation (Eq. (2.11)):

$$Y(\mathbb{I}) = 2\mathbb{I}, \quad Y(\text{Λ}) \text{Λ} = 7 \text{Λ} \text{Λ} = Y(\text{Λ}) \text{Λ} + \text{Λ} Y(\text{Λ}).$$

**Theorem 25.** (Universal property [53, Sect. 3 Theorem 2]) Let  $A$  be an algebra and  $L : A \rightarrow A$  an endomorphism. Then there is a unique morphism  $U : H_{CK} \rightarrow A$  such that  $U \circ B_+ = B_+ \circ L$  and  $U \circ m_{H_{CK}} = m_A \circ U$  and  $U \circ \mathbb{1}_{H_{CK}} = \mathbb{1}_A \circ U$ .

Especially, if  $A$  in Theorem 25 is a Hopf algebra itself, then  $U$  is a Hopf algebra morphism.

### Example 59: Rooted trees of Faà di Bruno Hopf algebra.

One obtains Connes-Kreimer trees for the inverse Faà di Bruno Hopf algebra by omitting the hairs,

$$\mathfrak{B}_1 = \mathbb{1}, \quad \mathfrak{B}_2 = \bullet, \quad \mathfrak{B}_3 = 2 \mathbb{I} + \bullet, \quad \mathfrak{B}_4 = 4 \mathbb{I} + \text{Λ} + 5 \mathbb{I} + \bullet.$$

Computing the coproduct of these forests, one confirms the result of Example 56. Note that by omitting hairs, all vertices have become equivalent, and the trees and their multiplicities appearing in  $\mathfrak{B}_n$  might no longer appear “natural”. A more “homogeneous” encoding of the coefficients of concatenated power series is realized by the trees  $\delta_k$  of the Connes-Moscovici Hopf algebra, see Example 60.

### Example 60: Rooted trees of Connes-Moscovici Hopf algebra.

The generators of the Connes-Moscovici Hopf algebra are obtained recursively by *natural growth*  $N : H_{\text{CK}} \rightarrow H_{\text{CK}}$ . This amounts to adding one new leaf at every possible vertex of the preceding forest. The first generators are

$$N(\mathbb{1}) = \bullet =: \delta_1, \quad N(\delta_1) = \text{I} =: \delta_2, \quad N(\delta_2) = \text{I} + \text{A} =: \delta_3$$

$$N(\delta_3) = \text{I} + \text{A} + 3 \text{B} + \text{C} =: \delta_4.$$

These weights can be computed from the tree factorial [68], and they show interesting behavior in QFT [82].

**Definition 80.** The *1-cocycle* (Definition 75)  $B_+$  of the Connes-Kreimer Hopf algebra  $H_{\text{CK}}$  (Definition 79) takes a disjoint union of trees  $T_1 \dots T_n$  as argument and joins all of them to a newly created root, producing a tree  $B_+(T_1 \dots T_n)$ .

### Example 61: Rooted trees, cocycle.

$$B_+(\mathbb{1}) = \bullet, \quad B_+(\bullet \bullet \bullet) = \text{A}, \quad B_+(\text{A}) = \text{I}.$$

### Example 62: Bamboos.

The *bamboos*, or *ladders*, are the rooted trees without branches, namely

$$b_0 = \mathbb{1}, \quad b_1 = \bullet, \quad b_2 = \text{I}, \quad b_n = \text{I} \Big\}^n, \quad Y(b_n) = nb_n.$$

All bamboos can be generated from the cocycle (Definition 80) by setting  $b_1 = B_+(\mathbb{1})$  and  $b_n = B_+(b_{n-1})$ .  $b_n$  has exactly  $n - 1$  edges. Explicit construction gives the coproduct

$$\Delta(b_n) = \sum_{k=0}^n b_{n-k} \otimes b_k.$$

The coproduct of bamboos is symmetric under exchange of the two factors, and both factors consist of bamboos exclusively. Hence, the bamboos form a cocommutative (Definition 64) sub Hopf algebra of  $H_{\text{CK}}$ . Especially, the sum of all bamboos is a grouplike (Definition 67) element

$$G_B := \sum_{n=0}^{\infty} b_n, \quad \Rightarrow \quad \Delta(G_B) = G_B \otimes G_B.$$

The antipode of bamboos can be written as

$$S(b_n) = \sum_{k=1}^n (-1)^k \sum_{s_1+\dots+s_k=n} b_{s_1} \cdots b_{s_k}.$$

We have seen in Eq. (2.17) that grouplike elements are the exponential function of primitive elements. Conversely, we expect to find primitive elements by taking the “logarithm” of grouplike elements. This operation can be made precise using a Dynkin operator.

**Definition 81.** The *Dynkin operator* is defined to be the convolution product (Definition 77) of the antipode with the degree operator (Definition 70):

$$S \star Y : H_{\text{CK}} \rightarrow H_{\text{CK}}, \quad (S \star Y)(h) = m(S \otimes Y) \Delta(h).$$

The Dynkin operator is an infinitesimal character Definition 78. Using the cocycle property (Definition 75) of  $B_+$  (Definition 80),  $\Delta(B_+(h)) = B_+(h) \otimes 1 + (\text{id} \otimes B_+) \Delta(h)$ , together with  $Y(\mathbb{1}) = 0$ , one finds that for all  $h \in H_{\text{CK}}$ , the coradical degree (Definition 73) falls,

$$\text{cor}((S \star Y)(h)) < \text{cor}(h). \quad (2.24)$$

Effectively, the Dynkin operator realizes a logarithm. Applied to the grouplike element  $G_B$  of Example 62, we obtain an infinite set of primitive forests, one for each degree. Let  $b_n$  be a bamboo (Example 62), then a primitive forest of degree  $n$  is given by

$$p_n = \frac{1}{n} (S \star Y)(b_n) = \frac{1}{n} \sum_{k=1}^n k S(b_{n-k}) b_k. \quad (2.25)$$

**Example 63: Rooted trees, primitive elements.**

$$p_1 = \bullet, \quad p_2 = \text{I} - \frac{1}{2} \bullet \bullet, \quad p_3 = \text{I} - \bullet \text{I} + \frac{1}{3} \bullet \bullet \bullet.$$

These elements are non-trivial examples of the bound Eq. (2.14):  $1 = \text{cor}(p_k) \leq |p_k| = k$ . When applied to arbitrary trees, the Dynkin operator does not necessarily produce a primitive element. For example  $F := (S \star Y)(\text{A}) = 3 \text{A} - 4 \bullet \text{I} + \bullet \bullet \bullet$  is not primitive, but  $\Delta_1(F) = 2 \bullet \otimes p_2 - 4p_2 \otimes \bullet$  and therefore  $\text{cor}(F) = 2 < 3 = \text{cor}(\text{A})$ , as claimed in Eq. (2.24).

**2.1.6 Fixed-Point Equations for Rooted Trees**

The cocycle (Definition 80) can be used to construct a fixed-point equation for some forest  $X(\alpha) \in H_{\text{CK}}$ , depending on a parameter  $\alpha$ . We restrict ourselves to the form

$$X(\alpha) = \mathbb{1} + \alpha B_+ (X(\alpha) \cdot Q(\alpha)). \quad (2.26)$$

Here,  $Q(\alpha) \in H_{\text{CK}}$  is a forest, the most relevant case for our later quantum field theory applications is

$$Q(\alpha) := X(\alpha)^w, \quad w \in \mathbb{R}. \quad (2.27)$$

If we allow for labelled rooted trees then every labelled vertex  $\bullet$  comes with its own cocycle  $B_+^\bullet$ . Summing over all such vertices, where we potentially assign different orders in  $\alpha$  to different vertices, we obtain a generalization of Eq. (2.26) that has the schematic form

$$X(\alpha) = \mathbb{1} + \sum_k \alpha^k B_+^{(k)} (X(\alpha) \cdot Q^k(\alpha)). \quad (2.28)$$

**Example 64: Linear fixed-point equation.**

The choice  $w = 0$  amounts to  $Q = \mathbb{1}$  and therefore the equation

$$X(\alpha) = \mathbb{1} + \alpha B_+ (X(\alpha)).$$

We call this a *linear* fixed-point equation, because the argument of  $B_+$  is a linear function of  $X(\alpha)$ . Clearly, the order zero solution is  $X(\alpha) = \mathbb{1} + \mathcal{O}(\alpha)$ . If we insert this into the fixed point equation, we obtain  $X(\alpha) = \mathbb{1} + \alpha B_+(\mathbb{1}) + \mathcal{O}(\alpha^2) = \mathbb{1} + \bullet + \mathcal{O}(\alpha^2)$ . By induction, the unique power-series solution of the linear fixed-point equation is given by the bamboos (Example 62),

$$X(\alpha) = \mathbb{1} + \alpha \bullet + \alpha^2 \bullet + \alpha^3 \bullet + \dots = \sum_{n=0}^{\infty} \alpha^n b_n.$$

Using the cocycle property (Definition 75), we see

$$\begin{aligned} \Delta(X(\alpha)) &= \Delta(\mathbb{1}) + \alpha B_+(X(\alpha)) \otimes \mathbb{1} + (\text{id} \otimes B_+) \Delta(X(\alpha)) \\ &= X(\alpha) \otimes \mathbb{1} + (\text{id} \otimes B_+) \Delta(X(\alpha)) \end{aligned}$$

which has the solution  $\Delta(X(\alpha)) = X(\alpha) \otimes X(\alpha)$ . The solution of a linear fixed point equation is grouplike (Definition 67). Taking coefficients in  $\alpha$ , we learn that the bamboos are cocommutative (compare Example 62).

The cocycle  $B_+$  (Definition 80) joins all its arguments to a new root. If  $B_+$  is given  $(w+1)$  factors as an argument, it will produce a root vertex with  $(w+1)$  children. Consequently, a parameter  $w \in \mathbb{N}_0$  defines the maximum fertility of the trees in the series  $X(\alpha)$ : There will be trees with up to  $(w+1)$  children per vertex. If  $w$  is negative or non-integer, then a formal series expansion is understood:

$$X(\alpha) = \mathbb{1} + Y(\alpha) \quad \Rightarrow \quad X(\alpha)^{w+1} := \sum_{n=0}^{\infty} \binom{w+1}{n} Y(\alpha)^n.$$

This series terminates for  $w+1 \in \mathbb{N}$ , otherwise it is infinite. In particular, the choice  $w = -2$  produces the geometric series

$$X(\alpha)^{-2+1} = \frac{1}{\mathbb{1} + Y(\alpha)} = \sum_{n=0}^{\infty} (-1)^n Y(\alpha)^n.$$

The general solution of the fixed point equation (2.28) is a series

$$X(\alpha) = \mathbb{1} + \sum_{k=1}^{\infty} \alpha^k x_k, \tag{2.29}$$

where the coefficients  $x_k \in H_{\text{CK}}$  are sums of rooted trees.

**Theorem 26.** (Kreimer, Bergbauer, Van Suijlekom, Foissy [54, 55, 83, 84]) Consider the Connes-Kreimer Hopf algebra  $H_{\text{CK}}$  (Definition 79). Let Eq. (2.29) be the unique power series solution of Eq. (2.28) where  $Q = X^w$ . Then

1.  $\Delta(X(\alpha)) = \sum_{j=0}^{\infty} X(\alpha)\alpha^j Q^j(\alpha) \otimes x_j$ .
2. The coefficients  $x_k$  of the solution  $X(\alpha)$  generate a sub Hopf algebra of  $H_{\text{CK}}$ .
3. If  $w \in \mathbb{N}_0$ , then  $x_k$  is a sum of rooted trees with at most  $w + 1$  children at each vertex.

### Summary of Sect. 2.1.

1. Power series are useful even if they do not converge as functions. Many “analytic” operations can be defined term-wise (Sect. 2.1.1).
2. Divergent power series contain information about their non-perturbative completion in the way the coefficients grow at high order (Sect. 2.1.2).
3. Hopf algebras are a systematic mathematical framework for operations that require a “deconcatenation”, given by the coproduct (Sect. 2.1.3).
4. In the Faà di Bruno Hopf algebra, the coproduct describes insertion of power series into each other, and the antipode gives the inverse power series. Elements can be denoted as rooted trees with hair (Sect. 2.1.4).
5. The Connes-Kreimer Hopf algebra of rooted trees is the general framework in which almost all Hopf algebras can be understood graphically. Its coproduct is the sum over all ways to cut a given tree horizontally into two pieces (Sect. 2.1.5).
6. Fixed point equations, expressed by the Hochschild cocycle  $B_+$ , can be solved by power series in rooted trees. A fixed point equation generates a sub Hopf algebra, and linear fixed point equations have grouplike solutions (Sect. 2.1.6).

## 2.2 Renormalization

In constructing the perturbative expansion for QFT observables, namely the Dyson series Eq. (1.34), we have so far ignored one conceptual problem: Every observable is given by an infinite series in the coupling parameter  $\alpha$ , therefore, no measurement can tell us the value of  $\alpha$  directly. If we do not know  $\alpha$ , we can not actually make predictions for real-world observables.

Conceptually, it is clear what we should do: We need to measure some observable, invert the series to obtain the numerical value of  $\alpha$ , and insert this value into the Dyson series of other observables which we want to predict. This process, adjusting some

*bare* parameters of the theory to match experimental values for the observables, is called *renormalization*. From the above description, it is clear that renormalization is not in any direct way related to “infinities”, or to QFT being “quantum”: That renormalization is necessary, and how it works in principle, is a consequence of the fact that the observables of the theory depend non-linearly on the parameters of the theory, renormalization occurs in a similar way also in hydrodynamics, statistical physics, and many other fields. We will consider the implications of renormalization for the finiteness of observables in QFT in Sect. 2.3.4, after having developed how renormalization works concretely.

### 2.2.1 Renormalization of a Formal Power Series

To understand the combinatorics of renormalization, we first examine an illustrative example without any reference to QFT. This section partially follows [63, 64, 85]. Assume that we are given a formal power series in a parameter  $\lambda_0$ , where coefficients depend on another variable  $s$ ,

$$f(\lambda_0, s) = \lambda_0 + f_{0,2}(s)\lambda_0^2 + f_{0,3}(s)\lambda_0^3 + \mathcal{O}(\lambda_0^4). \quad (2.30)$$

Our task is to evaluate this series as a function of  $s$ . We have no information about  $\lambda_0$ . Instead, we are given the value of the function at some point  $s = s_0$ , called *renormalization point*:

$$f(\lambda_0, s_0) =: \lambda. \quad (2.31)$$

This equation is called a *renormalization condition*. Since  $s_0$  is a constant, we can view the renormalization condition as a formal power series  $\lambda(\lambda_0)$ . The value  $\lambda$  is called *renormalized coupling*. Given this data, we can in principle invert the series Eq. (2.30) in order to find the value of  $\lambda_0$ . But in practice, we would like to express all predictions in terms of the observable  $\lambda$  instead of always doing the inversion whenever we measure a new value  $\lambda$ . Therefore, we define the *renormalized function*

$$f_R(\lambda, s) := f(\lambda_0(\lambda), s) \quad (2.32)$$

where

$$\lambda_0(\lambda) =: c_1\lambda + c_2\lambda^2 + c_3\lambda^3 + \dots =: Z_\lambda(\lambda) \cdot \lambda. \quad (2.33)$$

is the inverse series of Eq. (2.31). We have defined the *Z-factor*,  $Z_\lambda(\lambda)$ . Our task now reduces to a purely combinatorial problem for the series coefficients. First, determine the coefficients  $c_j$  of the Z-factor by inverting Eq. (2.31), and second, insert the series  $\lambda_0(\lambda)$  into Eq. (2.30) to produce the renormalized series Eq. (2.32).

Both are standard operations for formal power series (Sect. 2.1.1). Using Theorem 19, we find the  $Z$ -factor as in Example 40,

$$Z_\lambda(\lambda) = 1 - f_{0,2}(s_0)\lambda + (2f_{0,2}^2(s_0) - f_{0,3}(s_0))\lambda^3 + \dots$$

With the help of Theorem 20, we arrive at our renormalized function Eq. (2.32),

$$f_{\mathcal{R}}(\lambda, s) = \lambda + \underbrace{(f_{0,2}(s) - f_{0,2}(s_0))}_{=:f_2(s)}\lambda^2 + \left( f_{0,3}(s) - f_{0,3}(s_0) - 2f_{0,2}(s_0) \underbrace{(f_{0,2}(s) - f_{0,2}(s_0))}_{=:f_2(s)} \right) \lambda^3 + \dots$$

Explicit formulas for  $f_j$  and  $c_j$  can be constructed in terms of Bell polynomials (Definition 54).

Although we did not make any reference to physics, our result exhibits some typical properties one also observes for renormalization in QFT:

1. The renormalized function features expressions  $(f_{0,j}(s) - f_{0,j}(s_0))$  as “building blocks”. For Feynman graphs, they will correspond to subtraction of *superficial divergences*.
2. At order  $\lambda^n$  there are terms involving  $(f_{0,j}(s) - f_{0,j}(s_0))$  for  $j < n$ . For Feynman graphs, such terms can be identified with subgraphs of smaller size.
3. There are seemingly non-trivial signs and combinatoric factors. In fact, they arise from the inversion and concatenation of series (Sect. 2.1.1).

To transfer our findings to a more general setting, we rewrite them in the abstract language of the Faà di Bruno Hopf algebra  $H_{\text{FdB}}$  (Sect. 2.1.4). We take  $s, s_0$  as fixed parameters and let  $\lambda, \lambda_0$  be the power series argument. The bare function  $f$ , and the renormalized function  $f_{\mathcal{R}}$ , are supposed to be characters (Definition 76) in  $H_{\text{FdB}}$ :

$$\begin{aligned} n!c_n &= (\lambda_0(\lambda)) \mathfrak{C}_n, \\ n!f_{0,n} &= (f(\lambda_0)) \mathfrak{C}_n, \\ n!f_n &= (f_{\mathcal{R}}(\lambda)) \mathfrak{C}_n = (f(\lambda_0(\lambda))) \mathfrak{C}_n. \end{aligned}$$

Recall from eq. (2.18) that the coefficient extraction operators  $\mathfrak{C}_n$  act to the left, or rather, the characters are operators acting on the  $\mathfrak{C}_n$  and not vice versa.

**Definition 82.** The *kinematic renormalization operator*  $\mathcal{R}$  is the evaluation of a power series  $f(s, \lambda, \dots)$  at a fixed value  $s_0$  of the kinematic scale variable  $s$ ,

$$\mathcal{R}(f(\lambda, s)) := f_{\mathcal{R}}(\lambda, s_0).$$

In Eq. (2.32), the renormalized function is given as a concatenation of the unrenormalized function with the series  $\lambda_0(\lambda)$  from Eq. (2.33). In the Faà di Bruno Hopf

algebra, the coefficient of such concatenated series is expressed by the coproduct (Eq. (2.19)):

$$f_{\mathcal{R}} \mathfrak{C}_n = m(\lambda_0 \circ f) \Delta \mathfrak{C}_n = (\lambda_0 \star f) \mathfrak{C}_n.$$

By the renormalization condition Eq. (2.31),  $\lambda_0(\lambda)$  is the inverse series of  $f$ , evaluated at  $s = s_0$ . Using the kinematic renormalization operator (Definition 82), this reads

$$\lambda_0 \mathfrak{C}_n = (f(\lambda, s_0))^{-1} \mathfrak{C}_n = (\mathcal{R}(f))^{-1} \mathfrak{C}_n = \mathcal{R}(f) S \mathfrak{C}_n = \mathcal{R} \circ f \circ S \mathfrak{C}_n. \quad (2.34)$$

Despite the abstract algebraic language, there is an intuitive understanding of what is happening here: The operator  $(S \mathfrak{C}_n)$  extracts the  $n$ -th coefficient of the inverse of the function standing on the left of it, and that very function is  $f(\lambda_0, s)$ , evaluated at  $s = s_0$ . Consequently, the  $n$ -th coefficient of the renormalized series is

$$f_{\mathcal{R}} \mathfrak{C}_n = (\mathcal{R} f S \star f) \mathfrak{C}_n. \quad (2.35)$$

The combinatoric properties of the convolution product (Definition 77) ensure that we are multiplying and adding the correct coefficients on the right hand side. We can rewrite Eq. (2.35) in a “recursive” fashion by splitting off the augmentation ideal (Definition 65), namely  $P_{\text{Aug}} + \tilde{\mathbb{1}} = \text{id}$ , and noting that  $\Delta \mathfrak{C}_n$  contains a summand  $\mathfrak{C}_n \otimes \mathbb{1}$ . Further, we use  $\mathcal{R}(\mathcal{R}(f)) = \mathcal{R}(f)$  and Eq. (2.9),  $S = -m(S \otimes P_{\text{Aug}})\Delta$ , to arrive at

$$\begin{aligned} f_{\mathcal{R}} \mathfrak{C}_n &= m(\mathcal{R} f S \otimes f) \Delta \mathfrak{C}_n = m(\mathcal{R} f S \otimes f P_{\text{Aug}}) \Delta \mathfrak{C}_n + m(\mathcal{R} f S \otimes f)(\mathfrak{C}_n \otimes \mathbb{1}) \\ &= (\text{id} - \mathcal{R})(m(\mathcal{R} f S \otimes f P_{\text{Aug}}) \Delta \mathfrak{C}_n) = (\text{id} - \mathcal{R})(\mathcal{R} f S \star f P_{\text{Aug}}) \mathfrak{C}_n. \end{aligned}$$

These formulas hold for every coefficient. Therefore, they also hold for the overall renormalized power series  $f_{\mathcal{R}}(\lambda)$  (Eq. (2.32)) fulfilling the renormalization condition Eq. (2.31):

$$f_{\mathcal{R}}(t) = \mathcal{R} f S \star f = (\text{id} - \mathcal{R})(\mathcal{R} f S \star f P_{\text{Aug}}). \quad (2.36)$$

## 2.2.2 Classification of Feynman Amplitudes

The renormalization procedure as developed in Sect. 2.2.1 involves only a single power series. In most situations in QFT, renormalization will be applied to multiple power series simultaneously, namely to different Green functions (Definition 48). The goal of the present section is to establish a classification for the various Green functions which can appear in a given QFT.

**Definition 83.** [[86, 87]] Assume that  $\{\underline{p}_j\}$  are the external momenta to some Green function in momentum space. We define the *scale*  $s$  as the square of any non-vanishing linear combination of them such that  $s = 0$  only when all external momenta vanish. All other momenta are then expressed as dimensionless ratios, such as  $\theta_1 = \frac{\underline{p}_1 \underline{p}_2}{s}$ , which we collectively call *angles*  $\theta$ . Sometimes, we also express the internal masses as angles by scaling to  $s$ .

In momentum space, a  $n$ -point Green function has depends on  $(n - 1)$  independent momenta due to momentum conservation. By Lorentz covariance, it depends only on the  $(n - 1)$  magnitudes  $\underline{p}_i^2$  and the  $\frac{(n-1)(n-2)}{2}$  scalar products  $\underline{p}_i \underline{p}_j$ , which amounts to  $\frac{n(n-1)}{2}$  scalar variables in total. One of them is the scale, and there are  $\frac{n(n-1)}{2} - 1$  angles. This number is reduced by  $n$  if the external edges are required to be onshell (Definition 8).

### Example 65: Mandelstam variables of 4-point functions.

A 4-point scattering process, where masses are not counted as angles, has five angle variables. If the external edges are onshell, then one angle remains. It is typically expressed in terms of the Lorentz-invariant Mandelstam variables [88],

$$s := (\underline{p}_1 + \underline{p}_2)^2, \quad t := (\underline{p}_1 + \underline{p}_3)^2, \quad u := (\underline{p}_1 + \underline{p}_4)^2.$$

As always, all four momenta are counted as incoming. One can choose, for example,  $s$  as a scale, then  $\theta_1 = \frac{t}{s}$  and  $\theta_2 = \frac{u}{s}$  are angles. Only one of the two angles is independent because  $s + t + u = m_1^2 + m_2^2 + m_3^2 + m_4^2$ .

### Example 66: Scale invariance.

Spacial or temporal translations are generated by the operator  $\partial_k$ , rotations by  $x_i \partial_j - x_j \partial_i$  and scale transformations by  $x_j \partial_j + \Delta$ , where  $\Delta$  is a constant, the dimension of the field in question (we will compute it in Definition 105). All theories considered in the present thesis are invariant under translations and rotations, namely Poincaré transformations (Definition 3).

If the theory is additionally scale invariant, then the 2-point function (of a scalar field) is  $G^{(2)}(\underline{x}_1, \underline{x}_2) \propto (\underline{x}_{12})^{-\Delta}$ , where  $\underline{x}_{12} = \underline{x}_2 - \underline{x}_1$ . This function, thereby, only depends on one variable, the magnitude of the distance. If the theory would contain a mass, then the mass-dependence would enter in the form of an angle. This would break scale invariance. Likewise, the 3-point function of a scale-invariant theory has the form

$$G^{(3)} \propto |\underline{x}_{12}|^{-3\Delta} f(\theta_1, \theta_2),$$

where  $\theta_1 = \frac{|\underline{x}_{13}|}{|\underline{x}_{12}|}$  and  $\theta_2 = \frac{|\underline{x}_{23}|}{|\underline{x}_{12}|}$ . Morally speaking, scale invariance means that the dependence of Green functions on the scale variable is a monomial, that is, the dependence is qualitatively identical regardless of the particular value of the scale. The dependence on angle variables can be arbitrary.

The same relations hold for scale-invariant functions in momentum space. The 2-point function depends only on  $s := \underline{p}^2$ , while the 3-point function depends on  $s$  and two angles.

A similar, but not identical, situation arises for a non-scale-invariant theory, where we take the masses fixed, not expressing them as angles. In that case, one can consider *onshell* Green functions by setting  $\underline{p}_j^2 = m^2$  for every external  $\underline{p}$ . Both the 2-point function and the 3-point function are mere numbers in that case, there is no degree of freedom left.

### Example 67: Conformal invariance.

Conformal symmetry has the generators  $\underline{x}^2 \partial_j - 2x_j x_i \partial_i - 2\Delta \cdot \underline{x}_j$ . Conformal invariance is stronger than mere scale invariance. If a theory is not only scale invariant (Example 66), but also conformally invariant, then the 3-point function can no longer depend on angles in an arbitrary way, but it is entirely fixed to be

$$G^{(3)}(\underline{x}_1, \underline{x}_2, \underline{x}_3) \propto |\underline{x}_{12}|^{-\Delta} |\underline{x}_{13}|^{-\Delta} |\underline{x}_{23}|^{-\Delta}.$$

The first non-trivial correlation function of a conformally invariant theory is the 4-point function, depending on two angles. Generally, a conformally invariant  $n$ -point function has  $\frac{n(n-3)}{2}$  scalar degrees of freedom [89, 90].

**Definition 84.** The *tensor structure*  $T$  of a Green function  $G$  is, in a scalar theory, a monomial in the external momenta of the Green function. Especially, the mass dimension (Definition 4) is  $[T] = [G]$ .

Let  $g$  be the residue (Definition 26) of a Green function, and  $T$  be its tensor structure (Definition 84). In general,  $g$  can contain multiple different field types and the tensor structure  $T$  may also involve Dirac matrices or tensors corresponding to internal symmetries. By  $(g, T)$ , we denote the Green function with residue  $g$ , projected onto the tensor  $T$ . Here and in the following, we assume that  $T$  is *compatible* with  $g$ , that is, the number and type of kinematic variables in the tensor  $T$  matches the external fields in the residue  $g$ . These pairs  $(g, T)$  can be used to classify all the Green functions of a QFT. For a fixed residue, the sum over all tensors  $T$  is defined

as  $G^g := \sum_T T \cdot (g, T)$ . For a theory with a single scalar field, the external structure is simply the number of fields, we write  $G^{(n)} := G^{\phi^n}$  for a Green function with  $n$  external fields.

### Example 68: Decomposition of Green functions for scalar fields.

Consider massive  $\phi^4$  theory in  $D = 4$  dimensions (Example 3). The 2-point function contains summands proportional to  $\underline{p}^2$  and summands proportional to  $m^2$ , so there are two components,  $(\phi^2, \underline{p}^2)$  and  $(\phi^2, m^2)$ . Consequently,  $G^{(2)} = \underline{p}^2 f_1 + m^2 f_2$ , where  $f_1$  and  $f_2$  are functions of angles, that is, of scale-free ratios of momenta.

The 4-point function is not proportional to momenta, we write  $(\phi^4, 1)$ . This does not imply that the 4-point function is constant, it can still depend on angles, and on the scale in a way that is not a monomial with integer exponents. The 6-point function behaves like  $(\phi^6, \underline{p}^{-2})$ . The massive theory also has  $(\phi^6, m^{-2})$ . The massless theory has exactly one Green function for each  $n \in \mathbb{N}$ , namely  $(\phi^{2n}, s^{2-n})$  with the scale  $s := \underline{p}^2$ .

### Example 69: Decomposition of Green functions for QED.

The 2-point function of the fermion  $\psi$  in QED (see Example 23) is  $G^{\bar{\psi}\psi} = (\psi \bar{\psi}, p^\mu \gamma_\mu)$ , where  $\gamma_\mu$  are the Dirac matrices. The massless photon  $A_\mu$  has two different 2-point functions, a longitudinal one  $(A^\mu A^\nu, p^\mu p^\nu)$ , and a transversal one  $(A^\mu A^\nu, \eta^{\mu\nu} \underline{p}^2 - p^\mu p^\nu)$ . The tensors of amplitudes with a higher number of non-scalar particles can conveniently be classified in terms of spin-helicity variables [91–93].

### 2.2.3 Hopf Algebra of Feynman Graphs

**Definition 85.** The set of amplitudes needing renormalization  $\mathfrak{R}$  is a set of pairs  $(g, T) = r$ , where  $g$  is the residue (Definition 26) of a Green function, and  $T$  is a kinematic tensor structure compatible with  $g$ . The notion  $\mathfrak{R} = \infty$  means that  $\mathfrak{R}$  contains all amplitudes  $(g, T)$ .

For a connected Feynman graph  $\Gamma$ , we denote  $\Gamma \in \mathfrak{R}$  if  $\text{res}(\Gamma) = g$  for some  $(g, T) \in \mathfrak{R}$  and  $\mathcal{F}(\Gamma)$  projected onto  $T$  does not vanish.  $\Gamma \in \mathfrak{R}_+$  means that  $\Gamma \in \mathfrak{R}$  and  $|L_\Gamma| > 0$  (Definition 29). A non-connected graph  $\Gamma$  is  $\in \mathfrak{R}$  if all connected components are.

For the present section, the precise choice of  $\mathfrak{R}$  is irrelevant. In Sect. 2.3.4, we see why certain  $\mathfrak{R}$  are physically sensible.

**Example 70:  $\phi^n$  theory, amplitudes needing renormalization.**

For massive  $\phi^4$  theory in  $D = 4$  dimensions with propagator powers  $\nu_e = 1$ , we choose

$$\mathfrak{R} = \{(\phi^2, m^2), (\phi^2, p^2), (\phi^4, 1)\}.$$

$\phi^3$  theory in  $D = 6$  dimensions has

$$\mathfrak{R} = \{(\phi^2, m^2), (\phi^2, p^2), (\phi^3, 1)\}.$$

For the massless theory, leave out the  $m^2$  residue in both cases.

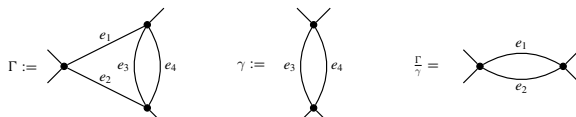
**Definition 86.** The Hopf algebra (Definition 69) of Feynman graphs  $H_F$  contains all Feynman graphs (Definition 24) as algebra elements. The product  $m$  is given by disjoint union, it is commutative.  $\mathbb{1}$  is the empty graph. Let  $\mathfrak{R}$  be a set of amplitudes needing renormalization (Definition 85), then the coproduct of a Feynman graph  $\Gamma \in H_F$  is

$$\Delta_{\mathfrak{R}}(\Gamma) = \sum_{\Gamma \supset \gamma \in \mathfrak{R}_+} \gamma \otimes \frac{\Gamma}{\gamma}.$$

Here,  $\gamma$  does not need to be connected, but every component must have at least one loop (Definition 29).  $\frac{\Gamma}{\gamma}$  denotes contraction (Definition 27).  $H_F$  is graded by the loop number and connected, the antipode follows from Eq. (2.9).

**Example 71: Dunce's cap, renormalization coproduct.**

Consider the dunce's cap from Example 12. It has exactly one proper subgraph  $\gamma$  with  $\text{res}(\gamma) \in \mathfrak{R}_+$  (Example 70), the multiedge  $\gamma = \{e_3, e_4\}$ . The cograph  $\frac{\Gamma}{\gamma}$  is a multiedge  $\{e_1, e_2\}$ . Note that  $\{e_1, e_2, e_3\} \notin \mathfrak{R}$  because this graph has 6 external edges.



Hence, the coproduct of the dunce's cap is

$$\Delta_{\mathfrak{R}}(\Gamma) = \mathbb{1} \otimes \Gamma + \Gamma \otimes \mathbb{1} + \{e_3, e_4\} \otimes \{e_1, e_2\}.$$

**Definition 87.** The *core Hopf algebra* of Feynman graphs is a Hopf algebra of Feynman graphs (Definition 86), where the coproduct  $\Delta_\infty$  is given by  $\mathfrak{R} = \infty$  (Definition 85). That is, there is a factor  $\gamma \otimes \frac{\Gamma}{\gamma}$  for every subgraph  $\gamma$  which has at least one loop.

### Example 72: Dunce's cap, core coproduct.

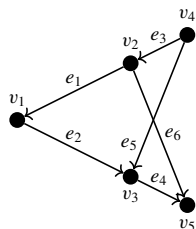
The dunce's cap from Example 71 has two subgraphs with 6 external edges. Contracting them, one obtains a tadpole (self-loop) on a single vertex. We denote the tadpole made of edge  $e_j$  by  $t_j$ . The core-coproduct (Definition 87) reads

$$\Delta_\infty(\Gamma) = \Delta_{\mathfrak{R}}(\Gamma) + \{e_1, e_2, e_3\} \otimes t_4 + \{e_1, e_2, e_4\} \otimes t_3.$$

**Definition 88.** In the Hopf algebra  $H_F$  (Definition 86), a graph  $\Gamma$  is said to be *primitive* (Definition 67) if  $\Gamma \in \mathfrak{R}_+$  (Definition 85) and there is no proper subgraph  $\gamma \subset \Gamma$  with  $\gamma \in \mathfrak{R}_+$ .

### Example 73: $\phi^4$ theory, primitive graphs.

All 1-loop Feynman graphs  $\Gamma$  with  $\Gamma \in \mathfrak{R}$  are primitive because they can not have proper subgraphs with at least one loop. The dunce's cap (Example 12) is not primitive due to the subgraph  $\gamma = \{e_3, e_4\} \in \mathfrak{R}_+$ . But there are primitive graphs with more than one loop in  $\phi^4$  theory, for example:



The fact that there is more than one primitive element in  $H_F$  has an interesting consequence for the Hochschild cocycle  $B_+$  (Definition 75). Namely, by lemma 22,  $B_+(\mathbb{1})$  is primitive, therefore, there must be multiple  $B_+$  in  $H_F$ , one for each primitive Feynman graph.

**Definition 89.** Let  $\Gamma \in H_F$  be a primitive (Definition 88) Feynman graph. We define the Hochschild 1-cocycle  $B_+^\Gamma : H_F \rightarrow \text{Aug}$  (Definition 75) such that  $B_+^\Gamma(\mathbb{1}) = \Gamma$  and

$$B_+^\Gamma(h) := \frac{1}{|I|} \sum_I \text{insert } h \text{ into } \Gamma,$$

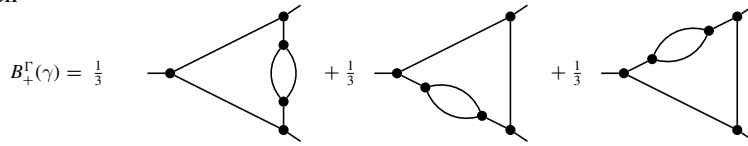
where  $I$  is the set of all possible insertion places of  $h$  into  $\Gamma$ . Here,  $h$  can be a product (=disjoint union) of multiple graphs, and the operation returns the empty graph in case  $h$  has too many, or incompatible, components.

### Example 74: Cocycle of Feynman graphs.

Let



then



We have mentioned in Sect. 2.1.5 that the Hopf algebra of rooted trees  $H_{CK}$  (Definition 79) is a universal description for all graded connected Hopf algebras (Theorem 25). Consequently, there is a mapping of Feynman graphs  $H_F$  (Definition 86) into  $H_{CK}$ .

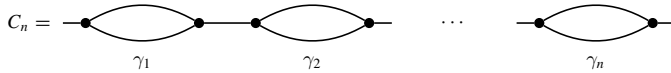
**Theorem 27.** (Kreimer [76, 94]) The following algorithm is a Hopf algebra homomorphism from  $H_F$  to a vertex-labelled  $H_{CK}$ . Let  $\Gamma \in H_F$  be a Feynman graph.

1. Let  $\gamma \subset \Gamma$  with  $\gamma \in \mathfrak{R}_+$  (Definition 85). Assume there are zero or more graphs  $\gamma' \subset \gamma$  with  $\gamma' \in \mathfrak{R}_+$ . If  $\frac{\gamma}{\bigcup \gamma'} \in \mathfrak{R}_+$ , but  $\gamma - \bigcup \gamma'$  is not in  $\mathfrak{R}_+$ , then  $\gamma$  corresponds to a vertex  $v_\gamma$ , labelled by  $\gamma$ , of a rooted tree.
2. If  $\gamma_1 \subset \gamma_2$  both correspond to vertices by point 1, then the vertex  $v_{\gamma_1}$  is attached below  $v_{\gamma_2}$ .
3. If  $\gamma \subset \gamma_1$  and  $\gamma \subset \gamma_2$  but  $\gamma_1 \not\subset \gamma_2$  and  $\gamma_2 \not\subset \gamma_1$ , then draw two trees, one where  $v_\gamma$  is attached below  $v_{\gamma_1}$  and one where  $v_\gamma$  is attached below  $v_{\gamma_2}$ .

Without the labels of the rooted trees, one can, in general, not reproduce the corresponding Feynman graph, compare Examples 78 and 79.

**Example 75: Chain graphs, rooted trees.**

The conditions in point 1 of Theorem 27 may appear intransparent. To clarify them, consider a chain of  $n$  multiedges in  $\phi^3$  theory (Example 70):



Every single  $\gamma_j$  is  $\in \mathfrak{R}$  and has one loop and does not have any non-trivial subgraphs, so each  $\gamma_j$  amounts to one vertex in the rooted tree. Now consider the connected subgraph  $\gamma' := \gamma_1 \cup e \cup \gamma_2$ . It is also  $\in \mathfrak{R}_+$  and, for example,

$$\frac{\gamma'}{\gamma_1} = \gamma_2 \cup e \in \mathfrak{R}_+.$$

Still,  $\gamma'$  does not map to a vertex in the rooted trees because  $\gamma' - \gamma_1 = \gamma_2 \cup e \in \mathfrak{R}_+$ . Restricting ourselves again to unlabelled trees, Theorem 27 yields (compare Example 58)

$$C_n \mapsto \underbrace{\bullet \bullet \cdots \bullet}_{n \text{ factors}}.$$

**Example 76: Dunce's cap, rooted trees.**

In the renormalization Hopf algebra, the dunce's cap has only a single subgraph (Example 71). Using unlabelled rooted trees, by Theorem 27

$$\Gamma \mapsto \bullet.$$

The coproduct (Definition 79) of this rooted tree exactly matches the one of  $\Gamma$ ,

$$\Delta_{\mathfrak{R}}(\Gamma) = \mathbb{1} \otimes \Gamma + \Gamma \otimes \mathbb{1} + \{e_3, e_4\} \otimes \{e_1, e_2\}$$

$$\Delta(\bullet) = \mathbb{1} \otimes \bullet + \bullet \otimes \mathbb{1} + \bullet \otimes \bullet.$$

As anticipated, the unlabelled trees are missing information:  $\bullet$  denotes both  $\{e_3, e_4\}$  and  $\{e_1, e_2\}$ , and we do not know if  $\{e_3, e_4\}$  is inserted into the left or right vertex of  $\{e_1, e_2\}$ .

**Example 77: Second chain graph, rooted trees.**

The graph  $S$  in Example 27 is called “second chain graph” because its subgraph is the second chain  $C_2$  from Example 75. Under Theorem 27, ignoring vertex labels,

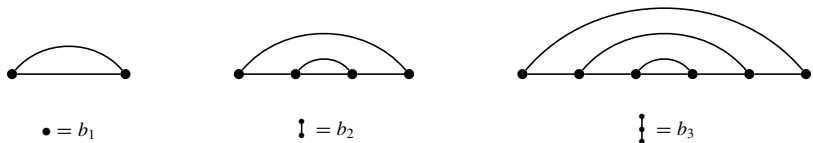
$$S \mapsto \text{Λ}.$$

Observe how  $C_2 = \gamma_1 \gamma_2 \mapsto \bullet\bullet$  is attached below the root vertex. The graphs with only one subgraph from Example 27 map to  $\Gamma/\gamma_i = \Gamma_i \mapsto \mathbb{I}$ . This is the same rooted tree as the dunce’s cap (Example 76), despite the Feynman graphs being different. The coproduct is

$$\begin{aligned} \Delta(S) = & S \otimes \mathbb{1} + \mathbb{1} \otimes S + (\gamma_1 \otimes S_1 + \gamma_2 \otimes S_2) + \gamma_1 \gamma_2 \otimes \gamma \\ \mapsto & \text{Λ} \otimes \mathbb{1} + \mathbb{1} \otimes \text{Λ} + 2 \bullet \otimes \mathbb{I} + \bullet\bullet \otimes \bullet. \end{aligned}$$

**Example 78: Bamboos from rainbows.**

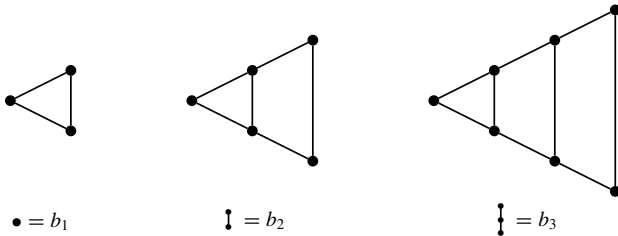
In Example 62 we saw that the bamboos are an interesting class of rooted trees. The *rainbow* Feynman graphs are a possible counterpart in  $H_F$ :



The coproduct (Definition 86) of the Feynman graphs clearly matches the coproduct of Example 62, as every subgraph and cograph of a rainbow graph is again a (smaller) rainbow graph.

**Example 79: Bamboos from ladders.**

As announced below Theorem 27, the mapping  $H_F \rightarrow H_{CK}$  is not invertible for unlabelled trees. As an illustration, the *ladder graphs* represent another class of Feynman graphs which are mapped to the (unlabelled) bamboos just like the rainbows (Example 78).



In  $\phi^3$  theory, the ladders contribute to the vertex  $\Gamma^{(3)}$ , the rainbows to the propagator  $\Gamma^{(2)}$ .

### 2.2.4 Renormalized Feynman Rules

The Feynman rules, by Definition 40, are a map that takes a Feynman graph as input and returns a number, or more generally a function of kinematic parameters. By Eq. (1.41), the Feynman rules are compatible with the product in the Hopf algebra of Feynman graphs  $H_F$  (Definition 86), hence they are a character (Definition 76). The cocycle  $B_+^\Gamma$  (Definition 89) of  $H_F$  corresponds to a linear operator for the Feynman rules, namely integration:

$$\mathcal{F}[B_+^\Gamma(h)] = \int d_\Gamma \mathcal{F}[h]. \quad (2.37)$$

Here  $\int d_\Gamma$  denotes the integral over the respective integration variables of the Feynman integral  $\mathcal{F}[\Gamma]$ , and it is understood that  $\mathcal{F}[h]$  is to be evaluated at the corresponding arguments.

Using Theorem 27, one can reformulate the Feynman rules to act not on graphs, but on labelled rooted trees. Besides being a useful tool to organize the combinatorial aspects of renormalization, these *tree Feynman rules* allow to construct simplified toy models that still respect the fundamental combinatorial properties of quantum field theory while skipping the technical difficulties of solving ordinary Feynman integrals [72, 95, 96].

#### Example 80: Toy model Feynman rules.

Let  $t \in H_{CK}$  be a forest of unlabelled rooted trees, and  $\epsilon \in \mathbb{R}$  a regularization parameter. One possible toy model [94, 95] is given by

$$\mathcal{F}[B_+(t)](s) := \int_0^\infty dx \frac{x^{-\epsilon}}{x+s} \mathcal{F}[t](x).$$

Morally, this resembles a theory with a single primitive.

Having established the Hopf algebra of Feynman graphs, renormalization now is conceptually very simple. All we have to do is apply Eq. (2.36) to Feynman graphs. For a more precise discussion of the various Hopf algebras involved in renormalization, see [62, 71, 97–99].

**Definition 90.** The *renormalized Feynman rules* are given by

$$\mathcal{F}_{\mathcal{R}} = S_{\mathcal{R}}^{\mathcal{F}} \star \mathcal{F} = (\text{id} - \mathcal{R}) (S_{\mathcal{R}}^{\mathcal{F}} \star \mathcal{F} P_{\text{Aug}}).$$

Here,  $\mathcal{F}$  are the Feynman rules (Definition 40),  $\star$  is the convolution product (Definition 77),  $S_{\mathcal{R}}^{\mathcal{F}}$  is the *counterterm* (Definition 91), and  $P_{\text{Aug}}$  projects onto Aug (Definition 65). We write  $\mathcal{F}_{\mathcal{R}}[\Gamma](L)$  to indicate the Feynman rules acting on  $\Gamma$ , evaluated at  $L$ .

**Definition 91.** The *counterterm* is the twisted antipode, given recursively by Eq. (2.9),

$$S_{\mathcal{R}}^{\mathcal{F}}[\Gamma] = -\mathcal{R} \left( m (S_{\mathcal{R}}^{\mathcal{F}} \otimes \mathcal{F} P_{\text{Aug}}) \Delta(\Gamma) \right) = -\mathcal{R} \left( (S_{\mathcal{R}}^{\mathcal{F}} \star \mathcal{F} P_{\text{Aug}}) \Gamma \right).$$

Here,  $\mathcal{R}$  denotes the renormalization operator to be made precise in Definition 99.

Note that in the power series setting Eq. (2.36), we have explicitly used kinematic renormalization conditions (Definition 82), and obtained the counterterm  $S_{\mathcal{R}}^{\mathcal{F}}[\Gamma] = \mathcal{R}(\mathcal{F}[S[\Gamma]])$ . This particular simplification only holds under certain conditions. By Definition 91, the counterterm involves nested applications of the renormalization operator and general  $S_{\mathcal{R}}^{\mathcal{F}}[\Gamma] \neq \mathcal{R}(S(\Gamma))$ . We will see this effect explicitly later in Example 108.

**Definition 92.** The *renormalized 1PI Green functions* arise from the combinatorial 1PI Green functions (Definition 47) via the renormalized Feynman rules (Definition 90),

$$G_{\mathcal{R}}^r := \mathcal{F}_{\mathcal{R}} [\Gamma^r] = \sum_{\Gamma \text{ 1PI, } \text{res}(\Gamma)=r} \alpha^{|\text{L}_{\Gamma}|} \text{sym}(\Gamma) \mathcal{F}_{\mathcal{R}}[\Gamma].$$

**Example 81: Dunce's cap, renormalized amplitude.**

The coproduct of the dunce's cap  $\Gamma$  has been computed in Example 71. If  $M^{(1)} = \{e_3, e_4\}$  is a 1-loop multiedge (Example 25) then  $S(M^{(1)}) = -M^{(1)}$ , and as always  $S(\mathbb{1}) = \mathbb{1}$ . Further,  $\mathcal{F}[\mathbb{1}] = 1$  and  $P_{\text{Aug}}(\mathbb{1}) = 0$  (Definition 65). Hence, the renormalized Feynman rules (Definition 90) of the dunce's cap are

$$\begin{aligned}\mathcal{F}_{\mathcal{R}}[\Gamma] &= (\text{id} - \mathcal{R}) m (\mathcal{R} \mathcal{F} S \otimes \mathcal{F} P_{\text{Aug}}) \Delta_{\mathcal{R}}(\Gamma) \\ &= (\text{id} - \mathcal{R}) \left( \mathcal{R} \mathcal{F} S(\mathbb{1}) \cdot \mathcal{F}[\Gamma] + 0 + \mathcal{R} \mathcal{F} S(\{e_3, e_4\}) \cdot \mathcal{F}[\{e_1, e_2\}] \right) \\ &= (\text{id} - \mathcal{R}) \left( \mathcal{F}[\Gamma] - \mathcal{R} \mathcal{F}[\{e_3, e_4\}] \cdot \mathcal{F}[\{e_1, e_2\}] \right). \\ \mathcal{S}_{\mathcal{R}}^{\mathcal{F}}[\Gamma] &= -\mathcal{R} \mathcal{F}[\Gamma] + \mathcal{R} \left( \mathcal{R} \mathcal{F}[\{e_3, e_4\}] \cdot \mathcal{F}[\{e_1, e_2\}] \right).\end{aligned}$$

As expected, the combinatorics of this procedure is non-trivial, but everything is encoded in the Hopf algebra coproduct (Definition 86).

We do not print the full result here because it is a complicated function. See Example 88. An explicit calculation shows that asymptotically for large scale  $s$ , the finite term scales like  $(\ln s/s_0)^2$  [100]. We will understand this in Theorem 37.

Unrenormalized Feynman rules are multiplicative for disjoint graphs (Eq. (1.41)), which has the interpretation of *locality*, namely that two processes are independent if they happen far apart from each other. Renormalization might potentially spoil this property. On the other hand, renormalized Green functions are what we ultimately observe, and one finds experimentally, and would expect from everyday experience and intuition, that processes are independent if they are arbitrarily far apart. Consequently, we demand as an axiom that also the renormalized Feynman rules are multiplicative,

$$\mathcal{F}_{\mathcal{R}}[h_1 \cdot h_2] \stackrel{!}{=} \mathcal{F}_{\mathcal{R}}[h_1] \cdot \mathcal{F}_{\mathcal{R}}[h_2]. \quad (2.38)$$

More precisely, we want  $\mathcal{F}_{\mathcal{R}}$  to be a character (Definition 76) on  $H_F$  (Definition 86). Effectively, this is a condition for the counterterm  $S_{\mathcal{R}}^{\mathcal{F}}$  (Definition 91), which needs to be a character as well. This requires [68, 97, 101, 102] that the renormalization operator  $\mathcal{R}$  is a *Rota-Baxter operator* [103, 104], it satisfies

$$\mathcal{R}(f(x)g(x)) + \mathcal{R}(f(x))\mathcal{R}(g(x)) \stackrel{!}{=} \mathcal{R}(\mathcal{R}(f(x))g(x)) + \mathcal{R}(f(x)\mathcal{R}(g(x))). \quad (2.39)$$

The most straightforward renormalization operator  $\mathcal{R}$  is the analogue of Definition 82, with the only difference that it acts on functions  $G$  which, in general, depend on more than one variable.

**Definition 93.** Let  $G \in \mathfrak{R}$  (Definition 85) be an amplitude needing renormalization. In the *kinematic renormalization scheme*, or *MOM-scheme*, or *BPHZ-scheme*, the renormalization operator  $\mathcal{R}$  evaluates  $G$  at a fixed value  $s_0, \theta_0$  of the angle and scale variables (Definition 83),

$$\mathcal{R} : G(s, \theta, m, \dots) \mapsto G(s_0, \theta_0, m, \dots).$$

The kinematic renormalization operator has the special property that

$$\mathcal{R}((\mathcal{R}f(s)) \cdot g(s)) = \mathcal{R}(f(s_0) \cdot g(s)) = f(s_0) \cdot g(s_0) = \mathcal{R}(f(s) \cdot g(s)) = (\mathcal{R}f(s)) \cdot (\mathcal{R}g(s)).$$

Thereby, it trivially fulfills the Rota-Baxter equation (2.39), and the couterterm (Definition 91) in kinematic renormalization indeed turns out to be  $S_{\mathcal{R}}^{\mathcal{F}}[\Gamma] = \mathcal{R}(S(\Gamma))$ .

Owing to the cocycle property (Definition 75), the renormalized Feynman rules (Definition 90) acting on  $B_+$  (Eq. (2.37)) decompose into subtraction of a superficial divergence,  $(\text{id} - \mathcal{R})$ , and renormalization of subdivergences,  $\mathcal{F}_{\mathcal{R}}[h]$  [54]:

$$\mathcal{F}_{\mathcal{R}}[B_+^\Gamma(h)] = (\text{id} - \mathcal{R}) \int d_\Gamma \mathcal{F}_{\mathcal{R}}[h] = (\text{id} - \mathcal{R}) \mathcal{F}[B_+^\Gamma(\mathcal{F}_{\mathcal{R}}[h])]. \quad (2.40)$$

### 2.2.5 Dyson-Schwinger Equations Revisited

In Sect. 1.3.11, we have introduced Dyson-Schwinger equations in a rather colloquial way. The Hopf algebra of Feynman graphs allows us to give them a much more concrete form.

By the DSE in Theorem 16, every internal edge in a kernel graph  $\Gamma$  (Definition 52) is to be replaced by the connected combinatorial 2-point function (Definition 49), given by the series  $(\Gamma^{(2)})^{-1}$ . Equivalently, one can “distribute” the factor  $\Gamma^{(2)}$  to the two vertices adjacent to the edge by using  $\Gamma^{(2)} = (\Gamma^{(2)})^{\frac{1}{2}} \cdot (\Gamma^{(2)})^{\frac{1}{2}}$ . The square root of a set of graphs is explained by its formal (Definition 53) series expansion,

$$\sqrt{1+t} = \sum_{n=0}^{\infty} \binom{\frac{1}{2}}{n} t^n = \sum_{n=0}^{\infty} \frac{(2n)!(-1)^{n+1}}{(n!)^2(2n-1)4^n} t^n = 1 + \frac{1}{2}t - \frac{1}{8}t^2 + \frac{1}{16}t^3 \mp \dots$$

Products of graphs are disjoint unions (Definition 86). Every  $n$ -valent internal vertex  $v \in V_\Gamma$  is adjacent to exactly  $n$  edges, and every edge is adjacent to two vertices. It turns out to be useful include the Green functions of adjacent edges together with the vertex into a single object, the invariant charge.

**Definition 94.** Let  $v$  be a  $n$ -valent vertex and  $\Gamma^v$  its combinatorial 1PI Green function (Definition 47). Let  $e \sim v$  be edges adjacent to  $v$  and  $\Gamma^e$  the 1PI propagator corresponding to  $e$ . The combinatorial *invariant charge* is

$$Q_v = \left( \frac{\Gamma^v}{\prod_{e \sim v} \sqrt{\Gamma^e}} \right)^{\frac{2}{n-2}}.$$

The exponent  $\frac{2}{n-2}$  in Definition 94 is a matter of convention, here it is chosen such that the loop number (Definition 29) matches the power of  $Q_v$ .

### Example 82: Invariant charges.

In scalar  $\phi^n$  theory, the invariant charges for the  $n$ -valent vertices are

$$Q_n = \frac{(\Gamma^{(n)})^{\frac{2}{n-2}}}{(\Gamma^{(2)})^{\frac{n}{n-2}}}, \quad Q_3 = \frac{(\Gamma^{(3)})^2}{(\Gamma^{(2)})^3}, \quad Q_4 = \frac{\Gamma^{(4)}}{(\Gamma^{(2)})^2}.$$

QED (Example 23) has a photon , and an electron , and a vertex  with invariant charge

$$Q_{\text{QED}} = \frac{(\Gamma^{\text{}})^2}{(\Gamma^{\text{}})^2 \Gamma^{\text{}}}.$$

QCD (Example 131) has gluons , quarks , and ghosts , and four different vertices:

$$Q_{\text{}} = \frac{(\Gamma^{\text{}})^2}{(\Gamma^{\text{}})^3}, \quad Q_{\text{}} = \frac{\Gamma^{\text{}}}{(\Gamma^{\text{}})^2}, \quad Q_{\text{}} = \frac{(\Gamma^{\text{}})^2}{(\Gamma^{\text{}})^2 \Gamma^{\text{}}}, \quad Q_{\text{}} = \frac{(\Gamma^{\text{}})^2}{(\Gamma^{\text{}})^2 \Gamma^{\text{}}}.$$

**Theorem 28.** (Combinatorial Dyson-Schwinger equations) Consider a scalar QFT with a single  $n$ -valent interaction term. Rescale  $\lambda_n^{\frac{2}{n-2}} =: \alpha$ . Let  $\Gamma^{(n)}$  be the  $n$ -point 1PI graphs (Definition 47), where  $\Gamma^{(n)}$  is divided by  $(i\lambda_n)$  such that the treelevel vertex is normalized to  $\mathbb{1}$ . Let  $\Gamma^{(2)}$  be the 1PI 2-point function (Definition 49). Let  $K^{(n)}$  be the set of kernel graphs (Definition 52) with residue  $\phi^n$ . Then the Dyson-Schwinger equations (Theorem 16) can be expressed using the Hochschild 1-cocycle  $B_+$  (Definition 89) as

$$\begin{aligned}\Gamma^{(2)} &= \mathbb{1} - \sum_{\Gamma \in K^{(2)}} \alpha^{|L_\Gamma|} \text{sym}(\Gamma) B_+^\Gamma (\Gamma^{(2)} \cdot Q_n^{|L_\Gamma|}) \\ \Gamma^{(n)} &= \mathbb{1} + \sum_{\Gamma \in K^{(n)}} \alpha^{|L_\Gamma|} \text{sym}(\Gamma) B_+^\Gamma (\Gamma^{(n)} \cdot Q_n^{|L_\Gamma|}).\end{aligned}$$

**Proof** The Cocycle  $B_+^\Gamma(h)$  (Definition 89) of Feynman graphs inserts the subgraph  $h$  into  $\Gamma$ , by the identification Eq. (2.37). This is exactly what is being done in a graphical Dyson-Schwinger equation (Theorem 16). To be shown is that the argument of  $B_+^\Gamma$  is sufficient to replace exactly all internal edges and vertices of  $\Gamma$ . Consider the propagator DSE. By Eq. (1.43), a graph  $\Gamma \in K^{(2)}$  has  $\frac{n}{n-2} |L_\Gamma| - 1$  internal edges and  $\frac{2}{n-2} |L_\Gamma|$  vertices. Therefore  $B_+^\Gamma$  requires the argument

$$(\Gamma^{(2)})^{-\left(\frac{n}{n-2} |L_\Gamma| - 1\right)} (\Gamma^{(n)})^{\frac{2}{n-2} |L_\Gamma|} = \Gamma^{(2)} \left( \frac{\Gamma^{(n)}}{(\Gamma^{(2)})^{\frac{n}{2}}} \right)^{\frac{2}{n-2} |L_\Gamma|} = \Gamma^{(2)} \cdot Q_n^{|L_\Gamma|}.$$

The vertices of this graph contribute  $\lambda_3^{\frac{2}{n-2} |L_\Gamma|} = \alpha^{|L_\Gamma|}$ . Analogous for the vertex DSE.  $\square$

### Example 83: Multiedge DSE, algebraic form.

In Example 35 we have introduced a simplified DSE for the propagator in  $\phi^3$  theory by setting the 3-valent vertex to its treelevel value. Thanks to our rescaling, this now amounts to

$$\Gamma^{(3)} = \mathbb{1}, \quad \Rightarrow \quad Q_3 = (\Gamma^{(2)})^{-3}.$$

The DSE has only one single kernel graph,  $\text{--}\circlearrowleft-$ , with symmetry factor (Theorem 15)  $\text{sym}(\text{--}\circlearrowleft-) = \frac{1}{2}$ . In the form of Theorem 28, the DSE reads

$$\Gamma^{(2)} = \mathbb{1} - \alpha \cdot \frac{1}{2} B_+^{\text{--}\circlearrowleft-} ((\Gamma^{(2)})^{-2}).$$

The exponent  $-2$  expresses that one can insert two  $(\Gamma^{(2)})^{-1}$  into the two internal edges of  $\text{--}\circ\text{--}$ .

There are also Dyson-Schwinger equations for those Green functions which do not require (superficial) renormalization. Consider a renormalizable scalar  $\phi^n$  theory, then these are all the combinatorial Green functions  $\Gamma^{(m)}$  with  $m > n$ . Let  $t$  be any of the trees with  $m$  external edges, built from  $n$ -valent vertices, then, by Eq. (1.42),  $t$  contains  $|V_t| = \frac{m-2}{n-2}$  vertices and  $|E_t| = \frac{m-n}{n-2}$  internal edges. Define

$$T^{(m)} := \frac{(\Gamma^{(n)})^{\frac{m-2}{n-2}}}{(\Gamma^{(2)})^{\frac{m-n}{n-2}}}$$

and let  $\bar{K}^{(m)}$  be the set of all 1PI kernel graphs  $\Gamma$  (Definition 52) with  $\text{res}(\Gamma) = \phi^m$ . Being kernels, these  $\Gamma$  do not contain subdivergences, but unlike the kernels in Theorem 28, they are not even superficially divergent. The DSE then takes the form

$$\Gamma^{(m)} = \sum_{\Gamma \in \bar{P}^{(m)}} \alpha^{|L_\Gamma|} \text{sym}(\Gamma) B_+^\Gamma (T^{(m)} \cdot Q_n^{|L_\Gamma|}). \quad (2.41)$$

Observe that this DSE is missing the summand  $\mathbb{1}$  because  $\Gamma^{(m)}$  has no treelevel vertex, and, being a 1PI Green function (Definition 47), so the tree  $T^{(m)}$  itself does not contribute to  $\Gamma^{(m)}$ .

Using Eq. (2.40), one can directly map Theorem 28 to a set of integral equations for renormalized Green functions.

**Definition 95.** The renormalized invariant charge is the renormalized Feynman rule (Definition 90) acting on the combinatorial invariant charge (Definition 94),

$$\mathcal{Q}(\alpha, L) := \mathcal{F}[Q(\alpha)](L), \quad \mathcal{Q}_{\mathcal{R}}(\alpha, L) := \mathcal{F}_{\mathcal{R}}[Q(\alpha)](L).$$

In kinematic renormalization (Definition 93), we must fix all angles at the renormalization point symmetrically, such that all Green functions involved in  $\mathcal{Q}_n$  are evaluated at the same scale.

**Theorem 29.** Let  $G_{\mathcal{R}}^r$  be the renormalized 1PI Green function (Definition 92 and 49) with residue  $r$ , where the treelevel term is normalized to unity. Let  $P^r$  be the set of 1PI kernel graphs (Definition 52) with residue  $r$  (which are free of subdivergences, and not necessarily superficially divergent). Let  $\mathfrak{R}$  as in Definition 85. Then the Dyson-Schwinger equations from Theorem 28 and Eq. (2.41) can be expressed using the Hochschild 1-cocycle  $B_+$  (Eq. (2.37)) as

$$G_{\mathcal{R}}^r = 1 \pm (\text{id} - \mathcal{R}) \sum_{\Gamma \in P^r} \alpha^{|\mathcal{L}_{\Gamma}|} \text{sym}(\Gamma) \mathcal{F} \left[ B_+^{\Gamma} \left( G_{\mathcal{R}}^r \cdot \mathcal{Q}_{\mathcal{R}}^{|\mathcal{L}_{\Gamma}|} \right) \right], \quad r \in \mathfrak{R}$$

$$G_{\mathcal{R}}^r = \sum_{\Gamma \in P^r} \alpha^{|\mathcal{L}_{\Gamma}|} \text{sym}(\Gamma) \mathcal{F} \left[ B_+^{\Gamma} \left( T^{(m)} \cdot \mathcal{Q}_{\mathcal{R}}^{|\mathcal{L}_{\Gamma}|} \right) \right], \quad r \notin \mathfrak{R}.$$

### Summary of Sect. 2.2.

1. Renormalization means to eliminate undetermined bare parameters from a theory, and express the predicted observables in terms of other observables whose value has been fixed in an experiment. In perturbation theory, this schematically amounts to insertion and reversion of power series, leading to the formula  $f_{\mathcal{R}} = S f \mathcal{R} \star f$  (Sect. 2.2.1).
2. In QFT, renormalization involves not just one power series, but a finite number of the Green functions of the theory. They can be classified with respect to their residue and their tensor structure (Sect. 2.2.2).
3. Feynman graphs form a Hopf algebra  $H_F$ . The coproduct is given by extraction and contraction of all subgraphs which are specified in a chosen set  $\mathfrak{R}$ . There is a homomorphism between Feynman graphs and rooted trees. The abstract Hochschild-1-cocycle  $B_+$  amounts, for Feynman graphs, to the insertion of subgraphs (Sect. 2.2.3).
4. Feynman rules are a character in  $H_F$ . The renormalized Feynman rules  $\mathcal{F}_{\mathcal{R}} = S_{\mathcal{R}}^{\mathcal{F}} \star \mathcal{F}$  are a character as well, they are determined by specifying one renormalization condition for each Green function in  $\mathfrak{R}$  (Sect. 2.2.4).
5. For Feynman amplitudes,  $B_+$  is the integral operator which appears in the Dyson-Schwinger equations. The Green functions in the argument of  $B_+$  can be regrouped so that they involve one invariant charge  $Q_v$  for each vertex  $v$  of the theory. Dyson-Schwinger equations for Green functions that are not in  $\mathfrak{R}$  are uniquely determined without specifying a renormalization condition for them (Sect. 2.2.5).

## 2.3 Divergences and Renormalizability

The alert physicist reader might wonder by now how we have introduced renormalization without any reference to “removing infinities”. This is not an accident: Renormalization is a rigorous method of expressing power series in terms of observable parameters, which themselves are given by power series. It is completely unrelated to the question if certain integrals are divergent, and it is necessary in just the same way if they are not. In the present section, we will see that renormalization also happens to eliminate certain types of divergences from the theory.

### 2.3.1 Divergences of Feynman Graphs

Before we discuss the general case, we consider a simple illustration for the qualitative behavior of Feynman integrals. Let  $L$  and  $n$  be integers,  $n + L \neq 0$  and consider the  $L$ -dimensional integral (ignoring integration constants)

$$\int_{\Lambda_0}^{\Lambda_1} d^L t \ t^n = \int_{\Lambda_0}^{\Lambda_1} dt \cdots \int_{\Lambda_0}^{\Lambda_1} dt \ t^n = \frac{n!}{(n+L)!} (\Lambda_1^{n+L} - \Lambda_0^{n+L}). \quad (2.42)$$

The limit  $\Lambda_1 \rightarrow \infty$  is called *ultraviolet (UV) limit* while  $\Lambda_0 \rightarrow 0$  is the *infrared (IR) limit*. This naming is motivated physically: Ultraviolet light carries higher energy (“ $t \rightarrow \infty$ ”) per photon than visible light, while infrared light carries less (“ $t \rightarrow 0$ ”).

Clearly, the expression Eq. (2.42) is divergent in the UV limit if  $n + L > 0$ . We call this phenomenon an *UV-divergence*. Similarly, the integral has an *IR-divergence* if  $n + L < 0$ . In the boundary case  $n + L = 0$ , the result will become a logarithm which is both UV-divergent and IR-divergent.

Now consider a Feynman integral in momentum space, Eq. (1.50),

$$\mathcal{F}[\Gamma] = \prod_{v \in V_\Gamma} (-i \lambda_{|v|}) \cdot \prod_{l \in L_\Gamma} \int \frac{d^D \underline{k}_l}{(2\pi)^D} \prod_{e \in E_\Gamma} (G_F(\underline{k}_e))^{\nu_e}. \quad (2.43)$$

By choosing spherical coordinates, we can split each  $D$ -dimensional integration  $d^D \underline{k}_l$  into a *scale*  $t_l$  and  $D-1$  *angles*  $\{\theta_l\}$ , compare Definition 83. The scale is to be integrated from 0 to  $\infty$  with a measure  $dt_l \ t_l^{D-1}$ , while the integration domain of the angles is compact. Next, for each integration scale  $t_l$ , we extract a common factor  $t$  such that  $t_l = t \cdot c_l$  and the quantities  $c_l$  represent the ratio between two scales, fixing e.g.  $c_1 = 1$ . There are  $|L_\Gamma|$  (Definition 29) integrations over different  $t_l$ , hence the integration over  $t$  has a measure  $dt \ t^{|L_\Gamma|D-1}$ .

**Definition 96.** Let  $t_l$  be as above. A *superficial UV divergence* is a divergence of the Feynman integral in the limit where all  $t_l \rightarrow \infty$  jointly, that is, the limit  $t \rightarrow \infty$  with finite  $c_l$ . Conversely, if the integral diverges in the case where only a subset of the  $t_l$  goes  $\rightarrow \infty$ , then it is said to have an *UV subdivergence*.

In the limit  $t \rightarrow \infty$ , the Feynman propagator Eq. (1.25) behaves like  $t^{-2}$ , regardless of the value of the mass  $m_e$ . Consequently, the integrand in Eq. (2.43) scales like

$$\prod_{e \in E_\Gamma} (G_F(\underline{k}_e))^{\nu_e} \sim \prod_{e \in E_\Gamma} (t^{-2})^{\nu_e} = t^{-2 \sum_{e \in E_\Gamma} \nu_e}, \quad t \rightarrow \infty.$$

Including the integration measure  $dt$   $t^{|L_\Gamma|D-1}$ , we find that in the superficial UV limit,  $t \rightarrow \infty$ , the Feynman integral Eq. (1.50) behaves like

$$\int_{\Lambda_1} dt t^{|L_\Gamma|D-1-2 \sum_{e \in E_\Gamma} \nu_e} \cdot (\text{angle integrations}) \propto (\Lambda_1^2)^{|L_\Gamma| \frac{D}{2} - \sum_{e \in E_\Gamma} \nu_e}, \quad \Lambda_1 \rightarrow \infty. \quad (2.44)$$

The exponent  $|L_\Gamma| \frac{D}{2} - \sum_{e \in E_\Gamma} \nu_e = -\omega_\Gamma$  is nothing but the negative superficial degree of convergence (Definition 43). This justifies the name: The Feynman integral is superficially UV-divergent if  $\omega_\Gamma \leq 0$ . A UV subdivergence (Definition 96) of  $\mathcal{F}[\Gamma]$  amounts to a superficial UV divergence of the integral of some subgraph  $\gamma \subset \Gamma$ . One finds that again, the sub-integral is divergent if  $\omega_\gamma \leq 0$ .

**Theorem 30.** (Weinberg power counting theorem [105]) The Feynman integral  $\mathcal{F}[\Gamma]$  of a Feynman graph  $\Gamma$  is UV-convergent if the superficial degree of convergence Definition 43 fulfills

1.  $\omega_\Gamma > 0$  and
2.  $\omega_\gamma > 0$  for all subgraphs  $\emptyset \neq \gamma \subset \Gamma$ .

Each factor  $t_l$  is the magnitude of a 4-momentum  $\underline{k}_l$ . Consequently, its mass dimension (Definition 4) is  $[t_l] = 1$  and the superficial degree of convergence equals the mass dimension of the overall Feynman integral:

$$\text{assuming } [\lambda_j] = 0, \quad [\mathcal{F}[\Gamma]] = -2\omega_\Gamma = |L_\Gamma| D - 2 \sum_{e \in E_\Gamma} \nu_e. \quad (2.45)$$

If the coupling constants  $\lambda_j$  themselves have a non-vanishing mass dimension, then

$$[\mathcal{F}[\Gamma]] = -2\omega_\Gamma + \sum_{v \in V_\Gamma} [\lambda_{|v|}]. \quad (2.46)$$

We further remark that the UV-limit in momentum space corresponds to a short-distance limit in position space. Instead of using the Feynman integral in momentum space (Eq. (2.43)), the same conclusions can be reached in position space or in the parametric representation, see e.g. [87]. Inspecting Eq. (1.58), we can confirm that the prefactor  $\Gamma(\omega_\Gamma)$  causes the expression to diverge as soon as  $\omega_\Gamma$  is a non-positive integer, in accordance with Theorem 30.

#### Example 84: Multiedges, mass dimension.

For the massless multiedge graphs, the only quantities with a nonvanishing mass dimension are the external momentum  $s := p^2$ , with  $[s] = 2$ , and potentially the coupling constants. The monomial  $s^n$  has mass dimension  $2n$ . Indeed, the integral of the 1-loop-multiedge (Example 25) is  $\mathcal{F}[M^{(1)}] \propto \lambda_3^2 s^{-\omega}$  as expected from Eq. (2.46),  $[\mathcal{F}[M^{(l)}]] = 2[\lambda_{l+2}] - 2\omega$ .

**Definition 97.** A Feynman integral  $\mathcal{F}[\Gamma]$  is said to be *logarithmically UV divergent* if the superficial degree of convergence (Definition 43), or equivalently the mass dimension (Eq. (2.45)), is  $\omega_\Gamma = 0$ . It is said to be *quadratically UV divergent* if  $\omega_\Gamma = -1$ , and so on.

Returning to our initial example Eq. (2.42), we can repeat the whole procedure for the infrared limit, analyzing “superficial” infrared divergences. The result is a statement analogous to Theorem 30, the *Lowenstein Zimmerman power counting theorem* [106].

Infrared singularities arise if the denominators in Feynman propagators (Eq. (1.25)) vanish at the lower integration limit, which is only possible for massless particles  $m_e = 0$ . However, the fact that  $k_e^2$  can be both positive or negative means that the denominator can also vanish in other regions of the integration domain, which can depend on the external kinematics. Consequently, there are two different classes of infrared divergences:

1. Infrared divergences in a closer sense are *soft* and *collinear* IR divergences, they occur in the limit of vanishing momentum in massless propagators. Although they make the individual integrals diverge, these divergences always cancel if one sums up all processes contributing to a physically observable process by the *Kinoshita Lee Nauenberg theorem* [107–110]. One can avoid them for example by giving a small artificial mass to internal edges or by choosing suitable momenta of external edges [111].

2. In a wider sense, singularities arise if massive propagators become singular, if they are onshell (Definition 8)  $\underline{k}_e^2 = m_e^2 > 0$ . Unlike UV and IR divergences, these situations reflect an expected physical behavior of scattering amplitudes, for example, a branch cut as soon as the total energy of external particles is sufficient to create a real intermediate state. The amplitude will not be holomorphic at such points, but, choosing appropriate integration contours and Riemann sheets, this will only affect particular external kinematic configurations, and the amplitude will be finite at other kinematic points. See Sect. 1.2.8 for some comments on the analytic structure of Feynman amplitudes.

We conclude that, although infrared singularities are a formidable challenge in concrete calculations, they are not conceptionally problematic for the topics discussed in the remainder of the present thesis. In the following, we will largely ignore infrared singularities and instead focus on the ultraviolet ones.

### 2.3.2 Analytic Regularization

Feynman integrals are UV-divergent if their superficial degree of convergence (Definition 43) is a non-positive integer, as can be seen from Eq. (1.58). To work with these expressions in a mathematically sensible way, we need to *regularize* them so that they become infinite only in some well-defined limit. The most basic regularization is a *cutoff* in the integral like  $\Lambda_0, \Lambda_1$  in Eq. (2.42). However, a cutoff breaks Lorentz invariance.

Breaking a symmetry in the regularization is not necessarily catastrophic, because a regularized amplitude is only an intermediate object without direct physical significance. But the missing symmetry makes computations cumbersome, the various cutoffs become increasingly intransparent if we consider subdivergences, and special care is required to make sure that symmetries are properly restored if the regulator is removed. We therefore concentrate on those regularization schemes that preserve Lorentz symmetry.

*Analytic regularization* amounts to choosing the powers of propagators in the Feynman integral to be  $\nu_e \notin \mathbb{N}$ . Physically, this means that we slightly change the short-distance, or high-energy, behavior of propagators. The resulting amplitude will be divergent in the *physical limit*  $\{\nu_e \rightarrow 1\}$ . We can introduce parameters  $\nu_e := 1 + \varepsilon_e$ , where the physical limit is  $\varepsilon_e \rightarrow 0$ . It is generally unnecessary to alter every single propagator, as long as the degree of convergence  $\omega_\gamma$  (Definition 43) becomes non-integer or positive for every subgraph  $\gamma$ .

**Example 85: Massless  $l$ -loop multiedges, analytic regularization.**

We can specialize the value of the multiedge from Example 26 to  $D = 4$  dimensions:

$$\mathcal{F}[M^{(l)}](s) = \frac{-\lambda_{l+2}^2 i^{l+1}}{(4\pi)^{2l}} \frac{\Gamma(\omega)}{\prod_e \Gamma(\nu_e)} \frac{1}{s^\omega} \frac{\prod_e \Gamma(2 - \nu_e)}{\Gamma(2(l+1) - \nu)}.$$

Here,  $\nu := \nu_1 + \dots + \nu_{l+1}$ . Choose,  $\nu_e =: 1 + \varepsilon$  with the same parameter  $\varepsilon$  for all edges. In that case  $\nu = l + 1 + (l+1)\varepsilon$  and  $\omega = (l+1)(1+\varepsilon) - 2l = 1 - l + (l+1)\varepsilon$ .

$$\mathcal{F}[M^{(l)}](s) = \frac{-\lambda_{l+2}^2 i^{l+1}}{(4\pi)^{2l}} \frac{\Gamma(1 - l + (l+1)\varepsilon)}{(\Gamma(1 + \varepsilon))^{l+1}} \frac{1}{s^\omega} \frac{(\Gamma(1 - \varepsilon))^{l+1}}{\Gamma((l+1) - (l+1)\varepsilon)}.$$

We are interested in a series expansion of the regularized amplitude in the regularization parameter(s). For the Euler gamma function (Definition 5), this is easily done:

$$\begin{aligned} z\Gamma(z) &= \Gamma(1+z), & \Gamma(z)\Gamma(1-z)\sin(\pi z) &= \pi, \\ \Gamma(1+z) &= \exp\left(-\epsilon\gamma_E + \sum_{m=2}^{\infty} \frac{(-z)^m}{m} \zeta(m)\right). \end{aligned} \quad (2.47)$$

Here,  $\gamma_E = 0,577\dots$  is Euler's constant [112], and the Riemann zeta function [113] is

$$\zeta(m) := \sum_{t=1}^{\infty} \frac{1}{t^m}. \quad (2.48)$$

**Example 86: Massless 1-loop multiedge, series expansion.**

The 1-loop multiedge from Example 85, with the choice  $\nu_e = 1 + \varepsilon$ , requires ratios like

$$\left(\frac{\Gamma(1-\epsilon)}{\Gamma(1+\epsilon)}\right)^n = \exp\left(2n\epsilon\gamma_E + 2n \sum_{m=1}^{\infty} \frac{\epsilon^{2m+1}}{2m+1} \zeta(2m+1)\right).$$

As expected, the regularized Feynman integral is a series which is divergent in the limit  $\varepsilon \rightarrow 0$ , that is, it contains a pole in  $\varepsilon$ :

$$\begin{aligned}\mathcal{F}[M^{(1)}](s) &= \frac{\lambda_3^2}{(4\pi)^2} \frac{1}{s^{2\epsilon}} \frac{1}{2\epsilon(1-2\epsilon)} \exp\left(2 \sum_{m=1}^{\infty} \frac{((-2)^{2m+1} + 2)\epsilon^{2m+1}}{2m+1} \zeta(2m+1)\right) \\ &= \frac{\lambda_3^2}{(4\pi)^2} \left( \frac{1}{2\epsilon} + 1 - \ln s + (2 - 2\ln s + (\ln s)^2)\epsilon + \dots \right).\end{aligned}$$

We have introduced analytic regularization as a technical tool to avoid divergences, but quantum corrections generally imply that propagators change their form and obtain non-integer exponents called *anomalous dimensions* (section 3.2.1). If one only includes a certain simple class of corrections, given by bamboo rooted trees, then the resulting full propagator is in fact equal to a free propagator with non-integer power, see section 3.2.3.

### 2.3.3 Dimensional Regularization

In Sect. 2.3.2, we saw that Feynman integrals can be regularized by letting the superficial degree of convergence  $\omega$  (Definition 43) be non-integer. Instead of choosing  $\nu_e \notin \mathbb{Z}$  as in Sect. 2.3.2, one can also introduce a non-integer dimension according to

$$D := D_0 - 2\epsilon,$$

where  $D_0 \in \mathbb{N}$ . This is *dimensional regularization* [114, 115], [116, Chap. 3.3]. To ensure that all mass dimensions (Definition 4) are consistent, one generally needs to introduce an arbitrary but fixed reference mass scale  $s_0$  as soon as  $D$  is altered, compare Definition 106.

The notion of a  $D$ -dimensional integral needs explanation in the case of  $D \notin \mathbb{N}$ . Precise constructions can be found in [114, 115], but the general idea is very much in the spirit of the above discussion of divergence in Eq. (2.44): One first splits off  $(D_0 - 1)$  spatial “angular” integrals which work as usual. The remaining  $(1 - 2\epsilon)$ -dimensional “radial” integral is then done by analytic continuation similar to Eq. (2.42). This analytic continuation is already implicit in the parametric integrand (Eq. (1.58)) which does contain  $D$  only as function arguments, but not as dimension of an integral. Similarly, the analytic continuation is unproblematic for Fourier transforms of monomials (Eq. (1.2)). In  $D = 4 - 2\epsilon$  dimensions, the massless Feynman propagator in position space (Eq. (1.24)) involves corrections of order  $\epsilon$ ,

$$G_F(x) = \int \frac{d^D k}{(2\pi)^D} \frac{i}{k^2} e^{-ikx} = \frac{i}{(2\pi)^2 \underline{x}^2} (1 + \epsilon (\gamma_E + \ln(\pi \underline{x}^2 / \underline{x}_0^2)) + \mathcal{O}(\epsilon^2)). \quad (2.49)$$

The value of a Feynman integral in dimensional regularization will be a Laurent series in  $\epsilon$ . If no infrared divergences are present then there are no poles of higher order than  $\epsilon^{-|L_\Gamma|}$  [117] (see Examples 87 and 89 and Theorem 57), otherwise, with IR divergences, poles can be  $\epsilon^{-2|\Gamma|}$  [118]. For one loop graphs, this IR pole gives rise to terms  $\propto (\ln(s/s_0))^2$ , known as *Sudakov double logarithms* [119]. Moreover, the pole terms in the Laurent series will generally depend on kinematic variables (in momentum-space). This is called *nonlocal divergence* because, after Fourier transform to position space, such terms are not proportional to  $\delta(x)$ .

**Lemma 31.** Let the  $n^{\text{th}}$  harmonic number be  $H_n := \sum_{j=1}^n j^{-1}$ , and define  $s := p^2$  to be the scale (Definition 83), where  $s_0 \in \mathbb{R}$  is an arbitrary, but fixed, reference scale. Then in  $D = 4 - 2\epsilon$  dimensions, the massless  $l$ -loop multiedge (Example 19) with propagators  $i(k^2)^{-1}$ , not including the symmetry factor (Theorem 15), has the Feynman integral

$$\mathcal{F}[M^{(l)}] = \frac{\lambda_{l+2}^2 (-is)^{l-1}}{(4\pi)^{2l} (l!)^2} \left( \frac{1}{\epsilon} + (2l+1)H_l - 1 + l(\ln(4\pi) - \gamma_E) - l \ln\left(\frac{s}{s_0}\right) \right) + \mathcal{O}(\epsilon).$$

**Proof** We skip the trivial prefactor  $(-i\lambda_{l+2})^2$ . Set  $D = 4 - 2\epsilon$  and  $\nu_e = 1$  in Example 25 to obtain

$$M^{(l)}(s) = \frac{s^{l-1-l\epsilon}}{(4\pi)^{l(2-\epsilon)}} (\Gamma(1-\epsilon))^{l+1} \frac{\Gamma(-l+1+l\epsilon)}{\Gamma(l+1-(l+1)\epsilon)}. \quad (2.50)$$

The only singular factor for  $\epsilon \rightarrow 0$  is the second gamma function in the numerator. Its series representation is Eq. (2.47),

$$\Gamma(-l+1+l\epsilon) = \frac{(-1)^{l-1}}{l!} \left( \frac{1}{\epsilon} + l\psi(l) + \mathcal{O}(\epsilon) \right).$$

Here,  $\psi(l)$  is the digamma function, with integer argument  $l > 0$  it has the value [120, §5.4]

$$\psi(l) = \sum_{k=1}^{l-1} \frac{1}{k} - \gamma_E = H_{l-1} - \gamma_E$$

where  $\gamma_E$  is Euler's constant. All other factors in Eq. (2.50) are regular for  $\epsilon \rightarrow 0$ , consequently their  $\mathcal{O}(\epsilon^1)$  coefficients need to be included to produce an overall  $\mathcal{O}(\epsilon^0)$  result. These are

$$\frac{1}{\Gamma(l+1-(l+1)\epsilon)} = \frac{1}{\Gamma(l+1)} + \epsilon(l+1) \frac{\psi(l+1)}{\Gamma(l+1)} + \mathcal{O}(\epsilon^2) = \frac{1}{l!} \left( 1 + \epsilon(l+1)(H_l - \gamma_E) + \mathcal{O}(\epsilon^2) \right),$$

$$\begin{aligned} (\Gamma(1-\epsilon))^{l+1} &= 1 + \epsilon(l+1)\gamma_E + \mathcal{O}(\epsilon^2), & s^{l-1-l\epsilon} &= s^{l-1} \left( 1 - \epsilon l \ln s + \mathcal{O}(\epsilon^2) \right), \\ (4\pi)^{-2l+l\epsilon} &= (4\pi)^{-2l} \left( 1 + \epsilon l \ln(4\pi) + \mathcal{O}(\epsilon^2) \right). \end{aligned}$$

Finally, use  $H_l = H_{l-1} + l^{-1}$  and include a factor  $i^{l+1}$  for  $l+1$  internal propagators.  $\square$

### Example 87: Massless 1-loop multiedge, dimensional regularization.

The 1-loop multiedge, by lemma 31, amounts to the Laurent series

$$\mathcal{F}[M^{(1)}] = \frac{\lambda_3^2}{(4\pi)^2} \left( \frac{1}{\epsilon} + 2 - \gamma_E + \ln(4\pi) - \ln\left(\frac{s}{s_0}\right) + \mathcal{O}(\epsilon) \right).$$

Compare to Example 86. Both series have a simple pole in the regulator and the finite term is  $-\ln(s)$  up to constants, which differ between the two regularizations. Similarly, the 2-loop multiedge in dimensional regularization is

$$\mathcal{F}[M^{(2)}](s) = \frac{-is\lambda_4^2}{4(4\pi)^4} \left( \frac{1}{\epsilon} + \frac{11}{2} - 2\gamma_E + 2\ln(4\pi) - 2\ln\left(\frac{s}{s_0}\right) + \mathcal{O}(\epsilon) \right).$$

### Example 88: Dunce's cap in dimensional regularization.

In a massless theory, the multiedge graph  $M^{(l)} \propto s^{-\omega}$  (Example 26) amounts to a propagator with the non-integer power  $\omega$ , see Examples 66 and 85. This means that a triangle graph, where the edges are replaced with multiedges, equals, up to prefactors, a massless triangle graph where the edges carry said non-integer propagator power. If two of the external edges are onshell then triangle graphs can be computed recursively like the multiedges (Example 26), and evaluate to Gamma functions. For arbitrary momenta, the triangle graph evaluates to Appel's hypergeometric  $F_4$  functions [121, 122]. Without any multiedge insertions, the graph is convergent in 4 dimensions and computed in [123, Eq. (2.11)].

The dunce's cap corresponds to the insertion of a 1-loop multiedge in one of the edges of the triangle. Its unrenormalized integral, without the symmetry factor  $\frac{1}{2}$ , reads [124] (compare also [125, 126])

$$\mathcal{F}[\Gamma](s_1, s_2, s_3) = \frac{1}{2(4\pi)^4} \left( \frac{1}{\epsilon^2} + \left( 5 - 2\gamma_E - 2\ln\left(\frac{s_3}{s_0}\right) + 2\ln(4\pi) \right) \frac{1}{\epsilon} + \text{finite terms} \right).$$

Again, the amplitude contains a nonlocal divergence.

**Example 89: Second chain graph in dimensional regularization.**

Consider the second chain graph. We have computed its integral in Example 27. Using  $D = 6 - 2\epsilon$ , and leaving out the prefactors  $\propto \frac{\lambda^2}{(4\pi)^{\frac{D}{2}}}$ , we find

$$\begin{aligned}\mathcal{F}[S_i] &= is^{1-2\epsilon} \frac{\Gamma(-1+\epsilon)\Gamma(-1+2\epsilon)\Gamma(2-2\epsilon)\Gamma^3(2-\epsilon)}{\Gamma(4-3\epsilon)\Gamma(4-2\epsilon)\Gamma(1+\epsilon)} \\ \mathcal{F}[S] &= -s^{1-3\epsilon} \frac{\Gamma^2(-1+\epsilon)\Gamma(-1+3\epsilon)\Gamma(2-3\epsilon)\Gamma^5(2-\epsilon)}{\Gamma(4-4\epsilon)\Gamma^2(4-2\epsilon)\Gamma(1+2\epsilon)}.\end{aligned}$$

Observe that the various integer arguments of the functions count the loops, subgraphs, edges etc. The factors  $\Gamma(-1 + \dots)$  are divergent for  $\epsilon \rightarrow 0$ , a series expansion results in

$$\begin{aligned}\mathcal{F}[S] &= -s \left( -\frac{1}{648\epsilon^3} + \frac{-35 + 9\gamma_E}{1944\epsilon^2} + \frac{1}{216\epsilon^2} \ln\left(\frac{s}{s_0}\right) \right. \\ &\quad \left. + \frac{-2984 + 18\gamma_E(70 - 9\gamma_E) + 9\pi^2}{23328\epsilon} + \frac{35 - 9\gamma_E}{648\epsilon} \ln\left(\frac{s}{s_0}\right) - \frac{1}{144\epsilon} \ln\left(\frac{s}{s_0}\right)^2 + \mathcal{O}(\epsilon^0) \right).\end{aligned}$$

Some of the pole terms depend on  $\ln \frac{s}{s_0}$ . These poles are nonlocal divergences.

Observe that the highest pole is of order  $\epsilon^{-3}$ , consistent with the graph having 3 loops, and that this one is a local divergence, independent of  $\ln \frac{s}{s_0}$ .

**Definition 98.** Let  $\Gamma$  be a Feynman graph in  $D_0 \in \mathbb{N}$  dimensions, free of IR-divergences, logarithmically UV-divergent (Definition 97), and without UV-subdivergences (Definition 96), and let  $0 < \nu_e \in \mathbb{N}$ . The *Feynman period* of  $\Gamma$  is given by the convergent integral

$$\mathcal{P}[\Gamma] = \prod_{e \in E_\Gamma} \int_0^\infty \frac{da_e}{\Gamma(\nu_e)} a_e^{\nu_e-1} \delta\left(1 - \sum_{e=1}^{|E_\Gamma|} a_e\right) \frac{1}{\psi^{\frac{D_0}{2}}}.$$

Especially, the Feynman period is independent of kinematics.

The proof for finiteness, and many more properties, can be found in [127–131]. The name *period* is borrowed from mathematics: A period is an absolutely convergent integral of a rational function with rational coefficients and an integration domain given by polynomial inequalities with rational coefficients [132].

**Theorem 32.** Let  $\Gamma$  be a Feynman graph without any subdivergences (Definition 96) in  $D_0 \in \mathbb{N}$  dimensions, free of IR-divergences, and logarithmically UV-divergent (Definition 97). Let  $s \propto \underline{p}^2$  be the momentum scale,  $s_0$  a

fixed reference scale, and  $\{\theta\}$  angles (Definition 83). Then the Feynman amplitude of  $\Gamma$  in dimensional regularization has the form

$$\mathcal{F}[\Gamma] = \Lambda \left( \frac{\mathcal{P}[\Gamma]}{|L_\Gamma|} \frac{1}{\epsilon} - \mathcal{P}[\Gamma] \ln \left( \frac{s}{s_0} \right) + C_\Gamma(\{\theta\}) + \mathcal{O}(\epsilon) \right).$$

Here,  $\Lambda = i^{|E_\Gamma|} (4\pi)^{|L_\Gamma|(-\frac{D_0}{2})} \prod_{v \in V_\Gamma} (-i\lambda_{|v|})$ , and  $\mathcal{P}[\Gamma]$  is the period (Definition 98), and  $C_\Gamma$  is a finite quantity which might depend on the angles  $\{\theta\}$ , but not on the scale  $s$ .

**Proof** Consider the Feynman rules in parametric space (Eq. (1.58)). Without subdivergences, the only divergence comes from  $\Gamma(\omega_\Gamma)$ . In dimensional regularization

$$\omega_\Gamma = \sum_{e \in E_\Gamma} \nu_e - |L_\Gamma| \frac{D_0}{2} + |L_\Gamma| \epsilon =: -n + |L_\Gamma| \epsilon,$$

where  $n \in \mathbb{N}_0$  and  $-n$  amounts to the unregularized superficial degree of divergence (Definition 97),  $n = 0$  by assumption. Let  $H_n = \sum_{k=1}^n \frac{1}{k}$  be the harmonic numbers. Using Eq. (2.47), we find

$$\Gamma(-n + |L_\Gamma| \epsilon) = \frac{\Gamma(1 + |L_\Gamma| \epsilon)}{\prod_{k=1}^n (-k + |L_\Gamma| \epsilon)} = \frac{(-1)^n}{n! |L_\Gamma| \epsilon} + \frac{(-1)^n}{n!} (H_n - \gamma_E) + \mathcal{O}(\epsilon). \quad (2.51)$$

By Theorem 14, we can extract the scale factor  $\phi_\Gamma = s \cdot \tilde{\phi}_\Gamma$  from the second Symanzik polynomial. With this, the Feynman rules in parametric space (Eq. (1.58)) read

$$\Lambda \cdot \Gamma(|L_\Gamma| \epsilon) s^{-|L_\Gamma| \epsilon} \prod_{e \in E_\Gamma} \int_0^\infty \frac{da_e}{\Gamma(\nu_e)} a_e^{\nu_e - 1} \delta \left( 1 - \sum_{e=1}^{|E_\Gamma|} a_e \right) \frac{\psi^{-\frac{D_0}{2} + (|L_\Gamma| + 1)\epsilon}}{\tilde{\phi}_\Gamma^{|L_\Gamma| \epsilon}}.$$

Expand in  $\epsilon$ .  $\Gamma(|L_\Gamma| \epsilon)$  has a simple pole  $\frac{1}{|L_\Gamma| \epsilon}$  by Eq. (2.51). Setting  $\epsilon = 0$  in the integral, we obtain the Feynman period (Definition 98), which is independent from angles. Next, expand  $(s/s_0)^{-|L_\Gamma| \epsilon} = e^{-|L_\Gamma| \epsilon \ln(s/s_0)}$  to first order. Finally, the constant term  $C_\Gamma$  is given by the order  $\epsilon^1$  of the integral, which will involve  $\tilde{\phi}_\Gamma$  and therefore depend on the angles. The exponent  $\epsilon$  in the prefactor  $\Lambda = i^{|E_\Gamma|} (4\pi)^{|L_\Gamma|(-\frac{D_0}{2})} \prod(-i\lambda_{|v|})$  can be left out, because it results in momentum-independent, non-singular contributions, which can always be absorbed into  $C_\Gamma$ .

Note the result is well-defined for any choice of the scale (Definition 83), since a rescaling  $s \rightarrow c \cdot s$  as  $c$  can be absorbed into  $C_\Gamma \rightarrow C_\Gamma - \ln c$ . A more rigorous proof, concerning especially the convergence of the integral and the precise dependence on angle variables, is given in [87, 133].  $\square$

Theorem 32 (together with analogous statements for other regularization schemes) is the core of renormalization theory, therefore it deserves some explanation. The statement of Theorem 32 is not that “every primitive graph depends on the overall momentum like  $\ln s$ ”. This is certainly false, to see this, consider any massive graph which has non-trivial analytic properties as soon as the energy is sufficient to create real massive intermediate particles. The masses are expressed in terms of angles such as  $\theta = m^2/s$ . If masses are fixed then  $\theta$  changes with  $s$ , and Theorem 32 has nothing to say about the behavior of the amplitude in this case, because  $C_\Gamma(\theta)$  can be any function. Instead, what we are asking is “If all energies and all masses are scaled with the same factor  $s$ , what does the amplitude do?”. The surprising answer of Theorem 32 is that this *does* change something, namely, it alters the amplitude by  $\mathcal{P}[\Gamma] \ln s$ . Phrased differently, primitive graphs are *not* exactly scale invariant.

### Example 90: Massless multiedge, period.

If we leave out tadpole graphs (Definition 30, compare the discussion in Sect. 5.1.4), then a multiedge (Example 19) has no subdivergence (Definition 96). Consequently, the prefactor of  $\frac{1}{\epsilon}$  in lemma 31 represents the period by Theorem 32. The only caveat is that we have to exclude a prefactor  $s^{l-1}$  from the multiedge. Concretely, in  $D = 4 - 2\epsilon$ , we find the following period for the  $l$ -loop multiedge  $M^{(l)}$ :

$$\mathcal{P}[M^{(l)}] = \frac{-(-1)^l}{l!(l-1)!}.$$

### Example 91: Second chain graph, nontrivial primitive.

In Example 63, we saw that the Connes-Kreimer Hopf algebra contains primitive elements other than  $\bullet$ . The first of these is  $p_2 := \mathbb{I} - \frac{1}{2} \bullet \bullet$ . Using Theorem 27, one possible realization of these trees as Feynman graphs are  $\mathbb{I} \simeq S_i$  and  $\bullet \simeq \gamma_i$  from Examples 27 and 77. Let  $P_2 := S_i - \frac{1}{2} \gamma_i \frac{i}{s} \gamma_i$ , where all momenta are to be taken equal to  $s$  (the momentum dependence would require more care if we had chosen a graph  $\mathbb{I}$  where the subgraph has a different external edge structure). Using Example 89, we find

$$\mathcal{F}[P_2] = is \left( \frac{11}{432} \frac{1}{\epsilon} - \frac{11}{216} \ln \left( \frac{s}{\mu} \right) + \frac{535 - 132\gamma_E}{2592} + \mathcal{O}(\epsilon) \right).$$

This is indeed the form predicted by Theorem 32, with a period  $\mathcal{P}[P_1] = \frac{11}{216}$ .

We will be using dimensional regularization with the sole purpose of making intermediate expressions finite. One can, however, take it at face value to obtain results in a truly different dimension of spacetime. Examples in that regard are [134–136]. A more drastic step is to extend  $D$  all the way to negative integers  $D = -n$ , interpreting an integral  $\int d^D \underline{x}$  as a derivative  $\partial_{\underline{x}}^n$ . This gives rise to the *negative dimensional integration method* to solve Feynman integrals [122, 137–139]. Recent more algebraic perspectives are [140, 141].

### 2.3.4 Renormalizability

#### 2.3.4.1 Amplitudes Needing Renormalization and Residues of the Lagrangian

We have based the renormalized Feynman rules (Definition 90) on the arbitrary set  $\mathfrak{R}$  of *amplitudes needing renormalization* (Definition 85), without discussing physically sensible choices. By construction, each amplitude  $G \in \mathfrak{R}$  is a power series which is assigned exactly one renormalization condition.

On the other hand, going back to the simplified example Sect. 2.2.1, we see that, in order to carry out the series inversion Eq. (2.33), the unrenormalized series needs to have a non-vanishing first order term. Translated to Feynman graphs, this means that each amplitude  $G \in \mathfrak{R}$  must have a non-vanishing treelevel term. But such a term corresponds to either a propagator or a vertex, that is, to one of the *residues of the Lagrangian  $\mathcal{L}$*  (Definition 51). We record this finding as a theorem:

**Theorem 33.** Renormalization of Feynman graphs based on the amplitudes  $\mathfrak{R}$  (Definition 85) is only possible if  $\mathfrak{R} \subseteq \mathcal{L}$  (Definition 51). Also, one needs to provide exactly one renormalization condition for each  $(g, T) \in \mathfrak{R}$ .

On the other hand, if  $\mathfrak{R} \subsetneq \mathcal{L}$  then there are constants in  $\mathcal{L}$  to which we do not assign values by any renormalization condition. Mathematically, this is possible, but physically questionable, since the result then contains unknown bare parameters. From now on, we assume that  $\mathfrak{R} = \mathcal{L}$ .

In concrete QFTs, the interplay between  $\mathfrak{R}$  and  $\mathcal{L}$  works as follows: We start with an “initial guess” of a Lagrangian. Then, by calculation (see Theorem 34), we obtain the set  $\mathfrak{R}$ , which might or might not be a subset of  $\mathcal{L}$ . In the latter case, we need to include additional monomials into the Lagrangian  $\mathcal{L}$  and repeat the calculation, until eventually Theorem 33 is satisfied. In general, this will force us to add all possible terms of given mass dimension (Definition 4) because quantum corrections lead to *operator mixing*, that is, a quantum correction originating from one such term will generally include all possible terms of the same mass dimension which are not forbidden by symmetries [142].

### Example 92: Renormalization of a massless scalar field.

Theorem 33 has an interesting, albeit slightly philosophical, consequence for massless theories: Starting with a massive interacting Lagrangian (Eq. (1.6)), we obtain a renormalized theory where the mass needs to be determined by renormalization conditions. We can choose the renormalized theory to be massless by imposing the renormalization condition  $m = 0$  for the renormalized mass term. In this way, effectively, we can leave out all mass terms and work with a massless Lagrangian from the start. The true reason is not that mass corrections can not arise, but that we demand them to vanish, compare [143]. Masslessness is a choice, not a result. Symmetries change the picture, as we will see in Sect. 5.1.1.

#### 2.3.4.2 Finiteness and Subdivergences

Another aspect in the process of renormalization is the question whether a renormalized amplitude will be finite. Let  $\Gamma$  be a 1-loop graph. It is UV-divergent if and only if  $\omega_\Gamma \leq 0$  (Theorem 30). By Definition 88,  $\Gamma$  is primitive iff  $\Gamma \in \mathfrak{R}$ . Now observe that by renormalization (Definition 90), a primitive graph is mapped to the renormalized Feynman rules

$$\mathcal{F}_{\mathcal{R}}[\Gamma] = (\text{id} - \mathcal{R}) \mathcal{F}[\Gamma] = \mathcal{F}[\Gamma] - \mathcal{R}\mathcal{F}[\Gamma]. \quad (2.52)$$

If  $\mathcal{R}$  denotes kinematic renormalization (Definition 93), then  $\mathcal{F}_{\mathcal{R}}[\Gamma]$  is finite by Theorem 32, because the residue of the pole in  $\epsilon$  is the period, which is independent of external momenta and therefore  $\mathcal{P}[\Gamma]_{\epsilon}^{\perp} - \mathcal{R}\mathcal{P}[\Gamma]_{\epsilon}^{\perp} = 0$ . In particular, every 1-loop graph is either convergent or primitive. We conclude that in kinematic renormalization, the renormalized Feynman rules of all 1-loop graphs are finite provided that  $\Gamma \in \mathfrak{R}$  for all 1-loop graphs  $\Gamma$  where  $\omega_\Gamma \leq 0$ .

In order to investigate the finiteness of arbitrary renormalized graphs, we need to provide more information about what the renormalization operator  $\mathfrak{R}$  in the counterterm  $S_{\mathcal{R}}^{\mathcal{F}}$  (Definition 91) concretely does. That is, we need to specify what it means to be a renormalization scheme. Since by Eq. (2.52), the renormalization of a primitive graph amounts to an overall subtraction  $\mathcal{F}[\Gamma] - \mathcal{R}\mathcal{F}[\Gamma]$ , it is plausible to *demand* from every renormalization scheme that it makes such expressions finite.

**Definition 99.** A *renormalization scheme* is a choice of a renormalization operator  $\mathcal{R}$  such that

1. The Rota-Baxter equation Eq. (2.39) is fulfilled, and
2. The renormalized Feynman rules (Definition 90)  $(\text{id} - \mathcal{R})\mathcal{F}[\Gamma]$  are finite for every primitive (Definition 88) Feynman graph  $\Gamma$ .

In all renormalization schemes, the treelevel term of a Green function by definition has the value unity, that is, we project onto the treelevel tensor (see Sect. 2.2.2).

**Theorem 34.** Assume that  $\Gamma \in \mathfrak{R}$  (Definition 85) whenever the superficial degree of convergence (Definition 43) is  $\omega_\Gamma \leq 0$ . Let  $\mathcal{R}$  be a renormalization scheme (Definition 99). Then the renormalized Feynman rules (Definition 90)  $\mathcal{F}_{\mathcal{R}} = S_{\mathcal{R}}^{\mathcal{F}} \star \mathcal{F}$  are finite.

**Proof** For a detailed proof, see [53, 77, 94, 144].

Use induction on the coradical degree. For primitive graphs,  $\mathcal{F}_{\mathcal{R}}$  is finite by definition (99). Assume that  $\mathcal{F}_{\mathcal{R}}(\gamma)$  is finite for all Feynman graphs  $\gamma$  with  $\text{cor}(\gamma) < n \in \mathbb{N}$ . By the Dyson-Schwinger equation (Theorem 28), the graphs of coradical degree  $n$  are of the form

$$\Gamma' = B_+^\Gamma(P(\{\gamma\})).$$

Here,  $\Gamma$  is a primitive (kernel) graph and  $P(\{\gamma\})$  is a polynomial in the graphs  $\gamma$  of coradical degree smaller than  $n$ . Using Eq. (2.38) (which needs the Rota-Baxter equation assumed in Definition 99) and the induction hypothesis, the renormalized Feynman rules  $\mathcal{F}_{\mathcal{R}}[P(\{\gamma\})] = P(\{\mathcal{F}_{\mathcal{R}}[\gamma]\})$  are finite. The renormalized amplitude of  $\Gamma'$  is, by Theorem 29,

$$\mathcal{F}_{\mathcal{R}}[\Gamma'] = (\text{id} - \mathcal{R}) \int d\Gamma \mathcal{F}_{\mathcal{R}}[P(\{\gamma\})].$$

The integral on the right hand side does not contain subdivergences, so  $(\text{id} - \mathcal{R})$  applied to it is finite by assumption. Similarly, one can establish that the counterterms  $S_{\mathcal{R}}^{\mathcal{F}}[\Gamma]$  (Definition 91) are local.

The non-Hopf algebra version of this theorem is known as *Zimmermann forest formula*, named after the forests of rooted trees corresponding to nested sub-divergences (Theorem 27). This combinatorial procedure (which we nowadays encode in the coproduct  $\Delta$ ), together with the kinematic renormalization operator  $\mathcal{R}$  (Definition 93), is called *BPHZ-renormalization* [145–147] (Definition 93). See also [116, 148, 149].  $\square$

On first sight, a simple subtraction like  $(\text{id} - \mathcal{R})$  might appear insufficient for quadratically divergent (Definition 97) integrals. However, our procedure works in full generality because we project onto the tensors. Consider an amplitude  $(g, T) \in \mathfrak{R}$ , where the tensor is  $T \propto (\underline{p}^2)^n$  with  $n \geq 1$ , that is, the underlying graph  $\Gamma$  is divergent of degree  $\omega_\Gamma = -2n$  (Definition 43). In that case, one also needs to include  $(g, 1), (g, \underline{p}^2), \dots, (g, (\underline{p}^2)^{n-1}) \in \mathfrak{R}$  because each of them will be divergent by power counting (Theorem 30). In total,  $n + 1$  renormalization conditions must be

provided. Each of these amplitudes can be treated with a simple subtraction, but all of the together are equivalent to a subtraction of the first  $(n + 1)$  powers of momenta in  $\mathcal{F}[\Gamma]$ .

### 2.3.4.3 Predictive Power of a Renormalized Theory

Theorem 34 implies that we can make any Feynman graph finite by including the residue of every possible subgraph into  $\mathfrak{R}$ . By doing this, we obtain the core Hopf algebra (Definition 87). If  $\mathfrak{R}$  contains infinitely many amplitudes, then, by Theorem 33, one needs to provide infinitely many renormalization conditions to give a physical meaning to the renormalized amplitude. This makes the theory *unpredictive*: No finite set of (measured) input values allows to predict all remaining observables.

**Definition 100.** A quantum field theory is called *renormalizable* if there is a finite set  $\mathfrak{R}$  (Definition 85) such that, if  $\Gamma$  is a superficially divergent graph (Definition 96) without subdivergences, then  $\Gamma \in \mathfrak{R}$ .

In detail, Definition 100 implies two conditions: (1) There are only finitely many residues  $g = \text{res}(\Gamma)$  of graphs such that  $\omega_\Gamma \leq 0$ . And (2) For each of these residues, there are only finitely many tensors  $T$  such that  $(g, T) \in \mathfrak{R}$ .

#### Example 93: Second chain graph, kinematic renormalization.

Consider the second chain graph from Example 27. It is not primitive and, correspondingly, has non-local divergences (Example 89). The appropriate set  $\mathfrak{R}$  for  $\phi^3$  theory is the one we chose in Example 70, fulfilling Lemma 35. We will use the notation  $S_i = S/\gamma_i$  and  $\gamma = S/(\gamma_1\gamma_2)$ , the corresponding rooted trees are shown in Example 77.

First, we renormalize  $S_1$ , which has one subgraph  $\gamma_2$  needing renormalization.

$$\Delta(S_1) = S_1 \otimes \mathbb{1} + \mathbb{1} \otimes S_1 + \gamma_2 \otimes \gamma, \quad \text{antipode: } S(S_1) = -S_1 + \gamma_2\gamma.$$

Eventually, all graphs are proportional to  $s$ , we leave out this overall factor. The counterterm and renormalized amplitude are

$$S_{\mathcal{R}}^{\mathcal{F}}[S_1] = \mathcal{R} \left( -\mathcal{F}[S_1] + \mathcal{R}(\mathcal{F}[\gamma_2]) \frac{i}{s} \mathcal{F}[\gamma] \right) = \left( \frac{1}{72\epsilon^2} + \frac{7}{144\epsilon} - \frac{\gamma_E + \ln s_0}{36\epsilon} + \mathcal{O}(\epsilon^0) \right) i.$$

If we take  $\mathcal{R}$  to be kinematic renormalization at  $s = s_0$  (Definition 93), then

$$\begin{aligned}\mathcal{F}_{\mathcal{R}}[S_1] &= \mathcal{F}[S_1] + S_{\mathcal{R}}^{\mathcal{F}}[S_1] + S_{\mathcal{R}}^{\mathcal{F}}[\gamma_2] \frac{i}{s} \mathcal{F}[\gamma] \\ &= \frac{1}{72} i \ln^2 \left( \frac{s}{s_0} \right) - \frac{11}{216} i \ln \left( \frac{s}{s_0} \right) + \mathcal{O}(\epsilon).\end{aligned}$$

As it should be, the result is finite for  $\epsilon \rightarrow 0$  and it vanishes at  $s = s_0$ .

Now consider the full graph  $S$  (not to be confused with the antipode) from Example 27.

$$\begin{aligned}\Delta(S) &= S \otimes \mathbb{1} + \mathbb{1} \otimes S + \gamma_1 \otimes S_1 + \gamma_2 \otimes S_2 + \gamma_1 \gamma_2 \otimes \gamma \\ S(S) &= -S + \gamma_1 S_1 + \gamma_2 S_2 - \gamma_1 \gamma_2 \gamma, \quad S(\gamma_1 \gamma_2) = \gamma_1 \gamma_2 \\ S_{\mathcal{R}}^{\mathcal{F}}[S] &= \mathcal{R} \left( -\mathcal{F}[S] + \mathcal{R}(\mathcal{F}[\gamma_1]) \mathcal{F}[S_1] + \mathcal{R}(\mathcal{F}[\gamma_2]) \mathcal{F}[S_2] - \mathcal{R}(\mathcal{F}[\gamma_1]) \mathcal{R}(\mathcal{F}[\gamma_2]) \mathcal{F}[\gamma] \right) \\ &= -\frac{1}{648 \epsilon^3} + \left( -\frac{37}{3888} + \frac{\gamma_E + \ln s_0}{216} \right) \frac{1}{\epsilon^2} + \mathcal{O}\left(\frac{1}{\epsilon}\right).\end{aligned}$$

The renormalized value of the second chain graph is (again, assuming kinematic renormalization)

$$\begin{aligned}\mathcal{F}_{\mathcal{R}}[S] &= \mathcal{F}[S] + S_{\mathcal{R}}^{\mathcal{F}}[S] + 2S_{\mathcal{R}}^{\mathcal{F}}[\gamma_i] \mathcal{F}[S_i] + S_{\mathcal{R}}^{\mathcal{F}}[\gamma_1 \gamma_2] \mathcal{F}[\gamma] \\ &= -\frac{1}{648} \ln^3 \left( \frac{s}{s_0} \right) + \frac{11}{1296} \ln^2 \left( \frac{s}{s_0} \right) - \frac{85}{3888} \ln \left( \frac{s}{s_0} \right) + \mathcal{O}(\epsilon).\end{aligned}$$

The superficial degree of convergence (Definition 43) is nothing but the negative mass dimension (Definition 4) of a graph, see Eq. (2.46), which in turn is given by counting the number of edges, vertices, and loops in a graph. Euler's formula (Eq. (1.42)) implies two other useful characterizations of renormalizability, which have been known long before the Hopf algebra theory of renormalization (e.g. [150]).

**Lemma 35.** A quantum field theory is renormalizable (Definition 100) if the superficial degree of convergence  $\omega_{\Gamma}$  (Definition 43) is independent of the loop number  $|L_{\Gamma}|$ , and  $\omega_{\Gamma} \leq 0$  for only finitely many residues of graphs.

**Lemma 36.** A quantum field theory is renormalizable (Definition 100) if all coupling constants  $\lambda_n$  in its Lagrangian (Definition 6) have mass dimension (Definition 4) zero.

### Example 94: Renormalizability of Liouville theory.

We introduced Liouville theory in Example 4, its Lagrangian is

$$\mathcal{L} = \frac{1}{2} \partial_\mu \phi \partial^\mu \phi - \exp(g\phi).$$

In two dimensions, classical Liouville theory is solved by mapping its solutions to modes of a free field via Bäcklund transformation [151]. As a quantum theory, Liouville theory is renormalizable in  $D = 2$  dimensions by lemma 36. It enjoyed significant attention in the 1980s [152, 153] for its connection to string theory [154].

In four dimensions, the coupling has mass dimension (Definition 4)  $[g] = 1$  and Liouville theory is not renormalizable by lemma 36. This requires to introduce additional constraints, apart from the usual renormalization conditions, in order to fully fix the Green functions [155–157]. Compare Example 144.

A slightly different perspective on renormalizability originates from Dyson-Schwinger equations. There, the renormalization condition, encoded in the operator  $\mathcal{R}$ , is a boundary condition for the solutions  $G_{\mathcal{R}}^r$  of the DSEs. A theory is renormalizable (Definition 100) if it involves only *finitely many* DSEs of the upper type in Theorem 29. Once the boundary conditions of these DSEs are fixed, all remaining  $G_{\mathcal{R}}^m$ , where  $m \notin \mathfrak{R}$ , can be computed without further renormalization, that is, without providing additional input data. Conceptually, it is not even necessary to expand the solutions of Dyson-Schwinger equations in perturbative series, see section 3.2.4 for other approaches. But even then, the fundamental notion of renormalizability stays the same. One possible renormalization procedure that explicitly avoids Feynman graphs is discussed in [158].

The topic of renormalizability is vast, but the space in this thesis is not. We are therefore content with a few stenographical comments without further explanation:

1. The LSZ formula (Theorem 5) requires *amputated* graphs. This means amputation of the renormalized full 2-point function, not just of the bare propagator.
2. The Hopf algebraic description of renormalization can be extended to also subtract infrared singularities, using a  $\mathcal{R}^*$ -operation in place of  $\mathcal{R}$  [117, 159–162].
3. An integral can be renormalized according to Definition 90 on the level of the integrand, see for example [87]. All integrals are then convergent and regularization is not needed.
4. Renormalization can be carried out graphically if one introduces a  $n$ -valent *counterterm vertex* with amplitude  $Z^{(n)} - 1$  for the  $Z$ -factor (Eq. (2.33)) of each amplitude  $(n) \in \mathfrak{R}$ .
5. It is possible to mix different regularization schemes, the counterterms will then in general depend on all the regulators. The results in kinematic renormalization are unaltered. This freedom is essential to the removal of tadpoles, see later in Sect. 5.1.4. If one uses a renormalization scheme that depends on the regulator

- (such as the MS-scheme to be introduced in Definition 110), the results differ for different choices of regulators.
6. All renormalization schemes (Definition 99) are, at least in perturbation theory, equivalent up to a changed, potentially  $\alpha$ -dependent renormalization point. This will be the topic of Chap. 4.
  7. A theory is called *superrenormalizable* if the coupling constants have positive mass dimension, or, equivalently, if there are finitely many graphs (not residues) with  $\omega_\Gamma \leq 0$ .
  8. The problem with non-renormalizable theories is that they need infinitely many renormalization conditions. If  $|\mathfrak{R}| = \infty$  but still the renormalization conditions are dictated by some other mechanism, the theory can potentially still be predictive. Compare Sect. 5.2.1.
  9. The question of divergences in quantum field theory might be less important than it at first appears: In general, quantum corrections lead to non-integer exponents of propagators, and it is well conceivable that the Feynman integrals with such propagators are not divergent at all, compare Sect. 3.2.3. Divergences are then an artifact of an unfortunate choice of series expansion. Nevertheless, renormalization is necessary and works as described, and it is still possible for such a theory to be non-predictive by requiring infinitely many renormalization conditions.
  10. The correspondence between a sensible series expansion and the mass dimensions of coupling constants (compare lemma 36) has been remarked as early as 1927 [163], before QFT was even formulated.
  11. The physical intuition that divergences would be cured by re-defining results in terms of observable quantities also dates earlier than Theorem 34. Bethe, observing the divergence in his computation of the Lamb shift, notes [164]:

This shift [of energy levels] comes out infinite in all existing theories, and has therefore always been ignored. However, it is possible to identify the most strongly divergent term in the level shift with an electromagnetic mass effect [...]. This effect should properly be regarded as already included in the observed mass of the electron, and we must therefore subtract from the theoretical expression, the corresponding expression for a free electron [...].

### Summary of Sect. 2.3.

1. Feynman integrals can be divergent. The superficial degree of convergence  $\omega_\Gamma$  determines whether an integral is UV-divergent (Sect. 2.3.1).
2. Divergent Feynman amplitudes can be regularized if one introduces non-integer powers  $\nu_e$  of the propagators. This is analytic regularization (Sect. 2.3.2).
3. Dimensional regularization amounts to choosing a non-integer spacetime dimension. A divergent graph without subdivergences then takes the form

$\mathcal{F}[\Gamma] \propto \mathcal{P}[\Gamma]/|L_\Gamma|^{\frac{1}{\epsilon}} - \mathcal{P}[\Gamma] \ln(s/\mu) + C_\Gamma$ , where  $\mathcal{P}[\Gamma]$  is the period, independent of kinematics (Sect. 2.3.3).

4. If one includes the amplitude of every superficially divergent graph into  $\mathfrak{R}$  then the renormalized Feynman rules are finite. If this is possible with a finitely large set  $\mathfrak{R}$  then the theory is called renormalizable. It needs only a finite amount of input data in order to predict all correlation functions (Sect. 2.3.4).

## 2.4 Digression: Order of Derivatives and Dimension of Spacetime

Having finished our survey of Hopf algebra renormalization theory, we return to the axioms on the Lagrangian at the very beginning of the thesis. In Definition 6, we demanded that a Lagrangian must not depend on higher than first derivatives of the field. The present section explores some motivation and consequences of this assumption, partially following [165].

In classical mechanics, Ostrogradsky's theorem [166] asserts that if a Lagrangian function contains time derivatives of higher than first order, the Hamilton function, or the total energy, is unbounded from below. To see this, consider a Lagrangian function  $L(x, \dot{x}, \ddot{x})$  depending on the second derivative with respect to time in the form of a monomial  $(\ddot{x})^n$ , where  $n \neq 1$ . The requirement that the first variation of the classical action vanishes,  $\delta S = 0$  (Eq. (1.7)), leads to the Euler-Lagrange equation (1.8),

$$\frac{\partial L}{\partial x} - \frac{d}{dt} \frac{\partial L}{\partial \dot{x}} + \frac{1}{2} \frac{d^2}{dt^2} \frac{\partial L}{\partial \ddot{x}} = 0.$$

Since  $\frac{\partial L}{\partial \ddot{x}} \sim \ddot{x}^{n-1}$ , this is a differential equation of fourth order in time, as opposed to second order for a conventional Lagrangian function depending only on  $x, \dot{x}$ .

The Hamiltonian formalism for this generalized Lagrangian is sometimes called *Ostrogradsky formalism*. Hamilton equations of motion are supposed to be first order differential equations, hence we need four canonical variables. Choose

$$q_1 := x, \quad q_2 := \dot{x}, \quad p_1 := \frac{\partial L}{\partial \dot{x}} - \frac{d}{dt} \frac{\partial L}{\partial \ddot{x}}, \quad p_2 := \frac{\partial L}{\partial \ddot{x}}.$$

With this definition, only  $p_1$  involves the third derivative  $\ddot{x}$ , the other three canonical variables only depend on  $\{x, \dot{x}, \ddot{x}\}$ . Inverting these relations, one can hence express the Langrangian in terms of  $q_1, q_2, p_2$ , without using  $p_1$ . The Hamilton function (Definition 9) is

$$H(q_1, q_2, p_1, p_2) := p_1 \dot{x} + p_2 \ddot{x}(q_1, q_2, p_2) - L(q_1, q_2, p_2). \quad (2.53)$$

This choice satisfies the Hamilton equations of motion (1.12) as expected,

$$\dot{q}_1 = \frac{\partial H}{\partial p_1}, \quad \dot{q}_2 = \frac{\partial H}{\partial p_2}, \quad \dot{p}_1 = -\frac{\partial H}{\partial q_1}, \quad \dot{p}_2 = -\frac{\partial H}{\partial q_2}.$$

A closer look at the Hamilton function Eq. (2.53) reveals that it is unbounded: The variable  $\dot{x} = q_2$  is an independent degree of freedom, not expressed through  $p_1$  (as it would be in the ordinary Hamilton formalism). The Lagrangian is independent of the variable  $p_1$ , hence the Hamilton function  $H$  Eq. (2.53) is linear in  $p_1$ , and hence unbounded.

In quantum mechanics, at least if interactions are present, generally all possible states of a system will participate in the dynamics. A theory with unbounded energy has no stable ground state [167] and a different structure of Hilbert space compared to our construction [168]. On physical grounds, it must be rejected, compare also the discussion in [169].

Canonical quantization (Sect. 1.2.2) involves certain additional subtleties regarding the correspondence between classical objects and quantum field operators as soon as higher derivatives are present [170]. A theory with second derivatives in the Lagrangian gives, qualitatively, a propagator

$$G_F(\underline{p}) = \frac{i}{\underline{p}^4 - m^4} = \frac{i}{(\underline{p}^2 + m^2)(\underline{p}^2 - m^2)},$$

which inevitably has poles at  $\underline{p}^2 = +m^2$  and  $\underline{p}^2 = -m^2$ . Depending on conventions and interpretation, one of them corresponds to a physically absurd particle called *Ostrogradsky ghost*, showing either a negative rest mass or negative probabilities.

On the other hand, for example  $\phi^3$  theory is a QFT with unbounded potential energy and yet at least a perturbative treatment is possible. It has been argued that, similarly, a higher-derivative QFT can be given meaning at least in the massless case by considering a delicate limit of vanishing masses [171, 172].

A different perspective on higher derivatives comes from dimensional analysis. A theory with  $n^{\text{th}}$  derivatives in the Lagrangian has a propagator which scales, for large momenta, as  $(\underline{p}^2)^{-n}$ . Using Eq. (1.2), we find the short-distance behavior in position space: A field with  $n^{\text{th}}$  derivatives propagates  $\sim (r^2)^{n-\frac{D}{2}}$ , see also Eq. (1.27). Assuming a flat  $D$ -dimensional spacetime with one time dimension, there are  $D-1$  spatial dimensions. The surface area of a sphere with radius  $r$  is

$$A_{D-1}(r) = \frac{2\pi^{\frac{D-1}{2}}}{\Gamma\left(\frac{D-1}{2}\right)} r^{D-2}. \quad (2.54)$$

Together, these two scaling laws mean that the total spatial flow of the field, that is the propagator integrated over the spherical surface, scales as  $r^{2n-D} \cdot r^{D-2} = (r^2)^{n-1}$ . Irrespective of the dimension of spacetime, the flow is conserved only in the case  $n=1$ , that is, for a Lagrangian with first derivatives only. This heuristic argument

implies that with  $n \neq 1$ , the theory will not be unitary, as indicated by the above Ostrogradsky ghosts.

At this point, we could settle for the conclusion that theories with higher than first derivatives are not sensible, were it not for quantum gravity. The latter is perturbatively non-renormalizable and introducing higher derivatives is one speculative way to solve the problem. We will discuss details in Sect. 5.2.1, after having developed all the necessary concepts. Nevertheless, we are confident that prohibiting higher derivatives in Definition 6 is at least a sensible choice for most of the typical cases in QFT.

## References

1. H.S. Wilf, *Generating functionology* (Academic, 1994), <https://www.math.upenn.edu/%7Ewilf/gfologyLinked2.pdf>
2. D.M. Jackson, A. Kempf, A.H. Morales, A robust generalization of the Legendre transform for QFT. *J. Phys. A: Math. Theor.* **50**, 225201 (2017)
3. D.M. Jackson, A. Kempf, A.H. Morales, Algebraic combinatorial Fourier and Legendre transforms with applications in perturbative quantum field theory (2019). <http://arxiv.org/abs/1805.09812>
4. D. Pavlovic, M. Escardo, Calculus in coinductive form, in *Proceedings. Thirteenth Annual IEEE Symposium on Logic in Computer Science (Cat. No.98CB36226)* (1998), pp. 408–417,
5. E.T. Bell, Exponential polynomials. *Ann. Math.* **35**, 258–277 (1934)
6. L. Comtet, *Advanced Combinatorics* (D. Reidel Publishing Company, Dordrecht, Holland, 1974)
7. D. Cvijovic, New identities for the partial Bell polynomials. *Appl. Math. Lett.* **24**, 1544–1547 (2011)
8. A. Schreiber, Inverse relations and reciprocity laws involving partial Bell polynomials and related extensions (2020). <http://arxiv.org/abs/2009.09201>
9. F. Qi, D.-W. Niu, D. Lim, Y.-H. Yao, Special values of the Bell polynomials of the second kind for some sequences and functions. *J. Math. Anal. Appl.* **491**, 124382 (2020)
10. J.-L. de Lagrange, Nouvelle methode pour resoudre les equations litterales par la moyen des series, *Mem. Acad. Royale des Sciences et Belles-Lettres de Berlin* (1770), pp. 251–326
11. Henrici, An algebraic proof of the Lagrange-Buermann Formula. *J. Math. Anal. Appl.* **8**, 218–224 (1964)
12. D. Merlini, R. Sprugnoli, M.C. Verri, Lagrange inversion: when and how. *Acta Appl. Math.* **94**, 233–249 (2006)
13. W.P. Johnson, The curious history of Faa du Bruno’s formula. *Am. Math. Mon.* **109**, 217–234 (2002)
14. É. Borel, *Leçons sur les Séries Divergentes, Nouvelles Leçons Sur La Théorie Des Fonctions* (Gauthier-Villars, Paris, 1901)
15. G.G. Stokes, On the discontinuity of arbitrary constants which appear in divergent developments. *Trans. Camb. Philos. Soc.* **10**, 105 (1864)
16. M.V. Berry, C.J. Howls, Hyperasymptotics for integrals with saddles. *Proc. Roy. Soc. Lond. Ser. A: Math. Phys. Sci.* **434**, 657–675 (1991)
17. O. Costin, On Borel summation and Stokes phenomena for rank-1 nonlinear systems of ordinary differential equations. *Duke Math. J.* **93**, 289–344 (1998)
18. I.M. Suslov, Divergent perturbation series. *J. Exp. Theor. Phys.* **127**, 1350 (2005)
19. D. Sauzin, Introduction to 1-summability and resurgence (2014). <http://arxiv.org/abs/1405.0356>

20. I. Aniceto, G. Başar, R. Schiappa, A primer on resurgent transseries and their asymptotics. *Physics Reports, A Primer on Resurgent Transseries and Their Asymptotics* **809**, 1–135 (2019)
21. D. Dorigoni, An introduction to resurgence, trans-series and alien calculus. *Ann. Phys.* **409**, 167914 (2019)
22. J. Zinn-Justin, Perturbation series at large orders in quantum mechanics and field theories: application to the problem of resummation. *Phys. Rep.* **70**, 109 (1981)
23. K. Yeats, Growth estimates for Dyson-Schwinger equations (2008). [arXiv:0810.2249](https://arxiv.org/abs/0810.2249) [math-ph]
24. G.V. Dunne, M. Unsal, WKB and Resurgence in the Mathieu Equation (2016). [arXiv:1603.04924](https://arxiv.org/abs/1603.04924) [math-ph]
25. P.J. Clavier, Borel-Écalle Resummation of a two-point function. *Ann. Henri Poincaré* **22**, 2103–2136 (2021)
26. M. Kontsevich, Y. Soibelman, Analyticity and resurgence in wall-crossing formulas. *Lett. Math. Phys.* **112**, 32 (2022)
27. A. Maiezza, J.C. Vasquez, Non-Wilsonian ultraviolet completion via transseries. *Int. J. Mod. Phys. A* **36**, 2150016 (2021)
28. M. Borinsky, D. Broadhurst, Resonant resurgence asymptotics from quantum field theory. *Nucl. Phys. B* **981**, 115861 (2022)
29. M.P. Bellon, E.I. Russo, Resurgent analysis of Ward-Schwinger-Dyson equations. *SIGMA. Symmetry, Integrab. Geometry: Methods Appl.* **17**, 075 (2021)
30. P.C. Argyres, M. Ünsal, The semi-classical expansion and resurgence in gauge theories: new perturbative, instanton, bion, and renormalon effects. *J. High Energy Phys.* **2012**, 63 (2012)
31. G. Basar, G.V. Dunne, M. Unsal, Resurgence theory, ghost-instantons, and analytic continuation of path integrals. *J. High Energy Phys.* **2013**, 41 (2013)
32. L. Klaczynski, Resurgent transseries & Dyson-Schwinger equations. *Ann. Phys.* **372**, 397–448 (2016)
33. M. Borinsky, Generating asymptotics for factorially divergent sequences. *Electron. J. Comb.* P4.1–P4.1 (2018)
34. G.V. Dunne, M. Unsal, Resurgence and trans-series in quantum field theory: the CP(N-1) model. *J. High Energy Phys.* **2012**, 170 (2012)
35. G.V. Dunne, M. Ünsal, Generating nonperturbative physics from perturbation theory. *Phys. Rev. D* **89**, 041701 (2014)
36. M. Borinsky, Renormalized asymptotic enumeration of Feynman diagrams. *Ann. Phys.* **385**, 95–135 (2017)
37. M. Borinsky, G.V. Dunne, Non-perturbative completion of Hopf-algebraic Dyson-Schwinger equations. *Nucl. Phys. B* **957**, 115096 (2020)
38. F.J. Dyson, Divergence of perturbation theory in quantum electrodynamics. *Phys. Rev.* **85**, 631–632 (1952)
39. A. Sommerfeld, Zur Quantentheorie der Spektrallinien. *Ann. Phys.* **356**, 1–94 (1916)
40. M. Gevrey, Sur la nature analytique des solutions des équations aux dérivées partielles. Premier mémoire. *Annales scientifiques de l’École Normale Supérieure* **35**, 129–190 (1918)
41. L. Euler, De seriebus divergentibus. *Novi Commentarii academiae scientiarum Petropolitanae* **5**, 205–237 (1760)
42. G.A. Edgar, Transseries for beginners (2009). <http://arxiv.org/abs/0801.4877>
43. B. Dahn, P. Göring, Notes on exponential-logarithmic terms. *Fundam. Math.* **127**, 45–50 (1987)
44. Y.S. Il'yashenko, Finiteness theorems for limit cycles. *Russ. Math. Surv.* **45**, 129–203 (1990)
45. J. Ecalle, *Introduction aux fonctions analysables et preuve constructive de la conjecture de Dulac*, Actualités Mathématiques (Hermann, Paris, 1992)
46. L. van den Dries, A. Macintyre, D. Marker, Logarithmic-exponential power series. *J. Lond. Math. Soc.* **56**, 417–434 (1997)
47. J. Hoeven, *Transseries and Real Differential Algebra*, 1st edn., Lecture Notes in Mathematics 1888 (Springer Berlin Heidelberg, 2006), 260 pp., <https://doi.org/10.1007/3-540-35590-1>

48. O. Costin, Exponential asymptotics, transseries, and generalized Borel summation for analytic rank one systems of ODE's (2006). <http://arxiv.org/abs/math/0608414>
49. R.B. Dingle, *Asymptotic Expansions: Their Derivation and Interpretation* (Academic, London, New York, 1973)
50. J. Ecalle, *Les fonctions ré surgentes*, Vol. 1, 3 vols., Publ. Math. Orsay (Orsay, 1981), 248 pp
51. L.F. Richardson, R.T. Glazebrook, The approximate arithmetical solution by finite differences of physical problems involving differential equations, with an application to the stresses in a masonry dam. Philos. Trans. Roy. Soc. Lond. Ser. A **210**, 307–357 (1911)
52. C. Kassel, *Quantum Groups*, Vol. 155, Graduate Texts in Mathematics (Springer, New York, NY, 1995). <http://link.springer.com/10.1007/978-1-4612-0783-2>
53. A. Connes, D. Kreimer, Hopf Algebras, Renormalization and Noncommutative Geometry Series, in *Quantum Field Theory: Perspective and Prospective*. ed. by C. DeWitt-Morette, J.-B. Zuber, N.A.T.O. Science (Springer, Netherlands, Dordrecht, 1999), pp.59–109
54. C. Bergbauer, D. Kreimer, Hopf algebras in renormalization theory: locality and Dyson-Schwinger equations from Hochschild cohomology. IRMA Lect. Math. Theor. Phys. **10**, 133–164 (2006)
55. D. Kreimer, E. Panzer, Renormalization and Mellin transforms. *Computer Algebra in Quantum Field Theory, Texts & Monographs in Symbolic Computation* (2013), pp. 195–223
56. S. Raianu, Coalgebras from formulas, in *Lecture Notes In Pure and Applied Mathematics*, Vol. 237 (2004), pp. 215–224. <http://math.csudh.edu/~sraianu/coalgfor.pdf>
57. J.W. Milnor, J.C. Moore, On the structure of Hopf algebras. Ann. Math. **81**, 211–264 (1965)
58. E. Abe, *Hopf Algebras*, Cambridge Tracts in Mathematics, vol. 74 (Cambridge University Press, Cambridge, 1980), p.300
59. G. Bogfjellmo, A. Schmeding, The geometry of characters of Hopf algebras, in *Computation and Combinatorics in Dynamics, Stochastics and Control*. Abel Symposia, Vol. 13 (2016), pp. 159–185,
60. G. Bogfjellmo, R. Dahmen, A. Schmeding, Character groups of Hopf algebras as infinite-dimensional Lie groups. Annales de l'Institut Fourier **66**, 2101–2155 (2016)
61. S.A. Joni, G.-C. Rota, Coalgebras and bialgebras in combinatorics. Stud. Appl. Math. **61**, 93–139 (1979)
62. A. Abdesselam, Feynman Diagrams in Algebraic Combinatorics (2002). <http://arxiv.org/abs/math/0212121>
63. H. Figueroa, J.M. Gracia-Bondia, J.C. Varilly, Faa di Bruno Hopf algebras (2005). <http://arxiv.org/abs/math/0508337>
64. H. Figueroa, J.M. Gracia-Bondía, Combinatorial Hopf algebras in quantum field theory. Rev. Math. Phys. **17**, 881–976 (2005)
65. A. Connes, D. Kreimer, *Lessons from Quantum Field Theory - Hopf Algebras and Spacetime Geometries* (1999). <http://arxiv.org/abs/hep-th/9904044>
66. R.P. Stanley, *Enumerative Combinatorics II*, Vol. 2, 2 vols., Cambridge Studies in Advanced Mathematics (Cambridge University Press, Cambridge, 1999). <https://www.cambridge.org/core/books/enumerative-combinatorics/D8DDDF7E8EBF0BCFE99F5E6918CE2A8>
67. A. Connes, H. Moscovici, Hopf algebras, cyclic cohomology and the transverse index theorem. Commun. Math. Phys. **198**, 199–246 (1998)
68. D. Kreimer, Chen's Iterated Integral represents the Operator Product Expansion (1999). <http://arxiv.org/abs/hep-th/9901099>
69. J.C. Butcher, Coefficients for the study of Runge-Kutta integration processes. J. Aust. Math. Soc. **3**, 185–201 (1963)
70. T. Krajewski, P. Martinetti, Wilsonian renormalization, differential equations and Hopf algebras (2008). <http://arxiv.org/abs/0806.4309>
71. Ch. Brouder, Runge-Kutta methods and renormalization. Eur. Phys. J. C - Part. Fields **12**, 521–534 (2000)
72. B.R. Jones, K. Yeats, *Tree Hook Length Formulae*. Feynman rules and B-series (2014). <http://arxiv.org/abs/1412.6053>

73. C. Runge, Ueber die numerische Auflösung von Differentialgleichungen. *Math. Ann.* **46**, 167–178 (1895)
74. W. Kutta, Beitrag zur näherungsweisen Integration totaler Differentialgleichungen. *Zeitschrift für Mathematik und Physik* **46**, 435–453 (1901)
75. J.P. Bell, S.N. Burris, K.A. Yeats, Counting rooted trees: the universal law  $t(n) \sim C\rho^{-n}n^{-3/2}$ . *Electron. J. Comb.* R63–R63 (2006)
76. D. Kreimer, On overlapping divergences. *Commun. Math. Phys.* **204**, 669–689 (1999)
77. D. Kreimer, Combinatorics of (perturbative) quantum field theory. *Phys. Rep. Renormalization Group Theory in the New Millennium. IV* **363**, 387–424 (2002)
78. R.L. Grossman, R.G. Larson, *Hopf-algebraic structures of families of trees* (1987). <http://arxiv.org/abs/0711.3877>
79. L. Foissy, Les algèbres de Hopf des arbres enracinés décorés, II. *Bulletin des Sciences Mathématiques* **126**, 249–288 (2002)
80. L. Foissy, Les algèbres de Hopf des arbres enracinés décorés, I. *Bulletin des Sciences Mathématiques* **126**, 193–239 (2002)
81. F. Chapoton, M. Livernet, Pre-Lie algebras and the rooted trees operad. *IMRN* **2001**(8), 395–408 (2000)
82. D.J. Broadhurst, D. Kreimer, Renormalization automated by Hopf algebra. *J. Symb. Comput.* **27**, 581 (1999)
83. W.D. van Suijlekom, Renormalization of Gauge fields: a Hopf algebra approach. *Commun. Math. Phys.* **276**, 773–798 (2007)
84. L. Foissy, General Dyson-Schwinger equations and systems. *Commun. Math. Phys.* **327**, 151–179 (2014)
85. B. Delamotte, A hint of renormalization. *Am. J. Phys.* **72**, 170–184 (2004)
86. F. Brown, D. Kreimer, Decomposing Feynman rules (2012). <http://arxiv.org/abs/1212.3923>
87. F. Brown, D. Kreimer, Angles, scales and parametric renormalization. *Lett. Math. Phys.* **103**, 933–1007 (2013)
88. S. Mandelstam, Determination of the pion-nucleon scattering amplitude from dispersion relations and unitarity. *General theory. Phys. Rev.* **112**, 1344–1360 (1958)
89. A.M. Polyakov, Conformal symmetry of critical fluctuations. *JETP Lett.* **12**, 381 (1970)
90. G. Mack, I.T. Todorov, Conformal-invariant green functions without ultraviolet divergences. *Phys. Rev. D* **8**, 1764–1787 (1973)
91. R. Penrose, Twistor algebra. *J. Math. Phys.* **8**, 345 (1967)
92. F.A. Berends, W.T. Giele, Recursive calculations for processes with n gluons. *Nucl. Phys. B* **306**, 759–808 (1988)
93. L. Dixon, Calculating Scattering Amplitudes Efficiently (1996). <http://arxiv.org/abs/hep-ph/9601359>
94. D. Kreimer, On the Hopf algebra structure of perturbative quantum field theories. *Adv. Theor. Math. Phys.* **2**, 303–334 (1998)
95. E. Panzer, Hopf algebraic Renormalization of Kreimer's toy model (2012). <http://arxiv.org/abs/1202.3552>
96. E. Panzer, Renormalization, Hopf algebras and Mellin transforms (2015). <http://arxiv.org/abs/1407.4943>
97. A. Connes, D. Kreimer, Renormalization in quantum field theory and the Riemann-Hilbert problem I: the Hopf algebra structure of graphs and the main theorem. *Commun. Math. Phys.* **210**, 249–273 (2000)
98. A. Connes, D. Kreimer, Renormalization in quantum field theory and the Riemann-Hilbert problem II: the beta-function, diffeomorphisms and the renormalization group. *Commun. Math. Phys.* **216**, 215–241 (2001)
99. C. Brouder, A. Frabetti, C. Krattenthaler, Non-commutative Hopf algebra of formal diffeomorphisms (2004). <http://arxiv.org/abs/math/0406117>
100. N.I. Usyukina, On a representation for the three-point function. *Theor. Math. Phys.* **22**, 210–214 (1975)

101. K. Ebrahimi-Fard, L. Guo, D. Kreimer, Integrable renormalization II: the general case. *Ann. Henri Poincaré* **6**, 369–395 (2005)
102. D. Manchon, Hopf Algebras in Renormalisation, in *Handbook of Algebra*, Vol. 5, ed. by M. Hazewinkel (North-Holland, 2008), pp. 365–427
103. G. Baxter, An analytic problem whose solution follows from a simple algebraic identity. *Pac. J. Math.* **10**, 731–742 (1960)
104. G.-C. Rota, Baxter algebras and combinatorial identities. I. *Bull. Am. Math. Soc.* **75**, 325–329 (1969)
105. S. Weinberg, High-energy behavior in quantum field theory. *Phys. Rev.* **118**, 838–849 (1960)
106. J.H. Lowenstein, W. Zimmermann, The power counting theorem for Feynman integrals with massless propagators. *Commun. Math. Phys.* **44**, 73–86 (1975)
107. D. Yennie, S. Frautschi, H. Suura, The infrared divergence phenomena and high-energy processes. *Ann. Phys.* **13**, 379–452 (1961)
108. T. Kinoshita, Mass singularities of Feynman amplitudes. *J. Math. Phys.* **3** (1962)
109. K. Harada, R. Kubo, Infrared singularity in the electron propagator in quantum electrodynamics. *Nucl. Phys. B* **191**, 181–188 (1981)
110. R. Akhoury, M.G. Sotiropoulos, V.I. Zakharov, The KLN theorem and soft radiation in gauge theories: abelian case. *Phys. Rev. D* **56**, 377–387 (1997)
111. A.A. Vladimirov, Method of calculating renormalization-group functions in the scheme of dimensional regularization. *Theor. Math. Phys.* **43**, 417–422 (1980)
112. L. Euler, De progressionibus harmonicis observationes. *Commentarii academiae scientiarum Petropolitanae* **7**, 150–161 (1740)
113. B. Riemann, Ueber die Anzahl der Primzahlen unter einer gegebenen Grösse, in *Bernard Riemann's gesammelte mathematische Werke und wissenschaftlicher Nachlass*, ed. by R. Dedekind, H.M. Weber, 1st ed. (Cambridge University Press, 1859), pp. 136–144
114. C.G. Bollini, J.J. Giambiagi, Dimensional renormalization: the number of dimensions as a regularizing parameter. *Il Nuovo Cimento B* **1971–1996**(12), 20–26 (1972)
115. G. 't Hooft, M. Veltman, Regularization and renormalization of gauge fields. *Nucl. Phys. B* **44**, 189–213 (1972)
116. B.W. Lee, Gauge theories, in *Methods in Field Theory, Les Houches Session 1975*, ed. by R. Balian and J. Zinn-Justin, Les Houches Session 28 (North Holland/World Scientific, 1981), pp. 79–140
117. K.G. Chetyrkin, V.A. Smirnov,  $R_*$ -operation corrected. *Phys. Lett. B* **144**, 419–424 (1984)
118. W.L. Van Neerven, Dimensional regularization of mass and infrared singularities in two-loop on-shell vertex functions. *Nucl. Phys. B* **268**, 453–488 (1986)
119. V. Sudakov, Vertex parts at very high-energies in quantum electrodynamics. *Sov. Phys. JETP* **3**, 65–71 (1956)
120. *DLMF: NIST Digital Library of Mathematical Functions*, <https://dlmf.nist.gov/>
121. E.E. Boos, A.I. Davydychev, Method for calculating vertex-type Feynman integrals. *Vestnik Moskovskogo Universiteta, Seriya 3. Fizika, Astronomiya* **28**, 8–12 (1987)
122. A.T. Suzuki, E.S. Santos, A.G.M. Schmidt, Massless and massive one-loop three-point functions in negative dimensional approach. *Eur. Phys. J. C* **26**, 125–137 (2002)
123. A.I. Davydychev, Recursive algorithm for evaluating vertex-type Feynman integrals. *J. Phys. A: Math. Gen.* **25**, 5587–5596 (1992)
124. N.I. Ussyukina, A.I. Davydychev, New results for two-loop off-shell three-point diagrams. *Phys. Lett. B* **332**, 159–167 (1994)
125. T. Gehrmann, G. Heinrich, T. Huber, C. Studerus, Master integrals for massless three-loop form factors: one-loop and two-loop insertions. *Phys. Lett. B* **640**, 252–259 (2006)
126. J.A. Gracey, Off-shell two loop QCD vertices. *Phys. Rev. D* **90**, 025014 (2014)
127. P. Belkale, P. Brosnan, Periods and Igusa Zeta functions (2003). <http://arxiv.org/abs/math/0302090>
128. O. Schnetz, Quantum periods: a census of  $\phi^4$ -transcendentals. *Commun. Num. Theor. Phys.* **4**, 1–48 (2010)

129. F.C.S. Brown, On the periods of some Feynman integrals (2010). <http://arxiv.org/abs/0910.0114>
130. S. Hu, O. Schnetz, J. Shaw, K. Yeats, Further investigations into the graph theory of  $\phi^4$ -periods and the  $c_2$  invariant. Ann. Inst. Henri Poincaré D **9**, 473–524 (2022)
131. E. Panzer, O. Schnetz, The Galois coaction on  $\phi^4$  periods. Commun. Num. Theory Phys. **11**, 657–705 (2017)
132. M. Kontsevich, D. Zagier, Periods, in *Mathematics Unlimited - 2001 and Beyond* (Springer, 2001), pp. 771–808
133. S. Bloch, H. Esnault, D. Kreimer, On motives associated to graph polynomials. Commun. Math. Phys. **267**, 181–225 (2006)
134. L. Zambelli, O. Zanusso, Lee-Yang model from the functional renormalization group. Phys. Rev. D **95**, 085001 (2017)
135. J.A. Gracey, Renormalization of scalar field theories in rational spacetime dimensions (2017). <http://arxiv.org/abs/1703.09685>
136. J.A. Gracey, Four loop renormalization of phi3 theory in six dimensions. Phys. Rev. D **92**, 025012 (2015)
137. I.G. Halliday, R.M. Ricotta, Negative dimensional integrals. I. Feynman graphs. Phys. Lett. B **193**, 241–246 (1987)
138. G.V. Dunne, I.G. Halliday, Negative dimensional integration. II. Path integrals and fermionic equivalence. Phys. Lett. B **193**, 247–252 (1987)
139. D.J. Broadhurst, Two-loop negative-dimensional integration. Phys. Lett. B **197**, 179–182 (1987)
140. A. Kempf, D.M. Jackson, A.H. Morales, How to (path-) integrate by differentiating. J. Phys: Conf. Ser. **626**, 012015 (2015)
141. D. Jia, E. Tang, A. Kempf, Integration by differentiation: new proofs, methods and examples. J. Phys. A: Math. Theor. **50**, 235201 (2017)
142. S.L. Adler, Einstein gravity as a symmetry-breaking effect in quantum field theory. Rev. Mod. Phys. **54**, 729–766 (1982)
143. S. Coleman, E. Weinberg, Radiative corrections as the origin of spontaneous symmetry breaking. Phys. Rev. D **7**, 1888–1910 (1973)
144. D. Kreimer, *Structures in Feynman Graphs – Hopf Algebras and Symmetries* (2002). <http://arxiv.org/abs/hep-th/0202110>
145. N.N. Bogoliubow, O.S. Parasiuk, Ueber die Multiplikation der Kausalfunktionen in der Quantentheorie der Felder. Acta Math. **97**, 227–266 (1957)
146. K. Hepp, Proof of the Bogoliubov-Parasiuk theorem on renormalization. Commun. Math. Phys. **2**, 301–326 (1966)
147. W. Zimmermann, Convergence of Bogoliubovs method of renormalization in momentum space. Commun. Math. Phys. **15**, 208–234 (1969)
148. E.R. Speer, Ultraviolet and infrared singularity structure of generic Feynman amplitudes. Annales de l'I.H.P. Physique théorique **23**, 1–21 (1975)
149. W.E. Caswell, A.D. Kennedy, Simple approach to renormalization theory. Phys. Rev. D **25**, 392–408 (1982)
150. S. Sakata, H. Umezawa, S. Kamefuchi, On the structure of the interaction of the elementary particles, I. The renormalizability of the interactions. Progress Theoret. Phys. **7**, 377–390 (1952)
151. A.V. Bäcklund, Zur Theorie der partiellen Differentialgleichung erster Ordnung. Math. Ann. **17**, 285 (1880)
152. E. Braaten, T. Curtright, C. Thorn, An exact operator solution of the quantum Liouville field theory. Ann. Phys. **147**, 365–416 (1983)
153. E. D'Hoker, R. Jackiw, Classical and quantal Liouville field theory. Phys. Rev. D **26**, 3517–3542 (1982)
154. A.M. Polyakov, Quantum geometry of bosonic strings. Phys. Lett. B **103**, 207–210 (1981)
155. E.P. Osipov, Feynman integral for exponential interaction in four-dimensional space-time. I. Theor. Math. Phys. **47**, 475–480 (1981)

156. G.V. Efimov, Formulation of a scalar quantum field theory with an essentially non-linear. Nucl. Phys. **74**, 657–668 (1965)
157. G.V. Efimov, Nonlinear interaction Lagrangians. Sov. Phys. JETP **21**, 7 (1965)
158. K.J. Costello, *Renormalisation and the Batalin-Vilkovisky formalism* (2007). <http://arxiv.org/abs/0706.1533>, preprint
159. K.G. Chetyrkin, F.V. Tkachov, Infrared R-operation and ultraviolet counterterms in the MS-scheme. Phys. Lett. B **114**, 340–344 (1982)
160. V.A. Smirnov, K.G. Chetyrkin,  $R_*$  operation in the minimal subtraction scheme. Theor. Math. Phys. **63**, 462–469 (1985)
161. F. Herzog, B. Ruijl, The  $R_*$ -operation for Feynman graphs with generic numerators. J. High Energy Phys. **2017**, 37 (2017)
162. R. Beekveldt, M. Borinsky, F. Herzog, The Hopf algebra structure of the  $R_*$ -operation. J. High Energy Phys. **2020**, 61 (2020)
163. W. Heisenberg, Über den anschaulichen Inhalt der quantentheoretischen Kinematik und Mechanik. Z. Phys. **43**, 172–198 (1927)
164. H.A. Bethe, The electromagnetic shift of energy levels. Phys. Rev. **72**, 339–341 (1947)
165. R.P. Woodard, The theorem of Ostrogradsky. Scholarpedia **10**, 32243 (2015)
166. M. Ostrogradsky, Mémoires sur les équations différentielles, relatives au problème des isopérimètres. Mem. Acad. St. Petersbourg **6**, 385–517 (1850)
167. H. Motohashi, T. Suyama, Quantum Ostrogradsky theorem. JHEP **09**, 032 (2020)
168. D. Braak, Integrability of the Rabi model. Phys. Rev. Lett. **107**, 100401 (2011)
169. G.W. Ford, R.F. O’Connell, The rotating wave approximation (RWA) of quantum optics: serious defect. Physica A **243**, 377–381 (1997)
170. Y.-M.P. Lam, Perturbation Lagrangian theory for scalar fields-ward-Takahashi identity and current algebra. Phys. Rev. D **6**, 2145–2161 (1972)
171. I.L. Buchbinder, S.L. Lyahovich, Canonical quantisation and local measure of R 2 gravity. Class. Quantum Gravity **4**, 1487–1501 (1987)
172. A. Ganz, K. Noui, Reconsidering the Ostrogradsky theorem: Higher-derivatives Lagrangians, Ghosts and Degeneracy. Class. Quant. Grav. **38**, 075005 (2021)

# Chapter 3

## Renormalized Green Functions in Kinematic Renormalization



This chapter deals with the renormalization group and the properties of renormalized Green functions in the kinematic renormalization scheme.

In Sect. 3.1, we see that the fact that Green functions need to be renormalized implies a certain structure for their dependence on the energy scale. We introduce a generic expansion of Green functions in powers of the logarithmic scale. We also introduce Mellin transforms, these are a version of Feynman integrals where the propagators are raised to arbitrary powers.

Section 3.2 deals with the different versions of the renormalization group equation. We derive the Callan-Symanzik equation, which describes how a renormalized Green function depends on the energy scale. We also demonstrate that the counterterms, which can be introduced as additional vertices of the theory, on the one hand can be computed naturally in the Hopf algebra framework, but on the other hand are related to the renormalization group functions. From that perspective, renormalization can be understood as a change of energy scale.

Section 3.3 describes a systematic framework for solving Dyson-Schwinger equations that has been developed in the past 20 years. It is based on series expansions of renormalized Green functions and aims to turn a Dyson-Schwinger equation into a combinatorial statement for these series coefficients. In the easiest cases, one obtains an explicit differential equation for the anomalous dimension of the Green function in question. We give a systematic derivation and review of the known results, and extend them to include the dependence on the regularization parameter  $\epsilon$  in dimensional regularization.

Section 3.4 is about the power-series solutions of some simple Dyson-Schwinger equations, and in particular about the large-order growth of the series coefficients. We generalize the previously known results with respect to a parameter that interpolates between linear and non-linear Dyson-Schwinger equations, and we show empirically that the large-order growth depends on this parameter in an interesting way.

### 3.1 Renormalization and Momentum-Dependence

We have established in Sect. 2.3.4 that renormalization amounts to the iterative subtraction of subdivergences. These subtractions do not only remove divergences, but they also impose a certain structure on the finite renormalized amplitudes. In the present section, we discuss some of the properties that are consequences of the renormalization process.

#### 3.1.1 Angles and Scales

In Definition 83, we have split the arguments of a Feynman amplitude into one scale variable  $s$  and arbitrary many scale-free angles  $\theta$ . From now on, we ignore the possible dependence on angles unless otherwise mentioned. This is not as much of a restriction as it seems. Observe that for a primitive graph (Theorem 32), the dependence on angles resides in the finite part  $C_\Gamma(\{\theta\})$ , unrelated to the scale dependence given by  $\mathcal{P}[\Gamma] \cdot L$ . In this, the angle dependence is analogous to the divergent part, which, for a primitive graph, is independent of the scale as well. Essentially the same recursive construction that leads to renormalizability (Sect. 2.3.4),  $\mathcal{F}_R(s/s_0) = (\mathcal{F}(s_0))^{-1} \star \mathcal{F}(s)$ , also allows a factorization of angles and scales [1–3],

$$\mathcal{F}_R(s, \theta) = \mathcal{F}_R(s) \Big|_{\theta \text{ fixed}} \star \mathcal{F}_R(\theta) \Big|_{s \text{ fixed}}. \quad (3.1)$$

In the remainder of Sect. 3.1, we will see that the scale-dependence of a renormalized amplitude is to a large extent fixed by the structure of renormalization. On the other hand, little can be said about the angle dependence, even though by Eq. (3.1), the Feynman rules factor “symmetrically” into a scale-dependent and an angle-dependent part. The pivotal reason is that the dependence of a primitive graph on scale is simply a linear function  $\mathcal{P}[\Gamma] \cdot L$  (Theorem 32), while the dependence on angles is much less restricted, albeit subject to the analytic conditions mentioned in Sect. 1.2.8.

#### 3.1.2 Expansion in Logarithmic Momenta

Unless otherwise stated, we assume that a renormalized Feynman graph  $\mathcal{F}_R[\Gamma]$  is projected to its treelevel tensor (Definition 84) and coupling constant. That is,  $\mathcal{F}_R[\Gamma]$  is a scalar under Lorentz transformations (Definition 2) and its power series starts with a constant independent of the coupling  $\alpha$ . More precisely, in kinematic renormalization,  $\mathcal{F}_R[\Gamma] = 1 + \mathcal{O}(\alpha)$ .

**Definition 101.** We express the external momenta as angles and scales (Definition 83), and we introduce some arbitrary *reference scale*  $s_0$ . Define the *logarithmic scale* as

$$L := \ln \frac{s}{s_0}.$$

The point  $L = 0$  amounts to  $s = s_0$ . In the present chapter, we restrict ourselves to kinematic renormalization (Definition 93) and choose  $s_0$  as the renormalization point. The renormalized Feynman rules (Definition 90) are a character (Eq. (2.38)) and hence, they are generated (with respect to the scale  $L$ ) by some infinitesimal character according to Eq. (2.16).

**Definition 102.** The infinitesimal character (Definition 78)  $\sigma$  which generates the Feynman rules (Definition 90) in kinematic renormalization is called *infinitesimal Feynman rule* and it is related to  $\mathcal{F}_{\mathcal{R}}$  via Eq. (2.16),

$$\mathcal{F}_{\mathcal{R}}[\Gamma](L) = \exp^*(L\sigma)[\Gamma], \quad \sigma[\Gamma] := \left. \frac{\partial}{\partial L} \mathcal{F}_{\mathcal{R}}[\Gamma] \right|_{L=0}.$$

The zeroth power  $\sigma_0[\Gamma] := \sigma^{*0}[\Gamma] = \mathcal{F}_{\mathcal{R}}[\Gamma]|_{L=0}$  extracts the value at the renormalization point. In kinematic renormalization,  $\sigma_0 = \tilde{\mathbb{1}}$  (Definition 63) because every renormalized graph vanishes at  $L = 0$  (Definition 93), except for the treelevel amplitude, which is rescaled to  $1 = \tilde{\mathbb{1}} \circ \mathbb{1}$ . The behavior in non-kinematic renormalization will be discussed in Sect. 4.1.1. The empty graph does not depend on momenta, so  $\sigma(\mathbb{1}) = 0$  in every renormalization scheme.

### Example 95: Infinitesimal character for a primitive graph.

For a primitive graph  $\Gamma$ , we know from Theorems 32 and 34 that  $\mathcal{F}_{\mathcal{R}}[\Gamma] = \Lambda \mathcal{P}[\Gamma] \cdot L + \Lambda C_{\Gamma}$ , where in kinematic renormalization  $C_{\Gamma} = 0$  at the renormalization point. Indeed, Definition 102 produces

$$\begin{aligned} \mathcal{F}_{\mathcal{R}}[\Gamma] &= \tilde{\mathbb{1}}(\Gamma) + L \cdot \sigma[\Gamma] + \frac{1}{2} L^2 \cdot m \circ (\sigma \otimes \sigma) \Delta(\Gamma) + \mathcal{O}(L^3) \\ &= 0 + L \cdot \Lambda \mathcal{P}[\Gamma] + 0 + \mathcal{O}(L^3). \end{aligned}$$

We used  $\Delta(\Gamma) = \Gamma \otimes \mathbb{1} + \mathbb{1} \otimes \Gamma$  and  $\sigma(\mathbb{1}) = 0$ . All higher orders in  $L$  vanish.

**Theorem 37** ([2]). Let  $\Gamma$  be a Feynman graph free of IR-divergences, then the renormalized Feynman rules (Definition 90), projected on the treelevel tensor (Definition 84), depend on the scale  $s$  (Definition 83) in the form

$$\mathcal{F}_{\mathcal{R}}[\Gamma](L) = \sum_{j=0}^{\text{cor}(\Gamma)} g_j(\theta) \cdot L^j.$$

Here,  $L$  is the logarithm of the scale (Definition 101) and  $\text{cor}(\Gamma)$  is the coradical degree (Definition 73). The coefficients  $g_j$  can be different for different renormalization schemes.

**Proof** The coefficients  $g_j$  will in general depend on  $\theta$  because the overall amplitude does. By Theorem 34, they are finite. Now, by Definition 102, the term proportional to  $L^n$  is given by

$$\frac{1}{n!} \sigma^{\star n}[\Gamma] = \frac{1}{n!} m \circ \sigma^{\otimes n} \circ \Delta^n(\Gamma).$$

The iterated coproduct  $\Delta^n$  (Definition 72) involves factors of  $\mathbb{1}$  for all  $\Gamma$  with  $\text{cor}(\Gamma) > n$  (Definition 73). But  $\sigma(\mathbb{1}) = 0$  and therefore  $\sigma^{\star n}(\Gamma) = 0$  in those cases.

Alternatively, the statement can also be shown from Dyson-Schwinger integral equations (Theorem 17), without using infinitesimal characters (Definition 102), upon noticing that

$$\int \frac{ds}{s} (\ln s)^n = \frac{(\ln s)^{n+1}}{n+1}.$$

The coradical degree is then the number of nested integrals. This gives a “pedestrian” derivation which does not require the Hopf algebra knowledge that an infinitesimal character *must* exist.  $\square$

**Lemma 38.** Let  $n > 1$ . In kinematic renormalization, the character  $\sigma^{\star n}[\Gamma]$ , and hence  $g_n$  in Theorem 37, are completely determined by values of proper subgraphs  $\gamma \subsetneq \Gamma$ .

**Proof** For a graph  $\Gamma$ ,  $c_n = \sigma^{\star n}[\Gamma] = m(\sigma \otimes \sigma^{\star(n-1)})\Delta(\Gamma)$ . But  $\sigma(\mathbb{1}) = 0$  in kinematic renormalization, therefore only  $\Delta_1(\Gamma)$  (Definition 66) contributes, consisting entirely of subgraphs.  $\square$

**Example 96: Second chain graph, scale dependence.**

Consider the graph  $S \simeq \Delta$  from Examples 27 and 93, where

$$\begin{aligned}\mathcal{F}_R[S] &= -\frac{1}{648} \ln^3\left(\frac{s}{s_0}\right) + \frac{11}{1296} \ln^2\left(\frac{s}{s_0}\right) - \frac{85}{3888} \ln\left(\frac{s}{s_0}\right), \\ \mathcal{F}_R[S_i] &= \frac{1}{72} i \ln^2\left(\frac{s}{s_0}\right) - \frac{11}{216} i \ln\left(\frac{s}{s_0}\right), \quad \mathcal{F}_R[\gamma] = \frac{1}{6} \ln\left(\frac{s}{s_0}\right).\end{aligned}$$

The infinitesimal Feynman rules (Definition 102), applied to these graphs, are

$$\sigma[S] = -\frac{85}{3888}, \quad \sigma[S_i] = -\frac{11}{216}i, \quad \sigma[\gamma] = \frac{1}{6}.$$

Note that  $\sigma[S_i]$  equals the period  $\mathcal{P}[P_2]$  of the 2-loop primitive  $P_2$  constructed from  $S_i$  in Example 91. Now, use  $\Delta(S_i) = \gamma_i \otimes \gamma$  to find that indeed

$$\exp^*(L\sigma)[S_i] = L\sigma[S_i] + \frac{1}{2} L^2 \sigma[\gamma_i] \sigma[\gamma] = -\frac{11}{216}iL + \frac{1}{2} \left(\frac{1}{6}\right) i \left(\frac{1}{6}\right) = \mathcal{F}_R[S_i].$$

As expected,  $\sigma^{*2}[S_i] = \frac{1}{2}\sigma[\gamma_i]\sigma[\gamma]$  is completely determined by the subgraph  $\gamma_i \simeq \gamma$ . The factor  $i$  is to correct the intermediate propagator  $\frac{i}{s}$ , we divide out the tensor  $s$  as usual.

By Example 77,  $\Delta(S) = S \otimes \mathbb{1} + \mathbb{1} \otimes S + 2\gamma_i \otimes S_i + \gamma_1 \gamma_2 \otimes \gamma$ . Further,  $\sigma[\gamma_1 \gamma_2] = 0$  and therefore

$$\begin{aligned}\sigma^{*2}[S] &= 2\sigma[\gamma_i]\sigma[S_i] = 2\left(\frac{1}{6}\right) i \left(-\frac{11}{216}i\right) = \frac{11}{648}, \\ \sigma^{*3}[S] &= 2\sigma[\gamma_i]\sigma^{*2}[S_i] + \sigma^{*2}[\gamma_1 \gamma_2]\sigma[\gamma] = 2\sigma[\gamma]^3 = 2i^2 \left(\frac{1}{6}\right)^3 = -\frac{1}{108}.\end{aligned}$$

With these numbers, we correctly reproduce Example 93,

$$\exp^*(L\sigma)[S] = L\sigma[S] + \frac{1}{2} L^2 \sigma^{*2}[S] + \frac{1}{6} \sigma^{*3}[S] = -\frac{85}{3888}L + \frac{11}{1296}L^2 - \frac{1}{648}L^3.$$

$\sigma[S]$  is the only non-trivial input, all higher orders in  $L$  are determined by subgraphs.

Summing over all graphs, and suppressing the dependence on angles, Theorem 37 delivers an expansion of the renormalized Green function, again projected to a treelevel tensor (Definition 84), in terms of logarithms,

$$G_{\mathcal{R}}^r(\alpha, L) = \sum_{j=0}^{\infty} \gamma_j^r(\alpha) \cdot L^j. \quad (3.2)$$

Observe that  $^j$  in  $L^j$  denotes a power while  $^r$  in  $\gamma^r$  is the residue  $r := \text{res}(G^r)$  (Definition 26). By Theorem 37, the functions  $\gamma_j^r$  obtain contributions only from graphs  $\Gamma$  with  $\text{cor}(\Gamma) \geq j$ . They are given by the infinitesimal Feynman rules (Definition 102) acting on the combinatorial Green functions (Definition 47),

$$\gamma_j^r(\alpha) = \frac{1}{j!} \sum_{\Gamma \text{ 1PI}, \text{res}(\Gamma)=r} \alpha^{|\Gamma|} \text{sym}(\Gamma) \cdot \sigma^{\star j}[\Gamma] = \frac{1}{j!} \sigma^{\star j}[\Gamma^r(\alpha)]. \quad (3.3)$$

### 3.1.3 Mellin Transforms

We can rewrite  $L$  (Definition 101) in Theorem 37 as derivatives,

$$L^j = \partial_\rho^j e^{L\rho} \Big|_{\rho=0} = \partial_\rho^j \left( \frac{s}{s_0} \right)^\rho \Big|_{\rho=0} \Rightarrow \mathcal{F}_{\mathcal{R}}[\gamma](L) = \sum_{j=0}^{\text{cor}(\gamma)} g_j(\theta) \partial_\rho^j \left( \frac{s}{s_0} \right)^\rho \Big|_{\rho=0}. \quad (3.4)$$

At this point, we assume that  $\gamma$  is a 1PI propagator-type graph for concreteness. Then  $s = \underline{p}^2$  is the external momentum of  $\gamma$  and  $g_j(\theta) = g_j$  is independent of angles. By Eq.(2.37),  $\mathcal{F}[B_+^\Gamma(\mathcal{F}_{\mathcal{R}}[\gamma])] = \int d_\Gamma \mathcal{F}_{\mathcal{R}}[\gamma]$ . In the momentum representation (Eq.(1.50)),  $\gamma$  replaces one of the edges in  $\Gamma$  according to

$$\frac{i}{s_p} \rightarrow \frac{i}{s_p} s_p \mathcal{F}_{\mathcal{R}}[\gamma](s) \frac{i}{s_p} = \frac{-1}{s_p} \mathcal{F}_{\mathcal{R}}[\gamma](s).$$

If we further assume the field to be massless, then  $s_p = s = \underline{p}^2$  and

$$\begin{aligned} \int d_\Gamma \mathcal{F}_{\mathcal{R}}[\gamma] &= \prod_{v \in V_\Gamma} (-i \lambda_{|v|}) \cdot \prod_{l \in L_\Gamma} \int \frac{d^D k_l}{(2\pi)^D} \frac{-1}{s} \sum_{j=0}^{\text{cor}(\gamma)} g_j(\theta) \partial_\rho^j \left( \frac{s}{s_0} \right)^\rho \Big|_{\rho=0} \prod_{e \neq l} \frac{i}{s_e} \\ &= - \sum_{j=0}^{\text{cor}(\gamma)} g_j(\theta) \partial_\rho^j \left( \frac{1}{s_0} \right)^\rho \prod_{v \in V_\Gamma} (-i \lambda_{|v|}) \cdot \prod_{l \in L_\Gamma} \int \frac{d^D k_l}{(2\pi)^D} \frac{1}{s^{1-\rho}} \prod_{e \neq l} \frac{i}{s_e} \Big|_{\rho=0} \\ &=: -\mathcal{F}_{\mathcal{R}}[\gamma] \left( \partial_\rho \right) \frac{1}{(s_0)^\rho} \prod_{v \in V_\Gamma} (-i \lambda_{|v|}) \tilde{F}_\gamma(\rho, 0, \dots, 0) \Big|_{\rho=0}. \end{aligned} \quad (3.5)$$

**Definition 103.** The *Mellin transform* of a Feynman graph  $\Gamma$  with  $E = |E_\Gamma|$  internal edges and  $L = |L_\Gamma|$  loops is defined by raising each of its propagators to an undetermined power  $\rho_e$ ,

$$\tilde{F}_\Gamma(\rho_1, \dots, \rho_E) := \int \frac{d^{LD}k}{(2\pi)^{LD}} \frac{1}{(\underline{k}_1^2)^{1-\rho_1}} \cdots \frac{1}{(\underline{k}_E^2)^{1-\rho_E}}$$

Up to global factors, the Mellin transform equals the integral  $\mathcal{F}[\Gamma]$  in analytic regularization (Sect. 2.3.2) with exponents  $\nu_j = 1 - \rho_j$ . By Eq. (2.45), the Mellin transform is proportional to the scale (Definition 83)  $s^{kD/2-E+\sum\rho_j}$ . For renormalization, we evaluate at  $s = s_0$ , therefore, we factor out this dependence and define

$$s^{k\frac{D}{2}-E+\sum_j \rho_j} F_\Gamma(\rho_1, \dots, \rho_E) := \tilde{F}_\Gamma(\rho_1, \dots, \rho_E).$$

If  $\Gamma$  is primitive and divergent (Definition 88) and we restrict ourselves to only one  $\rho \neq 0$ , then

$$F_\Gamma(\rho) = \sum_{j=0}^{\infty} c_j \rho^{j-1}. \quad (3.6)$$

That there is a pole term of first order, and no higher order poles, follows from the fact that the same is true for analytic regularization (Sect. 2.3.2). Indeed, without a pole, the graph would not be divergent in the physical limit, and with a pole of higher than first order, it would have non-local subdivergences and thus be not primitive, both contradicting the assumptions.

### Example 97: 1-loop multiedge, Mellin transform.

The Mellin transform can directly be read off from Example 25 (compare also Example 86):

$$F_{M^{(1)}}(\rho_1, \rho_2) = \frac{1}{(4\pi)^{\frac{D}{2}}} \frac{\Gamma(-\rho_1 - \rho_2 + 2 - \frac{D}{2}) \Gamma(\frac{D}{2} - 1 + \rho_1) \Gamma(\frac{D}{2} - 1 + \rho_2)}{\Gamma(D - 2 + \rho_1 + \rho_2) \Gamma(1 - \rho_1) \Gamma(1 - \rho_2)}.$$

For the sake of brevity, we skip all prefactors  $4\pi$ . Set  $\rho_2 = 0$  and  $D = 4 - 2\epsilon$ :

$$F_{M^{(1)}}(\rho, 0) \Big|_{D=4-2\epsilon} = \frac{\Gamma(\epsilon - \rho) \Gamma(1 - \epsilon + \rho) \Gamma(1 - \epsilon)}{\Gamma(2 - 2\epsilon + \rho) \Gamma(1 - \rho)}.$$

Conversely, set  $D = 4$  and use Eq. (2.47):

$$F_{M^{(1)}}(\rho_1, \rho_2) \Big|_{D=4} = \frac{-1}{(\rho_1 + \rho_2)(1 + \rho_1 + \rho_2)} \frac{\Gamma(1 - \rho_1 - \rho_2)\Gamma(1 + \rho_1)\Gamma(1 + \rho_2)}{\Gamma(1 + \rho_1 + \rho_2)\Gamma(1 - \rho_1)\Gamma(1 - \rho_2)}$$

Combining both the previous restrictions, we obtain

$$F_{M^{(1)}}(\rho, 0) \Big|_{D=4} = \frac{-1}{\rho(1 + \rho)}, \quad F_{M^{(1)}}(\rho, 0) \Big|_{D=6} = \frac{1}{\rho(1 + \rho)(2 + \rho)(3 + \rho)}.$$

As seen from the first equations, a Mellin transform is in general an arbitrarily complicated function, finding a simple rational function is an exotic special case.

The Mellin transform allows to write an explicit formula for the action of the cocycle  $B_+^\Gamma$  (Definition 89) on the level of Feynman rules. This is the mapping between different  $B_+$  announced in the universal property (Theorem 25), from the Hopf algebra of Feynman graphs to the Hopf algebra of formal power series in  $L$ . We assume that  $\gamma$  is inserted into edge  $e = 1$  in  $\Gamma$ , then Eq. (3.5) becomes

$$\mathcal{F}\left[B_+^\Gamma(\mathcal{F}_R[\gamma])\right](L) = - \prod_{v \in V_\Gamma} (-i\lambda_{|v|}) \mathcal{F}_R[\gamma](\partial_\rho) e^{L\rho} F_\Gamma(\rho) \Big|_{\rho=0}. \quad (3.7)$$

Kinematic renormalization (Definition 93) amounts to subtraction at  $L = 0$ , therefore

$$\mathcal{F}_R\left[B_+^\Gamma(\mathcal{F}_R(\gamma))\right](L) = - \prod_{v \in V_\Gamma} (-i\lambda_{|v|}) \mathcal{F}_R[\gamma](\partial_\rho) (e^{L\rho} - 1) F_\Gamma(\rho) \Big|_{\rho=0}. \quad (3.8)$$

The product of series  $\mathcal{F}_R[\gamma]$  and  $F_\Gamma$  in Eq. (3.8) can be reordered to obtain a representation of the cocycle as an integral operator:

$$\mathcal{F}_R\left[B_+^\Gamma(\mathcal{F}_R[\gamma])\right](L) = - \int_0^L dt \sum_{k=0}^{\text{cor}(\gamma)} c_k \frac{\partial^k}{\partial t^k} \mathcal{F}_R[\gamma](t). \quad (3.9)$$

The precise algebraic nature of these maps regarding the universal property is explained in [4]. Following Theorem 22, the integral  $-c_0 \int dt$  is the crucial ingredient to make this map a cocycle, all higher summands can be viewed as a coboundary  $b_0 L_0$  (Definition 74). In the more conventional language of physics,  $c_0$  defines the *leading-log-order* of an amplitude, while  $c_{j>0}$  give next-to-leading-log corrections, see Sect. 3.3.3.

### Example 98: Tree Feynman rules.

Using Eq. (3.9), we can assign an amplitude to every rooted tree. We chose the trees to be unlabeled, consequently  $\mathcal{F}_{\mathcal{R}}[\mathbb{1}] = 1$  is the only primitive of this model, and all other trees correspond to iteratively inserting this primitive into itself. Therefore, all renormalized Feynman rules can be expressed in terms of the coefficients of the Mellin transform Eq. (3.6), for example

$$\begin{aligned}\mathcal{F}_{\mathcal{R}}[\bullet] &= \mathcal{F}_{\mathcal{R}}[B_+(\mathbb{1})] = - \int_0^L dt c_0 \mathcal{F}_{\mathcal{R}}[\mathbb{1}] = -c_0 L, \\ \mathcal{F}_{\mathcal{R}}\left[\begin{array}{c} \bullet \\ | \end{array}\right] &= - \int_0^L dt (c_0(-c_0 t) + c_1 \partial_t(-c_0 t)) = \frac{1}{2} c_0^2 L^2 + c_0 c_1 L, \\ \mathcal{F}_{\mathcal{R}}\left[\begin{array}{c} \Lambda \\ | \end{array}\right] &= \mathcal{F}_{\mathcal{R}}(B_+(\mathcal{F}_{\mathcal{R}}[\bullet]^2)) = -\frac{1}{3} c_0^3 L^3 - c_0^2 c_1 L^2 - 2c_0^2 c_2 L, \\ \mathcal{F}_{\mathcal{R}}\left[\begin{array}{c} \Lambda \\ \Lambda \\ | \end{array}\right] &= \frac{1}{12} c_0^4 L^4 + \frac{2}{3} c_0^3 c_1 L^3 + c_0^2 (2c_0 c_2 + c_1^2) L^2 + c_0^2 (c_0 c_3 + 4c_1 c_2) L.\end{aligned}$$

Observe that the highest order in  $L$  is determined by  $c_0$ , the next-to-highest order involves  $\{c_0, c_1\}$ , and so on. This will be made precise in Sect. 3.3.3.

A priori, the tree Feynman rules must be computed recursively, by repeatedly using Eq. (3.9). However, it is possible to directly obtain the result for a given rooted tree. To that end, one considers all possible *tubings* of a tree, where a tubing can be understood as a graphical representation of cutting the tree into single vertices by a certain sequence of cuts. See [5] for details.

### Example 99: Toy model, Mellin transform.

For the toy model (Example 80) at  $\epsilon = 0$ , the Mellin transform is

$$F(\rho) = \int_0^\infty dx \frac{x^\rho}{x+1} = \frac{-\pi}{\sin(\pi\rho)} = -\frac{1}{\rho} \exp\left(\sum_{n=1}^\infty \zeta(2n) \frac{\rho^{2n}}{n}\right) = -\frac{1}{\rho} - \frac{\pi^2}{6}\rho - \frac{7\pi^4}{360}\rho^3 + \dots$$

We used Eq. (2.47) and  $\zeta(2n) = (-1)^{n+1} 2^{2n+1} B_{2n}/(2n)! \pi^{2n}$  with the Bernoulli numbers  $B_j$ . Consequently, the tree amplitudes (Example 98) for the toy model are

$$\begin{aligned}\mathcal{F}_{\mathcal{R}}[\mathbb{1}] &= 1, & \mathcal{F}_{\mathcal{R}}(\bullet) &= -L, & \mathcal{F}_{\mathcal{R}}\left[\begin{array}{c} \bullet \\ | \end{array}\right] &= \frac{1}{2} L^2, \\ \mathcal{F}_{\mathcal{R}}\left[\begin{array}{c} \Lambda \\ | \end{array}\right] &= -\frac{1}{3} L^3 - \frac{\pi^2}{6} L, & \mathcal{F}_{\mathcal{R}}\left[\begin{array}{c} \Lambda \\ \Lambda \\ | \end{array}\right] &= \frac{1}{12} L^4 + \frac{\pi^2}{6} L^2.\end{aligned}$$

### Summary of Sect. 3.1.

1. Feynman integrals, as well as entire amplitudes, factorize under the convolution product  $\star$  into a scale-dependent and an angle-dependent part (Sect. 3.1.1). We are mostly concerned with the scale dependent part.
2. We expanded the scale-dependence of the Feynman rules in powers of the logarithmic scale  $L$ . The infinitesimal Feynman rules  $\sigma$  extract the linear coefficient in  $L$ , and the exponential of the operator  $\sigma$  reproduces the full Feynman amplitude by acting with  $\sigma$  on subgraphs (Sect. 3.1.2).
3. The action of the cocycle  $B_+$  on Feynman graphs amounts to insertion of subgraphs. For the values of Feynman integrals, the action of  $B_+$  can be expressed as a series convolution with the Mellin transform of the underlying graph (Sect. 3.1.3).

## 3.2 Renormalization Group in Kinematic Renormalization

Up to this point, we have examined the scale-dependence of individual graphs. In the present section, we consider full Green functions and additionally use the information that they are solutions of Dyson-Schwinger equations.

### 3.2.1 Callan-Symanzik Equation

Our exposition of the renormalization group loosely follows [1, 6, 7]. The convolution product  $\star$  (Definition 77) is a homomorphism, this implies that it is linear under multiplication,  $L \cdot \sigma[\Gamma] = \sigma[L \cdot \Gamma]$ . A product can thus be expanded according to

$$\left((L_1 + L_2)\sigma\right) \star \left((L_1 + L_2)\sigma\right) = L_1^2 \sigma \star \sigma + L_1 L_2 \sigma \star \sigma + L_2 L_1 \sigma \star \sigma + L_2^2 \sigma \star \sigma.$$

Collecting all the prefactors, we obtain

$$\left((L_1 + L_2)\sigma\right) \star \left((L_1 + L_2)\sigma\right) = (L_1 + L_2)^2 \sigma \star \sigma.$$

The same argument applies to all higher monomials. Consequently, the Feynman rules (Definition 102) factorize with respect to scales.

**Lemma 39.** Let  $\mathcal{F}_{\mathcal{R}}$  be the renormalized Feynman rules in kinematic renormalization, given by Definition 102. Let  $L_1, L_2 \in \mathbb{R}$  be two arbitrary, but fixed scales, then

$$\mathcal{F}_{\mathcal{R}}|_{L_1+L_2}[\Gamma] = \mathcal{F}_{\mathcal{R}}[\Gamma](L_1 + L_2) = e^{\star(L_1+L_2)\sigma}\Gamma = (e^{\star L_1\sigma} \star e^{\star L_2\sigma})\Gamma = (\mathcal{F}_{\mathcal{R}}|_{L_1} \star \mathcal{F}_{\mathcal{R}}|_{L_2})\Gamma.$$

Algebraically, Lemma 39 means that the Feynman rules at fixed angles (Definition 83) form a group with respect to  $\star$ , this is the *renormalization group*. It is a Lie group, its generator are the infinitesimal Feynman rules  $\sigma$  (Definition 102) as can be seen from Eq. (2.16).

The star product  $\star$  does not directly correspond to an ordinary product, so despite Lemma 39, we generally have  $\mathcal{F}_{\mathcal{R}}[\Gamma](L_1 + L_2) \neq \mathcal{F}_{\mathcal{R}}[\Gamma](L_1) \cdot \mathcal{F}_{\mathcal{R}}[\Gamma](L_2)$ . But still, the renormalization group has deep consequences for the momentum-dependence of renormalized Green functions. To see this, recall that every physically sensible Green function satisfies a combinatorial DSE (Theorem 28),

$$\Gamma^r = \mathbb{1} \pm \sum_{\Gamma \in K^r} \alpha^{|L_\Gamma|} \text{sym}(\Gamma) B_+^\Gamma (\Gamma^r \cdot Q^{|L_\Gamma|}).$$

Denote the insertion into all  $k$ -loop kernels by

$$B_+^{r,k} = \sum_{|L_\Gamma|=k, \text{ res}(\Gamma)=r} \text{sym}(\Gamma) B_+^\Gamma. \quad (3.10)$$

We skip the superscript  $r$  for now. Then, the DSE becomes

$$\Gamma = \mathbb{1} \pm \sum_{k=1}^{\infty} \alpha^k B_+^k (\Gamma \cdot Q^k). \quad (3.11)$$

The combinatorial Green function  $\Gamma$  (Definition 47) is a series in  $\alpha$ . We obtain the 1PI Green function (Definition 92) by applying the renormalized Feynman rules,

$$G_{\mathcal{R}}(L, \alpha) = \mathcal{F}_{\mathcal{R}}[\Gamma(\alpha)](L). \quad (3.12)$$

We now want to translate Lemma 39 into a statement about the behavior of Eq. (3.12) under a shift in the scale  $L$  (Definition 101). We remark that such a shift can equivalently be viewed as a change of the renormalization point  $s_1 \leftrightarrow s_0$ ,

$$L' := \ln \frac{s}{s_2} = \ln \frac{s}{s_1} + \ln \frac{s_1}{s_2} = L + \delta, \quad \Leftrightarrow \quad s_2 = e^\delta \cdot s_1.$$

**Definition 104.** Let  $\mathcal{Q}_{\mathcal{R}}(\alpha, L)$  be the renormalized invariant charge (Definition 95). The *running coupling*  $\tilde{\alpha}$  at the energy scale  $L$  is defined as

$$\tilde{\alpha}(\alpha, L) := \alpha \mathcal{Q}_{\mathcal{R}}(\alpha, L).$$

In kinematic renormalization with renormalization point  $L = 0$ , we have  $\tilde{\alpha}(\alpha, 0) = \alpha$ .

**Lemma 40.** Let  $L, \delta \in \mathbb{R}$  be two arbitrary, but fixed, logarithmic scales (Definition 101). Let  $G_{\mathcal{R}}(\alpha, L)$  be a solution of a DSE in kinematic renormalization (Definition 93) and let  $\tilde{\alpha}$  be the running coupling (Definition 104). Then

$$G_{\mathcal{R}}(\alpha, L + \delta) = G_{\mathcal{R}}(\alpha, \delta) \cdot G_{\mathcal{R}}(\tilde{\alpha}(\alpha, \delta), L).$$

**Proof** Under a shift of scale, the Feynman rules transform according to Lemma 39:

$$\mathcal{F}_{\mathcal{R}}[\Gamma](\delta + L) = \left( \mathcal{F}_{\mathcal{R}} \Big|_{\delta} \star \mathcal{F}_{\mathcal{R}} \Big|_L \right) \Gamma = m \left( \mathcal{F}_{\mathcal{R}} \Big|_{\delta} \otimes \mathcal{F}_{\mathcal{R}} \Big|_L \right) \Delta(\Gamma).$$

$\Gamma$  fulfills the DSE Eq.(3.11), hence we know  $\Delta(\Gamma)$  from Theorem 26 and find:

$$\begin{aligned} \mathcal{F}_{\mathcal{R}}[\Gamma](L') &= \sum_{j=0}^{\infty} \mathcal{F}_{\mathcal{R}}[\Gamma \cdot Q^j](\delta) \cdot \alpha^j \mathcal{F}_{\mathcal{R}}[\Gamma_j](L) \\ &= \mathcal{F}_{\mathcal{R}}[\Gamma](\delta) \cdot \sum_{j=0}^{\infty} \left( \alpha \mathcal{F}_{\mathcal{R}}[Q](\delta) \right)^j \cdot \mathcal{F}_{\mathcal{R}}[\Gamma_j](L). \end{aligned} \quad (3.13)$$

Here we have used multiplicativity (Eq.(2.38)) to write  $\mathcal{F}_{\mathcal{R}}[Q^j] = \mathcal{F}_{\mathcal{R}}[Q]^j$ . The invariant charge  $\mathcal{F}_{\mathcal{R}}[Q](\delta) = \mathcal{Q}_{\mathcal{R}}(\alpha, \delta)$  (Definition 95) evaluated at a fixed  $\delta$  is simply a fixed number, it rescales the coupling  $\alpha$  according to Definition 104. In Eq.(3.13),  $\Gamma_j := [\alpha^j] \Gamma$  is the series coefficient of the Green function. The sum over  $j$  is nothing but the Green function, but at the running coupling.  $\square$

We emphasize how nicely the correspondence between Lemmas 39 and 40 fits with our understanding of the renormalization Hopf algebra as an “advanced variant of the Faà di Bruno Hopf algebra” (Sect. 2.1.4), compare Sect. 2.2.1: The  $\star$ -product in the Hopf algebra of Feynman graphs *really* amounts to inserting Green functions into each other, corresponding to insertion of power series.

**Definition 105.** Let  $G_{\mathcal{R}}^r$  be the renormalized 1PI Green function (Definition 92) in kinematic renormalization (Definition 93) with renormalization point  $L = 0$ , and let  $\tilde{\alpha}(\alpha, L)$  be the running coupling (Definition 104). The *anomalous dimension* in kinematic renormalization is defined as

$$\gamma^r(\alpha) := \frac{\partial}{\partial L} G_{\mathcal{R}}^r(\alpha, L) \Big|_{L=0} = \sigma[\Gamma^r].$$

The *Symanzik beta function* in kinematic renormalization is

$$\beta(\alpha) := \frac{\partial}{\partial L} \tilde{\alpha}(\alpha, L) \Big|_{L=0} = \alpha \sigma[Q].$$

Here,  $\sigma$  (Definition 102) is the infinitesimal Feynman rule.

The anomalous dimension expresses the fact that interaction in a quantum field theory can effectively change the mass dimension of the field, compare for example [8] or our discussion in Sect. 2.4.

**Theorem 41** ([9, 10]). In kinematic renormalization, with  $\beta, \gamma^r$  from Definition 105, the renormalized Green function, projected onto its treelevel tensor (Definition 84), satisfies the *Callan-Symanzik equation*,

$$\frac{\partial}{\partial L} G_{\mathcal{R}}^r(\alpha, L) = \left( \gamma^r(\alpha) + \beta(\alpha) \cdot \frac{\partial}{\partial \alpha} \right) G_{\mathcal{R}}^r(\alpha, L).$$

**Proof** Deriving Lemma 40 with respect to  $\delta$ , we obtain

$$\frac{\partial}{\partial \delta} \ln G_{\mathcal{R}}(\alpha, L + \delta) = \frac{\partial}{\partial \delta} \ln G_{\mathcal{R}}(\alpha, \delta) + \frac{\partial}{\partial \delta} \tilde{\alpha}(\alpha, \delta) \cdot \frac{\partial}{\partial \tilde{\alpha}(\delta)} \ln G_{\mathcal{R}}(\tilde{\alpha}(\delta), L).$$

Consider the point  $\delta = 0$ . According to kinematic renormalization conditions,  $\tilde{\alpha}(0) = \alpha$  and  $G_{\mathcal{R}}(\alpha, 0) = 1$ , therefore  $\partial_L \ln G|_{L=0} = \partial_L G|_{L=0}$  and

$$\frac{\partial}{\partial L} \ln G_{\mathcal{R}}(\alpha, L) = \frac{\partial}{\partial L} G_{\mathcal{R}}(\alpha, L) \Big|_{L=0} + \frac{\partial}{\partial L} \tilde{\alpha}(\alpha, L) \Big|_{L=0} \cdot \frac{\partial}{\partial \alpha} \ln G_{\mathcal{R}}(\alpha, L).$$

Identify Definition 105 to obtain the Callan-Symanzik equation.  $\square$

A variant of the Callan-Symanzik equation can be obtained if we exchange  $L \leftrightarrow \delta$  in Lemma 40 and then derive that equation with respect to  $\delta$  at  $\delta = 0$ :

$$\frac{\partial}{\partial L} G_{\mathcal{R}}^r(\alpha, L) = G_{\mathcal{R}}^r(\alpha, L) \cdot \gamma^r(\tilde{\alpha}(\alpha, L)) \Leftrightarrow \frac{\partial}{\partial L} \ln G_{\mathcal{R}}^r(\alpha, L) = \gamma^r(\tilde{\alpha}(\alpha, L)). \quad (3.14)$$

Further variants and generalizations of the Callan-Symanzik equation exist [11–15]. Recall that we project the Green function onto its tensor structure (Sect. 2.2.2). In realistic theories, there are multiple tensors, and hence multiple Green functions (Example 68). Each of them has their own  $\gamma^r$  and the Callan-Symanzik equation can involve additional terms, such as  $\gamma^m(\alpha) \frac{\partial}{\partial m}$  for a massive theory. For the present thesis, Theorem 41 is sufficiently general.

For our later calculations it is useful to rewrite the Callan-Symanzik equation in terms of the expansion functions  $\gamma_j^r(\alpha)$  of the log-expansion Eq.(3.2),

$$G_{\mathcal{R}}^r(\alpha, L) = \sum_{j=0}^{\infty} \gamma_j^r(\alpha) \cdot L^j. \quad (3.15)$$

**Theorem 42** ([6, 16, 17]). Let  $\gamma_j^r$  be the coefficients of the log expansion Eq.(3.15), where  $r$  is an index, not a power. Let  $\beta, \gamma$  be the beta function and anomalous dimension (Definition 105) of the corresponding Callan-Symanzik equation. Then

$$\gamma_{j>1}^r(\alpha) = \frac{1}{j} (\gamma^r(\alpha) + \beta(\alpha) \cdot \partial_\alpha) \gamma_{j-1}^r(\alpha).$$

**Proof** Act on Eq.(3.13) with the infinitesimal Feynman rules (Definition 102), or equivalently insert the expansion Eq.(3.2) into Theorem 41.  $\square$

**Lemma 43.** Assume  $G^r(\alpha, L)$  is a formal power series (Definition 53) in  $\alpha$ . Assume that  $\gamma^{(r)}$  and  $\beta$  have a non-vanishing term  $\propto \alpha$ . Then, the coefficients in Eq.(3.15) are of order

$$\gamma_k(\alpha) \in \mathcal{O}(\alpha^k) \quad \forall k \geq 0. \quad (3.16)$$

**Proof** Clearly  $\gamma_0(\alpha) = G(\alpha, L=0) \in \mathcal{O}(\alpha^0)$ . We have rescaled the DSE Eq.(3.11) such that the first correction is of order one,  $\Gamma = \mathbb{1} \pm \alpha B_+^1(\mathbb{1})$ . But  $B_+(\mathbb{1})$  is primitive by Theorem 22, therefore its amplitude is linear in  $L$  by Theorem 32 and consequently  $\gamma = \partial_L \Gamma \in \mathcal{O}(\alpha)$ . The higher  $k \geq 1$  follow from Theorem 42 by induction. It is even possible that some coefficients of the power series vanish and that  $\gamma_k(\alpha)$  actually starts with a higher order than  $k$ .  $\square$

**Lemma 44.** Consider  $\phi^n$  theory with vertex  $G_{\mathcal{R}}^v$  and propagators  $G_{\mathcal{R}}^e$  in kinematic renormalization (Definition 93). Let  $e \sim v$  denote that  $e$  is incident to  $v$ . Then, the beta function (Definition 105) can be computed from the various anomalous dimensions according to

$$\beta(\alpha) = \frac{2\alpha}{n-2} \left( \gamma^v(\alpha) - \frac{1}{2} \sum_{e \sim v} \gamma^e(\alpha) \right). \quad (3.17)$$

**Proof** The invariant charge (Definition 94) is a monomial in the various Green functions, consequently, the beta function is related to the various anomalous dimensions. Consider the logarithm  $\ln \mathcal{Q}_{\mathcal{R}} = \frac{2}{n-2} \ln G_{\mathcal{R}}^v - \sum_{e \sim v} \frac{1}{n-2} \ln G_{\mathcal{R}}^e$ . By Definition 105,

$$\beta(\alpha) = \alpha \partial_L \mathcal{Q}_{\mathcal{R}}|_{L=0} = \mathcal{Q}_{\mathcal{R}}(0) \cdot \partial_L \ln \mathcal{Q}_{\mathcal{R}}|_{L=0}.$$

In kinematic renormalization (Definition 93),  $\mathcal{Q}_{\mathcal{R}}(0) = 1$  and we obtain

$$\beta(\alpha) = \frac{\partial}{\partial L} \ln \mathcal{Q}_{\mathcal{R}}|_{L=0} = \frac{2\alpha}{n-2} \left( \partial_L G_{\mathcal{R}}^v|_{L=0} - \sum_{e \sim v} \frac{1}{2} \partial_L G_{\mathcal{R}}^e|_{L=0} \right).$$

□

### Example 100: $\phi^n$ theory, relation between anomalous dimensions.

In  $\phi^n$  theory, there are exactly  $n$  identical propagators attached to each vertex, hence

$$\beta(\alpha) = \alpha \sigma[\mathcal{Q}] = \frac{2\alpha}{n-2} \left( \gamma^{(n)}(\alpha) - \frac{n}{2} \gamma^{(2)}(\alpha) \right).$$

Concretely, in  $\phi^3$  theory,  $\beta = 2\alpha\gamma^{(3)} - 3\alpha\gamma^{(2)}$ . In  $\phi^4$  theory,  $\beta = \alpha\gamma^{(4)} - 2\alpha\gamma^{(2)}$ .

Finally, all the renormalization group equations can be rewritten for the running coupling (Definition 104). Use Definition 94 to find

$$\frac{\partial}{\partial L} \ln \mathcal{Q}_{\mathcal{R}} = \frac{2}{n-2} \frac{\partial}{\partial L} \ln G_{\mathcal{R}}^v - \sum_{e \sim v} \frac{1}{n-2} \frac{\partial}{\partial L} \ln G_{\mathcal{R}}^e.$$

Apply Theorems 41, 3.14 to each summand and use Lemma 44 to collect the terms:

$$\frac{\partial}{\partial L} \tilde{\alpha}(\alpha, L) = \tilde{\alpha} \frac{\partial}{\partial L} \ln \mathcal{Q}_{\mathcal{R}}(\alpha, L) = \beta(\tilde{\alpha}(\alpha, L)) = \left( \beta(\alpha) + \beta(\alpha) \frac{\partial}{\partial \alpha} \right) \mathcal{Q}_{\mathcal{R}}(\alpha, L). \quad (3.18)$$

Note that, by Definition 105,  $\beta$  is the derivative  $\partial_L \tilde{\alpha}$  at  $L = 0$ , while Eq. (3.18) holds for all  $L$ . Using separation of variables, one obtains a formal solution:

$$d\tilde{\alpha}(\alpha, L) \frac{1}{\beta(\tilde{\alpha}(\alpha, L))} = dL, \quad \tilde{\alpha}(\alpha, 0) = \alpha \quad \Rightarrow \quad L = \int_{\alpha}^{\tilde{\alpha}(L)} du \frac{1}{\beta(u)}. \quad (3.19)$$

### Example 101: Multiedge DSE, beta function and anomalous dimension.

In Example 35, we introduced a simplified DSE for the  $\phi^3$  propagator by setting  $G_R^{(3)} = \cancel{\llcorner} = 1$ . In that case, the 3-point function is not momentum-dependent and we have  $\gamma^{(3)} = 0$ . By Lemma 44, the beta function of this model is

$$\beta(\alpha) = -3\alpha\gamma^{(2)}(\alpha).$$

We want to stress that even if the vertex function is trivial, there still is a non-trivial running coupling (Eq. (3.18)). The  $L$ -dependence of the coupling is ultimately given by the anomalous dimension  $\gamma^{(2)}$  of the propagator. This relationship is called *propagator-coupling duality* in [18].

We can slightly generalize this model by letting the invariant charge (Definition 94) be  $Q = (G^{(2)})^w$ . In that case,  $w = -3$  is the ordinary physical choice and  $w = 0$  amounts to a linear DSE, and the beta function is

$$\beta(\alpha) = w \cdot \alpha\gamma^{(2)}(\alpha).$$

### 3.2.2 Counterterms and $\epsilon$ -dependence

So far, we have concentrated on renormalized quantities, most prominently the renormalized Green functions  $G_R$  (Definition 92). In our initial example (Sect. 2.2.1), we interpreted renormalization as a rescaling of the bare coupling constant by the *Z-factor*  $\lambda_0 =: Z_\lambda(\lambda) \cdot \lambda$  (Eq. (2.33)). Similar Z-factors can be introduced in the full QFT picture. Their form depends on the chosen regularization scheme. For concreteness, we work in dimensional regularization (Sect. 2.3.3) here and for the rest of the thesis, unless stated otherwise. This is not a restriction, unless one would want to introduce *renormalization* schemes that make explicit reference to some other type of regularization.

Consider the Lagrangian of massless  $\phi^n$  theory (Example 3). In this Lagrangian, two quantities can be rescaled: The coupling constant  $\lambda_n$ , and the field variable  $\phi$ . This matches the two residues  $\mathcal{L}$  of the Lagrangian (Example 34). Like in the DSE

(Theorem 29), we redefine the coupling  $\lambda_n^{\frac{2}{n-2}} =: \alpha$  to ensure that  $\alpha$  corresponds to the loop order of the graphs.

**Definition 106.** Let  $s_0$  be an arbitrary, but fixed, mass scale. For massless  $\phi^n$  theory, the *Z-factors* in dimensional regularization (Sect. 2.3.3) are

$$\alpha_0 := Z_\alpha(\alpha, \epsilon) s_0^\epsilon \cdot \alpha, \quad \phi_0 := (Z_\phi(\alpha, \epsilon))^{\frac{1}{2}} \cdot \phi.$$

The factor  $s_0^\epsilon$  in the definition of  $Z_\alpha$  is to make  $\alpha$  dimensionless regardless of  $\epsilon$ . It will cause significant effects later, therefore we want to stress that there is not the option to leave out  $s_0$  in order to simplify later calculations. If we were to leave it out, then the renormalized coupling would, for  $\epsilon \neq 0$ , obtain a non-vanishing mass dimension (Definition 4). In that case, we would be forced to introduce a new, arbitrary, mass scale into the theory at a later point in order to construct a sensible expansion in a massless parameter. In most cases, we will not write  $s_0^\epsilon$  explicitly, but rather implicitly redefine  $s_0^\epsilon \alpha \rightarrow \alpha$ .

In perturbation theory, a Z-factors is a power series in the renormalized coupling  $\alpha$ , and a Laurent series in the regulator  $\epsilon$ , it can always be chosen to not depend on masses [19]. For convenience, we introduce

$$Z^{(2)}(\alpha, \epsilon) := Z_\phi(\alpha, \epsilon), \quad Z^{(n)}(\alpha, \epsilon) := Z_{\alpha^{\frac{n-2}{2}}}(\alpha, \epsilon) s_0^{(\frac{n-2}{2})\epsilon} (Z_\phi(\alpha, \epsilon))^{\frac{n}{2}}. \quad (3.20)$$

The overall factor  $Z_{\alpha^{\frac{n-2}{2}}}$  in  $Z^{(n)}$  arises from our convention that  $G^{(n)}$  is rescaled to the treelevel,  $G^{(n)} = \lambda + \dots$ . With these factors, and absorbing  $s_0^\epsilon$  into  $\alpha$ , the  $n$ -point 1PI Green function (Definition 92) is renormalized according to

$$G_{\mathcal{R}}^{(n)}(\alpha, L) := Z^{(n)}(\alpha, \epsilon) \cdot G^{(n)}(Z_\alpha(\alpha, \epsilon) \cdot \alpha, L). \quad (3.21)$$

This explicitly requires  $G_{\mathcal{R}}^{(n)}$  to be 1PI, the factors would be different for a connected Green function, owing to Definition 49. Equation 3.21 is the analytic manifestation of the abstract relation  $\mathcal{F}_{\mathcal{R}} = S_{\mathcal{R}}^{\mathcal{F}} \star \mathcal{F}$  (Definition 90), where

$$S_{\mathcal{R}}^{\mathcal{F}} [\Gamma^{(j)}] \equiv Z^{(j)} \quad (3.22)$$

is the counterterm (Definition 91).

Equation 3.21 is structurally similar to the behavior of  $G_{\mathcal{R}}$  under finite changes of the energy scale (Lemma 40). Indeed, the Z-factors (Definition 106) are defined analogous to the running coupling (Definition 104). To express a renormalized amplitude at a given energy scale, the coupling constant is rescaled multiplicatively two times [20–23]. Firstly,  $Z_\alpha$  in Definition 106 ensures that the renormalized coupling  $\alpha$  takes its pre-described value at the renormalization point  $s_0$  (Eq. (2.31)). Secondly,

the invariant charge  $\mathcal{Q}_{\mathcal{R}}(L)$  (Definition 95) adjusts  $\alpha$  to its effective value at  $L \neq 0$ . Schematically,

$$\alpha_0 \xrightarrow{Z_\alpha s_0^\epsilon} \alpha \xrightarrow{\mathcal{Q}_{\mathcal{R}}(L)} \tilde{\alpha}(L). \quad (3.23)$$

The renormalized invariant charge (Definition 95) is related to its unrenormalized counterpart via the counterterm  $Z_\alpha$  (Definition 106),

$$\mathcal{Q}_{\mathcal{R}}(\alpha, L) = Z_\alpha s_0^\epsilon \cdot \mathcal{Q}(Z_\alpha \alpha, L). \quad (3.24)$$

At this point, we can state that multiplicative renormalization (Definition 106) and the  $L$ -dependence in the renormalization group are *one and the same thing*. Indeed, the exact same construction that has lead to the renormalization group in Sect. 3.2.1 is also used for renormalization itself. Schematically, we start with an un-renormalized DSE (Theorem 28) and insert the rescalings Eqs. (3.20) and (3.21) to obtain

$$\begin{aligned} G^{(2)}(\alpha_0) &= 1 - \sum_{k=1}^{\infty} \alpha_0^k B_+^{(2),k} (G^{(2)}(\alpha_0) \cdot \mathcal{Q}(\alpha_0)^k) \\ \Rightarrow Z^{(2)} G^{(2)}(Z_\alpha \cdot \alpha) &= Z^{(2)} \left( 1 - \sum_{k=1}^{\infty} (Z_\alpha \cdot \alpha)^k B_+^{(2),k} (G^{(2)}(\alpha) \cdot \mathcal{Q}(Z_\alpha \cdot \alpha)^k) \right). \end{aligned}$$

An analogous replacement is possible for the vertex-type DSE. Using Eq. (3.24), the general form is

$$G_{\mathcal{R}}^{(n)}(\alpha) = Z^{(n)} \pm \sum_{k=1}^{\infty} \alpha^k B_+^{(n),k} (G_{\mathcal{R}}^{(n)}(\alpha) \cdot \mathcal{Q}_{\mathcal{R}}(\alpha)^k). \quad (3.25)$$

The cocycle  $B_+$  is an integral operator, see Eq. (2.40). If we were to write Eq. (3.23) non-recursively, using the DSE Eq. (3.25), then we would obtain to every fixed order in  $\alpha$  an expression involving finitely many nested integrals, where the integration limits are the renormalization point  $s_0$  and the physical scale  $L$ . This construction is known as *Chen's lemma* [24], from this perspective the Hopf algebra (Definition 90) implements the combinatorics of the permuted integral boundaries. The *renormalization group* describes the fact that the intermediate renormalization scale  $s_0$  is arbitrary, that is, the process Eq. (3.23) can involve arbitrarily many intermediate steps, each of which comes with its own  $Z$ -factors. The convolution product  $\star$  (Definition 77) is the group operation of the renormalization group,  $Z = Z_1 \star Z_2$  just like, in Definition 90,  $\mathcal{F}_{\mathcal{R}} = Z \star \mathcal{F}$  where  $Z = S_{\mathcal{R}}^{\mathcal{F}}$  (Definition 91). Comparing Definition 102, we see that the renormalization group is generated by the infinitesimal Feynman rule  $\sigma$ . In the special case of a linear DSE, there is no non-trivial nesting and the resulting integrals can be written down explicitly, see Eq. (3.31).

The  $Z$ -factors depend on  $\epsilon$ , in order to work with them, we need to extend the renormalization group theory of Sect. 3.2.1 to include  $\epsilon$ -dependence of  $\gamma$ ,  $\beta$  and  $G_{\mathcal{R}}$ .

**Definition 107.** For  $\epsilon \neq 0$ , we extend Definition 104: the *running coupling* is defined as

$$\tilde{\alpha}(\alpha, \epsilon, L) := \alpha e^{-\epsilon L} Q_{\mathcal{R}}(\alpha, \epsilon, L).$$

The running coupling  $\tilde{\alpha}(\alpha, \epsilon, s)$  at a certain physical scale  $s$  (Definition 83), and at the physical dimension  $\epsilon = 0$ , is an observable, it is the numerical value of a scattering amplitude at that energy. Renormalization involves the arbitrary intermediate renormalization scale  $s_0$  in Eq. (3.23). Consequently,  $\tilde{\alpha}(s)$  must not change if we change  $s_0$ , that is,

$$0 = s_0 \cdot \frac{d\tilde{\alpha}}{ds_0} = \frac{d\tilde{\alpha}}{d \ln s_0} = \frac{\partial \tilde{\alpha}}{\partial \ln \alpha} \frac{d \ln \alpha}{d \ln s_0} + \frac{\partial \tilde{\alpha}}{\partial L} \frac{dL}{d \ln s_0}. \quad (3.26)$$

Owing to Definition 101,  $\frac{dL}{d \ln s_0} = -1$ . Equation 3.26 is valid for all values of  $L$ . Specify to  $L = 0$ , then the second summand, in the limit  $\epsilon = 0$ , becomes the beta function  $\beta(\alpha) := \frac{\partial \tilde{\alpha}}{\partial L}|_{L=0}$  from Definition 105,

$$0 = \frac{\partial \tilde{\alpha}}{\partial \alpha}\Big|_{L=0, \epsilon=0} \alpha s_0 \frac{d}{ds_0} \ln \alpha\Big|_{\epsilon=0} - \beta(\alpha).$$

On the other hand, for  $\epsilon \neq 0$ , owing to Definition 104 there will always be a trivial summand  $\epsilon \tilde{\alpha}$  in the derivative of  $\tilde{\alpha}$

$$0 = \frac{\partial \tilde{\alpha}}{\partial \alpha}\Big|_{L=0} \alpha s_0 \frac{d}{ds_0} \ln \alpha + \epsilon \tilde{\alpha}\Big|_{L=0} - \alpha \frac{\partial Q_{\mathcal{R}}}{\partial L}\Big|_{L=0}.$$

For later convenience, we *define* the  $\epsilon$ -dependent beta function to not contain the term  $\epsilon \tilde{\alpha}$ . In kinematic renormalization, we know that  $\tilde{\alpha}(\alpha, \epsilon = 0, L = 0) = \alpha$  and  $\partial_\alpha \tilde{\alpha} = 1$ . In other renormalization schemes, the latter derivative is non-trivial, and it turns out that one should include it into the definition of the beta function in order to obtain a Callan-Symanzik equation that has the same form in all renormalization schemes (see Theorem 53).

**Definition 108.** Let  $\mathcal{Q}_{\mathcal{R}}$  be the invariant charge (Definition 95). In dimensional regularization, the  $\epsilon$ -dependent *beta-function* is defined as

$$\beta(\alpha, \epsilon) := \frac{1}{\frac{\partial \tilde{\alpha}}{\partial \alpha} \Big|_{L=0}} \alpha \frac{\partial \mathcal{Q}_{\mathcal{R}}}{\partial L} \Big|_{L=0} = \alpha s_0 \frac{d}{ds_0} \ln \alpha(s_0, \alpha_0) \Big|_{\alpha_0 \text{ fixed}} + \frac{\tilde{\alpha} \epsilon}{\frac{\partial \tilde{\alpha}}{\partial \alpha}} \Big|_{L=0}.$$

In kinematic renormalization with renormalization point  $L = 0$ , and in the limit  $\epsilon \rightarrow 0$ , this reproduces Definition 105:

$$\beta(\alpha) := \alpha \frac{\partial}{\partial L} \mathcal{Q}_{\mathcal{R}}(\alpha, L) \Big|_{L=0} = \alpha s_0 \frac{d}{ds_0} \ln \alpha(s_0, \alpha_0) \Big|_{\alpha_0 \text{ fixed}}.$$

For the remainder of this section, we will again assume kinematic renormalization conditions. We stress again that the first equation in Definition 108 holds in all renormalization schemes (Definition 99), while the second one is only valid in kinematic renormalization (Definition 93).

Definition 108 implies an equation for the  $Z$ -factors. From Definition 106, one obtains

$$s_0 \frac{d}{ds_0} \ln \alpha = s_0 \frac{d}{ds_0} (\ln \alpha_0 - \ln Z_\alpha - \epsilon \ln s_0) = -s_0 \frac{d}{ds_0} \ln \alpha \cdot \frac{\partial}{\partial \ln \alpha} \ln Z_\alpha - \epsilon.$$

The first summand on the right hand can be expressed by the beta function (Definition 108), and therefore

$$\beta(\alpha, \epsilon) + (\beta(\alpha, \epsilon) - \alpha \epsilon) \alpha \frac{\partial}{\partial \alpha} \ln Z_\alpha(\alpha, \epsilon) = 0. \quad (3.27)$$

Comparing Eq. (3.27) with Eq. (3.18),  $\beta(\alpha) + \beta(\alpha) \partial_\alpha \ln \mathcal{Q}_{\mathcal{R}} = \alpha \partial_L \ln \mathcal{Q}_{\mathcal{R}}$ , we see that  $Z_\alpha$  is the  $L$ -independent part of  $\tilde{\alpha}$ , as stated in Eq. (3.23), while on the other hand  $\mathcal{Q}_{\mathcal{R}}$  is the finite part for  $\epsilon \rightarrow 0$ . Knowing either  $Z_\alpha$  or  $\beta(\alpha, \epsilon)$ , one can compute the other,

$$\begin{aligned} \beta(\alpha, \epsilon) &= \frac{-\epsilon}{\frac{\partial}{\partial \alpha} \ln (\alpha \cdot Z_\alpha(\alpha, \epsilon))} + \alpha \epsilon, \\ Z_\alpha(\alpha, \epsilon) &= \exp \left( - \int_0^\alpha \frac{du}{u} \frac{\beta(u, \epsilon)}{\beta(u, \epsilon) - u \epsilon} \right) = \prod_{j=1}^{\infty} \exp \left( \frac{1}{\epsilon^j} \int_0^\alpha \frac{du}{u} \left( \frac{\beta(u, \epsilon)}{u} \right)^j \right). \end{aligned} \quad (3.28)$$

For  $\epsilon \neq 0$ , not only the beta function, but also the anomalous dimension can obtain a non-trivial  $\epsilon$ -dependent part. It arises from the  $\epsilon$ -dependence of  $G_{\mathcal{R}}^{(2)}$  in Eq. (3.15),

$$\gamma^{(2)}(\alpha, \epsilon) := -s_0 \partial_{s_0} G_{\mathcal{R}}^{(2)}(\alpha, \epsilon).$$

Expressed in terms of Z-factors (Definition 106), using Eq. (3.21) and Definition 108, this means

$$\gamma^{(2)}(\alpha, \epsilon) = -(\beta(\alpha, \epsilon) - \alpha\epsilon) \partial_\alpha \ln Z_\phi(\alpha, \epsilon), \quad Z_\phi(\alpha, \epsilon) = \exp \left( - \int_0^\alpha du \frac{\gamma^{(2)}(u, \epsilon)}{\beta(u, \epsilon) - u\epsilon} \right). \quad (3.29)$$

The relations between the renormalization group functions and the counterterms are called *Gross-'t Hooft relations* [20, 25, 26]. Observe how they resemble the finite rescaling Eq. (3.19): As expected from Eq. (3.23), the Z-factor and the finite rescaling  $\alpha \rightarrow \tilde{\alpha}$  are structurally similar.

The  $\epsilon$ -dependent Green functions functions satisfy, in kinematic renormalization, all the properties from Sect. 3.2.1. We collect them in a theorem for later reference:

**Theorem 45.** In kinematic renormalization, with renormalization point  $L = 0$ , the renormalization group equations Theorems 41 and 42 and Eqs. (3.14) and (3.18) hold for  $\epsilon \neq 0$  in the form

$$\begin{aligned} \partial_L \ln G_{\mathcal{R}}(\alpha, \epsilon, L) &= \gamma(\tilde{\alpha}(\alpha, \epsilon, L), \epsilon), \\ \partial_L G_{\mathcal{R}}^r(\alpha, \epsilon, L) &= (\gamma^r(\alpha, \epsilon) + (\beta(\alpha, \epsilon) - \alpha\epsilon) \partial_\alpha) G_{\mathcal{R}}^r(\alpha, \epsilon, L), \\ \gamma_{j>1}^r(\alpha, \epsilon) &= \frac{1}{j} (\gamma^r(\alpha, \epsilon) + (\beta(\alpha, \epsilon) - \alpha\epsilon) \cdot \partial_\alpha) \gamma_{j-1}^r(\alpha, \epsilon), \\ \tilde{\alpha}(\alpha, \epsilon, L) \partial_L \ln \mathcal{Q}_{\mathcal{R}}(\alpha, \epsilon) &= \beta(\tilde{\alpha}(\alpha, \epsilon, L), \epsilon) \quad (\text{there is no } -\alpha\epsilon \text{ here}), \\ \partial_L \ln \mathcal{Q}_{\mathcal{R}}(\alpha, \epsilon) - \epsilon &= (\beta(\alpha, \epsilon) - \alpha\epsilon) \partial_\alpha \ln(\alpha \mathcal{Q}_{\mathcal{R}}(\alpha, \epsilon)). \end{aligned}$$

Moreover, for  $\phi^n$  theory, the relation from Lemma 44 is fulfilled even for  $\epsilon \neq 0$ ,

$$\beta(\alpha, \epsilon) = \frac{2\alpha}{n-2} \left( \gamma^{(n)}(\alpha, \epsilon) - \frac{n}{2} \gamma^{(2)}(\alpha, \epsilon) \right).$$

### 3.2.3 Grouplike Green Functions

Let  $\Gamma \in H_F$  be a grouplike (Definition 67) combinatorial Green function (Definition 47). We do not require at this point that  $\Gamma$  is a solution to a combinatorial DSE (Eq. 2.28). Owing to  $\Delta(\Gamma) = \Gamma \otimes \Gamma$ , we have  $(\sigma \star \sigma)\Gamma = \sigma[\Gamma] \cdot \sigma[\Gamma]$ . This holds as well for higher powers, and the Feynman rules (Definition 78) evaluate to

$$\exp^*(L\sigma)[\Gamma] = \mathbb{1} + L\sigma[\Gamma] + \frac{1}{2} L^2\sigma[\Gamma]\sigma[\Gamma] + \frac{1}{6} L^3\sigma[\Gamma]\sigma[\Gamma]\sigma[\Gamma] + \dots = e^{L\sigma[\Gamma]}.$$

In other words: The Feynman amplitude (Definition 102) of a grouplike Hopf algebra element is a *scaling solution* (Example 66), where the value  $\sigma[\Gamma(\alpha)] = \gamma_1(\alpha)$  is the exponent,

$$\mathcal{F}_{\mathcal{R}}[\Gamma](L) = e^{L\gamma_1(\alpha)} = \left(\frac{s}{s_0}\right)^{\gamma_1(\alpha)}. \quad (3.30)$$

We have used Definition 101 and the kinematic renormalization condition  $\sigma^{*0}(\Gamma) = \mathbb{1}$ . The same solution is also obtained from Lemma 39 and  $\Delta(\Gamma) = \Gamma \otimes \Gamma$ , via the functional equation

$$\mathcal{F}_{\mathcal{R}}[\Gamma](L_1 + L_2) = m (\mathcal{F}_{\mathcal{R}}|_{L_1} \otimes \mathcal{F}_{\mathcal{R}}|_{L_2}) \Delta(\Gamma) = \mathcal{F}_{\mathcal{R}}[\Gamma](L_1) \cdot \mathcal{F}_{\mathcal{R}}[\Gamma](L_2).$$

On the other hand, we know from Sect. 2.1.6 that the solution of a linear combinatorial Dyson–Schwinger equation is grouplike.

**Theorem 46.** Let  $\Gamma \in H_{CK}$  or  $\Gamma \in H_F$  be the solution of a linear DSE  $\Gamma = \mathbb{1} + \sum_k \alpha^k B_+^k(\Gamma)$  (Eq. 2.28). Then the following holds:

1.  $\Gamma$  is grouplike (Definition 67),  $\Delta(\Gamma) = \Gamma \otimes \Gamma$ .
2. The beta function (Definition 108) vanishes,  $\beta(\alpha, \epsilon) = 0$ .
3. The renormalized Green function in kinematic renormalization (Definition 93) for  $\epsilon = 0$  is  $\mathcal{F}_{\mathcal{R}}[\Gamma](L) = \exp(L\gamma_1(\alpha))$ , where  $\gamma_1(\alpha) = \gamma(\alpha)$  is the anomalous dimension (Definition 105).

**Proof** Point 1 was remarked in Example 64, and is a special case of Theorem 26. Point 2 follows from Definition 108 because in a linear DSE,  $Q = \mathbb{1}$  is momentum-independent. The general form in point 3 follows from the Callan–Symanzik equation (Theorem 41) using  $\beta(\alpha) = 0$ . In kinematic renormalization, we demand  $\mathcal{F}_{\mathcal{R}}[\Gamma]|_{L=0} = 1$ , hence there is no prefactor to  $e^{L\gamma}$ . Alternatively, use Theorem 42 to find  $\gamma_j = \frac{1}{j!} (\gamma_1)^j$ . With these coefficients, Eq. (3.2) takes the desired form. Clearly,  $\partial_L \mathcal{F}_{\mathcal{R}}[\Gamma]|_{L=0} = \gamma_1 = \gamma$  is the anomalous dimension (Definition 105).  $\square$

Compare Theorem 46 with Example 66: The scaling solution of a linear DSE is the 2-point function of a scale invariant theory. Moreover, for a scalar field theory, scale invariance implies conformal invariance [27], therefore, if a scalar theory is described by a linear DSE, then its correlation functions are severely restricted, see Example 67.

### Example 102: Infinite sums of rainbows or ladders.

Two realizations of grouplike Green functions in terms of Feynman graphs are the rainbows (Example 78) and ladders (Example 79). From Theorem 46, we know, without performing any explicit computation, that these infinite sums of Feynman graphs add up to a Green function of the form Eq. (3.30). The only remaining task is to determine  $\gamma_1(\alpha)$ , we will come back to this in Theorem 47.

Another class of grouplike graphs are the wheels with spokes, recently featured in Super Yang-Mills theory [28, 29].

The simple scaling form of grouplike Green functions holds only for  $\epsilon = 0$ . For  $\epsilon \neq 0$ , we have the Callan-Symanzik equation (45),

$$\partial_L G_{\mathcal{R}}(\alpha, \epsilon, L) = (\gamma(\alpha, \epsilon) - \epsilon \alpha \partial_\alpha) G_{\mathcal{R}}(\alpha, \epsilon, L).$$

Using separation of variables and the boundary condition  $G_{\mathcal{R}}(\alpha, \epsilon, 0) = 1$ , we find

$$G_{\mathcal{R}}(\alpha, \epsilon, L) = \exp \left( - \int_{\alpha e^{-\epsilon L}}^{\alpha} du \frac{\gamma(u, \epsilon)}{-u\epsilon} \right). \quad (3.31)$$

Compare this to the counterterm in Eq. (3.29),

$$Z_G(\alpha, \epsilon) = \exp \left( - \int_0^{\alpha} du \frac{\gamma(u, \epsilon)}{-u\epsilon} \right).$$

This is a particularly striking illustration of Eq. (3.23): Owing to the  $\epsilon$  in the denominator, the integral in Eq. (3.31) would be divergent, were it not for integration limits  $(\alpha - \alpha e^{-\epsilon L}) \sim -\epsilon L \alpha$ . The counterterm represents the divergent part of this integral, the renormalized Green function at  $L$  is a transition to the running coupling  $\alpha e^{-\epsilon L} = \tilde{\alpha}$  (Definition 107).

As an alternative to the integral in Eq. (3.31), one can derive a series solution of the linear DSE by iterating the renormalization group equation for  $\gamma_j(\alpha, \epsilon)$ ,

$$\gamma_j(\alpha, \epsilon) = \frac{1}{j} (\gamma_1(\alpha, \epsilon) - \alpha \epsilon \partial_\alpha) \gamma_{j-1}(\alpha, \epsilon).$$

The first order in  $\epsilon$  is

$$\begin{aligned} G_{\mathcal{R}}(\alpha, \epsilon, L) &= e^{L\gamma_1(\alpha, \epsilon)} - \frac{1}{2} \epsilon L^2 e^{L\gamma_1(\alpha, \epsilon)} \alpha \partial_\alpha \gamma_1(\alpha, \epsilon) + \mathcal{O}(\epsilon^2) \\ &= e^{L\gamma_1(\alpha)} \left( 1 + \epsilon \left( [\epsilon^1] \gamma_1(\alpha, \epsilon) - \frac{1}{2} L^2 \alpha \partial_\alpha \gamma_1(\alpha) \right) + \mathcal{O}(\epsilon^2) \right). \end{aligned} \quad (3.32)$$

Here, we have introduced  $\gamma_1(\alpha, \epsilon) =: \gamma_1(\alpha) + \epsilon[\epsilon^1]\gamma_1(\alpha, \epsilon) + \mathcal{O}(\epsilon^2)$ .

Grouplike Green functions allow us to make an argument about counterterms in the physical dimension  $\epsilon = 0$ : To finite order in  $\alpha$ , the counterterms (Definition 106) are a sum of poles in  $\epsilon$  and clearly infinite for  $\epsilon \rightarrow 0$ . But the full renormalized 2-point Green functions carry an anomalous dimension, which will generally be non-integer. For grouplike functions (Theorem 46), this anomalous dimension resembles analytic regularization (Sect. 2.3.2). In that case, the Feynman integrals are not actually divergent when the regulator is removed, and “the theory regularizes itself” [30]. The  $Z$ -factors are then finite. See Example 120 for the counterterm of a linear DSE. In the non-linear case, Eq. (3.2) represents an expansion “around analytic regularization” [30]. The true non-perturbative status of  $Z$ -factors is unclear, but it is well possible that they turn out finite in the general case as well. This would be fortunate, because, in the traditional view of canonical quantization, they are introduced as probabilities and hence  $Z \in [0, 1]$ . A detailed discussion of the latter aspect can be found in [31].

### 3.2.4 *Digression: History and Variants of the Renormalization Group*

The early developments, motivations and variants of the renormalization group are laid out in the foundational work [21]. For QFT, the renormalization group is intimately related to the quantum nature of the interaction, that is, the sum of all possible interactions as expressed by Dyson-Schwinger equations. Nonetheless, the renormalization group also appears in classical statistical physics [32, 33]. There, a change of scale amounts to averaging over microscopic degrees of freedom, in lattice models for example expressed by *Migdal-Kadanoff transformations* [34–37].

A first step towards the renormalization group equation in QFT was the *Gell-Mann-Low equation* [38, 39], which concerns the behavior of interactions in QED at very high energies. From today’s perspective, this analysis falls under *leading-log expansion*, to be introduced in Sect. 3.3.3. See [32] for a detailed discussion of this point and a comprehensive historical review. Interestingly, without developing a formal theory, [39] already contains many of the features of the later renormalization group theory. The crucial point seems to be that later work, culminating in the Callan-Symanzik equation (Theorem 41), realized that the renormalization group functions determine *all* scale dependence, while Gell-Mann and Low did not make a sharp distinction between the scale and the energy (compare Example 66), and consequently understood their results only as an asymptotic approximation for very small distances, i.e. high energies, where scale and energy actually become equivalent.

The running of the coupling (Definition 104) is governed (Eq. (3.18)) by the behavior of the beta function [40–42]. Especially, a value  $\alpha^*$  such that  $\beta(\alpha^*) = 0$  is a *fixed point* of the theory [43]. Once the energy scale  $L$  is such that  $\tilde{\alpha}(L) = \alpha^*$ , any further change of  $L$  will not change  $\tilde{\alpha}$  any more, and therefore, the theory becomes *scale invariant*. This observation, together with *Bjorken scaling* [44, 45], guided the

discovery of *asymptotic freedom* in QCD in the 1970s [46–49]: A theory of strong interaction should be such that at very large scales, its beta function vanishes.

In our above language (Definition 104), scale invariance means that the Dyson-Schwinger equations become linear, or that  $\mathcal{Q}_R(\alpha^*, L) = \mathbb{1}$ . Clearly,  $\alpha^* = 0$  is a fixed point, called *Gaussian fixed point* (because the free fields follow a Gaussian distribution, compare Theorem 3). It is conceivable that a theory has additional *non-trivial fixed points*  $\alpha^* \neq 0$ . This implies that the linear DSEs studied in Sect. 3.2.3 are not merely a technical example, but they are of high relevance for real-world QFT to describe theories at fixed points. Conversely, a non-vanishing beta function in the renormalization group (Theorem 42) can be interpreted as a “perturbation around conformal field theory” [16, Sect. 4.2].

One can view the renormalization group equations (RGE, Theorem 41) as yet another perspective—apart from implementing boundary conditions, rescaling Lagrangian parameters, and removing divergences as discussed in Sect. 2.3.4—on renormalizability. This is the perspective of *Wilson’s renormalization group* [21, 50–54]. The RGE determine how beta functions change with the scale. Renormalizability then amounts to whether or not an effective action (Definition 50) at high energies can have finite coupling constants, given the values we observe at lower energies. Even if the conclusions are similar, this view is philosophically the opposite compared to the “UV-finiteness” we usually demand: For us, the argument was that there must be no divergent high-energy unobservable quantum corrections to the processes we observe. In Wilson’s perspective, the theory at a very high, but finite, scale is the fundamental object and the question is if it gives rise to a low-energy theory with non-zero effective couplings. For a non-renormalizable theory, the couplings *decrease* polynomially as the scale is *lowered*, rendering them effectively zero at observable scales. This phenomenon is called *triviality* and it can also occur for renormalizable theories, for example, scalar  $\phi^4$  theory is assumed to be trivial in this sense [55], even though it is perturbatively renormalizable.

Computing the change of the effective action (as opposed to individual Green functions) with changing energy scales is the endeavour of *exact renormalization group theory* and the *Wetterich equation* [56–61]. A priori, this comes at the cost of manipulating, instead of functions, a potentially complicated functional like the effective action, but in concrete calculations one truncates the functional to finitely many functions. This setup appears particularly suitable for finding non-trivial fixed points [62]. Especially, it might be that quantum gravity, despite not being renormalizable when formulated as a perturbation of a free theory (see Sect. 5.2.1), has a sensible, finite, high-energy effective action, representing a non-trivial fixed point [63–66].

Finally, we have discussed the renormalization group only in terms of UV-behavior (for example by largely ignoring the presence of masses and their potential influence on the Callan–Symanzik equation). Especially for gauge theories, the IR-behavior is interesting as well and many analogous statements can be derived for the scaling behavior of theories in the infrared limit, see [32, 67–76].

### Summary of Sect.3.2.

1. Upon changing the energy scale, a renormalized Green function changes according to the Callan-Symanzik equation (Theorem 41). The change of the coupling parameter with changing energy scale is given by the beta function, such scale transformations generate the renormalization group. We concentrated on kinematic renormalization conditions in Sect. 3.2.1.
2. In Sect. 3.2.2, we extended the renormalization group to  $\epsilon \neq 0$  in dimensional regularization, still using kinematic renormalization. We saw that removing divergences is essentially the same process as rescaling to different energy scales. In this transformation, the invariant charge represents the finite  $L$ -dependent part, the counterterms a divergent,  $L$ -independent part. The latter are integrals of the renormalization group functions. The infinities in counterterms can be interpreted as coming from an infinitely large change of energy scale.
3. A linear DSE has grouplike combinatorial Green functions as solutions, and the corresponding analytic Green function is a simple monomial, called scaling solution. The functional form becomes more complicated when  $\epsilon \neq 0$  (Sect. 3.2.3).
4. Section 3.2.4 is a short survey of other aspects of renormalization group theory, which are not directly relevant for the present thesis. We observed that scaling solutions, or linear DSEs, are relevant for fixed-points of the renormalization group.

## 3.3 Dyson-Schwinger Equations, Third Act

Equipped with knowledge about the renormalization group, we can finally carry out our last attack on Dyson-Schwinger equations. The previous sections about DSEs, Sects. 1.3.11 and 2.2.5, have been rather superficial and served to introduce the general, conceptional features of Dyson-Schwinger equations. Conversely, the purpose of the present section is to find concrete solutions of a certain class of DSEs.

### 3.3.1 Propagator-DSE as Differential Equation

We want to learn how to compute the anomalous dimensions (Definition 105) systematically in kinematic renormalization. The method presented here was derived gradually over 15 years in [1, 17, 18, 30, 40, 77, 78].

For this section, we restrict ourselves to a massless theory, and a single (non-coupled) Dyson-Schwinger equation of propagator type. Conceptually, the method

can account for vertex corrections either by explicitly including kernel graphs (Definition 52) with vertex-type subgraphs into the propagator DSE, or by introducing an additional functional dependence of kernels on angle parameters (Definition 83) to allow for vertex-type DSEs. Both approaches greatly increase the computational difficulty and we will not pursue them further. It has been argued [79] that this approximation to DSEs is in the spirit of the Hartree-Fock method [80–82] in molecular physics: Instead of solving the full coupled system, one solves for one Green function at a time, keeping all others fixed.

The solution we are trying to find is a 1PI propagator Green function  $G_{\mathcal{R}}^{(2)} =: G_{\mathcal{R}}$  and the invariant charge (Definition 95) is a power of this Green function,

$$\mathcal{Q}_{\mathcal{R}} = G_{\mathcal{R}}^w. \quad (3.33)$$

Here, the exponent  $w \in \mathbb{Z}$  is chosen corresponding to the vertex valence of the theory, see Definition 94. We have encountered this setup already in Example 83. In kinematic renormalization, Eq. (3.33) implies  $\beta(\alpha, \epsilon) = w \cdot \alpha \gamma(\alpha, \epsilon)$  (Theorem 45). We shall see in Theorem 51 that the same holds for all renormalization schemes.

Despite the simplifications, the DSE can still involve infinitely many kernel graphs (Definition 52). We redefine the coupling constant such that it corresponds to the loop order  $|\Gamma|$  of the kernels, that is, the first non-vanishing kernel is of order  $\alpha^1$ , the next one  $\alpha^2$  etc. In this way, the DSE has a form similar to Theorem 29,

$$G_{\mathcal{R}} = 1 - (1 - \mathcal{R}) \sum_{k=1}^{\infty} \alpha^k B_+^{(k)} (G_{\mathcal{R}} \cdot \mathcal{Q}_{\mathcal{R}}^k) = 1 - (1 - \mathcal{R}) \sum_{k=1}^{\infty} \alpha^k B_+^{(k)} (G_{\mathcal{R}}^{1+wk}). \quad (3.34)$$

Here,  $B_+^{(k)}$  is the sum of all cocycles of grade  $k$ , it is the analogue of Eq. (3.10), but on the level of amplitudes, not on graphs. It is given by the Mellin transform (Definition 103) according to Eq. (3.8),

$$(1 - \mathcal{R}) B_+^{(k)} (G_{\mathcal{R}}^{1+wk}) = \sum_{\Gamma} \underbrace{G_{\mathcal{R}}(\alpha, \partial_{\rho_1}) \cdots G_{\mathcal{R}}(\alpha, \partial_{\rho_E})}_{E=1+wk \text{ factors}} \left( e^{L \sum_j \rho_j} - 1 \right) F_{\Gamma}(\rho_1, \dots, \rho_E) \Big|_{\rho=0}.$$

All graphs of order  $k$  have the same number  $E = |\Gamma|$  of internal edges, therefore we can sum up their Mellin transforms to obtain

$$F_k(\rho_1, \dots, \rho_E) := \sum_{\Gamma, |\Gamma|=k} F_{\Gamma}(\rho_1, \dots, \rho_E).$$

The DSE from Eq. (3.34) now reads

$$G_{\mathcal{R}}(\alpha, L) = 1 - \sum_{k=1}^{\infty} \alpha^k G_{\mathcal{R}}(\alpha, \partial_{\rho_1}) \cdots G_{\mathcal{R}}(\alpha, \partial_{\rho_E}) \left( \left( e^{L \sum_j \rho_j} - 1 \right) F_k(\rho_1, \dots, \rho_E) \Big|_{\rho=0} \right). \quad (3.35)$$

This is a *pseudodifferential equation* version of the DSE, that is, a differential equation of potentially infinite order. Expanding in  $L$  results in an equation for the anomalous dimension in kinematic renormalization,  $\gamma(\alpha) = \gamma_1(\alpha)$ ,

$$\gamma(\alpha) = -\sum_{k=1}^{\infty} \alpha^k G_{\mathcal{R}}(\alpha, \partial_{\rho_1}) \cdots G_{\mathcal{R}}(\alpha, \partial_{\rho_E}) \left( \left( \sum_j \rho_j \right) F_k(\rho_1, \dots, \rho_E) \Big|_{\rho=0} \right). \quad (3.36)$$

The Green functions  $G_{\mathcal{R}}$  on the right hand side are determined from the anomalous dimension by the renormalization group equation (Theorem 42), where  $\beta = w\alpha\gamma$ .

If the Mellin transform is known as a power series in  $\rho$ , computing  $\gamma(\alpha)$  from Eq. (3.36) is a merely combinatorial task, which can typically be done to hundreds of orders, e.g. [83] or even to all orders [17, 18]. Equation 3.35 in particular implies that all information about the behavior of  $G_{\mathcal{R}}$  for high orders in  $\alpha$  is encoded in the coefficients of the Mellin transforms, see [40–42]. A graphical interpretation of the coefficients of  $\gamma(\alpha)$  can be given in terms of chord diagrams [84–88]. By truncating the Mellin transform to a polynomial of low degree, the computation can be simplified even more [89, 90].

### 3.3.2 Insertions into a Single Edge

The differential equation Eq. (3.36) has the drawback that it contains differential operators inside the Green function, which requires the equation to be solved recursively. It would be more transparent to have an equation where the differential operators are explicitly given from the start, without having to construct them order-by-order. This can be achieved at least in the case where the following severe additional restrictions are imposed:

1. There are only kernel graphs of a single order, which we take to be  $k = 1$ .
2. The correction is only inserted into one of the edges at a time. Technically, this means that we restrict ourselves to one-parameter Mellin transforms  $F(\rho) := F(\rho, 0, \dots, 0)$ . It is possible to include all edges,  $F(\rho) := F(\rho, 0, \dots) + F(0, \rho, \dots)$ , but this will still miss the insertions into multiple edges *simultaneously*.

Under these conditions, the DSE (Theorem 17) takes the form

$$G(\alpha, s) = 1 + \alpha(1 - \mathcal{R}) \int dy K(s, y) G(\alpha, y)^{1+w}, \quad (3.37)$$

where  $K$  is the sum of all kernel graphs and  $w = -2$  in physical models. The DSE can be rewritten as a differential equation analogous to Eq. (3.35),

$$G_{\mathcal{R}}(\alpha, L) = 1 - \alpha \left( G_{\mathcal{R}}^{1+w}(\alpha, \partial_\rho) e^{L\rho} F(\rho) - G_{\mathcal{R}}^{1+w}(\alpha, \partial_\rho) F(\rho) \right) \Big|_{\rho=0}. \quad (3.38)$$

**Theorem 47.** Consider a DSE at the physical dimension  $\epsilon = 0$  of the form Eq. (3.37), where  $\mathbb{R} \ni w \neq 0$  and  $F(\rho)$  is the Mellin transform (Definition 103) of the sum of kernel graphs. Then, in kinematic renormalization (Definition 93), the anomalous dimension  $\gamma(\alpha)$  (Definition 105) is a solution of the pseudodifferential equation

$$\frac{1}{\rho \cdot F(\rho)} \Big|_{\rho \rightarrow \gamma(1+w\alpha\partial_\alpha)} \gamma(\alpha) = -\alpha.$$

If, in the same setup, the DSE is linear, that is  $w = 0$ , then  $\gamma(\alpha)$  satisfies the algebraic equation

$$\frac{1}{F(\gamma(\alpha))} = -\alpha \Leftrightarrow \gamma(\alpha) = F^{-1} \left( -\frac{1}{\alpha} \right).$$

On the right hand side,  $F^{-1}$  denotes the inverse function  $F^{-1}(F(t)) = t$ , not the function  $\frac{1}{F}$ .

**Proof** Conceptually, we use Eq. (3.4) in reverse direction, namely  $\partial_L^k e^{L\rho} = \rho^k e^{L\rho}$  and therefore

$$e^{L\rho} = \frac{1}{F(\rho)} \cdot F(\rho) e^{L\rho} = \frac{1}{F(\rho)} \Big|_{\rho \rightarrow \partial_L} \cdot F(\rho) e^{L\rho}.$$

Apply this differential operator to both sides of Eq. (3.38):

$$\frac{1}{F(\rho)} \Big|_{\rho \rightarrow \partial_L} G_{\mathcal{R}}(\alpha, L) = -\alpha G_{\mathcal{R}}^{1+w}(\alpha, \partial_\rho) e^{L\rho} \Big|_{\rho=0} + 0 = -\alpha G_{\mathcal{R}}^{1+w}(\alpha, L).$$

The operator on the left hand side is a power series in  $\partial_L$ , starting at linear order. The Callan-Symanzik equation (Theorem 41) in our case reads  $\partial_L G_{\mathcal{R}} = \gamma(\alpha)(1 + w\alpha\partial_\alpha)G_{\mathcal{R}}$ . Therefore, we can replace  $\partial_L$  and obtain

$$\begin{aligned} \frac{1}{F(\rho)} \Big|_{\rho \rightarrow \gamma(1+w\alpha\partial_\alpha)} G_{\mathcal{R}}(\alpha, L) &= -\alpha G_{\mathcal{R}}^{1+w}(\alpha, L) \\ \frac{1}{F(\rho)} \Big|_{\rho \rightarrow \gamma(1+w\alpha\partial_\alpha)} \left( 1 + \gamma(\alpha)L + \gamma_2(\alpha)L^2 + \dots \right) &= -\alpha \left( 1 + \gamma(\alpha)L + \gamma_2(\alpha)L^2 + \dots \right)^{1+w}. \end{aligned}$$

We will be interested in the order  $L^0$ . On the left hand side,

$$\gamma(1 + w\alpha\partial_\alpha)1 = \gamma(\alpha), \quad (\gamma(1 + w\alpha\partial_\alpha))^j 1 = j! \gamma_j(\alpha) = (\gamma(1 + w\alpha\partial_\alpha))^{j-1} \gamma(\alpha).$$

Consequently, if we reduce all powers of  $\rho$  in the differential equation by one, then the operator acts on  $\gamma(\alpha)$  instead of on 1. We obtain the claimed form of the pseudodifferential equation.

In this equation, unlike Eq. (3.37), the parameter  $w$  has an analytic, but no longer a combinatorial function, therefore we can allow  $w \in \mathbb{R}$ . The algebraic equation is the limit  $w \rightarrow 0$  of the differential equation.  $\square$

In the literature, differential equations like Theorem 47 have appeared for various concrete examples of Mellin transforms [1, 18, 40, 89]. However, we are not aware of a publication that explicitly states the general form of this differential equation for an arbitrary Mellin transform. Knowing a differential equation for the anomalous dimension allows to derive sophisticated statements about its behavior beyond perturbation theory [91–93], see Sect. 3.4.

We remark that for the original graphical DSE (Eq. (3.37)) in physical models, every choice  $w \notin \{-2, 0\}$  means that we insert subgraphs with non-standard prefactors, or only certain sets of subgraphs. The choice  $w = -2$  is the only one where all subgraphs are used with their conventional QFT multiplicities. The choice  $w = 0$  amounts to  $Q = 1$  (Eq. (3.33)) and therefore to a linear DSE. With  $w = -1$ , we obtain a non-recursive “DSE”, which has the 1-loop graph  $\gamma(\alpha) = -c_0\alpha$  as full solution, where  $c_0$  is the first coefficient of  $F(\rho)$  (Eq. (3.6)).

The physically most relevant cases  $w = 0$  (linear approximation, e.g. [30, 94, 95]) and  $w = -2$  (one inverse Green function inserted into the kernel, e.g. [18, 77, 83, 89–92]) have been discussed in the literature repeatedly. The setup of [83, 89, 90] is based on an invariant charge  $Q_{\mathcal{R}} = G_{\mathcal{R}}^{-3}$ , but still it is conceptually different from choosing  $w = -3$  in our formalism: With  $w = -3$ , we insert the entire correction  $G_{\mathcal{R}}^{-2}$  into only one of the two internal edges, while in [83, 89, 90], one copy  $G_{\mathcal{R}}^{-1}$  is inserted into each of the two edges. We remark that the restriction to insert only into a subset of the available edges can equivalently be formulated as the inclusion of additional primitive kernels, see [40, Sect. 5].

Finally, we remark that Theorem 47 represents a unique mapping between a DSE of the form Eq. (3.37) at  $\epsilon = 0$  and its perturbative solution. That is, knowing the anomalous dimension (as a power series) allows to reconstruct the Mellin transform of the kernel (as a power series for  $\epsilon = 0$ ). No two different Dyson-Schwinger equations of this form have the same solution in kinematic renormalization.

**Example 103: Toy model, linear DSE.**

The toy model (Example 80) gives rise to the renormalized DSE

$$G_{\mathcal{R}}(\alpha, s) = 1 - (1 - \mathcal{R}) \alpha \int_0^\infty \frac{dy}{1+y} (sy)^{-\epsilon} G_{\mathcal{R}}^{1+w}(\alpha, sy).$$

We have computed the Mellin transform  $F(\rho) = \frac{\pi}{\sin(\pi\rho)}$  in Example 99. By Theorem 47, the linear DSE, for  $\epsilon = 0$ , has the all-order solution  $G_{\mathcal{R}}(\alpha, L) = e^{L\gamma(\alpha)}$  with

$$\gamma(\alpha) = -\frac{1}{\pi} \arcsin(\pi\alpha) = -\alpha - \frac{\pi^2}{6}\alpha^3 - \frac{3\pi^4}{40}\alpha^5 - \frac{5\pi^6}{112}\alpha^7 - \dots$$

**Example 104: Multiedge DSE.**

We consider insertions into one of the edges of the the 1-loop multiedge (Example 24). Then the DSE reads

$$G_{\mathcal{R}}(\alpha, \epsilon, \underline{q}^2) = 1 - \lambda^2 \int \frac{d^D k}{(2\pi)^D} \frac{G_{\mathcal{R}}^{1+w}(\alpha, \epsilon, \underline{k}^2)}{\left(\underline{k} + \underline{q}\right)^2 \underline{k}^2} + \mathcal{R} \left( \lambda^2 \int \frac{d^D k}{(2\pi)^D} \frac{G_{\mathcal{R}}^{1+w}(\underline{k}^2)}{\left(\underline{k} + \underline{q}\right)^2 \underline{k}^2} \right).$$

If  $D = D_0 - 2\epsilon$ , then we obtain the form Eq. (3.37) by rescaling the coupling  $\alpha := \lambda(4\pi)^{-\frac{D_0}{2}}$ .

**Definition 109** ([96, 97]). For  $n \in \mathbb{N}$ , the *Catalan numbers*  $C_n$  are given by

$$C_n := \frac{1}{n+1} \binom{2n}{n}.$$

**Example 105: Multiedge linear DSE.**

The multiedge linear DSE amounts to setting  $w = 0$  in Example 104. The Mellin transform of the 1-loop multiedge in  $D = 4$  was computed in Example 97. In kinematic renormalization at  $\epsilon = 0$ , it has a scaling solution (Theorem 46), where the anomalous dimension is given by Theorem 47:

$$\frac{1}{\frac{-1}{\gamma(\alpha)(1+\gamma(\alpha))}} = -\alpha \Rightarrow \gamma(\alpha) = \frac{\sqrt{1+4\alpha} - 1}{2} = \sum_{n=1}^{\infty} (-1)^n C_{n-1} \alpha^n.$$

$C_n$  are the Catalan numbers (Definition 109). This solution has long been known [94]. In a similar way, the Mellin transform of the same kernel in  $D = 6$  is a rational function of degree four (see Example 97), leading to the anomalous dimension

$$\gamma(\alpha) = \frac{\sqrt{5 + 4\sqrt{1-\alpha}} - 3}{2}.$$

Observe that Theorem 47 does not make any reference to regularization. That is because essentially the Mellin transform acts as an analytically regularized integral. But even without explicit regularization, Theorem 47 is based on kinematic renormalization conditions (Definition 93). Earlier works on DSEs, such as [94, 95], do regulate the integrals using dimensional regularization (Sect. 2.3.3), but they impose kinematic renormalization conditions nonetheless. We will consider DSEs with non-kinematic renormalization conditions in Chap. 4.

### 3.3.3 *Leading-Log Expansion*

In Eqs. (3.2) and (3.15), we expanded the renormalized 1PI Green function in powers of the logarithmic scale  $L$  (Definition 101), where the coefficients  $\gamma_j(\alpha)$  are functions of the renormalized coupling  $\alpha$ . The *leading log expansion* is a reordering of the series, in powers of  $(\alpha \cdot L)$ :

$$G_R(\alpha, x) = 1 + \sum_{k=1}^{\infty} H_k(\alpha L) \alpha^{k-1}. \quad (3.39)$$

The function  $H_1(z)$  is the *leading-log contribution* to the Green function, and  $H_k(z)$  represents the next-to $k$  leading log part. They can be obtained systematically from DSEs by mapping to chord diagrams [98, 99], or from the renormalization group equation in the Hopf algebra [1, 7, 100]. In the language of rooted trees

(Sect. 2.1.5), the leading log approximation amounts to a weighting of all trees with their *tree factorial* [1, 101], which constitutes a special choice of tree Feynman rules (Example 98).

Using Eq. (3.9), we see that the leading-log order is the highest power in  $L$  for each graph, therefore it is given by the  $c_0$ -term of the Mellin transform (Definition 103). Phrased differently, we obtain the leading-log solution of any theory by setting  $c_{j \geq 1} = 0$  in the Mellin transform, and the next-to $k$  leading log by keeping only the first  $k$  coefficients  $c_j$  (compare Example 98). Equivalently,  $H_k$  depends on the first  $k$  coefficients  $c_k$  of the anomalous dimension in kinematic renormalization (Definition 93),

$$\gamma(\alpha) =: \sum_{j=1}^{\infty} c_j \alpha^j. \quad (3.40)$$

As remarked in Sect. 3.2.4, this observation was the starting point for renormalization group theory in QED in [39, 102]: Knowing the first coefficient of the beta function, one can resum leading logarithms to all orders. Concretely, for a DSE with one insertion point (Eq. (3.38)) which features the invariant charge  $\mathcal{Q}_{\mathcal{R}} = G_{\mathcal{R}}^w$  (Eq. (3.33)), where  $w \neq 0$ , one finds [7]:

$$\begin{aligned} H_1(z) &= \frac{1}{(1 - wc_1 z)^{\frac{1}{w}}}, & H_2(z) &= \frac{-c_2 \ln(1 - wc_1 z)}{wc_1 (1 - wc_1 z)^{\frac{1}{w}+1}}, \\ H_3(z) &= \frac{-w^2 c_1 (c_2^2 - c_1 c_3) z - wc_2^2 \ln(1 - wc_1 z) + \frac{c_2^2}{2} (1 + w) \ln^2(1 - wc_1 z)}{w^2 c_1^2 (1 - wc_1 z)^{\frac{1}{w}+2}}. \end{aligned} \quad (3.41)$$

### Example 106: Landau pole in QED.

The leading-log functions in Eq. (3.41) are only valid for a theory with a single Green function. QED (Example 23) contains two fields and three Green functions needing renormalization (the two propagators and the vertex). Thanks to the Ward identity to be discussed in Example 129, in terms of renormalization, QED effectively behaves like a theory with only one Green function and  $w = +1$ . We are interested in the leading log expansion of the running coupling  $\tilde{\alpha}$  (Definition 104). By Eq. (3.18), its momentum dependence is given by the beta function, so we have to replace  $\gamma$  with  $\beta$  in Eq. (3.41). In QED, the first coefficient of the beta function (where one factor of  $\alpha$  is removed by  $\alpha \mathcal{Q}_{\mathcal{R}} = \tilde{\alpha} \leftrightarrow \mathcal{Q}_{\mathcal{R}}$ ) is  $c_1 = \frac{\alpha}{3\pi} > 0$  [103, 104]. From Eq. (3.41), we obtain

$$\tilde{\alpha}(\alpha, L) = \frac{\alpha}{1 - \frac{\alpha}{3\pi} L}.$$

This is the famous first order correction to the running coupling, obtained by Gell-Mann and Low [39, 102]. We see that  $\tilde{\alpha}(\alpha, L^*) = \infty$  for a finite value  $L^*$ . This value is known as the Landau pole, or Moscow zero, of QED [38, 105, 106], indicating the breakdown of the leading-log expansion. The same pole will appear for all  $H_k$ , at the same  $L^*$ , unless the polynomials in the numerator cancel the pole. A slightly different perspective, based on Dyson-Schwinger equations rather than the leading-log expansion, is given in [41], with the outcome that the presence of a Landau pole depends on the asymptotic growth of primitive Feynman graphs.

Conversely, the leading log approximation in QED does not contain obvious poles for the infrared asymptotics  $L \rightarrow -\infty$ . Therefore, the leading-log expansion does not break down and  $H_k(z)$  would give the correct asymptotics for vanishing *scale*. However, this limit implies simultaneously a vanishing of the electron mass (see Example 66), so it is not the physical low-energy limit of QED.

The opposite situation occurs if the coefficient  $c_1$  is smaller than zero [42]. Then,  $H_1$  is not singular for  $L \rightarrow \infty$  and the leading-log expansion produces the correct UV asymptotics [32]. Such theories are called *asymptotically free* [48, 49, 61] since for high energies, they become free field theories. But this time, the leading log expansion breaks down for low scales  $L \rightarrow -\infty$ . Quantum chromodynamics (QCD) is a theory of this kind.

At the same time, the (experimentally verified) existence of the strong force is an argument for why the Landau pole in QED does not necessarily indicate a failure of quantum field theory as such, but only of the leading log approximation: The coupling of QCD at low energies becomes strong and perturbation theory breaks down, but the coupling stays finite nevertheless and QCD still describes experimentally observed properties of the strong force, as known e.g. from lattice calculations [107]. It might well be that something similar happens to QED at high energies. For example, a non-Gaussian UV fixed point has been proposed for QED [108], rendering it finite despite the diverging low-order perturbation series. Compare the discussions in Sects. 3.2.4 and 5.2.1.

### 3.3.4 Non-physical Spacetime Dimension

So far in Sect. 3.3, we have concentrated on the physical spacetime dimension  $D = D_0$ . But with small modifications, our theory is also applicable to the general case  $D = D_0 - 2\epsilon$ .

**Theorem 48.** Work in dimensional regularization (Sect. 2.3.3) with  $D = D_0 - 2\epsilon$ . Consider a DSE of the form Eq. (3.37), where  $\mathbb{R} \ni w \neq 0$  and  $F(\rho)$  is the  $\epsilon$ -dependent Mellin transform of the sum of kernel graphs. Then, in kinematic renormalization (Definition 93), the  $\epsilon$ -dependent anomalous dimension is a solution of the pseudodifferential equation

$$\frac{1}{\rho \cdot F(\rho)} \Big|_{\rho \rightarrow \gamma + (w\gamma - \epsilon)\alpha\partial_\alpha} \gamma(\alpha, \epsilon) = -\alpha.$$

The  $\epsilon$ -dependent solution of a linear DSE is given by the differential equation that arises by setting  $w = 0$ .

**Proof** The proof of Theorem 47 can be copied almost verbatim. The only difference is that we need the Mellin transform in  $D$  dimensions, including its  $\epsilon$ -dependence, and the Callan-Symanzik equation with  $\epsilon$ -dependence (Theorem 45),

$$(\gamma(\alpha, \epsilon) + (w\gamma(\alpha, \epsilon) - \epsilon)\alpha\partial_\alpha)G_R(\alpha, \epsilon, L) = \partial_L G_R(\alpha, \epsilon, L).$$

The linear case still contains the derivative operator  $-\epsilon\alpha\partial_\alpha$ , it does not reduce to an algebraic equation in the  $\epsilon$ -dependent case.  $\square$

The differential equation in Theorem 48 implies a highly non-trivial mixing of the various orders in  $\epsilon$ . This is because, in a series expansion of the anomalous dimension in  $\epsilon$ , the various orders no longer commute. For example, the quantity  $[\epsilon^0]\gamma\alpha\partial_\alpha([\epsilon^1]\gamma)$  is generally different from  $[\epsilon^1]\gamma\alpha\partial_\alpha([\epsilon^0]\gamma)$ . The situation becomes more manageable in the linear case ( $w = 0$ ):

**Theorem 49.** Consider a linear DSE ( $w = 0$ ) of the form Eq. (3.37) with  $\epsilon$ -dependent Mellin transform (Definition 103)  $F(\rho)$ . Let  $\frac{1}{F(\rho)} = T_0(\rho) + \epsilon T_1(\rho) + \mathcal{O}(\epsilon^2)$  and  $\gamma(\alpha, \epsilon) =: \gamma(\alpha) + \epsilon g(\alpha) + \mathcal{O}(\epsilon^2)$ , then

$$g(\alpha) = \frac{\alpha\partial_\alpha\gamma(\alpha) \cdot \left( \frac{1}{2}\partial_\rho^2 T_0(\rho) \Big|_{\rho \rightarrow \gamma(\alpha)} \right) - T_1(\gamma(\alpha))}{\left( \partial_\rho T_0(\rho) \Big|_{\rho \rightarrow \gamma(\alpha)} \right)}.$$

**Proof** We have to extract the order  $\epsilon^1$  from Theorem 48 in the linear case. First, observe that

$$\begin{aligned} [\epsilon^1] \left( (\gamma(\alpha, \epsilon) - \epsilon\alpha\partial_\alpha)^k \gamma(\alpha, \epsilon) \right) &= (\gamma(\alpha))^k g(\alpha) + \sum_{j=1}^k (\gamma(\alpha))^{k-j} (g(\alpha) - \alpha\partial_\alpha) (\gamma(\alpha))^j \\ &= (k+1) \cdot \gamma(\alpha)^k g(\alpha) - \frac{k(k+1)}{2} \gamma(\alpha)^{k-1} \alpha\partial_\alpha \gamma(\alpha). \end{aligned}$$

Let  $T_0(\rho) =: \sum_{k \geq 1} t_k \rho^k$ , then the first order in  $\epsilon$  of Theorem 48 is  $0 = T_1(\gamma(\alpha)) + [\epsilon^1]T_0(\gamma(\alpha), \epsilon)$ ,

$$\begin{aligned} 0 &= T_1(\gamma(\alpha)) + \sum_{k \geq 1} t_k \left( k \cdot \gamma(\alpha)^{k-1} g(\alpha) - \frac{k(k-1)}{2} \gamma(\alpha)^{k-2} \alpha \partial_\alpha \gamma(\alpha) \right) \\ &= T_1(\gamma(\alpha)) + g(\alpha) \left( \partial_\rho T_0(\rho) \Big|_{\rho \rightarrow \gamma(\alpha)} \right) - \alpha \partial_\alpha \gamma(\alpha) \left( \frac{1}{2} \partial_\rho^2 T_0(\rho) \Big|_{\rho \rightarrow \gamma(\alpha)} \right). \end{aligned}$$

□

### Example 107: Multiedge DSE, linear correction in $\epsilon$ .

The Mellin transform of the Multiedge is Example 97, a series expansion results in

$$\begin{aligned} T_0(\rho) &= -\rho - \rho^2 \\ T_1(\rho) &= 2 + 4\rho + \gamma_E \rho(1 + \rho) + (\pi \cot(\pi\rho) + 2\psi(\rho)) \rho(1 + \rho) \\ &= 1 + (3 - \gamma_E)\rho - \gamma_E \rho^2 - 2 \sum_{j=1}^{\infty} \zeta(2j+1)(\rho^{2j+1} + \rho^{2j+2}). \end{aligned}$$

Here,  $\psi(z) := \partial_z \Gamma(z)$  is the digamma function. Using the given series expansion and Eq. 2.47, one finds the alternative representation

$$(\pi \cot(\pi\rho) + 2\psi(\rho))\rho = \rho \partial_\rho \ln \frac{\Gamma(1+\rho)}{\Gamma(1-\rho)} - 1.$$

We have  $\partial_\rho T_0 = -1 - 2\rho$  and  $\frac{1}{2}\partial_\rho^2 T_0 = -1$ . The anomalous dimension  $\gamma(\alpha)$  for  $\epsilon = 0$  was derived in Example 105, consequently,

$$\begin{aligned} g(\alpha) &= \frac{\alpha \partial_\alpha \gamma(\alpha) + T_1(\gamma(\alpha))}{1 + 2\gamma(\alpha)} \\ &= 1 + \frac{\alpha}{1+4\alpha} + \frac{\gamma(\alpha)+1}{2\gamma(\alpha)+1} \left( 2\gamma(\alpha) \cdot \gamma_E + \rho \partial_\rho \ln \frac{\Gamma(1+\rho)}{\Gamma(1-\rho)} \Big|_{\rho \rightarrow \gamma(\alpha)} - 1 \right) \\ &= 1 + 2\alpha - 7\alpha^2 + (26 - 2\zeta(3))\alpha^3 + (-99 + 8\zeta(3))\alpha^4 + \dots \end{aligned}$$

Knowing the functions  $\gamma(\alpha)$  and  $g(\alpha)$ , the first-order solution in  $\epsilon$  of the linear DSE is given by Eq. (3.32).

### Summary of Sect. 3.3.

1. A DSE for propagator-type Green functions can be written as an implicit pseudodifferential equation where the Mellin transforms of the kernel graphs are the input data (Sect. 3.3.1).
2. If we further restrict ourselves to insertions into only a single internal edge of a single kernel graph, then the DSE turns into an explicit pseudodifferential equation for the anomalous dimension  $\gamma(\alpha)$  (Sect. 3.3.2). The expansion coefficients of the Mellin transform determine the coefficients of this differential equation.
3. The leading-log expansion is a reordering of the series expansion of  $G_R$  in powers of  $(\alpha \cdot L)$ . The next-to- $k$  leading-log approximation is determined by the first  $k$  coefficients of the anomalous dimension, or of the Mellin transform of the kernel. Depending on the sign of the first coefficient, the leading-log expansion describes the asymptotics of the theory either for  $L \rightarrow \infty$  or for  $L \rightarrow -\infty$  (Sect. 3.3.3).
4. In Sect. 3.3.4, we showed that for insertions into a single edge, essentially the same pseudodifferential equation holds for the full  $\epsilon$ -dependent anomalous dimension  $\gamma(\alpha, \epsilon)$  as for the earlier case of  $\epsilon = 0$ . However, it needs the  $\epsilon$ -dependent Mellin transform as input, which is in practice a much more complicated function than the  $\epsilon = 0$  case. For a linear DSE, we derived an explicit formula for the first coefficient  $[\epsilon^1]\gamma(\alpha, \epsilon)$ .

## 3.4 Asymptotics and Nonperturbative Contributions in MOM

In this section, we compute explicit series solutions to three concrete examples of DSEs in kinematic renormalization (Definition 93). We determine the growth of the series coefficients of the Green functions at high order in the coupling  $\alpha$ , and comment on its implications for non-perturbative completions by resurgence (Sect. 2.1.2).

### 3.4.1 Multiedge DSE at $D = 4$

The multiedge DSE has been introduced in Example 104. We stated the solution of the linear DSE in Example 105. The Mellin transform of this model, as computed in Example 97, is  $F(\rho) = \frac{-1}{\rho(1+\rho)}$ . By Theorem 47, the anomalous dimension  $\gamma(\alpha)$  for the nonlinear DSE,  $w \neq 0$ , is determined by the differential equation

$$(1 + \gamma(\alpha)(1 + w\alpha\partial_\alpha))\gamma(\alpha) = \alpha. \quad (3.42)$$

**Table 3.1** First perturbative coefficients of the anomalous dimension in MOM for the  $D = 4$  multiedge DSE as a function of the renormalized coupling  $\alpha$  for various powers  $w$  of the invariant charge  $Q = G^w$ . Only insertions into a single internal edge were performed, regardless of the value of  $w$

$w$	$\gamma(\alpha)$
5	$\alpha - 6\alpha^2 + 102\alpha^3 - 2640\alpha^4 + 87804\alpha^5 - 3483072\alpha^6 + 158329512\alpha^7 - 8050087584\alpha^8$
4	$\alpha - 5\alpha^2 + 70\alpha^3 - 1485\alpha^4 + 40370\alpha^5 - 1306370\alpha^6 + 48365100\alpha^7 - 2000065725\alpha^8$
3	$\alpha - 4\alpha^2 + 44\alpha^3 - 728\alpha^4 + 15368\alpha^5 - 384960\alpha^6 + 11004672\alpha^7 - 350628096\alpha^8$
2	$\alpha - 3\alpha^2 + 24\alpha^3 - 285\alpha^4 + 4284\alpha^5 - 75978\alpha^6 + 1530720\alpha^7 - 34237485\alpha^8$
1	$\alpha - 2\alpha^2 + 10\alpha^3 - 72\alpha^4 + 644\alpha^5 - 6704\alpha^6 + 78408\alpha^7 - 1008480\alpha^8$
0	$\alpha - \alpha^2 + 2\alpha^3 - 5\alpha^4 + 14\alpha^5 - 42\alpha^6 + 132\alpha^7 - 429\alpha^8$
-1	$\alpha$
-2	$\alpha + \alpha^2 + 4\alpha^3 + 27\alpha^4 + 248\alpha^5 + 2830\alpha^6 + 38232\alpha^7 + 593859\alpha^8$
-3	$\alpha + 2\alpha^2 + 14\alpha^3 + 160\alpha^4 + 2444\alpha^5 + 45792\alpha^6 + 1005480\alpha^7 + 25169760\alpha^8$
-4	$\alpha + 3\alpha^2 + 30\alpha^3 + 483\alpha^4 + 10314\alpha^5 + 268686\alpha^6 + 8167068\alpha^7 + 281975715\alpha^8$
-5	$\alpha + 4\alpha^2 + 52\alpha^3 + 1080\alpha^4 + 29624\alpha^5 + 988288\alpha^6 + 38377152\alpha^7 + 1689250176\alpha^8$

This ODE has a unique perturbative solution. Using a power series ansatz Eq. (3.40),

$$\gamma(\alpha) =: \sum_{j=1}^{\infty} c_j \alpha^j, \quad (3.43)$$

we computed the coefficients  $c_j$  symbolically up to order  $\alpha^{500}$ , for  $w \in \{-5, \dots, +5\}$  with the help of Wolfram Mathematica(tm) 13.2.

Results up to order  $\alpha^8$  are reported in Table 3.1. The sequence of coefficients for  $w = 1$  is part of the OEIS [109, A177384]. As remarked below Theorem 47, the case  $w = -3$  in our setup is not equivalent to insertion into both edges of the kernel graph, even if the latter also corresponds to  $w = -3$ . For  $w = -3$ , we obtain

$$\gamma(\alpha) = \alpha + 2\alpha^2 + 14\alpha^3 + 160\alpha^4 + 2444\alpha^5 + 45792\alpha^6 + 1005480\alpha^7 + 25169760\alpha^8 \mp \dots \quad (3.44)$$

Our result Eq. (3.44) coincides with the rational part of [83, Table 1], the latter work concerns the situation where  $G_R(\alpha, x)$  is inserted into both of the internal edges of the primitive. This overlap be understood heuristically: The rational contribution to  $\gamma(\alpha)$  arises from a rational Mellin transform. For the multiedge (Example 97), this is the Mellin transform  $F(\rho_1, \rho_2)$  where one of the  $\rho_j$  is set to zero. But restricting this Mellin transform to only one non-vanishing  $\rho$  exactly amounts to inserting into only one edge, as we do for Eq. (3.44).

The empirical values of Table 3.1 suggest for the coefficients of Eq. (3.43)

$$\begin{aligned} c_0 &= 0, \quad c_1 = 1, \quad c_2 = -(w+1), \quad c_3 = (1+w)(2+3w), \\ c_4 &= -(w+1)(2w+1)(7w+5), \quad c_5 = (1+w)(2+5w)(7+22w+17w^2). \end{aligned} \quad (3.45)$$

These formulae have been verified for  $w \in \{-30, 30\}$ . Observe how every  $c_{j \neq 1}$  contains a factor  $(w+1)$ , indicating that the higher coefficients vanish for the non-recursive DSE  $w = -1$  as expected. The limit  $w \rightarrow 0$ , that is, the coefficient  $w^0$  of  $c_j$ , must reproduce the solution of the linear DSE (Example 105), namely the Catalan numbers  $C_n$  (Definition 109):

$$[w^0]c_n = -(-1)^n C_{n-1} = (-1)^{n-1} \frac{1}{n} \binom{2(n-1)}{n-1}.$$

It turns out that the first order can be expressed in a similar fashion,

$$[w^1]c_n = \frac{1}{2}(-1)^{n-1} \left( 4^{n-1} - \binom{2(n-1)}{n-1} \right). \quad (3.46)$$

The anomalous dimension considered so far,  $\gamma(\alpha) =: \gamma^{\text{pert}}(\alpha)$ , is the perturbative solution to the differential equation Eq. (3.42). This ODE has also non-perturbative solutions [91, 92] of the form

$$\gamma^{\text{non-pert}}(\alpha) = \alpha^{\beta(w)} \exp \left( \frac{\lambda(w)}{\alpha} \right) (1 + b^{(1)}(w)\alpha + b^{(2)}(w)\alpha^2 + \dots). \quad (3.47)$$

We use the method of [92, Sect. V. A.] to determine the unknown coefficients.<sup>1</sup> The ansatz  $\gamma(\alpha) = \gamma^{\text{pert}}(\alpha) + \gamma^{\text{non-pert}}(\alpha)$  is inserted into Eq. (3.42) and the above coefficients  $c_j$  are used for  $\gamma^{\text{pert}}$ . The equation is then linearized in  $\gamma^{\text{non-pert}}$ . The resulting series in  $\alpha$  has to vanish, this leads to the expressions

$$\begin{aligned} \lambda(w) &= \frac{1}{w}, \quad \beta(w) = -\frac{3+2w}{w}, \quad b^{(1)}(w) = \frac{(1+w)(1+3w)}{w}, \\ b^{(2)}(w) &= \frac{(1+w)(1+5w+3w^2-5w^3)}{2w^2} \\ b^{(3)}(w) &= \frac{(1+w)(1+5w-4w^2-20w^3+45w^4+81w^5)}{6w^3} \\ b^{(4)}(w) &= \frac{(1+w)(1+3w-23w^2-9w^3+259w^4-327w^5-2421w^6-2139w^7)}{24w^4}. \end{aligned} \quad (3.48)$$

Setting  $w = -2$ , these expressions reproduce the results given in [91, (14)].

---

<sup>1</sup> The author thanks Gerald Dunne for suggesting the method.

**Table 3.2** First 50 digits of the Stokes constant  $S(w)$  for the non-linear DSE in  $D = 4$  in the asymptotic expansion Eq.(3.49). The numerical values coincide with the special values given in Eq.(3.51)

$w$	$S(w)$
5	-0.025296711447842155554062589810922604262477942805771
4	-0.027093755285804302538145834438779321901953254099492
3	-0.027514268695235967509951466619196206136028416088749
2	-0.022754314527304604570864961094569471756231077114904
1	-0.0054283179932662026367480341381320752861015892636883
-2	0.20755374871029735167013412472066868268445351496963
-3	0.12923567581109177871522936685966399491429288708430
-4	0.087977369959821254076048394021324447743442962588612
-5	0.065314016354658749144010387750377100215558556707446

The coefficients  $c_n$  of the perturbative solution of the non-linear DSE Eq.(3.42), grow factorially (Definition 60), which has been studied intensively [18, 89, 91, 110]. As indicated in Eq. 2.5, the asymptotic behavior of  $c_n$  is dictated by the non-perturbative solution Eq.(3.47), [111]. The same result can be obtained with the methods of [89]. For  $n \rightarrow \infty$ ,

$$c_n \sim S(w) \cdot \frac{1}{(-\lambda(w))^n} \cdot \Gamma(n - \beta(w)) \left( 1 + \frac{-\lambda(w) \cdot b^{(1)}(w)}{(n - \beta(w) - 1)} + \frac{(-\lambda)^2 \cdot b^{(2)}}{(n - \beta - 1)(n - \beta - 2)} + \frac{(-\lambda)^3 \cdot b^{(3)}}{(n - \beta - 1)(n - \beta - 2)(n - \beta - 3)} + \dots \right). \quad (3.49)$$

We computed 500 series coefficients of  $\gamma^{\text{pert}}(\alpha)$  and extracted their asymptotic behavior using order-70 Richardson extrapolation (Definition 61). This produced at least 50 significant digits and confirmed the expressions  $\lambda(s)$ ,  $\beta(s)$ ,  $b^{(1)}(s) \dots b^{(4)}(s)$  listed in Eq.(3.48). Numerical values for the Stokes constant  $S(s)$  is reported in Table 3.2.

Knowing the parameters Eq.(3.48) (and even the infinitely many other  $b^{(j)}$ ) does not yet fix the non-perturbative solution entirely. Our non-perturbative ansatz Eq.(3.47), in resurgence terminology, corresponds to a 1-instanton correction. There are infinitely many more terms  $\gamma^{\text{non-pert},k}$  of similar structure, each of which has coefficients determined from the asymptotic growth of the preceding one, see the discussion in Sect. 2.1.2. The true non-perturbative solution is a transseries (Definition 59)

$$\gamma(\alpha) = \gamma^{\text{pert}} + \sum_{k=1}^{\infty} t^k \gamma^{\text{non-pert},k}, \quad (3.50)$$

where  $t \in \mathbb{C}$  is a free parameter expressing the boundary condition of the first order DSE. For the case  $w = -2$ , all  $\gamma^{\text{non-pert},k}$  have been determined in [91].

### 3.4.2 Stokes Constant as a Function of the Exponent of the Invariant Charge

As remarked above, the ODE Eq. (3.49) from Theorem 47 contains the exponent  $w$  of the invariant charge  $\mathcal{Q}_R = G_R^w$  (Eq. (3.33)) as an arbitrary numerical parameter, void of combinatorial interpretation. Consequently, we can also insert non-integer  $w \in \mathbb{Q}$ . The asymptotic corrections in Eq. (3.49) are analytic in  $w$ . We numerically extract the Stokes constant  $S(w)$  as a function of  $w$  using Richardson extrapolation (Definition 61) as described below Eq. (3.49).

Firstly, we searched for values of  $w$  where the Stokes constant is a recognizable number, by comparing the numerical values to monomials in  $\sqrt{\pi}$ ,  $\sqrt{e}$ ,  $\ln(n)$  for  $n \in \{2, \dots, 10\}$ , and zeta values. We found the following, including  $S(-2)$  known from [91]:

$$\begin{aligned} S(w = -1) &= S(w = 0) = 0, & S\left(w = -\frac{3}{2}\right) &= \frac{2}{\pi e}, \\ S(w = -2) &= \frac{1}{\sqrt{\pi}e}, & S(w = -3) &= \frac{3}{\pi e^2}. \end{aligned} \quad (3.51)$$

In the cases  $w = 0$  and  $w = -1$ , the DSE has convergent perturbative solutions (Example 105), that is, the coefficients  $c_n$  in Eq. (3.43) do not grow factorially. Consequently,  $S(0) = 0$  and  $S(-1) = 0$ . It turns out that  $S(w)$  oscillates rapidly in the interval  $w \in (-1, 0)$ , with growing amplitude as  $w \rightarrow 0_-$ , see Fig. 3.1.

From the numerical data, we also conclude that  $S(w)$  approaches zero faster than polynomially if  $w \rightarrow 0_+$  from above. On the other hand, between  $w = -1$  and  $w = 0$

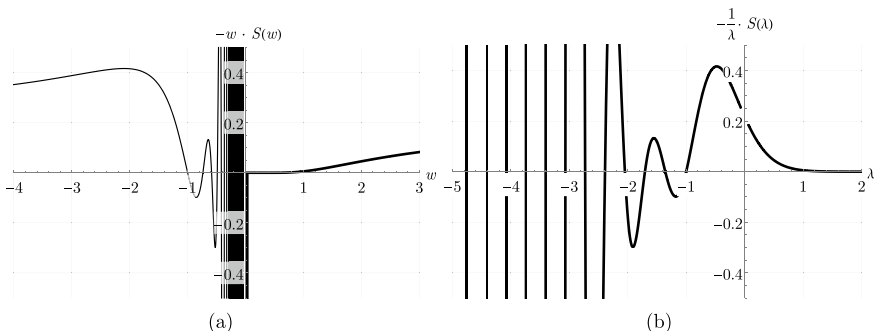


**Fig. 3.1** Stokes constant of the anomalous dimension of the  $D = 4$  multiedge DSE according to Eq. (3.49). The plot is generated from  $\sim 10^4$  individual evaluations of  $S(w)$ . The Stokes constant vanishes for  $w = 0$  (linear DSE) and  $w = -1$  (trivial DSE). Between these values, it is oscillating. In (b), the same data is shown as a function of  $\lambda = \frac{1}{w}$ , we see that the oscillations are regularly periodic in  $\lambda$ .

the function is oscillating with growing amplitude as  $w$  approaches zero from below. We determined the first 50 nontrivial zeros to six digits precision, starting with

$$z_j = \{-0.73658049, -0.586465, -0.488212, -0.418580, -0.366536, -0.326114, \dots\}.$$

For large  $j$ , we find  $j^2 \cdot (z_{j+1} - z_j) \rightarrow -3.000$  which indicates  $z_j \sim \frac{-3}{j} + \mathcal{O}\left(\frac{1}{j^2}\right)$ .

If we examine the Stokes constant as a function of  $\lambda = \frac{1}{w}$ , we see<sup>2</sup> that these oscillations are periodic in  $\lambda$ , with a period of  $\frac{1}{3}$  as  $\lambda \rightarrow -\infty$ , shown in Fig. 3.1b. To shed some light on the curious behavior of  $S(\lambda)$ , we also express Eq. (3.49) in terms of  $\lambda = \frac{1}{w}$ :

$$c_n \sim -\frac{1}{\lambda} S(\lambda) \frac{1}{\lambda^{n-1}} \Gamma(3\lambda + n + 2) \left(1 - \frac{\lambda^2 + 4\lambda + 3}{n} + \mathcal{O}\left(\frac{1}{n^2}\right)\right).$$

The heuristic physical interpretation of the parameter  $w$  is that it expresses the degree to which quantum corrections are taken into account: For  $w = -1$ , there are no quantum corrections, while  $w = 0$  corresponds to a linear DSE, which includes all nested quantum corrections, but not yet the multiple insertions into the same edge. Consequently, we expect that the anomalous dimension  $\gamma(\alpha)$  transitions smoothly between  $w = -1$  and  $w = 0$ , or in the region  $\lambda < -1$ . On the other hand, the summand  $3\lambda$  in  $\Gamma(n + 2 + 3\lambda)$  will compete with the growth of  $n$ . Assuming that the  $c_n$  do not vary strongly as  $\lambda$  changes, the prefactor  $S(\lambda)$  must absorb the shift, which leads to

$$S(\lambda) \sim \frac{1}{\Gamma(3\lambda + d(\lambda))}, \quad \lambda \rightarrow \infty. \quad (3.52)$$

Here,  $d(\lambda) = d_0 + d_1 \frac{1}{\lambda} + \dots$  is a subleading correction. Comparing with our numerical data, the formula Eq. (3.52) qualitatively reproduces a correct factorial growth of  $S(\lambda)$  for  $\lambda \rightarrow 0_+$ , and oscillations with period  $\frac{1}{3}$  in  $\lambda$ , see Fig. 3.2. We can even estimate the coefficients  $d_j$ , or find corrections to the formula Eq. (3.52), but we will not pursue this further as we are currently lacking the theoretical background to rigorously understand the behavior of  $S(\lambda)$ .

Prompted by the observations in Fig. 3.1, David Broadhurst has independently reached similar conclusions as stated above, but greatly extended them by finding a variant of Eq. (3.46) for all higher orders in  $w$ . With this, besides interesting number-theoretical and combinatorial findings, he was able to resum the first correction to the linear DSE [112]. It appears that, apart from this work, the behavior of Dyson-Schwinger equations as functions of a continuous parameter  $w$  has never been examined in the literature. The author is convinced that a more detailed analysis can be fruitful, especially since it might provide a “continuous” way to introduce non-perturbative features into a theory, thereby clarifying their qualitative properties.

---

<sup>2</sup> The author thanks David Broadhurst for suggesting this variable, and for further discussions of this topic.

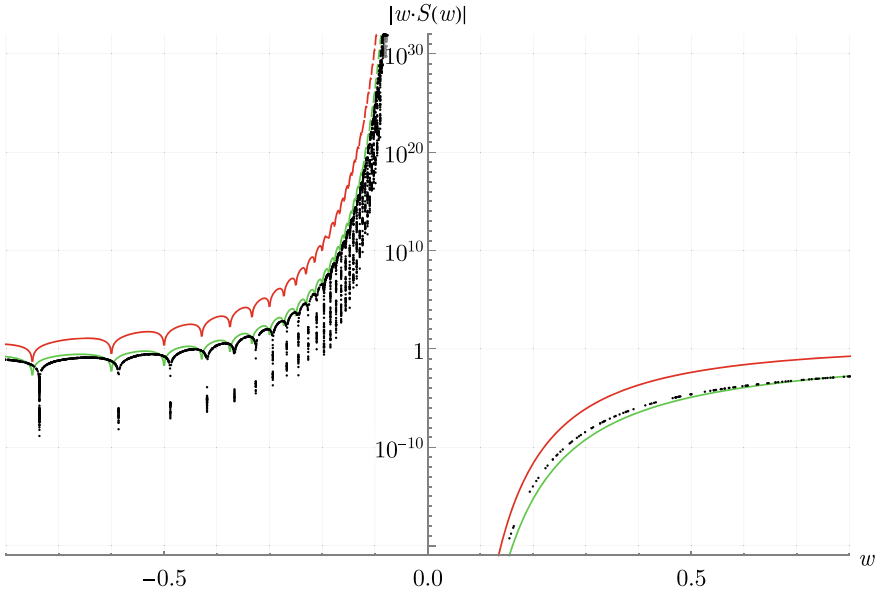


**Fig. 3.2** Comparison of our numerical data (black) with the heuristic function Eq. (3.52), plotted logarithmically as a function of  $w = \frac{1}{\lambda}$ . Red:  $\frac{1}{\lambda} S(\lambda)$  from Eq. (3.52) with  $d(\lambda) = 0$ . Green: The same function for  $d(\lambda) = 3$ . Visually, Eq. (3.52) reproduces the observed behavior of  $S(\lambda)$

### 3.4.3 Multiedge DSE at $D = 6$

We also examined the multiedge DSE (Example 104) for the case  $D = 6$ , which differs from the  $D = 4$  case only by a different Mellin transform, given in Example 97. Consequently, the ODE of Theorem 47 now takes the form

$$(3 + \gamma(1 + w\alpha\partial_\alpha))(2 + \gamma(1 + w\alpha\partial_\alpha))(1 + \gamma(1 + w\alpha\partial_\alpha))\gamma = -\alpha. \quad (3.53)$$

Again, we have computed the perturbative solution  $\gamma^{\text{pert}}(\alpha) = \sum_{j=0}^{\infty} c_j \alpha^j$  to order  $\alpha^{500}$  from this ODE, the first coefficients are

$$\begin{aligned} c_1 &= -\frac{1}{6}, & c_2 &= -\frac{11(w+1)}{6^3}, & c_3 &= -\frac{(w+1)(206+291w)}{6^5}, \\ c_4 &= -\frac{(w+1)(4711+14887w+11326w^2)}{6^7}, \\ c_5 &= -\frac{(w+1)(119762+622327w+1036764w^2+556165w^3)}{6^9}. \end{aligned}$$

Following the same procedure as in Sect. 3.4.1, we insert the first few  $c_j$  and the non-perturbative ansatz Eq. (3.47) into Eq. (3.53), linearize, and solve for the parameters

**Table 3.3** First 50 digits of the Stokes constant  $S(w)$  for the multiedge DSE in  $D = 6$ , from the asymptotics Eq. (3.49)

$w$	$10^6 \cdot S(w)$
5	-48.879979612936267148575174247043686402701421680529
4	-33.683126435179258367949154667346857343063662040223
3	-16.197057487106552084835982615789341267879644562145
2	-2.8749310663584041698420077656773118015156356312116
1	-0.0050376438522521046131658646410401520933414352165372
-2	87595.552909179124483795447421262990627388017406822
-3	17853.256793175269493347991077950813245133374820922
-4	6637.5931100379316509518941784586037225957017664650
-5	3384.1867616825132279651486289425088074650135043176

$\beta, \lambda, b^{(1)}, b^{(2)}, b^{(3)}$ . Equation 3.53 is of third order, unlike in the case  $D = 4$ , we find three linearly independent solutions:

$$\begin{aligned} \gamma(w) &= \left( -\frac{6}{w}, -\frac{12}{w}, -\frac{18}{w} \right), \quad \mathbf{f}(w) = \left( -\frac{35+29w}{6w}, -\frac{5+2w}{3w}, -\frac{15+13w}{2w} \right) \\ \mathbf{b}^{(1)}(w) &= \left( \frac{275+267w-8w^2}{6 \cdot 6^2 w}, \frac{-265-624w-359w^2}{3 \cdot 6^2 w}, \frac{-85-241w-156w^2}{2 \cdot 6^2 w} \right), \\ \mathbf{b}^{(2)}(w) &= \left( \frac{75625+83790w-101849w^2-177828w^3-67814w^4}{93312w^2}, \right. \\ &\quad \left. \frac{70225+339690w+602764w^2+465258w^3+131959w^4}{23328w^2}, \frac{7225+37950w+69779w^2+51628w^3+12574w^4}{10368w^2} \right), \\ \mathbf{b}^{(3)}(w) &= \left( \frac{20796875+8551125w-107422197w^2-206297091w^3-177713418w^4-90251478w^5-23658704w^6}{60466176w^3}, \right. \\ &\quad \left. \frac{-18609625-138592350w-424432473w^2-687305592w^3-624311121w^4-303609366w^5-62154089w^6}{7558272w^3}, \right. \\ &\quad \left. \frac{-614125-4453575w-12499453w^2-16989843w^3-11830354w^4-4259034w^5-758520w^6}{2239488w^3} \right). \end{aligned} \quad (3.54)$$

In order to match [92, Eqs. (41)–(43)], the coefficient  $b^{(1)}$  has to be multiplied by 3,  $b^{(2)}$  by 9 and  $b^{(3)}$  by 27.

In the ansatz Eq. (3.47), the solution with smallest absolute  $\lambda$  is dominant, this is the first entry of the vectors Eq. (3.54). Including order  $1/n^3$ , the large-order growth of  $c_n$  in Eq. (3.49) is determined entirely by the first component of the vectors Eq. (3.54). We have confirmed this behavior numerically from the first 500 coefficients  $c_n$  for  $w \in \{-5, \dots, +5\}$ . The Stokes constant  $S(w)$  is reported in Table 3.3, we reproduce the value [92, (15)] which was obtained by a similar method as in our case, but only for  $w = -2$ .

As for  $D = 4$  in Eq. (3.50), the full non-perturbative solution requires to know  $\gamma^{\text{non-pert}, k}$ , where this time  $k$  indicates contributions from all three fundamental solutions Eq. (3.54), and there are three independent transseries parameters  $t_1, t_2, t_3$ .

Moreover, the three non-perturbative solutions ‘overlap’, giving rise to terms  $\sim \ln(\alpha)$  in the full transseries solution. A detailed examination of the case  $w = -2$  is [93].

### 3.4.4 Toy Model

In the toy model (Example 103), the Mellin transform (Example 99) is not rational. Unlike the ODEs Eqs. (3.42) and (3.53), the equation from Theorem 47 is a pseudodifferential equation, that is, it is of infinite order:

$$\left. \frac{\sin(\pi u)}{\pi u} \right|_{u \rightarrow \gamma(1+w\alpha\partial_\alpha)} \gamma(\alpha) = -\alpha. \quad (3.55)$$

Inserting a non-perturbative ansatz (Eq. (3.47)) into Eq. (3.55), we do not obtain a polynomial equation, therefore one can not simply read off the parameters of Eq. (3.47). Instead, we computed a symbolic perturbative power series solution according Eq. (3.43),  $\gamma(\alpha) = \sum c_n \alpha^n$ , of Eq. (3.55). Since Eq. (3.55) contains infinitely many derivative operators, a series solution is harder to compute than in the previous cases Eqs. (3.42) and (3.53), our result includes order  $\alpha^{450}$ . As above, we numerically extracted the asymptotic behavior of  $c_j$  using Richardson extrapolation (Definition 61). The result has the form Eq. (3.49) for  $n$  odd. We find, empirically,

$$\beta(w) = -\frac{2+w}{w}. \quad (3.56)$$

Numerical values of the constants  $S(w)$ ,  $b^{(1)}(w)$  and  $b^{(2)}(w)$  are given in Table 3.4. We did not recognize these numbers as rationals, apart from the Stokes constant  $S(-2) = 2/\pi$ .

**Table 3.4** First digits of the Stokes constant  $S(w)$  and subleading corrections of the asymptotic growth Eq. (3.49) of the anomalous dimension in the toy model

$w$	$S(w)$	$b^{(1)}(w)$	$b^{(2)}(w)$
5	-0.32358439814031030546	33.713129682396588961	565.374787298670
4	-0.39133508371923490586	28.505508252042547410	405.630022359080
3	-0.48873615802624779599	23.352717957250113407	273.573399332400
2	-0.62073652944344889658	18.337005501361698274	169.862094180663
1	-0.59543401151910843904	13.869604401089358619	98.0525675224480
-2	0.63661977236758134308	-4.4674011002723396547	7.97883629535726
-3	0.52618629546780378450	-9.4831135561607547882	40.2545894932164
-4	0.41925649525660905756	-14.635903850953188791	98.9744451682625
-5	0.34358721547093244258	-19.843525281307230343	184.621956597118

### Summary of Sect. 3.4.

1. We computed the perturbative anomalous dimension for the multiedge DSE in  $D = 4$  to order  $\alpha^{500}$  for various  $w$ . We derived formulas for their asymptotic growth and first corrections for variable  $w$ , and verified them numerically (Sect. 3.4.1).
2. The Stokes constant  $S(w)$  can be computed numerically for non-integer  $w$ . We recognized that it is a smooth function, oscillating between  $w = 0$  and  $w = -1$ . We gave a tentative heuristic explanation for this observation (Sect. 3.4.2).
3. For the  $D = 6$  multiedge DSE, we derived the first coefficients for the asymptotic growth as a function of  $w$  and verified them numerically (Sect. 3.4.3).
4. For the toy model DSE, we extracted the first growth coefficients numerically (Sect. 3.4.4).

## References

1. D. Kreimer, E. Panzer, Renormalization and Mellin transforms, in *Computer Algebra in Quantum Field Theory*. Texts & Monographs in Symbolic Computation (2013), pp. 195–223. [arXiv:1207.6321](https://arxiv.org/abs/1207.6321)
2. F. Brown, D. Kreimer, “Angles, Scales and Parametric Renormalization”. Lett. Math. Phys. **103**, 933–1007 (2013). <https://doi.org/10.1007/s11005-013-0625-6>
3. F. Brown, D. Kreimer, Decomposing Feynman rules (2012). [arXiv:1212.3923](https://arxiv.org/abs/1212.3923)
4. E. Panzer, Hopf algebraic Renormalization of Kreimer’s toy model (2012). [arXiv:1202.3552](https://arxiv.org/abs/1202.3552)
5. P.-H. Balduf, A. Cantwell, K. Ebrahimi-Fard, L. Nabergall, N. Olson-Harris, K. Yeats, Tubings, chord diagrams, and Dyson–Schwinger equations (2023). [arXiv:2302.02019](https://arxiv.org/abs/2302.02019), preprint
6. C. Bergbauer, D. Kreimer, Hopf algebras in renormalization theory: locality and Dyson–Schwinger equations from Hochschild cohomology. IRMA Lect. Math. Theor. Phys. **10**, 133–164 (2006). arXiv:0506190
7. O. Krüger, Log expansions from combinatorial Dyson–Schwinger equations. Lett. Math. Phys. **110**, 2175–2202 (2020). <https://doi.org/10.1007/s11005-020-01288-8>
8. K. Johnson, Solution of the equations for the green’s functions of a two dimensional relativistic field theory. Il Nuovo Cimento (1955–1965) **20**, 773–790 (1961). <https://doi.org/10.1007/BF02731566>
9. C.G. Callan, Broken scale invariance in scalar field theory. Phys. Rev. D **2**, 1541–1547 (1970). <https://doi.org/10.1103/PhysRevD.2.1541>
10. K. Symanzik, Small distance behaviour in field theory and power counting. Commun. Math. Phys. **18**, 227–246 (1970). <https://doi.org/10.1007/BF01649434>
11. K. Symanzik, Massless theory in  $4-\epsilon$  dimensions. Lettere al Nuovo Cimento (1971–1985) **8**, 771–774 (1973). <https://doi.org/10.1007/BF02725853>
12. M. Gomes, B. Schroer, Comment on “New approach to the renormalization group”. Phys. Rev. D **10**, 3525–3531 (1974). <https://link.aps.org/doi/10.1103/PhysRevD.10.3525>
13. E. Brezin, J.C. Le Guillou, J. Zinn-Justin, Wilson’s Theory of Critical Phenomena and Callan–Symanzik Equations in 4-epsilon dimensions. Phys. Rev. D **8**, 434–440 (1973). <https://link.aps.org/doi/10.1103/PhysRevD.8.434>

14. S. Weinberg, New approach to the renormalization group. *Phys. Rev. D* **8**, 3497–3509 (1973). <https://link.aps.org/doi/10.1103/PhysRevD.8.3497>
15. S. W. MacDowell, Generalized callan-symanzik equations and the renormalization group. *Phys. Rev. D* **12**, 1089–1092 (1975). <https://link.aps.org/doi/10.1103/PhysRevD.12.1089>
16. D. Kreimer, Anatomy of a gauge theory. *Ann. Phys.* **321**, 2757–2781 (2006). <http://arxiv.org/abs/hep-th/0509135>
17. D. Kreimer, K. Yeats, An Etude in non-linear Dyson–Schwinger Equations. *Nuclear Physics B - Proceedings Supplements, Proceedings of the 8th DESY Workshop on Elementary Particle Theory* **160**, 116–121 (2006). <http://www.sciencedirect.com/science/article/pii/S0920563206006347>
18. D.J. Broadhurst, D. Kreimer, Exact solutions of Dyson-Schwinger equations for iterated one-loop integrals and propagator-coupling duality. *Nucl. Phys. B* **600**, 403–422 (2001). <http://arxiv.org/abs/hep-th/0012146>
19. J.C. Collins, Structure of counterterms in dimensional regularization. *Nucl. Phys. B* **80**, 341–348 (1974). <https://www.sciencedirect.com/science/article/pii/0550321374905215>
20. G. ’t Hooft, Dimensional regularization and the renormalization group. *Nucl. Phys. B* **61**, 455–468 (1973). <https://www.sciencedirect.com/science/article/pii/0550321373903763>
21. K.G. Wilson, J. Kogut, The renormalization group and the  $\epsilon$  expansion. *Phys. Rep.* **12**, 75–199 (1974). <http://www.sciencedirect.com/science/article/pii/0370157374900234>
22. L.S. Brown, Dimensional regularization of composite operators in scalar field theory. *Ann. Phys.* **126**, 135 (1980). <http://www.sciencedirect.com/science/article/pii/0003491680903772>
23. L.T. Adzhemyan, M.V. Kompaniets, Renormalization group and the-expansion: representation of the  $\beta$ -function and anomalous dimensions by nonsingular integrals. *Theor. Math. Phys.* **169**, 1450–1459 (2011). <https://doi.org/10.1007/s11232-011-0121-z>
24. D. Kreimer, “Chen’s iterated integral represents the operator product expansion (1999). <http://arxiv.org/abs/hep-th/9901099>
25. J.C. Collins, A.J. Macfarlane, New methods for the renormalization group. *Phys. Rev. D* **10**, 1201–1212 (1974). <https://link.aps.org/doi/10.1103/PhysRevD.10.1201>
26. D.J. Gross, Applications of the renormalization group to high-energy physics, in *Methods in Field Theory, Les Houches Session 1975*, ed. by R. Balian, J. Zinn-Justin, Les Houches Session 28 (North Holland/World Scientific, 1981), pp. 141–250. <https://doi.org/10.1142/0004>
27. A.N. Vasil’ev, M.M. Perekalin, Y.M. Pis’mak, On the possibility of conformal infrared asymptotic behavior in non-Abelian Yang-Mills theory. *Theor. Math. Phys.* **55**, 529–536 (1983). <https://doi.org/10.1007/BF01015163>
28. Ö. Gürdoğan, V. Kazakov, New Integrable 4D Quantum Field Theories from Strongly Deformed Planar  $\mathcal{N} = 4$  Supersymmetric Yang-Mills Theory. *Phys. Rev. Lett.* **117**, 201602 (2016). <https://link.aps.org/doi/10.1103/PhysRevLett.117.201602>
29. J. Caetano, O. Gurdogan, V. Kazakov, Chiral limit of  $N = 4$  SYM and ABJM and integrable Feynman graphs (2018). <arXiv:1612.05895>
30. D. Kreimer, Étude for linear Dyson–Schwinger equations, in *Traces in Number Theory, Geometry and Quantum Fields, Aspects of Mathematics E38* (Vieweg Verlag, Wiesbaden, 2008), pp. 155–160. <http://preprints.ihes.fr/2006/P/P-06-23.pdf>
31. L. Klaczynski, Haag’s theorem in renormalisable quantum field theories, doctoral Thesis (Humboldt-Universität zu Berlin, Mathematisch-Naturwissenschaftliche Fakultät, 2016). <https://edoc.hu-berlin.de/handle/18452/18100>
32. A.N. Vasilev, *The Field Theoretic Renormalization Group in Critical Behavior Theory and Stochastic Dynamics* (2004)
33. A. Wipf, *Statistical Approach to Quantum Field Theory: an Introduction*, Lecture Notes in Physics, vol. 864 (Springer, Heidelberg, New York, 2013), 390 pp
34. A.A. Migdal, Phase transitions in gauge and spin-lattice systems. *Zh. Eksp. Teor. Fiz.* **69**, 1457 (1975)
35. L.P. Kadanoff, Notes on Migdal’s recursion formulas. *Ann. Phys.* **100**, 359–394 (1976). <http://www.sciencedirect.com/science/article/pii/000349167690066X>

36. R. Lipowsky, H. Wagner, The Migdal-Kadanoff renormalization group scheme for the Ising model with a free surface. *Zeitschrift für Physik B Condensed Matter* **42**, 355–365 (1981). <https://doi.org/10.1007/BF01293202>
37. N. Benayad, J. Zittartz, Real-space renormalization group investigation of the three-dimensional semi-infinite mixed spin ising model. *Zeitschrift für Physik B Condensed Matter* **81**, 107–112 (1990). <https://doi.org/10.1007/BF01454221>
38. L.D. Landau, A.A. Abrikosov, I.M. Khalatnikov, An asymptotic expression for the photon Green function in quantum electrodynamics. *Dokl. Akad. Nauk SSSR* **95**, 1177–1180 (1954)
39. M. Gell-Mann, F.E. Low, Quantum electrodynamics at small distances. *Phys. Rev.* **95**, 1300–1312 (1954). <https://link.aps.org/doi/10.1103/PhysRev.95.1300>
40. K. Yeats, Growth estimates for Dyson-Schwinger equations (2008). [arXiv:0810.2249](https://arxiv.org/abs/0810.2249) [math-ph]
41. G. van Baalen, D. Kreimer, D. Uminsky, K. Yeats, The QED  $\beta$ -function from global solutions to Dyson–Schwinger equations. *Ann. Phys.* **324**, 205–219 (2009). <https://www.sciencedirect.com/science/article/pii/S0003491608000869>
42. G. van Baalen, D. Kreimer, D. Uminsky, K. Yeats, The QCD  $\beta$ -function from global solutions to Dyson–Schwinger equations. *Ann. Phys.* **325**, 300–324 (2010). <https://www.sciencedirect.com/science/article/pii/S0003491609002140>
43. K.G. Wilson, M.E. Fisher, Critical exponents in 3.99 dimensions. *Phys. Rev. Lett.* **28**, 240–243 (1972). <https://link.aps.org/doi/10.1103/PhysRevLett.28.240>
44. J.D. Bjorken, Asymptotic sum rules at infinite momentum. *Phys. Rev.* **179**, 1547–1553 (1969). <https://link.aps.org/doi/10.1103/PhysRev.179.1547>
45. C.G. Callan, D.J. Gross, Bjorken scaling in quantum field theory. *Phys. Rev. D* **8**, 4383–4394 (1973). <https://link.aps.org/doi/10.1103/PhysRevD.8.4383>
46. D. Gross, F. Wilczek, Ultraviolet behavior of non-abelian gauge theories. *Phys. Rev. Lett.* **30**, 1343–1346 (1973)
47. H. Politzer, Reliable perturbative results for strong interactions? *Phys. Rev. Lett.* **30**, 1346–1349 (1973)
48. S. Coleman, D.J. Gross, Price of asymptotic freedom. *Phys. Rev. Lett.* **31**, 851–854 (1973). <https://link.aps.org/doi/10.1103/PhysRevLett.31.851>
49. H.D. Politzer, Asymptotic freedom: an approach to strong interactions. *Phys. Rep.* **14**, 129–180 (1974). [http://www.sciencedirect.com/science/article/pii/0370157374900143](https://www.sciencedirect.com/science/article/pii/0370157374900143)
50. K.G. Wilson, Non-Lagrangian models of current algebra. *Phys. Rev.* **179**, 1499–1512 (1969). <https://link.aps.org/doi/10.1103/PhysRev.179.1499>
51. K.G. Wilson, Renormalization group and strong interactions. *Phys. Rev. D* **3**, 1818–1846 (1971). <https://link.aps.org/doi/10.1103/PhysRevD.3.1818>
52. W. Zimmermann, Normal products and the short distance expansion in the perturbation theory of renormalizable interactions. *Ann. Phys.* **77**, 570–601 (1973). [http://www.sciencedirect.com/science/article/pii/0003491673904302](https://www.sciencedirect.com/science/article/pii/0003491673904302)
53. J. Polchinski, Renormalization and effective Lagrangians. *Nucl. Phys. B* **231**, 269–295 (1984). [http://www.sciencedirect.com/science/article/pii/0550321384902876](https://www.sciencedirect.com/science/article/pii/0550321384902876)
54. H.E. Stanley, Scaling, universality, and renormalization: three pillars of modern critical phenomena. *Rev. Mod. Phys.* **71**, S358–S366 (1999). <https://link.aps.org/doi/10.1103/RevModPhys.71.S358>
55. D.J.E. Callaway, Triviality pursuit: can elementary scalar particles exist?. *Phys. Rep.* **167**, 241–320 (1988). <https://www.sciencedirect.com/science/article/pii/0370157388900087>
56. T.R. Hurd, Renormalization group proof of perturbative renormalizability. *Commun. Math. Phys.* **124**, 153–168 (1989). [https://projecteuclid.org/download/pdf\\_1/euclid.cmp/1104179080](https://projecteuclid.org/download/pdf_1/euclid.cmp/1104179080)
57. C. Wetterich, Average action and the renormalization group equations. *Nucl. Phys. B* **352**, 529–584 (1991). [http://www.sciencedirect.com/science/article/pii/055032139190099J](https://www.sciencedirect.com/science/article/pii/055032139190099J)
58. M. Reuter, Nonperturbative evolution equation for quantum gravity. *Phys. Rev. D* **57**, 971–985 (1998). [http://arxiv.org/abs/hep-th/9605030](https://arxiv.org/abs/hep-th/9605030)

59. H. Gies, J. Jaeckel, Renormalization flow of QED. Phys. Rev. Lett. **93**, 110405 (2004). <http://arxiv.org/abs/hep-ph/0405183>
60. J.M. Pawłowski, Aspects of the functional renormalisation group. Ann. Phys. **322**, 2831–2915 (2007). <https://www.sciencedirect.com/science/article/pii/S0003491607000097>
61. S. Nagy, Lectures on renormalization and asymptotic safety. Ann. Phys. **350**, 310–346 (2014). <http://www.sciencedirect.com/science/article/pii/S0003491614002061>
62. M. Reuter, N. Tetradis, C. Wetterich, The Large N Limit and the High Temperature Phase Transition for the  $\phi^4$  theory. Nucl. Phys. B **401**, 567–590 (1993). <http://arxiv.org/abs/hep-ph/9301271>
63. O. Lauscher, Untersuchungen zum nichtstörungstheoretischen Renormierungsverhalten der Quanten-Einstein-Gravitation (Johannes Gutenberg-Universität, Mainz, 2002), 306 pp. [https://publications.ub.uni-mainz.de/theses/frontdoor.php?source\\_opus=391&la=de](https://publications.ub.uni-mainz.de/theses/frontdoor.php?source_opus=391&la=de)
64. M. Reuter, F. Saueressig, Functional renormalization group equations, asymptotic safety, and quantum Einstein gravity (2007). <arXiv:0708.1317>
65. M. Niedermaier, M. Reuter, the asymptotic safety scenario in quantum gravity. Living Rev. Relativ. **9**, 5 (2006). <https://doi.org/10.12942/lrr-2006-5>
66. S. Weinberg, Effective field theory, past and future (2009). <arXiv:0908.1964>
67. T. Appelquist, J. Carazzone, Infrared singularities and massive fields. Phys. Rev. D **11**, 2856–2861 (1975). <https://link.aps.org/doi/10.1103/PhysRevD.11.2856>
68. C.P.K. Altes, E. de Rafael, Infrared structure of form factors in quantum electrodynamics and their behaviour at large momentum transfer. Nucl. Phys. B **106**, 237–268 (1976). <https://www.sciencedirect.com/science/article/pii/0550321376903801>
69. A.I. Alekseev, B.A. Arbuzov, V.A. Baikov, Infrared asymptotic behaviour of gluon green's functions in quantum chromodynamics. Theor. Math. Phys. **52**, 733–739 (1982). <https://link.springer.com/article/10.1007/BF01018412>
70. B.A. Arbuzov, Infrared asymptotics of gluon and quark propagators in QCD. Phys. Lett. B **125**, 497–500 (1983). <http://www.sciencedirect.com/science/article/pii/0370269383913345>
71. I. Antoniadis, E. Mottola, Four-dimensional quantum gravity in the conformal sector. Phys. Rev. D **45**, 2013–2025 (1992). <https://link.aps.org/doi/10.1103/PhysRevD.45.2013>
72. U. Ellwanger, M. Hirsch, A. Weber, Flow equations for the relevant part of the pure Yang–Mills action. Zeitschrift für Physik C Particles and Fields **69**, 687–697 (1996). <https://doi.org/10.1007/s002880050073>
73. R. Alkofer, C.S. Fischer, L. von Smekal, The infrared behaviour of the running coupling in Landau gauge QCD (2002). <http://arxiv.org/abs/hep-ph/0205125>
74. S. Moch, J.A.M. Vermaasen, A. Vogt, Three-loop results for quark and gluon form factors. Phys. Lett. B **625**, 245–252 (2005). <http://www.sciencedirect.com/science/article/pii/S0370269305011186X>
75. C.S. Fischer, A. Maas, J.M. Pawłowski, On the infrared behavior of Landau gauge Yang–Mills theory. Ann. Phys. **324**, 2408–2437 (2009). <https://www.sciencedirect.com/science/article/pii/S0003491609001468>
76. Z. Komargodski, A. Schwimmer, On renormalization group flows in four dimensions. J. High Energy Phys. **2011**, 99 (2011). <arXiv:1107.3987>
77. D.J. Broadhurst, D. Kreimer, Combinatorial explosion of renormalization tamed by Hopf algebra: 30-loop Pade-Borel resummation. Phys. Lett. B **475**, 63–70 (2000). <http://arxiv.org/abs/hep-th/9912093>
78. K. Yeats, *Rearranging Dyson-Schwinger Equations*, vol. 211, Memoirs of the American Mathematical Society 995 (American Mathematical Society, 2011). <https://www.ams.org/memo/0995/>
79. H.W. Hamber, L.H.S. Yu, Dyson's equations for quantum gravity in the Hartree–Fock approximation. Symmetry **13**, 120 (2021). <https://www.mdpi.com/2073-8994/13/1/120>
80. D.R. Hartree, The wave mechanics of an atom with a non-coulomb central field. Part II. Some results and discussion. Math. Proc. Camb. Philos. Soc. **24**, 111–132 (1928). <https://www.cambridge.org/core/journals/mathematical-proceedings-of-the-cambridge-philosophical-society/article/wave-mechanics-of-an-atom-with-a-noncoulomb-central-field-part-ii-some-results-and-discussion/5916E7A0DEC0A051B435688BE2ACD57E>

81. V. Fock, Näherungsmethode zur Lösung des quantenmechanischen Mehrkörperproblems. *Zeitschrift für Physik* **61**, 126–148 (1930). <https://doi.org/10.1007/BF01340294>
82. J.C. Slater, Note on Hartree's method. *Phys. Rev.* **35**, 210–211 (1930). <https://link.aps.org/doi/10.1103/PhysRev.35.210.2>
83. M. Bellon, F.A. Schaposnik, Renormalization group functions for the Wess-Zumino model: up to 200 loops through Hopf algebras. *Nucl. Phys. B* **800**, 517–526 (2008). [arXiv:0801.0727](https://arxiv.org/abs/0801.0727)
84. N. Marie, K. Yeats, A chord diagram expansion coming from some Dyson-Schwinger equations. *Commun. Number Theory Phys.* **07**, 251–291 (2013). <https://www.intlpress.com/site/pub/pages/journals/items/cntp/content/vols/0007/0002/a002/abstract.php>
85. J. Courtiel, K. Yeats, Terminal chords in connected chord diagrams (2016). [arXiv:1603.08596](https://arxiv.org/abs/1603.08596)
86. M. Hihn, K. Yeats, Generalized chord diagram expansions of Dyson-Schwinger equations. *Annales de l'Institut Henri Poincaré D* **6**, 573–605 (2019). <https://ems.press/journals/aihp/articles/16458>
87. K. Yeats, *A Combinatorial Perspective on Quantum Field Theory*. SpringerBriefs in Mathematical Physics, vol. 15 (Springer International Publishing, Cham, 2017). <http://link.springer.com/10.1007/978-3-319-47551-6>
88. A.A. Mahmoud, Chord diagrams and the asymptotic analysis of QED-type theories (2020). [arXiv:2011.04291 \[hep-th\]](https://arxiv.org/abs/2011.04291)
89. M.P. Bellon, Approximate differential equations for renormalization group functions in models free of vertex divergencies. *Nucl. Phys. B* **826**, 522–531 (2010). <https://www.sciencedirect.com/science/article/pii/S0550321309005896>
90. M. Bellon, An efficient method for the solution of Schwinger–Dyson equations for propagators. *Lett. Math. Phys.* **94**, 77–86 (2010). [arXiv:1005.0196](https://arxiv.org/abs/1005.0196)
91. M. Borinsky, G.V. Dunne, Non-perturbative completion of Hopf-algebraic Dyson-Schwinger equations. *Nucl. Phys. B* **957**, 115096 (2020). <https://www.sciencedirect.com/science/article/pii/S0550321320301826>
92. M. Borinsky, G. Dunne, M. Meynig, Semiclassical Trans-Series from the Perturbative Hopf-Algebraic Dyson-Schwinger Equations:  $\phi^3$  QFT in 6 Dimensions. *Symmetry Integr. Geom. Methods Appl.* **17**, 087 (2021). <https://doi.org/10.3842/SIGMA.2021.087>
93. M. Borinsky, D. Broadhurst, Resonant resurgent asymptotics from quantum field theory. *Nucl. Phys. B* **981**, 115861 (2022). [arXiv:2202.01513](https://arxiv.org/abs/2202.01513)
94. R. Delbourgo, A.C. Kalloniatis, G. Thompson, Dimensional renormalization: ladders and rainbows. *Phys. Rev. D* **54**, 5373–5376 (1996). <https://link.aps.org/doi/10.1103/PhysRevD.54.5373>
95. R. Delbourgo, D. Elliott, D.S. McAnally, Dimensional renormalization in Phi3 theory: ladders and rainbows. *Phys. Rev. D* **55**, 5230–5233 (1997). <https://link.aps.org/doi/10.1103/PhysRevD.55.5230>
96. P.J. Larcombe, The 18th century Chinese discovery of the Catalan numbers. *Math. Spectr.* **32**, 5–7 (1999). [https://www.math.ucla.edu/~pak/lectures/Cat/Larcombe-The\\_18th-century\\_Chinese\\_discovery\\_of\\_the\\_Catalan\\_numbers.pdf](https://www.math.ucla.edu/~pak/lectures/Cat/Larcombe-The_18th-century_Chinese_discovery_of_the_Catalan_numbers.pdf)
97. R.P. Stanley, *Catalan Numbers* (Cambridge University Press, Cambridge, 2015). <https://www.cambridge.org/core/books/catalan-numbers/5441FB5B09E9C01185834D9CBB9DFAD9>
98. L. Delage, Leading log expansion of combinatorial Dyson Schwinger equations (2016). [arXiv:1602.08705 \[math.CO\]](https://arxiv.org/abs/1602.08705)
99. J. Courtiel, K. Yeats, Next-to-k leading log expansions by chord diagrams. *Commun. Math. Phys.* **377**, 469–501 (2020). <https://doi.org/10.1007/s00220-020-03691-7>
100. O. Krüger, D. Kreimer, Filtrations in Dyson–Schwinger equations: next-to-j-leading log expansions systematically. *Ann. Phys.* **360**, 293–340 (2015). <https://www.sciencedirect.com/science/article/pii/S0003491615001979>
101. E. Panzer, Feynman integrals and hyperlogarithms. Doctoral Thesis (Humboldt-Universität zu Berlin, Berlin, 2015). [arXiv:1506.07243](https://arxiv.org/abs/1506.07243)
102. A. Petermann, E. Stueckelberg, La normalisation des constantes dans la théorie des quanta. <https://doi.org/10.5169/SEALS-112426>

103. E.A. Uehling, Polarization effects in the positron theory. Phys. Rev. **48**, 55–63 (1935). <https://link.aps.org/doi/10.1103/PhysRev.48.55>
104. R. Serber, Linear modifications in the Maxwell field equations. Phys. Rev. **48**, 49–54 (1935). <https://link.aps.org/doi/10.1103/PhysRev.48.49>
105. G. Feldman, R.E. Peierls, Modified propagators in field theory (with application to the anomalous magnetic moment of the nucleon). Proc. R. Soc. London. Ser. Math. Phys. Sci. **223**, 112–129 (1954). <https://royalsocietypublishing.org/doi/10.1098/rspa.1954.0103>
106. W.E. Pauli, *Niels Bohr and the Development of Physics: Essays Dedicated to Niels Bohr on the Occasion of His Seventieth Birthday* (McGraw-Hill Book Company, 1955), 195 pp
107. A. Sternbeck, P.-H. Balduf, A. Kizilersu, O. Oliveira, P.J. Silva, J.-I. Skullerud, A.G. Williams, Triple-gluon and quark-gluon vertex from lattice QCD in Landau gauge (2017). [arXiv:1702.00612](https://arxiv.org/abs/1702.00612)
108. J.B. Kogut, E. Dagotto, A. Kocic, New phase of quantum electrodynamics: a nonperturbative fixed point in four dimensions. Phys. Rev. Lett. **60**, 772–775 (1988). <https://link.aps.org/doi/10.1103/PhysRevLett.60.772>
109. N.J.A. Sloane (ed.), *The On-Line Encyclopedia of Integer Sequences* (2023). <https://oeis.org>
110. M. Borinsky, Generating asymptotics for factorially divergent sequences. Electron. J. Comb. P4.1–P4.1 (2018). <https://www.combinatorics.org/ojs/index.php/eljc/article/view/v25i4p1>
111. I. Aniceto, G. Başar, R. Schiappa, A primer on resurgent transseries and their asymptotics. Phys. Rep. **809**, 1–135 (2019). <https://www.sciencedirect.com/science/article/pii/S0370157319300730>
112. D. Broadhurst, *Airy Tadpoles and Dyson-Schwinger Equations*, Private communication (2022)

# Chapter 4

## Renormalization Group and DSEs in Non-kinematic Renormalization



The goal of the fourth chapter is to understand which features of renormalized Green functions and the renormalization group change if one uses non-kinematic renormalization conditions.

In Sect. 4.1, we generalize our previous constructions, both in the language of Hopf algebras as well as in terms of traditional renormalization group equations, to incorporate arbitrary renormalization schemes. We establish which properties do and which do not change in that case. In particular, we find that the anomalous dimension and the beta function still exist, but the concrete form of these functions depends on the scheme. We introduce the Minimal Subtraction scheme, arguably the most popular non-kinematic renormalization scheme, and discuss its most salient properties.

Section 4.2 is a practical interlude to explain how one solves a Dyson–Schwinger equation in terms of power series. This enables us to give concrete examples for the abstract renormalization group arguments, and to better understand what a renormalization scheme does in practice.

In Sect. 4.3, we introduce a novel way to parameterize renormalization schemes: Instead of abstractly describing the action of the renormalization operator, we can also specify the value that is assigned to a Green function at the renormalization point. Yet another description is to give the energy scale where the renormalized Green function is unity. Within perturbation theory, all descriptions are equivalent for theories described by a single Dyson–Schwinger equation. In particular, this allows us to understand every renormalization scheme as a kinematic renormalization scheme with some exotic renormalization point  $\delta$ , which might itself be a power series of the coupling. This systematic description of renormalization schemes and their relations is one of the main results of the present thesis.

In Sect. 4.5, we apply the new theory of renormalization conditions to some simple example Dyson–Schwinger equations. We determine the shift of renormalization point that corresponds to Minimal Subtraction, and examine the large-order growth of its series coefficients.

## 4.1 Non-kinematic Renormalization Schemes

Up to this point, we have exclusively used the kinematic renormalization scheme (MOM, Definition 93). MOM has two advantages: Firstly, it allows for a clear physical interpretation of the renormalization process, namely that renormalization means the redefinition of parameters in terms of their measured values, see Sect. 2.2.1. Secondly, it represents a boundary condition for renormalized Green functions,  $G_{\mathcal{R}}(\alpha, L = 0) = 1$ , which is particularly helpful in deriving the renormalization group (Sect. 3.2) and in solving Dyson–Schwinger equations, see Sects. 2.2.5 and 3.3. However, according to Definition 99, other renormalization schemes are conceivable. In the present section, we examine how the Green functions change in a different scheme.

### 4.1.1 General Infinitesimal Feynman Rules

A drawback of the MOM scheme is that the counterterms (Definition 106) are relatively complicated expressions. Conversely, the idea of the *Minimal Subtraction* scheme is to choose the simplest possible counterterms which are sufficient to make renormalized amplitudes finite:

**Definition 110.** Assume that the regularized Feynman amplitude is a Laurent series in a regularization parameter  $\epsilon$ , as it is in dimensional (Sect. 2.3.3) or analytic (Sect. 2.3.2) regularization. In the *Minimal Subtraction scheme* (MS), the renormalization operator  $\mathcal{R}$  extracts the pole part from its argument Laurent series,

$$\hat{\mathcal{R}} \left( \sum_{k=-n}^{\infty} \epsilon^k c_k \right) := \sum_{k=-n}^{-1} \epsilon^k c_k.$$

In *modified Minimal Subtraction* (MS-bar,  $\overline{\text{MS}}$ ), those parts of the  $n = 0$  summand, which are powers of  $\ln(4\pi)$  or  $\gamma_E$ , are extracted, too. The presence and precise form of such factors depends on the theory in question. To distinguish from MOM, we will denote the quantities in MS with a hat –  $\hat{G}$ ,  $\hat{Z}$ , and quantities in MS-bar with a bar –  $\bar{G}$ ,  $\bar{Z}$ .

Unlike with MOM, a MS-renormalized amplitude does not satisfy any particular pre-defined boundary condition at  $\epsilon = 0$ , apart from being finite. We stress that Minimal Subtraction is not the same as dimensional regularization (Sect. 2.3.3), even if the two are often used in conjunction. For example (see Sect. 4.2.2), one can perfectly use dimensional regularization, but with kinematic renormalization conditions instead of Minimal Subtraction.

We write  $\mathcal{R}'$  for an arbitrary renormalization scheme (Definition 99), while  $\hat{\mathcal{R}}$  and  $\bar{\mathcal{R}}$  indicate MS and MS-bar (Definition 110), and  $\mathcal{R}$  is reserved for kinematic renormalization at  $L = 0$  (Definition 93). Acting on a Laurent series, the kinematic renormalization operator  $\mathcal{R}$  amounts to a subtraction of *all* orders at  $L = 0$ , not only the pole terms as in Definition 110:

$$\mathcal{R} \left( \sum_{k=-n}^{\infty} \epsilon^k c_k \right) = \sum_{k=-n}^{\infty} \epsilon^k c_k.$$

In this notation, the fact that we subtract at  $L = 0$  is not visible explicitly, compare Sect. 4.2.2.

**Example 108: Second chain graph in MS.**

In Example 93 we computed the integral of the second chain graph in MOM for  $D = 6 - 2\epsilon$ . Now we repeat the computation in MS, where we skip powers of the coupling constant  $\lambda_3^2/(4\pi)^2$ . The reference scale  $s_0$  in  $L = \ln \frac{s}{s_0}$  (Definition 101) does not have any specific significance for the renormalized Green function. The renormalized 1-loop multiedge (Example 87) in MS is

$$\mathcal{F}_{\hat{\mathcal{R}}}[\gamma] = \frac{1}{6}L + \left( -\frac{4}{9} + \frac{\gamma_E}{6} \right).$$

In MOM, the operator  $\mathcal{R}$  (Definition 93) can be concatenated and multiplied without restrictions, this is not true for  $\hat{\mathcal{R}}$  in MS. Recall that a renormalization operator is only required to satisfy the Rota–Baxter equation (Eq. (2.39)). For our concrete example, the MS-counterterm (Definition 91) of  $S_1$  is

$$S_{\hat{\mathcal{R}}}^{\mathcal{F}}[S_1] = -\hat{\mathcal{R}}[\mathcal{F}[S_1]] - \hat{\mathcal{R}}(\hat{\mathcal{R}}(\mathcal{F}[\gamma_2]) \cdot i \cdot \mathcal{F}[\gamma]) \neq \hat{\mathcal{R}}(-\mathcal{F}[S_1] + \mathcal{F}[\gamma_2] \cdot i \cdot \mathcal{F}[\gamma]).$$

For  $S_1$ , we obtain the following counterterm and renormalized integral:

$$\begin{aligned} S_{\hat{\mathcal{R}}}^{\mathcal{F}}[S_1] &= \left( \frac{1}{72\epsilon^2} - \frac{11}{432\epsilon} \right) i, \\ \mathcal{F}_{\hat{\mathcal{R}}}[S_1] &= \frac{1}{72}iL^2 - \left( \frac{1}{8} - \frac{\gamma_E}{36} \right) iL + \left( \frac{791}{2592} - \frac{\gamma_E}{8} + \frac{\gamma_E^2}{72} \right) i. \end{aligned}$$

Now consider the full graph  $S$ . Again,  $S_{\hat{\mathcal{R}}}^{\mathcal{F}}$  is computed recursively using Definition 91.

$$\begin{aligned}
S_{\hat{\mathcal{R}}}^{\mathcal{F}}[\gamma i \gamma] &= -\hat{\mathcal{R}}(\mathcal{F}[\gamma] \cdot i \cdot \mathcal{F}[\gamma]) + 2\hat{\mathcal{R}}(\hat{\mathcal{R}}(\mathcal{F}[\gamma]) \cdot i \cdot \mathcal{F}[\gamma]) \stackrel{2.39}{=} \hat{\mathcal{R}}(\mathcal{F}[\gamma]) \cdot i \cdot \hat{\mathcal{R}}(\mathcal{F}[\gamma]), \\
S_{\hat{\mathcal{R}}}^{\mathcal{F}}[S] &= -\hat{\mathcal{R}}(\mathcal{F}[S] - \hat{\mathcal{R}}(\mathcal{F}[\gamma_i]) \cdot i \cdot \mathcal{F}[S_i] + \hat{\mathcal{R}}(\mathcal{F}[\gamma]) \cdot i \cdot \hat{\mathcal{R}}(\mathcal{F}[\gamma]) \cdot i \cdot \mathcal{F}[\gamma]) \\
&= -\frac{1}{648\epsilon^3} + \frac{11}{3888\epsilon^2} + \frac{13}{23328\epsilon}, \\
\mathcal{F}_{\hat{\mathcal{R}}}[S] &= \mathcal{F}[S] + S_{\hat{\mathcal{R}}}^{\mathcal{F}}[S] + 2S_{\hat{\mathcal{R}}}^{\mathcal{F}}[\gamma_i]\mathcal{F}[S_i] + S_{\hat{\mathcal{R}}}^{\mathcal{F}}[\gamma_1\gamma_2]\mathcal{F}[\gamma] \\
&= -\frac{1}{648}L^3 + \left(\frac{1}{48} - \frac{\gamma_E}{216}\right)L^2 + \left(-\frac{389}{3888} + \frac{\gamma_E}{24} - \frac{\gamma_E^2}{216}\right)L \\
&\quad + \frac{24155}{139968} - \frac{389\gamma_E}{3888} + \frac{\gamma_E^2}{48} - \frac{\gamma_E^3}{648} + \frac{\zeta(3)}{324}.
\end{aligned}$$

Comparing with MOM (Example 93), not only does the renormalized integral in MS contain a constant term independent of  $L$ , but also the coefficients of the non-constant terms are significantly more complicated. On the other hand, the counterterms in MS are very simple rational functions. Observe further that for each graph, the highest coefficient in  $L$  agrees between MS and MOM, as we will prove in Theorem 58.

By Definition 102, the Feynman rules  $\mathcal{F}_{\mathcal{R}}$  in MOM are the exponential of the infinitesimal Feynman rule  $\sigma$ . The exponential formula relies on the condition  $\mathcal{F}_{\mathcal{R}}|_{L=0} = \tilde{\mathbb{1}}\mathbb{1}$ . To extend the procedure to non-kinematic schemes, we need to extract the amplitude at  $L = 0$ .

**Definition 111.** Let  $\mathcal{R}'$  denote any renormalization scheme (Definition 99). Let  $s_0 \in \mathbb{R}$  be the reference scale (Definition 101). The operator  $\tau : H_F \rightarrow \mathbb{R}$  extracts the value at  $s_0$ ,

$$\tau[\Gamma] := \mathcal{F}_{\mathcal{R}'}[\Gamma] \Big|_{s=s_0} = \mathcal{R} \circ \mathcal{F}_{\mathcal{R}'}[\Gamma], \quad \tau[\mathbb{1}] = 1.$$

Here,  $\mathcal{R}$  is the kinematic renormalization operator (Definition 93).

In MOM with renormalization point  $s_0$ , we have  $\tau = \tilde{\mathbb{1}} \circ \mathbb{1}$ , as a MOM-renormalized amplitude vanishes at  $L = 0$  for any graph except the empty graph.  $\tau$  is an evaluation of  $\mathcal{F}_{\mathcal{R}'}$  at a specific point, therefore, by Eq. (2.38), it constitutes a character (Definition 76):

$$\tau[\gamma_1 \cdot \gamma_2] = \mathcal{F}_{\mathcal{R}'}[\gamma_1 \cdot \gamma_2] \Big|_{s=s_0} = (\mathcal{F}_{\mathcal{R}'}[\gamma_1] \cdot \mathcal{F}_{\mathcal{R}'}[\gamma_2]) \Big|_{s=s_0} = \tau[\gamma_1] \cdot \tau[\gamma_2]. \quad (4.1)$$

**Theorem 50** (Compare [1, 2]). Let  $L = \ln \frac{s}{s_0}$  and  $\sigma = \partial_L \mathcal{F}_{\mathcal{R}}|_{L=0}$  (Definition 102), where  $\mathcal{F}_{\mathcal{R}}$  is renormalized in MOM with renormalization point  $L = 0$ . Let  $\mathcal{R}'$  be an arbitrary renormalization scheme (Definition 99) with the corresponding operator  $\tau$  (Definition 111). The renormalized Feynman rules in  $\mathcal{R}'$  are given by

$$\mathcal{F}_{\mathcal{R}'}[\Gamma](L) = (\mathcal{F}_{\mathcal{R}'}(0) \star \mathcal{F}_{\mathcal{R}}(L))\Gamma = (\tau \star \exp^*(L\sigma))\Gamma.$$

**Proof** Let  $\mathcal{R}$  be the evaluation of the amplitude at  $s_0$  (Definition 93). By construction, a counterterm  $S_{\mathcal{R}'}^{\mathcal{F}}$  (Eq. (3.22)) does not depend on momenta (i.e. it is local), this implies  $\mathcal{R}(S_{\mathcal{R}'}^{\mathcal{F}}) = S_{\mathcal{R}'}^{\mathcal{F}}$ . Use Definitions 90 and 111:

$$\begin{aligned}\mathcal{F}_{\mathcal{R}'} &= S_{\mathcal{R}'}^{\mathcal{F}} \star \mathcal{F} = (\mathcal{R} \circ S_{\mathcal{R}'}^{\mathcal{F}}) \star \mathcal{F} = (\mathcal{R} \circ S_{\mathcal{R}'}^{\mathcal{F}}) \star (\mathcal{R} \circ \mathcal{F}) \star (\mathcal{R} \circ \mathcal{F})^{-1} \star \mathcal{F} \\ &= (\mathcal{R} \circ (S_{\mathcal{R}'}^{\mathcal{F}} \star \mathcal{F})) \star S_{\mathcal{R}}^{\mathcal{F}} \star \mathcal{F} = \mathcal{R}(\mathcal{F}_{\mathcal{R}'}) \star \mathcal{F}_{\mathcal{R}} = \tau \star \mathcal{F}_{\mathcal{R}}.\end{aligned}$$

Here,  $\mathcal{F}_{\mathcal{R}}$  are the Feynman rules in kinematic renormalization (Definition 102), with renormalization point  $s_0$  as used by  $\mathcal{R}$ .  $\square$

Owing to the Rota–Baxter equation (Eq. (2.39)) in Definition 99, renormalized Feynman rules, regardless of the scheme, are multiplicative with respect to disjoint unions (Eq. (2.38)),

$$\mathcal{F}_{\mathcal{R}'}[\Gamma_1 \cdot \Gamma_2](L) = m(\tau \otimes e^{*\mathcal{L}\sigma}) \Delta(\Gamma_1)\Delta(\Gamma_2) = \mathcal{F}_{\mathcal{R}'}[\Gamma_1](L) \cdot \mathcal{F}_{\mathcal{R}'}[\Gamma_2](L). \quad (4.2)$$

### Example 109: Second chain graph in MS, exponential formula.

In Example 108, we computed

$$\begin{aligned}\tau[\gamma] &= \mathcal{F}_{\hat{\mathcal{R}}}[\gamma]\Big|_{s=s_0} = -\frac{4}{9} + \frac{\gamma_E}{6}, \quad \tau[S_i] = \left(\frac{791}{2592} - \frac{\gamma_E}{8} + \frac{\gamma_E^2}{72}\right)i, \\ \tau[S] &= \frac{24155}{139968} - \frac{389\gamma_E}{3888} + \frac{\gamma_E^2}{48} - \frac{\gamma_E^3}{648} + \frac{\zeta(3)}{324}.\end{aligned}$$

The MOM-coefficients are known from Example 93,

$$\sigma[\gamma] = \frac{1}{6}, \quad \sigma[S_i] = -\frac{11}{216}i, \quad \sigma[S] = -\frac{85}{3888}.$$

The summands of Theorem 50 are:

$$\begin{aligned}
 (\tau \star \tilde{\mathbb{1}}) S &= \tau[S] = \frac{24155}{139968} - \frac{389\gamma_E}{3888} + \frac{\gamma_E^2}{48} - \frac{\gamma_E^3}{648} + \frac{\zeta(3)}{324} \\
 (\tau \star L\sigma) S &= \bar{L} \left( \underbrace{\tau[S]\sigma[1]}_{=0} + \underbrace{\tau[1]\sigma[S]}_{=1} + 2\tau[\gamma]\sigma[S_i] + \underbrace{\tau[\gamma\gamma]\sigma[\gamma]}_{=\tau[\gamma]^2} \right) \\
 &= L \left( -\frac{85}{3888} + 2 \left( -\frac{4}{9} + \frac{\gamma_E}{6} \right) i \left( -\frac{11}{216} i \right) + \left( -\frac{4}{9} + \frac{\gamma_E}{6} \right)^2 i^2 \frac{1}{6} \right) \\
 &= \left( -\frac{389}{3888} + \frac{\gamma_E}{24} - \frac{\gamma_E^2}{216} \right) L, \\
 \left( \tau \star \frac{1}{2} L\sigma \star L\sigma \right) S &= \frac{L^2}{2} \left( 2\tau[\gamma] \cdot \sigma[\gamma] \cdot \sigma[\gamma] + 2\sigma[\gamma] \cdot \sigma[S_i] \right) = \left( \frac{1}{48} - \frac{\gamma_E}{216} \right) L^2, \\
 \left( \tau \star \frac{1}{6} (L\sigma)^{\star 3} \right) S &= -\frac{1}{648} L^3.
 \end{aligned}$$

These are the correct coefficients of  $\mathcal{F}_{\hat{\mathcal{R}}}[S]$  as computed in Example 108.

### 4.1.2 Renormalization Group Functions at the Physical Dimension

In Sect. 3.2, we discussed the renormalization group in MOM. We found that the renormalization group functions  $\beta, \gamma$  (Definitions 105 and 108) in kinematic renormalization simultaneously enjoy the following properties:

1. They are the  $L$ -derivative of  $G_{\mathcal{R}}$  or  $\mathcal{Q}_{\mathcal{R}}$  at  $L = 0$  (Definition 105).
2. They are the coefficients in the Callan–Symanzik equation (Theorem 45).
3. If  $Q$  (Definition 94) is a monomial in the combinatorial Green functions  $\Gamma^{(j)}$ , then an analogous relation (Theorem 45) holds between  $\beta$  and the corresponding  $\gamma^{(j)}$ .
4. The beta function is the derivative of the renormalized coupling  $\alpha(\alpha_0)$  with respect to the reference scale  $s_0$  at fixed  $\alpha_0$  (Definition 108).
5. The  $Z$ -factors are integrals of the renormalization group functions, or  $\beta$  and  $\gamma$  are derivatives of the  $Z$ -factors (Eqs. (3.28) and (3.29)).

In deriving these properties in Sect. 3.2, we repeatedly used the kinematic renormalization condition  $G_{\mathcal{R}}(L = 0) = 1$ . In non-kinematic renormalization schemes, all points except the first one are still satisfied by one set of functions  $\beta, \gamma$  (which are, however, different functions than in MOM). Only the first point is exclusive to MOM. In a concrete renormalization scheme, one will typically be able to compute the  $Z$ -factors unequivocally, therefore we take the last point as a definition:

**Definition 112.** In dimensional regularization, and for all renormalization schemes (Definition 99), the  $\epsilon$ -dependent renormalization group functions are defined as derivatives of the counterterms  $Z'$  (Eq.(3.22)):

$$\begin{aligned}\beta'(\alpha, \epsilon) &:= \frac{-\epsilon}{\partial_\alpha \ln (\alpha \cdot Z'_\alpha(\alpha, \epsilon))} + \alpha \epsilon \\ \gamma'^{(n)}(\alpha, \epsilon) &:= -(\beta'(\alpha, \epsilon) - \alpha \epsilon) \partial_\alpha \ln Z'^{(n)}(\alpha, \epsilon)\end{aligned}$$

For kinematic renormalization, this definition coincides with the earlier Definitions 105 and 108.

**Theorem 51.** Let the functions  $\beta', \gamma'$  be defined as in Definition 112. Then:

1.  $Z'_\alpha(\alpha, \epsilon) = \exp \left( - \int_0^\alpha \frac{du}{u} \frac{\beta'(u, \epsilon)}{\beta'(u, \epsilon) - u\epsilon} \right),$
2.  $Z'_\phi(\alpha, \epsilon) = \exp \left( - \int_0^\alpha du \frac{\gamma'^{(2)}(u, \epsilon)}{\beta'(u, \epsilon) - u\epsilon} \right),$
3.  $Z'_\alpha(\alpha, \epsilon) = (Z'_\phi(\alpha, \epsilon))^w \quad \text{if and only if} \quad \beta'(\alpha, \epsilon) = w\alpha \gamma'^{(2)}(\alpha, \epsilon).$

**Proof** These are Eqs.(3.28), (3.29) and Theorem 45. They follow from Definition 112 upon solving for the  $Z$ -factors as shown in Sect. 3.2.2.  $\square$

What remains to be shown is that the so-defined renormalization group functions satisfy the Callan–Symanzik equation (Theorem 41).

In kinematic renormalization,  $\mathcal{F}_{\mathcal{R}}$  is multiplicative under  $\star$  with respect to scale, see Lemma 39. In an arbitrary renormalization scheme, the latter equation is modified. Using Theorem 50, we have in general

$$\begin{aligned}\mathcal{F}_{\mathcal{R}'}[\Gamma](L_1 + L_2) &= (\tau \star e^{\star L_1 \sigma} \star e^{\star L_2 \sigma}) \Gamma = \left( \mathcal{F}_{\mathcal{R}'} \Big|_{L_1} \star \mathcal{F}_{\mathcal{R}} \Big|_{L_2} \right) \Gamma \quad (4.3) \\ &\neq \left( \mathcal{F}_{\mathcal{R}} \Big|_{L_1} \star \mathcal{F}_{\mathcal{R}'} \Big|_{L_2} \right) \Gamma.\end{aligned}$$

In terms of analytic Green functions, Eq.(4.3) becomes the following lemma.

**Lemma 52.** Let  $\Gamma$  be the solution of a combinatorial DSE (Eq. (2.28)) and  $G_{\mathcal{R}'}(\alpha, L) = (\tau \star e^{*L})\Gamma(\alpha)$  the renormalized analytic Green function according to Theorem 50. Let  $\tilde{\alpha}(\alpha) := \alpha\tau[Q(\alpha)] = \alpha Q_{\mathcal{R}'}(\alpha, 0)$ , then

$$G_{\mathcal{R}'}(\alpha, L) = G_{\mathcal{R}'}(\alpha, 0) \cdot G_{\mathcal{R}}(\tilde{\alpha}(\alpha), L).$$

Here,  $G_{\mathcal{R}}$  is the renormalized Green function in MOM (Definition 93).

**Proof** The coproduct of  $\Gamma$  is given by Theorem 26. Upon identification  $e^{*L\sigma} = \mathcal{F}_{\mathcal{R}}$  (Definition 102), we find

$$\begin{aligned} \mathcal{F}_{\mathcal{R}'}[\Gamma](L) &= m(\tau \otimes \mathcal{F}_{\mathcal{R}}(L))\Delta(\Gamma) = \sum_{j=0}^{\infty} \tau[\Gamma \alpha^j Q^j] \cdot \mathcal{F}_{\mathcal{R}}[\Gamma_j](L) \\ &= \tau[\Gamma] \cdot \mathcal{F}_{\mathcal{R}}[\Gamma](L) \Big|_{\alpha \rightarrow \alpha\tau[Q]}. \end{aligned}$$

We have used Eq. (4.1). By Definition 111, the first factor is  $G_{\hat{\mathcal{R}}}(\alpha, 0)$ .  $\square$

By Lemma 52, the non-kinematic Green function obtains an overall prefactor  $G_{\mathcal{R}'}(\alpha, 0) =: \gamma'_0(\alpha)$ . Qualitatively, the behavior is indicated in Fig. 4.1.

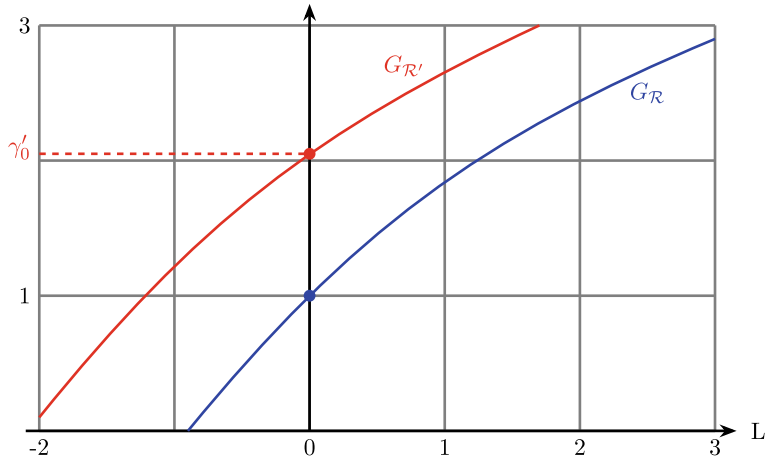


**Fig. 4.1** Sketch of a Green function in MOM with renormalization point  $L = 0$  (blue) and in different scheme (red), both for the same value of the coupling. The value  $\gamma'_0 = \tau[G] = G_{\mathcal{R}'}(0)$  is indicated in red. By Lemma 52, the Green functions are not merely multiples of each other, so  $G_{\mathcal{R}'} \neq \gamma'_0 \cdot G_{\mathcal{R}}$ , because the coupling  $\alpha$  is transformed, too. See [3] for a similar figure

**Theorem 53.** Let  $\Gamma$  be the solution of a combinatorial DSE (Eq.(2.28)) and  $G_{\mathcal{R}'}(\alpha, L) = (\tau \star e^{\star L})\Gamma(\alpha)$  the renormalized analytic Green function according to Theorem 50. Then, for  $\epsilon = 0$ , the Callan–Symanzik equation (Theorem 41) holds,

$$\frac{\partial}{\partial L} G_{\mathcal{R}'}(\alpha, L) = \left( \gamma'(\alpha) + \beta'(\alpha) \frac{\partial}{\partial \alpha} \right) G_{\mathcal{R}'}(\alpha, L),$$

where

$$\begin{aligned} \tilde{\alpha}(\alpha) &:= \alpha \tau[\mathcal{Q}(\alpha)] = \alpha \mathcal{Q}_{\mathcal{R}'}(\alpha, 0), & \gamma'_0(\alpha) &:= \tau[G(\alpha)] = G_{\mathcal{R}'}(\alpha, 0), \\ \beta'(\alpha) &= \frac{\beta(\tilde{\alpha}(\alpha))}{\frac{\partial \tilde{\alpha}(\alpha)}{\partial \alpha}} & \gamma'(\alpha) &= \gamma(\tilde{\alpha}(\alpha)) - \frac{\beta'(\alpha)}{\gamma'_0(\alpha)} \frac{\partial \gamma'_0(\alpha)}{\partial \alpha}. \end{aligned}$$

**Proof** One can obtain the general Callan–Symanzik equation by repeating the steps of Sect. 3.2, but using the renormalized Feynman rules Theorem 50. Lemma 52 then takes the place of Lemma 40. Firstly, we derive Lemma 52 with respect to  $\alpha$ :

$$\frac{\partial}{\partial \alpha} G_{\mathcal{R}'}(\alpha, L) = \frac{\partial}{\partial \alpha} \gamma'_0(\alpha) \cdot G_{\mathcal{R}'}(\tilde{\alpha}, L) + \gamma'_0(\alpha) \frac{\partial}{\partial \alpha} \tilde{\alpha}(\alpha) \cdot \frac{\partial}{\partial \tilde{\alpha}} G_{\mathcal{R}'}(\tilde{\alpha}, L).$$

We want to make a connection with the MOM Green function  $G_{\mathcal{R}}(\alpha, L)$ , which satisfies the Callan–Symanzik equation (Theorem 41). Write this equation with the variable  $\tilde{\alpha}$  instead of  $\alpha$ :

$$\frac{\partial}{\partial \tilde{\alpha}} G_{\mathcal{R}}(\tilde{\alpha}, L) = \frac{1}{\beta(\tilde{\alpha})} \frac{\partial}{\partial L} G_{\mathcal{R}}(\tilde{\alpha}, L) - \frac{\gamma(\tilde{\alpha})}{\beta(\tilde{\alpha})} G_{\mathcal{R}}(\tilde{\alpha}, L).$$

Insert this above:

$$\begin{aligned} \frac{\partial}{\partial \alpha} G_{\mathcal{R}'}(\alpha, L) &= \frac{\partial}{\partial \alpha} \gamma'_0(\alpha) \cdot G_{\mathcal{R}'}(\tilde{\alpha}, L) + \frac{\gamma'_0(\alpha)}{\beta(\tilde{\alpha})} \cdot \frac{\partial \tilde{\alpha}(\alpha)}{\partial \alpha} \left( \frac{\partial}{\partial L} G_{\mathcal{R}}(\tilde{\alpha}, L) - \gamma(\tilde{\alpha}) G_{\mathcal{R}}(\tilde{\alpha}, L) \right) \\ &= \left( \frac{\partial \gamma'_0(\alpha)}{\partial \alpha} - \gamma(\tilde{\alpha}) \frac{\gamma'_0(\alpha)}{\beta(\tilde{\alpha})} \frac{\partial \tilde{\alpha}(\alpha)}{\partial \alpha} \right) G_{\mathcal{R}}(\tilde{\alpha}, L) + \frac{\gamma'_0(\alpha)}{\beta(\tilde{\alpha})} \frac{\partial \tilde{\alpha}(\alpha)}{\partial \alpha} \frac{\partial}{\partial L} G_{\mathcal{R}}(\tilde{\alpha}, L). \end{aligned}$$

Owing to Lemma 52, the  $L$ -derivative of  $G_{\mathcal{R}'}$  is expressible in terms of  $G_{\mathcal{R}}$ :

$$G_{\mathcal{R}}(\tilde{\alpha}, L) = \frac{1}{\gamma'_0(\alpha)} G_{\mathcal{R}'}(\alpha, L), \quad \frac{\partial}{\partial L} G_{\mathcal{R}}(\tilde{\alpha}, L) = \frac{1}{\gamma'_0(\alpha)} \partial_L G_{\mathcal{R}'}(\alpha, L).$$

Eventually, we find the Callan–Symanzik equation

$$\left( \gamma(\tilde{\alpha}) \frac{\partial \tilde{\alpha}(\alpha)}{\partial \alpha} - \frac{\beta(\tilde{\alpha})}{\gamma'_0(\alpha)} \frac{\partial \gamma'_0(\alpha)}{\partial \alpha} \right) G_{\mathcal{R}'}(\alpha, L) + \beta(\tilde{\alpha}) \frac{\partial}{\partial \alpha} G_{\mathcal{R}'}(\alpha, L) = \frac{\partial \tilde{\alpha}(\alpha)}{\partial \alpha} \frac{\partial}{\partial L} G_{\mathcal{R}'}(\alpha, L)$$

□

The concrete formulas for  $\beta'$ ,  $\gamma'$  in Theorem 53 are only moderately useful because they require to know the MOM functions  $\beta$ ,  $\gamma$ . But these relations allow us to prove the well-definedness of  $\beta'$ ,  $\gamma$  for  $\epsilon = 0$ , which would otherwise be unclear from Definition 112. Remember that we always redefine the coupling such that the first quantum correction appears in order  $\alpha^1$ , compare Eq. (3.34).

**Lemma 54.** Assume that in MOM, the power series (Definition 53)  $\beta(\alpha)$  and  $\gamma(\alpha)$  have non-vanishing terms  $\propto \alpha^1$ , and no constant terms. Then, to every finite order in perturbation theory, the renormalization group functions  $\beta'$ ,  $\gamma'$  from Theorem 53 have finite series coefficients for  $\epsilon \rightarrow 0$ , and contain no pole terms in  $\alpha$ .

**Proof**  $\beta'$ ,  $\gamma'$  are computed from evaluations and derivatives of the renormalized quantities  $\mathcal{Q}_{\mathcal{R}'}$ ,  $G_{\mathcal{R}'}$ . The individual factors are therefore finite by Definition 99 and Theorem 34.

We have to show that the fractions appearing in Theorem 53 are not singular. It is

$$\frac{\partial \tilde{\alpha}(\alpha)}{\partial \alpha} = \mathcal{Q}_{\mathcal{R}'}(\alpha, 0) + \alpha \frac{\partial \mathcal{Q}_{\mathcal{R}'}(\alpha, L)}{\partial \alpha} \Big|_{L=0}.$$

The first summand can not vanish in general because it has the structure  $\mathcal{Q}_{\mathcal{R}'}(\alpha, L) = 1 + C_0(\alpha) + C_1(\alpha) \cdot L$  where  $C_1$  is, to leading order  $\alpha^1$ , given by the periods of the involved graphs (Theorem 32). The series  $C_0(\alpha)$  starts at order  $\alpha^1$  and depends on the renormalization scheme. It is conceivable that  $\mathcal{Q}_{\mathcal{R}'}(\alpha^*, 0) = 0$  for some value  $\alpha^* \neq 0$ , but in the limit  $\alpha \rightarrow 0$ , we have  $\mathcal{Q}_{\mathcal{R}'} \rightarrow 1$  at least to finite order in perturbation theory. The denominator of  $\beta'(\tilde{\alpha})$  is of order  $\alpha^0$  and  $\beta'$  is a power series without pole terms in  $\alpha$ . The same holds for  $\gamma'(\tilde{\alpha})$  because, if  $\gamma'_0(\alpha) \in \mathcal{O}(\alpha^k)$  then  $\partial_\alpha \gamma'_0(\alpha) \in \mathcal{O}(\alpha^{k-1})$  and  $\beta \cdot \gamma'_0 \in \mathcal{O}(\alpha^k)$ . □

**Lemma 55.** In every renormalization scheme  $\mathcal{R}'$ , the renormalization group functions  $\beta'(\alpha)$ ,  $\gamma'(\alpha)$  appearing in Theorem 53 are the limit  $\epsilon \rightarrow 0$  of the functions  $\beta'(\alpha, \epsilon)$ ,  $\gamma'(\alpha, \epsilon)$  computed from the counterterms by Definition 112.

**Proof** Start from Eq. (3.26),

$$0 = s_0 \cdot \frac{d\tilde{\alpha}}{ds_0} = \frac{d\tilde{\alpha}}{d \ln s_0} = \alpha s_0 \frac{\partial \tilde{\alpha}}{\partial \alpha} \frac{d \ln \alpha}{ds_0} - \frac{\partial \tilde{\alpha}}{\partial L},$$

and repeat the steps of Sect. 3.2.2. Especially, note how Definition 108 already contains the derivative  $\frac{\partial \hat{\alpha}}{\partial \alpha}$ , which vanishes in MOM but is present in the beta function of general schemes in Theorem 53.  $\square$

In its current form, the relationships between  $\beta, \gamma$  and  $\beta', \gamma'$  in Theorem 53 only hold for  $\epsilon = 0$ . We will come back to the  $\epsilon$ -dependence of  $\beta', \gamma'$  in Sect. 4.3.

### 4.1.3 Properties of Minimal Subtraction

In this section, we derive two important properties of the Minimal Subtraction scheme.

**Theorem 56.** In Minimal Subtraction (Definition 110), the renormalization group functions (Definition 112) do not depend on the regularization parameter  $\epsilon$ ,

$$\hat{\beta}(\alpha, \epsilon) = \hat{\beta}(\alpha), \quad \hat{\gamma}(\alpha, \epsilon) = \hat{\gamma}(\alpha).$$

**Proof** By Lemma 55, the renormalization group functions  $\hat{\beta}, \hat{\gamma}$  appearing in the counterterms of MS are the same ones which appear in the Callan–Symanzik equation. By Lemma 54, they are finite for  $\epsilon = 0$ , therefore, they can not contain pole terms in  $\epsilon$ . What remains to be shown is that they do not contain positive powers, either.

By Definition 110,  $\hat{Z}$  contains no positive powers of  $\epsilon$ . Therefore, using Theorem 51,

$$-\frac{\hat{\beta}(\alpha, \epsilon)}{\beta(\alpha, \epsilon) - \alpha\epsilon} = \frac{\hat{\beta}(\alpha, \epsilon)}{\alpha\epsilon} \sum_{k=0}^{\infty} \left( \frac{\hat{\beta}(\alpha, \epsilon)}{\alpha\epsilon} \right)^k \text{ must only contain negative powers of } \epsilon.$$

Assume that  $\hat{\beta}(\alpha, \epsilon) = \dots + c \cdot \epsilon$ , then the fraction  $\hat{\beta}/\epsilon$  contains a summand  $c$  which is not of negative order in  $\epsilon$ . Therefore  $\hat{\beta}(\alpha, \epsilon)$  can not contain positive order terms in  $\epsilon$ . Hence it does not depend on  $\epsilon$  at all. An analogous argument applies to  $\hat{\gamma}(\alpha, \epsilon)$ .  $\square$

Using the integral representation Theorem 51, the counterterms are completely determined by the renormalization group functions  $\hat{\beta}, \hat{\gamma}$ . In MOM, one needs to know the full  $\epsilon$ -dependence of  $\beta(\alpha, \epsilon)$  to compute the counterterm  $Z_\alpha(\alpha, \epsilon)$ , even to compute only the pole parts of  $Z_\alpha$ . In MS, by Theorem 56, we only have functions of a single variable  $\alpha$ . Consequently, one can reconstruct the counterterm entirely from the renormalization group functions  $\hat{\beta}, \hat{\gamma}$  at the physical dimension.

We expand  $Z$  in orders of the pole term  $\epsilon^{-1}$ , similarly to the expansion of the Green function in terms of  $L$  (Eq.(3.2)):

$$\hat{Z}_\alpha(\alpha, \epsilon) =: \sum_{j=0}^{\infty} \hat{z}_j(\alpha) \epsilon^{-j}. \quad (4.4)$$

**Theorem 57.** (Scattering type formula [2, 4, 5], [6, Sect. 7]) Consider a single DSE with  $Q = G^w$  (Eq.(3.33)). In MS, the coefficients of the counterterm Eq.(4.4) satisfy  $\hat{z}_{j<0} = 0$  and  $\hat{z}_0(\alpha) = 1$  and

$$\alpha^2 \partial_\alpha \hat{z}_1(\alpha) = \hat{\beta}(\alpha), \quad \alpha^2 \partial_\alpha \hat{z}_{j>1}(\alpha) = \hat{\gamma}(\alpha) \left( 1 + \hat{\beta}(\alpha) \alpha \partial_\alpha \right) \hat{z}_{j-1}(\alpha).$$

Here,  $\hat{\gamma}(\alpha)$  is the anomalous dimension in MS.

**Proof** Insert Eq.(4.4) into the analogue of the Callan–Symanzik equation for the  $Z$ -factor, (Eq.(3.27)),

$$\hat{\beta}(\alpha) \hat{Z}_\alpha(\alpha, \epsilon) + (\hat{\beta}(\alpha) - \alpha \epsilon) \alpha \frac{\partial}{\partial \alpha} \hat{Z}_\alpha(\alpha, \epsilon) = 0. \quad (4.5)$$

The resulting series is

$$\sum_{j=0}^{\infty} \hat{\beta}(\alpha) \hat{z}_j(\alpha) \epsilon^{-j} + \sum_{j=0}^{\infty} \hat{\beta}(\alpha) \alpha \frac{\partial}{\partial \alpha} \hat{z}_j(\alpha) \epsilon^{-j} = \sum_{j=0}^{\infty} \alpha^2 \frac{\partial}{\partial \alpha} \hat{z}_{j+1}(\alpha) \epsilon^{-j}.$$

Compare orders in  $\epsilon$ . By Definition 110,  $\hat{z}_0 = 1$  and therefore  $\partial_\alpha z_0 = 0$ . From this,  $\alpha^2 \partial_\alpha \hat{z}_1 = \hat{\beta}$ .  $\square$

The second equation in Theorem 57 can be integrated term by term with the boundary condition that  $[\alpha^n] \hat{z}_j(\alpha) = 0$  whenever  $n < j$ .

It is instructive to note the duality of MOM and MS renormalization conditions. For concreteness, we assume a DSE of type Eq.(3.34) with  $Q = G^w$ .

- In kinematic renormalization (Definition 93), the order  $L^0$  in  $G_R(\alpha, \epsilon, L)$  vanishes for all  $\epsilon$ . This makes the log-expansion Eq.(3.2) “simple”, it only depends on  $\gamma_1(\alpha, \epsilon)$ , which is the anomalous dimension. The counterterms are given by Theorem 51, which involves the non-trivial dependence of  $\gamma(\alpha, \epsilon)$  on  $\epsilon$ .
- In Minimal Subtraction (Definition 110), the anomalous dimension  $\hat{\gamma}(\alpha, \epsilon) = \hat{\gamma}(\alpha)$  is independent of  $\epsilon$ , and the complete counterterm  $\hat{Z}(\alpha, \epsilon)$  is determined entirely from  $\hat{\gamma}(\alpha)$ . This makes renormalization of concrete graphs “simple”.

Conversely, the renormalized Green function Eq. (3.2) now involves a non-trivial function  $\hat{\gamma}_0(\alpha, \epsilon) = G_{\mathcal{R}}|_{L=0}$ .

Further aspects of this dichotomy will be discussed in Sect. 4.4.

#### 4.1.4 Renormalization Scheme Independent Quantities

Having established Minimal Subtraction, we now perform a quick survey of renormalization-scheme independent quantities. To this end, recall that grouplike elements of the Hopf algebra (Definition 67) satisfy  $\Delta(\Gamma) = \Gamma \otimes \Gamma$ . In Sect. 3.2.3, we examined them in kinematic renormalization. From Theorem 50, we read off their Feynman amplitude for  $\epsilon = 0$  in arbitrary schemes:

$$\mathcal{F}_{\mathcal{R}'}[\Gamma](L) = \mathcal{F}_{\mathcal{R}'}[\Gamma] \Big|_{s=s_0} \cdot \left( \frac{s}{s_0} \right)^{\gamma'_1(\alpha)} =: \gamma'_0(\alpha) \cdot \left( \frac{s}{s_0} \right)^{\gamma'_1(\alpha)}. \quad (4.6)$$

This is a scaling solution just like Eq. (3.30), only with a non-trivial prefactor  $\gamma'_0$ . Both  $\gamma'_0$  and  $\gamma'_1$  are functions of the renormalized coupling  $\alpha$ .

**Theorem 58.** (Compare [7, Sect. 4]) The following quantities are invariant under change of the renormalization scheme (Definition 99):

1. The first coefficient of the anomalous dimension and of the beta function (Definition 105) in the limit  $\epsilon = 0$ .
2. The highest pole in  $\epsilon$  of the counterterms (Definition 106) for every fixed order in  $\alpha$ .
3. The coefficient  $g_{\text{cor}(\Gamma)}$  of the highest order term in the log expansion Theorem 37.
4. The anomalous dimension of a linear DSE (Theorem 46) for  $\epsilon = 0$ .

**Proof** 1. The first coefficient is given by 1-loop graphs, which are, in particular, primitive. By Theorem 32, the coefficient of their scale-dependence is the period, which is independent of renormalization schemes.

2. By Theorem 51, the Z-factor is the exponential of a sum of type  $\sum_j \left( \frac{\gamma(\alpha, \epsilon)}{\epsilon} \right)^j$ . A term proportional to  $\alpha^n$  can arise from  $1 \leq j \leq n$  because the anomalous dimension has no constant term,  $[\alpha^0]\gamma = 0$ . However,  $j$  is the order of the pole. Therefore, the highest possible pole arises when  $j = n$ , and in that case, the numerator is  $([\alpha^1]\gamma)^j$ , so it is entirely determined by the first coefficient. These coefficients are independent of the renormalization scheme by point 1. A similar argument applies to  $Z_\alpha$  and  $\beta$ .

3. The statement is obvious for primitive graphs since the period (Definition 98) is independent of renormalization conditions.

The dependence of  $\mathcal{F}_{\mathcal{R}'}$  on the renormalization scheme, by Theorem 50, is entirely encoded in the operator  $\tau$  (Definition 111). We therefore have to demonstrate that

the highest order coefficient is independent of  $\tau$ . Apply Theorem 50 to a cocycle (Definition 89)  $\Gamma = B_+(\gamma)$ , using the reduced coproduct (Definition 66)

$$\begin{aligned} (\tau \star e^{\star L\sigma}) B_+(\gamma) &= \tau[B_+(\gamma)] \cdot 1 + m(\tau \otimes e^{\star L\sigma} \circ B_+) \Delta(\gamma) \\ &= \tau[B_+(\gamma)] + \tau[\gamma] \cdot e^{\star L\sigma} B_+(\mathbb{1}) + e^{\star L\sigma} B_+(\gamma) + m(\tau \otimes e^{\star L\sigma} \circ B_+) \Delta_1(\gamma). \end{aligned}$$

Assume that  $\text{cor}(\gamma) = n$ , then  $\text{cor}(B_+^\Gamma(\gamma)) = n + 1$  by Theorem 22, and  $\Delta_1(\gamma)$  contains factors with coradical degree of at most  $n - 1$ . The above sum contains only one summand of order  $L^{n+1}$ ,

$$[L^{n+1}] (\tau \star e^{\star L\sigma}) B_+(\gamma) = [L^{n+1}] e^{\star L\sigma} B_+(\gamma) = [L^{n+1}] \mathcal{F}_R(\Gamma).$$

The right hand side is independent of  $\tau$ , so is the left hand side.

4. On an algebraic level, this was remarked in [8, Ex. 5.12]. From Theorem 46 we know that  $\beta(\alpha) = 0$  in MOM. By Theorem 53,  $\beta'(\alpha) = 0$  in all schemes. Furthermore,  $\mathcal{Q}_{R'} = 1$  in every renormalization scheme since, regardless of the scheme, we still scale the treelevel graph to unity (Definition 99). Hence  $\tilde{\alpha} = \alpha$  for  $\epsilon = 0$  and the statement follows from Theorem 53.  $\square$

Point 4 of Theorem 58 fits with Lemma 52: If there is no renormalization of the coupling constant, then the only difference between renormalization schemes is a finite overall factor  $G_R(\alpha, 0) = \gamma'_0(\alpha)$ . Point 1. in Theorem 58 actually holds for the second order coefficients as well, see Theorem 65.

### Summary of Sect. 4.1.

1. The renormalized Feynman rules in any renormalization scheme can be expressed by a variant of the exponential formula,  $\mathcal{F}_{R'} = \tau \star e^{\star L\sigma}$ , where  $\sigma$  are the infinitesimal Feynman rules in kinematic renormalization and the operator  $\tau$  evaluates at  $L = 0$  (Sect. 4.1.1).
2. The Callan–Symanzik equation holds for non-kinematic renormalization schemes, and the renormalization group functions are simultaneously derivatives of the counterterms. The only difference of the general case from the MOM case is that in MOM, the renormalization group functions are derivatives of renormalized Green functions with respect to  $L$  at the point  $L = 0$  (Sect. 4.1.2).
3. The renormalization group functions in MS are independent of  $\epsilon$ , and the MS-counterterms  $\hat{Z}$  can be reconstructed completely from knowing the renormalization group functions at  $\epsilon = 0$  (Sect. 4.1.3).
4. In all renormalization schemes, the analytic Green function of a linear DSE for  $\epsilon = 0$  is a scaling solution with an overall prefactor depending on the scheme. The exponent, that is the anomalous dimension, is the same in all schemes. The leading coefficients of the series expansion of various quantities are independent of the renormalization scheme (Sect. 4.1.4).

## 4.2 Recursively Solving a DSE

By now, we have introduced technical details of the renormalization group which might not be entirely obvious from standard textbooks. To convince ourselves of their soundness, it is useful to have a concrete example at hand. Therefore, before we continue with the theoretical development, we discuss, within a particularly accessible setting, how the various quantities can be computed concretely.

### 4.2.1 Expansion of the Kernel of the DSE

We work in dimensional regularization (Sect. 2.3.3), where  $\epsilon$  is the regularization parameter. Our starting point is a propagator DSE of type Eq. (3.37),

$$\begin{aligned} G_{\mathcal{R}}(\alpha, \epsilon, s) &= 1 - \alpha(1 - \mathcal{R}) \int dy K(s, y) G_{\mathcal{R}}(\alpha, \epsilon, y)^{1+w} \\ &= Z(\alpha, \epsilon) - \alpha \int dy K(s, y) G_{\mathcal{R}}(\alpha, y)^{1+w}. \end{aligned} \quad (4.7)$$

The integration variable is generally a vector, and  $\alpha$  is a rescaled coupling constant. The renormalization scheme  $\mathcal{R}$  (Definition 99) does not need to be a kinematic one. We have introduced the counterterm  $Z(\alpha, \epsilon) := Z^{(2)}(\alpha, \epsilon)$  where  $\alpha$  is the renormalized coupling. In our setup, we have  $Z_\alpha = Z^w$ , and the two different renormalization group functions (Definition 108) are related by Theorem 51,

$$\beta(\alpha, \epsilon) = w \cdot \alpha \gamma(\alpha, \epsilon). \quad (4.8)$$

It turns out that for an order-by-order solution of Eq. (4.7), we need to know the Mellin transform (Definition 103) of the kernel graph with arguments  $-k\epsilon$ , where  $k \in \mathbb{N}_0$  is arbitrary. Observe that this quantity depends on  $\epsilon$  in two different ways: Firstly, the Mellin transform itself is taken at a spacetime dimension  $D_0 - 2\epsilon$ , and secondly, its argument is  $-k\epsilon$ . Concretely, we expand each summand of Eq. (3.6) in  $\epsilon$ , and we factor out trivial powers of  $(4\pi)$ . For the multiedge (Example 104), this expansion reads

$$F(-k\epsilon) =: (4\pi)^{-\frac{D}{2}} e^{-\gamma_E \epsilon} \sum_{n=-1}^{\infty} f_n^{(k)} \epsilon^n. \quad (4.9)$$

Using the Mellin transform from Example 97, we find

$$\sum_n f_n^{(k)} \epsilon^n = e^{\gamma_E \epsilon} \frac{\Gamma\left(-\frac{D}{2} + 2 + k\epsilon\right) \Gamma\left(\frac{D}{2} - 1\right) \Gamma\left(\frac{D}{2} - 1 - k\epsilon\right)}{\Gamma(1 + k\epsilon) \Gamma(D - 2 - k\epsilon)}.$$

It remains to expand the gamma functions using Eq. (2.47). In  $D = 4 - 2\epsilon$  dimensions,

$$\Gamma := \frac{\Gamma((k+1)\epsilon)\Gamma(1-(k+1)\epsilon)\Gamma(1-\epsilon)}{\Gamma(1+k\epsilon)\Gamma(2-(k+2)\epsilon)} = \frac{e^{-\gamma_E}}{(k+1)(1-(k+2)\epsilon)\epsilon} \exp\left(\sum_{m=2}^{\infty} T_m^{(k)} \epsilon^m\right),$$

where  $T_m^{(k)} := (m-1)! \left((-1)^m (k+1)^m + (k+1)^m + 1 - (-k)^m - (k+2)^m\right) \zeta(m)$ . (4.10)

Expanding the prefactor in a geometric series, we obtain the coefficients of Eq. (4.9),

$$f_n^{(k)} = \sum_{t=-1}^n \frac{(k+2)^{t+1}}{k+1} \frac{1}{(n-t)!} \sum_{m=0}^{n-t} B_{n-t,m} \left(0, T_2^{(k)}, T_3^{(k)}, \dots, T_{n-t+1-m}^{(k)}\right). \quad (4.11)$$

Here  $B_{n,k}$  are the Bell polynomials (Definition 54).

### Example 110: Coefficients for the 1-loop multiedge in $D = 4 - 2\epsilon$ .

Unlike the Mellin transform at exactly  $D = 4$  (Example 97), the coefficients of Eq. (4.11) do involve zeta values and powers of  $\pi^2$ :

$$\begin{aligned} f_{-1}^{(0)} &= 1, & f_0^{(0)} &= 2, & f_1^{(0)} &= 4 - \frac{\pi^2}{12}, & f_2^{(0)} &= 8 - \frac{\pi^2}{6} - \frac{7\zeta(3)}{3}, \\ f_{-1}^{(1)} &= \frac{1}{2}, & f_0^{(1)} &= \frac{3}{2}, & f_1^{(1)} &= \frac{9}{2} - \frac{\pi^2}{24}, & f_2^{(1)} &= \frac{27}{2} - \frac{\pi^2}{8} - \frac{26\zeta(3)}{6}. \end{aligned}$$

For  $D = 6 - 2\epsilon$  dimensions, we have that

$$\frac{\Gamma(-1+(k+1)\epsilon)\Gamma(2-\epsilon)\Gamma(2-(k+1)\epsilon)}{\Gamma(1+k\epsilon)\Gamma(4-(k+2)\epsilon)} = \frac{\epsilon-1}{(3-(k+2)\epsilon)(2-(k+2)\epsilon)} \cdot \Gamma.$$

The gamma functions on the right hand side are the same as in  $D = 4 - 2\epsilon$ , consequently their series expansion is again given by the polynomials  $T_m^{(k)}$  from Eq. (4.10):

$$f_n^{(k)} = \sum_{t=-1}^n \left(-(k+1) + \frac{k}{2^{t+1}} - \frac{k-1}{3^{t+2}}\right) \frac{(k+2)^t}{2(k+1)} \frac{1}{(n-t)!} \sum_{m=0}^{n-t} B_{n-t,m} \left(0, T_2^{(k)}, \dots, T_{n-t+1-m}^{(k)}\right). \quad (4.12)$$

As a last example, we consider the toy model (Example 99):

$$\int_0^\infty \frac{dy}{1+y} y^{-(k+1)\epsilon} = \frac{-\pi}{\sin(\pi(k+1)\epsilon)} = -\Gamma((k+1)\epsilon)\Gamma(1-(k+1)\epsilon) =: \sum_{n=-1}^{\infty} f_n^{(k)} \epsilon^n.$$

The Bernoulli numbers  $B_n$  [9] vanish when  $n > 1$  is odd, therefore we can write

$$f_n^{(k)} := \frac{-1}{(k+1)} \sum_{m=0}^{n+1} \frac{1}{(n+1)!} B_{n+1,m} \left( 0, T_2^{(k)}, \dots, T_{n+2-m}^{(k)} \right), \quad T_n^{(k)} := (2\pi(k+1))^n \frac{|B_n|}{n}. \quad (4.13)$$

Observe that, in order to compute  $f_n^{(k)}$ , it is irrelevant whether the Mellin transform (Example 97) is a simple rational function at  $\epsilon = 0$  or not. The “analytic” approach (solving the ODE in Theorem 47) is only feasible in practice in very limited cases, whereas our current “brute force” approach is applicable also for more complicated kernels, as long as  $f_n^{(k)}$  can be determined with reasonable effort.

### 4.2.2 Series Solution of the DSE

As always, the Green function  $G_{\mathcal{R}}(\alpha, \epsilon, L)$  is scaled to its treelevel tensor, consequently, the order-zero solution of Eq. (4.7) is

$$G_{\mathcal{R}}^{(0)}(\alpha, \epsilon, q^2) := 1. \quad (4.14)$$

Inserting this into the right hand side of the DSE (Eq. (4.7)), the integral amounts to the Mellin transform (Eq. (4.9)) at the argument zero, that is,  $F(-k\epsilon)$  with  $k = 0$ . We will assume for concreteness that our kernel is the 1-loop multiedge at  $D = 4 - 2\epsilon$ , all other cases are qualitatively similar. The correct choice to absorb trivial prefactors is then  $\alpha = \lambda(4\pi)^{-2}$ , and the order one solution of the DSE is given by the coefficients  $f_n^{(0)}$ :

$$\begin{aligned} G_{\mathcal{R}}^{(1)}(\alpha, \epsilon, q^2) &= 1 - \alpha(1 - \mathcal{R}) \left[ (4\pi)^\epsilon e^{-\gamma_E \epsilon} \left( \frac{q^2}{s_0} \right)^{-\epsilon} \sum_{r=-1}^{\infty} f_r^{(0)} \epsilon^r \right] \\ &= Z^{(1)}(\alpha, \epsilon) - \alpha(4\pi e^{-\gamma_E})^\epsilon \left( \frac{q^2}{s_0} \right)^{-\epsilon} \sum_{r=-1}^{\infty} f_r^{(0)} \epsilon^r. \end{aligned} \quad (4.15)$$

Here,  $s_0$  is an arbitrary reference mass scale introduced for dimensional reasons. We have used that a renormalization operator  $\mathcal{R}$  (Definition 99) is local, that is, it results in a counterterm summand  $Z^{(1)}$  that is independent of  $q^2$ :

$$Z^{(1)}(\alpha, \epsilon) = 1 + \alpha(4\pi e^{-\gamma_E})^\epsilon \mathcal{R} \left[ \sum_{r=-1}^{\infty} f_r^{(0)} \epsilon^r \right].$$

We restrict ourselves to the following family of renormalization operators, which is parametrized by a number  $\epsilon_{\max} \in \mathbb{Z} \cup \{\pm\infty\}$ . Namely, we assume that the renormalization operator extracts the orders up to  $\epsilon_{\max}$  of a given Laurent series  $f(\epsilon)$ :

$$\mathcal{R}[f(\epsilon)] = \mathcal{R} \left[ \sum_{n=-\infty}^{\infty} f_n \epsilon^n \right] := \sum_{n=-\infty}^{\epsilon_{\max}} f_n \epsilon^n. \quad (4.16)$$

Three different options will be relevant to us:

1. If we chose  $\epsilon_{\max} = -\infty$ , then  $\mathcal{R} = 0$  and we compute the unrenormalized Green function.
2. If we chose  $\epsilon_{\max} = +\infty$ , then  $\mathcal{R}$  subtracts the complete function  $f(\epsilon)$ . Due to the prefactor  $(q^2/s_0)^{-\epsilon}$  in Eq. (4.15), this amounts to kinematic renormalization (Definition 93) at the renormalization point  $s_0$ .
3. The choice  $\epsilon_{\max} = -1$  amounts to Minimal Subtraction (Definition 110).

In concrete computations, to obtain the correct solution at  $\epsilon = 0$  to order  $\alpha^n$ , it is sufficient to chose  $\epsilon_{\max} > n$ . This is because every step in the iteration multiplies by  $\epsilon^{-1}$ . For a linear DSE, it is even sufficient to let  $\epsilon_{\max} = 1$  to obtain the correct MOM-solution at  $\epsilon = 0$ .

In order to streamline computations of higher orders, we define the coefficients  $g_{t,r}^{(1)}$ , which encode both the counterterm and the finite part of  $G_{\mathcal{R}}^{(1)}$ :

$$g_{1,r}^{(1)} := -f_r^{(0)}, \quad g_{0,r}^{(1)} := \begin{cases} -g_{1,r}^{(1)} & r \leq \epsilon_{\max} \\ 0 & \text{else.} \end{cases}$$

With this notation, the renormalized solution to order one, Eq. (4.15), reads

$$G_{\mathcal{R}}^{(1)}(\alpha, \epsilon, q^2) = 1 + \alpha \sum_{t=0}^1 (4\pi e^{-\gamma_E})^{t\epsilon} \left( \frac{q^2}{s_0} \right)^{-t\epsilon} \sum_{r=-1}^{\infty} g_{t,r}^{(1)} \epsilon^r. \quad (4.17)$$

The 1-loop multiedge kernel graph gives rise to a factor  $(4\pi e^{-\gamma_E})^{t\epsilon}$ , which eventually produces finite contributions  $\propto \gamma_E$  and  $\propto \ln(4\pi)$ . In MS renormalization, these terms are present in the finite part of  $\hat{G}_{\mathcal{R}}$  while in MS-bar renormalization they are assigned to the MS-bar-counterterm  $\bar{Z}$  and thus absent from  $\hat{G}_{\mathcal{R}}$ . To facilitate computations, we will absorb them into the momentum variable. In this way, choosing  $\epsilon_{\max} = -1$ , we obtain the MS-bar Green function of the new momentum variable, but our counterterm will be  $\hat{Z}$  in MS, not in MS-bar:

$$\hat{x} := \frac{q^2}{s_0}, \quad \bar{x} := \frac{e^{\gamma_E} q^2}{4\pi s_0} \equiv \frac{q^2}{\bar{s}_0}, \quad \hat{G}_{\mathcal{R}}(\hat{x}) \equiv \bar{G}_{\mathcal{R}}(\bar{x}). \quad (4.18)$$

If we chose  $\epsilon_{\max} = \infty$ , that is, kinematic renormalization, then we can understand the transition  $\hat{x} \leftrightarrow \bar{x}$  as a constant rescaling of the renormalization point  $s_0 \leftrightarrow 4\pi e^{\gamma_E} s_0 =: \bar{s}_0$ . Had we chosen a different kernel, such as the toy model (Example 103), then the factor  $(4\pi e^{-\gamma_E})$  would be different or not arise at all. In any case, we skip all decorations  $\bar{x}$ ,  $\hat{x}$ , knowing that they can always be chosen to absorb superfluous constants. Observe that those constants have already been factored out of  $f_n^{(k)}$  in Eq. (4.9).

**Example 111: Multiedge DSE, first order coefficients.**

Consider the DSE of the 1-loop multiedge in  $D = 4 - 2\epsilon$  dimensions. At 1-loop order, the solution is independent from the exponent  $w$  in the invariant charge Eq. (3.33). In MOM renormalization, the coefficients of the solution are

$$\begin{aligned} g_{1,-1}^{(1)} &= -1, & g_{1,0}^{(1)} &= -2, & g_{1,1}^{(1)} &= -4 + \frac{\pi^2}{12}, \\ g_{0,-1}^{(1)} &= 1, & g_{0,0}^{(1)} &= 2, & g_{0,1}^{(1)} &= 4 - \frac{\pi^2}{12}. \end{aligned}$$

In MS-bar renormalization, that is,  $\epsilon_{\max} = -1$  in Eq. (4.16) and  $(4\pi e^{-\gamma_E})$  is absorbed as in Eq. (4.18), we have

$$\begin{aligned} g_{1,-1}^{(1)} &= -1, & g_{1,0}^{(1)} &= -2, & g_{1,1}^{(1)} &= -4 + \frac{\pi^2}{12}, \\ g_{0,-1}^{(1)} &= 1, & g_{0,0}^{(1)} &= 0, & g_{0,1}^{(1)} &= 0. \end{aligned}$$

Even if the only difference between MS-bar and MOM is in the counterterm  $g_{0,r}^{(1)}$ , this does not imply that the renormalized Green functions are equal.

Higher orders of the renormalized Green function are computed iteratively. Assume we know the order- $m$ -solution in the form

$$G_{\mathcal{R}}^{(m)}(\alpha, \epsilon, x) = 1 + \sum_{n=1}^m \alpha^n \sum_{t=0}^n x^{-t\epsilon} \sum_{r=-n}^{\infty} g_{t,r}^{(n)} \epsilon^r =: 1 + \sum_{n=1}^m \alpha^n G_n(x, \epsilon),$$

where we defined functions  $G_n(x, \epsilon)$ . The latter do not depend on the order  $m$ . Next, we write a generic expansion of the invariant charge Eq. (3.33) according to

$$G_{\mathcal{R}}^{(m)}(\alpha, \epsilon, x) \cdot \mathcal{Q}_{\mathcal{R}}(\alpha, \epsilon, x) \equiv \left( G_{\mathcal{R}}^{(m)}(\alpha, \epsilon, x) \right)^{w+1} =: 1 + \sum_{n=1}^m \alpha^n \sum_{t=0}^n x^{-t\epsilon} h_t^{(n)}(\epsilon). \quad (4.19)$$

The auxiliary functions  $h_t^{(n)}(\epsilon)$  are Laurent series in  $\epsilon$  with the highest pole order  $\epsilon^{-n}$ . They are given by Faa di Bruno's formula (Theorem 20) and the Binomial theorem,  $B_{n,k}$  are Bell polynomials (Definition 54):

$$\begin{aligned} \frac{1}{(G_{\mathcal{R}}^{(m)}(x))^{-w-1}} &= \frac{1}{(-w-2)!} \sum_{n=0}^{\infty} \alpha^n \frac{1}{n!} \sum_{k=1}^n (-s-2+k)! B_{n,k} (1!G_1, 2!G_2, \dots), \quad w < -1 \\ \left(G_{\mathcal{R}}^{(m)}(x)\right)^{w+1} &= (w+1)! \sum_{n=0}^{\infty} \alpha^n \frac{1}{n!} \sum_{k=0}^{s+1} \frac{1}{(w+1-k)!} B_{n,k} (1!G_1, 2!G_2, \dots), \quad w > -1. \end{aligned} \quad (4.20)$$

Knowing the functions  $h_t^{(n)}(\epsilon)$ , we integrate the sum Eq.(4.19) term-wise. Each summand corresponds to a Mellin transform  $F(-t\epsilon)$  in Eq.(4.9), solving the integral amounts to multiplication with a suitable series  $\sum_n f_n^{(t)} \epsilon^n$ . Symbolically, the result is

$$g_{1,r}^{(1)} = -f_r^{(0)}, \quad \bar{g}_{t,r}^{(n)} = - \sum_{u=-1}^{n+r-1} \left( [\epsilon^{r-u}] \bar{h}_{t-1}^{(n-1)} \right) f_u^{(t-1)}, \quad t \geq 1.$$

The overall minus sign is the  $(-\alpha)$  in Eq.(4.7). With these new coefficients, the next order solution of the DSE is

$$G_{\mathcal{R}}^{(m+1)}(\alpha, \epsilon, x) = G_{\mathcal{R}}^{(1)}(\alpha, \epsilon, x) + (1 - \mathcal{R}) \sum_{n=2}^{m+1} \alpha^n \sum_{t=1}^n x^{-t\epsilon} \sum_{r=-n}^{\infty} g_{t,r}^{(n+1)} \epsilon^r. \quad (4.21)$$

To renormalize, we compute the counterterm  $Z^{(m+1)}(\alpha, \epsilon)$  according to Eq.(4.16),

$$\begin{aligned} g_{0,r}^{(n)} &:= \begin{cases} -\sum_{t=1}^n g_{t,r}^{(n)}, & r \leq \epsilon_{\max} \\ 0, & \text{else,} \end{cases} \\ Z^{(m+1)}(\alpha, \epsilon) &= 1 + \sum_{n=1}^{m+1} \alpha^n \sum_{r=-n}^{\infty} g_{0,r}^{(n)} \epsilon^r = 1 + \sum_{n=1}^{m+1} \alpha^n \sum_{r=-n}^{\epsilon_{\max}} g_{0,r}^{(n)} \epsilon^r. \end{aligned}$$

As explained above Eq.(4.18), if we use  $\epsilon_{\max} = -1$ , the quantity  $Z$  represents the MS (not MS-bar) counterterm, even though  $G_{\mathcal{R}}$  in that case is the MS-bar renormalized Green function. In any case, the renormalized Green function to order  $m+1$  reads

$$\begin{aligned} G_{\mathcal{R}}^{(m+1)}(\alpha, \epsilon, x) &= \sum_{n=1}^{m+1} \alpha^n \sum_{u=0}^n x^{-u\epsilon} \sum_{r=-n}^{\infty} g_{u,r}^{(n)} \epsilon^r \\ &= Z^{(m+1)}(\alpha, \epsilon) + \sum_{n=1}^{m+1} \alpha^n \sum_{t=1}^n x^{-t\epsilon} \sum_{r=-n}^{\infty} g_{t,r}^{(n)} \epsilon^r. \end{aligned} \quad (4.22)$$

Algebraically, our algorithm of solving the DSE can be understood as iterated matrix products, compare [10].

### Example 112: Multiedge linear DSE in MOM, coefficients.

Consider the linear DSE,  $w = 0$ , of the 1-loop multiedge in  $D = 4 - 2\epsilon$  dimensions and MOM renormalization. The 1-order solution is Example 111. At two loops, the coefficients  $g_{2,j}^{(2)}$  appear for the first time:

$$\begin{aligned} g_{2,-2}^{(2)} &= \frac{1}{2} & g_{2,-1}^{(2)} &= \frac{5}{2}, & g_{2,0}^{(2)} &= \frac{19}{2} - \frac{\pi^2}{12}, & g_{2,1}^{(2)} &= \frac{65}{2} - \frac{5\pi^2}{12} - \frac{16\zeta(3)}{3}, \\ g_{1,-2}^{(2)} &= -1 & g_{1,-1}^{(2)} &= -4, & g_{1,0}^{(2)} &= -12 + \frac{\pi^2}{6}, & g_{1,1}^{(2)} &= -32 + \frac{2\pi^2}{3} + \frac{14\zeta(3)}{3}, \\ g_{0,-2}^{(2)} &= \frac{1}{2} & g_{0,-1}^{(2)} &= \frac{3}{2}, & g_{0,0}^{(2)} &= \frac{5}{2} - \frac{\pi^2}{12}, & g_{0,1}^{(2)} &= -\frac{1}{2} - \frac{\pi^2}{4} + \frac{2\zeta(3)}{3}. \end{aligned}$$

### Example 113: Multiedge nonlinear DSE in MOM, coefficients.

Consider the same situation as in Example 112, but this time a non-linear DSE with  $w = 3$ . The order one solution stays the same, but at two loops we find

$$\begin{aligned} g_{2,-2}^{(2)} &= 2g_{1,-1}^{(2)} = 10, & g_{2,0}^{(2)} &= 38 - \frac{\pi^2}{3}, & g_{2,1}^{(2)} &= 130 - \frac{5\pi^2}{3} - \frac{64\zeta(3)}{3}, \\ g_{1,-2}^{(2)} &= -4g_{1,-1}^{(2)} = -16, & g_{1,0}^{(2)} &= -48 + \frac{2\pi^2}{3}, & g_{1,1}^{(2)} &= -128 + \frac{8\pi^2}{3} + \frac{56\zeta(3)}{3}, \\ g_{0,-2}^{(2)} &= 2g_{0,-1}^{(2)} = 6, & g_{0,0}^{(2)} &= 10 - \frac{\pi^2}{3}, & g_{0,1}^{(2)} &= -2 - \pi^2 + \frac{8\zeta(3)}{3}. \end{aligned}$$

### Example 114: Multiedge nonlinear DSE in MS, coefficients.

Consider the same DSE with  $w = 3$ , but this time in MS-bar renormalization, as introduced in Example 111. The coefficients of the second order solution are

$$\begin{aligned} g_{2,-2}^{(2)} &= 2 & g_{1,-1}^{(2)} &= 10, & g_{2,0}^{(2)} &= 38 - \frac{\pi^2}{3}, & g_{2,1}^{(2)} &= 130 - \frac{5\pi^2}{3} - \frac{64\zeta(3)}{3}, \\ g_{1,-2}^{(2)} &= -4 & g_{1,-1}^{(2)} &= -8, & g_{1,0}^{(2)} &= -16 + \frac{\pi^2}{3}, & g_{1,1}^{(2)} &= -32 + \frac{2\pi^2}{3} + \frac{28\zeta(3)}{3}, \\ g_{0,-2}^{(2)} &= 2 & g_{0,-1}^{(2)} &= -2, & g_{0,0}^{(2)} &= 0 & g_{0,1}^{(2)} &= 0. \end{aligned}$$

We emphasize that the “highest order”, the coefficients  $g_{n,r}^{(n)}$ , coincide between MS and MOM. This is a consequence of (or rather reason for) Theorem 58.

### 4.2.3 Expansions of the Renormalized Green Function

The all-order perturbative solution  $G_{\mathcal{R}}(\alpha, \epsilon, x)$  of Eq.(4.7) is defined as the limit  $m \rightarrow \infty$  in Eq.(4.22), effectively it is an infinite sum over the orders  $\alpha^m$  in the coupling. But the form Eq.(4.22) is not yet practically useful because it contains pole terms, which only cancel if all summands of a given order are included. We can expose the log-expansion (Eq.(3.2)), with the identification of the logarithmic scale  $L = \ln x$  (Eq.(4.18) and Definition 101), by expanding

$$x^{-t\epsilon} = e^{-Lt\epsilon} = 1 - t\epsilon L + \frac{1}{2}t\epsilon^2 L^2 \mp \dots$$

Reordering Eq.(4.22), we obtain

$$G_{\mathcal{R}}(\alpha, \epsilon, x) = Z(\alpha, \epsilon) + \sum_{k=0}^{\infty} L^k \sum_{t=1}^{\infty} \frac{(-t)^k}{k!} \sum_{n=t}^{\infty} \alpha^n \sum_{r=-n}^{\infty} g_{t,r}^{(n)} \epsilon^{k+r}. \quad (4.23)$$

From this, we read off the expansion functions

$$\gamma_k(\alpha, \epsilon) = \sum_{t=1}^{\infty} \frac{(-t)^k}{k!} \sum_{n=t}^{\infty} \alpha^n \sum_{r=-n}^{\infty} g_{t,r}^{(n)} \epsilon^{k+r}, \quad (4.24)$$

especially, the limit  $\gamma_k(\alpha, \epsilon = 0) =: \gamma_k(\alpha)$  is

$$\gamma_k(\alpha) = \sum_{t=1}^{\infty} \frac{(-t)^k}{k!} \sum_{n=t}^{\infty} \alpha^n g_{t,-k}^{(n)}, \quad \gamma_1(\alpha) = - \sum_{t=1}^{\infty} t \sum_{n=t}^{\infty} \alpha^n g_{t,-1}^{(n)}. \quad (4.25)$$

#### Example 115: Multiedge linear DSE, anomalous dimension.

Consider the DSE from Example 112. In MOM,  $\gamma_0(\alpha, \epsilon) = 1$  and we find

$$\begin{aligned} \gamma_1(\alpha, \epsilon) &= \alpha - \alpha^2 + 2\alpha^3 - 5\alpha^4 + 14\alpha^5 - 42\alpha^6 + 132\alpha^7 \mp \dots \\ &\quad + (2\alpha - 7\alpha^2 + (26 - 2\zeta(3))\alpha^3 + (-99 + 8\zeta(3))\alpha^4 + \dots)\epsilon + \mathcal{O}(\epsilon^2). \end{aligned}$$

The  $[\epsilon^0]$ - part of  $\gamma_1$  is indeed the anomalous dimension known from Example 105,

$$\gamma(\alpha) = \gamma_1(\alpha) = \frac{\sqrt{1+4\alpha}-1}{2} = - \sum_{n=1}^{\infty} (-1)^n C_{n-1} \alpha^n.$$

The  $[\epsilon^1]$ -part coincides with our analytic calculation in Example 107.

**Example 116: Multiedge nonlinear DSE, expansion functions.**

The DSE with  $w = 3$  in MOM results in

$$\gamma_1(\alpha, \epsilon) = \alpha - 4\alpha^2 + 44\alpha^3 \mp \dots + (2\alpha - 28\alpha^2 + (572 - 56\zeta(3))\alpha^3 + \dots)\epsilon + \mathcal{O}(\epsilon^2).$$

In MS-bar, for  $w = 3$ , we find

$$\begin{aligned}\gamma_0(\alpha, \epsilon) &= 1 - 2\alpha + 22\alpha^2 \pm \dots + \\ &\left( \left( -4 + \frac{\pi^2}{12} \right) \alpha + (98 - \pi^2 - 12\zeta(3))\alpha^2 \mp \dots \right) \epsilon + \mathcal{O}(\epsilon^2), \\ \gamma_1(\alpha, \epsilon) &= \alpha - 12\alpha^2 + 212\alpha^3 \mp \dots + \left( 2\alpha + \left( -60 + \frac{\pi^2}{3} \right) \alpha^2 \mp \dots \right) \epsilon + \mathcal{O}(\epsilon^2).\end{aligned}$$

**Example 117: Multiedge linear DSE, constant term in MS.**

In MS-bar, the function  $\gamma_0(\alpha, \epsilon)$  is not fixed by renormalization conditions. An explicit calculation for the linear DSE in  $D = 4 - 2\epsilon$ , using Example 4.25, results in

$$\begin{aligned}\gamma_0(\alpha, \epsilon) &= 1 - 2\alpha + \frac{11}{2}\alpha^2 + \left( -17 + \frac{2\zeta(3)}{3} \right) \alpha^3 + \left( \frac{447}{8} - \frac{10\zeta(3)}{3} \right) \alpha^4 + \dots \\ &+ \left( \left( -4 + \frac{\pi^2}{12} \right) \alpha + \left( \frac{49}{2} - \frac{\pi^2}{4} - 3\zeta(3) \right) \alpha^2 + \dots \right) \epsilon + \mathcal{O}(\epsilon^2).\end{aligned}$$

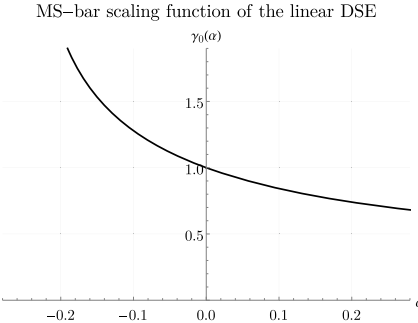
Using the coefficients up to order  $\alpha^{25}$  and the series-lookup function of the OEIS [11], one discovers a closed formula for  $[\epsilon^0]\gamma_0$ . Firstly, laborious experimentation results in

$$\begin{aligned}\ln \gamma_0 - \ln \left( \frac{\sqrt{1+4\alpha} - 1}{2\alpha(1+4\alpha)^{\frac{1}{4}}} \right) &= \zeta(3) \left( 2\frac{\alpha^3}{3} - 8\frac{\alpha^4}{4} + 30\frac{\alpha^5}{5} - 112\frac{\alpha^6}{6} + 420\frac{\alpha^7}{7} \mp \dots \right) \\ &+ \zeta(5) \left( 2\frac{\alpha^5}{5} - 12\frac{\alpha^6}{6} + 56\frac{\alpha^7}{7} - 240\frac{\alpha^8}{8} \pm \dots \right) + \zeta(7) \dots.\end{aligned}$$

The coefficients of  $\frac{\alpha^{j+m-1}}{j+m-1}$  in the term proportional to  $\zeta(m)$  are, as has been checked empirically to order  $\alpha^{25}$ , given by the binomial coefficient  $2\binom{2j+m-3}{j-1}$ . We assume that this holds universally, then all series over  $\alpha$  and then the remaining series in  $\zeta(m)$  can be summed explicitly. The end result for  $[\epsilon^0]\gamma_0$  is

$$\gamma_0(\alpha) = e^{\gamma_E(1-\sqrt{1+4\alpha})} \frac{\sqrt{1+4\alpha}-1}{2\alpha(1+4\alpha)^{\frac{1}{4}}} \frac{\Gamma(\frac{3}{2}-\frac{1}{2}\sqrt{1+4\alpha})}{\Gamma(\frac{1}{2}+\frac{1}{2}\sqrt{1+4\alpha})} = \frac{\gamma}{\alpha} \sqrt{\frac{d\gamma}{d\alpha}} e^{-2\gamma\gamma_E} \frac{\Gamma(1-\gamma)}{\Gamma(1+\gamma)}.$$

In this equation,  $\gamma \equiv \gamma(\alpha)$  is the anomalous dimension from Example 115. We note at this point that such a fraction of gamma functions is common in the computation of multiedge Feynman graphs, compare for example [12]. Indeed, we will understand its precise relation to the multiedge amplitude (Example 25) in Theorem 70.



Compare also [3] for similar and additional figures.

### Example 118: Multiedge linear DSE, $D=6$ , constant term.

In a very similar fashion to Example 117, one finds empirically for the linear multiedge DSE in  $D = 6$  dimensions the following functions:

$$\begin{aligned}\gamma(\alpha) &= \frac{\sqrt{5+4\sqrt{1+\alpha}}-3}{2}, \\ \gamma_0(\alpha) &= \frac{6\gamma}{\alpha} \sqrt{\frac{d(6\gamma)}{d\alpha}} e^{\gamma(1-2\gamma_E)} \frac{\Gamma(1-\gamma)}{\Gamma(1+\gamma)}.\end{aligned}$$

The anomalous dimension coincides with the expression quoted in Example 105, derived from Theorem 47.

### Example 119: Toy model linear DSE, constant term.

For the linear DSE of the toy model (Example 103), empirical calculation results in the tentative formula

$$\gamma_0(\alpha) = 1 + \left(\frac{\pi^2\alpha^2}{4}\right) + \frac{5}{2} \left(\frac{\pi^2\alpha^2}{4}\right)^2 + \dots = (1 - \pi^2\alpha^2)^{-\frac{1}{4}} = \sqrt{\frac{d\gamma}{d\alpha}}.$$

Here,  $\gamma = -\frac{1}{\pi} \arcsin(\pi\alpha)$  is the anomalous dimension from Example 103.

For simple kernels such as the ones introduced in Sect. 4.2.1, we can typically reach orders  $\sim \alpha^{20}$  with a few hours computation time in Wolfram Mathematica. For computing the anomalous dimension in MOM, the analytic methods introduced in Sect. 3.3 are tremendously more efficient: A power-series solution to the ODE in Theorem 47 for the 1-loop multiedge in  $D = 4$  dimensions can be obtained to hundreds of orders within minutes.

Nonetheless, the present brute-force algorithm for solving the DSE has two benefits. Firstly, it allows a seamless computation of the full  $\epsilon$ -dependence of all quantities, especially also the counterterms, and secondly, it is not restricted to the MOM scheme. Therefore, it is indispensable to verify our theoretical study of “exotic” cases in the renormalization group.

### Example 120: Multiedge linear DSE, MS counterterm.

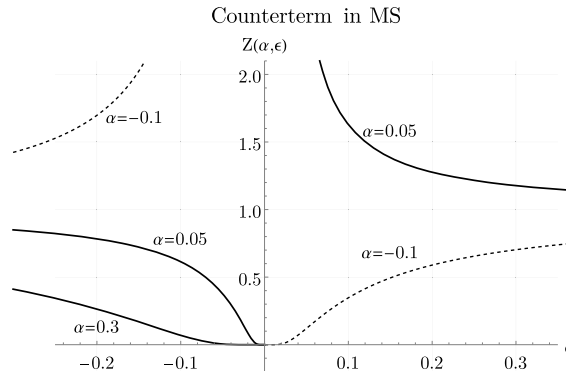
Our calculation (up to order  $\alpha^{25}$ ) delivers for the counterterm in MS the series coefficients

$$\ln \hat{Z}(\alpha, \epsilon) = \frac{1}{\epsilon} \left( \alpha - \frac{\alpha^2}{2} + 2 \frac{\alpha^3}{3} - 5 \frac{\alpha^4}{4} + 14 \frac{\alpha^5}{5} - 42 \frac{\alpha^6}{6} \pm \dots \right).$$

Once more, we recognize the Catalan numbers and introduce  $\gamma = \gamma(\alpha) = \frac{1}{2} (\sqrt{1+4\alpha} - 1)$  from Example 115, which for  $\epsilon = 0$  is the anomalous dimension both in MS and in MOM (Theorem 58). The counterterm is indeed the integral of  $\gamma(\alpha)$ , as expected from Theorem 51:

$$\hat{Z}(\alpha, \epsilon) = \exp \left( -\frac{1}{\epsilon} \sum_{n=1}^{\infty} (-1)^n C_{n-1} \frac{\alpha^n}{n} \right) = \left( \frac{e^{2\gamma}}{1+\gamma} \right)^{\frac{1}{\epsilon}} = e^{\frac{1}{\epsilon} \int_0^{\alpha} \frac{du}{u} \gamma(u)}. \quad (4.26)$$

Technically,  $\hat{Z}(\alpha, \epsilon)$  is a transseries (Definition 59) in  $\epsilon$ .



Compare also [3] for similar figures.

As long as  $\alpha$  and  $\epsilon$  have opposite signs, this function has the limit  $\hat{Z}(\alpha, 0_+) = 0$  when  $\epsilon \rightarrow 0$ , see the figure. Compared to its perturbative expansion, where every single term diverges as  $\epsilon \rightarrow 0$ , the resummed counterterm shown in Eq. (4.26) is a remarkably well-behaved function of  $\epsilon$ . This is in line with [13] and a comment made in [14]: The all-order-solution Example 115 “regulates itself” by its anomalous dimension, and the DSE (Eq. (4.7)) does not contain a non-trivial counterterm at all. Compare the discussion at the end of Sect. 3.2.3.

#### 4.2.4 Exact Solutions of the Toy Model

Using the algorithm described above, one can solve the toy model DSE (Example 103) for various values of  $w$ . In general, the results show the expected behavior, but we made two curious observations which are worth mentioning.

Firstly, using kinematic renormalization and  $w = -\frac{1}{2}$ , the perturbative anomalous dimension turns out to be  $\gamma(\alpha) = -\alpha + \mathcal{O}(\epsilon)$ . This result was verified up to order  $\alpha^{500}$  using Theorem 47. We therefore assume that it holds to all orders in  $\alpha$ , which means that for  $w = -\frac{1}{2}$ , the non-linear toy model DSE has a perturbative solution comparable to the non-recursive DSE ( $w = -1$ ). Indeed,  $w = -1$  corresponds to an anomalous dimension  $\gamma(\alpha) = -\alpha$ , where we have rescaled  $\frac{6\alpha}{\pi^2} \rightarrow \alpha$  to eliminate trivial factors. Let  $L := \ln x$ , then the non-recursive DSE (Example 103) gives rise to the Callan–Symanzik equation (Theorem 41)

$$\frac{\partial}{\partial L} G_{\mathcal{R}}(\alpha, L) = \gamma(\alpha) \left( 1 + w\alpha \cdot \frac{\partial}{\partial \alpha} \right) G_{\mathcal{R}}(\alpha, L) = -\alpha G_{\mathcal{R}}(\alpha, L) + \alpha^2 \frac{\partial}{\partial \alpha} G_{\mathcal{R}}(\alpha, L).$$

The general solution of this partial differential equation is

$$G_{\mathcal{R}}(\alpha, L) = \alpha F_{-1} \left( L - \frac{1}{\alpha} \right),$$

where  $F_{-1}$  is an arbitrary function. The requirement  $\partial_L G_{\mathcal{R}}|_{L=0} = \gamma(\alpha) = -\alpha$  and the boundary condition  $G(\alpha, 0) = 1$  fix  $F_{-1}(u) = -u$ .

Although the anomalous dimension  $\gamma(\alpha) = -\alpha$  of  $w = -1$  coincides with the (supposed) one at  $w = -\frac{1}{2}$ , the latter gives rise to a slightly different Callan–Symanzik equation, namely

$$\frac{\partial}{\partial L} G_{\mathcal{R}}(\alpha, L) = -\alpha G_{\mathcal{R}}(\alpha, L) + \frac{1}{2} \alpha^2 \frac{\partial}{\partial \alpha} G_{\mathcal{R}}(\alpha, L).$$

This time, the general solution is

$$G_{\mathcal{R}}(\alpha, L) = \alpha^2 F_{-\frac{1}{2}} \left( L - \frac{2}{\alpha} \right).$$

The condition  $G_{\mathcal{R}}(\alpha, 0) = 1$  translates to  $F_{-\frac{1}{2}}(u) = \frac{1}{4}u^2$  and we find

$$G_{\mathcal{R}}(\alpha, L) = \frac{1}{4}\alpha^2 L^2 - \alpha L + 1. \quad (4.27)$$

At least within perturbation theory, Eq. (4.27) represents an *exact* solution of a non-linear DSE. The same DSE with  $w = -\frac{1}{2}$  in Minimal Subtraction (Definition 110) gives rise to an anomalous dimension which seems to be a factorially divergent power series, and has no simple polynomial solution  $\hat{G}_{\mathcal{R}}$ .

The phenomenon occurs in reverse direction if we choose  $w = -2$ . In Minimal Subtraction, we find  $\hat{\gamma}(\alpha) = -\alpha$  at least up to order  $\alpha^{18}$ . By Theorem 56, the latter is true even for  $\epsilon \neq 0$ . Assume again that  $\hat{\gamma}(\alpha) = -\alpha$  holds to all orders of  $\alpha$ , then the Callan–Symanzik equation (Theorem 41) reads

$$\frac{\partial}{\partial L} G_{\hat{\mathcal{R}}}(\alpha, \epsilon, L) = -\alpha G_{\hat{\mathcal{R}}}(\alpha, \epsilon, L) + 2\alpha^2 \frac{\partial}{\partial \alpha} G_{\hat{\mathcal{R}}}(\alpha, \epsilon, L).$$

In MS, the Green function does not satisfy some simple boundary condition, therefore we can not derive an exact solution for  $G_{\hat{\mathcal{R}}}$  from this differential equation. The MOM anomalous dimension for  $w = -2$  is factorially divergent as its Stokes constant does not vanish (Table 3.4).

It is unclear whether the toy model contains any concrete physical information, but nevertheless, the observations in this subsection serve as an example for how different renormalization conditions can give rise to qualitative different analytic features of the solution of the same DSE. As we shall see in Theorem 59, these solutions are physically equivalent, but, owing to renormalization of the coupling constant, they are expressed in terms of expansion parameters which are related non-linearly and therefore the corresponding series can look truly different. Concretely, the shift between MOM and MS can transform a factorially divergent power series (Definition 60) into a trivial polynomial  $\hat{\gamma}(\alpha) = -\alpha$ .

### Summary of Sect. 4.2.

1. We consider propagator-type DSEs where the series expansion of the Mellin transform of the kernel is assumed to be known (Sect. 4.2.1).
2. Starting from the treelevel  $G_{\mathcal{R}}^{(1)} = 1$ , the DSE can be solved order by order by algebraic operations on the Mellin coefficients. MOM and MS renormalization conditions can be implemented easily (Sect. 4.2.2).
3. The resulting Green function is a triple series in  $\alpha$ ,  $\epsilon$  and  $L$ . The expansion functions  $\gamma_j(\alpha, \epsilon)$  or the counterterm  $Z(\alpha, \epsilon)$  can be obtained by reordering the series (Sect. 4.2.3).
4. The non-linear DSE of the toy model seems to have simple perturbative solutions in two particular cases. This is an example for the fact that different renormalization conditions can give rise to qualitatively different perturbative solutions (Sect. 4.2.4).

## 4.3 Shifted Kinematic Renormalization Point

We have examined non-kinematic renormalization schemes already in Sect. 4.1. In the present section, we extend the previous analysis in two respects:

1. We consider the full  $\epsilon$ -dependence of all quantities in dimensional regularization.
2. In Theorem 50, non-kinematic renormalization schemes were expressed in terms of the quantity  $\tau[\Gamma] = G_{\mathcal{R}'}(L = 0) = \gamma'_0(\alpha)$ . In the present section, we instead take the value  $\delta$  as the primary object, defined as  $L = -\delta \neq 0$ , where  $G_{\mathcal{R}'}(L = -\delta) = 1$ .

### 4.3.1 Shifted Green Function

By Theorem 50, a non-kinematic Green function  $G_{\mathcal{R}'}$  has the value  $G_{\mathcal{R}'}(L) = 1$  not at the point  $L = 0$ , but at some point  $\delta$ . Instead of knowing the amplitude at  $L = 0$ , given by  $\tau$  (Definition 111), one can also ask at which point  $L = -\delta$  the Green function is unity. In practice, the latter is often more physically sensible because, to limited order in perturbation theory, we expect our results to be accurate as long as the quantum corrections ( $G_{\mathcal{R}'} - 1$ ) are small. Consequently, a non-kinematic Green function will be reliable in the vicinity of  $L = -\delta$ , and not necessarily for small  $L$  [15, 16]. The set up is shown in Fig. 4.2.

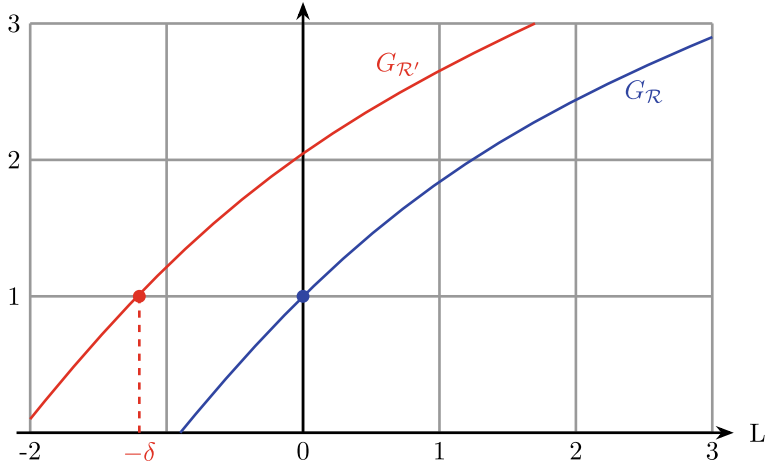


**Fig. 4.2** Sketch of a Green function in MOM with renormalization point  $L = 0$  (blue) and in shifted MOM according to Definition 113 with  $\delta = 1.2$  (red), both for the same value of the coupling. See [3] for similar figures

**Definition 113.** Let  $L = \ln \frac{s}{s_0}$  be the logarithmic scale (Definition 101) and let  $\delta(\alpha, \epsilon)$  be a power series (Definition 53) in  $\alpha$  and  $\epsilon$ , regular at the origin. Let  $\mathcal{F}_R$  be the Feynman amplitude in kinematic renormalization (Definition 93) with renormalization point  $L = 0$ . The *shifted kinematic renormalization scheme*  $\mathcal{F}_{R'}(L)$  is defined by the renormalization condition

$$\mathcal{F}_{R'}(-\delta) \stackrel{!}{=} \tilde{\mathbb{1}} = \mathcal{F}_R(0).$$

**Theorem 59.** Let  $G_{R'}$  be a renormalized Green function in any renormalization scheme (Definition 99), which is a solution of a DSE. Let  $\tau$  (Definition 111) be the extraction of the value at  $L = 0$  in  $R'$ , and let  $\sigma = \partial_L|_{L=0}$  be the infinitesimal Feynman rule in MOM (Definition 102). Then,  $G_{R'}$  is the Green function (of the same DSE) in a shifted kinematic scheme (Definition 113), provided the equation

$$\tau = \exp^*(\delta \cdot \sigma)$$

can be satisfied with some power series  $\delta(\alpha, \epsilon) \in \mathbb{R}[[\alpha, \epsilon]]$  (Definition 53).

**Proof** With Definition 113,  $\mathcal{F}_{\mathcal{R}'}(0) = \mathcal{F}_{\mathcal{R}}(\delta)$  is not unity. We can extract the value with the operator  $\tau$  from Definition 111. On the other hand,  $\mathcal{F}_{\mathcal{R}}(\delta)$  is given by the ordinary exponential formula Definition 102. Consequently, the relation between  $\tau$  and  $\delta$  must be the one claimed above, and if it is, then  $\mathcal{F}_{\mathcal{R}'}(L + \delta) = \mathcal{F}_{\mathcal{R}}(L)$ .  $\square$

In perturbation theory, the condition of Theorem 59 can certainly be fulfilled: The operator  $\tau$ , applied to a combinatorial Green function (Definition 47), results in a formal power series in  $\alpha$  with finite coefficients as  $\epsilon \rightarrow 0$ . Then,  $\delta$  can be obtained by taking the combinatorial logarithm of this series. Algebraically, this is realized by the Dynkin operator Definition 81, but one can understand its mechanism also by solving a DSE order by order as in Sect. 4.2: At every new order, the Green function contains a higher power in  $L$ , and by shifting  $L \rightarrow L + \delta$ , one can always add a new free constant to adjust the absolute value. We will derive concrete algorithms to find  $\delta$  in Sect. 4.4.

### Example 121: Multiedge DSE, manually computing the shift.

Consider the multiedge DSE in  $D = 4 - 2\epsilon$  from Example 111. The first-order solution is simply the kernel graph, in MOM it reads

$$G_{\mathcal{R}}(\alpha, \epsilon, L) = 1 + \alpha L + \mathcal{O}(\epsilon).$$

We use MS as an example of a non-kinematic renormalization scheme. In MS, the solution is

$$G_{\mathcal{R}'}(\alpha, \epsilon, L) = 1 + \alpha(L - 2) + \mathcal{O}(\epsilon).$$

Both Green functions are solutions to the same DSE, so by Theorem 59, it should be possible to find a shift  $\delta$  such that the MS-solution is a shifted kinematic scheme. That is, by Definition 113, we want  $G_{\mathcal{R}'}(-\delta) = 1$ . Indeed, we can read off this value from the explicit solutions:  $G_{\mathcal{R}'}(\alpha, \epsilon, 2) = 1 + \mathcal{O}(\epsilon)$ , therefore,

$$\delta = -2 + \mathcal{O}(\epsilon) + \mathcal{O}(\alpha).$$

The extension of this “brute force algorithm” to higher orders in  $\alpha$  and  $\epsilon$  will be described in Sect. 4.4.2

There are two rather philosophical obstacles to the relation between  $\sigma$  and  $\tau$  in Theorem 59:

1. If  $\sigma[\Gamma] = 0$ , then the right hand side is unity. If  $G_{\mathcal{R}}$  is taken to be  $\mathcal{Q}_{\mathcal{R}}$ , then this case amounts to a fixed-point of the renormalization group. Moreover, this obstacle can arise in an empty DSE, that is, in a theory without any quantum corrections. The classification of such cases in full generality is rather complicated since a theory might have multiple beta functions, vanishing at different points. Geometrically, this case is simple to visualize:  $\sigma$  computes the derivative of  $G_{\mathcal{R}}$ , and if this value

is zero somewhere then  $G_{\mathcal{R}}$  can potentially have an absolute extreme value at that point and thus be not surjective. If in that case  $\gamma'_0$  is outside of the values of  $G_{\mathcal{R}}$ , then no shift can be found to relate  $G_{\mathcal{R}}$  and  $G_{\mathcal{R}'}$ . Phrased differently: To find a shift, it is necessary that  $G_{\mathcal{R}'}$  is unity *somewhere*, and the non-vanishing of the anomalous dimension and beta function guarantees that  $G_{\mathcal{R}'}$  is monotonic and thus surjective.

2. Beyond perturbation theory, the operators  $\sigma, \tau$  can, in principle, give rise to arbitrary functions with unknown analytic properties. In that case, we can not trivially resort to the combinatorial logarithm to solve for  $\delta$ .

Both points will be irrelevant for the rest of the thesis because we only consider reasonably well-behaved DSEs in perturbation theory. There is, however, one very relevant caveat to the shift between renormalization schemes: Theorem 59 requires both Green functions to be solutions of the same combinatorial DSE. If the underlying graphs do not satisfy a DSE at all, then the exponential formula (Definition 102) does not hold to start with and, in general, it is impossible to find a  $\delta(\alpha, \epsilon)$  to relate the schemes. The chain approximation (Sect. 4.5.4) is an example for the latter problem.

Before we turn to concrete algorithms for computing  $\delta$ , we will first examine some general properties of the shifted scheme (Definition 113).

### 4.3.2 Shifted Counterterms

**Definition 114.** Let  $\delta(\alpha, \epsilon)$  be the shifted renormalization point from Definition 113 and  $\mathcal{Q}_{\mathcal{R}'}$  be the invariant charge (Definition 95) in the shifted theory. We define two *shifted couplings*  $\alpha'$  and  $\tilde{\alpha}$  in analogy to Definitions 104, 107 and 106:

$$\begin{aligned}\alpha'(\alpha, \epsilon) &:= \alpha e^{-\epsilon\delta(\alpha, \epsilon)}, & \mathcal{Q}_0(\alpha, \epsilon) &:= \mathcal{Q}_{\mathcal{R}'}(\alpha, \epsilon, 0) \\ \tilde{\alpha}(\alpha, \epsilon) &:= \alpha'(\alpha, \epsilon) \cdot \mathcal{Q}_0(\alpha, \epsilon) = \alpha e^{-\epsilon\delta(\alpha, \epsilon)} \mathcal{Q}_{\mathcal{R}'}(\alpha, \epsilon, 0).\end{aligned}$$

In the special case of  $\mathcal{Q}_{\mathcal{R}} = \mathbb{1}$  (linear DSE), the shifted couplings coincide,  $\alpha' = \tilde{\alpha}$ . Observe that all series in Definition 114 start with a linear term in the coupling, therefore, using series reversion (Theorem 19) and concatenation (Theorem 20), one can compute the transformations between any pair of the three couplings  $\{\alpha, \alpha', \tilde{\alpha}\}$ . We will often indicate the dependence of functions by the corresponding decoration, for example  $\tilde{\mathcal{Q}}_0(\tilde{\alpha}, \epsilon) := \mathcal{Q}_0(\alpha(\tilde{\alpha}), \epsilon)$  and  $\mathcal{Q}'_0(\alpha', \epsilon) := \mathcal{Q}_0(\alpha(\alpha'), \epsilon)$ .

**Lemma 60.** Let  $G_{\mathcal{R}'}$  be a solution of a DSE in shifted kinematic renormalization (Definition 113). Then

$$G_{\mathcal{R}'}(\alpha, \epsilon, L) = G_{\mathcal{R}'}(\alpha, \epsilon, 0) \cdot G_{\mathcal{R}}(\tilde{\alpha}(\alpha, \epsilon, \delta), \epsilon, L). \quad (4.28)$$

**Proof** For the analytic Green function, the renormalization condition Definition 113 is

$$G_{\mathcal{R}'}(\alpha, \epsilon, L) = G_{\mathcal{R}}(\alpha, \epsilon, L + \delta). \quad (4.29)$$

The right hand side is known from Lemma 40.  $\square$

The behavior of counterterms under a change of renormalization point is in principle straightforward from their definition, but great care is required regarding which quantity is a function of which variable. For clarity, we restrict ourselves to a theory with only a single Green function  $G_{\mathcal{R}}$  and two  $Z$ -factors,  $Z_\alpha$  for the coupling and  $Z_G$  for  $G_{\mathcal{R}}$ . The renormalized Green function  $G_{\mathcal{R}}$  in MOM (Definition 93) is related to the unrenormalized one via Definitions 106 and Eq. 3.25,

$$G_{\mathcal{R}}(\alpha, \epsilon, L) = Z_G(\alpha, \epsilon) \cdot G(\alpha Z_\alpha(\alpha, \epsilon), \epsilon, L). \quad (4.30)$$

Firstly, we consider a linear Dyson–Schwinger equation, that is, the invariant charge (Definition 94) is  $Q = 1$  and consequently  $Z_\alpha = 1$ , and Eq. (4.30) becomes

$$G_{\mathcal{R}}(\alpha, \epsilon, L) = Z_G(\alpha, \epsilon) G(\alpha, \epsilon, L). \quad (4.31)$$

By Definition 114,  $\tilde{\alpha}(\alpha, \epsilon) = \alpha'(\alpha, \epsilon)$  for a linear DSE. Let

$$\gamma'_0(\alpha, \epsilon) := G_{\mathcal{R}'}(\alpha, \epsilon, 0) = G_{\mathcal{R}}(\alpha, \epsilon, L = \delta(\alpha, \epsilon)). \quad (4.32)$$

Combining Lemma 60 and Eq. (4.31), the shifted Green function is

$$\begin{aligned} G_{\mathcal{R}'}(\alpha, \epsilon, L) &= \gamma'_0(\alpha, \epsilon) \cdot G_{\mathcal{R}}(\alpha'(\alpha, \epsilon), \epsilon, L) \\ &= \gamma'_0(\alpha, \epsilon) \cdot Z_G(\alpha'(\alpha, \epsilon), \epsilon) \cdot G(\alpha'(\alpha, \epsilon), \epsilon, L). \end{aligned} \quad (4.33)$$

Naively, from Definition 106, we expect the form

$$G_{\mathcal{R}'}(\alpha, \epsilon, L) \stackrel{?}{=} Z'_G(\alpha, \epsilon) G(\alpha Z'_\alpha(\alpha, \epsilon), \epsilon, L). \quad (4.34)$$

This would mean that  $\alpha Z'_\alpha \stackrel{?}{=} \alpha' = \alpha e^{-\epsilon\delta}$ . In other words, with the definition Eq. (4.34), the solution of a linear Dyson–Schwinger equation obtains a non-

vanishing coupling counterterm  $Z'_\alpha \stackrel{?}{=} e^{-\epsilon\delta}$ . This is not only “unintuitive”, but it also violates equations such as  $Z_\alpha = Z_G^w$ , which would otherwise guarantee that  $Z_\alpha = 1$  if  $w = 0$ . We therefore *decide* that  $\alpha'$  is the proper variable for  $G_{\mathcal{R}'}$ , so that in Eq.(4.33), no  $Z_\alpha$  is necessary. We stress that this is a choice, not a theorem. Essentially, it is the same choice that we commented on below Definition 106 for factoring  $s_0^\epsilon$  out of the definition of  $Z_\alpha$ . We absorb  $e^{-\epsilon\delta}$  into the definition of the coupling  $\alpha'$  in the same way that we absorbed  $s_0^\epsilon$  into  $\alpha$  in Eq.(3.23). With this understanding, we define

$$\begin{aligned} G'_{\mathcal{R}}(\alpha', \epsilon, L) &:= G_{\mathcal{R}'}(\alpha(\alpha', \epsilon), \epsilon, L) \\ \gamma'_0(\alpha', \epsilon) &:= G'_{\mathcal{R}}(\alpha', \epsilon, 0) = \gamma_0(\alpha(\alpha', \epsilon), \epsilon). \end{aligned} \quad (4.35)$$

**Definition 115.** Let  $\mathcal{R}'$  be a shifted kinematic renormalization scheme (Definition 113). We take the shifted coupling  $\alpha'$  from Definition 114 as a natural variable and define the *shifted counterterms*  $Z'_G(\alpha', \epsilon)$ ,  $Z'_\alpha(\alpha', \epsilon)$  by the relation

$$G'_{\mathcal{R}}(\alpha', \epsilon, L) =: Z'_G(\alpha', \epsilon) \cdot G(\alpha' Z'_\alpha(\alpha', \epsilon), \epsilon, L).$$

The counterterms for the linear DSE can now be read off from comparing Eq.(4.33) and Definition 115:

$$\begin{aligned} Z'_\alpha(\alpha', \epsilon) &= 1, \\ Z'_G(\alpha', \epsilon) &= \gamma'_0(\alpha', \epsilon) Z_G(\alpha', \epsilon). \end{aligned} \quad (4.36)$$

In the second equation, we insert  $\alpha'$  as a variable into  $Z_G$ , without any implicit transformation  $\alpha(\alpha')$ .

### Example 122: Multiedge linear DSE, shifted counterterm.

Consider the linear multiedge DSE from Example 120. We introduce a shift  $\delta = -3$ . Equation 4.35 then takes the form

$$\begin{aligned} \gamma'_0(\alpha', \epsilon) &= 1 - 3\alpha' + \frac{15}{2}\alpha'^2 - \frac{39}{2}\alpha'^3 + \frac{435}{8}\alpha'^4 - \frac{6441}{40}\alpha'^5 + \dots \\ &\quad + \left( -\frac{3}{2}\alpha' + \frac{33}{2}\alpha'^2 + \left( -\frac{393}{4} + 6\zeta(3) \right)\alpha'^3 + \dots \right) \epsilon + \mathcal{O}(\epsilon^2). \end{aligned}$$

According to Eq.(4.36), the shifted counterterm is

$$\ln Z'_G(\alpha', \epsilon) = \left( \alpha' - \frac{\alpha'^2}{2} + 2\frac{\alpha'^3}{3} - 5\frac{\alpha'^4}{4} + 14\frac{\alpha'^5}{5} \mp \dots \right) \frac{1}{\epsilon}$$

$$- \alpha' - \frac{1}{2}\alpha'^2 + \left( \frac{8}{3} - \frac{2}{3}\zeta(3) \right) \alpha'^3 + \left( -\frac{39}{4} + 2\zeta(3) \right) \alpha'^4 + \dots + \mathcal{O}(\epsilon).$$

The singular term of this series coincides with the un-shifted one from Example 120.

**Theorem 61.** Let  $\mathcal{R}'$  be a shifted kinematic renormalization scheme (Definition 113), and let  $\alpha'$  be the shifted coupling (Definition 114). Let  $Z_G, Z_\alpha$  be the counterterms in kinematic renormalization without shift, and let

$$\gamma'_0(\alpha', \epsilon) := G'_{\mathcal{R}}(\alpha', \epsilon, 0), \quad Q'_0(\alpha', \epsilon) := Q'_{\mathcal{R}}(\alpha', \epsilon, 0) = Q_{\mathcal{R}'}(\alpha(\alpha'), \epsilon, 0).$$

Then, the shifted counterterms of Definition 115 are given by

$$Z'_\alpha(\alpha', \epsilon) = Q'_0(\alpha', \epsilon) \cdot Z_\alpha(\alpha' Q'_0(\alpha', \epsilon), \epsilon), \quad Z'_G(\alpha', \epsilon) = \gamma'_0(\alpha', \epsilon) \cdot Z_G(\alpha' Q'_0(\alpha', \epsilon), \epsilon).$$

**Proof** For a non-linear DSE, from Lemma 60, we obtain

$$G_{\mathcal{R}'}(\alpha, \epsilon, L) = \gamma'_0(\alpha, \epsilon) \cdot G_{\mathcal{R}}(\tilde{\alpha}(\alpha, \epsilon), \epsilon, L).$$

Note the presence of  $\tilde{\alpha} = \alpha' Q_0(\alpha, \epsilon)$  from Definition 114. We take  $\alpha'$  as a natural variable and define the shifted  $Z$ -factors according to Definition 115. The un-shifted Green function is given by Eq. (4.30), therefore

$$\gamma'_0(\alpha, \epsilon) \cdot Z_G(\tilde{\alpha}, \epsilon) G(\tilde{\alpha} Z_\alpha(\tilde{\alpha}, \epsilon), \epsilon, L) = Z'_G(\alpha', \epsilon) G(\alpha' Z'_\alpha(\alpha', \epsilon), \epsilon).$$

Comparing factors, and writing everything as a function of  $\alpha'$ , we obtain the claimed expressions.  $\square$

### 4.3.3 Shifted Renormalization Group Functions

Knowing the shifted counterterms from Theorem 61, we can compute the corresponding renormalization group functions from Definition 112. We deliberately expressed our shifted functions in terms of  $\alpha'$ , not  $\alpha$ , because in this way, we can use the same derivations as in Sect. 3.2.2, only replacing  $\alpha$  by  $\alpha'$ . This fits with our remark Eq. (3.23): Renormalization and change of energy scale are one and the same operation, that is, with a shifted renormalization point, we obtain identical results, up to a different value of the coupling.

**Theorem 62.** Consider an arbitrarily shifted kinematic renormalization scheme, where the counterterms are given by Theorem 61 as functions of  $\alpha'$  (Definition 114). The shifted renormalization group functions  $\beta'(\alpha', \epsilon)$ ,  $\gamma'(\alpha', \epsilon)$  are computed as in Definition 112, where every  $\alpha$  is replaced by  $\alpha'$ . Then, the Callan–Symanzik equation (Theorem 45) holds for the shifted Green function Eq. (4.35) as a function of  $\alpha'$ :

$$\left( \gamma'(\alpha', \epsilon) + (\beta'(\alpha', \epsilon) - \alpha' \epsilon) \frac{\partial}{\partial \alpha'} \right) G'_{\mathcal{R}}(\alpha', \epsilon, L) = \frac{\partial}{\partial L} G'_{\mathcal{R}}(\alpha', \epsilon, L).$$

**Proof** Owing to our definitions in Sect. 4.3.2, Definition 115 is exactly the same as the un-shifted relation Eq. (4.30), only with every  $\alpha$  replaced by  $\alpha'$  and  $Z$  replaced by  $Z'$ . Moreover, thanks to Definition 112, the  $Z$ -factors are related to the renormalization group functions exactly as in the un-shifted case, up to replacing  $\gamma \rightarrow \gamma'$  and  $\beta \rightarrow \beta'$ . Effectively,  $G'_{\mathcal{R}}(\alpha, \epsilon, L)$  can be expressed in terms of  $\gamma'$ ,  $\beta'$  exactly the same way that  $G_{\mathcal{R}}(\alpha, \epsilon, L)$  is expressed by  $\gamma$ ,  $\beta$ , and both are based on the same un-renormalized Green function  $G$ . Consequently, both satisfy the same Callan–Symanzik equation Theorem 45.

A different perspective is to use Theorem 59: The shifted kinematic Green function is equal to some non-kinematic Green function, and by Lemma 55, the latter satisfies the familiar Callan–Symanzik equation and the counterterm relations of Definition 112.  $\square$

Similarly to Eq. (3.2), the shifted Green function (Eq. (4.35)) can be expanded in the logarithmic scale (Definition 101):

$$G'_{\mathcal{R}}(\alpha', \epsilon, L) := \sum_{j=0}^{\infty} \gamma'_j(\alpha', \epsilon) L^j. \quad (4.37)$$

In this equation, all quantities are functions of  $\alpha'$  from Definition 114. But, unlike earlier notation,  $\gamma'_j(\alpha') \neq \gamma_j(\alpha(\alpha'))$ .

**Lemma 63.** Let  $G'_{\mathcal{R}}(\alpha, \epsilon, L)$  be a renormalized Green function in a shifted kinematic scheme (Definition 113) which is a solution of a DSE. Let  $\gamma'_j(\alpha', \epsilon)$  be the coefficients of the log expansion Eq. (4.37). Then,

$$\gamma'_{j>1}(\alpha', \epsilon) = \frac{1}{j} \left( \gamma'(\alpha', \epsilon) + (\beta'(\alpha', \epsilon) - \alpha' \epsilon) \cdot \frac{\partial}{\partial \alpha'} \right) \gamma'_{j-1}(\alpha', \epsilon).$$

**Proof** Insert the expansion Eq.(4.37) into the Callan–Symanzik equation (Theorem 62).  $\square$

By Theorems 62 and 63, the shifted renormalization group is entirely expressed in terms of shifted couplings  $\alpha'$ , shifted Green functions  $G_{\mathcal{R}'}$  and shifted renormalization group functions  $\beta', \gamma'$ . On the other hand, for a given shift  $\delta$ , the expansion functions can also be computed directly from the un-shifted ones.

**Theorem 64.** Let  $\gamma'_j(\alpha', \epsilon)$  be the expansion functions from Eq.(4.37), where  $G'_{\mathcal{R}}$  is a shifted Green function according to Eq.(4.35) and Definition 113, and let  $\gamma_j(\alpha, \epsilon)$  be the corresponding expansion functions in MOM from Eq.(3.2). Let  $\alpha(\alpha') = \alpha'e^{+\epsilon\delta'(\alpha', \epsilon)}$ , where  $\delta'(\alpha', \epsilon) = \delta(\alpha(\alpha'), \epsilon)$  from Definition 114. Then,

$$\begin{aligned}\gamma'_k(\alpha', \epsilon) &= \gamma'_0(\alpha', \epsilon) \cdot \gamma_k(\tilde{\alpha}(\alpha', \epsilon), \epsilon) \\ \gamma'_k(\alpha', \epsilon) &= \sum_{j=k}^{\infty} \binom{j}{k} \gamma_j(\alpha(\alpha', \epsilon), \epsilon) \delta^{j-k}(\alpha(\alpha'), \epsilon).\end{aligned}$$

**Proof** The first equation follows if we insert the expansion Eq.(4.37) into Lemma 60.

From Definition 113, we obtain

$$G_{\mathcal{R}'}(\alpha, \epsilon, L) = G_{\mathcal{R}}(\alpha, \epsilon, L + \delta).$$

Insert the expansions Eqs.(3.2) and (4.37),

$$\sum_{j=0}^{\infty} \gamma'_j(\alpha, \epsilon) L^j = \sum_{j=1}^{\infty} \gamma_j(\alpha, \epsilon) (L + \delta)^j.$$

Expand the right hand side with the binomial theorem and consider order  $L^k$ .

$$\sum_{j=0}^{\infty} \gamma_j(\alpha, \epsilon) \sum_{k=0}^j \binom{j}{k} L^k \delta^{j-k} = \sum_{k=0}^{\infty} L^k \sum_{j=k}^{\infty} \binom{j}{k} \gamma_j(\alpha, \epsilon) \delta^{j-k}.$$

$$\gamma'_k(\alpha, \epsilon) = \sum_{j=k}^{\infty} \binom{j}{k} \gamma_j(\alpha, \epsilon) \delta^{j-k}.$$

This is a function of  $\alpha$ , so we need to insert  $\alpha(\alpha')$  everywhere.  $\square$

So far, we have worked with the full  $\epsilon$ -dependent functions, which is necessary for a consistent treatment of counterterms. If we are only interested in the  $\epsilon = 0$  case, then the situation simplifies considerably.

**Theorem 65.** Assume that the MOM expansion functions  $\gamma_k(\alpha)$  from Eq. (3.2) are formal power series and satisfy the Callan–Symanzik equation Theorem 41, and the kinematic renormalization point is shifted by a factor  $\delta(\alpha)$  according to Definition 113, which is a power series in  $\alpha$ . Assume further that  $G_{\mathcal{R}}$  is a solution to a DSE of type Eq. (3.34), where the invariant charge (Definition 94) is  $Q = G^w$ . Then, in the limit  $\epsilon = 0$ ,

1. The shifted anomalous dimension and beta functions of Theorem 62, for  $\epsilon = 0$ , are

$$\gamma'(\alpha) := \frac{\gamma(\alpha)}{1 + w\gamma(\alpha) \cdot \alpha\partial_\alpha\delta(\alpha)}, \quad \beta'(\alpha) := w\alpha\gamma'(\alpha),$$

2. The shifted anomalous dimension satisfies  $\gamma'(\alpha) = \gamma(\alpha) + \mathcal{O}(\alpha^3)$ , and the shifted beta function satisfies  $\beta'(\alpha) = \beta(\alpha) + \mathcal{O}(\alpha^4)$ .

**Proof** 1. Consider the limit  $\epsilon \rightarrow 0$  in Theorem 64. In that limit,  $\alpha' \rightarrow \alpha$  and the  $\epsilon$ -dependence of all quantities can be left out because they are regular (Lemma 54). Compute the derivative of this series, using the fact that  $\gamma_j(\alpha)$  satisfy the Callan–Symanzik equation (Theorem 42), and identify the resulting series to obtain

$$\begin{aligned} \alpha\partial_\alpha\gamma'_k(\alpha) &= -\frac{\gamma}{w\gamma}\gamma'_k + \frac{1}{w\gamma} \sum_{j=k+1}^{\infty} \frac{j!(k+1)\gamma_j\delta^{j-1-k}}{(j-1-k)!(k+1)!} + \alpha\partial_\alpha\delta \cdot \sum_{j=k}^{\infty} \frac{j!(k+1)\gamma_j\delta^{j-k-1}}{(j-k-1)!(k+1)!} \\ (k+1)\gamma'_{k+1} &= \frac{\gamma}{1 + w\gamma\alpha\partial_\alpha\delta} \cdot \gamma'_k + \frac{s\gamma}{1 + w\gamma\alpha\partial_\alpha\delta} \cdot \alpha\partial_\alpha\gamma'_k. \end{aligned}$$

This is again the Callan–Symanzik equation, but with a different anomalous dimension and beta function as claimed.

2. Follows from 1. and Lemma 43 upon noticing that  $\gamma(\alpha) \cdot \alpha\partial_\alpha \ln \delta(\alpha) \in \mathcal{O}(\alpha^2)$ .  $\square$

For the linear DSE,  $w = 0$ , we recover  $\gamma'(\alpha) = \gamma(\alpha)$ , known from Theorem 58. Point 2. is an extension of point 1 in Theorem 58.

**Lemma 66.** For a linear DSE, the shifted anomalous dimension  $\gamma'(\alpha', \epsilon)$  is

$$\gamma'(\alpha', \epsilon) = \gamma(\alpha', \epsilon) + \epsilon \partial_{\alpha'} \ln \gamma'_0(\alpha', \epsilon).$$

Here,  $\gamma(\alpha', \epsilon)$  is the un-shifted anomalous dimension where the argument is  $\alpha'$ , that is, we do not insert the transformation  $\alpha(\alpha')$ . Especially,  $[\epsilon^0]\gamma'(\alpha, \epsilon) = [\epsilon^0]\gamma(\alpha, \epsilon)$ , so  $\gamma$  and  $\gamma'$  coincide for  $\epsilon = 0$ .

**Proof** First note that in the linear case,  $\beta'(\alpha', \epsilon) = 0$ . Using Definition 112 on Eq. (4.36) results in

$$\gamma'(\alpha', \epsilon) = \epsilon \alpha' \epsilon \partial_{\alpha'} \ln Z_G(\alpha', \epsilon) = \partial_{\alpha'} \ln \gamma'_0(\alpha', \epsilon) + \alpha' \epsilon \partial_{\alpha'} \ln Z_G(\alpha', \epsilon).$$

The last summand is the un-shifted anomalous dimension with argument  $\alpha'$ .  $\gamma'$  is regular in  $\epsilon$ , since it appears in the Callan–Symanzik equation (Theorem 62) where  $G_{\mathcal{R}'}$  is regular and non-vanishing for  $\epsilon \rightarrow 0$ . The difference of  $\gamma$  and  $\gamma'$  is proportional to  $\epsilon$  because neither of them contains poles in  $\epsilon$ .  $\square$

### Summary of Sect. 4.3.

1. All solutions of the same DSE, but in different renormalization schemes, are identical up to different renormalization points. In non-kinematic renormalization schemes, the renormalization point  $\delta(\alpha, \epsilon)$  is a function of  $\alpha$  (Sect. 4.3.1).
2. In order to obtain the correct counterterms and renormalization group functions for  $\epsilon \neq 0$ , one needs to introduce a shifted coupling  $\alpha' = \alpha e^{-\epsilon \delta}$  (Sect. 4.3.2).
3. For a given shift  $\delta(\alpha)$ , the shifted counterterms and renormalization group functions can be computed from the un-shifted ones, and they satisfy all the usual renormalization group equations (Sect. 4.3.3).

## 4.4 MS as a Shifted MOM Scheme

All renormalization schemes can be interpreted as shifted kinematic renormalization schemes (Definition 113), where the renormalization point  $\delta(\alpha, \epsilon)$  in general depends both on  $\alpha$  and on  $\epsilon$ . This follows from Theorem 59, and is valid up to the exceptions discussed there. In the present section, we narrow down the setting to a comparison between kinematic renormalization and concretely Minimal Subtraction, instead of arbitrary non-kinematic schemes.

### 4.4.1 Relation Between MS and MOM

As described in Sect. 4.1.1, kinematic renormalization (Definition 93) has pleasant analytic features and straightforward interpretation, while Minimal Subtraction (Definition 93) is technically easiest for solving Feynman integrals. Moreover, in MS, but presumably not in MOM, the beta function is expected to be dominated by primitive diagrams (Definition 88) [17]. In Sect. 4.2.4, we saw explicit examples for the fact that the perturbative beta function can differ substantially between MS and MOM. Finally, we can expect that low-order perturbation theory is reliable where quantum corrections are small, that is, in the vicinity of the renormalization point  $\delta$ , not necessarily near  $L = 0$  [15, 16]. For all these reasons, we want to improve our understanding of the relationship between MS and MOM by concretely determining the shift  $\delta(\alpha, \epsilon)$ .

The qualitative situation is sketched in Fig. 4.3: The Green function  $\hat{G}_R$  in MS is some function of  $\alpha$ ,  $\epsilon$  and  $L$  and we want to determine the values  $L = -\delta(\alpha, \epsilon)$  where it has unit value. There are three approaches to finding  $\delta$ :

1. Compute the MS solution  $\hat{G}_R$  and determine  $\delta$  from the condition Definition 113, by reversing the series.
2. Compute the MOM solution and the MS solution and determine  $\delta$  without extensive series reversions.
3. Derive  $\delta$  from a known MOM solution without explicitly computing the MS solution.

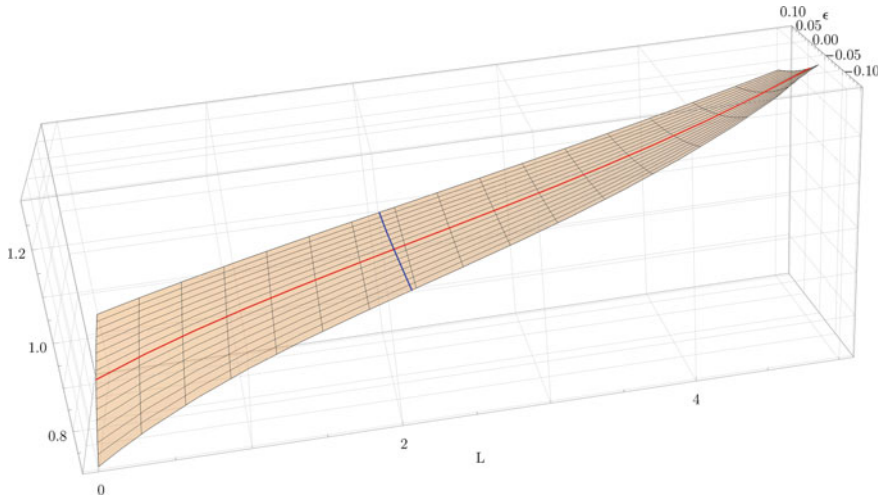


**Fig. 4.3** Sketch of the situation discussed in the present section. The orange surface is a Green function  $\hat{G}_R(\alpha, \epsilon, L)$  in MS-bar for some fixed value of  $\alpha$ . The red line indicates its value for  $\epsilon = 0$ . Our goal is to find the blue line. The blue line is the function  $-\delta(\alpha, \epsilon)$ , for the same fixed value of  $\alpha$ , where  $\tilde{G}_R(\alpha, \epsilon, -\delta) = 1$

We shall discuss the first approach in Sect. 4.4.2, the second one in Sect. 4.4.3 and the third one in Sect. 4.4.4.

In all cases, we will actually be working with MS-bar and not MS (Definition 110) in order to eliminate trivial constants. The transition between MOM and MS is described in Sect. 4.2.2, and for our concrete examples it is given in [3]. Moreover, we again restrict ourselves to propagator-DSEs of type Eq. (3.34) where  $\mathcal{Q} = G^w$  with  $w \in \mathbb{Q}$ .

#### 4.4.2 Brute-Force Computation

With the algorithm described in Sect. 4.2, we can in principle find the MS-bar solution  $\bar{G}_{\mathcal{R}}(\bar{\alpha}, \epsilon, L)$  to any finite order, and then determine  $\delta(\alpha, \epsilon)$  by “reversing” the resulting series in  $L$ . A first order computation was shown in Example 121.

In the framework of shifted kinematic renormalization (Sect. 4.3), the MS-bar Green function is to be interpreted as the shifted Green function, that is, it is expressed in the variable  $\bar{\alpha}$ , corresponding to  $\alpha'$  in Definition 114. The shifted renormalization condition (Definition 113),

$$\bar{G}_{\mathcal{R}}(\bar{\alpha}, \epsilon, -\bar{\delta}) \stackrel{!}{=} 1, \quad (4.38)$$

represents a linear system for the expansion coefficients of the power series  $\delta(\bar{\alpha}, \epsilon)$ . In practice, finding the inverse series  $\bar{\delta}(\bar{\alpha}, \epsilon)$  of Eq. (4.38) is a computationally demanding task since we are dealing with a double series where the coefficients are large polynomials in  $\pi^2$  and zeta values.

In solving Eq. (4.38), observe that we are performing the transformations of Sect. 4.3 in “reverse direction”. Concretely, in Sect. 4.3, we started with a MOM-renormalized amplitude, expressed as a function of  $\alpha$ , and computed the shifted amplitude, expressed via  $\bar{\alpha} = \alpha e^{-\epsilon\delta(\alpha, \epsilon)}$ . In the present case, the coupling that we are using in MS represents  $\bar{\alpha}$ , and we have  $\alpha = \bar{\alpha}e^{+\epsilon\bar{\delta}(\bar{\alpha}, \epsilon)}$ , where

$$\bar{\delta}(\bar{\alpha}, \epsilon) = \delta(\alpha(\bar{\alpha}), \epsilon). \quad (4.39)$$

If  $G_{\mathcal{R}}(\alpha, \epsilon, L)$  is the solution of the same DSE in MOM, then

$$\bar{G}_{\mathcal{R}}(\bar{\alpha}, \epsilon, L) = G_{\mathcal{R}}(\alpha(\bar{\alpha}), \epsilon, L + \bar{\delta}(\bar{\alpha}, \epsilon)).$$

To be explicit: The shift  $\delta(\alpha, \epsilon)$  that translates from MOM to MS, for  $\epsilon \neq 0$ , is not the same as the function  $\bar{\delta}(\bar{\alpha}, \epsilon)$  in the opposite direction, because they depend on different variables. This conundrum disappears as soon as one consistently uses  $\bar{\alpha}$  as the name of the coupling in MS, but it is not obvious from Definition 110 why in MS, one would suddenly give a different name to the coupling compared to MOM. Owing to  $\bar{\alpha} = \alpha + \mathcal{O}(\epsilon)$ , the functions  $\bar{\delta}(\bar{\alpha})$  and  $\delta(\alpha)$  coincide for  $\epsilon = 0$ , so the distinction is unnecessary as long as we are only interested in  $\epsilon = 0$ .

### Example 123: Multiedge linear DSE, brute force shift.

In Example 117, we quoted the constant term  $\bar{\gamma}_0(\bar{\alpha}, \epsilon)$ , similarly, all higher  $\bar{\gamma}_j(\bar{\alpha}, \epsilon)$  can be determined from the coefficients (Example 112). Here,  $\bar{\alpha}$  is merely the name of the variable, it is not computed from some underlying  $\alpha$ . Knowing the power series  $\bar{G}_{\mathcal{R}}(\bar{\alpha}, \epsilon, L)$ , we obtain from Eq. (4.38):

$$\begin{aligned}\bar{\delta}(\bar{\alpha}, \epsilon) &= -2 + \frac{3}{2}\bar{\alpha} + \left(-\frac{19}{6} + \frac{2}{3}\zeta(3)\right)\bar{\alpha}^2 + \left(\frac{103}{12} - \frac{4}{3}\zeta(3)\right)\bar{\alpha}^3 + \dots \\ &\quad + \left(-2 + \frac{\pi^2}{12} + \left(\frac{9}{2} - 3\zeta(3)\right)\bar{\alpha} + \left(-\frac{403}{24} + \frac{\pi^2}{90} + 5\zeta(3)\right)\bar{\alpha}^2 + \dots\right)\epsilon + \mathcal{O}(\epsilon^2).\end{aligned}$$

With this, we compute  $\alpha(\bar{\alpha}) = \alpha e^{+\epsilon\bar{\delta}(\bar{\alpha}, \epsilon)}$ . We invert the latter series to find  $\bar{\alpha}(\alpha)$ , which results in

$$\begin{aligned}\delta(\alpha, \epsilon) &= -\frac{1}{\epsilon} \ln \frac{\bar{\alpha}(\alpha)}{\alpha} = \bar{\delta}(\bar{\alpha}(\alpha), \epsilon) \\ &= -2 + \frac{3}{2}\alpha + \left(-\frac{19}{6} + \frac{2}{3}\zeta(3)\right)\alpha^2 + \left(\frac{103}{12} - \frac{4}{3}\zeta(3)\right)\alpha^3 + \dots \\ &\quad + \left(-2 + \frac{\pi^2}{12} + \left(\frac{15}{2} - 3\zeta(3)\right)\alpha + \left(-\frac{761}{24} + \frac{\pi^4}{90} + \frac{23}{3}\zeta(3)\right)\alpha^2 + \dots\right)\epsilon + \mathcal{O}(\epsilon^2).\end{aligned}$$

As expected, the functions  $\delta$  and  $\bar{\delta}$  coincide for  $\epsilon = 0$ , but they differ for  $\epsilon \neq 0$ .

#### 4.4.3 Relation of the Shift to Renormalization Group Functions

The brute force method (Eq.(4.38)) is computationally demanding for  $\epsilon \neq 0$ . It becomes significantly faster if we restrict ourselves to  $\epsilon = 0$ . In that case, the distinction Definition 4.39 does not exist,  $\bar{\alpha} = \alpha$  and  $\bar{\delta} = \delta$ . Furthermore, we can accelerate the computation by exploiting the particular analytic structure of  $\bar{G}_{\mathcal{R}}$ .

First, consider a linear DSE,  $w = 0$ . In MS-bar, it has a scaling solution (Eq. (4.6)),

$$\bar{G}_{\mathcal{R}}(\alpha, L) = \bar{\gamma}_0(\alpha) \cdot L^{\gamma(\alpha)}. \quad (4.40)$$

By Theorem 58, the anomalous dimension  $\gamma(\alpha)$  of a linear DSE is independent of the renormalization scheme.

**Theorem 67.** Consider two perturbative solutions of the same linear Dyson–Schwinger equation (Eq. (3.34) with  $Q = 1$ ). Let  $\gamma(\alpha)$  be the anomalous dimension and assume that both  $\gamma_0(\alpha)$  and  $\gamma'_0(\alpha) = 1 + \mathcal{O}(\alpha)$  are formal power series (Definition 53) starting with unity. Then, the Green functions are equal up to an  $\alpha$ -dependent shift  $\delta$  (Definition 113) given by the power series

$$\delta(\alpha) = \frac{1}{\gamma(\alpha)} \ln \left( \frac{\gamma'_0(\alpha)}{\gamma_0(\alpha)} \right).$$

**Proof** In the linear case,  $w = 0$ , the renormalized Green function has the form Eq. (4.40). Using Definition 113, we demand  $\gamma'_0 = \gamma_0 \delta^\gamma$ , which leads to the claimed formula. The functions  $\gamma(\alpha)$ ,  $\gamma_0(\alpha)$  and  $\gamma'_0(\alpha)$  are power series and  $\gamma'_0(\alpha)/\gamma_0(\alpha) = 1 + \mathcal{O}(\alpha)$  by assumption. Therefore  $\ln(\gamma'_0/\gamma_0) \in \mathcal{O}(\alpha)$  and the pole  $1/\alpha$  of  $1/\gamma(\alpha)$  from Lemma 43 is cancelled. The claimed formula  $\delta(\alpha) = \frac{1}{\gamma} \ln \frac{\gamma'_0}{\gamma_0}$  is a formal power series indeed.  $\square$

In MOM, we have  $\gamma_0(\alpha) = 1$  by the renormalization condition Definition 93. In MS-bar, the solution will have some  $\bar{\gamma}_0(\alpha) \neq 1$ . Theorem 67 thus specializes to

$$\delta(\alpha) = \frac{\ln \bar{\gamma}_0(\alpha)}{\gamma(\alpha)}. \quad (4.41)$$

**Lemma 68.** Consider a DSE of the form Eq. (4.7) and let  $f_n^{(k)}$  be the expansion coefficients of the kernel (Eq. (4.9)). Then, the shift  $\delta$  between MS-bar and MOM (Definition 113), regardless of  $w$ , starts with

$$\delta(\alpha) = -\frac{f_0^{(0)}}{f_{-1}^{(0)}} + \mathcal{O}(\alpha).$$

**Proof** By explicit calculation, the first coefficients of an explicit perturbative solution of Eq. (4.7) in MOM respectively MS-bar are

$$\begin{aligned} \gamma(\alpha) &= -f_{-1}^{(0)}\alpha + (w+1)\left(-2f_{-1}^{(0)}f_0^{(1)} - 2f_0^{(0)}f_{-1}^{(1)} + 2f_{-1}^{(0)}f_0^{(0)}\right)\alpha^2 + \mathcal{O}(\alpha^3), \\ \bar{\gamma}_1(\alpha) &= -f_{-1}^{(0)}\alpha + (w+1)\left(-2f_{-1}^{(0)}f_0^{(1)} - 2f_0^{(0)}f_{-1}^{(1)} + f_{-1}^{(0)}f_0^{(0)}\right)\alpha^2 + \mathcal{O}(\alpha^3), \\ \bar{\gamma}_0(\alpha) &= 1 + \alpha f_0^{(0)} + \mathcal{O}(\alpha^2), \quad \alpha \partial_\alpha \hat{G}|_{x=1} = \alpha f_0^{(0)} + \mathcal{O}(\alpha^2). \end{aligned}$$

Using Theorems 41 and 65, the anomalous dimension in MS is

$$\bar{\gamma}(\alpha) = \frac{\bar{\gamma}_1(\alpha)}{\bar{\gamma}_0(\alpha) + w\alpha \partial_\alpha \bar{G}|_{x=1}} = \frac{\bar{\gamma}_1(\alpha)}{1 + (w+1)\alpha f_0^{(0)} + \mathcal{O}(\alpha^2)} = \gamma(\alpha) + \mathcal{O}(\alpha^3).$$

$\square$

Note that  $f_{-1}^{(0)} \neq 0$  in physically sensible kernels, because the pole  $\frac{1}{\rho}$  in the “regulator”  $\rho$  expresses that the kernel graph is primitively divergent. Remarkably,  $\delta(0) \neq 0$  unless  $f_0^{(0)} = 0$ , so the shift does not necessarily vanish for vanishing coupling. This result does not depend on the invariant charge in the DSE, but just on the kernel.

### Example 124: Multiedge DSE, first order of shift.

For the multiedge DSE, the first coefficients  $f_n^{(k)}$  are listed in Example 110,  $f_{-1}^{(0)} = 1$  and  $f_0^{(0)} = 2$ . By Lemma 68,

$$\delta(\alpha) = -2 + \mathcal{O}(\alpha).$$

This coincides with our earlier finding in Example 123.

**Theorem 69.** Let  $G_{\mathcal{R}}(\alpha, x)$  and  $\tilde{G}_{\mathcal{R}}(\alpha, x)$  be the perturbative solutions of the same propagator-type Dyson–Schwinger equation (4.7) with  $w \neq 0$ , where  $G_{\mathcal{R}}$  uses kinematic renormalization and  $\tilde{G}_{\mathcal{R}}$  uses Minimal Subtraction. Assume that the anomalous dimensions (Definition 112)  $\gamma(\alpha), \tilde{\gamma}(\alpha)$  are power series with a non-vanishing term  $\propto \alpha$ . Then there is a unique power series  $\delta(\alpha)$  such that  $G_{\mathcal{R}}(\alpha, L + \delta(\alpha)) = \tilde{G}(\alpha, L)$  (Definition 113) for all  $L$ , given by Lemma 68 and

$$\frac{\partial}{\partial \alpha} \delta(\alpha) = \frac{1}{w\alpha} \left( \frac{1}{\tilde{\gamma}(\alpha)} - \frac{1}{\gamma(\alpha)} \right) = \frac{\gamma(\alpha) - \tilde{\gamma}(\alpha)}{w\alpha\tilde{\gamma}(\alpha)\gamma(\alpha)}.$$

**Proof** The fact that MS and MOM are related via a change in renormalization point is known from Theorem 59. We need to show that  $\delta(\alpha)$  is a well-defined power series.

From Theorem 65 we know how shifting the kinematic renormalization point induces a change in the anomalous dimension. Solving the latter relation for  $\delta(\alpha)$  produces the claimed expression.

By Lemma 43 and point 2 of Theorem 65, using the assumption, the denominator of the last fraction in the present theorem is proportional to  $\alpha^3$ . But, since  $\tilde{\gamma}(\alpha)$  is the anomalous dimension in MS, the numerator is  $\gamma(\alpha) - \tilde{\gamma}(\alpha) \in \mathcal{O}(\alpha^3)$  by Theorem 65. Therefore the right hand side is a well defined power series in  $\alpha$ . It uniquely defines the power series  $\delta(\alpha)$  up to a constant summand, which is fixed by Lemma 68.  $\square$

There are at least three approaches to calculate  $\delta(\alpha)$  as soon as one knows the solutions both in MOM and MS-bar. The first approach uses Theorem 69, where the anomalous dimensions  $\gamma(\alpha), \tilde{\gamma}(\alpha)$  can be extracted from the corresponding  $Z$ -factors according to Definition 112.

The second approach utilizes the renormalization group equation in MS-bar derived in Theorem 65,

$$(k+1)\bar{\gamma}_{k+1}(\alpha) = \frac{\gamma(\alpha)}{1 + w\gamma(\alpha)\alpha\partial_\alpha\delta(\alpha)} \cdot (1 + w\alpha\partial_\alpha)\bar{\gamma}_k(\alpha). \quad (4.42)$$

If any two of the MS functions  $\hat{\gamma}_k(\alpha)$ , together with the MOM anomalous dimension  $\gamma(\alpha)$ , are known, then  $\delta(\alpha)$  can be computed. For example, using  $\bar{\gamma}_0$  and  $\bar{\gamma}_1$ , one has

$$\frac{\partial}{\partial\alpha}\delta(\alpha) = \frac{\gamma \cdot \hat{\gamma}_0 - \bar{\gamma}_1}{w\alpha \cdot \bar{\gamma}_1} + \frac{1}{\bar{\gamma}_1} \frac{\partial}{\partial\alpha}\bar{\gamma}_0 \quad (\text{for } w \neq 0). \quad (4.43)$$

The third approach is to compute all MS-bar functions  $\bar{\gamma}_j(\alpha)$  up to some desired maximum  $j$  and additionally all MOM functions  $\gamma_j(\alpha)$ . Next, one writes a power series ansatz for  $\delta(\alpha)$  and uses this to formally compute the powers  $\delta(\alpha)^k$ . Then the right side of Eq. (4.37),

$$G'_{\mathcal{R}}(\alpha', \epsilon, L) := \sum_{j=0}^{\infty} \gamma'_j(\alpha', \epsilon) L^j \quad (4.44)$$

is a linear system for the unknown coefficients of  $\delta(\alpha)$  which can be solved.

The resulting  $\delta(\alpha)$  agrees in all three approaches. The difference between them is about which input data they need, and how computationally efficient they are. The third approach produces one order higher in  $\alpha$  compared to the first two, for the same order of input data, because it does not use derivatives.

In all approaches, we need both the MOM- and the MS-bar solution in order to compute  $\delta(\alpha)$ . As long as we restrict ourselves to  $\epsilon = 0$ , it is not possible to obtain  $\delta(\alpha)$  without knowing data from both of the renormalized Green functions.

#### 4.4.4 Deriving the Shift from the MOM Solution

As outlined above, we can find the shift function  $\delta(\alpha, \epsilon)$  if we are given two different renormalized Green functions. On the other hand, for  $\epsilon = 0$ , the renormalization point is really only a single number, and the rest of the Green function is determined from the DSE. It is therefore conceivable that one can alternate between MOM and MS from first principles, without needing to explicitly know both Green functions.

Definition 110 makes explicit reference to the  $\epsilon$ -dependence of counterterms. This already indicates that in order to go from MOM to MS or vice versa, we need to know the solution in one of the schemes for  $\epsilon \neq 0$ . For systematic derivations, we need an analytic statement comparable to the condition  $G_{\mathcal{R}}(\alpha, \epsilon, 0) = 1$  for MOM. This is Theorem 56 condition that the shifted anomalous dimension  $\gamma'(\alpha, \epsilon)$  is independent of  $\epsilon$ .

**Theorem 70.** Consider a linear DSE of type Eq. (3.37). Let  $\gamma(\alpha, \epsilon) = \partial_L G_{\mathcal{R}}(\alpha, \epsilon, L)|_{L=0}$  be the anomalous dimension in MOM. Then, the solution in MS-bar at  $L = 0$  has the amplitude

$$G_{\bar{\mathcal{R}}}(\alpha, \epsilon, L = 0) = \bar{\gamma}_0(\alpha, \epsilon) = \exp \left( - \int_0^\alpha du \frac{\gamma(u, \epsilon) - \gamma(u, 0)}{u\epsilon} \right).$$

Here,  $G_{\bar{\mathcal{R}}}(\alpha, \epsilon, L)$  is a function of  $\alpha$ , not of  $\bar{\alpha}$ , compare Eqs. (4.32) to (4.35).

**Proof** Use Theorem 66, where  $\gamma'$  represents the anomalous dimension in MS. By Theorem 56, the latter is independent from  $\epsilon$ . By Theorem 65, it coincides with the MOM anomalous dimension  $\gamma(\alpha)$  for  $\epsilon = 0$ . Therefore

$$\bar{\gamma}(\alpha, \epsilon) = \gamma(\alpha) + \epsilon \partial_\alpha \ln \bar{\gamma}_0(\alpha, \epsilon).$$

In Theorem 66,  $\alpha'$  is merely a renamed variable, since all quantities are functions of  $\alpha'$ .  $\square$

**Lemma 71.** Consider a linear DSE of type Eq. (3.37) for  $\epsilon = 0$ , where  $\gamma(\alpha)$  is the anomalous dimension and  $g(\alpha)$  is the coefficient given by Theorem 49. Then, the shift between MS and MOM (Definition 113) is

$$\delta(\alpha) = -\frac{1}{\gamma(\alpha)} \int_0^\alpha \frac{du}{u} g(u).$$

**Proof** For a linear DSE,  $\gamma'_0$  directly corresponds to  $\delta$  via Theorem 67. Insert Theorem 70 into Eq. (4.41):

$$\delta(\alpha) = \frac{1}{\gamma(\alpha)} [\epsilon^0] \ln \bar{\gamma}_0(\alpha) = -\frac{1}{\gamma(\alpha)} [\epsilon^0] \int_0^\alpha du \frac{\gamma(u, \epsilon) - \gamma(u, 0)}{u\epsilon}$$

$\square$

The further transition from MS-bar to MS is a trivial rescaling, discussed in Sect. 4.2 and in [3]. Using Lemma 71 and Theorem 49, we can indeed deduce the MS amplitude of a linear DSE directly from the Mellin transform in a comparable way as we can for MOM (Theorem 46). Especially, we can obtain the solution in MS with purely analytic operations, without solving the DSE order by order. This result represents one of the key findings of the present thesis.

### Example 125: Multiedge linear DSE, exact shift.

From Example 107, we know

$$g(\alpha) = 1 + \frac{\alpha}{1+4\alpha} + \frac{\gamma(\alpha)+1}{2\gamma(\alpha)+1} \left( 2\gamma(\alpha) \cdot \gamma_E + \rho \partial_\rho \ln \frac{\Gamma(1+\rho)}{\Gamma(1-\rho)} \Big|_{\rho \rightarrow \gamma(\alpha)} - 1 \right),$$

where  $\gamma = \frac{1}{2} (\sqrt{1+4\alpha} - 1)$  from Example 105. This function satisfies  $\frac{d\gamma(\alpha)}{d\alpha} = \frac{1}{\sqrt{1+4\alpha}} = \frac{1}{2\gamma(\alpha)+1}$ . Consequently,  $\frac{du}{2\gamma(u)+1} = d\gamma(u)$ . Upon integration, we obtain

$$\ln \bar{\gamma}_0(\alpha) = - \int_0^\alpha \frac{du}{u} g(u) = \ln \frac{\gamma(\alpha)}{\alpha} - \frac{1}{4} \ln(1+4\alpha) - 2\gamma(\alpha)\gamma_E + \ln \frac{\Gamma(1-\gamma(\alpha))}{\Gamma(1+\gamma(\alpha))}.$$

This confirms the formula we had found empirically in Example 117. By Lemma 71, the shift between MS-bar and MOM is

$$\begin{aligned} \bar{\delta}(\alpha) &= \frac{\ln \bar{\gamma}_0(\alpha)}{\gamma(\alpha)} = \frac{1}{\gamma(\alpha)} \ln \frac{\gamma(\alpha)}{\alpha} - \frac{\ln(1+4\alpha)}{4\gamma(\alpha)} - 2\gamma_E + \frac{1}{\gamma(\alpha)} \ln \frac{\Gamma(1-\gamma(\alpha))}{\Gamma(1+\gamma(\alpha))} \\ &= -2 + \frac{3}{2}\alpha + \left( -\frac{19}{6} + \frac{2}{3}\zeta(3) \right) \alpha^2 + \left( \frac{103}{12} - \frac{4}{3}\zeta(3) \right) \alpha^3 + \dots \end{aligned}$$

The first coefficient coincides with Example 124. We stress again that this shift  $\bar{\delta}(\alpha)$  was derived exactly and from first principles, without heuristically matching a series expansion and without doing any explicit calculation in MS-bar.

### Example 126: Toy model linear DSE, exact shift.

For the linear toy model DSE (Example 103), the function  $\bar{\gamma}_0(\alpha)$  is particularly simple, see Example 119. Using Lemma 71, we conclude

$$\delta(\alpha) = \frac{\pi \ln(1-\alpha^2\pi^2)}{4 \arcsin(\alpha\pi)} = -\frac{\pi^2}{4}\alpha - \frac{\pi^4}{12}\alpha^3 - \frac{73\pi^6}{1440}\alpha^5 - \mathcal{O}(\alpha^7).$$

Observe that this time, the constant coefficient  $[\alpha^0]\delta(\alpha)$  vanishes, in accordance with Lemma 68, since for the toy model  $f_0 = f_0^{(0)} = 0$ .

### Summary of Sect. 4.4.

1. Each of the two renormalization schemes MS and MOM has conceptually unique features which make them indispensable in certain applications. Therefore, it is highly desirable to find the precise relation between the two Green functions, in the form of a shift  $\delta(\alpha, \epsilon)$  of the renormalization point (Sect. 4.4.1).
2. Knowing the MS-solution explicitly to some finite order in perturbation theory, one can compute  $\delta(\alpha, \epsilon)$  by finding the point where the amplitude is unity (Sect. 4.4.2).
3. Skipping the full  $\epsilon$ -dependence, one can infer  $\delta(\alpha)$  in various ways from the log-expansion of the MS-solution (Sect. 4.4.3). For a linear DSE,  $\delta(\alpha)$  is determined explicitly from  $\gamma(\alpha)$  and  $\tilde{\gamma}_0(\alpha)$  alone (Theorem 67).
4. Conceptually, it is possible to derive  $\delta(\alpha, \epsilon)$  and the full MS-solution from the MOM-solution at  $\epsilon \neq 0$  (Sect. 4.4.4), which in turn only depends on the Mellin transform of the kernel. For linear DSEs, we derived an explicit formula which allows to compute  $\delta(\alpha)$  from a given,  $\epsilon$ -dependent Mellin transform (Lemma 71 and Theorem 49).

## 4.5 Shift Between MS and MOM in Non-linear Examples

In the present section, we present empirical results for the shift  $\delta(\alpha)$  for non-linear Dyson–Schwinger equations, computed with the methods discussed in Sect. 4.4.3.

### 4.5.1 Multiedge DSE in $D=4$ Dimensions

The multiedge DSE was introduced in Example 104. The shift between MS and MOM can be derived exactly in the linear case (Example 125). For the non-linear versions of the DSE, the solutions in kinematic renormalization have been discussed in Sect. 3.4.1. Again, we restrict ourselves to MS-bar and skip the transformation to MS.

We computed the coefficients  $g_{t,r}^{(n)}$  of Sect. 4.2 in MS for  $w \in \{-5, \dots, +5\}$  symbolically at least up to order  $\alpha^{11}$ . By using numerical approximations of the various constants  $\zeta(n)$  and  $\pi^m$ , we reached order  $\alpha^{20}$ . The first three orders of the leading-log expansion fulfill Eq. (3.41), which has been checked for all choices of  $w$ . The shift from MOM- to MS-bar-renormalization has been computed as discussed in Sect. 4.4.3. The first coefficients are reported in Table 4.1.

We are interested in the asymptotic behavior of the power series  $\bar{\delta}(\alpha)$  at high order. To this end, we use the expansion Eq. (3.43),

**Table 4.1** Non-linear multiedge DSE in  $D = 4$  dimensions.  $\bar{\delta}(\alpha)$  is the shift of the renormalization point between MOM- and MS-scheme Definition 113. Shown are the first four terms of its perturbative power series.  $f_{n+1}/f_n$  is the growth rate of the function  $f(\alpha)$  to be introduced in Eq. (4.53)

$w$	$\bar{\delta}(\alpha)$	$f_{n+1}/f_n$
5	$-2 + 9\alpha + (-139 + 14\zeta(3))\alpha^2 + \left(3464 + \frac{7\pi^4}{12} - 233\zeta(3)\right)\alpha^3$	$30.22 \pm 0.09$
4	$-2 + \frac{15}{2}\alpha + \left(-\frac{575}{6} + 10\zeta(3)\right)\alpha^2 + \left(\frac{23525}{12} + \frac{\pi^4}{3} - \frac{410}{3}\zeta(3)\right)\alpha^3$	$25.09 \pm 0.06$
3	$-2 + 6\alpha + \left(-\frac{182}{3} + \frac{20}{3}\zeta(3)\right)\alpha^2 + \left(\frac{2911}{3} + \frac{\pi^4}{6} - \frac{214}{3}\zeta(3)\right)\alpha^3$	$19.96 \pm 0.04$
2	$-2 + \frac{9}{2}\alpha + \left(-\frac{67}{2} + 4\zeta(3)\right)\alpha^2 + \left(\frac{773}{2} + \frac{\pi^4}{15} - 31\zeta(3)\right)\alpha^3$	$14.80 \pm 0.02$
1	$-2 + 3\alpha + \left(-\frac{43}{3} + 2\zeta(3)\right)\alpha^2 + \left(\frac{305}{3} + \frac{\pi^4}{60} - \frac{29}{3}\zeta(3)\right)\alpha^3$	$9.60 \pm 0.01$
0	$-2 + \frac{3}{2}\alpha + \left(-\frac{19}{6} + \frac{2}{3}\zeta(3)\right)\alpha^2 + \left(\frac{103}{12} - \frac{4}{3}\zeta(3)\right)\alpha^3$	
-1	-2	
-2	$-2 - \frac{3}{2}\alpha - \frac{29}{6}\alpha^2 - \left(\frac{94}{3} - \frac{1}{3}\zeta(3)\right)\alpha^3$	$5.8 \pm 1.8$
-3	$-2 - 3\alpha + \left(-\frac{53}{3} + \frac{2}{3}\zeta(3)\right)\alpha^2 - \left(\frac{578}{3} + \frac{\pi^4}{60} - \frac{17}{3}\zeta(3)\right)\alpha^3$	$10.50 \pm 0.11$
-4	$-2 - \frac{9}{2}\alpha + \left(-\frac{77}{2} + 2\zeta(3)\right)\alpha^2 - \left(\frac{2365}{4} + \frac{\pi^4}{15} - 22\zeta(3)\right)\alpha^3$	$15.69 \pm 0.05$
-5	$-2 - 6\alpha + \left(-\frac{202}{3} + 4\zeta(3)\right)\alpha^2 - \left(\frac{4003}{3} + \frac{\pi^4}{6} - \frac{166}{3}\zeta(3)\right)\alpha^3$	$20.85 \pm 0.07$

$$\gamma(\alpha) =: \sum_{j=1}^{\infty} c_j \alpha^j, \quad \bar{\delta}(\alpha) := \sum_{j=0}^{\infty} d_j \alpha^j. \quad (4.45)$$

The asymptotics of  $c_j$  in MOM is known from Eq. (3.49). To visualize it, we consider

$$\frac{c_{n+1}/\Gamma(n+1-\beta(w))}{-c_n/\Gamma(n-\beta(w))} \equiv \frac{-c_{n+1}}{(n+\frac{3+2w}{w})c_n} = w - b^{(1)}(w) \frac{1}{n^2} + \mathcal{O}\left(\frac{1}{n^3}\right). \quad (4.46)$$

There is no  $1/n$  correction to this quantity, hence it converges quickly, see Fig. 4.4a.

Similarly to Eq. (4.46), we examine the ratio of successive  $d_n$ ,

$$\frac{-d_n}{(n-\beta(w))d_{n-1}} = \frac{-d_n}{(n+\frac{3+2w}{w})d_{n-1}}, \quad (4.47)$$

where we used the same parameter  $\beta(w) = \frac{-3-2w}{w}$  (from Eq. (3.48)) as in Eq. (4.46). A priori, this choice is a guess, but the results shown in Fig. 4.4b, suggest that it is correct. Consequently, we write for  $d_n$  an ansatz similar to Eq. (3.49),

$$d_n \sim \tilde{S}(w) \cdot (-\tilde{F}(w))^n \cdot \Gamma\left(n - \tilde{\beta}(w)\right) \left(1 + \frac{\tilde{b}^{(1)}(w)}{(n - \tilde{\beta}(w) - 1)} + \dots\right). \quad (4.48)$$

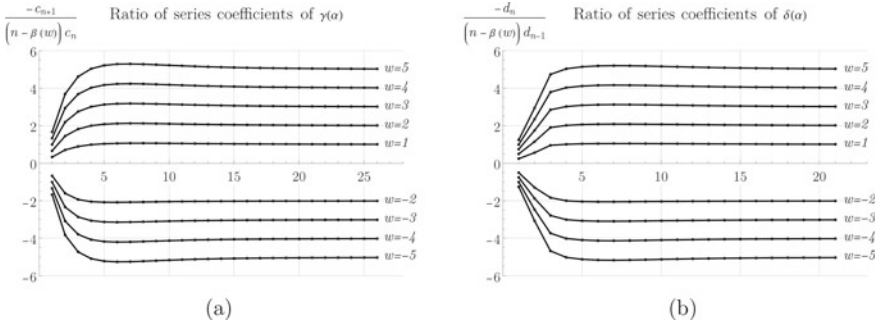


**Fig. 4.4** Multiedge DSE in  $D = 4$  dimensions. **a** Ratio of successive coefficients  $c_n$  of the anomalous dimension  $\gamma(\alpha) = \sum c_n \alpha^n$ . The denominator  $(n - \beta(w))$  is chosen to match the known asymptotics Eq. (3.49). The ratio quickly converges towards the limit  $w$ , see Eq. (4.46). **b** Ratio of successive coefficients  $d_n$  from Eq. (4.45). This ratio behaves very similarly to the ratio in (a), indicating that the leading growth rate of the coefficients is the same. See [3] for similar plots

**Table 4.2** Numerical findings of the growth parameters of  $\tilde{\delta}(\alpha)$  according to Eq. (4.48). They are consistent with Eqs. (3.2) and (3.48).  $\tilde{\delta}(\alpha)$  was computed including order  $\alpha^{n_{\max}}$

$w$	$n_{\max}$	$\tilde{S}(w)/w$	$\tilde{F}(w)$	$\tilde{\beta}(w)$	$\tilde{b}^{(1)}(w)$
5	24	$-0.02532 \pm 0.00037$	$4.987 \pm 0.062$	$-3.59 \pm 0.12$	$-2.61 \pm 0.18$
4	27	$-0.02709 \pm 0.00019$	$3.993 \pm 0.036$	$-3.74 \pm 0.08$	$-2.79 \pm 0.11$
3	32	$-0.02749 \pm 0.00011$	$2.997 \pm 0.017$	$-3.99 \pm 0.04$	$-3.10 \pm 0.06$
2	38	$-0.02272 \pm 0.00010$	$1.999 \pm 0.009$	$-4.50 \pm 0.03$	$-3.74 \pm 0.05$
1	38	$-0.00541 \pm 0.00009$	$0.999 \pm 0.007$	$-6.00 \pm 0.04$	$-5.97 \pm 0.12$
-2	21	$0.2080 \pm 0.0018$	$-1.998 \pm 0.012$	$-1.49 \pm 0.05$	$-0.74 \pm 0.08$
-3	21	$0.1295 \pm 0.0014$	$-2.995 \pm 0.026$	$-1.99 \pm 0.07$	$-1.10 \pm 0.11$
-4	21	$0.0882 \pm 0.0011$	$-3.993 \pm 0.040$	$-2.24 \pm 0.09$	$-1.30 \pm 0.14$
-5	21	$0.0655 \pm 0.0009$	$-4.991 \pm 0.054$	$-2.40 \pm 0.10$	$-1.43 \pm 0.15$

We extract the free parameters using Richardson extrapolation (Definition 61) of orders 2 to 5, where we use their mean as the estimation of the true value, and the largest absolute difference between any of these four extrapolations as uncertainty. The results are reported in Table 4.2. They are consistent with  $\tilde{S}(w) = w \cdot S(w)$ ,  $\tilde{F}(w) = w$  and  $\tilde{\beta}(w) = \beta(w) - 1$  within around 1% relative uncertainty. Unlike the analysis of  $\gamma(\alpha)$  in Sect. 3.4.1, the quoted of “rational numbers” should be understood as educated guesswork rather than numerical proofs, given the relatively poor accuracy of the numerical data. We refrain from deducing any closed formula for  $\tilde{b}^{(1)}(w)$  at this point.

Motivated by the formula Eq. (4.48), we directly compare the coefficients  $d_n$  to  $c_{n+1}$ . Using Eq. (4.48) with Table 4.2, we expect that  $d_n/c_{n+1} \rightarrow 1$ . By Eq. (3.48),  $w \cdot \lambda(w) = 1$  in our case, but we include this factor for consistency, and examine the ratio

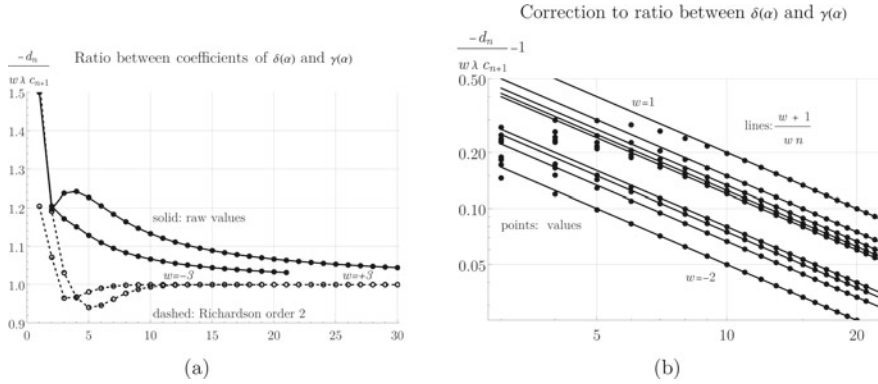


**Fig. 4.5** **a** Ratio of the coefficients  $d_n$  and  $c_n$ , of the shift  $\delta(\alpha) = \sum d_n \alpha^n$  and the anomalous dimension  $\gamma(\alpha) = \sum c_n \alpha^n$ , for  $w = -3$  and  $w = 3$ , other choices of  $w$  look similar. The solid lines are the raw values, the dashed lines indicate the order-2 Richardson extrapolation. The ratio  $-d_n/c_{n+1}$  approaches unity in the limit  $n \rightarrow \infty$ . **b** Deviation of the ratio from its asymptotic value unity. Each sequence corresponds to one value of  $w$ , solid lines represent the functions  $\frac{w+1}{wn}$ . The deviation between data points and functions is very small, this indicates the vanishing of quadratic corrections, see Table 4.3. See [3] for similar plots

$$\frac{-d_n}{w \lambda c_{n+1}} \sim r(w) + r_1(w) \frac{1}{n} + r_2(w) \frac{1}{n^2} + \dots, \quad n \rightarrow \infty. \quad (4.49)$$

This ratio is plotted in Fig. 4.5. As before, the free parameters of Eq. (4.49) are extracted using Richardson extrapolation (Definition 61). We confirm numerically that  $r(w) = 1 \pm 10^{-5}$ . The results for the corrections  $r_j$  are reported in Table 4.3. We emphasize the relatively low uncertainties, which indicate that the ratio Eq. (4.49) converges quickly. From the numerical results, we guess the expressions

$$r(w) = 1, \quad r_1(w) = \frac{w+1}{w}, \quad r_{j \geq 2}(w) = 0. \quad (4.50)$$

Together with the known behavior of  $c_{n+1}$  (Eq. (3.49)), and  $\beta(w) = -(3 + 2w)/w$ , we can give an explicit formula for the corrections to the leading asymptotics of  $d_n$ :

$$d_n \sim S(w)(-w)^{n+1} \Gamma(n - \beta(w) + 1) \cdot \left( 1 + \frac{\frac{1+3w+2w^2}{w^2}}{n - \beta(w)} + \frac{\frac{1+4w+4w^2-6w^3-7w^4}{2w^4}}{(n - \beta(w))(n - \beta(w) - 1)} + \mathcal{O}\left(\frac{1}{n^3}\right) \right). \quad (4.51)$$

The subleading coefficient is consistent with the value  $\tilde{b}^{(1)}(w)$  which we found in Table 4.2.

For the higher order corrections in Table 4.3, the uncertainties are increasing. If we nonetheless speculate that Eq. (4.50) is correct for all  $r_j$ , we obtain

**Table 4.3** Parameters of the ratio  $d_n/c_{n+1}$  for  $D = 4$  from Eq. (4.49).  $r_0 = 1$  is not included,  $r_{\geq 2}$  is consistent with zero as claimed in Eq. (4.50)

$w$	$r_1(w)$	$r_2(w)$	$r_3(w)$	$r_4(w)$	$r_5(w)$
5	$1.20002 \pm 0.00012$	$0.0003 \pm 0.0019$	$0.005 \pm 0.031$	$0.09 \pm 0.50$	$1.3 \pm 7.9$
4	$1.25000 \pm 0.00001$	$0.0000 \pm 0.0002$	$0.000 \pm 0.003$	$0.01 \pm 0.05$	$0.18 \pm 0.95$
3	$1.33333 \pm 0.00001$	$0.0000 \pm 0.0001$	$0.000 \pm 0.001$	$0.01 \pm 0.01$	$0.00 \pm 0.02$
2	$1.50000 \pm 0.00001$	$0.0000 \pm 0.0001$	$0.000 \pm 0.001$	$0.00 \pm 0.01$	$0.00 \pm 0.01$
1	$2.00000 \pm 0.00001$	$0.0000 \pm 0.0001$	$0.000 \pm 0.001$	$0.00 \pm 0.01$	$0.00 \pm 0.01$
-2	$0.50000 \pm 0.00001$	$0.0000 \pm 0.0001$	$0.000 \pm 0.001$	$0.00 \pm 0.01$	$0.00 \pm 0.02$
-3	$0.66667 \pm 0.00001$	$0.0000 \pm 0.0002$	$0.000 \pm 0.002$	$0.01 \pm 0.03$	$0.07 \pm 0.39$
-4	$0.75001 \pm 0.00004$	$0.0001 \pm 0.0005$	$0.001 \pm 0.007$	$0.02 \pm 0.09$	$0.20 \pm 1.24$
-5	$0.80001 \pm 0.00006$	$0.0002 \pm 0.0009$	$0.002 \pm 0.012$	$0.03 \pm 0.17$	$0.4 \pm 2.3$

$$d_n = - \left( 1 + \frac{w+1}{wn} \right) \cdot c_{n+1} + e_n. \quad (4.52)$$

Empirically, the remainder  $e_n$  falls off faster than exponentially, see Fig. 4.6a. This asymptotic statement for factorially divergent power series (Sect. 2.1.1) can be translated to a relation between the corresponding generating functions<sup>1</sup>:

$$\bar{\delta}(\alpha) = -\frac{\gamma(\alpha)}{\alpha} - \frac{w+1}{w} \int^{\alpha} \frac{da}{a} \frac{\gamma(a)}{a} + f(\alpha), \quad w \neq 0. \quad (4.53)$$

From our data, we can extract the first coefficients of the power series  $f(\alpha) := \sum_{n=1}^{\infty} f_n \alpha^n$ . These coefficients contain, besides rational factors, zeta values, which appear in  $\delta(\alpha)$  but not in  $\gamma(\alpha)$ , so they can not arise from the first two summands of Eq. (4.53). Figure 4.6b suggests that the coefficients  $f_n$  grow geometrically, not factorially. The growth rate is reported in the last column of Table 4.1. This geometric growth indicates that  $f(\alpha)$  is a convergent power series around  $\alpha = 0$ .

### 4.5.2 Multiedge DSE in $D=6$ Dimensions

For the 6-dimensional case (Example 104), the procedure is completely analogous to the one described in the previous Sect. 4.5.1. We use the same symbols as in the  $D = 4$  case in order to not clutter notation. Again, results for the linear DSE have been reported earlier (Examples 105 and 118) and will not be discussed here.

The power series coefficients of the shift  $\bar{\delta}(\alpha)$  have been computed symbolically up to order  $\alpha^{10}$ , and numerically at least to order  $\alpha^{20}$ , the first coefficients are reported

---

<sup>1</sup> The author thanks Michael Borinsky for pointing out this implication of Eq. (4.52).

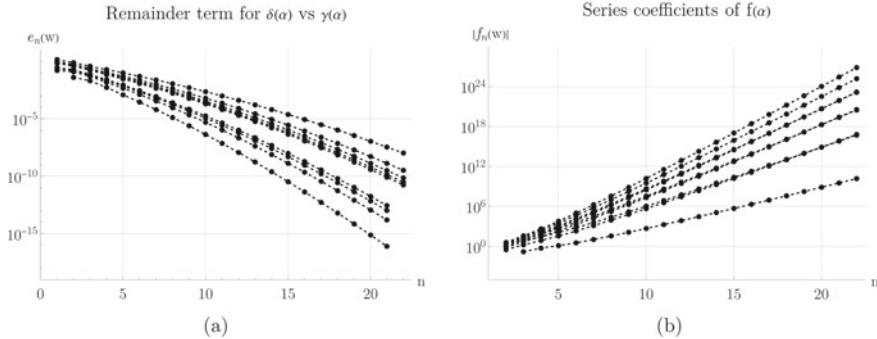


**Fig. 4.6** **a** Remainder coefficients  $e_n$  from Eq. (4.52), for different values of  $w$ . This is a logarithmic plot, they decay faster than exponentially. **b** Coefficients of the function  $f(\alpha)$  in Eq. (4.53). The coefficients grow geometrically (linearly in this logarithmic plot), which suggests that  $f(\alpha)$  is an analytic function. See [3] for similar plots

**Table 4.4** First perturbative coefficients of  $\delta(\alpha)$  for  $D = 6$  dimensions

$w$	$\delta(\alpha)$
5	$-\frac{8}{3} - \frac{61}{24}\alpha + \left(-\frac{80213}{7776} + \frac{7}{18}\zeta(3)\right)\alpha^2 - \left(\frac{8813575}{139968} + \frac{7\pi^4}{2592} - \frac{2563}{1296}\zeta(3)\right)\alpha^3$
4	$-\frac{8}{3} - \frac{305}{144}\alpha + \left(-\frac{331345}{46656} + \frac{5}{18}\zeta(3)\right)\alpha^2 - \left(\frac{119812205}{3359232} + \frac{\pi^4}{648} - \frac{2255}{1944}\zeta(3)\right)\alpha^3$
3	$-\frac{8}{3} - \frac{61}{36}\alpha + \left(-\frac{52325}{11664} + \frac{5}{27}\zeta(3)\right)\alpha^2 - \left(\frac{14842891}{839808} + \frac{\pi^4}{1296} - \frac{1177}{1944}\zeta(3)\right)\alpha^3$
2	$-\frac{8}{3} - \frac{61}{48}\alpha + \left(-\frac{38381}{15552} + \frac{1}{9}\zeta(3)\right)\alpha^2 - \left(\frac{3947825}{559872} + \frac{\pi^4}{3240} - \frac{341}{1296}\zeta(3)\right)\alpha^3$
1	$-\frac{8}{3} - \frac{61}{72}\alpha + \left(-\frac{24437}{23328} + \frac{1}{18}\zeta(3)\right)\alpha^2 + \left(\frac{1560359}{839808} + \frac{\pi^4}{12960} - \frac{319}{3888}\zeta(3)\right)\alpha^3$
0	$-\frac{8}{3} - \frac{61}{144}\alpha + \left(-\frac{10493}{46656} + \frac{1}{54}\zeta(3)\right)\alpha^2 + \left(\frac{518095}{3359232} - \frac{11}{972}\zeta(3)\right)\alpha^3$
-1	$-\frac{8}{3}$
-2	$-\frac{8}{3} + \frac{61}{144}\alpha - \frac{17395}{46656}\alpha^2 - \left(-\frac{114361}{209952} + \frac{11}{3888}\zeta(3)\right)\alpha^3$
-3	$-\frac{8}{3} + \frac{61}{72}\alpha + \left(\frac{31339}{23328} + \frac{1}{54}\zeta(3)\right)\alpha^2 - \left(-\frac{359005}{104976} - \frac{\pi^4}{12960} + \frac{187}{3888}\zeta(3)\right)\alpha^3$
-4	$-\frac{8}{3} + \frac{61}{48}\alpha + \left(-\frac{45283}{15552} + \frac{1}{18}\zeta(3)\right)\alpha^2 - \left(-\frac{11830593}{1119744} - \frac{\pi^4}{3240} + \frac{121}{648}\zeta(3)\right)\alpha^3$
-5	$-\frac{8}{3} + \frac{61}{36}\alpha + \left(-\frac{59227}{11664} + \frac{1}{9}\zeta(3)\right)\alpha^2 - \left(-\frac{20089615}{839808} - \frac{\pi^4}{1296} + \frac{913}{1944}\zeta(3)\right)\alpha^3$

in Table 4.4. The ratio of successive coefficients (Eq. (4.47)), this time with  $\beta(w)$  from Table 4.5, is shown in Fig. 4.7a. The plot suggests that  $d_n$  grow at a similar rate as  $c_n$ .

We extracted numerical estimates of the parameters in Eq. (4.48) with the procedure explained in Sect. 4.5.1. The results are reported in Table 4.5 and are consistent with  $\tilde{S}(w) = w \cdot S(w)$ ,  $\tilde{F}(w) = -w/6$  and  $\tilde{\beta}(w) = \beta_1(w) - 1$ .

**Table 4.5** Numerical findings of the growth parameters of  $\tilde{\beta}(\alpha)$  for the  $D = 6$  multiedge DSE, according to Eq. (4.48). They are consistent with Table 3.3 and Eq. (3.54)

$w$	$n_{\max}$	$10^6 \cdot \tilde{S}(w)/w$	$\tilde{F}(w)$	$\tilde{\beta}(w)$
5	24	$-50.1 \pm 4.5$	$-0.833 \pm 0.018$	$-7.00 \pm 0.37$
4	27	$-34.5 \pm 2.4$	$-0.666 \pm 0.012$	$-7.25 \pm 0.23$
3	29	$-16.6 \pm 1.2$	$-0.500 \pm 0.007$	$-7.72 \pm 0.19$
2	29	$-2.97 \pm 0.28$	$-0.333 \pm 0.006$	$-8.68 \pm 0.26$
1	26	$-0.0054 \pm 0.0015$	$-0.167 \pm 0.006$	$-11.64 \pm 0.75$
-2	21	$87900 \pm 1600$	$0.333 \pm 0.005$	$-2.92 \pm 0.12$
-3	21	$18000 \pm 560$	$0.500 \pm 0.009$	$-3.90 \pm 0.21$
-4	21	$6690 \pm 290$	$0.666 \pm 0.013$	$-4.39 \pm 0.26$
-5	21	$3410 \pm 180$	$0.833 \pm 0.018$	$-4.69 \pm 0.29$

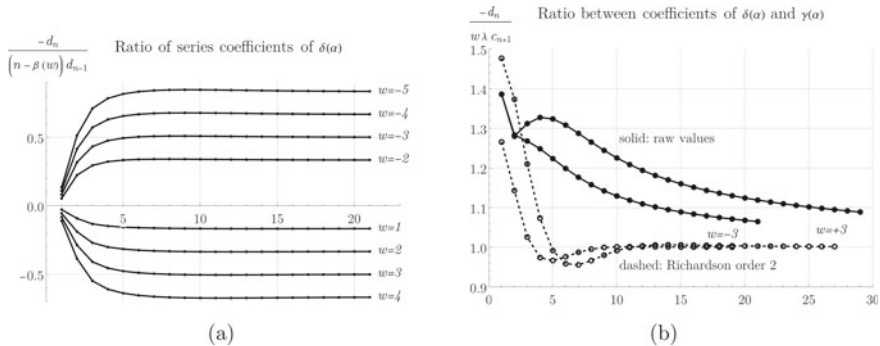


**Fig. 4.7** **a** Ratio of successive coefficients  $d_n$  of  $\delta(\alpha)$  (Eq. (4.45)), divided by the assumed leading asymptotic behavior from Eq. (3.54), for the multiedge DSE in  $D = 6$ . We see that the asymptotic value of this ratio is  $-w/6$ . **b** Ratio between the coefficients  $d_n$  of  $\delta(\alpha)$  and the coefficients  $c_{n+1}$  of  $\gamma(\alpha)$ . Compared to Fig. 4.5a, the raw values converge more slowly, but not the Richardson extrapolation. This indicates the presence of a significant subleading correction, see Table 4.6. See [3] for plots of different  $w$

The ratio from Eq. (4.49),

$$\frac{-d_n}{w \lambda(w) c_{n+1}} = \frac{d_n}{6c_{n+1}},$$

is depicted in Fig. 4.7b for two particular values of  $w$ . The asymptotic parameters, according to Eq. (4.49), are reported in Table 4.6. The convergence of this ratio is much less rapid than for the case  $D = 4$  above. We find empirically  $r_1(w) = (2.12 + 2.15w)/w$ , but the uncertainties are too large to exactly identify rational numbers. This is reflected by the large absolute values we obtain for the  $1/n^2$ -correction  $r_2(w)$ , see Table 4.6.

**Table 4.6** Numerical parameters of the ratio  $d_n/(6c_{n+1})$  for  $D = 6$  from Eq.(4.49)

$w$	$r(w)$	$r_1(w)$	$r_2(w)$
5	$1.0010 \pm 0.0017$	$2.573 \pm 0.072$	$-6.91 \pm 0.84$
4	$1.0007 \pm 0.0019$	$2.685 \pm 0.072$	$-7.3 \pm 1.4$
3	$1.0007 \pm 0.0024$	$2.863 \pm 0.078$	$-8.4 \pm 1.8$
2	$1.0010 \pm 0.0026$	$3.21 \pm 0.11$	$-11.2 \pm 1.8$
1	$1.0032 \pm 0.0048$	$4.22 \pm 0.23$	$-22.3 \pm 1.3$
-2	$1.0000 \pm 0.0002$	$1.083 \pm 0.003$	$-1.10 \pm 0.34$
-3	$1.0002 \pm 0.0004$	$1.441 \pm 0.012$	$-1.80 \pm 0.07$
-4	$1.0003 \pm 0.0007$	$1.619 \pm 0.018$	$-2.33 \pm 0.16$
-5	$1.0004 \pm 0.0008$	$1.726 \pm 0.022$	$-2.71 \pm 0.22$

For  $D = 4$  (Sect. 4.5.1), the suspected vanishing of  $r_{j \geq 2}$  allowed us to explicitly deduce the asymptotics of  $d_n$ , Eq.(4.51). This is not possible in  $D = 6$  since the  $r_{j \geq 2}$  do not vanish. Our findings suggest that the leading growth coincides with the one of  $c_{n+1}$ , that is

$$d_n \sim S(w)w \left(\frac{w}{6}\right)^n \Gamma\left(n + 1 + \frac{35 + 29w}{6w}\right). \quad (4.54)$$

### 4.5.3 Toy Model

The DSE of the toy model was introduced in Example 103, the shift for the linear case is given in Example 126.

We solved the non-linear toy model DSE for  $w \in \{-5, \dots, +4\}$  symbolically to order  $\alpha^{16}$ . Numerically, we reached order  $\alpha^{23}$ , but since  $c_n = 0$  for every even  $n$ , we effectively have only 12 coefficients at our disposal for asymptotic analysis. The leading-log functions  $H_1$ ,  $H_2$  and  $H_3$  agree with the general formula Eq.(3.41) given by [18] for the appropriate choice  $c_1 = 1$ ,  $c_2 = 0$ ,  $c_3 = \pi^2/2$  and for all values of  $w$ . Especially, we confirm  $H_2 = H_4 = H_6 = 0$ , and, for  $w = -2$ , the formula for  $H_1$  from [19, Corollary 3.6.4].

By Lemma 68, the shift  $\delta(\alpha)$  does not have a constant term in the toy model, compare Example 126. We compute and analyze the series expansion Eq.(4.45) of the shift in the same way we did in Sect. 4.5.1 and 4.5.2 for the multiedge DSE. The first coefficients for the shift are reported in Table 4.8, while Table 4.7 contains the numerical estimates for their growth parameters.

In the toy model, both  $c_n$  and  $d_n$  from Eq.(4.45) vanish for even  $n$ . Consequently, the ratio Eq.(4.49) is not well defined. Instead, we mimic the latter ratio by considering the following two ratios for odd  $n$ :

**Table 4.7** Numerical findings of the growth parameters of  $\bar{\delta}(\alpha)$  in the toy model, according to Eq. (4.48).  $\tilde{S}(w)$  is consistent with Table 3.4

$w$	$n_{\max}$	$\tilde{S}(w)/w$	$\tilde{F}(w)$	$\tilde{\beta}(w)$
4	23	$-0.389 \pm 0.010$	$3.985 \pm 0.081$	$-2.50 \pm 0.21$
3	23	$-0.485 \pm 0.015$	$2.988 \pm 0.068$	$-2.68 \pm 0.24$
2	23	$-0.612 \pm 0.023$	$1.991 \pm 0.059$	$-3.02 \pm 0.31$
1	23	$-0.572 \pm 0.037$	$0.996 \pm 0.056$	$-4.09 \pm 0.56$
-2	23	$0.6382 \pm 0.0067$	$1.997 \pm 0.012$	$-0.991 \pm 0.050$
-3	23	$0.5275 \pm 0.0076$	$2.994 \pm 0.024$	$-1.322 \pm 0.071$
-4	23	$0.4202 \pm 0.0069$	$3.991 \pm 0.037$	$-1.488 \pm 0.082$
-5	23	$0.3443 \pm 0.0060$	$4.988 \pm 0.051$	$-1.588 \pm 0.088$

**Table 4.8** First coefficients of  $\delta(\alpha)$  in the toy model, up to order  $\alpha^{11}$ . Here,  $A := (\alpha\pi)^2/4$ 

$w$	$\alpha\bar{\delta}(\alpha(A))$
5	$-6A - \frac{2009}{3}A^2 - \frac{11563106}{45}A^3 - \frac{173306477104}{945}A^4 - \frac{1228737945883358}{6075}A^5 - \frac{46235332362117842849}{147015}A^6$
4	$-5A - \frac{1130}{3}A^2 - \frac{4316822}{45}A^3 - \frac{59632972484}{1323}A^4 - \frac{461687074578658}{14175}A^5 - \frac{34025588969113725668}{1029105}A^6$
3	$-4A - \frac{554}{3}A^2 - \frac{1263424}{45}A^3 - \frac{10282878575}{1323}A^4 - \frac{46540947260036}{14175}A^5 - \frac{398737839692532122}{205821}A^6$
2	$-3A - \frac{217}{3}A^2 - \frac{1233338}{225}A^3 - \frac{4881119933}{6615}A^4 - \frac{3528108924854}{23625}A^5 - \frac{1074400592111547046}{25727625}A^6$
1	$-2A - \frac{55}{3}A^2 - \frac{106898}{225}A^3 - \frac{135875429}{6615}A^4 - \frac{272890120256}{212625}A^5 - \frac{2770658834393158}{25727625}A^6$
0	$-A - \frac{4}{3}A^2 - \frac{146}{45}A^3 - \frac{8864}{945}A^4 - \frac{417682}{14175}A^5 - \frac{9095176}{93555}A^6$
-1	0
-2	$A + 7A^2 + 242A^3 + 17771A^4 + 2189294A^5 + 404590470A^6$
-3	$2A + 41A^2 + \frac{92518}{25}A^3 + \frac{503885698}{735}A^4 + \frac{1639676026462}{7875}A^5 + \frac{266517331818761291}{2858625}A^6$
-4	$3A + \frac{370}{3}A^2 + \frac{4782122}{225}A^3 + \frac{48904622516}{6615}A^4 + \frac{887103429351554}{212625}A^5 + \frac{88600913717695595572}{25727625}A^6$
-5	$4A + \frac{826}{3}A^2 + \frac{3478864}{45}A^3 + \frac{287007344207}{6615}A^4 + \frac{185545372999796}{4725}A^5 + \frac{53252838327756373006}{1029105}A^6$

$$R^{(\delta)} := \sqrt{\frac{d_{n+2}}{(n - \beta(w) + 1)(n - \beta(w) + 2)d_n}}, \quad R^{(\delta/\gamma)} := \frac{d_n}{w \cdot (n - \beta(w) + 1)c_n}. \quad (4.55)$$

Empirically (for details and plots see [3]),  $R^{(\delta)}$  approaches the limit  $|w|$ , which suggests that  $d_n$  scale asymptotically  $\sim w^n \Gamma(n - \beta(w) + 1)$ , with (approximately) the same  $\beta(w)$  (Eq. (3.56)) as the coefficients  $c_n$  of  $\gamma(\alpha)$ .

The quantity  $R^{(\delta/\gamma)}$  allows us to fix the Stokes constant. One finds empirically that the limit of  $R^{(\delta/\gamma)}$  is  $1.00 \pm 0.02$ , suggesting that the Stokes constant agrees with the one of  $\gamma(\alpha)$ . Table 4.7 contains estimates of the asymptotic growth. Even for the anomalous dimension  $\gamma(\alpha)$ , the subleading asymptotic corrections are only known numerically (Table 3.4), we make no attempt to identify rational values for the corrections of  $\delta(\alpha)$ . All in all, we estimate the following asymptotic growth for the coefficients of  $\delta(\alpha)$  in the toy model:

$$d_n \sim S(w)w^{n+1}\Gamma\left(n + \frac{2+2w}{w}\right). \quad (4.56)$$

Some coefficients of the counterterm  $Z$  of the toy model in kinematic renormalization are listed in the appendix of [3]. They satisfy the relations of Theorem 51.

#### 4.5.4 The Chain Approximation in $D=4$

The chain approximation is a model where MS and MOM can not be related by a shift  $\delta(\alpha)$ , we discuss it here to show that the above theory is indeed nontrivial and requires the validity of Dyson–Schwinger equations. We restrict ourselves to  $D = 4 - 2\epsilon$  and consider renormalized quantities only at  $\epsilon = 0$ .

The chain approximation of the multiedge propagator DSE contains the sum of all chain graphs, that is, multiedges where a chain of subgraphs is inserted into one of the edges, without recursive insertions. From a Hopf-algebra perspective, the chain graphs correspond to corollas  $C_j$ ,

$$C_1 = \bullet, \quad C_2 = \text{I}, \quad C_3 = \text{A}, \quad C_4 = \text{AA}.$$

The second chain graph from Example 27 is  $S \simeq C_3$  in this sequence. The chain approximation is non-recursive by nature, and it is not generated by a DSE. Nevertheless, it is sometimes viewed as an intermediate step between the linear ( $w = 0$ ) and the full recursive ( $w = -2$ ) DSE, see for example [20]. The first function of the log-expansion (Eq. (3.2)) in MOM is

$$\gamma_1(\alpha) = - \sum_{n=1}^{\infty} (n-1)!(-\alpha)^n = e^{\frac{1}{\alpha}} \int_{\frac{1}{\alpha}}^{\infty} \frac{dt}{t} e^{-t}. \quad (4.57)$$

The resummed series is the exponential integral (Example 44). Explicit computation of the higher  $\gamma_t(\alpha)$  in MOM produces coefficients which can again be identified,

$$\gamma_{t \geq 1} = (-1)^t \frac{1}{t!} \sum_{n=t}^{\infty} (n-1)!(-\alpha)^n, \quad k\gamma_k(\alpha) = \alpha \cdot \alpha \partial_{\alpha} \gamma_{k-1}(\alpha)$$

$$\Rightarrow \partial_L G_{\mathcal{R}}(\alpha, L) = \gamma_1(\alpha) + \alpha \cdot \alpha \partial_{\alpha} G_{\mathcal{R}}(\alpha, L). \quad (4.58)$$

Although the last equation is reminiscent of the Callan–Symanzik equation Theorem 41 for a beta function  $\beta(\alpha) = \alpha$ , it is structurally different. The function  $\gamma_1(\alpha)$  is not the anomalous dimension of this model in the conventional physical sense, because it is not a prefactor of  $G_{\mathcal{R}}(\alpha, L)$ .

In Minimal Subtraction, we find by explicit calculation

$$\begin{aligned} \bar{\gamma}_0(\alpha) &= 1 - 2\alpha + \frac{11}{2}\alpha^2 - \left( \frac{37}{3} + \frac{2}{3}\zeta(3) \right)\alpha^3 + \left( \frac{169}{4} - \frac{1}{120}\pi^4 + \frac{1}{2}\zeta(3) \right)\alpha^4 + \dots \\ &=: \sum_{r=0}^{\infty} r_k(-\alpha)^k. \end{aligned}$$

The coefficients grow approximately as  $r_k \sim (k-1)!$ . The other expansion functions  $\bar{\gamma}_{t>0}(\alpha)$  empirically do not contain zeta values and are purely rational. The first of them is

$$\bar{\gamma}_1(\alpha) = \alpha - 3\alpha^2 + 10\alpha^3 - 38\alpha^4 + 168\alpha^5 - 872\alpha^6 + 5296\alpha^7 \pm \dots = \sum_{n=1}^{\infty} c_n(-\alpha)^n. \quad (4.59)$$

Empirically, the coefficients agree with [A010842] [11],  $c_n = (n-1)![x^{n-1}] \frac{e^{2x}}{x-1}$ .

The higher  $\bar{\gamma}_j$ , but not  $\bar{\gamma}_0$ , satisfy the recursion

$$k\bar{\gamma}_k(\alpha) = \alpha \cdot \alpha \partial_{\alpha} \bar{\gamma}_{k-1}(\alpha),$$

which is reminiscent of Theorem 42.  $\bar{\gamma}_0$  can not possibly satisfy the same equation because it is the only function to contain zeta values. Again, the function  $\bar{\gamma}(\alpha) = \alpha$  can not be interpreted as the anomalous dimension in the conventional physical sense.

For the chain approximation, it is not possible to consistently define a shift  $\delta(\alpha)$  between MS and MOM. The algorithms of Sect. 4.4.3 are not even applicable since they require a value  $w$  from the DSE. The brute-force algorithm (Sect. 4.4.2) does produce some solution  $\delta(\alpha)$  if the series are truncated. However, the solutions differ depending on whether  $\bar{\gamma}_0$  was included in the linear system or not. This was to be expected because the underlying formula  $\tau = e^{*\delta\sigma}$  (Theorem 59) is only valid for solutions of Dyson–Schwinger equations.

Regarding the physical validity of the chain approximation, we conclude the following: It is surely valid as an “approximation” in the sense that it includes a proper subset of the graphs of the full solution  $w = -2$ . Moreover, the would-be “anomalous dimension” Eq. (4.57) qualitatively resembles the true solution, see Fig. 4.8.

However, the chain approximation is not self-consistent in perturbation theory, it does not satisfy a Callan–Symanzik equation and therefore transforms inconsistently

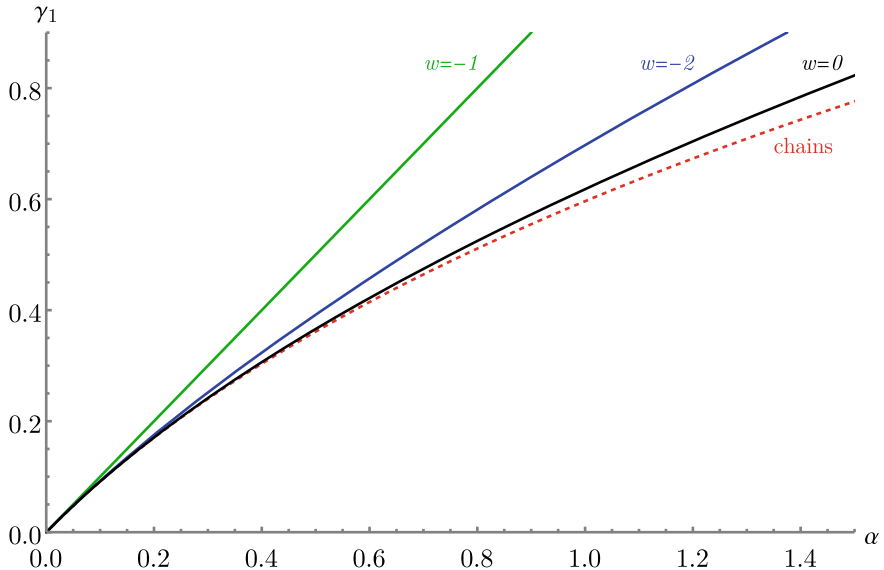


**Fig. 4.8** The function  $\gamma_1(\alpha)$  in MOM for different variants of the multiedge DSE in  $D = 4$  (Example 104). Green: trivial solution  $\gamma = \alpha$  for  $w = -1$ . Black: linear DSE (Example 115). Blue: exact parametric solution for  $w = -2$  from [21]. Red: chain approximation Eq. (4.57). Even if these four functions have significantly different properties in perturbation theory,  $w = 0$  and  $w = -1$  being convergent series while the other ones are asymptotic, their graphs look similar

in the renormalization group. Concretely, in different renormalization schemes, the chain approximation will give rise to physically inequivalent solutions, which can not be mapped one another by rescaling of arguments. The combinatorial reason for this is obvious: The chain approximation does not arise from a DSE and therefore does not have the “recursive” features to be expected from a QFT amplitude. Our verdict is that the chain approximation, without further justifications, is not a valid model to establish *combinatorial* properties of QFT, such as the presence of renormalons [22–24], because it systematically misses one of the key features of QFT combinatorics.

### Summary of Sect. 4.5.

1. For the non-linear multiedge DSE in  $D = 4$ , the shift  $\delta(\alpha)$  is given by a factorially divergent power series very similar to the anomalous dimension  $\gamma(\alpha)$ . From our numerical data, we guessed closed formulas for all the asymptotic coefficients and gave a tentative equation which relates  $\delta(\alpha)$  and  $\gamma(\alpha)$  up to an unknown convergent power series (Sect. 4.5.1).
2. For the non-linear multiedge DSE in  $D = 6$ , the asymptotic growth of the coefficients of  $\delta(\alpha)$  is very similar to the one of  $\gamma(\alpha)$ . This time, we did not find an explicit formula for all subleading corrections (Sect. 4.5.2).

3. The non-liner toy model DSE, again, behaves qualitatively similar to the multiedge case, but the concrete relation between  $\gamma$  and  $\delta$  is even less accurate than in 2 (Sect. 4.5.3).
4. The chain approximation does not satisfy a Dyson–Schwinger equation and its amplitudes are truly different in different renormalization schemes. We argued that the chain approximation is systematically inconsistent and should not be used for combinatorial arguments, even if in specific renormalization schemes, it empirically gives rise to similar Green functions as the other models (Sect. 4.5.4).

## References

1. D.J. Broadhurst, D. Kreimer, Renormalization automated by Hopf algebra. *J. Symb. Comput.* **27**, 581 (1999). [arXiv:hep-th/9810087](https://arxiv.org/abs/hep-th/9810087)
2. D. Kreimer, E. Panzer, Renormalization and Mellin transforms. Computer Algebra in Quantum Field Theory, Texts & Monographs in Symbolic Computation (2013), pp. 195–223. [arXiv:1207.6321](https://arxiv.org/abs/1207.6321)
3. P.-H. Balduf, Dyson–Schwinger equations in minimal subtraction. *Annales de l’Institut Henri Poincaré D* (2023). <https://doi.org/10.4171/ihpd/169>. <https://ems.press/journals/aihpda/articles/1023930>
4. G. ’t Hooft, Dimensional regularization and the renormalization group. *Nuclear Phys. B* **61**, 455–468 (1973). <https://www.sciencedirect.com/science/article/pii/0550321373903763>
5. A. Connes, D. Kreimer, Renormalization in quantum field theory and the Riemann–Hilbert problem II: the beta-function, diffeomorphisms and the renormalization group. *Commun. Math. Phys.* **216**, 215–241 (2001) [arxiv:hep-th/0003188](https://arxiv.org/abs/hep-th/0003188)
6. A. Connes, M. Marcolli, *Noncommutative Geometry, Quantum Fields and Motives*, vol. 55. Colloquium Publications (American Mathematical Society, Providence, Rhode Island, 2007). <http://www.ams.org/coll/055>
7. D. Kreimer, Chen’s Iterated Integral represents the Operator Product Expansion (1999). [arXiv:hep-th/9901099](https://arxiv.org/abs/hep-th/9901099)
8. E. Panzer, Renormalization, Hopf algebras and Mellin transforms (2015). [arxiv:1407.4943](https://arxiv.org/abs/1407.4943)
9. J. Bernoulli, *Ars conjectandi, opus posthumum. Accedit Tractatus de seriebus infinitis, et epis-tola gallic é scripta de ludo pilae reticularis* (impensis Thurnisiorum, fratrum, Basileae, 1713)
10. K. Ebrahimi-Fard, J.M. Gracia-Bondia, L. Guo, J.C. Varilly, Combinatorics of renormalization as matrix calculus. *Phys. Lett. B* **632**, 552–558 (2006). [arXiv:hep-th/0508154](https://arxiv.org/abs/hep-th/0508154)
11. N.J.A. Sloane (ed.), *The On-Line Encyclopedia of Integer Sequences* (2023). <https://oeis.org>
12. K. Bönisch, F. Fischbach, A. Klemm, C. Nega, R. Safari, Analytic structure of all loop banana amplitudes. *J. High Energy Phys.* **05**, 066 (2021). [arXiv:2008.10574](https://arxiv.org/abs/2008.10574)
13. G. Mack, I.T. Todorov, Conformal-invariant green functions without ultraviolet divergences. *Phys. Rev. D* **8**, 1764–1787 (1973). <https://link.aps.org/doi/10.1103/PhysRevD.8.1764>
14. D. Kreimer, Étude for linear Dyson–Schwinger equations, in *Traces in Number Theory, Geometry and Quantum Fields*. Aspects of Mathematics E38 (Vieweg Verlag, Wiesbaden, 2008), pp. 155–160. <http://preprints.ihes.fr/2006/P/P-06-23.pdf>
15. W. Celmaster, R.J. Gonsalves, Renormalization-prescription dependence of the quantum-chromodynamic coupling constant. *Phys. Rev. D* **20**, 1420 (1979). <https://link.aps.org/doi/10.1103/PhysRevD.20.1420>
16. W. Celmaster, R.J. Gonsalves, Quantum-chromodynamics perturbation expansions in a coupling constant renormalized by momentum-space subtraction. *Phys. Rev. Lett.* **42**, 1435 (1979). <https://link.aps.org/doi/10.1103/PhysRevLett.42.1435>

17. A.J. McKane, Perturbation expansions at large order: results for scalar field theories revisited. *J. Phys. A: Math. Theor.* **52**, 055401 (2019). [arXiv:1807.00656](https://arxiv.org/abs/1807.00656)
18. O. Krüger, Log expansions from combinatorial Dyson–Schwinger equations. *Lett. Math. Phys.* **110**, 2175–2202 (2020). <https://doi.org/10.1007/s11005-020-01288-8>
19. E. Panzer, Hopf algebraic Renormalization of Kreimer’s toy model (2012). [arXiv:1202.3552](https://arxiv.org/abs/1202.3552)
20. M. Borinsky, G.V. Dunne, Non-perturbative completion of Hopf-algebraic Dyson-Schwinger equations. *Nuclear Phys. B* **957**, 115096 (2020). <http://www.sciencedirect.com/science/article/pii/S0550321320301826>
21. D.J. Broadhurst, D. Kreimer, Exact solutions of Dyson-Schwinger equations for iterated one-loop integrals and propagator-coupling duality. *Nuclear Phys. B* **600**, 403–422 (2001). [arXiv:hep-th/0012146](https://arxiv.org/abs/hep-th/0012146)
22. M. Beneke, Renormalons. *Phys. Rep.* **317**, 1–142 (1999). <https://www.sciencedirect.com/science/article/pii/S0370157398001306>
23. D. Espriu, R. Tarrach, Ambiguities in QED: renormalons versus triviality. *Phys. Lett. B* **383**, 482–486 (1996). <https://www.sciencedirect.com/science/article/pii/0370269396007794>
24. G.V. Dunne, M. Meynig, Instantons or renormalons? a comment on phi4\_4 theory in the MS scheme (2021). [arXiv:2111.15554](https://arxiv.org/abs/2111.15554)

# Chapter 5

## Field Diffeomorphisms and Symmetries



The fifth chapter deals broadly with the role of symmetries in renormalization theory, and specifically with the invariance of scalar quantum fields under a non-linear change of the field variable.

In Sect. 5.1.1, we discuss from an abstract perspective how symmetries are treated in a renormalizable quantum field theory: They take the form of Ward identities between renormalized Green functions, or of ideals in the renormalization Hopf algebra. For the scalar fields considered in the present thesis, an important Hopf ideal is spanned by tadpole graphs, we discuss under which conditions it is allowed to ignore all tadpole contributions.

Section 5.2 is about non-linear redefinitions of the field variable. Such a redefinition is a diffeomorphism, that is, a differentiable mapping. We show that a diffeomorphism changes the offshell Green functions, but leaves the S-matrix invariant. For Feynman rules in position space, a diffeomorphism is relatively straightforward, while the Feynman rules in momentum space involve momentum-dependent vertices that can cancel adjacent edges. We show that these cancellations conspire, to all orders in perturbation theory, to reproduce the expected result from position space.

In Sect. 5.3, we consider a specific class of diffeomorphisms, essentially given by exponential functions. Such diffeomorphisms have particularly nice combinatorial properties because the vertices are proportional to each other. This is an interesting model because a similar, but more complicated, mechanism is at work in quantum gravity: There are vertices of arbitrary valence, but there is only one coupling constant, hence the higher order vertices are powers of the lower order ones.

In Sect. 5.4, we examine the counterterms and divergences of a field diffeomorphism. A diffeomorphism of any renormalizable theory is perturbatively non-renormalizable. However, for the special case of exponential diffeomorphisms introduced above, the number of independent counterterms reduces significantly.

## 5.1 Symmetries and Hopf Ideals

We have so far only considered a one-component scalar quantum field, which is sufficient to establish most of the principles of renormalization. In the present section, we examine how symmetries are encoded in the Hopf algebra.

### 5.1.1 Symmetries

**Theorem 72** (Coleman-Mandula-Haag [1, 2]). Under technical conditions listed in the cited works, every symmetry group  $G$  of the  $S$ -matrix (Definition 18) is isomorphic to the direct product of

1. The Poincaré group (Definition 3),
2. The group of supersymmetric transformations between bosons and fermions,
3. Internal symmetry groups of the fields (Definition 116).

All our quantum field theories are Poincaré-symmetric by construction (Definition 6), supersymmetry has never been observed experimentally in particle physics, consequently, the most relevant part of  $G$  for us is the *internal* symmetry.

**Definition 116.** An *internal symmetry* of a quantum field theory, defined by a Lagrangian  $\mathcal{L}$  (Definition 5), is a group  $G$  such that the quantum field operators are representations of  $G$ , acted upon by an unitary operator  $U(g)$  which leaves the action (Definition 7) invariant:

$$\int d^D \underline{x} U^\dagger(g) \mathcal{L} U(g) = \int d^D \underline{x} \mathcal{L} = S[\phi], \quad \forall g \in G.$$

#### Example 127: Gauge transformation of complex scalar field.

If the field variable  $\phi$  of a scalar field (Example 6) is not real, but complex, then the theory can have a global  $U(1)$  symmetry given by the transformations, which are independent of spacetime:

$$\phi \mapsto e^{i\alpha} \phi, \quad \phi^* \mapsto e^{-i\alpha} \phi^*, \quad \alpha \in \mathbb{R}.$$

These transformations are given by one real parameter, the gauge group is the Lie group  $U(1)$ . A square of fields transforms as  $\phi^* \phi \mapsto \phi^* e^{-i\alpha} e^{i\alpha} \phi = \phi^* \phi$ . Consequently, to be symmetric under these transformations, the Lagrangian must be a function of products  $\phi^* \phi$ . The complex analogue of the  $\phi^4$ -Lagrangian is

$$\mathcal{L} = -\frac{1}{2} \partial_\mu \phi^* \partial^\mu \phi - \frac{\lambda_4}{4!} (\phi^* \phi)^2.$$

An internal symmetry (Definition 116) is *local* if the transformation parameters depend on spacetime. In that case, the kinetic term of the Lagrangian gives rise to derivatives of the transformation parameter, which destroy the symmetry of the action. In order to restore symmetry, one needs to introduce a second field, which couples to the original one in a particular way called *gauge covariant derivative* and which transforms in a way to absorb the superfluous terms. This field is called *gauge boson*, the corresponding QFT is a *gauge theory*.

### Example 128: Gauge transformation in QED.

Quantum electrodynamics (Example 23) contains two fields, the potential  $A^\mu(\underline{x}) := (\Phi(\underline{x}), \mathbf{A}(\underline{x}))$ , and the fermion field  $\psi(\underline{x})$ . The Lagrangian is

$$\mathcal{L} = \bar{\psi} (i \gamma^\mu D_\mu - m) \psi - \frac{1}{4} F_{\mu\nu} F^{\mu\nu}, \quad D_\mu := \partial_\mu - ie A_\mu.$$

The Lagrangian of the fermion field  $\psi$  alone, without coupling to  $A^\mu$ , has the freedom to globally transform under the group  $U(1)$ ,  $\psi(\underline{x}) \mapsto e^{-ie\alpha} \psi(\underline{x})$ . Here,  $e$  is the electromagnetic charge of the fermion and  $\alpha$  is a constant.

The potential  $A^\mu$  has a gauge freedom  $A^\mu(\underline{x}) \mapsto A^\mu(\underline{x}) - \partial^\mu \alpha(\underline{x})$  for any differentiable function  $\alpha(\underline{x})$ , because all observables are functions of the field strength tensor  $F_{\mu\nu} := \partial_\mu A_\nu - \partial_\nu A_\mu$ . Consequently, also the pure electromagnetic Lagrangian  $F_{\mu\nu} F^{\mu\nu}$  is gauge invariant.

If  $\psi$  is coupled to  $A^\mu$  with the interaction term  $e\bar{\psi}\gamma^\mu A_\mu$ , arising from the gauge covariant derivative  $D_\mu$ , then the gauge transformation of  $\psi$  can be promoted to a local transformation as well, because the transformation of  $A^\mu$  cancels the non-invariant term arising from  $\psi$ . The photon field  $A^\mu$  is the gauge boson of QED since it allows the fermion field to be locally gauge invariant.

Internal symmetries are often related to the spin of particles, this is plausible by the following heuristics: The free part of quantum field theory of higher spin particles is typically based on the *Fierz-Pauli-Dirac* Lagrangian [3–5]. There, a particle with integer spin  $n$  is represented by a symmetric tensor with  $n$  indices (As Fierz pointed out later [6], this setup equivalently describes a non-local scalar field [7]). Nevertheless, by representation theory of the Lorentz group [8], a massless particle has only two degrees of freedom. This entails that many of the tensor entries are not

independent, and the form of possible interaction terms is restricted. A symmetry then amounts to the equivalence of different choices of the two independent degrees of freedom. For spin 1 and spin 2 massless unconfined particles, one finds that the Maxwell equations ([9], Example 7) and the Einstein equations ([10], Sect. 5.2.1)—together with their corresponding local gauge symmetries—follow automatically from Lorentz covariance [11–13]. Similarly, for spin 3 or higher, there are only very few consistent types of interactions [14–19].

Within a gauge theory, the  $n$ -point Green functions (Definition 14) are a priori not well defined, because with a suitable local gauge transform, the field can be altered almost arbitrarily at any given point. In order to calculate Green functions, one needs to fix the gauge and introduce fictitious particles with opposite statistics, called *gauge ghost particles*, which cancel superfluous degrees of freedom. This procedure gives rise to additional terms in the Lagrangian, and to corresponding vertices and propagators in Feynman graphs. The choice of gauge is arbitrary [20] within the limit that it must not destroy renormalizability of the theory [21, 22]. Physical observables are independent of the chosen gauge, compare [23]. We skip details because in the present thesis, we never need gauge fixing explicitly.

### 5.1.2 Ward Identities

As seen in Example 128, gauge invariance of the theory crucially depends on the presence, and precise numerical relation, of certain monomials in the Lagrangian. During renormalization, each monomial is rescaled by its corresponding Z-factor (Sect. 3.2.2), which depend on the energy scale in question. The renormalized QFT is gauge invariant if and only if the classical theory is, and all monomials in question are rescaled with the same Z-factor.

**Definition 117.** Consider a QFT where the underlying Lagrangian has an internal symmetry (Definition 116). A *Ward identity* or *Slavnov-Taylor identity* is an algebraic relation between the Z-factors (Definition 106) of those terms of the Lagrangian which are involved in the symmetry, which ensures that the symmetry is preserved in presence of the Z-factors.

#### Example 129: Ward identity in QED.

The Z-factors for the QED Lagrangian (Example 23) can be chosen as (e.g. [24])

$$\mathcal{L} = Z_2 \bar{\psi} \left( i\gamma^\mu \partial_\mu + \frac{Z_1}{Z_2} e\gamma^\mu A_\mu - Z_m m \right) \psi - \frac{1}{4} Z_3 F_{\mu\nu} F^{\mu\nu}.$$

If the renormalized theory is to be gauge invariant, then the gauge-covariant derivative must retain its form  $D_\mu = \partial_\mu - ieA_\mu$  after renormalization. This is possible only if the Ward identity (Definition 117)

$$\frac{Z_1}{Z_2} = 1 \quad \Leftrightarrow \quad Z_1 = Z_2$$

holds. This identity was suspected by Dyson in [25], and little after proven in a remarkably short article [26] by Ward.

From the perspective of Feynman graphs, the Ward identity in QED holds because one obtains all vertex graphs by adding exactly one more vertex into any of the internal fermion edges of the propagator graphs, see [27–29].

The concrete value of  $Z$ -factors depends on renormalization conditions [30]. If one uses kinematic renormalization (Definition 93), then the momentum of the individual edges of the vertex at the renormalization point must match the corresponding 2-point functions, [31, 32]. In Minimal Subtraction (Definition 110), Ward identities typically hold without additional constraints [27, 33]. Further, the concrete form of Ward identities heavily depends on the chosen gauge [34–36]. Finally, a Ward identity is valid in a regularized theory (where the regulator is not yet removed) only under the condition that the regularization procedure respects the symmetry, compare for example [37, 38]. A main reason for the popularity of dimensional regularization (Sect. 2.3.3) is that this regularization scheme does not spoil Ward identities in QED and QCD, while, for example, cutoff regularization does.

By Definition 117, Ward identities are equations for the  $Z$ -factors. Alternatively, they be expressed as identities for renormalized Green functions, compare for example [39].

### Example 130: Alternative forms of the Ward identity in QED.

The Ward identity in QED can be stated in the following forms. We do not claim that all forms are equivalent in full generality.

1.  $Z_1 = Z_2$  (Example 129)
2. The transversally projected 1PI vertex is the difference of electron propagators,

$$\left( \underline{p}_2 - \underline{p}_1 \right)^\mu G_{\mathcal{R},\mu}^{\nwarrow}(\underline{p}_1, -\underline{p}_2) = G_{\mathcal{R}}^{\nearrow}(\underline{p}_1) - G_{\mathcal{R}}^{\nearrow}(\underline{p}_2),$$

where  $\underline{p}_1, -\underline{p}_2$  are the momenta of the two electron edges entering the vertex.

3. The vertex at zero momentum transfer is the derivative of the electron propagator,

$$G_{\mathcal{R},\mu}^{\nwarrow}(\underline{p}, -\underline{p}) = -\frac{\partial}{\partial p^\mu} G_{\mathcal{R}}^{\nearrow}(\underline{p}).$$

4. All renormalized photon  $n$ -point  $S$ -matrix elements are transversal,

$$p_1^{\mu_1} G_{\mathcal{R}, \mu_1, \dots}^{(n)}(\underline{p}_1, \dots) = 0 \quad \text{for } \underline{p}_1^2 = 0.$$

5. The renormalized photon propagator is massless.

### Example 131: QCD.

Quantum Chromodynamics (QCD) is a gauge theory similar to QED (Example 23), but for an underlying non-Abelian symmetry group  $SU(3)$ . It can be formulated in terms of gauge-covariant derivatives  $D_\mu = \partial_\mu + ieA_\mu$  just like QED. The gauge field  $A_\mu^a = t^a A_\mu$  represents gluons, it carries an index  $a \in \{1, \dots, 8\}$  of the  $SU(3)$  adjoint representation matrix  $t^a$ . Since  $SU(3)$  is not Abelian, the structure constants  $f^{abc}$ , defined as  $[t^a, t^b] = if^{abc}t^c$ , do not vanish, and the field strength tensor involves a quadratic term in  $A_\mu^a$ ,

$$F_{\mu\nu}^a = \frac{1}{-ig} [D_\mu, D_\nu] = \partial_\mu A_\nu^a t^a - \partial_\nu A_\mu^a t^a + g f^{abc} A_\mu^b A_\nu^c t^a,$$

where  $g$  is the QCD coupling constant.

Unlike QED (Example 23), the Lagrangian of the gluon field in QCD, called *Yang-Mills Lagrangian* [40], contains cubic and quartic summands, expressing a self-interaction among gluons:

$$\mathcal{L}_{\text{QCD}} = -\frac{1}{4} \left( \partial_\mu A_\nu^a - \partial_\nu A_\mu^a + g f^{abc} A_\mu^b A_\nu^c \right) \left( \partial^\mu A^{a\nu} - \partial^\nu A^{a\mu} + g f^{abc} A^{b\mu} A^{c\nu} \right).$$

Possible gauges that do not spoil renormalizability are discussed in [22]. The case of the Abelian gauge group  $U(1)$  in QED (Example 23) is reproduced from  $\mathcal{L}_{\text{QCD}}$  in the case of vanishing structure constants  $f^{abc}$ .

For theories with more than one vertex, such as QCD, each vertex comes with an invariant charge (see Example 82) and a beta function (Definition 105), which determines how the amplitude of that vertex changes with the energy scale (Definition 104). The presence of a symmetry should not depend on the energy scale, therefore a Ward identity should hold all energy scales. Consequently, all vertices involved in the Ward identity must scale with the same beta function. This entails that their invariant charges must agree.

### Example 132: Slavnov-Taylor identities in QCD.

The gluon in Quantum chromodynamics (Example 131) is a massless spin-1 particle, it has only two degrees of freedom, which are transversal [8, 11, 12, 41].

The Yang-Mills Lagrangian (Example 131) has a 3-valent and a 4-valent gluon vertex. The 3-gluon vertex scales  $\sim p$  for the incoming momenta. If two 3-gluon vertices are joined with an intermediate gluon propagator  $\sim \frac{1}{q^2}$ , then the overall amplitude of this 4-valent tree scales as  $q^0$ , and it has summands which do not vanish when projected onto the external momenta. The 4-gluon vertex cancels this non-transversal term.

In order for the cancellation to work at all energy scales, both types of graphs, the 4-point function and the product of two 3-point functions, must scale identically. Consequently, the invariant charges (Example 82) which determine their scaling (Definition 104), must agree:

$$\sqrt{Q_{\text{---}}}, \sqrt{Q_{\text{---}}} = Q_{\text{---}}.$$

$Q_{\text{---}}$  already contains the appropriate factor for the intermediate gluon propagator.

Inspecting the cancellation mechanism for non-transversal terms in other vertices, one finally arrives at  $Q_{\text{---}} = Q_{\text{---}} = Q_{\text{---}} = Q_{\text{---}}$ . These are the Slavnov-Taylor identities [27, 42, 43]. They express that QCD has only one beta function, which scales *all* vertices simultaneously.

A more conventional notation is to write the Slavnov-Taylor identities directly for the  $Z$ -factors, or, equivalently, as identities for combinatorial 1PI Green functions:

$$\frac{Z_{\text{---}}}{Z_{\text{---}}} = \frac{Z_{\text{---}}}{Z_{\text{---}}} = \frac{Z_{\text{---}}}{Z_{\text{---}}} = \frac{Z_{\text{---}}}{Z_{\text{---}}}, \quad \text{or, at fixed angles,} \quad \frac{\Gamma_{\text{---}}}{\Gamma_{\text{---}}} = \frac{\Gamma_{\text{---}}}{\Gamma_{\text{---}}} = \frac{\Gamma_{\text{---}}}{\Gamma_{\text{---}}} = \frac{\Gamma_{\text{---}}}{\Gamma_{\text{---}}}.$$

Much like in QED (Example 129), the validity of the Slavnov-Taylor identities can be established order by order in perturbation theory by considering the involved Feynman graphs. But the QCD graphs often involve non-trivial symmetry factors (Sect. 1.3.8). Here, the mechanism of Example 30 comes into play, ensuring that symmetry factors match when vertices are being merged and split.

Another interesting perspective on the Slavnov-Taylor identities is the *corolla polynomial* [44–47]. It encodes a combinatorial algorithm to obtain the full QCD integrand from the graphs of scalar  $\phi^3$  theory. The validity of the Slavnov-Taylor identities, and therefore gauge symmetry and transversality of the resulting theory, is then a consequence of the fact that all gluon graphs arise from the same algebraic operations, applied to the same underlying scalar graphs.

By Definition 117, a Ward identity reduces the number of independent  $Z$ -factors and hence the number of necessary renormalization conditions. If the Ward identities in QED and QCD would not hold, then all vertices need their individual, independent

renormalization conditions. The quantized theory is then no longer gauge invariant, and the bosons (photon or gluon) are massive, completely altering the nature of their interactions. Nonetheless, QED and QCD would be renormalizable (Definition 100) by power counting (Theorem 30) even without Ward identities. As phrased by 't Hooft and Veltman [48, Chap. 13.1]:

Indeed, Ward identities have nothing to do with renormalizability but everything to do with unitarity.

### 5.1.3 Hopf Ideals

On the level of Feynman graphs, a Ward identity (Definition 117) amounts to setting certain classes of graphs equal, or, alternatively, assigning the value of zero to their difference. In order to be a physical symmetry, such identification must hold for all momentum scales  $L$  (Definition 83).

**Example 133: Ward identity in QED, identification of graphs.**

The Ward identity  $Z_1 - Z_2 = 0$  in QED (Example 129) is, with our sign convention (Definition 49),  $S_{\mathcal{R}}^{\mathcal{F}}[\Gamma^{\text{W}}] + S_{\mathcal{R}}^{\mathcal{F}}[\Gamma^{\text{F}}] = 0$ . Here,  $\Gamma^r$  is the combinatorial 1PI Green function (Definition 47). At 1-loop level, we denote the Ward identity by

$$\text{Diagram } + \text{Diagram} = 0.$$

This is meant to hold for the corresponding renormalized amplitudes for all momenta  $p$ , but only if the vertex has zero momentum transfer, as in point 3 in Example 130.

By Definition 102 Theorem 50, and Lemma 39, the behavior of  $\mathcal{F}_{\mathcal{R}}[\Gamma]$  under change of momentum scale is encoded in the coproduct  $\Delta(\Gamma)$ :

$$\frac{\partial}{\partial L} \mathcal{F}_{\mathcal{R}}[\Gamma^a](L) = (\sigma \star \tau \star e^{L\sigma}) \Gamma^a = (\sigma \star \mathcal{F}_{\mathcal{R}}(L)) \Gamma^a = m (\sigma \otimes \mathcal{F}_{\mathcal{R}}) \Delta(\Gamma^a).$$

If we want a Ward identity to hold at all scales, then the coproduct of the graphs involved in that identity must behave in an appropriate way. To understand the mechanism, we firstly consider the solution  $\Gamma^a$  of a Dyson-Schwinger equation (Theorem 28)  $\Gamma^a = 1 + \alpha B_+(\Gamma^a Q_a)$ , and we let  $\gamma_j^a = [\alpha^j] \Gamma^a$ . By Theorem 26,

$$\Delta(\Gamma^a) = \sum_j \Gamma^a Q_a^j \alpha^j \otimes \gamma_j^a.$$

If  $\gamma_j^a = 0$  for all  $j$ , then  $\partial_L \mathcal{F}_{\mathcal{R}}[\Gamma^a](L) = 0$  and  $\mathcal{F}_{\mathcal{R}}[\Gamma^a] = 0$  holds at all scales.

Now consider the sum of two solutions to different DSEs,  $\Gamma^a + \Gamma^b =: W$ . We have

$$\Delta(W) = \Delta(\Gamma^a + \Gamma^b) = \sum_j \alpha^j \left( \Gamma^a Q_a^j \otimes \gamma_j^a + \Gamma^b Q_b^j \otimes \gamma_j^b \right).$$

In general,  $Q_a \neq Q_b$  and the summands do not factorize into the form  $(\Gamma^a + \Gamma^b) \otimes (\gamma_j^a + \gamma_j^b)$ . Consequently, even if we demand  $\gamma_j^a + \gamma_j^b = 0$  for all  $j < n$  then, at order  $n$ , not all factors in the coproduct of  $\gamma_n^a + \gamma_n^b$  will necessarily vanish. Expressed in terms of Feynman rules, this means that even if the Ward identity is enforced for all graphs of loop order  $j < n$ , the corresponding identity at order  $n$  will still depend on the scale non-trivially. If we demand  $\mathcal{F}_R[\Gamma^a + \Gamma^b](L) = 0$  at some scale  $L$ , then this identity will generally not hold for other values of  $L$ .

If some identity of the form  $W = 0$  is supposed to be valid for all scales  $L$ , then we must require  $\Delta(W) \subseteq W \otimes H + H \otimes W$ . That is,  $W$  generates a Hopf ideal (Definition 71). In that case, we can impose  $W = 0$  and by Theorem 21, the quotient  $U := \frac{H}{W}$  is closed under the coproduct and antipode. The Hopf algebra  $U$  represents the theory where the Ward identity is imposed, it replaces the ordinary renormalization Hopf algebra  $H$ . This algebraic perspective on symmetries is described in [49, 50].

### Example 134: Ward identity in QED as a Hopf ideal.

To see a nontrivial effect for the coproduct, we need to examine non-primitive (Definition 88) graphs. We look at the non-primitive 2-loop graphs of QED (Example 23). A fully worked out example for QCD (Example 131), including primitive graphs, spans 9 pages in [50].

By (2) we denote two different orientations of the same graph (Definition 17). Let

$$\begin{aligned} \Gamma^{\nearrow} &:= \text{---} \bullet \text{---} + \text{---} \bullet \text{---} + \text{---} \bullet \text{---} \\ \Gamma^{\nwarrow} &:= (2) \text{---} \bullet \text{---} + \text{---} \bullet \text{---} + \text{---} \bullet \text{---} + (2) \text{---} \bullet \text{---} + \text{---} \bullet \text{---} \end{aligned}$$

The last graph of  $\Gamma^{\nwarrow}$  does not contribute because its 3-photon subgraph vanishes due to Furry's theorem [51]. The reduced coproducts (Definition 66) are

$$\begin{aligned} \Delta_1(\Gamma^{\nearrow}) &= \text{---} \otimes \text{---} + 2 \text{---} \otimes \text{---} + \text{---} \otimes \text{---} \\ \Delta_1(\Gamma^{\nwarrow}) &= 2 \text{---} \otimes \text{---} + 3 \text{---} \otimes \text{---} + \text{---} \otimes \text{---}. \end{aligned}$$

Define  $W_2 := \Gamma^{\nwarrow} + \Gamma^{\nearrow}$  and observe

$$\Delta_1(W_2) = \left( \text{wavy line} + \text{wavy line} \right) \otimes \left( \text{wavy line} + \text{wavy line} \right) + \text{wavy line} \otimes \left( \text{wavy line} + \text{wavy line} \right) \\ + \text{circle} \otimes \left( \text{wavy line} + \text{wavy line} \right) + \left( \text{wavy line} + \text{wavy line} \right) \otimes \text{wavy line}.$$

The Ward identity (Example 129) at one-loop level is

$$0 = \left( S_{\mathcal{R}}^{\mathcal{F}}[\Gamma^{\nwarrow}] + S_{\mathcal{R}}^{\mathcal{F}}[\Gamma^{\nearrow}] \right) \Big|_{\text{1 loop}} = \text{wavy line} + \text{wavy line} =: W_1.$$

We see that  $\Delta_1(W_2) \subseteq W_1 \otimes H + H \otimes W_1$ , so  $W_2$  indeed lies in a Hopf ideal (Definition 71). Further,

$$S_{\mathcal{R}}^{\mathcal{F}}[W_2] = -\mathcal{R}[W_2] - \mathcal{R} [S_{\mathcal{R}}^{\mathcal{F}}[W_1] \cdot H + S_{\mathcal{R}}^{\mathcal{F}}[H] \cdot W_1] = -\mathcal{R}[W_2].$$

But if we impose the Ward identity in general, not only at one-loop level, then  $-\mathcal{R}[W_2] = 0$ . Note that this construction is not tautological: If  $W_2$  would not lie in a Hopf ideal, then  $S_{\mathcal{R}}^{\mathcal{F}}[W_2]$  would contain additional summands which we have no information about. Demanding that  $S_{\mathcal{R}}^{\mathcal{F}}[W_2] = 0$ , in that case, would lead to identities between one-loop graph other than  $W_1 = 0$ . The Ward identity would then not be compatible with renormalization.

### 5.1.4 Tadpoles

In Sect. 1.3.1, we announced to leave out all tadpole graphs (Definition 30). In the present section, we motivate this decision. Tadpoles have only one external momentum, which vanishes by momentum conservation, hence they are independent of momenta altogether. The second Symanzik polynomial (Definition 39) of a tadpole  $T$  is

$$\phi_T = \psi_T \cdot \sum_{e \in E_T} m_e^2 a_e.$$

This leads to a parametric Feynman integral (Eq. 1.57) of the form

$$\mathcal{F}[T] = \frac{i^{|E_T|}}{(4\pi)^{|L_T| \frac{D}{2}}} \prod_{v \in V_T} (-i\lambda_{|v|}) \prod_{e \in E_T} \int_0^\infty \frac{da_e}{\Gamma(\nu_e)} \frac{a_e^{\nu_e-1}}{\psi_\Gamma^{\frac{D}{2}}} \exp \left( -\sum_{e \in E_T} m_e^2 a_e \right). \quad (5.1)$$

For a massless theory, all  $m_e = 0$  and the integrand is a rational function of the parameters  $a_e$ . By Theorem 14 and Definition 43, it is homogeneous of degree  $\omega_T -$

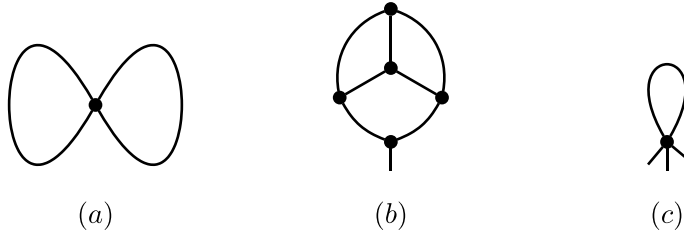


**Fig. 5.1** Three contributions of tadpole graphs. **a** vacuum graph. **b** 1-point function. **c** 3-point function

$|E_T|$ . An integral from 0 to  $\infty$  over a homogeneous function is divergent. This means that  $\mathcal{F}[T]$  for a massless tadpole  $T$  will be infinite, regardless of the values of  $\nu_e$  and  $D$ . Observe that Eq. (5.1) for  $m_e = 0$  is not the same as the period (Definition 98): The latter is the same integrand, but integrated over a compact domain given by the constraint  $\sum a_e = 1$ .

It is not possible to regularize massless tadpole graphs using either analytic (Sect. 2.3.2) or dimensional (Sect. 2.3.3) regularization. One can, however, regularize the integral by introducing an UV- and an IR- cutoff like in Eq. (2.42). Once the integrals are regularized, they factorize at single intermediate edges according to Eq. (1.60).

We will now argue that one can choose to leave out tadpoles from calculations as claimed in Sect. 1.3.1. Firstly, vacuum graphs (Fig. 5.1a) can be considered a special class of tadpoles. They are not observable in QFT because their contribution is always cancelled when Green functions are normalized (Theorem 6). Hence, they can be left out.

Secondly, the 1-point function  $G^{(1)}(\underline{x})$  consists entirely of tadpoles (Fig. 5.1b). Their amplitude is position-independent and  $G^{(1)}(\underline{x}) = G^{(1)}$  is a mere number; it can depend on masses. Effectively, tadpoles lead to a global shift  $\langle \phi(\underline{x}) \rangle \rightarrow \langle \phi(\underline{x}) \rangle + \delta(m)$ . One can remove it by imposing the renormalization condition Eq. (1.19),

$$\langle \phi(\underline{x}) \rangle \stackrel{!}{=} 0.$$

Thereby, one leaves out all tadpoles, massless or not, which contribute to the 1-point function.

Thirdly, tadpoles can contribute to ( $n \geq 2$ )-valent Green functions  $G^{(n)}(x)$ , if they involve a vertex of sufficiently high valence (Fig. 5.1c). There, the tadpoles constitute a mass-dependent shift of the corresponding vertex amplitude. In kinematic renormalization (Definition 93), the renormalized value of every vertex is fixed by a renormalization condition, therefore, tadpole contributions are always absorbed into this value, and all graphs which include tadpoles evaluate to zero in kinematic renormalization,

$$\mathcal{F}_{\mathcal{R}}[\Gamma] = \mathcal{F}_{\mathcal{R}}\left[\frac{\Gamma}{T}\right] \cdot (\mathcal{F}[T] - C_T) = \mathcal{F}_{\mathcal{R}}\left[\frac{\Gamma}{T}\right] \cdot 0 = 0.$$

**Theorem 73.** In kinematic renormalization, all graphs that contain tadpoles vanish, and they can be left out from the start.

Theorem 73 does not imply that we are forced to use cutoff regularization for all graphs. Tadpoles are a Hopf ideal (Definition 71) [44, 52], this means that it is possible to first use cutoff regularization so that tadpoles factorize, then divide by the tadpole Hopf ideal and then remove cutoff regularization. In the remaining tadpole-free sub Hopf algebra, we are free to use any regularization scheme of our choice.

In the Minimal Subtraction scheme (Definition 110), we are facing an obstacle: The latter is explicitly based on dimensional or analytic regularization, but tadpoles can not be regularized this way. Consequently, one must introduce a second, explicit, renormalization condition for tadpoles, independent of the ordinary MS renormalization condition. Tadpoles introduce a new, arbitrary, mass scale into the otherwise massless theory, therefore one typically demands them to vanish, but this is a choice, not a theorem, compare Example 92. We stress that such a choice, without altering the theory, is only possible for tadpoles because they are momentum-independent. If tadpoles vanish, then all multiedge graphs  $M^{(l)}$  (Example 19) are primitive (Definition 88) since their cographs are tadpoles.

The situation is different for massive tadpoles. They do not vanish automatically in MS renormalization conditions, and this time, the theory has a mass which they can depend on. Consequently, tadpoles will show up as non-vanishing cographs and massive multiedges are not primitive unless we use kinematic renormalization. We can still leave out tadpoles, but this requires to engineer a non-vanishing mass counterterm which absorbs them. If we choose to do so, then we are leaving the conventional MS scheme by imposing a non-MS renormalization condition specifically on tadpole graphs.

### Example 135: Violation of the tadpole Hopf ideal.

A massive theory in the Minimal Subtraction scheme (Definition 110) is an example that Hopf ideals are only necessary, but not sufficient, for Ward identities to hold. The combinatorics, and hence the Hopf algebra structure, of the massive theory is the same for all renormalization schemes. If we choose MOM, then the tadpole Hopf ideal is respected by default. The renormalized Feynman rules in MS violate the Hopf ideal, restoring it amounts to an additional condition. The Hopf ideal implies that it is consistent to impose this condition, but not that the condition must be imposed.

**Summary of Sect. 5.1.**

1. A quantum field theory can have different types of symmetries. We restrict our attention to internal gauge symmetries (Sect. 5.1.1).
2. A symmetry of the classical action does not automatically hold in the renormalized quantum theory because in renormalization, the monomials of the Lagrangian are rescaled by scale-dependent  $Z$ -factors. A Ward identity expresses that certain  $Z$ -factors scale identically, preserving the original symmetry (Sect. 5.1.2).
3. In the abstract Hopf algebra formulation of renormalization, Ward identities generate Hopf ideals by formally setting certain classes of graphs equal (Sect. 5.1.3).
4. Tadpole graphs form a Hopf ideal as well, it is algebraically consistent to set all tadpoles to zero. The Feynman rules in kinematic renormalization respect this ideal and tadpoles vanish automatically. For Minimal Subtraction, leaving out tadpoles is a dedicated choice (Sect. 5.1.4).

## 5.2 Diffeomorphisms of Scalar Fields

Intuitively, it should be possible to describe the same physical system by different choices of variables. In the present section, we examine the behavior of a scalar quantum field theory under non-linear transformations of the field variable. We derive the Feynman rules for the transformed theory both in position space and in momentum space, and we establish that the transformation indeed does not alter physical observables.

### 5.2.1 *Digression: The Numerous Problems of Quantum Gravity*

General relativity [10] is based on the Einstein-Hilbert Lagrangian [53],

$$\mathcal{L} = \sqrt{\det g} R, \quad (5.2)$$

where the field degrees of freedom are the entries of the curved metric tensor  $g_{\mu\nu}$ , the non-static analogue of the Minkowski metric (Definition 1).  $R$  denotes the scalar Riemann curvature, which is the trace of the curvature tensor  $R^\tau_{\mu\nu\lambda}.$  With a tedious calculation, we find  $R$  concretely in terms of  $g$  (for example [54, Eq. (36)]):

$$\begin{aligned} R := g^{\mu\nu} R_{\mu\nu}^\tau &= g^{\mu\nu} g^{\rho\sigma} \left( (\partial_\rho \partial_\sigma g_{\mu\nu} - \partial_\rho \partial_\mu g_{\nu\sigma}) \right. \\ &\quad \left. + g^{\tau\omega} \left( \frac{1}{2} \partial_\mu g_{\omega\sigma} \partial_\tau g_{\nu\rho} - \frac{3}{4} \partial_\mu g_{\tau\sigma} \partial_\nu g_{\omega\rho} + \partial_\mu g_{\nu\tau} \partial_\rho g_{\omega\sigma} - \partial_\mu g_{\nu\omega} \partial_\tau g_{\rho\sigma} + \frac{1}{4} \partial_\mu g_{\tau\omega} \partial_\nu g_{\rho\sigma} \right) \right). \end{aligned} \quad (5.3)$$

Here,  $g^{\mu\nu}$  is the inverse matrix of  $g_{\mu\nu}$ , which can be expressed as a Neumann series [55], and to obtain the Lagrangian (Eq. (5.2)), we still need to multiply  $R$  by  $\sqrt{\det g}$ , which is another power series in  $g_{\mu\nu}$ . General relativity is a gauge theory (Sect. 5.1.1), the gauge group is the group of general coordinate transformations in 4-dimensional spacetime.

Quantum Einstein gravity is the quantum field theory obtained from the Einstein-Hilbert Lagrangian Eq. (5.2), where the metric tensor is interpreted as a graviton particle. Irrespective of technical details, a superficial inspection of Eq. (5.3) already indicates two qualitative features of quantum gravity in perturbation theory: Firstly, due to the power series expansion of  $\sqrt{g}$ , there are  $n$ -graviton-vertices of every valence  $n \in \mathbb{N}$ . And secondly, since all summands in Eq. (5.3) involve second derivatives, the vertices scale as

$$v_n \sim \underline{p}^2. \quad (5.4)$$

The graviton propagator constructed from Eq. (5.2) scales as  $\underline{p}^{-2}$ . This scaling behavior has two closely related consequences for the  $n$ -graviton Feynman amplitudes  $G^{(n)}$ :

1. There are infinitely many Green functions  $G^{(n \geq 2)}$  which are superficially divergent (Definition 96).
2. For a concrete function  $G^{(n)}$ , the degree of divergence (Definition 43) of the contributing graphs grows indefinitely with loop number.

By Lemma 35, a theory with these properties is not renormalizable. As introduced in section 2.2.1, renormalization amounts to redefinition of finitely many constants in terms of their observable values. The above behavior of quantum gravity poses a double problem:

1. For each  $G^{(n)}$ , one would need an experimental input to fix their  $Z$ -factors, hence infinitely many measurements to render the complete theory predictive.
2. The interpretation of these experiments as measuring a coupling constant would be questionable, since the divergent part of  $G^{(n)}$  is an unknown power series in momenta, not just a constant.

Probably, this naive picture is too pessimistic [56] and the two infinite sets mentioned above are not mutually independent. But even in that case, one infinite set of unknown parameters remains to be determined by renormalization.

The theorist's conclusion appears to be that a quantum theory with Lagrangian Eq. (5.2) is impossible. But experiments confirm that both quantum theory, and general relativity, exist in nature, therefore the conclusion that they are mutually exclusive

is unacceptable. Over the last century, countless approaches to the renormalization problem of quantum gravity have been proposed. We review four of the more popular ones.

The first possible solution is to introduce a graviton propagator which scales  $\sim p^{-4}$  [57–63]. One prominent 4th-order theory of gravity is *conformal gravity*, given by the Weyl equations [64–69]. In Sect. 2.4, we have presented various arguments against propagators of 4th order, but they might not apply to the case of gravity: Since gravity is associated with a curved spacetime, it is not obvious whether Eq. 2.54 gives the correct short-distance scaling and the argument about conserved fluxes does not necessarily exclude  $n \neq 1$ . Similarly, the presence of Ostrogradsky ghosts can possibly be avoided by viewing the massless 4th order propagator as a particular limit of massive fields [58].

A second approach to the renormalization problem is the assumption that, instead of changing the propagator, the spacetime dimension changes for short distances, being effectively 2-dimensional, which would render gravity renormalizable [70–72]. We know from everyday experience and from various theoretical considerations [73, 74] that spacetime is 4-dimensional on observable scales. But these arguments do not apply to scales well below the size of nuclei. Several hypothetical mechanisms describe how and why spacetime can effectively become 2-dimensional at short distances [75–78].

Thirdly, quantum gravity in 4 dimensions can potentially still be finite, despite being perturbatively non-renormalizable, by having a non-trivial UV fixed point (see Sect. 3.2.4). This possibility has a certain overlap with the first two. For example, by quantum corrections, the propagator for high energies could deviate from the  $p^{-2}$  scaling (Definition 105), or the scaling behavior of propagators can even be taken as a *definition* of the dimension of spacetime at this scale [78–81]. From that perspective, whether spacetime changes its dimension or the propagator obtains a non-standard power is almost the same question.

Fourthly, it is conceivable that, due to the tensorial character of gravity, the mere scaling of the vertex (Eq. (5.4)) is too imprecise to capture the true behavior and that the infinitely many involved counterterms are not independent. An example of this phenomenon are the Slavnov-Taylor identities in QCD (Example 132): There are seven different divergent Green functions in QCD, but all of their counterterms are related and a single measurement—determining the physical value of the QCD coupling constant  $g$ —is sufficient to uniquely determine all seven divergent amplitudes. The hope is that for gravity, being based on the gauge group of arbitrary coordinate transformations, a similar mechanism might be at play, involving infinitely many Ward identities to fix all but finitely many counterterms [56, 82]. This approach to the renormalization problem fits into a broader set of considerations, that a theory with non-polynomial interaction can potentially be renormalizable if its amplitudes have certain special properties [83–86]. A necessary condition for the validity of such Ward identities is that they form a Hopf ideal (Definition 71) in the core Hopf algebra (Definition 87) which underlies the perturbation theory of gravity, compare Sect. 5.1.3. It has been verified that they do in gravity [54, 87–89].

Even if Hopf ideals are present, the Feynman rules can potentially violate them, compare Example 135. To check the validity of Ward identities, we would need to examine concrete Feynman rules of quantum gravity. Unfortunately, the construction of a QFT from the Einstein-Hilbert Lagrangian (Eq. (5.2)) faces significant technical and philosophical challenges. De Witt [90] observes that

Some of the field variables possess no conjugate momenta; the momenta conjugate to the remaining field variables are not all dynamically independent; the field equations themselves are not linearly independent, and some of them involve no second time derivatives [...].

In general relativity, the Hamiltonian (Definition 10), a cornerstone of canonical quantization (Sect. 1.2.2), vanishes identically, and it is not obvious which quantity should be interpreted as the total energy [91]. Moreover, scattering theory relies on the existence of asymptotic states (Definition 18) in infinite distances, which, in a globally curved spacetime, might propagate in a different effective metric, or might not exist at all.

Often, one defines the graviton  $h_{\mu\nu}$  to be a small perturbation around a background spacetime  $b_{\mu\nu}$ , by  $h_{\mu\nu} := g_{\mu\nu} - b_{\mu\nu}$ . This approach suffers from ambiguities by possibly inequivalent choices of background metrics  $b_{\mu\nu}$  and field variables  $h_{\mu\nu}$ . The obvious choice  $b_{\mu\nu} = \eta_{\mu\nu}$ , excludes the physical possibility of non-trivial topologies of the universe, but conversely, if  $b_{\mu\nu}$  is not a flat metric, then one faces all the problems of formulating QFT on a curved background [92–94]. Various different definitions of background and graviton field have been considered [35, 90, 95–99], including non-linear redefinitions (Definition 118) of  $h_{\mu\nu}$  [100]. At least, it has been established that gravity can not be formulated as a non-linear transformation of a free spin-2 field [101]. The perturbative formulations of quantum gravity considered so far typically reproduce (non quantum) general relativity in treelevel graphs [102–105], but this does not imply that they are the correct framework to compute quantum corrections.

Alternatively, one identifies the full metric tensor  $g_{\mu\nu}$  as the graviton field variable, but this results in a strongly coupled theory, making perturbation theory inapplicable. Many issues with the construction of quantum gravity are related to the identification of suitable physical observables, field variables, or gauge conditions [100], and the question unanswered so far is whether there exists any choice such that the above Ward identities render gravity renormalizable.

As a side remark, small perturbative deviations from a background field [106] and Feynman graphs [107] are also useful in general relativity itself, irrespective of its possible quantization. Moreover, as mentioned in Sect. 1.2.8, there are several approaches to construct the (physically observable)  $S$ -matrix of quantum gravity without defining any microscopic quantum field theory at all.

The present thesis does not propose a solution to the renormalization of quantum gravity. But the quantum field diffeomorphisms to be examined in the subsequent sections can be viewed as a toy model for a quantum field theory where vertices are proportional to inverse propagators. We will see in Theorem 92 that the diffeomorphism field indeed satisfies infinitely many Ward identities, but nevertheless, infinitely many counterterms remain undetermined. Morally, the two sets of

undetermined counterterms mentioned above are being reduced to just one infinite set of undetermined quantities. Examining the diffeomorphism toy model does not solve the gravity problem, but it helps to clarify what type of mechanism is needed concretely to make Ward identities work in the proposed sense.

### 5.2.2 Field Diffeomorphisms

In the present chapter, we consider diffeomorphisms of the field variable in quantum field theory. This setting is different from non-linear coordinate transformations in general relativity (Sect. 5.2.1), which are often called diffeomorphism as well.

**Definition 118.** Let  $\phi(\underline{x})$  be the variable of a scalar quantum field, and let  $a_n \in \mathbb{C}$ , where  $a_0 = 1$ . A (global) *field diffeomorphism* is a transformation of  $\phi$  to a new field variable  $\rho$ , related by a formal power series (Definition 53),

$$\phi(\underline{x}) = \sum_{n=0}^{\infty} a_n \rho^{n+1}(\underline{x}).$$

Likewise, with a set of coefficients  $b_n$ , we denote the inverse diffeomorphism by

$$\rho(\underline{x}) =: \sum_{n=1}^{\infty} \frac{b_{n+1}}{n!} \phi^n(\underline{x}). \quad (5.5)$$

The coefficients  $a_n$  and  $b_n$  in Definition 118 are related by Theorem 19,

$$\begin{aligned} a_n &= \frac{1}{(n+1)!} \sum_{k=1}^n B_{n+k,k}(0, -b_3, -b_4, -b_5, \dots) \\ b_{n+2} &= \sum_{k=1}^n \frac{(n+k)!}{n!} B_{n,k}(-1!a_1, -2!a_2, \dots, -n!a_n). \end{aligned} \quad (5.6)$$

Here,  $B_{n,k}$  are the Bell polynomials (Definition 54). The diffeomorphism (Definition 118) is called *global* in the sense of a global symmetry, which does not depend on the position (Sect. 5.1.1). Conversely, it could be called local in the sense that it is a transformation between fields at the same spacetime point.

Field diffeomorphisms of this type have been examined in the literature repeatedly and for different reasons. Some motivations are the following:

1. Non-linear field redefinitions do not alter the  $S$ -matrix (Definition 18), which has been established in various different frameworks (Theorem 80, [48, 108–114]). This invariance is frequently used to simplify the Lagrangian, for example in gauge theories [115, ch. 6.3], in non-local interactions [116], or in effective field theories [117].
2. Linear shifts in the field variable of an interacting field alter the type of interaction, but they do not impede renormalizability, which is important for theories with spontaneous symmetry breaking [118, 119].
3. By power counting, the Feynman graphs of a field diffeomorphism reside in the core Hopf algebra (Definition 87). The same is true for quantum Einstein gravity (Sect. 5.2.1). This makes field diffeomorphisms a toy model for the algebraic behavior of gravity.
4. For quantum gravity, it is notoriously difficult to identify the correct field variables, see Sect. 5.2.1. A better understanding of field diffeomorphisms can help to classify and restrict the possible choices.
5. By a field diffeomorphism, the Lagrangian of a theory with non-polynomial interaction can be transformed to a theory with polynomial interaction but non-standard kinetic term [120]. This has been used to examine the possibility of non-polynomial interactions in QFT, see Example 144.

In the present chapter, we touch upon most of these points, but the focus will be on the offshell Green functions, divergences and renormalizability of field diffeomorphisms. The perturbation theory of scalar field diffeomorphisms has been studied recently [108, 109, 111]. The remainder of the present chapter will follow the author's own works [110, 121].

For a diffeomorphism (Definition 118), the underlying field  $\phi$  can be either a free (Example 1) or an interacting (Example 6) field. We concentrate mostly on the first case, because it already gives rise to all the non-trivial phenomena of field diffeomorphisms, whereas an underlying interaction only makes calculations more cumbersome without adding qualitatively new effects. We write the free Lagrangian of the underlying field  $\phi$  in the form Eq.(1.5),

$$\mathcal{L} = \frac{1}{2}\phi(\underline{x})\hat{s}\phi(\underline{x}). \quad (5.7)$$

By Wick's theorem (Theorem 2), the correlation functions of  $\phi$  are products of Feynman propagators (Eq.(1.24))

$$G_F(\underline{x}_1, \underline{x}_2) := G_F(\underline{x}_2 - \underline{x}_1) = \int \frac{d^D k}{(2\pi)^D} \frac{i}{s_k} e^{-ik(\underline{x}_2 - \underline{x}_1)}, \quad (5.8)$$

where  $s_k$  is the offshell variable (Definition 8).

**Example 136: Analogy between QCD and a scalar field diffeomorphism.**

Consider the diffeomorphism (Definition 118)  $a_1 = \frac{-g}{2}$  and  $a_{n>1} = 0$ , that is,  $\phi(\underline{x}) = \rho(\underline{x}) - \frac{g}{2}\rho^2(\underline{x})$ . If the underlying field  $\phi$  is a free field (Eq.(5.7)) with offshell variable (Definition 8)  $s_p = \underline{p}^2$ , then, using  $\partial_\mu\rho^2 = 2\rho\partial_\mu\rho$ , the Lagrangian of  $\rho$  is

$$\mathcal{L} = \frac{1}{2} (-\partial_\mu\rho + g \rho\partial_\mu\rho) (-\partial^\mu\rho + g \rho\partial^\mu\rho).$$

This Lagrangian is reminiscent of the Yang-Mills-Lagrangian of QCD (Example 131), up to the tensor structure which is necessarily different between a scalar field and a vector-valued gauge field.

### 5.2.3 Diffeomorphism Feynman Rules in Position Space

We examine the Feynman rules of the field diffeomorphism  $\rho(\underline{x})$  (Definition 118) in position space. The time ordered correlation functions  $\tilde{G}^{(n)}(\underline{x}_1, \dots, \underline{x}_n) = \langle T\rho(\underline{x}_1) \cdots \rho(\underline{x}_n) \rangle$  (Definition 14) of  $\rho$  can be computed by expanding the series  $\rho(\phi(\underline{x}))$  in Definition 118 in powers of  $\phi(\underline{x})$ .

The 1-point function  $\langle T\rho(\underline{x}) \rangle$  is

$$\tilde{G}^{(1)}(\underline{x}) = \langle \rho(\underline{x}) \rangle = \sum_{n=1}^{\infty} \frac{b_{n+1}}{n!} \langle T\phi(\underline{x}) \cdots \phi(\underline{x}) \rangle.$$

By Wick's theorem (Theorem 2), the correlation functions  $\langle T\phi^n(\underline{x}) \rangle$  are propagators (Eq. (5.8)) evaluated at the same spacetime point,

$$\langle T\phi(\underline{x}) \rangle = 0, \quad \langle T\phi^2(\underline{x}) \rangle = G_F(\underline{0}), \quad \langle T\phi^4(\underline{x}) \rangle = 3 \cdot G_F(\underline{0}) \cdot G_F(\underline{0}), \quad \dots$$

These products correspond to tadpole graphs (Sect. 5.1.4). We demand that they vanish,

$$G_F(\underline{0}) \stackrel{!}{=} 0. \tag{5.9}$$

Equivalently, we demand that Eq. (1.19) holds for the transformed field,  $\langle \rho(\underline{x}) \rangle \stackrel{!}{=} 0$ .

For the 2-point function, the expansion of the diffeomorphism (Definition 118) reads

$$\tilde{G}^{(2)}(\underline{x}_1, \underline{x}_2) = \langle T\rho(\underline{x}_1)\rho(\underline{x}_2) \rangle = \sum_{t_1=1}^{\infty} \sum_{t_2=1}^{\infty} \frac{b_{t_1+1}b_{t_2+1}}{t_1!t_2!} \langle T\phi^{t_1}(\underline{x}_1)\phi^{t_2}(\underline{x}_2) \rangle.$$

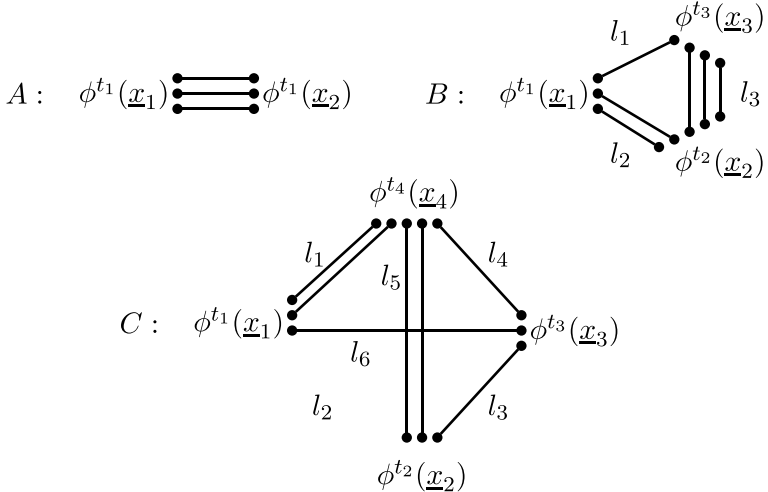


**Fig. 5.2** Contributions to connected correlation functions in position space. Each dot represents a factor of  $\phi$ . Graphs where dots of the same monomial  $\phi^j$  (i.e. same spacetime-point) are connected, are excluded due to Eq. 5.9.  $A$  : 2-point function,  $B$  : 3-point function,  $C$  : 4-point function, where  $l_2 = 0$

The right hand side are correlation functions of a free field  $\phi$ . By Wick's theorem and vanishing of tadpoles Eq. (5.9), the terms contributing to the 2-point function consist of an arbitrary number of edges between the two spacetime points  $x_1$  and  $x_2$ . They can be interpreted as Feynman graphs on two external vertices, see graph  $A$  in Fig. 5.2. There are  $t_1!$  different Wick contractions for each summand, consequently

$$\tilde{G}^{(2)}(\underline{x}_1, \underline{x}_2) = \sum_{t_1=1}^{\infty} \frac{b_{t_1+1}^2}{t_1! t_1!} t_1! G_F^{t_1}(\underline{x}_2 - \underline{x}_1) = \sum_{t=1}^{\infty} \frac{b_{t+1}^2}{t!} G_F^t(\underline{x}_2 - \underline{x}_1). \quad (5.10)$$

The time-ordered 3-point function is sketched in graph  $B$  in Fig. 5.2 and can be written as

$$\tilde{G}^{(3)}(\underline{x}_1, \underline{x}_2, \underline{x}_3) = \sum_{t_1=1}^{\infty} \sum_{t_2=1}^{\infty} \sum_{t_3=1}^{\infty} \frac{b_{t_1+1} b_{t_2+1} b_{t_3+1}}{t_1! t_2! t_3!} \langle \phi^{t_1}(\underline{x}_1) \phi^{t_2}(\underline{x}_2) \phi^{t_3}(\underline{x}_3) \rangle.$$

Let  $l_1, l_2, l_3$  be the number of propagators between the points as indicated in Fig. 5.2, then

$$\begin{aligned} t_1 &= l_1 + l_2, & t_2 &= l_2 + l_3, & t_3 &= l_1 + l_3 \\ \Leftrightarrow l_1 &= \frac{1}{2}(t_1 + t_3 - t_2), & l_2 &= \frac{1}{2}(t_1 + t_2 - t_3), & l_3 &= \frac{1}{2}(t_2 + t_3 - t_1). \end{aligned}$$

Rewriting the sums over  $t_i$  in terms of  $l_i$ , the non-tadpole part of the 3-point function reads

$$\tilde{G}^{(3)}(\underline{x}_1, \underline{x}_2, \underline{x}_3) = \sum_{\substack{l_j \in \mathbb{N}_0 \\ l_1 + l_2 + l_3 \geq 2}} \frac{b_{l_1+1} b_{l_2+1} b_{l_3+1}}{l_1! l_2! l_3!} G_F^{l_1}(\underline{x}_2 - \underline{x}_1)^{l_2} G_F(\underline{x}_3 - \underline{x}_2)^{l_3} G_F^{l_3}(\underline{x}_3 - \underline{x}_1). \quad (5.11)$$

The construction of higher  $\tilde{G}^{(n)}$  follows the same scheme, the resulting sum can always be interpreted as a sum over all possible graphs involving exactly  $n$  vertices. A graph contributing to  $\tilde{G}^{(4)}$  is shown in Fig. 5.2 C. Equivalently, this construction can be viewed as a sum over complete graphs  $K_n$  on  $n$  vertices, where each edge of  $K_n$  is replaced by any number, including zero, of propagators. A detailed examination shows that the combinatorial prefactors have the form analogous to Eq. (5.11) in the general case.

**Theorem 74** ([110]). Let  $\rho$  be a diffeomorphism (Definition 118) of a free scalar field  $\phi$  with propagator  $G_F(\underline{z})$  in position space (Eq. 5.8). Assume that tadpoles vanish, and let  $k = \frac{n(n-1)}{2}$ . Then, the time-ordered  $n$ -point amplitude (Definition 14) of  $\rho$  in position space is

$$\tilde{G}^{(n)}(\underline{x}_1, \dots, \underline{x}_n) = \sum_{\substack{l_1, \dots, l_k \in \mathbb{N}_0 \\ t_j \geq 1 \forall j}} \frac{b_{t_1+1} \cdots b_{t_n+1}}{l_1! \cdots l_k!} G_F^{l_1}(\underline{x}_1 - \underline{x}_2) G_F^{l_2}(\underline{x}_1 - \underline{x}_3) \cdots G_F^{l_k}(\underline{x}_{n-1} - \underline{x}_n)$$

The indices  $l_i$  are labels of the edges of a completely connected graph on  $n$  vertices, and  $t_j$  are the sum of all  $l_i$  incident to the vertex  $j$ , compare Fig. 5.2. Each  $l_i$  contributes to precisely two distinct  $t_j$  and each pair  $\{t_i, t_j\}$  shares precisely one  $l_i$  and the summation is such that no  $t_j$  is zero.

The index  $t_j$  of  $b_{t_j}$  depends on  $(n-1)$  of the summation indices  $l_j$ , consequently, the  $k$  sums in Theorem 74 are not independent from each other. The prefactor obtained in Theorem 74,

$$\frac{b_{t_1+1} \cdots b_{t_n+1}}{l_1! \cdots l_k!}, \quad (5.12)$$

equals the prefactor of an ordinary Feynman graph in position space (Definition 41): The numerator represents vertex Feynman rules, where a  $j$ -valent vertex has the amplitude  $\frac{b_j}{j!}$ . In the graphs constructed in Theorem 74, all  $n$  vertices are external, therefore, the symmetry factor (Theorem 15) arises entirely from permutations of the multiedges,  $l!$  for each  $G_F^{l_i}$ . This factor is the denominator in Eq. (5.12). Consequently, Theorem 74 reproduces the known Feynman rules in position space (Definition 41). The case of field diffeomorphisms is special only insofar as the resulting graphs do not contain internal vertices, and therefore no integrations.

### 5.2.4 Diffeomorphism Feynman Rules in Momentum Space

Applied to a free Lagrangian (Eq.(5.7)), a diffeomorphism (Definition 118) gives rise to a theory with an infinite set of interaction vertices.

**Lemma 75** ([110]). Let  $\rho$  be the diffeomorphism (Definition 118) of a free field (Eq.(5.7)) with offshell variable  $s$  (Definition 8). Then,  $\rho$  has vertices of every valence  $n \geq 2$  with Feynman rule

$$iv_n := i \frac{1}{2} \sum_{k=1}^{n-1} a_{n-k-1} a_{k-1} (n-k)! k! \sum_{P \in Q^{(n,k)}} s_P.$$

Here,  $Q^{(n,k)}$  is the set of all possibilities to choose  $k$  out of  $n$  external edges without distinguishing the order,  $P$  is one of these sets and  $s_P$  is the offshell variable corresponding to the momenta in  $P$ .

#### Example 137: Diffeomorphism vertices.

Let  $s$  be the offshell variable (Definition 8), with the usual shorthand notation  $s_{i+j} := s_{p_i+p_j}$ . The first vertices from Lemma 75 read

$$\begin{aligned} iv_2 &= is_1, \\ iv_3 &= 2ia_1(s_1 + s_2 + s_3), \\ iv_4 &= 6ia_2(s_1 + s_2 + s_3 + s_4) + 4ia_1^2(s_{1+2} + s_{1+3} + s_{2+3}). \end{aligned}$$

In general, it is not possible to reduce the offshell variables  $s_{i+j+\dots}$ , appearing in Lemma 75, to polynomials in the  $n$  external offshell variables  $\{s_i\}$ , except for the special cases  $s = p^2$  or  $s = p^2 - m^2$  [108].

**Theorem 76** ([110]). Let  $\phi$  be a scalar field with interacting Lagrangian (Eq.(1.6)),

$$\mathcal{L} = \frac{1}{2} \phi \hat{s} \phi - \sum_{t=3}^{\infty} \frac{\lambda_t}{t!} \phi^t,$$

and let  $\rho$  be a diffeomorphism (Definition 118) of  $\phi$ . Then,  $\rho$  has vertices  $iv_n$  according to Lemma 75, and additionally, for each  $n \geq 3$ ,  $t \leq n$ , a vertex

$$-iw_n^{(t)} = -i\lambda_t B_{n,t}(1!a_0, 2!a_1, 3!a_2, 4!a_3, \dots),$$

where  $B_{n,t}$  are the Bell polynomials (Definition 54).

For scalar fields where the propagator is of quadratic order in momentum, so  $s_p = p^2$  or  $s_p = p^2 + m^2$ , all propagator-cancelling theories are diffeomorphisms of a free field.

**Theorem 77.** Consider a scalar field theory  $\rho$  with propagator (Definition 8)  $s = \underline{p}^2 - m^2$ , where  $m^2 \geq 0$ .

1. If  $\rho$  has interaction vertices  $i v_n = k_n \cdot (p_1^2 + \dots + p_n^2) + r_n \forall n > 2$  where  $k_n, r_n \in \mathbb{R}$ , then  $\rho$  is a unique diffeomorphism of a field  $\phi$  such that the vertices of  $\phi$  are independent of momenta,  $i v'_n = i r'_n$  where  $r'_n \in \mathbb{R}$ .
2. If  $\rho$  is a massless field and has interaction vertices  $i v_n = k_n \cdot (p_1^2 + \dots + p_n^2)$ , with arbitrary  $k_n \in \mathbb{R}$ , then  $\rho$  is a diffeomorphism of a free massless scalar field.
3. There is no diffeomorphism between two power-counting renormalizable theories.

**Proof** The statements are a corollary of Theorem 76. Consider the general form of a vertex of the diffeomorphism theory,  $i v_n - i w_n^{(t)}$ . For  $s = \underline{p}^2 - m^2$ , this vertex is of the form stated in point 1. In this setting, both the diffeomorphism parameters  $\{a_n\}$  and the coupling constants  $\{\lambda_i\}$  are free parameters. Using the formulas in Lemma 75 and Theorem 76, one can determine these parameters to reproduce any given sets  $\{k_n, r_n\}$ .

A theory with propagator  $\sim \underline{p}^{-2}$  can only be power-counting renormalizable (Lemma 35) if no vertex is proportional to squared momenta. The most general form of such a scalar theory is the interacting Lagrangian of Theorem 76. By Lemma 75, every diffeomorphism of such a theory contains vertices scaling as  $\underline{p}^2$  and is therefore not renormalizable.  $\square$

### 5.2.5 Propagator Cancellations and the Connected Perspective

From now on, we restrict ourselves to an underlying free field. The vertices of the diffeomorphism (Lemma 75) are proportional to inverse offshell variables (Definition 8). Hence, they are capable of cancelling a propagator  $\frac{i}{s_e}$  (Eq.(5.8)), by the identity

$$s_e \cdot \frac{i}{s_e} = i.$$

If a Feynman graph contains vertices  $i v_n$  (Lemma 75) then the corresponding Feynman amplitude can have a different topology than the graph, in the sense that not every propagator of the graph appears as a factor  $\frac{i}{s_e}$  in the amplitude.



**Fig. 5.3** Illustration of splitting the vertex  $iv_7$  into  $iv_4 \xrightarrow{e} iv_5$ . Figure taken from [110]

The sum over offshell variables  $s_P$  in the vertex  $iv_n$  (Lemma 75) corresponds to all possibilities to choose  $k$  out of the  $n$  external edges. Pictorially, such a choice means splitting the external edges of the vertex into two disjoint sets. The same splitting happens if we replace the vertex  $iv_n$  by two smaller vertices  $iv_j \xrightarrow{s_P} iv_k$ , where  $j + k - 2 = n$  and  $s_P$  is the intermediate propagator joining  $iv_j$  and  $iv_k$ . The mechanism is depicted in Fig. 5.3.

The product  $iv_j \xrightarrow{s_P} iv_k = -iv_j \xrightarrow{s_P} iv_k$  has the opposite sign as the corresponding term in  $iv_n$ , and a closer examination [110] shows that the combinatorial factors match so that both terms exactly cancel each other. The only remaining summands in  $iv_n$  (Lemma 75) are those which do not correspond to splitting the vertex, that is, those where the partition  $P$  is a single external edge  $e$ . Such terms are proportional to an external offshell variable  $s_P = s_e$ .

$$\left( iv_n + \sum_{v_j \star v_k = v_n} iv_j \frac{i}{s_P} iv_k \right) \Big|_{\text{Terms not proportional to an external}} s_e = 0. \quad (5.13)$$

Here, the product  $v_j \star v_k$  denotes summation over all ways to choose the valences  $j, k$  and also all possible permutations of external edges. By Eq. (5.13), the connected tree-level  $n$ -point amplitude is proportional to the external offshell variables  $s_e$ , it has the form

$$-ib_n(s_1 + \dots + s_n) =: iV_n \quad (5.14)$$

where  $b_n \in \mathbb{R}$  is independent of kinematics.

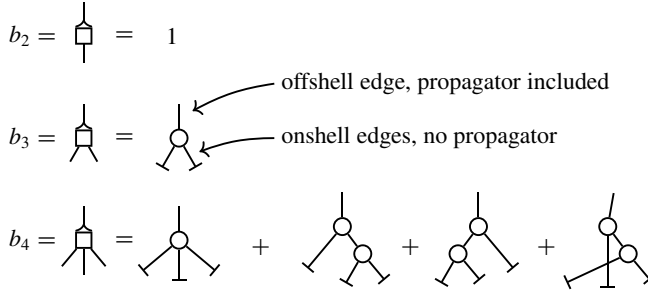
**Definition 119.** For  $n \geq 3$ , the *tree sums*  $b_n$  are defined as the sum of all connected tree-level Feynman graphs of the field  $\rho$  with a total of  $n$  external edges, where  $n - 1$  external edges are onshell (i.e.  $s_e = 0$  for these edges  $e$ ) and the last external edge is offshell. The propagator  $\frac{i}{s_e}$  of this offshell edge  $e$  is included in  $b_n$ . Finally,  $b_2 := 1$ .

**Example 138: Diffeomorphism tree sums.**

An explicit calculation of the first tree sums  $b_n$  (Definition 119), using Lemma 75, yields

$$\begin{aligned} b_3 &= \frac{i}{x_{1+2}} \cdot 2ia_1(x_1 + x_2 + x_{1+2}) \Big|_{x_1=0=x_2} = -2a_1, \\ b_4 &= -6a_2 + 12a_1^2. \end{aligned}$$

Graphically, we denote the tree sums  $b_n$  by a square vertex, and indicate the cancelled offshell external edge by an arrow. For the ordinary vertices  $i v_n$ , we indicate an onshell edge by a perpendicular line (figure taken from [110]):



**Theorem 78** ([108, 110, 111]). The tree sums  $b_n$  (Definition 119) are the coefficients  $b_n$  of the inverse diffeomorphism (Definition 118), for arbitrary offshell variable  $s_p$  (Definition 8).

**Example 139: Berends-Giele relations and Parke-Taylor formula.**

In QCD (Example 131), the  $n$ -gluon currents  $\hat{J}_\zeta^x(1, 2, \dots, n)$  are defined as the connected  $(n+1)$ -point gluon Green functions where precisely one leg is offshell. They can be constructed recursively with the Berends-Giele (BG) relations [122]. The definition of  $\hat{J}_\zeta^x$  is almost verbatim Definition 119 of the tree sums  $b_{n+1}$ . Consequently, the proof of Theorem 78 in [108] is strikingly similar to the derivation of BG relations in [122].

The maximum helicity violating (MHV) amplitudes in QCD are those onshell (Definition 8)  $n$ -gluon amplitudes where precisely two out of  $n$  external onshell gluons have a different helicity than the remaining ones. To leading order in  $N$  of the gauge group  $SU(N)$ , their matrix element is given by the Parke-Taylor formula [123],

$$|M_{\text{MHV}}(1^-, 2^-, 3^+, \dots)|^2 = \frac{g^{2n-4}}{2^{2n-4}} \frac{N^{n-2}(N^2-1)}{n} (p_1 \cdot p_2)^4 \sum_P \frac{1}{(p_1 \cdot p_2)(p_2 \cdot p_3) \cdots (p_n \cdot p_1)}$$

where  $P$  ranges over all permutations of  $1, \dots, n$ . The Parke-Taylor formula is a consequence of Berends-Giele relations.

In this sense, the connected amplitudes  $iV_n \sim ib_n$  in Eq. (5.14) are a scalar analogue of the MHV-amplitudes in QCD. Especially, if we restrict the diffeomorphism to Example 136, which closely resembles QCD, then the tree-level matrix element with one external edge offshell is the square of Eq. (5.14),

$$|V_n|^2 = |b_n|^2 \sum_{i=1}^n s_i^2 = g^{2n-4} ((2n-1)!!)^2 \sum_{i=1}^n (p_i \cdot p_i)^2.$$

This amplitude vanishes in the onshell limit  $p^2 = 0$ , see Theorem 80.

A scalar field diffeomorphism (Example 136) is not QCD, therefore we can not expect to precisely recover the Parke-Taylor formula, but it is interesting to observe that, despite the striking difference in tensor structure, qualitatively similar amplitudes arise.

The fact that the tree sums  $b_n$  (Definition 119) are mere numbers, without any remaining internal propagators, motivates to use these tree sums as *metavertices* in computing connected correlation functions. This approach is dubbed *connected perspective*, as opposed to the *ordinary perspective*, where the vertex Feynman rules are given by Lemma 75. The Feynman rules of the connected perspective differ from the ordinary momentum space Feynman rules (Definition 42).

**Theorem 79** ([110, 121]). Assume that tadpoles vanish. The connected  $n$ -point amplitude (Definition 14) of a diffeomorphism  $\rho$  (Definition 118) of a free field (Eq. (5.7)) is obtained by summing over all graphs  $\Gamma$  (Definition 24) such that

1. Each internal edge  $e \in \Gamma$  contributes a propagator factor  $\frac{i}{s_e}$ .
2.  $\Gamma$  is built from  $(k > 2)$ -valent metavertices with Feynman rule  $iV_k = -ib_k(s_1 + s_2 + \dots + s_k)$ . Keeping a summand  $s_e$  in this amplitude amounts to cancelling the adjacent edge  $e$ .
3. The metavertices do not cancel internal edges of  $\Gamma$ .
4. The Graph  $\Gamma$  does not contain internal metavertices, that is, every metavertex is adjacent to at least one external edge.

When using Theorem 79, all cancellations have been taken into account, and the topology of the graph equals the topology of the corresponding amplitude. The metavertex Feynman rule (Eq. (5.14)) implies that all graphs are proportional to at least one external offshell variable. Consequently, every non-trivial graph of the connected perspective vanishes as soon as all external momenta are taken onshell (Definition 8). An analogous statement holds if the underlying theory is interacting, where only the original interaction vertices remain in the onshell limit.

**Theorem 80** ([110]). Let  $\rho$  be a diffeomorphism (Definition 118) of a free or interacting scalar field  $\phi$ . Assume that tadpoles vanish. Then, as soon as all external momenta are onshell, the time ordered Green functions (Definition 14) of  $\rho$  coincide with the ones of  $\phi$ . The diffeomorphism does not alter the  $S$ -matrix (Definition 18).

We can understand the Feynman rules of the connected perspective (Theorem 79) from the diffeomorphism Feynman rules in position space (Theorem 74), compare Fig. 5.4. The metavarites in the connected perspective, cancelling the adjacent external propagator, can be identified as the external powers  $\phi^j(x)$  in position space. This correspondence indicates that the perturbative treatment in momentum space—which involves significant combinatorial effort in [108, 110, 121]—has indeed yielded the correct results.

### 5.2.6 Two-Point Function in Momentum Space

**Lemma 81.** Assume that tadpoles vanish (Sect. 5.1.4). Let  $\rho$  be a field diffeomorphism (Definition 118) of a free field. Then, the connected 2-point function  $\bar{G}_2$  (Definition 20) of  $\rho$ , excluding the two external propagators, is a sum of multiedges  $M^{(l)}$  (Example 19),

$$\bar{G}_2(s) = -is + \sum_{l=1}^{\infty} (-ib_{l+2}s)^2 \frac{\mathcal{F}[M^{(l)}](s)}{(l+1)!}.$$

**Proof** Using the Feynman rules of the connected perspective (Theorem 79), the connected amplitude with two external momenta  $\bar{G}_2$  is supported on Feynman graphs with up to two metavarites. Excluding tadpoles, the only remaining graph topology is that of  $l$ -loop multiedges  $M^{(l)}$ . The metavarites have valence  $(l+2)$  and Feynman rule  $iV_{l+2} = -ib_{l+2} \cdot s$  (Eq. (5.14)), see Fig. 5.5.  $\square$

Even if all multiedges are 1PI graphs (Definition 46),  $\bar{G}_2$  is the connected, not the 1PI 2-point function. If tadpoles vanish then multiedge graphs are primitive, so their divergence is local (Theorem 32). In dimensional regularization (Sect. 2.3.3), we split  $\bar{G}_2$  (Lemma 81) into a finite and a divergent part,

$$\bar{G}_2(s) =: -is \left( 1 + \bar{G}_2^{\text{fin}}(s) + \bar{G}_2^{\text{div}}(s) \right) + \mathcal{O}(\epsilon).$$

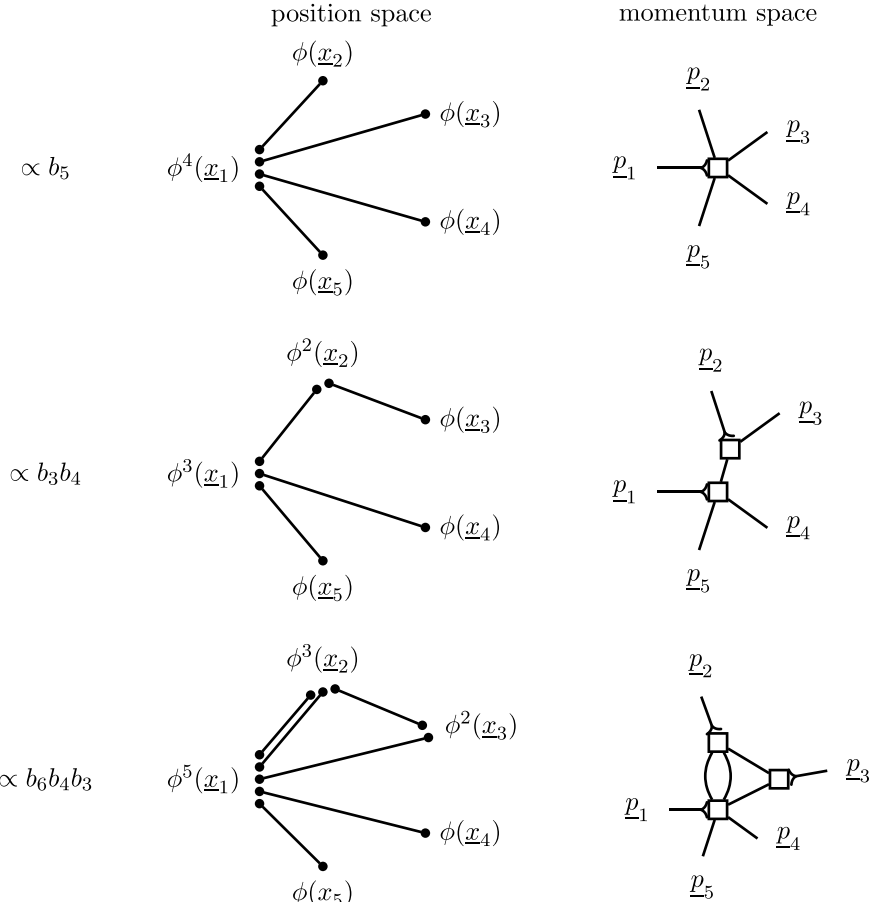


**Fig. 5.4** Correspondence between momentum space (Theorem 79) and position space (Theorem 74) Feynman rules for a diffeomorphism  $\rho$  (Definition 118). A momentum  $\underline{p}_i$  is the Fourier transform of a position  $\underline{x}_i$ . Metavertices are indicated by squares, the edge which is cancelled is marked with an arrow

$$\begin{aligned} \bar{G}_2(s) &= - + \text{---} + \text{---} + \text{---} + \dots \\ &= -is + (-ib_3s)^2 \frac{1}{2!} \mathcal{F}[M^{(1)}](s) + (-ib_4s)^2 \frac{1}{3!} \mathcal{F}[M^{(2)}](s) + \dots \end{aligned}$$

**Fig. 5.5** The amputated connected two-point-amplitude  $\bar{G}_2$  in momentum-space in the connected perspective. Both external propagators are being cancelled

The divergent part is  $\bar{G}_2^{\text{div}}(s) := \hat{\mathcal{R}}[\bar{G}_s(s)]$ , where  $\hat{\mathcal{R}}$  is the MS subtraction operator (Definition 110). It is specific to the 2-point function that  $\bar{G}_2$  contains only local divergences  $\bar{G}^{\text{div}}$ . In general, the diffeomorphism requires a systematic recursive renormalization procedure. We come back to this question in Sect. 5.4.

**Example 140: Massless two-point function of diffeomorphism.**

If we restrict ourselves to an underlying theory with offshell variable  $s = \underline{p}^2$ , then the finite and divergent part of  $\bar{G}_2$  are given by Lemma 31,

$$\begin{aligned}\bar{G}_2^{\text{div}}(s) &= -\frac{b_{l+2}^2 (-is)^l}{(4\pi)^{2l} (l!)^2 (l+1)!} \\ \bar{G}_2^{\text{fin}}(s) &= -\sum_{l=1}^{\infty} \frac{b_{l+2}^2}{(l+1)!} \frac{(-is)^l}{(4\pi)^{2l} (l!)^2} \left( (2l+1)H_l - 1 - l\gamma_E + l \ln(4\pi) - l \ln \frac{s}{s_0} \right).\end{aligned}$$

As expected from Theorem 80, we reproduce the free connected 2-point function  $-is$ , i.e. the inverse propagator (Eq. (5.8)) in the onshell limit  $s \rightarrow 0$ :

$$\lim_{s \rightarrow 0} \frac{i}{s} \bar{G}_2(s) = 1.$$

Moreover, if we demand that  $\bar{G}_2(s) = -is$  for all  $s \neq 0$  then necessarily all  $b_{n>2} = 0$  and  $\rho$  is equal to the underlying free theory. Demanding the 2-point function to be that of a free field is sufficient that the theory is free altogether, compare Theorem 1.

**Summary of Sect. 5.2.**

- The quantization of general relativity faces numerous technical and philosophical obstacles. Quantum gravity is unrenormalizable by power counting. Various remedies are conceivable. One of them is that quantum gravity might still be predictive if the counterterms are related by infinitely many Ward identities (Sect. 5.2.1).
- A field diffeomorphism is a non-linear global redefinition of the field variable. Diffeomorphisms have applications in various settings in QFT (Sect. 5.2.2).
- In position space, the Feynman rules of a diffeomorphism are straightforward from the definitions. They give rise to graphs without internal vertices, that is, without integrations (Sect. 5.2.3).
- In momentum space, the Feynman rules of a diffeomorphism contain vertices of any valence, which scale like inverse propagators. Every diffeomorphism is unrenormalizable by powercounting (Sect. 5.2.4).
- Momentum space Feynman rules can be simplified dramatically for connected amplitudes by introducing metavertices, which do not cancel internal edges of graphs (Sect. 5.2.5).
- The connected 2-point function is given by a sum of all multiedge graphs. For an underlying massless theory, the resulting amplitude can be computed explicitly (Sect. 5.2.6).

### 5.3 Exponential Diffeomorphism

In the field diffeomorphisms introduced in Sect. 5.2, the parameters  $\{a_n\}$  have been left undetermined. In the present section, we examine a certain family of diffeomorphisms where these parameters are powers of a single constant.

#### 5.3.1 Field Transformations

**Definition 120.** Let  $u \in \mathbb{N}$  and  $\lambda \in \mathbb{C}$ . The *exponential diffeomorphism* is defined as the diffeomorphism (Definition 118) with parameters

$$b_n = \begin{cases} 1 & n = 2 \\ \lambda^{n-2} & \exists k \in \mathbb{N}_0 : uk = n - 2 \\ 0 & \text{else.} \end{cases}$$

Definition 120 implies that the connected  $n$ -point function (Definition 20) is proportional to  $\lambda^{n-2}$ . In the following, we examine which transformation function  $\rho(\phi)$  or  $\phi(\rho)$  corresponds to the choice of coefficients given in Definition 120.

**Definition 121** ([124]). The *generalized hypergeometric function* is

$${}_pF_q \left( \{a_1, \dots, a_p\}, \{b_1, \dots, b_q\} \mid z \right) := \sum_{k=0}^{\infty} \prod_{i=1}^p \frac{\Gamma(k + a_i)}{\Gamma(a_i)} \prod_{j=1}^q \frac{\Gamma(b_j)}{\Gamma(k + b_j)} \frac{z^k}{k!}.$$

**Definition 122** ([125]). The *hyperbolic function* of order  $u$  of the  $r^{\text{th}}$  kind is

$$H_{u,r}(x) := \sum_{k=0}^{\infty} \frac{x^{uk+r}}{\Gamma(uk + 1 + r)}.$$

**Lemma 82** ([121]). Hyperbolic (Definition 122) and hypergeometric (Definition 121) functions are related via

$$H_{u,1}(z) = z \cdot \begin{cases} {}_1F_1(1; 2|z), & u = 1 \\ {}_0F_{u-1}\left(\{\}; \left\{\frac{2}{u}, \frac{3}{u}, \dots, \frac{u-1}{u}, \frac{u+1}{u}\right\} \middle| \left(\frac{z}{u}\right)^u\right) & u \geq 2. \end{cases}$$

**Lemma 83.** The exponential diffeomorphism (Definition 120) amounts to the field redefinition  $\rho(\phi)$  of the form

$$\rho(\underline{x}) = \frac{1}{\lambda} H_{u,1}(\lambda \phi(\underline{x})),$$

where  $H_{u,1}$  is the hyperbolic function (Definition 122).

**Proof** Using the diffeomorphism coefficients of Definition 120, the mapping  $\rho(\phi)$  is the series Definition 118,

$$\rho(x) = \sum_{n=1}^{\infty} \frac{b_{n+1}}{n!} \phi^n(x) = \phi \sum_{k=0}^{\infty} \frac{(\lambda \phi)^{ku}}{(uk + 1)!} = \phi \sum_{k=0}^{\infty} \frac{(\lambda \phi)^{ku}}{\Gamma(uk + 2)}.$$

This series is the hyperbolic function of order  $r = 2 - 1 = 1$  (Definition 122).  $\square$

The diffeomorphism given by Lemma 83 satisfy the differential equation [125]

$$\frac{d^u}{d\phi^u} \rho = \lambda^u \cdot \rho.$$

The solutions  $\rho(\phi)$  are sums of terms  $\rho \propto e^{q_i \lambda \phi}$  where  $q_i$  are  $u^{\text{th}}$  roots of unity, see Example 141. This fact motivates the name *exponential diffeomorphisms*.

### Example 141: Inverse exponential diffeomorphism.

For small  $u$ , the hyperbolic functions in Lemma 83 evaluate to

$$u = 1 : \quad \rho = \lambda^{-1} (e^{\lambda \phi} - 1),$$

$$u = 2 : \quad \rho = (2\lambda)^{-1} (e^{\lambda \phi} - e^{-\lambda \phi}) = \lambda^{-1} \sinh(\lambda \phi),$$

$$u = 3 : \quad \rho = (3\lambda)^{-1} \left( e^{\lambda \phi} + (-1)^{\frac{1}{3}} e^{-(1)^{\frac{1}{3}} \lambda \phi} + (-1)^{\frac{2}{3}} e^{(-1)^{\frac{2}{3}} \lambda \phi} \right).$$

Next, consider the diffeomorphism in the opposite direction, the function  $\phi(\rho)$ . Using Eq.(5.6), the diffeomorphism coefficients  $a_n$  can be computed in principle from the  $b_n$  in Definition 120, but there seems to be no easy explicit formula unless  $u = 1$ . One obtains

$$\begin{aligned} u = 1 : \quad a_n &= \frac{(-1)^n \lambda^n}{n+1}, \\ u > 1 : \quad a_n &= \begin{cases} \frac{(-1)^k \lambda^n}{(n+1)!} \cdot \alpha_k, & n = k \cdot u \\ 0 & \text{else,} \end{cases} \end{aligned} \quad (5.15)$$

where the sequences  $\{\alpha_k\}_{k \in \mathbb{N}}$  have been interpreted in terms of Whitney numbers [126].

### Example 142: Coefficients of the exponential diffeomorphism.

The case  $u = 1$  in Eq.(5.15) amounts to  $\alpha_n = n!$ . By explicit calculation, one obtains the sequences  $\{\alpha_k\}$ . Some of them can be identified empirically from the OEIS [127]:

$$\begin{aligned} u = 2 : \quad &\{1, 9, 225, 11025, 893025, \dots\} \quad [127, \text{A001818}], \\ u = 3 : \quad &\{1, 34, 5446, 2405116, 2261938588, \dots\} \quad [127, \text{A292750}], \\ u = 4 : \quad &\{1, 125, 124125, 477257625, \dots\}. \end{aligned}$$

### Example 143: Forward exponential diffeomorphism.

In the special cases  $u = 1, 2$ , the function  $\phi(\rho)$  can be obtained by inverting the function  $\rho(\phi)$  from Example 141:

$$\begin{aligned} u = 1 : \quad \phi &= \lambda^{-1} \ln(1 + \lambda\rho), \\ u = 2 : \quad \phi &= \lambda^{-1} \operatorname{asinh}(\lambda\rho) = \lambda^{-1} \ln(\sqrt{1 + (\lambda\rho)^2} + \lambda\rho). \end{aligned}$$

It is instructive to write down the Lagrangian for  $u = 1$  in the case  $s = p^2 - m^2$ ,

$$\mathcal{L} = -\frac{1}{2} \partial_\mu \phi \partial^\mu \phi - \frac{1}{2} m^2 \phi^2 = -\frac{1}{2} \frac{1}{(1 + \lambda\rho)^2} \partial_\mu \rho \partial^\mu \rho - \frac{1}{2} \frac{m^2}{\lambda^2} \ln^2(1 + \lambda\rho). \quad (5.16)$$

Setting  $m = 0$  and defining a field  $\varrho := 1 + \lambda\rho$ , Eq.(5.16) reads

$$\mathcal{L} = -\frac{1}{2\lambda^2} \cdot \varrho^{-2} \cdot \partial_\mu \varrho \partial^\mu \varrho. \quad (5.17)$$

This form vaguely reminds of the Einstein-Hilbert-Lagrangian (Eq.(5.2))  $\mathcal{L} \sim \sqrt{g} \cdot g^{-2} \partial_\mu g \partial_\nu g$ . Alternatively, from Eq.(5.15) we find  $a_n = \frac{(-1)^n g^n}{n+1}$  and the Lagrangian can be written as

$$\mathcal{L} = \frac{1}{2} (-\partial_\mu \rho + g \rho \partial_\mu \rho - g^2 \rho^2 \partial_\mu \rho + g^3 \rho^3 \partial_\mu \rho \mp \dots)^2.$$

To first order, this Lagrangian equals the choice of Example 136, which we argued to be analogous to QCD. Conversely, for the present case, the analogue to the Parke-Taylor formula (Example 139) has the particularly simple form

$$|V_n|^2 = g^{2n-4} \sum_{i=1}^n \left( \underline{p}_i \cdot \underline{p}_i \right)^2.$$

The rough qualitative analogy between field diffeomorphisms and gauge theory is probably of little help in practice, but it is pleasing to see that both the QCD-analogue and the gravity-analogue correspond to particularly simple, natural choices of diffeomorphisms—the first to a quadratic function, the second to an exponential one.

### 5.3.2 Correlation Functions of the Exponential Diffeomorphism

**Lemma 84** ([121]). Let  $\rho(x)$  be an exponential diffeomorphism (Definition 120), for a fixed  $u \in \mathbb{N}$ , of a free field  $\phi$  with propagator  $G_F(\underline{z})$  in position space. Assume that tadpoles vanish. Then, the connected full two-point function (Definition 20) of  $\rho$  in position space is

$$\bar{G}_2(\underline{z}) = \frac{1}{\lambda} H_{u,1}(\lambda^2 G_F(\underline{z})),$$

where  $H_{u,1}$  is the hyperbolic function (Definition 122).

#### Example 144: Exponential superpropagator.

Consider the massless theory with offshell variable  $s = \underline{p}^2$ , its propagator is Eqs.(1.27) and (2.49). One obtains the same functions as in Example 141. Especially, for  $u = 1$ , the resulting function is known as the *exponential superpropagator*,

$$\begin{aligned} \bar{G}_2(\underline{z}) &= \lambda^{-3} \left( e^{\lambda^2 G_F(\underline{z})} - 1 \right) \\ &= \lambda^{-2} \left( \exp \left( \frac{i\Gamma(1-\epsilon)\lambda^2}{(\underline{z}^2)^{1-\epsilon} 4\pi^{2-\epsilon}} \right) - 1 \right) = \lambda^{-2} \left( e^{\frac{i\lambda^2}{\underline{z}^2 (2\pi)^2}} - 1 \right) + \mathcal{O}(\epsilon). \end{aligned}$$

The superpropagator in position space is finite in the limit  $\epsilon \rightarrow 0$  as long as  $\underline{z}^2 \neq 0$ . But, in stark contrast to the free propagator  $G_F$  (Eq.(1.27)), or the perturbative 2-point function of any renormalizable theory, this function has an essential singularity at  $\underline{z}^2 = 0$  and it is not a tempered distribution [128]. Qualitatively, in order to remove the essential singularity, one needs to add terms of the form  $(\partial_\mu \partial^\mu)^n \delta(\underline{z})$  for all integers  $n$ . In a Fourier transform to position space (Eq.(1.2)), these terms become summands  $\propto (\underline{p}^2)^n$ . As always in renormalization, the counterterms are only well-defined up to a finite contribution. Consequently, the superpropagator in momentum space allows the addition of an arbitrary power series  $f(\underline{p}^2)$ . Consequently, the renormalized superpropagator is unpredictable, one can essentially *choose* what this function should be. The diffeomorphism is a non-renormalizable theory (Theorem 77), the non-predictive Fourier transform is exactly what is expected in such a case ([30], Sect. 2.3.4.3). We know the Feynman integrals of multiedges from Lemma 31. The infinitely many free constants correspond to the freedom to add finite terms into the counterterm of each  $M^{(l)}$ . The overall counterterm is not a constant, but a power series in  $\underline{p}^2$ , see Example 140.

By a field diffeomorphism, Liouville theory (Example 94) can be turned into a theory with polynomial interaction, but with the exponential superpropagator as 2-point function. Intuitively, 4-dimensional Liouville theory can be rendered predictive if one succeeds to remove the ambiguity from the superpropagator. Various prescriptions with conflicting results have appeared in the literature [86, 129–131].

The higher  $n$ -point functions of the exponential diffeomorphism (Definition 120) in position space are computable from Theorem 74. In the case  $u = 1$ , none of the  $b_n$  vanishes and the sum in Theorem 74 simplifies to

$$\tilde{G}^{(n)}(\underline{x}_1, \dots, \underline{x}_n) = \frac{1}{\lambda^n} \sum_{\substack{l_1, \dots, l_k \in \mathbb{N}_0 \\ t_j \geq 1 \ \forall j}} \frac{\lambda^{2l_1} \cdots \lambda^{2l_k}}{l_1! \cdots l_k!} G_F^{l_1}(\underline{x}_1 - \underline{x}_2) G_F^{l_2}(\underline{x}_1 - \underline{x}_3) \cdots G_F^{l_k}(\underline{x}_{n-1} - \underline{x}_n). \quad (5.18)$$

On the other hand, for  $u = 1$ , the connected 2-point function (Lemma 84) is the exponential superpropagator (Example 144),

$$\tilde{G}_2(\underline{z}) := \sum_{l=0}^{\infty} \frac{\lambda^{2l}}{l!} G_F^l(\underline{z}).$$

The sum Eq.(5.18) amounts to all ways to connect the  $n$  spacetime points by superpropagators. This implies yet another interpretation of the exponential diffeomorphism (Definition 120): The latter is the unique choice of parameters  $b_n$  for which the position-space correlation functions factorize into products of superpropagators.

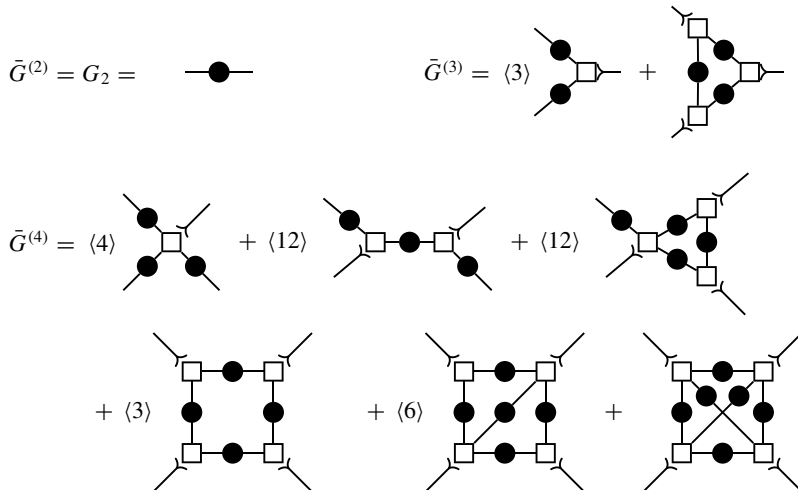
**Theorem 85** ([121]). Let  $\rho$  be an exponential diffeomorphism (Definition 120) of a free field. Assume further that tadpoles vanish. Then the connected Green functions  $\bar{G}^{(n>2)}$  (Definition 20) of  $\rho$  in momentum space are given by a sum over all the following connected graphs  $\Gamma$ :

1.  $\Gamma$  contains at most  $n$  vertices.
2. The  $j$ -valent vertices of  $\Gamma$  are metavertices  $V_j = -i\lambda^{n-2}(s_1 + \dots + s_j)$ .
3. There is at most one edge directly between any two metavertices.
4. Edges correspond to superpropagators in momentum space  $\bar{G}_2(s)$  (Example 144).
5. Every metavertex cancels precisely one of the  $n$  external edges, the uncancelled external edges are superpropagators  $\bar{G}_2(s)$ .
6.  $\Gamma$  carries a symmetry factor (Theorem 15) unity.

On first sight, Theorem 85 appears to be similar to Dyson-Schwinger equations (Theorem 16). But that impression is misleading: Theorem 85 does not describe fixed-point equations. To compute  $\bar{G}_n$ , assuming  $\bar{G}_2$  is known, only finitely many integrals remain to be solved and none of them involves  $\bar{G}_n$  itself.

#### Example 145: Green functions of the exponential diffeomorphism.

For the 2-, 3- and 4-point function, the graphs obtained from Theorem 85 are shown below. The brackets  $\langle k \rangle$  indicate a sum over  $n$  permutations (Definition 17).



In a Dyson-Schwinger equation (Example 37), the full 3-point function itself appears inside the integrals of  $\bar{G}^{(3)}$ , in the present case, it does not.

### Summary of Sect. 5.3.

- If the parameters of a diffeomorphism are chosen to be powers of one constant, then the diffeomorphism simplifies considerably and becomes a hypergeometric function. In the simplest such case, where the transformation is an exponential function, the resulting Lagrangian is qualitatively reminiscent of quantum gravity (Sect. 5.3.1).
- In position space, the correlation functions of the exponential diffeomorphism factorize into superpropagators. The superpropagator is not a tempered distribution and, it requires infinitely many renormalization conditions. Once the superpropagator is fixed, the higher correlation functions in momentum space are given by finitely many integrals (Sect. 5.3.2).

## 5.4 Divergences of Field Diffeomorphisms

In this section, we extend the formalism of the connected perspective (Sect. 5.2.4) to incorporate counterterms. We concentrate on the combinatorial properties and skip questions of physical interpretation. Moreover, the general proofs of the statements in the present section are rather tedious, but unilluminating combinatorial exercises. Instead of reproducing them here, we generally refer to the original article [121].

### 5.4.1 Metacounterterms

The connected perspective (Theorem 79) is based on metavertices which do not cancel adjacent internal edges. For a consistent treatment of divergences in the connected perspective, we need to define *metacounterterms*  $C_k$  which share the combinatorial properties of metavertices: they absorb all possible internal cancellations and appear in graphs without changing the graph topology. For brevity and concreteness, we only consider metacounterterms for the case that the underlying field (Definition 118) is a free field, we work in dimensional regularization (Sect. 2.3.3) and Minimal Subtraction (Definition 110), we assume that the divergent part of a 1-loop multiedge (Example 87) is independent of momenta, and we assume the vanishing of tadpoles (Sect. 5.1.4).

Metacounterterms can be classified by three integers  $j, k, l$  corresponding to the graphs they arise from. A metacounterterm  $C_{n,k}^{(l)}$  cancels the superficial divergence of graphs with

- $n$  external edges,
- $k \leq n$  external edges offshell (which implies precisely  $k$  metavertices), and
- $l$  loops.

A graph with  $n$  external edges can not have more than  $n$  external edges offshell, consequently we define

$$C_{n,k>n}^{(l)} := 0 \quad \forall n, k, l.$$

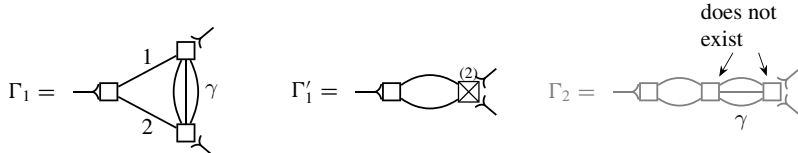
**Theorem 86** ([121]). Consider a diffeomorphism (Definition 118) of a free field. Assume that tadpoles vanish. Then, all connected Green functions  $\bar{G}^{(n)}$  (Definition 20) can be rendered finite if metacounterterms are included according to the following rules:

1. Construct the graphs of the connected perspective according to Theorem 79.
2. Proceed according to the BPHZ renormalization algorithm (Theorem 34), recursively replacing divergent subgraphs  $\gamma \subset \Gamma$  by their corresponding metacounterterm which subtracts the divergence. Finally, remove the superficial divergence.
3. The metacounterterm  $C_{n,k}$  is inserted in place of a graph on  $k$  metavertices, it cancels exactly  $k$  out of its  $n$  adjacent edges simultaneously.
4. Neither metavertices nor metacounterterms cancel internal edges of the graph.
5. There are neither internal metavertices nor internal metacounterterms.

In terms of cancellations, the only difference between metavertices and metacounterterms is that the former, by Eq. (5.14), cancel exactly one of their adjacent external edges, while metacounterterms  $C_{n,k}$  cancel  $k \leq n$  adjacent external edges.

#### Example 146: Metacounterterm in the 3-point-function.

The requirement of not cancelling internal edges automatically selects the correct parts of the metacounterterms. Consider the three-loop graph  $\Gamma_1$ :



$\Gamma_1$  has a divergent subgraph  $\gamma \subset \Gamma_1$ . This subdivergence is removed by the counterterm graph  $\Gamma'_1$  where a metacounterterm  $C_{4,2}^{(2)}$  (indicated by a crossed-out vertex) is inserted into the cograph  $\frac{\Gamma_1}{\gamma}$ . On the other hand, the graph  $\Gamma_2$  amounts to a different orientation of  $\gamma$  in the same cograph. However,  $\Gamma_2$  is not present in the connected perspective since it has an internal metavertex. This restriction is automatically respected by the metacounterterm  $C_{4,2}^{(2)}$ : When can-

canceling two edges, only those graphs contribute to  $C_{4,2}^{(2)}$  where the two cancelled edges are incident to two distinct metavertices, see the following figure:

$$\text{Diagram} = C_{4,2}^{(2)} = -\hat{\mathcal{R}} \left[ \text{Diagram} + \text{Diagram} + \text{Diagram} \right]$$

The third diagram is labeled "does not exist".

If we label the edges of  $C_{4,2}^{(2)}$  as 1, 2, 3, 4, then the graphs shown in the above figure are proportional to sums of two external momenta, that is, terms such as  $s_{1+2}$ , but not to  $s_j$  where  $j \in \{1, 2, 3, 4\}$ . Phrased differently: The cancellations of adjacent edges, which are caused by  $C_{4,2}^{(2)}$ , stem from metavertices of the underlying graphs, but not from the amplitudes  $\mathcal{F}[\Gamma]$  of the graphs themselves, because the latter always depend on sums  $s_{i+j}$  and not on individual  $s_i$ .

#### 5.4.2 Metacounterterms for Less Than 3 Edges Offshell

If all external edges are onshell, i.e.  $k = 0$  in  $C_{n,k}^{(l)}$ , then the amplitudes of the connected perspective vanish, consequently there is no divergence.

$$C_{n,0}^{(l)} = 0 \quad \forall n, l \quad \Rightarrow \quad C_{n,0} = 0. \quad (5.19)$$

If only one external edge is offshell, the amplitude is supported on graphs with a single metavertex. Such graphs are tadpoles and we assume them to vanish. We therefore have

$$C_{n,1}^{(l)} = 0 \quad \forall n, l \quad \Rightarrow \quad C_{n,1} = 0. \quad (5.20)$$

Graphically, these two identities are shown in Fig. 5.6.

As discussed in Sect. 5.2.6, the 2-point-function  $n = 2$  is supported on  $l$ -loop multiedge graphs  $M^{(l)}(s)$  which have no subdivergence and therefore do not require metacounterterms for subdivergences. Consequently, to render the 2-point function finite, all that is needed is the counterterm  $C_{2,2}$ . The  $l$ -loop metacounterterm for the 2-point-function is the divergent part  $-M_{\text{div}}^{(l)}$  of  $M^{(l)}$ ,

$$\begin{array}{ccc} \vdots & \text{Diagram} & = 0 \\ & \vdots & \end{array} \quad \begin{array}{ccc} \vdots & \text{Diagram} & = 0 \\ & \vdots & \end{array}$$

**Fig. 5.6** The metacounterterms  $C_{n,k}$  for connected amplitudes vanish identically if  $k = 0$  or  $k = 1$ , i.e. zero or one external edge is offshell

**Fig. 5.7** Metacounterterm  $C_{3,2}^{(l)}$  according to Eq.(5.22). For the indicated orientation of cancelled edges, only two graphs contribute

**Fig. 5.8** Metacounterterm  $C_{4,2}^{(l)}$  according to Eq.(5.23) for one of six orientations

$$C_{2,2}^{(l)}(s) = -(-ib_{l+2}s)^2 \frac{M_{\text{div}}^{(l)}(p^2)}{(l+1)!} = b_{l+2}^2 s^2 \frac{M_{\text{div}}^{(l)}(p^2)}{(l+1)!}. \quad (5.21)$$

For  $n > 2$  external edges, the metacounterterm with  $k = 2$  offshell edges still represents the superficial divergence of a graph on 2 metavertices i.e. a multiedge. The only difference to the case  $n = 2$  in Eq.(5.21) is that for  $n > 2$ , there are multiple possible orientations of the 2-vertex multiedge.

With  $n = 3$  external edges and  $k = 2$ , one of the metavertices is adjacent to one external edge and the other one to the remaining two, see Fig.5.7, and there are three ways to choose which two edges are offshell. The  $l$ -loop metacounterterm reads

$$C_{3,2}^{(l)} = \frac{b_{l+2}b_{l+3}}{(l+1)!} \left( s_1(s_2+s_3)M_{\text{div}}^{(l)}(s_1) + s_2(s_1+s_3)M_{\text{div}}^{(l)}(s_2) + s_3(s_1+s_2)M_{\text{div}}^{(l)}(s_3) \right). \quad (5.22)$$

With  $n = 4$  external edges and  $k = 2$  metavertices, two different configurations of multiedges are possible: Either each metavertex is adjacent to two external edges, or one of them to three and one to only one external edge. In the former case, the multiedge depends on a sum offshell variable  $s_{i+j}$ . There are six possibilities to choose two out of four edges offshell, each of them contributes four graphs as shown in Fig.5.8; the sum can be written as

$$C_{4,2}^{(l)} = \langle 4 \rangle \cdot b_{l+2}b_{l+4}s_1(s_2+s_3+s_4) \frac{M_{\text{div}}^{(l)}(s_1)}{(l+1)!} + \langle 3 \rangle \cdot b_{l+3}^2(s_1+s_2)(s_3+s_4) \frac{M_{\text{div}}^{(l)}(s_{1+2})}{(l+1)!}. \quad (5.23)$$

As expected,  $C_{4,2}^{(l)}$  again cancels exactly two out of its four external edges. Observe that  $M_{\text{div}}^{(l)}(s_1)$  in general is a monomial in  $s_1$ , and consequently the edge  $e_1$  gets cancelled multiple times.

Computing the higher valent metacounterterms, this pattern continues:

$$\begin{aligned} C_{5,2}^{(l)} &= \langle 5 \rangle \cdot b_{l+2} b_{l+5} s_1 (s_2 + s_3 + s_4 + s_5) \frac{M_{\text{div}}^{(l)}(s_1)}{(l+1)!} \\ &\quad + \langle 10 \rangle \cdot b_{l+3} b_{l+4} (s_1 + s_2) (s_3 + s_4 + s_5) \frac{M_{\text{div}}^{(l)}(s_{1+2})}{(l+1)!}. \end{aligned} \quad (5.24)$$

**Lemma 87** ([121]). The  $l$ -loop metacounterterm  $C_{n,k}^{(l)}$  with  $n$  edges, two of which are cancelled, is

$$C_{n,2}^{(l)} = \frac{1}{2} \sum_{j=1}^{n-1} \langle K_j \rangle b_{l+1+j} b_{l+n+1-j} (s_1 + \dots + s_j) (s_{j+1} + \dots + s_n) \frac{M_{\text{div}}^{(l)}(s_{1+\dots+j})}{(l+1)!},$$

where  $K_j = \binom{n}{j}$ , and  $\langle K_j \rangle$  indicates a symmetric sum over permutations (Definition 17).

### Example 147: 1-loop metacounterterms for the massless theory.

Assume that  $M_{\text{div}}^{(1)}$  is independent of momenta, this is true for example in  $D = 4 - 2\epsilon$  dimensions for quadratic propagators (Example 87). Then, the explicit prefactors in Lemma 87 constitute the only momentum-dependence. The product  $(s_1 + \dots + s_j)(s_{j+1} + \dots + s_n)$  contains  $j \cdot (n-j)$  summands. There are  $K_j = \binom{n}{j}$  such terms and the sum is symmetric. The elementary symmetric polynomial of order two in  $n$  variables is

$$E_2(s_1, s_2, \dots, s_n) = \left\langle \frac{n(n-1)}{2} \right\rangle s_1 s_2,$$

where  $\langle j \rangle$  denotes permutations (Definition 17).  $E_2(s_1, \dots, s_n)$  has  $\frac{n(n-1)}{2}$  factors, therefore

$$\langle K_j \rangle (s_1 + \dots + s_j)(s_{j+1} + \dots + s_n) = 2 \binom{n-2}{j-1} E_2(s_1, \dots, s_n)$$

and

$$C_{n,2}^{(1)} = E_2(s_1, \dots, s_n) M_{\text{div}}^{(1)} \sum_{j=1}^{n-1} \binom{n-2}{j-1} b_{j+2} b_{n-j+2}.$$

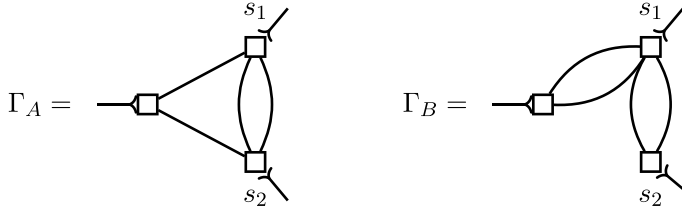


**Fig. 5.9** The two topologies of two-loop graphs contributing to the connected three-vertex correlation function where all three edges are cancelled. Each graph has three different permutations  $s_1 \rightarrow s_2 \rightarrow s_3$ , they are not indicated

If we further restrict ourselves to the exponential diffeomorphism (Definition 120) for  $u = 1$ , then  $b_{n+2} = \lambda_n$ . In  $D = 4 - 2\epsilon$  and for  $s = \underline{p}^2$ , the multiedge is the only divergent 1-loop graph, there are no divergent 1-loop graphs which involve  $k \geq 3$  metavertices. Therefore,  $\sum_k C_{n,k}^{(1)} = C_{n,2}^{(1)}$  actually represents the complete 1-loop counterterm. We can give its amplitude explicitly since we know the divergent part of the multiedge from Example 90:

$$C_n^{(1)} \equiv C_{n,2}^{(1)} = -\lambda^n \frac{2^{n-3}}{(4\pi)^2} \frac{1}{\epsilon} E_2(s_1, \dots, s_n).$$

For  $k > 2$  external edges offshell, the amplitudes in the connected perspective are no longer based on multiedge graphs exclusively. For  $k = 3$ , the new topology is triangle graphs, where each of the three internal edges is replaced by a multiedge. Additionally, there are contributions of two adjacent multiedges, see Fig. 5.9 for the topology at 2-loop order. The general principle of metacounterterms works as above, but from  $k = 3$  on, it is necessary to subtract subdivergences. A more detailed exposition can be found in [121]

#### Example 148: 3-point 2-loop metacounterterm for the massless theory.

Consider the massless theory with  $s = \underline{p}^2$  in  $D = 4 - 2\epsilon$ . At two loops, the metacounterterm  $C_{3,3}^{(2)}$  involves the graph topologies shown in Fig. 5.9. Divergent parts of the multiedges are derived in Lemma 31, the divergent part of the dunce's cap is quoted in Example 88. Together, and including permutations and symmetry factors, they give rise to the metacounterterm

$$C_{3,3}^{(2)} = i s_1 s_2 s_3 \frac{3}{4(4\pi)^4} \left( (b_3 b_4^2 + b_3^2 b_5) \frac{1}{\epsilon^2} - b_3 b_4^2 \frac{1}{\epsilon} \right).$$

### 5.4.3 1PI Counterterms

The metacounterterms  $C_{n,k}^{(l)}$  (Sect. 5.4.1) cancel the divergences of connected amplitudes, considered in the connected perspective. If we want to use the ordinary perspective, that is, the Feynman rules Lemma 75, then we need 1PI counterterms  $c_{n,k}^{(l)}$ . Their indices  $n, l, k$  have the same meaning as for the metacounterterms in Sect. 5.4.1. The sum  $c_n^{(l)} := \sum_{k=0}^n c_{n,k}^{(l)}$  represents the  $l$ -loop counterterm of the 1PI  $n$ -point function, that is, the  $l$ -loop order of the conventional counterterm  $Z^{(n)}$  in the sense of Definitions 106 and 91.

We know the metacounterterms from Sect. 5.4.2. At the same time, being counterterms for connected amplitudes, they correspond to all possible trees of 1PI counterterms  $c_{n,k}^{(l)}$  and 1PI vertices  $i v_n$  (Lemma 75). Extracting the 1PI counterterms is a question of combinatorics, namely a Legendre transform (Definition 55), they do not require any new evaluation of integrals.

In the present section, we demonstrate with a few explicit examples how the 1-loop 1PI counterterms can be obtained. Firstly, for the 2-point function, the 1PI one-loop amplitude and the amputated connected amplitude (Eq. (5.21)) are identical, therefore

$$C_2^{(1)} = C_{2,2}^{(1)} = b_3^2 s^2 \frac{M_{\text{div}}^{(1)}}{2} = c_2^{(1)}. \quad (5.25)$$

For the 3-point function, the connected 3-point divergence is the product of the 1PI 3-point divergence  $c_3^{(1)}$  and three adjacent connected 2-point divergences, see Fig. 5.10. To one-loop order, this product can contain only one divergent term in total, either  $c_3^{(1)}$  or one of the propagator counterterms  $c_{2,2}$ , consequently

$$C_3^{(1)} = c_3^{(1)} + \langle 3 \rangle i v_3 \frac{i}{s_1} c_{2,2}^{(1)}(s_1). \quad (5.26)$$

Here,  $\langle 3 \rangle$  denotes 3 permutations (Definition 17).

First consider the case of  $n = 3$  where all external edges are onshell, i.e.  $C_{3,0}^{(1)}$ . Then the metacounterterms  $C_3^{(1)}$  and  $C_2^{(1)}$  vanish due to Eqs. (5.19), and (5.26) simplifies to

$$0 = c_{3,0}^{(1)} + 0. \quad (5.27)$$

Now let one of the edges be offshell. The metacounterterm  $C_{3,1}^{(1)}$  vanishes due to Eq. (5.20), but one of the terms  $c_{2,2}^{(1)}$  in Eq. (5.26) remains, so

$$C_{3,1}^{(1)} = 0 = c_{3,1}^{(1)} + \langle 3 \rangle b_3(-is_1) \frac{i}{s_1} c_{2,2}^{(1)}(s_1). \quad (5.28)$$

This implies that

$$\text{eq. (5.25): } \text{Diagram}^{(1)} = \text{Diagram}^{(1)} = b_3^2 s^2 \frac{M_{\text{div}}^{(1)}}{2}$$

$$\text{eq. (5.28): } \underbrace{\text{Diagram}^{(1)}}_{=0} = \text{Diagram}^{(1)} + \text{Diagram}^{(1)} + \text{Diagram}^{(1)} + \text{Diagram}^{(1)}$$

$$\text{eq. (5.29): } \text{Diagram}^{(1)} = - \text{Diagram}^{(1)} = -b_3 \cdot b_3^2 s_1^2 \frac{M_{\text{div}}^{(1)}}{2}$$

**Fig. 5.10** Graphical representation for the computation of  $c_{3,1}^{(1)}$ . The perpendicular line indicates an external edge which must not be cancelled by the adjacent vertex

$$-\mathcal{R} \left[ \text{Diagram}^{(1)} + \text{Diagram}^{(1)} \right] = \text{Diagram}^{(1)} = \text{Diagram}^{(1)} + \text{Diagram}^{(1)} + \text{Diagram}^{(1)}$$

**Fig. 5.11** Graphical notation for the computation of  $c_{3,2}^{(1)}$ . The metacounterterm has been taken from Fig. 5.7

$$c_{3,1}^{(1)} = -\langle 3 \rangle b_3 c_{2,2}^{(1)}(s_1) = -b_3^3 (s_1^2 + s_2^2 + s_3^2) \frac{M_{\text{div}}^{(1)}}{2}. \quad (5.29)$$

For  $c_{3,2}^{(1)}$ , the metacounterterm  $C_{3,2}^{(1)}$  does not vanish, see Eq. (5.22). The construction of  $c_{3,2}^{(1)}$  is shown in Fig. 5.11, it yields

$$\begin{aligned} c_{3,2}^{(1)} &= C_{3,2}^{(1)} - \langle 3 \rangle (-ib_3 s_1) \frac{i}{s_2} c_{2,2}^{(1)}(s_2) - \langle 3 \rangle (-ib_3 s_2) \frac{i}{s_1} c_{2,2}^{(1)}(s_1) \\ &= \langle 6 \rangle b_3 (b_4 - b_3^2) s_1 s_2 \frac{M_{\text{div}}^{(1)}}{2} = b_3 (b_4 - b_3^2) \frac{M_{\text{div}}^{(1)}}{2} \cdot 2E_2(s_1, s_2, s_3). \end{aligned} \quad (5.30)$$

To streamline notation, we assumed that  $M_{\text{div}}^{(1)}$  is independent of momenta.

Finally,  $C_{3,3}^{(1)} = 0$  as there is no divergent connected graph that cancels three external edges at one loop (Example 147), therefore

$$c_{3,3}^{(1)} = 0. \quad (5.31)$$

This finishes our survey of 3-point 1PI counterterms at 1 loop order.

The higher  $n$ -point 1PI counterterms can be constructed similarly. For  $n = 4$  and  $k = 0$ , the mechanism is depicted in Fig. 5.12. The resulting 1PI counterterm is

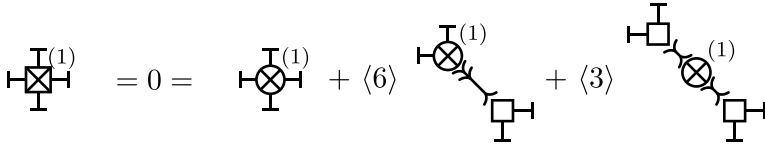


**Fig. 5.12** Construction of the onshell 4-point metacounterterm from metavertices 1PI counterterms. The metacounterterm  $C_{4,0}^{(1)}$  vanishes, see Fig. 5.6

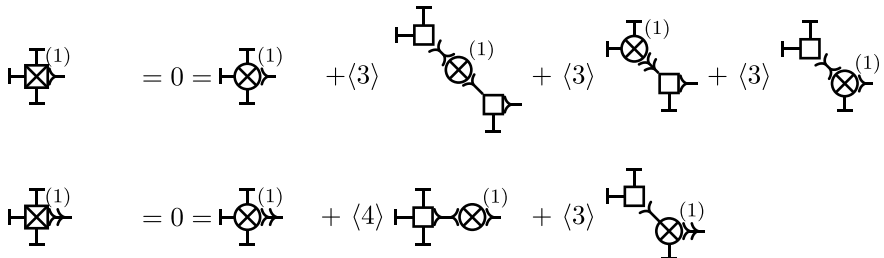


**Fig. 5.13** 4-valent metacounterterm with one external leg offshell, which can be cancelled once or twice, indicated by arrows. Edges with perpendicular lines must not be cancelled

$$c_{4,0}^{(1)} = -\langle 3 \rangle c_{3,1}^{(1)} \frac{i}{s_{1+2}} (-ib_3 s_{1+2}) = -b_3^4 (s_{1+2}^2 + s_{1+3}^2 + s_{1+4}^2) \frac{M_{\text{div}}^{(1)}}{2} \frac{1}{\epsilon}. \quad (5.32)$$

Observe that this 1PI counterterm does not vanish, even if the corresponding metacounterterm  $C_{4,0}^{(1)}$  does (Eq. (5.19)). With one external edge offshell, the metacounterterm  $C_{4,1}^{(1)}$  still vanishes (Eq. (5.20)) and we obtain the 1PI counterterm as shown in Fig. 5.13. Equation (5.29) implies that the second and third graph cancel and therefore

$$c_{4,1}^{(1)} = \langle 4 \rangle (b_4 - 3b_3^2) b_3^2 \frac{1}{2} M_{\text{div}}^{(1)} s_1^2 - \langle 4 \rangle 2b_3^2 (b_4 - b_3^2) \frac{1}{2} M_{\text{div}}^{(1)} (s_{1+2} + s_{1+3} + s_{1+4}) s_1.$$

This is the first instance of a 1PI counterterm which cancels a single of its external edges twice, as indicated by a double arrow in Fig. 5.13.

The structure of higher  $c_{n,k}^{(1)}$  is restricted by two mechanisms. Firstly, by power-counting, the one-loop 1PI counterterm  $c_n^{(1)}$  is proportional to two powers of offshell variables, hence, five different dependencies are possible: Square of an external offshell variable  $s_j^2$ , square of an internal one  $s_{i+j+\dots}^2$ , two different external ones  $s_i s_j$ , two different internal ones  $s_{i+j+\dots} s_{k+l+\dots}$  or a mixture of both types  $s_j s_{k+l+\dots}$ .

Secondly, since  $M_{\text{div}}^{(1)}$  is independent of momenta by assumption, the metacounterterms  $C_{n,k}^{(1)}$  are polynomials in only the external offshell variables  $s_j$ , but not in internal ones  $s_{i+j+\dots}$ . Both observations together severely restrict the structure of  $c_{n,k}^{(1)}$ . A rigorous proof requires a tedious recursive construction of trees, we skip the technical details and merely quote the results from [121].

**Lemma 88** ([121]). Assume that  $M^{(1)}$  is the only divergent 1-loop graph and that its divergent part  $M_{\text{div}}^{(1)}$  is independent of momenta. The summand in  $c_n^{(1)}$ , which is proportional to a square of an external offshell variable, is

$$+ (n-1)! a_{n-2} b_3^2 \frac{M_{\text{div}}^{(1)}}{2} (s_1^2 + \dots + s_n^2),$$

where  $a_n$  is given by Eq. (5.6).

**Lemma 89** ([121]). Assume that  $M^{(1)}$  is the only divergent 1-loop graph and  $M_{\text{div}}^{(1)}$  is independent of momenta. In the 1PI counterterm  $c_n^{(1)}$ , the contributions proportional to  $s_p^2$ , the square of the offshell variable of some partition  $p$  of the external momenta, is

$$b_3^2 \frac{M_{\text{div}}^{(1)}}{2} \frac{1}{2} \sum_{k=2}^{n-2} \sum_{p \in Q^{(n,k)}} k! a_{k-1} a_{n-k-1} (n-k)! s_p^2$$

where  $Q^{(n,k)}$  denotes the set of all possibilities to choose  $k$  out of  $n$  external legs.

**Lemma 90.** Assume that  $M^{(1)}$  is the only divergent 1-loop graph and that its divergent part  $M_{\text{div}}^{(1)}$  is independent of momenta. If  $b_n = \lambda^{n-2}$  then  $c^{(1)}$  does not contain any summands which are proportional to  $s_e \cdot s_f$ , where  $e \neq f$  can be external or internal offshell variables.

**Theorem 91.** For the exponential diffeomorphism (Definition 120),  $b_n = \lambda^{n-2}$ , the 1-loop counterterm  $c_n^{(1)}$  has the same structure as the 1PI vertex  $v_n$  (Lemma 75), up to a non-linear replacement of the offshell variable (Definition 8),

$$c_n^{(1)} = v_n \Big|_{s_e \rightarrow s_e \cdot \frac{M_{\text{div}}^{(1)}}{2} \lambda^2 s_e}.$$

**Proof** Add the contributions of Lemma 88 and 89 to obtain

$$\begin{aligned} c_n^{(1)} &= (n-1)! a_{n-2} b_3^2 \frac{M_{\text{div}}^{(1)}}{2} \left( s_1^2 + \dots + s_n^2 \right) + b_3^2 \frac{M_{\text{div}}^{(1)}}{2} \frac{1}{2} \sum_{k=2}^{n-2} \sum_{p \in Q^{(n,k)}} a_{n-k-1} a_{k-1} (n-k)! k! s_p^2 \\ &= \frac{1}{2} \sum_{k=1}^{n-2} \sum_{p \in Q^{(n,k)}} a_{n-k-1} a_{k-1} (n-k)! k! s_p^2 b_3^2 \frac{M_{\text{div}}^{(1)}}{2}. \end{aligned}$$

This equals the vertex Lemma 75 up to the claimed replacement of  $s_e$ . Given  $b_n = \lambda^{n-2}$ , Lemma 90 guarantees the absence of other terms.  $\square$

Theorem 91 asserts that if we set

$$is_{\mathcal{R}} := is - (is)^2 b_3^2 \frac{M_{\text{div}}^{(1)}}{2}, \quad (5.33)$$

then

$$iv_{\mathcal{R},n} := \frac{1}{2} \sum_{k=1}^{n-1} a_{n-k-1} a_{k-1} (n-k)! k! \sum_{p \in Q^{(n,k)}} is_{\mathcal{R},p} = iv_n + c_n^{(1)}$$

is a “renormalized” vertex in the sense that using  $iv_{\mathcal{R},n}$  in place of  $iv_n$ , all one-loop divergences are removed from the theory. The “renormalization” Eq. (5.33) is a divergent non-linear rescaling of a quantity, much like the rescaling  $\alpha = \alpha_0 + \mathcal{O}(\alpha_0^2)$  in conventional renormalization (Eq. (2.33)), only that it is not a rescaling of a coupling parameter, but, in a certain sense, a non-linear rescaling of spacetime. This finding is exciting, but it can not be generalized to higher loop orders, see Example 149. The failure at higher loop order is plausible from the involved Feynman graphs: From two loops on, there are divergent graphs which are not of propagator type, such as the dunce’s cap (Fig. 5.9). The divergence of non-propagator graphs can not possibly be cancelled by modifications of the propagator alone, because, even in ordinary renormalization, they require the presence of vertex counterterms.

Interestingly, this finding is reminiscent of quantum gravity (Sect. 5.2.1), uncoupled to matter: All 1-loop divergences can be removed by suitable redefinitions [132], but 2-loop divergences, at least in some formulation of gravity, require counterterms which are not present in the original Lagrangian [133, 134].

#### Example 149: 2-loop 1PI counterterms of the exponential diffeomorphism.

Consider the exponential diffeomorphism (Definition 120) with  $u = 1$ ,  $b_n = \lambda^{n-2}$ , of a massless field with  $s = \underline{p}^2$  in  $D = 4 - 2\epsilon$  dimensions. Then, the 1PI 2-loop counterterms are [121]

$$\begin{aligned}
c_{2,2}^{(2)} &= \frac{is^3}{24(4\pi)^4} \lambda^4 \left( \frac{1}{\epsilon} - 6 \frac{1}{\epsilon^2} \right), \\
c_{3,1}^{(2)} &= \frac{i(s_1^3 + s_2^2 + s_3^2)}{24(4\pi)^4} \lambda^5 \left( 6 \frac{1}{\epsilon^2} - \frac{1}{\epsilon} \right), \\
c_{3,2}^{(2)} &= -\frac{2i(s_1^2 s_2 + s_1^2 s_3 + s_2^2 s_1 + s_2^2 s_3 + s_3^2 s_1 + s_3^2 s_2)}{4(4\pi)^4} \lambda^5 \frac{1}{\epsilon^2}, \\
c_{3,3}^{(2)} &= \frac{3i s_1 s_2 s_3}{4(4\pi)^4} \lambda^5 \left( \frac{1}{\epsilon^2} - \frac{1}{\epsilon} \right).
\end{aligned}$$

Their tensor structure is not proportional to the vertex  $i v_3 = 2ia_2(s_1 + s_2 + s_3)$  (Example 137). This shows that, contrary to the 1-loop counterterms in Theorem 91, the 2-loop counterterms can not be generated by a rescaling of the momenta in the bare vertices like Eq.(5.33). Compare Example 145: The 3-point function  $\tilde{G}^{(3)}$  involves a triangle graph with superpropagators as edges. From 2 loops on, this graph is divergent, and requires a renormalization condition, even if the superpropagators themselves are finite (by a non-linear rescaling of  $s$ ).

We conclude that it is not possible to renormalize a field diffeomorphism by rescaling the offshell variable, not even in the special case of an exponential diffeomorphism (Definition 120). Instead, we need 1PI counterterms of all valences  $n \geq 2$ .

#### 5.4.4 Ward Identities of the Field Diffeomorphism

The non-vanishing metacounterterms  $C_n^{(l)}$  (Sect. 5.4.1) are proportional to at least two different external offshell variables  $s_j$ . Conversely, the 1PI counterterms of the same order can be proportional to inner offshell variables  $s_{i+j}$ , too, see for example Eq.(5.32). This means that the 1PI counterterms do not necessarily vanish in the onshell limit  $s_j \rightarrow 0$  of the external edges. Consequently, there must be identities amongst the 1PI counterterms which ensure that they do not contribute to the  $S$ -matrix (Definition 18) once all graphs are added up.

This behavior is completely analogous to the 1PI vertices  $i v_n$  Lemma 75 which, unlike the metavertices  $i V_n$  (Eq.(5.14)), contain such internal offshell variables in order to fulfil Eq.(5.13). Consequently, there is an analogue of Eq.(5.13) for counterterms, the following Ward identity (Definition 117):

**Theorem 92.** Consider a diffeomorphism (Definition 118) of a free field. Let  $c_n^{(l)} := \sum_{k=0}^n c_{n,k}^{(l)}$  be the  $l$ -loop  $n$ -valent 1PI counterterms and let

$$\Gamma_2 := -is - \sum_{l=1}^{\infty} c_2^{(l)}(s), \quad \Gamma_{n \geq 3} := iv_n + \sum_{l=1}^{\infty} c_n^{(l)},$$

and assume that tadpoles vanish (Sect. 5.1.4). Then, for  $n \geq 2$ ,

$$\begin{aligned} 1. \quad & \left[ \Gamma_n \frac{1}{\Gamma_2} (-is) \right]_{\text{only } s \text{ offshell}} = iv_n \Big|_{\text{only } s \text{ offshell}}, \\ 2. \quad & \sum_{\Gamma_j \star \Gamma_k = \Gamma_n} \left[ \Gamma_j \frac{1}{\Gamma_2} \Gamma_k \right]_{\text{onshell}} = -\Gamma_n \Big|_{\text{onshell}}, \end{aligned}$$

where the product  $\star$  implies that  $j + k = n + 2$  and the sum extends over all orientations of the involved graphs.

**Proof** First note that

$$\frac{1}{\Gamma_2} = \frac{i}{s - ic_2} = \frac{i}{s} \sum_{j=0}^{\infty} \left( \frac{i}{s} c_2 \right)^j$$

is the non-amputated chain of all 1PI 2-point counterterms, which equals the 2-point metacounterterm.  $\frac{1}{\Gamma_2} \cdot (-is)$  is the same chain where the outermost propagator is removed.

For any  $n \geq 3$ , the connected  $n$ -point correlation function vanishes if not more than one external edge is offshell due to Theorem 79. Consequently, its divergent part vanishes and  $C_{n,0} = C_{n,1} = 0$ , see Eqs. (5.19) and (5.20). It suffices to consider connected graphs where all internal edges are cancelled since the remaining graphs are products of the former type.

First prove point 1. Use induction on  $n$ . For  $n = 2$ , the statement becomes  $(-is) = iv_2$  which is true. For  $n = 3$ , since  $c_2$  vanishes onshell, the connected graph where only  $s$  is offshell is  $\Gamma_3 \frac{1}{\Gamma_2} (-is)$  where  $\Gamma_2$  is the counterterm of edge  $s$ . But  $C_{3,1} = 0$  and hence only the regular term survives of this sum, which is  $iv_3$  as claimed in point 1. Now assume the claim holds for  $j < n$ . Then, in the sum of all connected graphs, all divergent contributions cancel where  $s$  is adjacent to a  $j$ -valent counterterm, either directly or via a string of propagator counterterms. The only non-vanishing terms are those where a  $n$ -valent counterterm is involved. But again, the sum over all divergent terms has to vanish and the only remaining term is  $iv_n$ . This proves point 1.

For point 2, the case  $n = 2$  reads  $\Gamma_2|_{\text{onshell}} = -\Gamma_2|_{\text{onshell}}$  which is true since  $\Gamma_2|_{\text{onshell}} = 0$ . The same holds for  $n = 3$  since, by Eq. (5.19),  $\Gamma_3|_{\text{onshell}} = 0$ .

Assume point 2 holds for  $j, k < n$ . The onshell connected amplitude can only be proportional to powers of internal momenta  $s_e$ . If there is only one such internal

momentum, corresponding to one internal edge  $e$ , then all terms proportional to  $s_e$  arise from  $\Gamma_j \frac{1}{\Gamma_2(e)} \Gamma_k$ . Since these terms are not present in the end result, we know  $\Gamma_n$  must absorb them. If there is more than one edge, pick one and call it  $e$ . Then, there are two subtrees  $T_j, T_k$ , each of which has valence  $< n$  and only one external edge offshell, namely  $e$ . But by Eq. (5.20), such trees do not contain divergent terms. In fact, as a consequence of point 1, such trees do not even contain powers of internal momenta since they are made from tree-level vertices  $i v_k$  and such trees evaluate to  $b_j$  by Theorem 78. Therefore, the only relevant contribution stems from trees with exactly one internal multi-cancelled edge, which proves point 2.  $\square$

The compatibility of Theorem 92 with locality is expressed by the fact that such identifications between different  $n$ -point-functions represent Hopf ideals in the core Hopf algebra [88, 89]. Note also that Eq. (5.13) is the tree-level version of statement 2. Technically, only statement 1 of Theorem 92 requires the vanishing of tadpoles, i.e.  $C_{n,1} = 0$ , whereas statement 2 holds regardless. Furthermore, Theorem 92 is compatible with BCFW relations [135, 136], in the sense that the overall divergence of a connected graph is given by products of *onshell* subtrees, each of which vanishes.

The Ward identities of Theorem 92 play exactly the same role as they do in renormalizable theories: They implement a symmetry. In the case of field diffeomorphisms, the symmetry in question is invariance of the  $S$ -matrix (Theorem 80) under field diffeomorphisms. Point 2 of Theorem 92 ensures that, even at loop level, no counterterms arise which could alter the  $S$ -matrix.

Theorem 92 allows for a generalization of the lemmas at the end of Sect. 5.4.3. Point 1 of Theorem 92 can equivalently be written in the form

$$\Gamma_n \Big|_{\text{only } s \text{ offshell}} = \left[ i v_n \frac{i}{s} \Gamma_2(s) \right]_{\text{only } s \text{ offshell}}.$$

Upon expanding the series  $c_n^{(l)}$ , this implies

$$c_n^{(l)} \Big|_{\text{only } s \text{ offshell}} = \left[ v_n s^{-1} c_2^{(l)}(s) \right]_{\text{only } s \text{ offshell}}.$$

Consequently, the part of  $c_n^{(l)}$  proportional to powers of a single offshell variable is always given by the 2-point counterterm, Lemma 88 holds to all orders in perturbation theory. Similarly, inserting point 1 of Theorem 92 into point 2 produces

$$-\Gamma_n \Big|_{\text{onshell}} = \sum_{\Gamma_j \star \Gamma_k = \Gamma_n} \left[ i v_n \frac{i}{s} \Gamma_k \right]_{\text{onshell}} = \sum_{\Gamma_j \star \Gamma_k = \Gamma_n} \left[ i v_n \frac{i}{s} \Gamma_2(s) \frac{i}{s} i v_k \right]_{\text{onshell}}$$

and thereby also Lemma 89 holds to all orders.

It is Lemma 90 which fails at higher than one-loop order: To all orders, those parts of the counterterms which have the same momentum dependence as the vertices  $i v_n$

can be obtained by replacing  $-is \rightarrow \Gamma_2(s)$ . But starting from two-loop order, there are additional kinematic form factors in the counterterms which are not obtained in this way.

In renormalizable theories, by Lemma 35, each divergent amplitude has one single tensor structure and renormalization amounts to determining the scalar prefactor  $Z$  of this tensor. In the present case, on the other hand, a single amplitude obtains at higher loop order infinitely many additional tensor structures, each of which requires their own  $Z$  factor. Not all of these terms can be constructed recursively from Theorem 92, even if an infinite family can. It is this effect which ultimately renders the theory non-predictive despite the validity of Theorem 92.

This negative result for field diffeomorphisms does not directly translate to gravity (Sect. 5.2.1). The latter has a highly non-trivial tensor structure and we would need a dedicated examination to find out if, for a fixed  $n$ -graviton amplitude, the number of independent tensors can grow in a similarly uncontrolled way as it can for scalar fields. Such examination is beyond the scope of the present thesis.

### Summary of Sect. 5.4.

1. Divergences of connected amplitudes of a field diffeomorphism can be cancelled by metacounterterms, which work analogously to metavertices (Sect. 5.4.1). They are computed from Feynman graphs in the connected perspective (Sect. 5.4.2).
2. Ordinary counterterms, which cancel divergences of 1PI graphs, can be reconstructed from the metacounterterms by a Mellin transform (Sect. 5.4.3). For an exponential diffeomorphism, and only at 1-loop order, all counterterms amount to a non-linear rescaling of the offshell variable (Theorem 91).
3. A field diffeomorphism satisfies infinitely many Ward identities, which ensure that counterterms do not alter the  $S$ -matrix. These identities are not sufficient to render the theory predictive, as another infinite class of counterterms remains undetermined (Sect. 5.4.4).

## References

1. S. Coleman, J. Mandula, All possible symmetries of the  $S$  matrix. *Phys. Rev.* **159**, 1251–1256 (1967)
2. R. Haag, J.T. Lstrok;opuszański, M. Sohnius, All possible generators of supersymmetries of the  $S$ -matrix. *Nucl. Phys. B* **88**, 257 (1975)
3. M. Fierz, Über die relativistische Theorie kräftefreier Teilchen mit beliebigem Spin. *Helvetica Physica Acta* **12** (1939)
4. A. Sagnotti, Higher spins and current exchanges (2010)
5. A. Sagnotti, Notes on strings and higher spins. *J. Phys. Math. Theor.* **46**, 214006 (2013)
6. M. Fierz, Non-local fields. *Phys. Rev.* **78**, 184184 (1950)

7. H. Yukawa, Quantum theory of non-local fields. Part I. Free fields. *Phys. Rev.* **77**, 219–226 (1950)
8. E. Wigner, On unitary representations of the inhomogeneous Lorentz group. *Ann. Math.* **40**, 149 (1939)
9. J.C. Maxwell, A dynamical theory of the electromagnetic field. *Philos. Trans. R. Soc. Lond.* **155**, 459–512 (1865)
10. A. Einstein, Die Grundlage der allgemeinen Relativitätstheorie. *Annalen der Physik* **49**, 769 (1916)
11. S. Weinberg, Photons and gravitons in S-matrix theory: derivation of charge conservation and equality of gravitational and inertial mass. *Phys. Rev. B* **135**, B1049–B1056 (1964)
12. S. Weinberg, Photons and gravitons in perturbation theory: Derivation of Maxwell's and Einstein's equations. *Phys. Rev. B* **138**, B988–B1002 (1965)
13. J. Schwinger, Sources and gravitons. *Phys. Rev.* **173**, 1264–1272 (1968)
14. Y. Iwasaki, Consistency condition for propagators. *Phys. Rev. D* **2**, 2255–2256 (1970)
15. V. Alba, K. Diab, Constraining conformal field theories with a higher spin symmetry in d=4 (2013). [arXiv:1307.8092](https://arxiv.org/abs/1307.8092)
16. E.S. Fradkin, A.N. Vasil'ev, On the gravitation interaction of massless higher-spin fields. *Phys. Lett. B* **189**, 89–95 (1987)
17. E.S. Fradkin, M.A. Vasiliev, Cubic interaction in extended theories of massless higher-spin fields. *Nucl. Phys. B* **291**, 141–171 (1987)
18. N. Boulanger, P. Sundell, S. Leclercq, On the uniqueness of minimal coupling in higher-spin gauge theory. *J. High Energy Phys.* **2008**, 056056 (2008)
19. D.A. McGady, L. Rodina, Higher-spin massless S matrices in four dimensions. *Phys. Rev. D* **90**, 084048 (2014)
20. P.M. Lavrov, I.V. Tyutin, Canonical formalism of gauge theories with reducible constraints. *Sov. Phys. J.* **28**, 576–579 (1985)
21. B.W. Lee, J. Zinn-Justin, Spontaneously broken gauge symmetries. II. Perturbation theory and renormalization. *Phys. Rev. D* **5**, 3137–3155 (1972)
22. G. Curci, R. Ferrari, Slavnov transformations and supersymmetry. *Phys. Lett. B* **63**, 91–94 (1976)
23. E.S. Fradkin, I.V. Tyutin, S matrix for Yang-Mills and gravitational fields. *Phys. Rev. D* **2**, 2841–2857 (1970)
24. Ch. Brouder, A. Frabetti, Renormalization of QED with planar binary trees. *Eur. Phys. J. C Part. Fields* **19**, 715–741 (2001)
25. F.J. Dyson, The S matrix in quantum electrodynamics. *Phys. Rev.* **75**, 1736–1755 (1949)
26. J.C. Ward, An identity in quantum electrodynamics. *Phys. Rev.* **78**, 182 (1950)
27. G. 'tHooft, Renormalization of massless Yang-Mills fields. *Nucl. Phys. B* **33**, 173–199 (1971)
28. W.D. Van Suijlekom, The Hopf algebra of Feynman graphs in quantum electrodynamics. *Lett. Math. Phys.* **77**, 265–281 (2006)
29. W.D. van Suijlekom, Renormalization of gauge fields: A Hopf algebra approach. *Commun. Math. Phys.* **276**, 773–798 (2007)
30. W. Celmaster, R.J. Gonsalves, Renormalization-prescription dependence of the quantum-chromodynamic coupling constant. *Phys. Rev. D* **20**, 1420 (1979)
31. B.W. Lee, J. Zinn-Justin, Spontaneously broken gauge symmetries. I. Preliminaries. *Phys. Rev. D* **5**, 3121–3137 (1972)
32. J.A. Gracey, H. Kissler, D. Kreimer, On the self-consistency of off-shell Slavnov-Taylor identities in QCD (2019). [arXiv:1906.07996](https://arxiv.org/abs/1906.07996)
33. G. 't Hooft, M. Veltman, Combinatorics of gauge fields. *Nucl. Phys. B* **50**, 318–353 (1972)
34. D.M. Capper, G. Leibbrandt, Ward identities in a general axial gauge. I. Yang-Mills theory. *Phys. Rev. D* **25**, 1002–1008 (1982)
35. D.M. Capper, G. Leibbrandt, Ward identities in a general axial gauge. II. Quantum gravity. *Phys. Rev. D* **25**, 1009–1018 (1982)
36. D.F. Litim, J.M. Pawłowski, Flow equations for Yang-Mills theories in general axial gauges. *Phys. Lett. B* **435**, 181–188 (1998)

37. G. Keller, M. Salmhofer, C. Kopper, Perturbative renormalization and effective Lagrangians in Phi44. *Helv. Phys. Acta* **65**, 32–52 (1992)
38. U. Ellwanger, M. Hirsch, A. Weber, Flow equations for the relevant part of the pure Yang-Mills action. *Zeitschrift für Physik C Particles and Fields* **69**, 687–697 (1996)
39. M. Sars, Parametric representation of Feynman amplitudes in gauge theories (2015)
40. C.N. Yang, R.L. Mills, Conservation of isotopic spin and isotopic gauge invariance. *Phys. Rev.* **96**, 191–195 (1954)
41. S. Weinberg, Feynman rules for any spin. *Phys. Rev.* **133**, B1318–B1332 (1964)
42. A.A. Slavnov, Ward identities in gauge theories. *Theor. Math. Phys.* **10**, 99–107 (1972)
43. J.C. Taylor, Ward identities and charge renormalization of the Yang-Mills field. *Nucl. Phys. B* **33**, 436–444 (1971)
44. D. Kreimer, M. Sars, W.D. van Suijlekom, Quantization of gauge fields, graph polynomials and graph homology. *Ann. Phys.* **336**, 180–222 (2013)
45. D. Kreimer, K. Yeats, Properties of the corolla polynomial of a 3-regular graph. *Electron. J. Comb.* P41–P41 (2013)
46. D. Prinz, The corolla polynomial for spontaneously broken gauge theories. *Math. Phys. Anal. Geom.* **19**, 18 (2016)
47. M. Berghoff, A. Knispel, Complexes of marked graphs in gauge theory. *Lett. Math. Phys.* **110**, 2417–2433 (2020)
48. G. 't Hooft, M. Veltman, Diagrammar (Geneva, 1973). <http://cds.cern.ch/record/186259/files/CERN-73-09.pdf?version=1>
49. D. Kreimer, Structures in Feynman Graphs–Hopf algebras and symmetries (2002). <http://arXiv.org/abs/hep-th/0202110>
50. D. Kreimer, Anatomy of a gauge theory. *Ann. Phys.* **321**, 2757–2781 (2006)
51. W.H. Furry, A symmetry theorem in the positron theory. *Phys. Rev.* **51**, 125–129 (1937)
52. F. Brown, D. Kreimer, Angles, scales and parametric renormalization. *Lett. Math. Phys.* **103**, 933–1007 (2013)
53. D. Hilbert, Die Grundlagen der Physik (Erste Mitteilung.). Nachrichten von der Gesellschaft der Wissenschaften zu Göttingen, Mathematisch-Physikalische Klasse **1915**, 395–408 (1915)
54. D. Prinz, Algebraic structures in the coupling of gravity to gauge theories (2018). [arxiv.org/abs/1812.09919](http://arxiv.org/abs/1812.09919)
55. C.G. Neumann, *Untersuchungen über das logarithmische und Newton'sche Potential* (B.G. Teubner, Leipzig, 1877)
56. D. Kreimer, A remark on quantum gravity. *Ann. Phys.* **323**, 49–60 (2008)
57. A. Pais, G.E. Uhlenbeck, On field theories with non-localized action. *Phys. Rev.* **79**, 145–165 (1950)
58. P.D. Mannheim, Solution to the ghost problem in fourth order derivative theories. *Found. Phys.* **37**, 532–571 (2007)
59. L. Modesto, L. Rachwa & Istrok;, Universally finite gravitational and gauge theories. *Nucl. Phys. B* **900**, 147–169 (2015)
60. A. Salvio, A. Strumia, Quantum mechanics of 4-derivative theories. *Eur. Phys. J. C* **76**, 227 (2016)
61. J.A. Gracey, R.M. Simms, Higher dimensional higher derivative Phi4 theory. *Phys. Rev. D* **96**, (2017). <https://doi.org/10.1103/PhysRevD.96.025022>
62. A. Ganz, K. Noui, Reconsidering the Ostrogradsky theorem: higher-derivatives Lagrangians, ghosts and degeneracy. *Class. Quant. Grav.* **38**, 075005 (2021)
63. F. Briscese, L. Modesto, Unattainability of the trans-Planckian regime in nonlocal quantum gravity. *JHEP* **09**, 056 (2020)
64. H. Weyl, Eine neue Erweiterung der Relativitätstheorie. *Annalen der Physik* **364**, 101–133 (1919)
65. K.S. Stelle, Renormalization of higher-derivative quantum gravity. *Phys. Rev. D* **16**, 953–969 (1977)
66. S.L. Adler, Einstein gravity as a symmetry-breaking effect in quantum field theory. *Rev. Mod. Phys.* **54**, 729–766 (1982)

67. A. Zee, Einstein gravity emerging from quantum Weyl gravity. *Ann. Phys.* **151**, 431–443 (1983)
68. P.D. Mannheim, Conformal gravity challenges string theory (2007). [arXiv:0707.2283](https://arxiv.org/abs/0707.2283)
69. P.D. Mannheim, Alternatives to dark matter and dark energy. *Prog. Part. Nucl. Phys.* **56**, 340–445 (2006)
70. S.M. Christensen, M.J. Duff, Quantum gravity in 2 + epsilon dimensions. *Phys. Lett. B* **79**, 213–216 (1978)
71. R. Gastmans, R. Kallosh, C. Truffin, Quantum gravity near two dimensions. *Nucl. Phys. B* **133**, 417–434 (1978)
72. I. Jack, D.R.T. Jones, The epsilon-expansion of two-dimensional quantum gravity. *Nucl. Phys. B* **358**, 695–712 (1991)
73. P. Ehrenfest, Welche Rolle spielt die Dreidimensionalität des Raumes in den Grundgesetzen der Physik? *Annalen der Physik* **366**, 440–446 (1920)
74. J.H.C. Scargill, Can life exist in 2 + 1 dimensions? *Phys. Rev. Res.* **2**, 013217 (2020)
75. G.'t Hooft, Dimensional reduction in quantum gravity. *Conf. Proc. C* **930308**, 284–296 (1993)
76. J. Ambjørn, J. Jurkiewicz, R. Loll, Emergence of a 4D world from causal quantum gravity. *Phys. Rev. Lett.* **93**, 131301 (2004)
77. E.P. Verlinde, On the origin of gravity and the laws of newton, version 1. *J. High Energy Phys.* **04**, 029 (2011)
78. S. Carlip, Dimension and dimensional reduction in quantum gravity. *Class. Quantum Gravity* **34**, 193001 (2017)
79. M. Saravani, S. Aslanbeigi, A. Kempf, Spacetime curvature in terms of scalar field propagators. *Phys. Rev. D* **93**, 045026 (2016)
80. A. Kempf, Quantum gravity on a quantum computer? *Found. Phys.* **44**, 472–482 (2014)
81. F. Antonsen, K. Bormann, Propagators in curved space, version 1 (1996), [arXiv:hep-th/9608141](https://arxiv.org/abs/hep-th/9608141). <https://doi.org/10.48550/arXiv.hep-th/9608141>
82. D. Kreimer, Not so non-renormalizable gravity, in *Quantum Field Theory: Competitive Models*. ed. by B. Fauser, J. Tolksdorf, E. Zeidler (Birkhäuser, Basel, 2009), pp.155–162
83. S. Kamefuchi, H. Umezawa, On the structure of the interaction of the elementary pasticles, IV. On the interaction of the second kind. *Prog. Theor. Phys.* **9**, 529–549 (1953)
84. B.S. DeWitt, Gravity: a universal regulator? *Phys. Rev. Lett.* **13**, 114–118 (1964)
85. G. Lazarides, A.A. Patani, Q. Shafi, High-energy behavior in a model nonpolynomial Lagrangian field theory. *Phys. Rev. D* **6**, 2780–2788 (1972)
86. S. Okubo, Note on the second kind interaction. *Prog. Theor. Phys.* **11**, 80–94 (1954)
87. A. Bley, Cutkosky cuts at core Hopf algebra. MA thesis, Humboldt-Universität zu Berlin, Berlin, 2016, 42 pp., <http://www2.mathematik.hu-berlin.de/~kreimer/wp-content/uploads/Bley.pdf>
88. D. Kreimer, W.D. van Suijlekom, Recursive relations in the core Hopf algebra. *Nucl. Phys. B* **820**, 682–693 (2009)
89. D. Prinz, Gauge symmetries and renormalization (2022), [arXiv:2001.00104](https://arxiv.org/abs/2001.00104)
90. B.S. DeWitt, Quantum theory of gravity. I. The canonical theory. *Phys. Rev.* **160**, 1113–1148 (1967)
91. J.N. Goldberg, Conservation laws in general relativity. *Phys. Rev.* **111**, 315–320 (1958)
92. S.J. Avis, C.J. Isham, D. Storey, Quantum field theory in anti-de Sitter space-time. *Phys. Rev. D* **18**, 3565–3576 (1978)
93. L. Parker, Aspects of quantum field theory in curved space-time: effective action and energy-momentum tensor, in *Recent Developments in Gravitation: Cargèse 1978*. ed. by M. Lévy, S. Deser, N.A.T.O. Advanced (Study Institutes Series (Springer, US, Boston, MA, 1979), pp.219–273
94. B.S. DeWitt, Quantum field theory in curved spacetime. *Phys. Rep.* **19**, 295–357 (1975)
95. W.E. Thirring, An alternative approach to the theory of gravitation. *Ann. Phys.* **16**, 96–117 (1961)
96. R.P. Feynman, Quantum theory of gravitation. *Acta Phys. Polon.* **24**, 697–722 (1963)

97. B.S. DeWitt, Quantum theory of gravity. II. The manifestly covariant theory. *Phys. Rev.* **162**, 1195–1239 (1967)
98. B.S. DeWitt, Quantum theory of gravity. III. Applications of the covariant theory. *Phys. Rev.* **162**, 1239–1256 (1967)
99. D.M. Capper, G. Leibbrandt, M.R. Medrano, Calculation of the graviton self-energy using dimensional regularization. *Phys. Rev. D* **8**, 4320–4331 (1973)
100. C.J. Isham, A. Salam, J. Strathdee, Is quantum gravity ambiguity-free? *Phys. Lett. B* **46**, 407–411 (1973)
101. F.A. Berends, G.J.H. Burgers, H. van Dam, On spin three self interactions. *Zeitschrift für Physik C Particles and Fields* **24**, 247–254 (1984)
102. M.J. Duff, Quantum tree graphs and the Schwarzschild solution. *Phys. Rev. D* **7**, 2317–2326 (1973)
103. G.U. Jakobsen, General relativity from quantum field theory. Master thesis, 2020. [arXiv:2010.08839v1](https://arxiv.org/abs/2010.08839v1)
104. Y. Iwasaki, Quantum theory of gravitation vs. classical theory: fourth-order potential. *Prog. Theor. Phys.* **46**, 1587–1609 (1971)
105. J.F. Donoghue, Introduction to the effective field theory description of gravity (1995), <http://arxiv.org/abs/gr-qc/9512024>
106. A. Einstein, Näherungsweise Integration der Feldgleichungen der Gravitation. *Sitzungsber. Preuss. Akad. Wiss.* **1**, 688 (1916)
107. J. Blümlein, A. Maier, P. Marquard, G. Schäfer, Gravity in binary systems at the fifth and sixth post-Newtonian order (2022). [arXiv:2208.04552](https://arxiv.org/abs/2208.04552)
108. D. Kreimer, K. Yeats, Diffeomorphisms of quantum fields. *Math. Phys. Anal. Geom.* **20**, 16, 16 (2017)
109. D. Kreimer, A. Velenich, Field diffeomorphisms and the algebraic structure of perturbative expansions. *Lett. Math. Phys.* **103**, 171–181 (2013)
110. P.-H. Balduf, Perturbation theory of transformed quantum fields. *Math. Phys. Anal. Geom.* **23**, 33 (2020)
111. A.A. Mahmoud, K. Yeats, Diffeomorphisms of Scalar Quantum Fields via Generating Functions (2020). [arXiv:2007.12341](https://arxiv.org/abs/2007.12341) [math-ph]
112. A.A. Mahmoud, On the enumerative structures in quantum field theory (2020). [arXiv:2008.11661](https://arxiv.org/abs/2008.11661)
113. M. Omote, Point canonical transformations and the path integral. *Nucl. Phys. B* **120**, 325–332 (1977)
114. K.M. Apfeldorf, H.E. Camblong, C.R. Ordóñez, Field redefinition invariance in quantum field theory. *Mod. Phys. Lett. A* **16**, 103–112 (2001)
115. B.W. Lee, Gauge theories, in *Methods in Field Theory, Les Houches Session 1975*, ed. by R. Balian, J. Zinn-Justin. Les Houches Session 28 (North Holland/World Scientific, 1981), pp. 79–140
116. I.V. Chebotarev, V.A. Guskov, S.L. Ogarkov, M. Bernard, S-matrix of nonlocal scalar quantum field theory in basis functions representation. *Particles* **2**, 103–139 (2019)
117. M. Ruhdorfer, J. Serra, A. Weiler, Effective field theory of gravity to all orders. *J. High Energy Phys.* **05**, 083 (2020)
118. A.N. Vasilev, *The Field Theoretic Renormalization Group in Critical Behavior Theory and Stochastic Dynamics* (2004)
119. M.E. Peskin, D.V. Schroeder, *An Introduction to Quantum Field Theory* (1995), 842 pp., <https://cds.cern.ch/record/257493>
120. M.K. Volkov, Quantum field model with unrenormalizable interaction. *Commun. Math. Phys.* **7**, 289–304 (1968)
121. P.-H. Balduf, Propagator-cancelling scalar fields (2021). [arXiv:2102.04315](https://arxiv.org/abs/2102.04315) [math-ph]
122. F.A. Berends, W.T. Giele, Recursive calculations for processes with n gluons. *Nucl. Phys. B* **306**, 759–808 (1988)
123. S.J. Parke, T.R. Taylor, Amplitude for n-gluon scattering. *Phys. Rev. Lett.* **56**, 2459–2460 (1986)

124. C.F. Gauss, Disquisitiones generales circa seriem infinitam. *Commentationes Societatis Regiae Scientiarum Gottingensis, Recentiores classis mathematicae*, 227–270 (1813)
125. A. Ungar, Generalized hyperbolic functions. *Am. Math. Mon.* **89**, 688–691 (1982)
126. J. Engbers, D. Galvin, C. Smyth, Restricted Stirling and Lah number matrices and their inverses (2017), [arXiv:1610.05803](https://arxiv.org/abs/1610.05803)
127. N.J.A. Sloane (ed.), *The On-Line Encyclopedia of Integer Sequences* (2023), <https://oeis.org>
128. A.M. Jaffe, Form factors at large momentum transfer. *Phys. Rev. Lett.* **17**, 661–663 (1966)
129. H. Lehmann, K. Pohlmeyer, On the superpropagator of fields with exponential coupling. *Commun. Math. Phys.* **20**, 101–110 (1971)
130. R.J. Blomer, F. Constantinescu, On the zero-mass superpropagator. *Nucl. Phys. B* **27**, 173–192 (1971)
131. C.G. Bollini, J.J. Giambiagi, On the exponential superpropagator. *J. Math. Phys.* **15**, 125–128 (1974)
132. G. 't Hooft, M.J.G. Veltman, One loop divergencies in the theory of gravitation. *Ann. Inst. H. Poincaré Phys. Theor. A* **20**, 69–94 (1974)
133. M.H. Goroff, A. Sagnotti, The ultraviolet behavior of Einstein gravity. *Nucl. Phys. B* **266**, 709–736 (1986)
134. S. Abreu, F. Febres Cordero, H. Ita, M. Jaquier, B. Page, M.S. Ruf, V. Sotnikov, Two-loop four-graviton scattering amplitudes. *Phys. Rev. Lett.* **124**, 211601 (2020)
135. R. Britto, F. Cachazo, B. Feng, New recursion relations for tree amplitudes of gluons. *Nucl. Phys. B* **715**, 499–522 (2005)
136. R. Britto, F. Cachazo, B. Feng, E. Witten, Direct proof of tree-level recursion relation in Yang-Mills theory. *Phys. Rev. Lett.* **94**, 181602 (2005)

# Chapter 6

## Conclusion



### 6.1 Summary

We have examined the high-order perturbative renormalization of quantum field theory. Besides an extensive review of known concepts, we have reached the following results:

1. We extended the differential-equation version of Dyson-Schwinger equations to incorporate  $\epsilon$ -dependence (Sect. 3.3.4). For non-linear DSEs, the resulting equation is complicated, but we found an explicit formula for the order- $\epsilon$ -coefficient of the anomalous dimension of a linear DSE (Theorem 49).
2. We examined three popular example DSEs for an undetermined exponent  $w \in \mathbb{Z}$  of the invariant charge  $Q$ , and derived the leading asymptotic behavior of the coefficients of their anomalous dimensions (Sects. 3.4.1, 3.4.3 and 3.4.4). These results have been published in the author's article [1].
3. We found two seemingly exact solutions of non-linear toy model DSEs (Sect. 4.2.4) and two tentative exact values for the Stokes constant of the  $D = 4$  multiedge DSE (Sect. 3.4.1), all of which are contained in [1].
4. We computed the Stokes constant of the asymptotic growth of series coefficients as a function of  $w \in \mathbb{Q}$ . The result is a smooth, oscillating function, singular as  $w \rightarrow 0_-$ . We gave a tentative explanation (Sect. 3.4.2). This phenomenon is published so far only as a footnote in [1].
5. We analyzed counterterms and renormalization group equations in detail, for different renormalization conditions and including the full  $\epsilon$ -dependence. We related all quantities to the Hopf algebra formulation of renormalization (Sects. 3.2, 4.1 and 4.3). Although these statements are in principle known, the author is not aware of an exposition at a similar level of detail in the literature.

This study led us to the conclusion that Green functions in kinematic renormalization and in Minimal Subtraction are equivalent up to a different choice of renormalization point  $\delta(\alpha, \epsilon)$ , which, in perturbation theory, is a power series in  $\alpha$  and  $\epsilon$ .

6. We derived multiple formulas to compute  $\delta(\alpha, \epsilon)$  under the condition that the Green function is known both in MOM and in MS. To compute the  $\epsilon$ -independent part  $\delta(\alpha)$ , it is sufficient to know the renormalized Green functions for  $\epsilon = 0$  (Sects. 4.4.2 and 4.4.3). The case  $\epsilon = 0$  had been published in [1], the case  $\epsilon \neq 0$  is new.
7. We computed the shifts  $\delta(\alpha)$  for the three non-linear example DSEs and examined their power series coefficients. We found that the coefficients grow similarly to the ones of the anomalous dimension. These results are contained in [1].
8. For a linear DSE, we gave an explicit relation between the solution in MS at  $\epsilon = 0$  and the solution in MOM at  $\epsilon \neq 0$ . Using the above result, this allows us to compute the solution of a linear DSE in MS from the  $\epsilon$ -dependent Mellin transform alone, in a similar way as the MOM-solution can be found directly from the Mellin transform (Sect. 4.4.4). This result constitutes a central new contribution of the present thesis.
9. We examined the chain approximation and found that it does not arise from a Dyson-Schwinger equation. Physically, this means that it violates the fundamental principle of quantum mechanics, that all possible quantum processes must be included. Consequences of this shortcoming are that the chain approximation does not fulfil the renormalization group equations and it has inequivalent solutions in different renormalization schemes (Sect. 4.5.4). We conclude that the chain approximation is not a valid model for combinatorial properties of QFT. Parts of this argument are contained in [1].
10. We stated, skipping most of the proofs, the Feynman rules of a field diffeomorphism in momentum space and in position space. A diffeomorphism constitutes a perturbatively non-renormalizable theory, but its  $S$ -matrix coincides with the underlying field (Sect. 5.2). These results have been published in [2].
11. There is exactly one choice of diffeomorphism parameters with remarkably pleasant combinatorial properties, the exponential diffeomorphism (Sect. 5.3). In this case, the 2-point function is entirely undetermined, but once it has been fixed, all higher Green functions can be computed non-recursively, involving only finitely many Feynman graphs. This has been discussed in the author's preprint [3].
12. We examined the structure of divergences of a field diffeomorphism, following the preprint [3]. The outcome is that the divergences satisfy infinitely many Ward identities, which ensure that there are no divergent terms in the  $S$ -matrix. However, these identities still leave infinitely many divergences unconstrained. We conclude that the diffeomorphism theory is truly unrenormalizable (Sect. 5.4).
13. We included five remarks beyond the scope of the present thesis (Sects. 1.2.8, 1.3.9, 2.4, 3.2.4 and 5.2.1). They do not contain any new insights, but are perhaps useful for future doctoral candidates, as they concern topics which are rarely discussed explicitly in typical introduction courses.

## 6.2 Outlook: Numerical Integration of Feynman Periods

Apart from renormalization conditions and field diffeomorphisms, which have been presented in the main part of the thesis, the author devoted significant time of his doctorate to a third project, the numerical integration of Feynman periods. To keep the thesis at a reasonable length, the present section contains only a short outlook. The detailed results, together with a discussion of algorithms and implementation, have been published in [4].

### 6.2.1 Symmetries of the Period

The Feynman period  $\mathcal{P}[\Gamma]$  (Definition 98) is the coefficient of the logarithm of the scale and of the first-order pole in  $\epsilon$  (Theorem 32), of a primitive (Definition 88) Feynman amplitude. Equally,  $\mathcal{P}[\Gamma] = c_0$  is the first term of the Mellin transform (Definition 103) of the graph,

$$F_\Gamma(\rho) = \sum_{j=0}^{\infty} c_j \rho^{j-1}.$$

As discussed in Sect. 3.3, the Mellin transform is the input needed for Dyson–Schwinger equations in order to compute the all-order perturbative Green function  $G_R$  and inform a resurgence analysis (Sect. 2.1.2) of the non-perturbative properties (Sect. 3.4).

To derive the full Green function, we need to know the entire series expansion of the Mellin transform, for all (infinitely many) kernel graphs (Definition 52) of the DSE in question. Computing all of these series is beyond our current capabilities. The three examples discussed in the main text—the multiedge (Example 104) in  $D = 4$  and  $D = 6$ , and the toy model (Example 103)—were based on the intuition that a good approximation to the DSE can be obtained by considering the full Mellin transform of only a single kernel graph. The present section follows the opposite approach: Include as many kernel graphs as possible, but only the first coefficient of their Mellin transform. If the Mellin transform is truncated after  $c_0$ , then the DSE effectively becomes trivial, that is, its solution  $G_R$  is merely a sum of the primitive kernel graphs, without any insertions of divergent subgraphs.

We restrict ourselves to massless  $\phi^4$  theory in  $D = 4$  spacetime dimensions, and to the 4-point function. The resulting amplitudes are then contributions to the  $\beta$ -function (Definition 112) of  $\phi^4$  theory.

Computing the  $\beta$ -function to high loop order is relevant for conceptual questions of QFT, such as the existence of renormalons, see [5]. Moreover, as mentioned in Sect. 4.4.1, it is believed that in Minimal Subtraction, the beta function is dominated by primitive graphs, although a theoretical derivation of this result is still lacking [6]:

Since there are no citations given to substantiate these claims, their status is uncertain. The second of the [historic papers claiming that the beta function is dominated by primitive graphs] was written by the present author, but he recalls only that there was a general belief in the correctness of the assertion at the time.

For further applications, and concrete values, of the  $\beta$ -function in  $\phi^4$  theory, see [7–10].

**Definition 123.** A *n-edge-cut* of a graph  $\Gamma$  (Definition 24) is a set  $E_C := \{e_1, \dots, e_n\} \subset E_\Gamma$  such that removing the edges  $E_C$ ,  $\Gamma$  is split into at least two connected components (Definition 22), where none of the components is a single vertex. For us, a cut is always vertex-induced, that is, it is given by a partition of vertices, and  $E_C$  are those edges that join one part of the partition to the other.

Recall that the vertex-induced cuts form a vector space, the cut space (Definition 36).

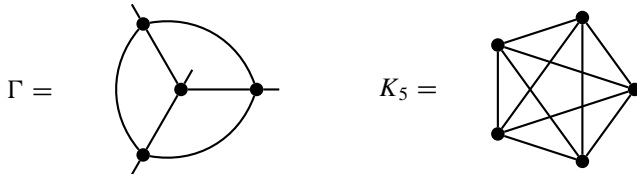
**Lemma 93.** In massless  $\phi^4$  theory in  $D = 4$  dimensions, a graph  $\Gamma$  is primitive if and only if it is internally 6-edge connected (Definition 22). That is, it has no  $k$ -edge-cut (Definition 123) with  $k < 6$ .

**Proof** Let  $\Gamma = \Gamma_1 \cup \Gamma_2$  be a split into two connected components. By Eq. 1.43,  $\phi^4$  theory does not contain graphs with an odd number of external edges. Therefore, all three graphs  $\Gamma, \Gamma_1, \Gamma_2$  have an even number of external edges, and there are no cuts with an odd number of edges.

By Lemma 35, a superficially divergent graph of  $\phi^4$  theory has 2 or 4 external edges. Assume that  $\Gamma$  has a divergent subgraph  $\gamma$ . Then  $\gamma$  has 2 or 4 external edges, that is,  $\gamma$  is connected to  $\frac{\Gamma}{\gamma}$  with 2 or 4 edges. Consequently,  $\Gamma$  has a 2-cut or a 4-cut. Conversely, if  $\Gamma$  is 6-connected, then there is no subgraph with less than 6 external edges, and therefore all subgraphs are convergent.  $\square$

**Definition 124.** A *completion* of a graph  $\Gamma$  is the graph  $\Gamma' = \Gamma \cup v$ , where  $v$  is an additional vertex and all external edges of  $\Gamma$  are incident to  $v$ , such that  $\Gamma'$  does not have any external edges. A *decompletion* of a completion  $\Gamma'$  is obtained by removing any vertex of  $\Gamma$ .

Every 4-point graph has a unique completion (Definition 124). On the other hand, a single completed graph typically gives rise to multiple non-isomorphic decompletions.

**Example 150: Wheel with spokes, completion.**

The graph  $\Gamma$  is called *wheel on three spokes*, its period is  $\mathcal{P}[\Gamma] = 6\zeta(3)$  [11] and its completion is  $K_5$ . In this particular case, all decompletions of  $K_5$  are isomorphic to  $\Gamma$ .

**Definition 125.** A *n-vertex-cut* of a graph  $\Gamma$  (Definition 24) is a set  $V_C := \{v_1, \dots, v_n\} \in V_\Gamma$  such that removing the vertices  $V_C$ ,  $\Gamma$  is split into at least two connected components Eq.(22), where none of the components is a single vertex.

The period  $\mathcal{P}[\Gamma]$  (Definition 98) is symmetric under certain operations on the graph  $\Gamma$ . Below, we list the known symmetries, a precise description can be found in [12–14].

Completion:	If $\Gamma_1$ and $\Gamma_2$ have the same completion $\Gamma'$ , then $\mathcal{P}[\Gamma_1] = \mathcal{P}[\Gamma_2]$ .
Product:	If $\Gamma = \Gamma_1 \cup \Gamma_2$ is a 3-vertex cut (Definition 125), then $\mathcal{P}[\Gamma] = \mathcal{P}[\Gamma_1] \cdot \mathcal{P}[\Gamma_2]$ .
Fourier:	If $\Gamma$ is a planar graph with planar dual $\tilde{\Gamma}$ , then $\mathcal{P}[\Gamma] = \mathcal{P}[\tilde{\Gamma}]$ .
Extended Fourier:	If the planar dual $\tilde{\Gamma}$ of a graph contains one vertex $v$ of valence higher than 4, construct the completion, remove $v$ , and take the planar dual again. If the result is a valid graph in $\phi^4$ theory, then its period coincides with $\mathcal{P}[\Gamma]$ . Repeat until the resulting graph has either none or more than one vertex of higher valence.
Twist:	If $\Gamma$ has a 4-vertex cut (Definition 125), then a pairwise exchange of the edges adjacent to the cut vertices does not alter the period.
Fourier split:	Assume that $\Gamma$ has a 4-vertex cut $\Gamma = \Gamma_1 \cup \Gamma_2$ (Definition 125). Taking the planar dual of one of the components, and reconnecting in a particular way, does not alter the period, $\mathcal{P}[\Gamma] = \mathcal{P}[\tilde{\Gamma}_1 \cup \Gamma_2]$ .

### 6.2.2 Numerical Quadrature

The number of primitive graphs grows factorially (Definition 60) with the loop number [15, 16]. There is a single period at 1 loop (the multiedge Example 19), a single one at 3 loops (the wheel with 3 spokes Example 150), but there are already more than 13000 periods at 10 loops. Even if by now the periods of hundreds of graphs are known analytically [12, 17–21], a sensible study of the high-order asymptotics of

periods requires significantly more data. One therefore resorts to numerical calculation of Feynman periods. We remark that the algorithm presented here is by no means the only modern development for numerically solving Feynman integrals. Besides established packages like FIESTA [22] and SecDec [23], there are for example recent approaches which try to estimate the integral with machine learning methods [24]. For our own project, we used a new integration algorithm developed by Borinsky [25, 26].

The integral in Definition 98,

$$\mathcal{P}[\Gamma] = \prod_{e \in E_\Gamma} \int_0^\infty \frac{da_e}{\Gamma(\nu_e)} a_e^{\nu_e - 1} \delta \left( 1 - \sum_{e=1}^{|E_\Gamma|} a_e \right) \frac{1}{\psi^2}, \quad (6.1)$$

is of high dimensionality, the method of choice for numerical quadrature is a Monte Carlo integration [27]. However, a direct Monte Carlo integration of Eq. 6.1 is impossible because the integrand has poles at the boundaries of the integration domain. The poles can be removed by splitting the integration domain into finitely many *Hepp sectors* [28], and scaling the integration variables in each of the sectors such that the new integrand is regular. Each of the sectors can be integrated numerically, for example with the Monte Carlo algorithm. This *sector decomposition* [29–32] can be automated, but for a given primitive  $\phi^4$ -graph  $\Gamma$ , it results in  $2^{|E_\Gamma|} = 4^{|L_\Gamma|}$  sectors. Consequently, the numerical computation of the period, for a single graph of 10 or more loops, requires the evaluation of millions of sector integrals.

The magnitudes of the individual sector integrals vary significantly. Borinsky [26] has achieved a breakthrough in computation efficiency by weighting each sector according to the Hepp bound (Definition 126), recently investigated by Panzer [14]. Using this weighting, a Monte-Carlo integration concentrates the sampling to sectors which give the largest contributions to the end result. The algorithm requires a table of Hepp bounds for all  $4^{|L_\Gamma|}$  Hepp sectors. This table, and not so much the actual computing time, is the limiting factor with regards to loop number. Computing 18-loop  $\phi^4$ -periods requires slightly more than 1TB of RAM.

**Definition 126.**[14, 28] Let  $\Gamma$  be a Feynman graph and  $\sigma$  a permutation of the edges  $E_\Gamma$ , and let the graph  $G_k^\sigma := \{\sigma(1), \dots, \sigma(k)\}$  be the first  $k$  edges in  $\sigma$ . Let  $S_n$  be the symmetric group of all  $|E_\Gamma|!$  permutations of  $E_\Gamma$ . The *Hepp bound* of a Feynman graph  $\Gamma$  is the rational function

$$\mathcal{H}[\Gamma] := \sum_{\sigma \in S_n} \frac{1}{\omega(G_1^\sigma) \cdots \omega(G_{|E_\Gamma|-1}^\sigma)},$$

where  $\omega(G_k^\sigma)$  is the superficial degree of convergence (Definition 43) of the graph  $G_k^\sigma$ .

The Hepp bound is indeed a bound of the period, which was its original motivation in the study of convergence of Feynman integrals [28]:

$$\mathcal{H}[\Gamma] \cdot \left| T_{\Gamma}^{(1)} \right|^{-2} \leq \mathcal{P}[\Gamma] \leq \mathcal{H}[\Gamma], \quad (6.2)$$

where  $T_{\Gamma}^{(1)}$  is the set of all spanning trees (Definition 35).

The Hepp bound (Definition 126) satisfies all known symmetries of the period. Moreover, there are pairs of graphs where the Hepp bounds coincide, but the two graphs are not related by any of the known symmetries. This probably indicates that there are still undiscovered symmetries of the period.

### Example 151: Wheel with spokes, Hepp bound.

The wheel with three spokes from Example 150 has 6 edges and therefore, the sum in Definition 126 is over  $6! = 720$  permutations. Its Hepp bound (Definition 126) is  $\mathcal{H}[\Gamma] = 84$ . There are 12 spanning trees (Definition 35) and Eq. 6.2 is satisfied:

$$\frac{8}{12} = \mathcal{H}[\Gamma] \cdot 12^{-2} \leq 6\zeta(3) \leq \mathcal{H}[\Gamma] = 84.$$

This example indicates that the Hepp bound is a rather crude approximation of the period.

### 6.2.3 Results

Our own contribution consists of two parts. Firstly, we implemented all known symmetries of the period (Sect. 5.1.1) as a new C++ program. The extended dual symmetry has been mentioned in [12], but apparently it has not actually been used in current implementations. It is also possible to combine the Fourier split with the extended Fourier symmetry on the components. The extended Fourier symmetry sometimes leads to sequences of many intermediate graphs until it finally produces a symmetric  $\phi^4$ -graph. This entails that, to find all symmetries of a given graph, the program typically has to construct thousands of candidate graphs, which is computationally demanding. Details of the implementation, as well as more statistical information regarding the symmetries, will be reported elsewhere.

We generated all completed (Definition 124) 4-point graphs of  $\phi^4$  theory up to 14 loops using nauty [33], and filtering for primitive graphs according to Lemma 93. For the graphs up to 13 loops, we determined the precise count of all known symmetries, including the extended Fourier split, see Table 6.1. The number of symmetries we find is slightly higher than what has been reported so far in the literature [12, 14]. The number of cases where Hepp bounds coincide, but the coincidence is not explained by a known symmetry, is therefore actually lower than the numbers in [14]. Nevertheless, from 8 loops on, there are unexplained identities. We have verified in every single case that if two graphs are related by a known symmetry, their Hepp bounds coincide.

**Table 6.1** Statistical information on  $\phi_4^4$ -periods. **L** Loop order of the decompletion; Total number of... **Decomp.** non-isomorphic decompletions (= primitive 4-valent graphs); **Planar dec.** planar completions; **Irred. compl.** 3-vertex-irreducible completions; **Twist** twist identities; **F** extended Fourier identities; **T+F** Twist and extended Fourier combined; **F split** extended Fourier splits; **Indep. periods** independent irreducible periods exploiting all known symmetries; **Hepp** numerically distinct Hepp bounds at machine precision; **Unexpl. Hepp**: Unique Hepp bounds coinciding for (sets of) graphs not related by known symmetries. This number is not equal 'independent periods'-'distinct Hepp bounds' since sometimes, more than two sets have the same identical Hepp bounds

L	Decomp.	Planar dec.	Irred. compl.	Twists	F	T+F	F split	Indep. periods	Hepp	Unexpl. Hepp
5	3	2	1	0	0	0	0	1	1	0
6	10	5	4	0	0	0	0	4	4	0
7	44	19	11	1	2	2	2	9	9	0
8	248	58	41	9	3	10	9	31	29	2
9	1688	235	190	48	14	55	53	134	129	5
10	13094	880	1182	336	21	350	334	819	776	42
11	114016	3623	8687	2387	43	2420	2276	6197	6030	158
12	1081529	14596	74204	18680	60	18728	17040	55196	54552	618
13	11048898	60172	700242	155547	90	155630	138164	543535	541196	2246
14	120451435		7160643	1386809	117			5773724		

One identity means a reduction of the number of independent graphs by one. The symmetry counts refer to irreducible graphs only, the reducible ones have additional symmetries. Note that many identities can be interpreted both as twist or as planar dual identity at the same time, and that planar duals are overall very rare

Our second contribution is the actual numerical computation of Feynman periods. The article [26] already contains a C++ reference implementation. We did some trivial modifications on this program in order to fine-tune it especially for  $\phi_4^4$ -periods. Moreover, the whole process—generation of graphs, numerical integration, and computation of symmetry factors,  $n$ -edge cuts (Definition 123) and other statistical quantities—has been fully automated, reading and saving all intermediate steps directly to compressed files, and ran on various computers at Humboldt-Universität zu Berlin since late 2020.

We deliberately chose to compute *all* completed graphs, and not just the remaining ones after application of symmetries, because this allows us to verify that expected symmetries are satisfied in every single case. No computation time is wasted because, after verification of symmetries, we combine the individual results of all symmetric graphs to obtain higher accuracy in the end result.

We have computed all periods up to 12 loops to at least  $90 \cdot 10^{-6}$  relative accuracy, and all 13-loop periods to at least  $290 \cdot 10^{-6}$  relative accuracy. Moreover, we have computed a total of over  $3 \cdot 10^5$  randomly selected graphs with 14 to 18 loops. The precise numbers are reported in Table 6.2. In total, we computed more than 1.1 million completed graphs, which amounts to the period values of round about 12 million non-isomorphic graphs of the 4-point function in  $\phi_4^4$  theory.

**Table 6.2** Statistical information on the graphs considered in this work. **L** Loop order; **computed** Number of numerically computed completed primitives, without using symmetries; **proportion** ratio of the computed completed primitives to the total number at that loop order; **rel. error** average/maximum relative uncertainty, in ppm, after imposing symmetries, where the average is taken over all computed graphs. The uncertainty refers to the computed graphs only, not also the ones constructed. **irreducible** number of irreducible graphs computed, **Hepp** number of distinct Hepp bounds within the irreducible graphs, **5 σ-d** number of irreducible graphs which are at least  $5\sigma$ -distinct from any other computed graph. **constr.** number of completed primitives, including the computed ones, constructed from the computed graphs by symmetries

L	Computed	Proportion	Rel. error	Irreducible	Hepp	5σ-d	Constr.
5	2	1	85/85	1	1	1	–
6	5	1	86/90	4	4	4	–
7	14	1	80/89	11	9	9	–
8	49	1	74/90	41	29	28	–
9	227	1	70/90	190	129	127	–
10	1354	1	68/90	1182	776	578	–
11	9722	1	69/90	8687	6030	1563	–
12	81305	1	57/90	55196	54706	3002	–
13	755643	1	218/288	700242	541196	1346	–
14	215738	$2.8 \cdot 10^{-2}$	246/289	208121	205335	1030	273462
15	99212	$1.1 \cdot 10^{-3}$	222/308	97178	96177	1198	142040
16	9996	$1.0 \cdot 10^{-5}$	219/273	9733	9733	997	21437
17	5144		172/261	5043	5043	999	11578
18	789		113/220	7 64	764	579	1448

In all cases, the numerical results satisfy the expected symmetries. Moreover, the periods agree, within the numerical accuracy, in all cases where Hepp bounds agree. The correspondence between symmetries, Hepp bounds, and numerical results indicates that our implementation of symmetries is likely correct.

Although we know some symmetries of the period, it would still be possible that even more periods coincide by unknown symmetries, perhaps even if their Hepp bounds are unequal. We tried to estimate a lower bound on the number of distinct periods. To this end, we counted how many numerical periods are distinct from all others of the same loop order by at least five standard deviations. However, due to the high number of periods, our numerical accuracy is not sufficient to tell most of them apart, and the so-obtained lower bound is weak, see Table 6.2.

In the cases where we computed only a random sample of periods, we used the symmetries to construct all symmetric graphs, whose value thereby is known as well. The latter periods are, however, not usable for the estimation of the asymptotics, because using them would distort the random sample of graphs, giving more weight to graphs which have more symmetries.

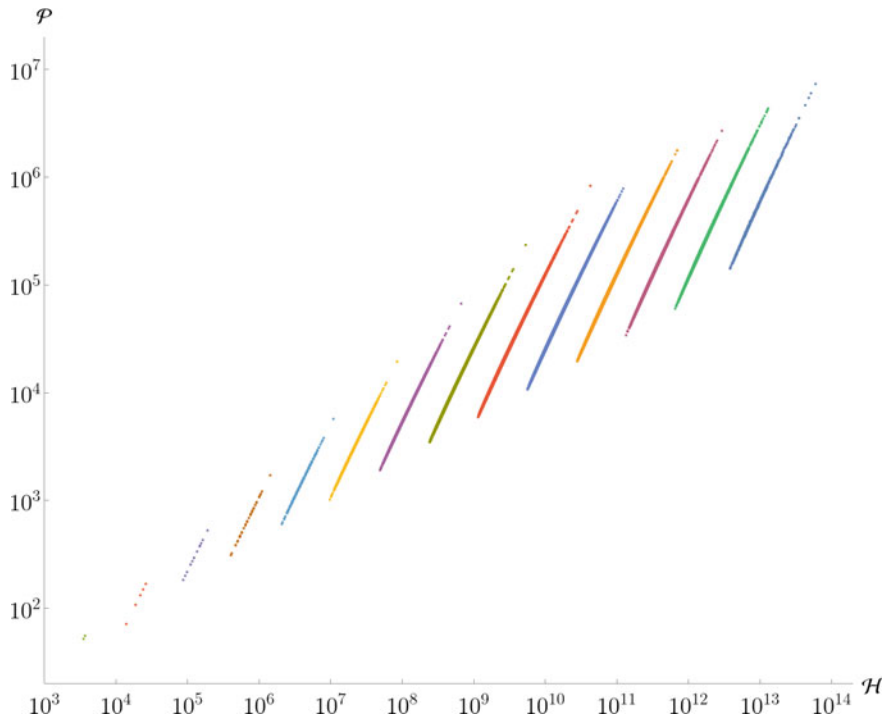


**Fig. 6.1** All computed periods, as a function of their Hepp bound (Definition 126). Colours indicate loop order, starting from 5 loops on the left. We see that, within the same loop order, the period is strongly correlated with the Hepp bound. This plot contains 1.1 million data points. Compare similar plots in [4]

At this point, we do not report the concrete numerical values we obtained, because the results would need significant explanation, which is beyond the scope of this thesis. As an illustration, Fig. 6.1 shows all our periods. The complete results can be found in [4].

## References

1. P.-H. Balduf, DysonSchwinger equations in minimal subtraction. Ann. Inst. Henri Poincaré D (2023). <https://doi.org/10.4171/aihp/169>
2. P.-H. Balduf, Perturbation theory of transformed quantum fields. Math. Phys. Anal. Geom. **23**, 33 (2020)
3. P.-H. Balduf, Propagator-cancelling scalar fields (2021). [arXiv:2102.04315](https://arxiv.org/abs/2102.04315) [math-ph]
4. P.-H. Balduf, Statistics of Feynman amplitudes in  $\phi^4$ -theory. J. High Energy Phys. **2023**, 160 (2023). [https://doi.org/10.1007/JHEP11\(2023\)160](https://doi.org/10.1007/JHEP11(2023)160). 73 pages. [arXiv:2305.13506](https://arxiv.org/abs/2305.13506) [hep-th]
5. G.V. Dunne, M. Meynig, Instantons or Renormalons? A Comment on phi4\_4 Theory in the MS Scheme (2021). [ARXIV: 2111.15554](https://arxiv.org/abs/2111.15554)

6. A.J. McKane, Perturbation expansions at large order: results for scalar field theories revisited. *J. Phys. A: Math. Theor.* **52**, 055401 (2019)
7. D.J. Broadhurst, D. Kreimer, Knots and numbers in  $\phi^4$  theory to 7 loops and beyond. *Int. J. Mod. Phys. C* **06**, 519–524 (1995)
8. L.T. Adzhemyan, M.V. Kompaniets, Five-loop numerical evaluation of critical exponents of the  $\varphi^4$  theory. *J. Phys: Conf. Ser.* **523**, 012049 (2014)
9. M.V. Kompaniets, E. Panzer, Minimally subtracted six loop renormalization of  $O(n)$  - symmetric  $\phi^4$  theory and critical exponents. *Phys. Rev. D* **96**, 036016 (2017)
10. M.V. Kompaniets, E. Panzer, Renormalization group functions of  $\phi^4$  theory in the MS-scheme to six loops. *PoS LL2016*, 038 (2016)
11. D.Z. Freedman, K. Johnson, J.I. Latorre, Differential regularization and renormalization: a new method of calculation in quantum field theory. *Nucl. Phys. B* **371**, 353–414 (1992)
12. O. Schnetz, Quantum periods: a census of  $\phi^4$ -transcendentals. *Commun. Num. Theor. Phys.* **4**, 1–48 (2010)
13. S. Hu, O. Schnetz, J. Shaw, K. Yeats, Further investigations into the graph theory of  $\phi^4$ -periods and the  $c_2$  invariant. *Ann. Inst. Henri Poincaré D* **9**, 473–524 (2022)
14. E. Panzer, Hepp’s bound for Feynman graphs and matroids. *Ann. Inst. Henri Poincaré D* **10**, 31–119 (2022)
15. M. Borinsky, Renormalized asymptotic enumeration of Feynman diagrams. *Ann. Phys.* **385**, 95–135 (2017)
16. M. Borinsky, *Graphs in Perturbation Theory: Algebraic Structure and Asymptotics*, Springer Theses (Springer International Publishing, Cham, 2018).
17. E. Nasrollahpouramami, *Periods of Feynman Diagrams and GKZD-Modules*, (2016). [ARXIV: 1605.04970](#)
18. M. Borinsky, O. Schnetz, Recursive computation of Feynman periods. *J. High Energy Phys.* **2022**, 291 (2022)
19. F.C.S. Brown, On the periods of some Feynman integrals (2010). [ARXIV: 0910.0114](#)
20. F. Brown, O. Schnetz, Single-valued multiple polylogarithms and a proof of the zig-zag conjecture. *J. Number Theory* **148**, 478–506 (2015)
21. E. Panzer, O. Schnetz, The Galois coaction on  $\phi^4$  periods. *Commun. Number Theory Phys.* **11**, 657–705 (2017)
22. A.V. Smirnov, N.D. Shapurov, L.I. Vysotsky, FIESTA5: numerical high-performance Feynman integral evaluation (2021). [ARXIV: 2110.11660](#)
23. S. Borowka, J. Carter, G. Heinrich, Numerical evaluation of multi-loop integrals for arbitrary kinematics with SecDec 2.0. *Comput. Phys. Commun.* **184**, 396–408 (2013)
24. D. Mâtre, R. Santos-Mateos, Multi-variable integration with a neural network. *J. High Energy Phys.* **2023**, 221 (2023)
25. M. Borinsky, H.J. Munch, F. Tellander, *Tropical Feynman integration in the Minkowski regime* (2023). [ARXIV: 2302.08955](#)
26. M. Borinsky, Tropical Monte Carlo quadrature for Feynman integrals. *Ann. Inst. Henri Poincaré D* **10**, 635–685 (2023)
27. N. Metropolis, A.W. Rosenbluth, M.N. Rosenbluth, A.H. Teller, E. Teller, Equation of state calculations by fast computing machines. *J. Chem. Phys.* **21**, 1087–1092 (1953)
28. K. Hepp, Proof of the Bogoliubov-Parasiuk theorem on renormalization. *Commun. Math. Phys.* **2**, 301–326 (1966)
29. T. Binoth, G. Heinrich, An automatized algorithm to compute infrared divergent multi-loop integrals. *Nucl. Phys. B* **585**, 741–759 (2000)
30. C. Bogner, S. Weinzierl, Resolution of singularities for multi-loop integrals. *Comput. Phys. Commun.* **178**, 596–610 (2008)
31. A.V. Smirnov, V.A. Smirnov, Hepp and Speer sectors within modern strategies of sector decomposition. *J. High Energy Phys.* **2009**, 004–004 (2009)
32. T. Kaneko, T. Ueda, A geometric method of sector decomposition. *Comput. Phys. Commun.* **181**, 1352–1361 (2010)
33. B.D. McKay, A. Piperno, Practical graph isomorphism, II. *J. Symb. Comput.* **60**, 94–112 (2014)

# Author's Curriculum Vitae

## Academic Positions

- 2/2023–present    **Postdoctoral fellow** University of Waterloo, Canada.  
Group of Prof. Karen Yeats, department of Combinatorics and Optimization, Faculty of Mathematics.
- 10/2018–9/2022    Wissenschaftlicher Mitarbeiter (doctoral candidate research assistant) Humboldt-Universität zu Berlin, Germany. Most of my working time was spent towards my research and Ph.D. The position included 2 h weekly teaching duties.
- 7/2017–10/2018    Studentische Hilfskraft (graduate student assistant) Humboldt-Universität zu Berlin, Germany.

## Education

- 10/2018–1/2023    Doctorate, Humboldt Universität zu Berlin, Institut für Physik.  
Supervisor Prof. Dirk Kreimer, *structure of local quantum field theories*  
Doctoral thesis *High-order renormalization of scalar quantum fields*  
Final grade *summa cum laude* (with distinction, the best out of 4 possible grades)
- 10/2015–9/2018    Master of Science (Physik), Humboldt-Universität zu Berlin, Germany  
Focus: Elementary particle physics  
Master's thesis *The propagator and diffeomorphisms of an interacting theory*, Thesis supervisor Prof. Dirk Kreimer  
Final grade: 1.0 (on a scale from 1.0 to 5.0 where 1.0 is best and 5.0 is fail)

8/2013–7/2014	Undergraduate student exchange, Lunds Universitet, Sweden Self-organized exchange year with a variety of courses in physics, mathematics, and Swedish language
10/2011–10/2015	Bachelor of Science (Physik), Friedrich-Schiller Universität Jena, Germany. Bachelor's thesis <i>Numerische Untersuchung von gluonischen Zwei- und Dreipunktfunktionen im Rahmen der Gitter-QCD</i> , Thesis supervisors Prof. Andras Wipf and Dr. André Sternbeck Final grade: 1.3 (on a scale from 1.0 to 5.0 where 1.0 is best and 5.0 is fail)
7/2003–6/2010	Abitur, Niklas-Luhmann-Gymnasium Oerlinghausen, Germany

## Teaching

### At University of Waterloo

1/2024–4/2024	Instructor <i>SYDE 112: Calculus 2 for systems design engineering</i> . $3 \times 1$ h weekly lecture, in person.
5/2023–9/2023	Instructor <i>MATH 225: Applied linear algebra 2</i> . 23 students, $3 \times 1$ h weekly lecture, in person. Developed course materials, assignment problems and example solutions, supervised 1 teaching assistant.

### At Humboldt-Universität zu Berlin

10/2021–12/2021	Teaching Assistant <i>Mathematische Grundlagen der Physik</i> . $2 \times 2$ h weekly tutorial in person. Marked weekly assignments.
10/2021–2/2022	Teaching Assistant <i>Physik für Agrarwissenschaftler</i> . Voluntary unpaid. 2 h tutorial every 2 weeks, online. Developed practice problems, marked solutions, held exam preparation meetings, marked exam. My tutorial was nominated for the price for good teaching at Humboldt-Universität.
10/2020–3/2021	Teaching Assistant <i>Klassische theoretische Physik</i> . 2 h weekly tutorial, online. Marked weekly assignments.
10/2020–3/2021	Teaching Assistant <i>Physik für Agrarwissenschaftler</i> . 2 h tutorial every 2 weeks, online. Wrote homework solutions.
4/2020–9/2021	Teaching Assistant <i>Experimentalphysik für Biologen und Chemiker 2</i> . 2 h weekly tutorial, online.

- 10/2019–3/2020 Teaching Assistant *Klassische theoretische Physik*.  
2 h weekly tutorial, in person. Marked weekly assignments.
- 10/2019–3/2020 Teaching Assistant *Physik für Agrarwissenschaftler*.  
2 h tutorial every 2 weeks, in person. Wrote homework solutions.
- 10/2018–3/2029 Teaching Assistant *Analysis 1*.  
Marked weekly assignments, wrote homework solutions.

## Services to the Scientific Community

- 6/2023 Co-organizer of the contributed minisymposium *Many Perspectives on Hopf Algebras in Combinatorics* at CanaDAM 2023, Winnipeg, Canada. Chair for one of two sessions.
- 8/2022 Co-organizer of the Ph.D.-student conference *(In)Credible Research 2022*, online at Charité, Berlin, Germany. Took part in the 6 months planning process, suggested and invited speakers, chair for multiple presentations.
- 4/2022 Helped at *Graph Complexes in quantum field theory*, Berlin, Germany.
- 8/2020 Chairman of *HU-Docs—Doctoral candidate network of Humboldt-Universität zu Berlin* (re-elected in 9/2021, until 9/2022). The club works Berlin-wide to improve the situation of international and German doctoral candidates and help them find their way in the city and the German academic system. As chairman, I was leading a team of 8 voluntary board members and one paid student assistant. I published peer-reviewed article (#3) about living conditions of doctoral candidates.
- 7/2019 Board member of *HU-Docs*. I was responsible for the weekly meeting on campus Adlershof, co-organized a 2-day excursion to Dresden, updated the website and designed advertising material.
- 4/2018 Helped at *23. Berliner Tag der Mathematik*, Berlin, Germany.
- 4/2017 Helped at *22. Berliner Tag der Mathematik*, Berlin, Germany.

## Conferences and Workshops

Talks given at conferences are listed under *Talks*, organization work done at conferences under *Services to the scientific community*.

- 9/2023    *Structural Aspects of Signatures and Rough Paths*, Oslo, Norway
- 6/2023    *Canadian Discrete and Algorithmic Mathematics—CanaDAM 2023*, Winnipeg, Canada
- 4/2023    *Math and Computing Research Discovery Days*, Waterloo, Canada
- 8/2022    *(In)Credible Research 2022*, Berlin, Germany
- 4/2022    *Graph Complexes in quantum field theory*, Berlin, Germany
- 7/2021    *52. Herbstschule für Hochenergiephysik Maria Laach*, Bad Honnef, Germany
- 3/2021    *Spring school on asymptotic methods and applications*, online Cambridge, UK
- 11/2020    *Algebraic structures in perturbative quantum field theory*, online Paris, France
- 6/2018    *Summer school on structures in local quantum field theory*, Les Houches, France

## Publications

An index<sup>a</sup> indicates that the authors are listed in alphabetical order.

### Submitted

- 6<sup>a</sup>   P.-H. Balduf, A. Cantwell, K. Ebrahimi-Fard, L. Nabergall, N. Olson-Harris, K. Yeats: *Tubings, chord diagrams, and Dyson–Schwinger equations*, Feb. 3, 2023. Submitted to *The Journal of the London Mathematical Society*. Preprint: [ARXIV 2302.02019 \[MATH.CO\]](#), 59 pages.

## Appeared

- 5 P.-H. Balduf: *Statistics of Feynman amplitudes in  $\phi^4$ -theory*. In *Journal of High Energy Physics* 11 (2023). [DOI 10.1007/JHEP11\(2023\)160](https://doi.org/10.1007/JHEP11(2023)160), 73 pages. [ARXIV 2305.13506 \[hep-th\]](https://arxiv.org/abs/2305.13506).
- 4 P.-H. Balduf: *Dyson-Schwinger Equations in Minimal Subtraction*. In: *Annales de l'Institut Henri Poincaré D* 169 (2023). [DOI 10.4171/aihp/169](https://doi.org/10.4171/aihp/169), 50 pages. [ARXIV2109.13684 \[hep-th\]](https://arxiv.org/abs/2109.13684).
- 3 P.-H. Balduf and A. Glück: *Fallbeispiele der Promotionsbedingungen für interne und externe Promovierende an der Humboldt-Universität zu Berlin*. In: *Qualität in der Wissenschaft* 3+4 (2022). 7 pages. Underlying results available from [docs.hu-berlin.de](https://docs.hu-berlin.de).
- 2 P.-H. Balduf: *Perturbation Theory of Transformed Quantum Fields* In: *Mathematical Physics Analysis and Geometry* 23, 33 (2020). [DOI 10.1007/s11040-020-09357-z](https://doi.org/10.1007/s11040-020-09357-z), 37 pages. [ARXIV 1905.00686 \[math-ph\]](https://arxiv.org/abs/1905.00686).
- 1 A. Sternbeck, P.-H. Balduf, A. Kızılersü, O. Oliveira, P.J. Silva, J. Skullerud, A. G. Williams: *Triple-gluon and quark-gluon vertex from lattice QCD in Landau gauge*, Feb 2, 2017. Proceedings of Science. Talk given at 34th annual International Symposium on Lattice Field Theory, 7 pages. [ARXIV 1702.00612 \[hep-lat\]](https://arxiv.org/abs/1702.00612).

## Preprint

- a P.-H. Balduf: “Propagator-cancelling scalar fields”, Feb 8, 2021. [ARXIV 2102.04315 \[math.ph\]](https://arxiv.org/abs/2102.04315), 46 pages.

# Appendix A

## Curious Quotes from the Literature

The ideas and results presented in this paper lead to many questions.

Erik Verlinde [34]

Eine physikalische Theorie glauben wir dann anschaulich zu verstehen, wenn wir uns in allen einfachen Fällen die experimentellen Konsequenzen dieser Theorie qualitativ denken können, und wenn wir gleichzeitig erkannt haben, daß die Anwendung der Theorie niemals innere Widersprüche enthält.

Werner Heisenberg [35]

An elucidation of the mathematical nature of quantum field theory is greatly desirable, particularly in view of current metaphysical pronouncements on this subject.

More pertinently, one neither knows entirely satisfactory calculational techniques in elementary particle physics nor, what is more fundamental, whether any proposed schemes have any solutions in principle.

William M. Frank [36]

Quantum mechanics itself is not at all a mystery to me.

Gerard 't Hooft [37]

I've analyzed this method both by doing a number of problems, and by a mathematical high-class elegant technique—I can do high class mathematics too, but I don't believe in it, that's the difference. [...] I'm lousy at proving things—I always make a mistake. [...]

So I always have to check with calculations; and I'm very poor at calculations  
— I always get the wrong answer.

Richard P. Feynman [38]

Well, brothers and sisters, I am here today to tell you: If you love these formulas, you need no longer hide in the shadows! The answer to all of these woes is here.

Gerald A. Edgar [39]

Section II contains the proof. Although at times this attains mathematical levels of obscurity, we make no claim for corresponding standards of rigor.

Sidney Coleman & Jeffrey Mandula [40]

Generalized hyperbolic functions [...] have a compelling intrinsic beauty.

Abraham Ungar [41]

Here I argue that mathematical soundness only is not enough when we are interested in processes of physical content.

Alfredo T. Suzuki [42]

The Yang-Mills theory with zero mass obviously does not exist, because a zero mass field would be obvious; it would come out of nuclei right away.

Richard P. Feynman [38]

The success of the quark-constituent picture both for resonances and for deep-inelastic electron and neutrino processes makes it difficult to believe quarks do not exist.

The problem is that quarks have not been seen.

Kenneth G. Wilson [43]

Indeed, we do not believe that physical quarks exist.

David J. Gross, [44], p. 209]

Knowledge of the effective potential is knowledge of the structure of spontaneous symmetry breakdown. Unfortunately, we do not know the effective potential.

Sidney Coleman & Erick Weinberg [45]

This result stands out from other multi-loop calculations because it is very likely correct.

Oliver Schnetz [12]

The aim of the present paper is to discuss in some detail established results on the field

[of quantum gravity]. In some strong sense, the review could be finished at once, because there are none.

Enrique Alvarez [46]

The appearance of this tiny fundamental length is a gentle reminder that, with conceptual problems no longer barring the way to performing the calculations, the practical interest attached to such refinements of gravitational dynamics is, and for the foreseeable future will remain, nil.

Julian Schwinger [47]

It would be difficult to pretend that the gravitational infrared divergence problem is very urgent. My reasons for now attacking this question are (1) Because I can [...] (2) Because something might go wrong, and that would be interesting.

Unfortunately, nothing does go wrong.

Steven Weinberg [48]

Durch mehrere Wahrnehmungen veranlasst, habe ich sorgfältige und vielfach wiederholte Versuche über die Fortleitung der Contaktelektricität in Metallen angestellt und Resultate erhalten, zu deren schleunigster Mittheilung ich mich um so mehr bewogen fühle, als meine geringe, ziemlich verkümmerte Musse mir es nicht verstattet, das Ende dieser Untersuchung so bald herbeizuführen.

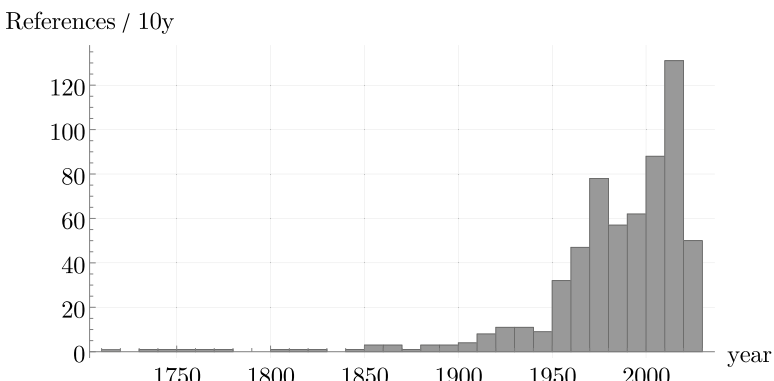
Georg S. Ohm [49]

## Appendix B

# Statistics

Including appendices and foreword, the thesis is 77380 words long. There are 4770 inline mathematical formulae, and 823 display formulae. This illustrates the scale of the project in Sect. 6.2.3: We have computed 16 period graphs for every word in this thesis.

The thesis contains references to 634 works, 552 of which are articles (including preprints and conference papers), 43 books, 15 book sections, 9 theses, and the rest other types of documents. The average document is from the year 1984, that is, 38 years old. The distribution below shows maxima corresponding to the main topics discussed in the thesis—1930s QFT basics, 1970s renormalization group theory and 2010s Hopf algebra theory:



Relying on references which are typically 40 years old might appear somewhat bizarre. But a trend towards older references has been observed empirically in many fields [50], and it is sometimes interpreted as a sign that scientific progress is slowing down [51]. The supposed mechanism is that, if the references of a work are decades old, this indicates that recent publications contribute little to the progress of the field.

The author is sceptical about this mechanism. The present thesis uses and refers to dozens of recent articles, the high average age arises mainly because we opted to refer to original sources even for widely known basics. But beyond the age of cited work, other indicators for a slowdown of scientific progress have been observed, despite an exponential growth in number of published papers [52–55]. The interpretation of these findings is disputed [56], and details of the claim—such as a slowdown in total numbers, or rather in productivity per researcher, or per money spent—vary, as well as the supposed reasons—incentive to work on well-funded mainstream questions instead of risky projects, overloading by the flood of published papers, by bureaucracy, teaching and communication tasks or simply the unbearable employment conditions of early career researchers. Our own findings [57] and the ongoing postdoc crisis [58–61]—postdoc positions sitting vacant because they are too unattractive to even apply—do support the last explanation, even if all the points are to some degree entangled. In any case, the author is much less concerned about the age of his references than about the employment situation of early career researchers.

## Appendix C

# Lied vom Schreiberling

Im Frühling fängt die Arbeit an,  
der Schreiberling beginnt sein Werk  
und manches dann noch nebendran,  
denn guter Mut hat ihn bestärkt.

Der Sommer schnell vorüber ging,  
die Seiten werden langsam mehr,  
gar freudig zeigt der Schreiberling  
die lange Schriftenrolle her.

Zum Mittag gibt es Pizzabrot  
und Pizza auch im Abendrot.  
Die Mensa ist von Kreuzberg fern  
und selber kocht er nicht so gern.

Der neue Tag bricht bald schon an,  
doch was macht noch der Schreibermann?  
Er legt sich nicht so bald zur Ruh,  
denn seine Frist rückt auf ihn zu.

Was nebenbei so liegen bleibt,  
dafür ist später keine Zeit.  
An Forschung lieg ihm gar nichts mehr,  
oh wenn es doch vorüber wär.

Der Schreiberling, der Schreiberling,  
der kleckst mit Tinte vor sich hin!  
Die Finger blau, die Augen rot,  
beim Schreiberling herrscht große Noth.

Er schreibt bei Tag und auch bei Nacht,  
wenn andrer schläft, ist er noch wach,  
noch ein Kapitel wird gebraucht,  
und dieses schreibt er schließlich auch.

Was bleibt von dieser Arbeitszeit  
wo ruhen kaum vergönnt ist?  
Kein Sommer zwar in Heiterkeit,  
doch immerhin Erkenntnis.

mit Alexandra Glück

# Appendix D

## List of Examples

- 1 Free scalar field, Lagrangian
- 2 Scalar field, field differential operator
- 3  $\phi^n$  theory, Lagrangian
- 4 Liouville theory, Lagrangian
- 5 Free scalar field, classical solution
- 6 Interacting scalar fields, classical equations of motion
- 7 Classical electrodynamics
- 8 Free scalar field, Hamiltonian density
- 9 Free scalar field, Four-point function
- 10 Permutations of four-point amplitude
- 11  $\phi^3$  theory, connected Feynman graphs
- 12 Dunce's cap
- 13 Dunce's cap, loops
- 14 Dunce's cap, graph matrices
- 15 Dunce's cap, trees
- 16 Dunce's cap, cut space and cycle space
- 17 Dunce's cap, first Symanzik polynomial
- 18 Dunce's cap, second Symanzik polynomial
- 19 Multiedges, Symanzik polynomials
- 20  $\phi^3$  theory, Feynman rules in position space
- 21 Multiedges, Feynman integral in position space
- 22  $\phi^3$  theory, Feynman rules in momentum space
- 23 Quantum electrodynamics
- 24 Multiedges, Feynman integral in momentum space
- 25 Massless 1-loop multiedge
- 26 Massless  $l$ -loop multiedges
- 27 Second chain graph
- 28 Contraction of the four-point function
- 29 Automorphism group of a 2-loop graph
- 30 Cutting a 2-loop graph
- 31 Dunce's cap as an electrical network
- 32 Dunce's cap, currents in the edges
- 33  $\phi^3$  theory, 1PI graphs
- 34  $\phi^n$  theory, residues of the Lagrangian
- 35  $\phi^3$  propagator, combinatorial Dyson-Schwinger equation

- 36  $\phi^3$  propagator, simplified combinatorial DSE
- 37  $\phi^3$  vertex, combinatorial Dyson-Schwinger equation
- 38  $\phi^3$  propagator, simplified integral DSE
- 39 Some values of Bell polynomials
- 40 First coefficients of the inverse series
- 41 First coefficients of the concatenation of series
- 42 Divergence of the QED perturbation series
- 43 Borel transform of factorially divergent series
- 44 Exponential integral
- 45 Algebra of quadratic matrices
- 46 Polynomials as algebra and coalgebra
- 47 Polynomials as bialgebra
- 48 Polynomials as Hopf algebra
- 49 Polynomials, coradical degree
- 50 Polynomials, Hopf algebra characters
- 51 Polynomials, infinitesimal characters
- 52 Faà di Bruno Hopf algebra, coproducts and antipodes
- 53 Series concatenation as trees
- 54 Series inversion as trees
- 55 Faà di Bruno Hopf algebra, inverse operators
- 56 Faà di Bruno Hopf algebra, coproduct of inverse operators
- 57  $\phi^3$  theory, counting treelevel graphs
- 58 Rooted trees, coproducts and antipodes
- 59 Rooted trees of Faà di Bruno Hopf algebra
- 60 Rooted trees of Connes-Moscovici Hopf algebra
- 61 Rooted trees, cocycle
- 62 Bamboos
- 63 Rooted trees, primitive elements
- 64 Linear fixed-point equation
- 65 Mandelstam variables of 4-point functions
- 66 Scale invariance
- 67 Conformal invariance
- 68 Decomposition of Green functions for scalar fields
- 69 Decomposition of Green functions for QED
- 70  $\phi^n$  theory, amplitudes needing renormalization
- 71 Dunce's cap, renormalization coproduct
- 72 Dunce's cap, core coproduct
- 73  $\phi^4$  theory, primitive graphs
- 74 Cocycle of Feynman graphs
- 75 Chain graphs, rooted trees
- 76 Dunce's cap, rooted trees
- 77 Second chain graph, rooted trees
- 78 Bamboos from rainbows
- 79 Bamboos from ladders
- 80 Toy model Feynman rules
- 81 Dunce's cap, renormalized amplitude
- 82 Invariant charges
- 83 Multiedge DSE, algebraic form
- 84 Multiedges, mass dimension
- 85 Massless  $l$ -loop multiedges, analytic regularization
- 86 Massless 1-loop multiedge, series expansion
- 87 Massless 1-loop multiedge, dimensional regularization
- 88 Dunce's cap in dimensional regularization
- 89 Second chain graph in dimensional regularization

- 90 Massless multiedge, period
- 91 Second chain graph, nontrivial primitive
- 92 Renormalization of a massless scalar field
- 93 Second chain graph, kinematic renormalization
- 94 Renormalizability of Liouville theory
- 95 Infinitesimal character for a primitive graph
- 96 Second chain graph, scale dependence
- 97 1-loop multiedge, Mellin transform
- 98 Tree Feynman rules
- 99 Toy model, Mellin transform
- 100  $\phi^n$  theory, relation between anomalous dimensions
- 101 Multiedge DSE, beta function and anomalous dimension
- 102 Infinite sums of rainbows or ladders
- 103 Toy model, linear DSE
- 104 Multiedge DSE
- 105 Multiedge linear DSE
- 106 Landau pole in QED
- 107 Multiedge DSE, linear correction in  $\epsilon$
- 108 Second chain graph in MS
- 109 Second chain graph in MS, exponential formula
- 110 Coefficients for the 1-loop multiedge in  $D = 4 - 2\epsilon$
- 111 Multiedge DSE, first order coefficients
- 112 Multiedge linear DSE in MOM, coefficients
- 113 Multiedge nonlinear DSE in MOM, coefficients
- 114 Multiedge nonlinear DSE in MS, coefficients
- 115 Multiedge linear DSE, anomalous dimension
- 116 Multiedge nonlinear DSE, expansion functions
- 117 Multiedge linear DSE, constant term in MS
- 118 Multiedge linear DSE,  $D = 6$ , constant term
- 119 Toy model linear DSE, constant term
- 120 Multiedge linear DSE, MS counterterm
- 121 Multiedge DSE, manually computing the shift
- 122 Multiedge linear DSE, shifted counterterm
- 123 Multiedge linear DSE, brute force shift
- 124 Multiedge DSE, first order of shift
- 125 Multiedge linear DSE, exact shift
- 126 Toy model linear DSE, exact shift
- 127 Gauge transformation of complex scalar field
- 128 Gauge transformation in QED
- 129 Ward identity in QED
- 130 Alternative forms of the Ward identity in QED
- 131 QCD
- 132 Slavnov-Taylor identities in QCD
- 133 Ward identity in QED, identification of graphs
- 134 Ward identity in QED as a Hopf ideal
- 135 Violation of the tadpole Hopf ideal
- 136 Analogy between QCD and a scalar field diffeomorphism
- 137 Diffeomorphism vertices
- 138 Diffeomorphism tree sums
- 139 Berends-Giele relations and Parke-Taylor formula
- 140 Massless two-point function of diffeomorphism
- 141 Inverse exponential diffeomorphism
- 142 Coefficients of the exponential diffeomorphism
- 143 Forward exponential diffeomorphism

- 144 Exponential superpropagator
- 145 Green functions of the exponential diffeomorphism
- 146 Metacounterterm in the 3-point-function
- 147 1-loop metacounterterms for the massless theory
- 148 3-point 2-loop metacounterterm for the massless theory
- 149 2-loop 1PI counterterms of the exponential diffeomorphism
- 150 Wheel with spokes, completion
- 151 Wheel with spokes, Hepp bound

# Bibliography

1. P.-H. Balduf, Dyson-Schwinger equations in minimal subtraction. *Annales de l'Institut Henri Poincaré D* **169** (2023). <https://doi.org/10.4171/aihp/169>
2. P.-H. Balduf, Perturbation theory of transformed quantum fields. *Math. Phys. Anal. Geom.* **23**, 33 (2020)
3. P.-H. Balduf, Propagator-cancelling scalar fields (2021). [arXiv:2102.04315](https://arxiv.org/abs/2102.04315) [math-ph]
4. P.-H. Balduf, Statistics of Feynman amplitudes in  $\phi^4$ -theory. *J. High Energy Phys.* **2023**, 160 (2023)
5. G.V. Dunne, M. Meynig, Instantons or renormalons? A comment on phi4\_4 theory in the MS scheme (2021). [arXiv: 2111.15554](https://arxiv.org/abs/2111.15554)
6. A.J. McKane, Perturbation expansions at large order: results for scalar field theories revisited. *J. Phys. A: Math. Theor.* **52**, 055401 (2019)
7. D.J. Broadhurst, D. Kreimer, Knots and numbers in  $\phi^4$  theory to 7 loops and beyond. *Int. J. Modern Phys. C* **06**, 519–524 (1995)
8. L.T. Adzhemyan, M.V. Kompaniets, Five-loop numerical evaluation of critical exponents of the  $\phi^4$  theory. *J. Phys.: Conf. Ser.* **523**, 012049 (2014)
9. M.V. Kompaniets, E. Panzer, Minimally subtracted six loop renormalization of  $O(n)$  - symmetric  $\phi^4$  theory and critical exponents. *Phys. Rev. D* **96**, 036016 (2017)
10. M.V. Kompaniets, E. Panzer, Renormalization group functions of  $\phi^4$  theory in the MS-scheme to six loops. *PoS LL2016*, 038 (2016),
11. D.Z. Freedman, K. Johnson, J.I. Latorre, Differential regularization and renormalization: a new method of calculation in quantum field theory. *Nuclear Phys. B* **371**, 353–414 (1992)
12. O. Schnetz, Quantum periods: A census of  $\phi^4$ -transcendentals. *Commun. Num. Theor. Phys.* **4**, 1–48 (2010)
13. S. Hu, O. Schnetz, J. Shaw, K. Yeats, Further investigations into the graph theory of  $\phi^4$ -periods and the  $c_2$  invariant. *Annales de l'Institut Henri Poincaré D* **9**, 473–524 (2022)
14. E. Panzer, Hepp's bound for Feynman graphs and matroids. *Annales de l'Institut Henri Poincaré D* **10**, 31–119 (2022)
15. M. Borinsky, Renormalized asymptotic enumeration of Feynman diagrams. *Ann. Phys.* **385**, 95–135 (2017)
16. M. Borinsky, *Graphs in Perturbation Theory: Algebraic Structure and Asymptotics*, Springer Theses (Springer International Publishing, Cham, 2018). <http://link.springer.com/10.1007/978-3-030-03541-9>

17. E. Nasrollahpoursamami, Periods of Feynman diagrams and GKZ D-modules (2016). [arXiv:1605.04970](https://arxiv.org/abs/1605.04970)
18. M. Borinsky, O. Schnetz, Recursive computation of Feynman periods. J. High Energy Phys. **2022**, 291 (2022)
19. F.C.S. Brown, On the periods of some Feynman integrals (2010). [arXiv:0910.0114](https://arxiv.org/abs/0910.0114)
20. F. Brown, O. Schnetz, Single-valued multiple polylogarithms and a proof of the zig-zag conjecture. J. Number Theory **148**, 478–506 (2015)
21. E. Panzer, O. Schnetz, The Galois coaction on  $\phi^4$  periods. Commun. Number Theory Phys. **11**, 657–705 (2017)
22. A.V. Smirnov, N.D. Shapurov, L.I. Vysotsky, FIESTA5: numerical high-performance Feynman integral evaluation (2021). [arXiv:2110.11660](https://arxiv.org/abs/2110.11660)
23. S. Borowka, J. Carter, G. Heinrich, Numerical evaluation of multi-loop integrals for arbitrary kinematics with SecDec 2.0. Comput. Phys. Commun. **184**, 396–408 (2013)
24. D. Maître, R. Santos-Mateos, Multi-variable integration with a neural network. J. High Energy Phys. **2023**, 221 (2023)
25. M. Borinsky, H.J. Munch, F. Tellander, Tropical Feynman integration in the Minkowski regime (2023). [arXiv:2302.08955](https://arxiv.org/abs/2302.08955)
26. M. Borinsky, Tropical Monte Carlo quadrature for Feynman integrals. Annales de l’Institut Henri Poincaré D **10**, 635–685 (2023)
27. N. Metropolis, A.W. Rosenbluth, M.N. Rosenbluth, A.H. Teller, E. Teller, Equation of state calculations by fast computing machines. J. Chem. Phys. **21**, 1087–1092 (1953)
28. K. Hepp, Proof of the Bogoliubov-Parasiuk theorem on renormalization. Commun. Math. Phys. **2**, 301–326 (1966)
29. T. Binoth, G. Heinrich, An automatized algorithm to compute infrared divergent multi-loop integrals. Nuclear Phys. B **585**, 741–759 (2000)
30. C. Bogner, S. Weinzierl, Resolution of singularities for multi-loop integrals. Comput. Phys. Commun. **178**, 596–610 (2008)
31. A.V. Smirnov, V.A. Smirnov, Hepp and Speer sectors within modern strategies of sector decomposition. J. High Energy Phys. **2009**, 004–004 (2009)
32. T. Kaneko, T. Ueda, A geometric method of sector decomposition. Comput. Phys. Commun. **181**, 1352–1361 (2010)
33. B.D. McKay, A. Piperno, Practical graph isomorphism, II. J. Symb. Comput. **60**, 94–112 (2014)
34. E.P. Verlinde, “On the Origin of Gravity and the Laws of Newton”, version 1. J. High Energy Phys. **04**, 029 (2011)
35. W. Heisenberg, Über den anschaulichen Inhalt der quantentheoretischen Kinematik und Mechanik. Zeitschrift für Physik **43**, 172–198 (1927)
36. W.M. Frank, Comparison theorems for convergence of regularized field theories. Ann. Phys. **29**, 175–216 (1964)
37. G. ’t Hooft, Dimensional reduction in quantum gravity. Conf. Proc. C **930308**, 284–296 (1993)
38. R.P. Feynman, Quantum theory of gravitation. Acta Phys. Polon. **24**, 697–722 (1963)
39. G.A. Edgar, Transseries for beginners (2009). [arXiv:0801.4877](https://arxiv.org/abs/0801.4877)
40. S. Coleman, J. Mandula, All possible symmetries of the S matrix. Phys. Rev. **159**, 1251–1256 (1967)
41. A. Ungar, Generalized hyperbolic functions. Amer. Math. Mon. **89**, 688–691 (1982)
42. A. Suzuki, Analytic result for the one-loop massless triangle Feynman diagram (2007)
43. K.G. Wilson, Confinement of quarks. Phys. Rev. D **10**, 2445–2459 (1974)
44. D.J. Gross, Applications of the renormalization group to high-energy physics, in *Methods in Field Theory, Les Houches Session 1975*, ed. by R. Balian, J. Zinn-Justin, Les Houches Session 28 (North Holland/World Scientific, 1981), pp. 141–250
45. S. Coleman, E. Weinberg, Radiative corrections as the origin of spontaneous symmetry breaking. Phys. Rev. D **7**, 1888–1910 (1973)
46. E. Alvarez, Quantum gravity, in *Lecture Notes in Physics*, vol. 669, ed. by J. Kowalski-Glikman, G. Amelino-Camelia, Lecture Notes in Physics (Springer, Berlin, Heidelberg, 2005), pp. 31–58
47. J. Schwinger, Sources and gravitons. Phys. Rev. **173**, 1264–1272 (1968)

48. S. Weinberg, Infrared photons and gravitons. Phys. Rev. **140**, B516–B524 (1965)
49. G.S. Ohm, Vorlfige Anzeige des Gesetzes, nach welchem Metalle die Contactelektricität leiten. Annalen der Physik **80**, 79–88 (1825)
50. A. Verstak, A. Acharya, H. Suzuki, S. Henderson, M. Iakhiae, C.C.Y. Lin, N. Shetty, On the shoulders of giants: the growing impact of older articles, version 1 (2014). [arXiv:1411.0275](https://arxiv.org/abs/1411.0275)
51. M. Clancy, Do Academic Citations Measure the Impact of New Ideas?. New Things Under the Sun (2022)
52. J.S.G. Chu, J.A. Evans, Slowed canonical progress in large fields of science. Proc. Natl. Acad. Sci. **118**, e2021636118 (2021)
53. J.A. Evans, Is scientific progress slowing? with James Evans: Big Brains podcast, Podcast, Chicago (2022). <https://news.uchicago.edu/scientific-progress-slowing-james-evans>
54. N. Bloom, Are ideas getting harder to find? Amer. Econ. Rev. **110**, 41 (2020)
55. S. Alexander, Is Science Slowing Down? - LessWrong, LessWrong (2018). <https://www.lesswrong.com/posts/v7c47vja3mavY3QC/is-science-slowing-down>
56. A. Guzey, How life sciences actually work: findings of a year-long investigation, guzey.com (2019). <https://guzey.com/how-life-sciences-actually-work/>
57. P.-H. Balduf, A. Glück, Fallbeispiele der Promotionsbedingungen für interne und externe Promovierende an der Humboldt- Universität zu Berlin. Qualität in der Wissenschaft **3+4**, 7 (2022)
58. A. Bahr, K. Eichhorn, S. Kubon, #IchBinHanna. Prek ä re Wissenschaft in Deutschland, 2nd edn. (Suhrkamp, 2022). <https://www.suhrkamp.de/buch/ichbihanna-t-9783518029756>
59. K. Langin, As professors struggle to recruit postdocs, calls for structural change in academia intensify (2022). <https://www.science.org/content/article/professors-struggle-recruit-postdocs-calls-structural-change-academia-intensify>
60. Postdocs in crisis: science cannot risk losing the next generation. Nature **585**, 160 (2020)
61. B. Nogrady, Pandemic amplifies postdoc struggles. The Scientist Magazine® (2021). <https://www.the-scientist.com/news-opinion/pandemic-amplifies-postdoc-struggles-69558>